# I. Discovery and Development of Nickel-Catalyzed 1,2-Dicarbofunctionalization Reactions of Alkenes

# II. Synthesis and Reactivity of Nucleophilic Calcium Fluoride Complexes with Oxygenic Ligand Frameworks

A thesis presented

by

Omar Apolinar

to

The Scripps Research Institute Graduate Program
and
Oxford Medical Sciences Division

in partial fulfilment of the requirements
for the degree of
Doctor of Philosophy
in the subject of

Chemistry/Biochemistry (TSRI/OU)

for

The Scripps Research Institute
La Jolla, California
and
The University of Oxford
Lincoln College, Oxford, UK

September 2024

©2024 by Omar Apolinar
All rights reserved

# Acknowledgements

For my Ph.D. studies, I was privileged to split my time between The Scripps Research Institute and the University of Oxford as part of the Skaggs-Oxford programme. I owe an enormous gratitude to the people at both locations for supporting me through the highs and lows of a joint doctoral degree spanning two continents.

At Scripps, I am immensely grateful for my supervisor Prof. Keary M. Engle throughout my graduate school journey. His guidance, advice, and passion for chemistry have all shaped me into the chemist that I am today. I am also thankful to my many colleagues in the Engle lab especially the team nickel family. Words cannot express how indebted I am to Dr. Joseph Derosa and Dr. Van T. Tran for their mentorship, friendship, and love for chemistry. If it was not for them, I would not have excelled at all in my chemistry adventures in graduate school. For instance, both helped me craft the sulfonamide directed Ni-catalyzed 1,2-DCF reaction system which is a significant part of my thesis. I would also like to thank Dr. Taeho Kang and Dr. Zi-Qi Li for their collaboration on a multitude of projects and for their authentic friendship. Specifically, Dr. Taeho Kang was a tremendous player in assisting me in achieving the first enantioselective Ni-catalyzed reaction for the Engle lab. Dr. Zi-Qi Li was such a hardworking labmate and a big help with the ketone directed Ni-catalyzed 1,2-DCF reaction system. I will always cherish working beside them including all those late-night lab hours especially during the pandemic which made me feel not so lonely. I would also like to acknowledge Dr. Tanner C. Jankins and postdoc Dr. Nana Kim for sharing with me all their organometallic chemistry wisdom. Dr. Tanner C. Jankins always pushed me

for excellence but at the same time made lab a fun time with all his silly shenanigans. Dr. Nana Kim was an amazing friend, and I always admired her intelligence and strong work ethic which has inspired me to strive for myself. Both of them were key to inspiring me to dive into main group organometallic chemistry at the University of Oxford.

I also want to thank older graduate students Drs. John A. Gurak, Jr., Zhen Liu, Mingyu Liu, Rei Matsuura, Andrew M. Romine, Lucas J. Oxtoby, Alena M. Vasquez, and postdoctoral fellows Drs. Yang Gao and Malkanthi K. Karunananda. I was so lucky to meet these kind, clever, hardworking and funny group members who easily welcomed me to the Engle lab family.

Next, I would like to acknowledge Dr. Huiqi Ni who was a part of my cohort and a good fume hood neighbor. I appreciate all those years that she brightened up our workspace with her cheerfulness and hard work. I would like to thank Camille Z. Rubel, who is a year below me, for her help on my enantioselective Ni-catalyzed reaction and for inspiring me with her driven work style. I also want to appreciate other Engle lab postdoctoral fellows that I overlapped with which include Drs. Zhonglin Liu, Phillippa Cooper, Amit K. Simlandy, Yeongyu Hwang, Skyler D. Mendoza and Johny M. Nguyen. I also would like to acknowledge other younger students in the Engle lab, namely Juntao Sun, Shenghua Yang, Wenji He, Madison Wagner, and Yilin Cao. It has been a great pleasure to have them onboard as the next generation of Engle lab members.

During my third year, I had the chance to mentor a UCSD undergraduate, Pranali G. Bedekar. I am grateful for her help in synthesizing a ton of substrates and ligands that were not easy to make and very time consuming.

I want to thank the past and present Engle lab's administrative staffs, Carrie Gabaldon, Kalee Brown, and Kathy Fritz. I am very grateful for Keary's family, Dr. Jae Engle, Oliver Engle, and our lab mascots Hermione, and Kingsly for giving the lab a good atmosphere.

Outside of the Engle lab, I am thankful to my friend Joong Phan from the Yu lab who is one of the smartest persons I know. I will forever cherish all the time he came down to visit me and talk about chemistry or just vent. In addition, I'm grateful to Brett Garabedian, Gabe Kline, Dr. Stone Woo, Hailee Parrett, Batuujin Burendei, Dr. Jinny C. Lee, Dr. Kelly Eberle, Dr. Brendyn Smith for being good friends and I will never forget you all.

During graduate school, I had opportunities to collaborate with amazing chemists in academia and industry outside of Scripps. Specifically, I'd like to thank our computational chemistry collaborators Prof. Peng Liu and his student Turki M. Alturaifi at University of Pittsburgh. Their computational studies and insights were essential to my major project. Additionally, I want to appreciate our industrial collaborators, Drs. Steven R. Wisniewski and Michael A. Schmidt from Bristol Myers Squibb especially for their intellectual contributions.

Regarding research facilities, I want to thank Dee-hua Huang and Laura Pasternack for top-notch NMR instrumentation at Scripps. I am very much indebted to the automated synthetic facility (ASF) members, Brittany Sanchez, Emily Sturgell, Quynh N. Wong, and Jason Chen for taking all the mass spectrometry and chiral SFC data. I also want to thank Arnold L. Rheingold, Jake, B. Bailey, and Milan Gembicky in UCSD for their X-ray crystallography contributions.

I would also like to thank the Skaggs-Oxford members that started from the Scripps side, namely Caroline Cuoco, Drs. Tossapol Pholcharee, and Tai Chaiamarit. For the past five years, Caroline has been on the same journey as me and I would not want anyone else to accompany me on this trek. I appreciate both Drs. Tossapol and Tai for their guidance especially the last parts of the joint doctoral programme.

At Oxford, I also had the honor to work with several awesome colleagues in the Aldridge group. First, I would like to deeply thank Prof. Simon Aldridge for taking me in and making me feel welcomed irrespective of my background. I will always remember the countless subgroup meetings which consisted of talking about chemistry for hours at end. His genuine curiosity-driven interest in chemistry was inspiring and his sage guidance led me to be successful in a new field in such a short time as well. I would like to thank Dr. Debotra Sarkar (Deb), Job J. C. Struijs, and Jianqin Tang (JT) for their immense friendship and help with chemistry. I will forever cherish the long discussions, the glove box sessions, and the jokes with Deb and JT as it made lab an easy place to work. I am grateful to Job J. C. Struijs for his help mainly with X-ray crystallography but also for his friendliness. All of them have a strong work ethic and I learned so much from them. All other Aldridge lab members have helped me greatly at one point or another, and I am grateful for their support. Specifically, I would like to acknowledge Lewis Wales, Dr. Maximilian Dietz, Aidan Murray, Dr. Mathias Ellwanger, Eve Poland and Tihomir Gluharev (Part II student) for their camaraderie.

My projects were in collaboration with the Gouverneur group, so would also like to thank Prof. Véronique Gouverneur for supporting me with my research interests and including me in the Gouverneur group meetings. I will always remember her warmth and

passion for chemistry. With regards to Gouverneur group members, I would like to acknowledge Calum Patel and Dr. Anirban Mondal for their good friendship, chemistry discussions, and laughs. I am also grateful for Gabija Poskaite, Ella Oglivy, Dr. Thomas Schlatzer, Caleb Doyle, Joseph Ford, Claire Dooley, and Sebastiano Ortalli for being so welcoming and supportive. I would like to thank Dr. Nick Rees for help with anything NMR related.

The Skaggs-Oxford crew from the Oxford side, Lauren Alexandrescu, Priyadarshini Chatterjee, and Peter R. Hall were all vital support that I appreciate dearly. We are all deeply grateful for Prof. Ian A. Wilson, Dawn Gibbons, Carmella Elan-Gaston, and Prof. Matthew C. Whitby to manage the logistics of the program.

Every now and then, I managed to sneak out of lab, and when I did I would either go to the Oxford Oratory, Black Friars, the Catholic Chaplaincy, or to the Rose and Crown. I am grateful to those communities for making Oxford so memorable. Specifically, I would like to thank my Oxford friends James, Edward, Ben, Renzo, Stefanos, Matthew, Karol, Elton, Nathan, Santo, Fr. Jack, Will & Eleanor, Sean & MC, Dominic, Agatha, Katharina, Rebecca, Zamely, Catherine, Isabel, Honor, Susannah, Joan & Pawel, Benedict, Pavol, Mateusz, Anton, the Wills, etc. I love you all!

Lastly, I would like to thank my friends and family from San Diego for supporting me during the past five years. My Mom, Dad, and my brother Jose always supported and encouraged me the entire way even if they did not understand what I was going through. I dedicate this thesis to Our Lady of Walsingham/Immaculate Conception, and I am eternally grateful to the three who give testimony in heaven the Father, the Son, and the Holy Spirit. Amen.

# Table of Contents

Acknowledgements ..... i
Table of Contents ..... vi
List of Tables ..... xiii
List of Figures ..... xv
List of Schemes ..... xvii
Abbreviations and Acronyms ..... xxiii
Abstract ..... xxvi

**Part I. Discovery and Development of Nickel-Catalyzed 1,2-Dicarbofunctionalization Reactions of Alkenes** ..... **1**

**Chapter 1: Introduction** ..... **2**

1.1. Conspectus ..... 3
1.2. Overview of Alkene Difunctionalization ..... 4
1.2.1. Significance of Alkenes ..... 4
1.2.2. Alkene 1,2-Difunctionalization under Transition Metal Catalysis ..... 5
1.2.3. Alkene 1,2-Dicarbofunctionalization under Transition Metal Catalysis ..... 6
1.2.4. Difficulties with Alkene 1,2-Dicarbofunctionalization Strategy ..... 7
1.3. Early Examples of Transition Metal Catalyzed 1,2-Dicarbofunctionalization of Alkenes ..... 8
1.3.1. Synopsis of non-Nickel Catalyzed 1,2-Dicarbofunctionalization ..... 8
1.4. Non-Stereoselective Nickel-Catalyzed 1,2-Dicarbofunctionalization of Alkenes ..... 9
1.4.1. Importance of Nickel as a Base Metal Catalyst ..... 9
1.4.2. Two-Component Ni-Catalyzed 1,2-Dicarbofunctionalization ..... 10
1.4.3. Three-Component Ni-Catalyzed 1,2-Dicarbofunctionalization ..... 10
1.5. Asymmetric Nickel- and Palladium- Catalyzed 1,2-Dicarbofunctionalization of Alkenes ..... 20
1.5.1. Background ..... 20

1.5.2. Two-Component Enantioselective 1,2-Dicarbofunctionalization of Alkenes via Migratory Insertion ..... 22
1.5.3. Two-Component Enantioselective 1,2-Dicarbofunctionalization of Alkenes via Radical Capture ..... 28
1.5.4. Three-Component Enantioselective 1,2-Dicarbofunctionalization of Alkenes via Migratory Insertion ..... 28
1.5.5. Three-Component Enantioselective 1,2-Dicarbofunctionalization of Alkenes via Radical Capture ..... 32
1.5.6. Miscellaneous Mechanisms ..... 35
1.6. References ..... 37

**Chapter 2: Experimental Methods** ..... 52

2.1. Chromatographic Techniques ..... 53
2.1.1. Silica Gel Column Chromatography ..... 53
2.1.2. Preparative Thin Layer Chromatography ..... 53
2.1.3. Supercritical Fluid Chromatography ..... 53
2.2. Spectroscopic and Analytical Techniques ..... 53
2.2.1. NMR Spectroscopy ..... 53
2.2.2. High Resolution Mass Spectroscopy ..... 54
2.2.3. X-Ray Crystallography ..... 54
2.3. Computational Methods ..... 54
2.4. References ..... 56

**Chapter 3: Nickel-Catalyzed 1,2-Diarylation of Alkenyl Ketones: A Comparative Study of Carbonyl-Directed Reaction Systems** ..... 59

3.1. Introduction ..... 60
3.2. Results and Discussion ..... 61
3.2.1. Reaction Optimization ..... 61
3.2.2. Comparison of Other Carbonyl-Directed Reaction Systems ..... 63
3.2.3. Substrate Scope ..... 65
3.2.4. Product Diversification ..... 69
3.2.5. Mechanistic Experiments ..... 70

3.3. Conclusion ..... 74
3.4. Experimental ..... 74
3.4.1. General Information ..... 74
3.4.2. Arylboronic Acid Neopentylglycol Ester Synthesis ..... 75
3.4.3. Alkenyl Ketone Substrate Synthesis ..... 75
3.4.4. General Procedure for Ni-Catalyzed 1,2-Diarylation of Alkenyl Ketones . 76
3.4.5. Unsuccessful/Low-Yielding Examples ..... 100
3.4.6. Control Experiment with $\gamma,\delta$-Unsaturated Ketone ..... 101
3.4.7. Proposed Catalytic Cycle ..... 101
3.4.8. $^{1}$H NMR and $^{13}$C NMR Resonances of Ketone Substrates ..... 101
3.4.9. Deuterium Incorporation Experiment ..... 102
3.5. References ..... 102
3.6. Contributions ..... 108

**Chapter 4: Sulfonamide Directivity Enables Nickel-Catalyzed 1,2-Diarylation of Diverse Alkenyl Amines ..... 109**

4.1. Introduction ..... 110
4.2. Results and Discussion ..... 111
4.2.1. Reaction Optimization ..... 111
4.2.2. Substrate Scope ..... 114
4.2.3. Control Experiments ..... 117
4.2.4. Tether Length Effects ..... 118
4.2.5. Proposed Catalytic Cycle ..... 119
4.2.6. Diversification of Representative Products ..... 120
4.3. Conclusion ..... 122
4.4. Experimental ..... 123
4.4.1. General Information ..... 123
4.4.2. Arylboronic Acid Neopentylglycol Ester Synthesis ..... 123
4.4.3. Alkenyl Sulfonamide and Miscellaneous Substrate Synthesis ..... 124
4.4.4. General Procedure for Ni-Catalyzed 1,2-Diarylation of Alkenyl Sulfonamides ..... 125

4.4.5. Miscellaneous Experiments for Nickel-Catalyzed 1,2-Diarylation of Alkenes ..... 157
4.5. References ..... 158
4.6. Contributions ..... 165

**Chapter 5: Three Component Asymmetric Nickel-Catalyzed 1,2-Dicarbofunctionalization of Unactivated Alkenes via Stereoselective Migratory Insertion ..... 166**

5.1. Introduction ..... 167
5.2. Results and Discussion ..... 169
5.2.1. Reaction Optimization ..... 169
5.2.2. Substrate Scope ..... 174
5.2.3. Experimental Mechanistic Investigations ..... 177
5.2.4. Proposed Catalytic Cycle ..... 178
5.2.5. Additional Experiments ..... 179
5.2.6. Computational Studies ..... 180
5.3. Conclusion ..... 184
5.4. Experimental ..... 184
5.4.1. General Information ..... 184
5.4.2. Aryl/alkenylboronic Acid Neopentylglycol Ester Synthesis ..... 185
5.4.3. Ligand Synthesis ..... 185
5.4.4. Alkenyl Sulfonamide and Miscellaneous Substrate Synthesis ..... 186
5.4.5. Screens and Trends for Nickel-Catalyzed 1,2-Dicarbofunctionalization of Alkenes ..... 188
5.4.6. General Procedure for Nickel-Catalyzed 1,2-Dicarbofunctionalization of Alkenes ..... 191
5.5. References ..... 219
5.6. Contributions ..... 225

**Chapter 6: New Vistas and Conclusion ..... 226**

6.1. Summary and Perspective ..... 227
6.2. Nickel-Catalyzed Hydroarylation of Trisubstituted Alkenes ..... 228

6.3. Nickel-Catalyzed 1,2-Arylalkylation of Unactivated Alkenes ..... 230
6.4. Advancements in Nickel-Catalyzed 1,2-Difunctionalization of Unactivated Alkenes using Sulfonamide Directing Groups ..... 231
6.5. Conclusion ..... 232
6.6. References ..... 233

**Part II. Synthesis and Reactivity of Nucleophilic Calcium Fluoride Complexes with Oxygenic Ligand Frameworks ..... 235**

**Chapter 7: Introduction ..... 236**

7.1. Conspectus ..... 237
7.2. Calcium Difluoride ..... 238
7.2.1. Physical Properties ..... 238
7.2.2. Applications ..... 239
7.3. Cluster Calcium Fluoride Complexes ..... 239
7.3.1. Background and Motive ..... 239
7.3.2. Calcium Fluoride Complexes of Titanium ..... 240
7.3.3. Molecular Calcium Fluoride Cages ..... 242
7.4. Well-Defined Molecular Calcium Fluoride Complexes ..... 243
7.4.1. β-Diketiminate-Supported Calcium Fluoride Complexes ..... 243
7.4.2. TACD-Supported Calcium Fluoride Complexes ..... 245
7.4.3. NON-Supported Calcium Fluoride Complexes ..... 246
7.4.4. Impetus for More Well-Defined Calcium Fluoride Complexes for Fluoride Anion Delivery ..... 248
7.5. References ..... 249

**Chapter 8: Experimental Techniques ..... 252**

8.1. Inert Atmosphere Schlenk Techniques ..... 253
8.2. Spectroscopic and Analytical Techniques ..... 253
8.2.1. NMR Spectroscopy ..... 253
8.2.2. Elemental Analysis ..... 254
8.2.3. X-Ray Crystallography ..... 254

8.3. References ..... 254

**Chapter 9: Synthesis and Reactivity of Nucleophilic Ca–F Complexes with TACN-based Ligands ..... 256**

9.1. Introduction ..... 257

9.2. Results and Discussion ..... 259

9.2.1. Synthesis and Attempted Fluorination of [K($\eta^6$-benzene)][(*t*-BuTACN)Ca] and (*t*-BuTACN-H)Ca ..... 259

9.2.2. Synthesis and Initial Fluorination Attempt of (*t*-BuTACN-Me)Ca ..... 262

9.2.3. Synthesis of [M][{(*t*-BuTACN-Me)Ca}$_2$F] Complexes ..... 264

9.2.4. Synthesis of [NMe$_4$][{(*t*-BuTACN-Me)CaF}$_2$] ..... 267

9.2.5. Reactivity of [K(2.2.2-crypt)][{(*t*-BuTACN-Me)Ca}$_2$F] ..... 269

9.3. Conclusions ..... 271

9.4. Experimental ..... 272

9.4.1. General Information ..... 272

9.4.2. Ligand Synthesis ..... 273

9.4.3. Preparation of [K($\eta^6$-benzene)][(*t*-BuTACN)Ca] ..... 274

9.4.4. Preparation of (*t*-BuTACN-H)Ca ..... 275

9.4.5. Preparation of (*t*-BuTACN-Me)Ca ..... 276

9.4.6. Preparation of [K(2.2.2-cryptand)][(*t*-BuTACN)Ca] ..... 277

9.4.7. Preparation of [M][{(*t*-BuTACN-Me)Ca}$_2$F] Complexes ..... 278

9.4.8. Preparation of [NMe$_4$][{(*t*-BuTACN-Me)CaF}$_2$] ..... 282

9.4.9. $^{19}$F DOSY NMR Spectra of Compounds **9.8** and **9.9** ..... 284

9.4.10. Reactivity of [K(2.2.2-cryptand)][{(*t*-BuTACN-Me)Ca}$_2$F] with Electrophiles ..... 285

9.5. References ..... 287

9.6. Contributions ..... 292

**Chapter 10: Future Directions and Conclusions ..... 293**

10.1. Summary and Perspective ..... 294

10.2. Leveraging Bulky 1,4,7-Triazacyclononane Ligands for Monomeric Calcium Fluoride Complexes ..... 295

10.2.1. Synthesis of K[(*t*-BuAdmTACN)Ca] ..... 295
10.2.2. Desymmetrization Attempts with K[(*t*-BuAdmTACN)Ca] ..... 297
10.2.3. Fluorination Attempts of (*t*-BuAdmTACN-Me)Ca ..... 298
10.3. Progress Towards Acyclic Molecular Calcium Fluorides using an O-Donor Boryloxy Ligand ..... 298
10.3.1. Synthesis of $Ca(OB(NDippCH)_2(THF)_2$ ..... 298
10.3.2. Fluorination Attempts of $Ca(OB(NDippCH)_2(THF)_2$ ..... 300
10.4. Conclusions ..... 302
10.5. References ..... 303

**Appendix I: X-Ray Crystallography Data** ..... **A1**

**Appendix II: Additional NMR Data** ..... **A22**

**Appendix III: Kinetic Data** ..... **A90**

**Appendix IV: SFC Data** ..... **A100**

**Appendix V: Computational Data** ..... **A114**

# List of Tables

**Table 3.1.** Reaction optimization table ..... 63
**Table 3.2.** Comparison of 1,2-diarylation conditions ..... 65
**Table 3.3.** Electrophile scope ..... 66
**Table 3.4.** Nucleophile scope ..... 67
**Table 3.5.** Ketone and alkene scope ..... 69
**Table 3.6.** Initial rate trends ..... 73
**Table 3.S1.** Aryl boronic acid neopentylglycol esters **3.S1–3.S11** ..... 75
**Table 3.S2.** Unsuccessful/low-yielding heteroaryl iodides ..... 100
**Table 3.S3.** Unsuccessful/low-yielding arylboronic acid neopentyl glycol esters. ..... 100
**Table 3.S4.** Unsuccessful/low-yielding alkenyl ketones ..... 100
**Table 3.S5.** NMR resonances of alkenes illustrating inductive effects ..... 101
**Table 4.1.** Optimization of 1,2-diarylation reaction ..... 113
**Table 4.2.** Electrophile and nucleophile scope ..... 115
**Table 4.3.** Sulfonamide and alkene scope ..... 117
**Table 4.4.** Tether length effects on 1,2-diarylation ..... 119
**Table 4.S1.** Aryl boronic acid neopentylglycol esters **(4.S1–4.S12)** used in this investigation ..... 123
**Table 4.S2.** Starting materials used in this study: alkenyl sulfonamides **4.S13**, **4.S14**, **4.S15,** and **4.S16**; alkenyl sulfonates **4.S17–4.S26**; and alkenyl amine **4.S27**. Failed or low yielding alkenyl amine starting materials include **4.S28–S35** ..... 124
**Table 4.S3.** Effect of catalyst loading on product yield ..... 157
**Table 5.1.** Directing group optimization of asymmetric 1,2-diarylation reaction ..... 170
**Table 5.2.** Ligand optimization of asymmetric 1,2-diarylation reaction ..... 172
**Table 5.3.** Deviation from optimized reaction conditions of asymmetric 1,2-diarylation reaction ..... 173
**Table 5.4.** Electrophile scope ..... 174
**Table 5.5.** Nucleophile scope ..... 176
**Table 5.6.** Alkene scope and limitations ..... 177

**Table 5.S1.** Aryl/alkenylboronic acid neopentylglycol esters (**5.S1–5.S19**) used in this study ..... 185
**Table 5.S2.** Commercially procured chiral ligands (**5.11**, **5.12**, **Bn-biOx**, **5.29** and **5.30**) used in this study ..... 185
**Table 5.S3.** Known Chiral Ligands (**5.13**, **5.14**, **5.15**, **5.16**, **5.22**, and **5.24–5.28**) ..... 186
**Table 5.S4.** Starting materials used in this study: alkenyl sulfonamides **5.1,** and **5.S20–5.S28**; sulfonyl chloride **5.S29**; alkenyl sulfonates **5.S30–5.S34** and **5.S36**; and alkenyl amine **5.S35** ..... 186
**Table 5.S5.** Low yielding electrophile and nucleophile examples ..... 190
**Table 5.S6.** Migratory insertion energy barrier values for all unique conformers computed at the DFT level ..... A122
**Table 6.1.** Preliminary screening of Ni-catalyzed hydroarylation reaction ..... 228
**Table 6.2.** Preliminary screening of Ni-catalyzed 1,2-arylalkylation reaction ..... 231
**Table 9.1.** Tabulated Ca–F–Ca bond angles and Ca–F bond lengths of complexes **9.6-9.8** ..... 267

# List of Figures

**Figure 1.1.** Dewar–Chatt–Duncanson model between nickel and ethylene ..... 5
**Figure 1.2.** Timeline (1996–2023) of Ni- and Pd-catalyzed 1,2-DCF of alkenes ..... 21
**Figure 3.1.** Background and synopsis of work ..... 61
**Figure 3.S1.** Comparison of the transition states for the substrate coordinating as the a) ketone (**TS1**), b) neutral enolate (**TS2, TS4, TS5**) and c) anionic enolate (**TS3**)..... A115
**Figure 3.S2.** Computed energy profiles for reductive elimination ..... A117
**Figure 3.S3.** Effect of aryl boronate electronic properties on reaction rate. Initial rate data and Hammett plot ..... A94
**Figure 3.S4.** Effect of aryl iodide electronic properties on reaction rate. Initial rate data and Hammett plot ..... A96
**Figure 3.S5.** Effect of aryl ketone electronic properties on reaction rate. Initial rate data and Hammett plot ..... A99
**Figure 3.S6.** Proposed mechanism ..... 101
**Figure 4.1.** Control experiments upon 1,2-diarylation reaction. ..... 117
**Figure 4.2.** Proposed catalytic cycle having directing group with X-type coordination upon migratory insertion. $L^1$ and $L^2$ represent neutral donors including DMFU, alkene substrate, solvent, etc. ..... 120
**Figure 5.1.** Proposed catalytic cycle of asymmetric 1,2-diarylation reaction ..... 179
**Figure 5.2.** Computed reaction energy profile of asymmetric 1,2-diarylation reaction . 182
**Figure 5.3.** Enantioselectivity-determining migratory insertion transition states..... 183
**Figure 5.S1.** Plot of log(e.r.) vs Hammett values of electrophiles at –10 °C ..... 188
**Figure 5.S2.** Plot of log(e.r.) vs Hammett values of electrophiles at 0 °C ..... 189
**Figure 5.S3.** Plot of log(e.r.) vs Hammett values of nucleophiles at –10 °C..... 190
**Figure 5.S4**. Lowest-energy conformers of the migratory insertion transition states. Gibbs free energies are with respect to the arylnickel(II) intermediate **5.82** ..... A120
**Figure 5.S5**. Lowest-energy conformers of the migratory insertion transition states with 4-iodobenzonitrile. Gibbs free energies are with respect to the most stable transition state **TS2a_CN** ..... A121

**Figure 5.S6.** Alternative transmetalation and reductive elimination pathways ..... A124
**Figure 5.S7.** Other possible reductive elimination transition states. All Gibbs free energies and enthalpies are with respect to the most stable transition state **TS4**. The COD ligand has a monodentate coordination in **TS4b** and **TS4c** ..... A125
**Figure 5.S8.** Computed transmetalation pathways with boronic acid and boronic ester. All Gibbs free energies and enthalpies are with respect to Ni(II) complex **5.84** ..... A126
**Figure 5.S9.** Isomers of the phenyl iodide–Ni(0) reactant complex ..... A126
**Figure 7.1.** Unit cell of $CaF_2$ from the fluoride anion perspective ..... 239
**Figure 7.2.** X-ray structure of a fluoro(aryloxo)calcium molecular cage ..... 243
**Figure 9.S1.** $^{19}F$ DOSY NMR spectrum of complex **9.8** in THF-$d_8$ ..... 285
**Figure 9.S2.** $^{19}F$ DOSY NMR spectrum of compound **9.9** in THF-$d_8$ ..... 285

# List of Schemes

**Scheme 1.1.** General 1,2-difunctionalization of alkenes scheme.....6
**Scheme 1.2.** General catalytic cycle of 1,2-DCF of alkenes.....7
**Scheme 1.3.** Common pitfalls for 1,2-DCF of alkenes.....8
**Scheme 1.4.** Genesis of 1,2-DCF of alkenes under Pd catalysis .....9
**Scheme 1.5.** Differing physical properties of Ni vs Pd: A) oxidation states, B) oxidative addition, C) atomic radius and electronegativity, and D) β-hydride elimination.....10
**Scheme 1.6.** Alkene substrate classes and stabilization strategies of three component Ni-catalyzed 1,2-DCF.....11
**Scheme 1.7.** A/B) Ni-Catalyzed 1,2-DCF of acrylate-type substrates.....12
**Scheme 1.8.** Ni-catalyzed 1,2-difluoroalkylarylation of enamides.....12
**Scheme 1.9.** 1,2-Diarylation of A) styrenyl aldimines and B/C) vinyl arenes .....13
**Scheme 1.10.** 1,2-Carboacylation of norbornenes .....14
**Scheme 1.11.** A) Ni-catalyzed 1,2-arylalkylation of β,γ-unsaturated carbonyls. B) Ni-catalyzed 1,2-dialkylation of β,γ- and γ,δ-unsaturated alkenyl carbonyls.....15
**Scheme 1.12.** Regiodivergent Ni-catalyzed 1,2-DCF of allyl amines using pyrimidine directing groups.....16
**Scheme 1.13.** A/B) Ni-catalyzed imine-directed 1,3- and 1,2-DCF of γ,δ-unsaturated ketimines. C) Ni-catalyzed 1,3-DCF of γ,δ-unsaturated α-cyanoesters .....17
**Scheme 1.14.** Ni-catalyzed reductive 1,2-perfluoroalkylacylation of allylic substrates...17
**Scheme 1.15.** A) Ni-catalyzed 1,2-diarylation of alkenyl amides. B) Ni-catalyzed 1,2-allylmethylation of *N*-allyl heterocycles. C) Ni-catalyzed 1,2-diarylation of alkenyl carboxylates.....18
**Scheme 1.16.** Photocatalytic 1,2-arylalkylation of unactivated alkenes.....19
**Scheme 1.17.** General scheme of non-stereoselective and asymmetric Ni- and Pd-catalyzed 1,2-DCF of alkenes.....21
**Scheme 1.18.** Component type and mechanisms of enantioinduction in Ni- and Pd-catalyzed 1,2-DCF of alkenes.....22
**Scheme 1.19.** Pd-catalyzed 1,2-DCF of cyclopentadiene-tethered alkenyl triflates.....23

**Scheme 1.20.** Ni-catalyzed two-component enantioselective 1,2-carbocyanation of alkenes linked with electrophiles....24
**Scheme 1.21.** Ni-catalyzed two-component enantioselective 1,2-DCF of alkenes linked with arylboranes....24
**Scheme 1.22.** Pd-catalyzed two-component enantioselective 1,2-DCF of acrylamides possessing a tethered aryltriflate....25
**Scheme 1.23.** Redox-neutral two-component enantioselective 1,2-DCFs of aryl-(pseudo) halide tethered alkenes....26
**Scheme 1.24.** Ni-catalyzed two-component enantioselective reductive 1,2-DCF of alkenes....27
**Scheme 1.25.** Ni-catalyzed two-component enantioselective 1,2-DCF of alkenes linked with carbamoyl halides....27
**Scheme 1.26.** Ni-catalyzed two-component enantioselective 1,2-DCF via radical capture....28
**Scheme 1.27.** Ni-catalyzed three-component enantioselective 1,2-homodiarylation of styrenes....29
**Scheme 1.28.** Enantioselective three-component 1,2-DCF of vinylboronic esters....30
**Scheme 1.29.** A) Enantioselective three-component 1,2-DCF of allylic esters. B) Enantioselective three-component reductive 1,2-DCF of vinyl amides. C) Enantioselective three-component reductive 1,2-DCF of 3,3,3-trifluoropropene....31
**Scheme 1.30.** A) Enantioselective, three-component metallaphotoredox catalyzed 1,2-DCF of vinyl phosphonates....31
**Scheme 1.31.** A) Enantioselective three-component Pd-catalyzed 1,2-diarylation of 1,3-dienes. B) Enantioselective three-component Pd-catalyzed 1,2-diarylation of 1,3-dienes. C) Enantioselective three-component Pd-Catalyzed 1,2-diarylation of unactivated alkenes with AQ auxiliary....33
**Scheme 1.32.** Enantioselective Pd-catalyzed 1,2-DCF of activated alkenes via enantiodetermining migratory insertion....33
**Scheme 1.33.** Enantioselective three-component Ni-catalyzed 1,2-diarylation of activated alkenes via enantiodetermining migratory insertion....34

**Scheme 1.34.** Enantioselective three-component Ni-catalyzed reductive 1,2-diarylation of unactivated alkenes with AQ auxiliary ..... 34
**Scheme 1.35.** Enantioselective three-component Pd-catalyzed 1,2-DCF of vinylboronic esters via enantiodetermining metallate rearrangement ..... 35
**Scheme 1.36.** Enantioselective three-component Pd-catalyzed 1,2-DCF of vinylboronic esters via enantiodetermining metallate rearrangement ..... 36
**Scheme 3.1.** Diversification of a representative product. (a) *m*CPBA, TFA, anhydrous DCM, r.t. (b) $H_2NOH$•HCl, TFA, 70 ˚C. (c) $Ph_3PCH_2Br$, *n*-BuLi, THF, 70 ˚C. (d) $LiAlH_4$, $AlCl_3$, $Et_2O$/DCM, r.t. (e) $NaBH_4$, THF, reflux ..... 70
**Scheme 3.2.** Mechanistic experiments ..... 71
**Scheme 3.3.** DFT calculations upon several migratory insertion transition states ..... 72
**Scheme 3.S1.** Synthesis of NaOMe ..... 75
**Scheme 3.S2.** Synthesis of alkenyl ketone substrates using a classical Barbier allylation with subsequent Dess–Martin oxidation ..... 75
**Scheme 3.S3.** Synthesis of the *γ*,*δ*-unsaturated ketone **3.S31** ..... A32
**Scheme 3.S4.** Synthesis of *α*-methyl *β*,*γ*-unsaturated ketone **3.S32** ..... A34
**Scheme 3.S5.** Synthesis of the *δ*,*ε*-unsaturated ketone **3.S33** ..... A35
**Scheme 3.S6.** Synthesis of the internal *β*,*γ*-unsaturated ketone **3.S34** ..... A36
**Scheme 3.S7.** Nickel-catalyzed 1,2-diarylation of alkenyl ketones ..... 76
**Scheme 3.S8.** Low-yielding 1,2-diarylation of γ,δ-unsaturated ketone in the absence of DMFU ..... 101
**Scheme 3.S9.** Mechanistic experiment with deuterated alcohol solvent. Compounds ***d*-3.1** and ***d*-3.S12** were isolated together, and the yield was determined from the combined mass and $^1$H NMR analysis of the mixture ..... 102
**Scheme 4.1.** Previous reports and synopsis of new findings ..... 111
**Scheme 4.2.** Diversification of 1,2-diarylated products as a linchpin technology. Percentages represent isolated yields ..... 121
**Scheme 4.3.** HLF cyclization of a representative product ..... 122
**Scheme 4.S1.** Synthesis of alkenyl sulfonamides **4.S36**, **4.S37**, **4.S38**, **4.S39**, **4.38**, and **4.S40**. These compounds were synthesized using adapted versions of literature procedures describing the preparation of similar compounds ..... 124

**Scheme 4.S2.** Synthesis of alkenyl sulfonamides **4.S41–4.S43**, **4.S46**, **4.S47**, and **4.S49–4.S50**. These compounds were synthesized using adapted versions of literature procedures describing the preparation of similar compounds ..... A46
**Scheme 4.S3.** Synthesis of α-methyl alkenyl sulfonamide **4.S54**. This compound was synthesized using an adapted version of a literature procedure describing the preparation of a similar compound ..... A56
**Scheme 4.S4.** Synthesis of N-methyl alkenyl sulfonamide **4.39**. This compound was synthesized using an adapted version of a literature procedure describing the preparation of a similar compound ..... A57
**Scheme 4.S5.** Synthesis of N-methyl alkenyl sulfonamide **4.40**. This compound was synthesized using an adapted version of a literature procedure describing the preparation of a similar compound ..... A58
**Scheme 4.S6.** Attempts of 1,2-diarylation with O-containing directing groups ..... 157
**Scheme 4.S7.** Synthesis of secondary alkyl amines **4.63–4.67** ..... A65
**Scheme 4.S8.** Synthesis of 4-Cs protected pyrrolidine **4.68** ..... A70
**Scheme 5.1.** Precedents and synopsis of this work ..... 169
**Scheme 5.2.** Mechanistic experiments of asymmetric 1,2-diarylation reaction ..... 178
**Scheme 5.3.** Additional experiments of asymmetric 1,2-diarylation reaction ..... 180
**Scheme 5.S1.** Synthesis of BiOX ligands **5.17, 5.18, 5.19, 5.20**, **5.21** and **5.23**. These compounds were synthesized using adapted versions of literature procedures describing the preparation of similar compounds ..... 186
**Scheme 5.S2.** Synthesis of alkenyl sulfonamides **1a**, **1f**, **1h**, **1p**, **1s**, and **1u**. These compounds were synthesized using adapted versions of literature procedures describing the preparation of similar compounds ..... 187
**Scheme 5.S3.** Synthesis of alkenyl sulfonamides **5.S41–5.S45**, **5.71**, and **5.73–5.75**. These compounds were synthesized using adapted versions of literature procedures describing the preparation of similar compounds ..... A79
**Scheme 5.S4.** Synthesis of N-methyl alkenyl sulfonamide **5.71**. This compound was synthesized using an adapted version of a literature procedure describing the preparation of a similar compound ..... A84
**Scheme 5.S5.** Deprotection of representative product **5.10** ..... A86

**Scheme 6.1.** Preliminary screening of Ni-catalyzed hydroarylation reaction.....229
**Scheme 6.2.** A) Ni-catalyzed 1,2-carboamination of alkenyl sulfonamides with N–O electrophiles. B) Ni-catalyzed 1,2-carbosulfenylation of alkenyl sulfonamides.....232
**Scheme 7.1.** Synthesis of a titanium calcium fluoride cluster from [Cp*$TiF_3$] and Ca/Hg alloy .....241
**Scheme 7.2.** Synthesis of a titanium calcium fluoride cluster from [Cp*$TiF_3$] and in situ formed $CaF_2$.....242
**Scheme 7.3.** Synthesis of a NacNac-stabilized calcium fluoride complex via $Me_3SnF$ .244
**Scheme 7.4.** Synthesis of a NacNac-stabilized calcium fluoride complex via C–F bond activation .....245
**Scheme 7.5.** Synthesis of a TACD-stabilized calcium fluoride complex via C–F bond activation .....246
**Scheme 7.6.** Synthesis of a NON-stabilized calcium fluoride complex via C–F bond activation. .....247
**Scheme 9.1.** Precedents and synopsis of the disclosed work.....259
**Scheme 9.2.** Synthesis and X-ray structures of anionic and neutral calcium complexes **9.2** and **9.3** (ellipsoids set at 50% probability level; H atoms omitted and arenes shown in wireframe format for clarity). (a) $Ca(HMDS)_2(THF)_2$, KHMDS, and $C_6D_6$. (b) $Ca(HMDS)_2(THF)_2$ and $C_6D_6$.....260
**Scheme 9.3.** Unsuccessful fluorination attempts of complex **9.2**.....261
**Scheme 9.4.** Unsuccessful fluorination attempts of complex **9.3**.....262
**Scheme 9.5.** Synthesis and X-ray structures of Ca complexes **9.4** and **9.5** (ellipsoids set at 50% probability level; H atoms omitted and arenes shown in wireframe format for clarity).....264
**Scheme 9.6.** Synthesis and X-ray structures of Ca–F–Ca complex **9.6** (ellipsoids set at 50% probability level; H atoms omitted and arenes shown in wireframe format for clarity).....265
**Scheme 9.7.** Synthesis and X-ray structures of Ca–F–Ca complex **9.6** (ellipsoids set at 50% probability level; H atoms omitted and arenes shown in wireframe format for clarity).....266
**Scheme 9.8.** Synthesis of dinuclear calcium difluoride complex **9.9** .....268

**Scheme 9.9**. Reactivity of Ca–F complex **9.6** with organic electrophiles. Percentage yield by $^{19}F$ NMR using fluorobenzene as internal standard ..... 270
**Scheme 9.10.** Stacked crude $^{1}H$ NMR spectra of reactions with compound **9.6** and independent synthesis of [K(2.2.2-crypt)][{(*t*-BuTACN-Me)Ca}$_2$(μ-Cl)] ..... 271
**Scheme 9.S1.** Reaction of complex **9.6** with 1-adamantanecarbonyl chloride..... 285
**Scheme 9.S2.** Reaction of complex **9.6** with triphenylcarbenium tetrakis(pentafluorophenyl)borate ..... 285
**Scheme 9.S3.** Reaction of complex **9.6** with chlorotriphenylsilane ..... 286
**Scheme 9.S4.** Reaction of complex **9.6** with tosyl chloride ..... 286
**Scheme 9.S5.** Independent synthesis of complex **9.14** with KCl/2.2.2-cryptand combination ..... 287
**Scheme 10.1.** A uranium complex supported by (*t*-BuAdmTACN) and its reactivity thereof..... 296
**Scheme 10.2.** Synthesis of (*t*-BuAdmTACN) 10.1 and complex K[(t-BuAdmTACN)Ca] **10.2** ..... 296
**Scheme 10.3.** Desymmetrization attempts of complex K[(*t*-BuAdmTACN)Ca] **10.2** ...297
**Scheme 10.4**. Telescoping fluorination experiment of complex (*t*-BuAdmTACN-Me)Ca **10.3** ..... 298
**Scheme 10.5**. Precedents with N-heterocyclic boryloxy and synopsis of inspired work. ..... 299
**Scheme 10.6**. Synthesis and X-ray structure of calcium complex **10.6**..... 300
**Scheme 10.7**. Initial fluorination attempts of calcium complex **10.6** ..... 301
**Scheme 10.8**. Fluorination of calcium complex **10.6** with $Me_3SnF$ ..... 301

# Abbreviations and Acronyms

| | |
|---|---|
| (*rac*) | Racemic |
| Å | Ångström ($10^{-10}$ metres) |
| Ac | Acetyl |
| acac | acetylacetonates |
| Adm | Adamantyl |
| Am | Amyl |
| aq | Aqueous |
| atm | Atmosphere (Pressure Unit) |
| Ar | Aryl |
| BINAP | 2,2'-Bis(diphenylphosphino)-1,1'-binaphthyl |
| biOx | Bioxazoline |
| bipy | 2,2'-Bipyridine |
| Bn | Benzyl |
| Boc | *tert*-Butyloxycarbonyl |
| BOX | Bisoxazoline |
| BPin | 4,4,5,5-Tetramethyl-1,3,2-dioxaborolan-2-yl |
| Bu | Butyl |
| C–C | Carbon–Carbon (Bond) |
| C–H | Carbon–Hydrogen (Bond) |
| Cbz | Carboxybenzyl |
| cod | 1,5-Cyclooctadiene |
| Cy | Cyclohexyl |
| d.r. | Diastereoisomeric Ratio |
| dba | Dibenzylideneacetone |
| DCC | *N*,*N'*-Dicyclohexylcarbodiimide |
| DCE | 1,2-Dichloroethane |
| DCF | Dicarbofunctionalization |
| DCM | Dichloromethane |
| DFT | Density Functional Theory |
| DG | Directing Group |

| | |
|---|---|
| DIPT | Diisopropyl Tartrate |
| DMAP | 4-(Dimethylamino)pyridine |
| DMFU | Dimethyl fumarate |
| EDO | Electron-deficient olefin |
| ee | Enantiomeric Excess |
| e.r. | Enantiomeric ratio |
| equiv. | Equivalent(s) |
| ESI | Electrospray Ionization |
| Et | Ethyl |
| FG | Functional group |
| FI | Field Ionization |
| g | Gram(s) |
| h | Hour(s) |
| Hex | Hexane |
| HPLC | High Performance Liquid Chromatography |
| HRMS | High Resolution Mass Spectrometry |
| Hz | Hertz |
| *i* | *Iso* |
| IR | Infrared Spectroscopy |
| L | Neutral Ligand |
| M | Moles per liter (mol/L) |
| M.p. | Melting Point |
| Me | Methyl |
| MHz | Megahertz |
| min | Minute(s) |
| mL | Milliliter(s) |
| mol | Mole(s) |
| *n* | Normal |
| nep | Neopentyl glycolato |
| NHC | *N*-Heterocyclic Carbene |
| NMR | Nuclear Magnetic Resonance Spectroscopy |
| Nu | Generic Nucleophile |
| PET | Positron Emission Tomography |

| | |
|---|---|
| PG | Protecting Group |
| Ph | Phenyl |
| Pin | Pinacol |
| Piv | Dimethylpropanoyl (Pivaloyl) |
| Pr | Propyl |
| R | Generic Carbogenic Fragment (Aryl or Alkyl Group) |
| r.r. | Regioisomeric ratio |
| R–$BX_n$ | Generic Organoboron Reagent |
| R–M | Generic Organometallic Reagent |
| $R_f$ | Retention Factor |
| RT | Room Temperature |
| $S_N2$ | Bimolecular Nucleophilic Substitution |
| *t* | Tertiary (*tert*) |
| TACN | 1,4,7-Triazacyclononane |
| *t*-AmylOH | 2-Methyl-2-butanol |
| TMAF | Tetramethylammonium Fluoride |
| Tf | Trifluoromethanesulfonyl (Triflyl) |
| TFA | Trifluoroacetic Acid or Trifluoroacetate (Depending on Context) |
| TFAA | Trifluoroacetic Anhydride |
| THF | Tetrahydrofuran |
| TLC | Thin Layer Chromatography |
| Tol | Tolyl |
| Tris | 2,4,6-triisopropylbenzene sulfonyl group |
| Ts | *para*-Toluenesulfonyl (Tosyl) |
| TS | Transition State |
| VSEPR | Valence Shell Electron Pair Repulsion |
| X | Anionic Ligand |
| δ | Chemical Shift |
| µL | Microliter(s) |
| °C | Degrees Celsius |

# Abstract

*Part I. Discovery and Development of Nickel-Catalyzed 1,2-Dicarbofunctionalization Reactions of Alkenes.*

While much success has been achieved in the realm of 1,2-dicarbofunctionalization of alkenes under nickel catalysis, yet there remains a paucity in using weak directing groups, dicarbofunctionalizing multisubstituted alkenes, and implementing asymmetric variants. In our investigations, we developed a method where we can leverage weak ketone native directing groups for the 1,2-diarylation of unactivated alkenes with excellent regioselectivity. Additionally, we serendipitously discovered that sulfonamides are uniquely effective in directing 1,2-dicarbofunctionalization of unactivated alkenes including 1,2-disubstituted and trisubstituted alkenes. In light of these findings, we demonstrate an enantioselective variant which was plausible by tuning the steric bulk of the sulfonamide directing group and finding the adequate flexibility of a chiral N,N-ligand.

*Part II. Synthesis and Reactivity of Nucleophilic Calcium Fluoride Complexes with Oxygenic Ligand Frameworks.*

The inorganic salt $CaF_2$ is insoluble in water and in organic solvents making it difficult to study *in situ*. While efforts have been made in the solid state, solution state investigations would greatly shed more light into the nature of the nucleophilicity of the Ca–F bond. The majority of the known soluble, well-defined, calcium fluoride complexes are typically stabilized by amido-type ligands, and with only one ligand archetype

showing fluoride delivery capabilities. We sought to investigate O-donor ligand scaffolds that may also stabilize calcium fluoride complexes and improve fluoride anion delivery compared to the amido-supported counterpart. In our investigations, we found that the TACN ligand was appropriate owing to its macrocyclic design, which encapsulates calcium. However, a novel desymmetrizing method of a (TACN)Ca complex had to be developed which allowed leeway for the synthesis of various dinuclear calcium mono- and difluoride complexes. Fluoride anion delivery upon electrophiles was found to be enhanced when compared to the notorious NON ligand framework.

# PART I

# DISCOVERY AND DEVELOPMENT OF NICKEL-CATALYZED 1,2-DICARBOFUNCTIONALIZATION REACTIONS OF ALKENES

# CHAPTER 1

## INTRODUCTION

Adapted with permission from:

Derosa, J.; Apolinar, O.; Kang, T.; Tran, V. T.; Engle, K. M. Recent Developments in Nickel-Catalyzed Intermolecular Dicarbofunctionalization of Alkenes. *Chem. Sci.* **2020**, *11*, 4287–4296. Copyright © 2020 Royal Chemical Society.

Kang, T.; Apolinar, O.; Engle, K. M. Ni- and Pd-Catalyzed Enantioselective 1,2-Dicarbofunctionalization of Alkenes. *Synthesis* **2024**, *56*, 1–15. Copyright © 2023 Thieme.

## 1.1. CONSPECTUS

The booming of transition metal–catalyzed cross-coupling reactions in the 1970s has proven monumental as it impacted not only modern chemical synthesis, but extended to applications in the industrial setting as well.[1a] Much of the early investigations were conducted with the base metal nickel as a catalyst; however, difficulties in characterization due to the paramagnetic properties of nickel led many to resort to nickel's fellow group-10 member, palladium.[1b] With facile analysis of reactions catalyzed by this metal and its more robust catalytic activity, much of the cross-coupling literature last century ended up revolving around palladium catalysis.

The following decades after the golden cross-coupling era led to a more sophisticated case of cross-coupling where a conjunctive linker is introduced joining both coupling partners in the resultant product. Although these so called conjunctive cross-coupling reactions were initially investigated with palladium catalysts, it turned out that nickel is better suited given its different chemical properties. Consequently, a nickel-catalyzed 1,2-dicarbofunctionalization (DCF) renaissance emerged mainly targeting alkenes as they are widely available and easy to procure. Currently, unactivated alkenes still remain a challenge in this area.

Part I of this Thesis describes our efforts to further advance the discovery and development of nickel-catalyzed 1,2-DCF reactions of unactivated alkenes with native directing groups. In Chapter 1, we offer a summary of the field of nickel catalysis and the purpose of this work. We begin by providing an overview of the transition-metal-catalyzed alkene 1,2-difunctionalization strategy (Section 1.2) before moving towards early examples of transition-metal-catalyzed alkene 1,2-difunctionalization excluding nickel

(Section 1.3). We then segue into a discussion of the non-stereoselective, nickel-catalyzed 1,2-DCF of alkenes (Section 1.4). Finally, we showcase the current state of asymmetric nickel and palladium-catalyzed 1,2-DCF of alkenes (Section 1.5).

Chapter 2 discusses the experimental methods used in the investigations. Chapters 3–5 revolve around research that was carried out by the author in collaboration with several coworkers (see Acknowledgments) from August 2019 to July 2022 in the Engle laboratory at The Scripps Research Institute. Chapter 3 focuses on the exploration of weak native directing groups, namely ketones, in 1,2-DCF of unactivated alkenes. Chapter 4 describes the discovery and optimization of 1,2-DCF of unactivated alkenes enabled by native sulfonamide directing groups. In Chapter 5, we showcase the first asymmetric 1,2-DCF of unactivated alkenes via aryl/alkenylnickel migratory insertion, which was facilitated by a bulky sulfonamide directing group and chiral bioxazoline ligand. Finally, Chapter 6 offers a conclusion and outlook on the field.

## 1.2. OVERVIEW OF ALKENE DIFUNCTIONALIZATION

### 1.2.1. Significance of Alkenes

Alkenes are a ubiquitous functional group found in all classes of organic molecules ranging from feedstock chemicals to blockbuster drug molecules. They are important due to their ubiquity and their vast potential for diverse functionalization in the context of organic synthesis and methodology. Alkenes have served as an excellent starting point for a fair amount of the classical organic chemistry reactions, for example but not limited to dihalogenation, dihydroxylation, and catalytic hydrogenation.[1c] Over the past several

decades, more focus has been geared towards the catalysis area, allowing for more molecular complexity to be achieved.

### 1.2.2. Alkene 1,2-Difunctionalization under Transition Metal Catalysis

Transition metal catalysts have been vital in functionalizing alkenes due to the accessibility of d-orbital electrons upon reaction. Furthermore, as depicted in the Dewar–Chatt–Duncanson model (Figure 1.1), the favorable interaction of the filled d-orbitals with the empty π* antibonding orbital of the alkenes allows elongation and activation of the C=C bond, allowing its functionalization to occur.[2]

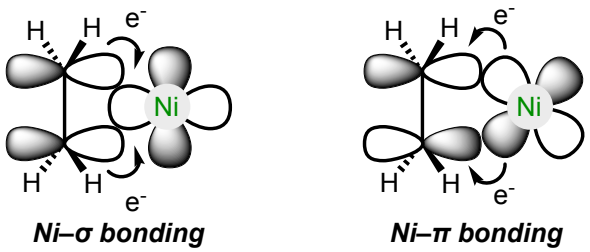


**Figure 1.1.** Dewar–Chatt–Duncanson model between nickel and ethylene.

Historically alkenes have been found useful in transition-metal-catalyzed difunctionalization reactions where installation of two adjacent groups is achieved in one synthetic step, allowing for rapid elaboration of molecular complexity from a simple, planar starting material (Scheme 1.1). A large body of catalytic alkene difunctionalizations have been reported in the realm of homodifunctionlizations,[3] intramolecular difunctionalizations,[4] and difunctionalizations of electronically biased systems such as polarized or conjugated alkene starting materials.[5] On the other hand, regioselective three-component 1,2-difunctionalizations of alkenes have historically proven to be cumbersome but have emerged a flourishing field of study in recent years.

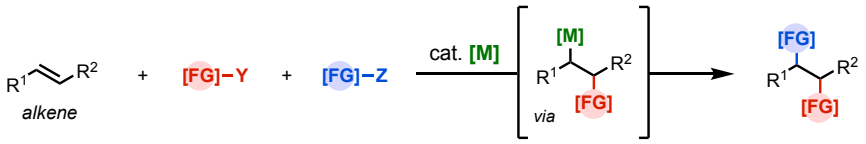


***Scheme 1.1.*** General depiction of 1,2-difunctionalization of alkenes.

### 1.2.3. Alkene 1,2-Dicarbofunctionalization under Transition Metal Catalysis

Traditional transition-metal-catalyzed cross-couplings have served as a strong driving force for the rapid construction of molecular complexity via C–C bond formation using carbogenic electrophiles and nucleophiles.[6,7] Several decades of development in the cross-coupling paradigm have generated a highly modular repertoire for bond making in organic synthesis. Nonetheless, the incorporation of an alkene as a third component has only recently come about as a feasible catalytic strategy.[8,9] In such a reaction, two carbogenic coupling partners are coupled across the C=C bond, resulting in 1,2-DCF. In the chemical literature, these types of transformations are usually referred to as conjunctive cross-couplings since they involve the two coupling partners that could be used in classical cross-couplings as well as a third linking component that can conjoin the other two fragments.

Mechanistically, 1,2-DCF reactions share a putative C($sp^3$)–metal intermediate in their respective catalytic cycles upon reaction with a first coupling partner (Scheme 1.2). Some plausible pathways to generate such intermediate include migratory insertion, nucleometallation, or radical addition followed by radical capture with the transition metal catalyst. Subsequently, the C($sp^3$)–metal intermediate reacts with a second coupling partner via elementary steps such as migratory insertion, oxidative addition, or transmetalation followed by reductive elimination to give the regioselective 1,2-dicarbofunctionalized

products. Such methodologies pose synthetic advantages yet possess several similar difficulties in selectivity control.

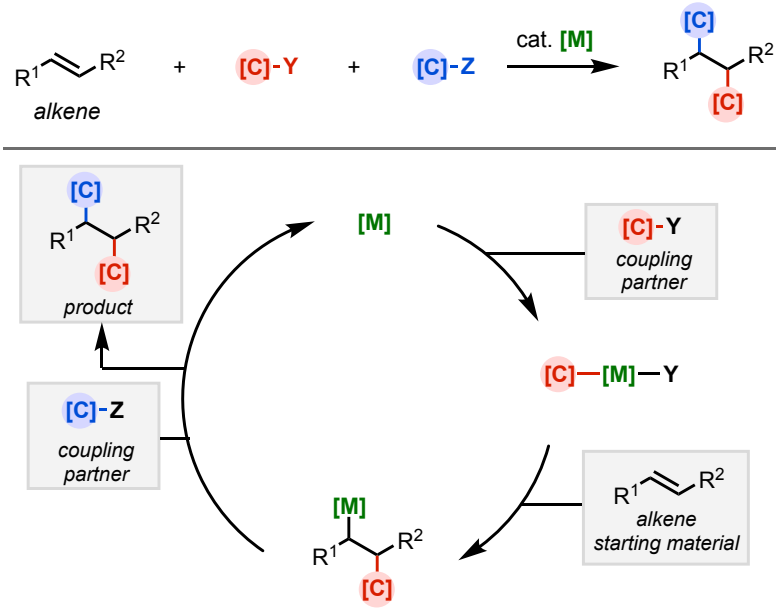


***Scheme 1.2.*** General catalytic cycle of 1,2-DCF of alkenes.

### 1.2.4. Difficulties with Alkene 1,2-Dicarbofunctionalization Strategy

Even though regioselective three-component 1,2-DCF of alkenes under transition metal catalysis is a vital synthetic tool, there are several setbacks en route to the desired product.[8,9] Generally speaking, regioselectivity can be difficult to control when there is no electronic or steric bias between two alkenyl carbon atoms. Another issue emerges when the reaction between the alkene and the first coupling partner is not kinetically favored, resulting in no productive catalysis or undesired two-component cross- or homocoupling between the coupling partners. The Achilles heel of this reaction paradigm is that the C($sp^3$)–metal intermediate is generally kinetically unstable, which can lead to undesired processes such as β-hydride elimination to enable chain-walking or classical Heck arylation, or protodemetallation to favor hydroarylation (Scheme 1.3).

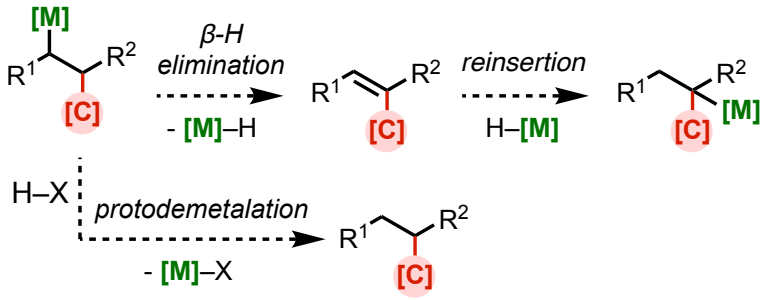


***Scheme 1.3.*** Common pitfalls for 1,2-DCF of alkenes.

## 1.3. EARLY EXAMPLES OF TRANSITION METAL CATALYZED 1,2-DICARBOFUNCTIONALIZATION OF ALKENES

### 1.3.1. Synopsis of non-Ni Catalyzed 1,2-Dicarbofunctionalization

The genesis of 1,2-DCF can be traced back to seminal work by Catellani and coworkers.[10] A quintessential report from her group showcased a Pd-catalyzed 1,2-DCF of norbornenes with aryl bromides and terminal alkynes as the coupling partners (Scheme 1.4). In terms of the mechanism, the authors postulated that the catalytic cycle proceeds via successive carbopalladation across the alkene and then the alkyne, with β-hydride elimination as the final step. In this report, the *in situ* furnished alkylpalladium intermediate is uncooperative towards β-hydride elimination because of the conformationally restrained nature of the norbornene, highlighting a vital rule in obtaining high selectivity in multicomponent 1,2-DCF systems. Most effort in the subsequent decades was geared towards expanding the scope of alkene substrates and coupling partners in 1,2-DCF, governing regioselectivity, and employing techniques to control selectivity. In this sense, progress during the past ten years in nickel catalysis has uncovered new opportunities in reactivity, which is more than what could be accomplished with palladium catalysis.

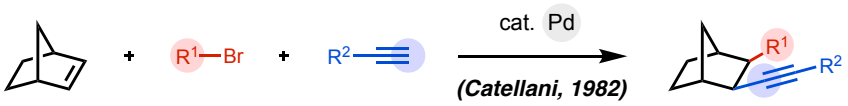


***Scheme 1.4.*** Genesis of 1,2-DCF of alkenes under Pd catalysis.

## 1.4. NON-STEREOSELECTIVE NICKEL-CATALYZED 1,2-DICARBOFUNCTIONALIZATION OF ALKENES

### 1.4.1. Importance of Nickel as a Base Metal Catalyst

Over the past few decades, the base metal nickel has attracted a lot of attention in the synthetic and methodological aspects of organic chemistry. Historically referred to as the "Spirited Horse", nickel has emerged as a competent catalyst owing to its multitude of enabling properties compared to palladium (Scheme 1.5).[11] As nickel is a first-row transition metal, it possesses readily accessible oxidation states ($Ni^0$ to $Ni^{IV}$) whereas traditional palladium cross-coupling reactions rely on $Pd^0/Pd^{II}$ catalytic cycles.[12] As a result, upon oxidative addition, nickel can react with coupling partners in either the two- or one-electron processes.[13] Nickel also has a smaller radius[14] and is more electropositive[15] than palladium, which both contribute to nickel having a slower β–H elimination process since a more strained geometry in the transition state and a weaker β-agostic interaction are prevalent.[16] Altogether, these advantageous properties for nickel over palladium give it the edge opening the repertoire for the type of carbogenic coupling partners in play allowing new synthetic methodologies and thus novel organic products to be obtained that would otherwise be difficult for palladium. A less notable but nontrivial feature is the drastically higher abundance and lower cost of nickel compared to palladium, which impacts industrial chemists on both the financial and environmental fronts.[17] Despite

concerning toxicity constraints (20 ppm for Ni and 10 ppm for Pd), companies are motivated to take more nickel catalysis into their current and future portfolios.

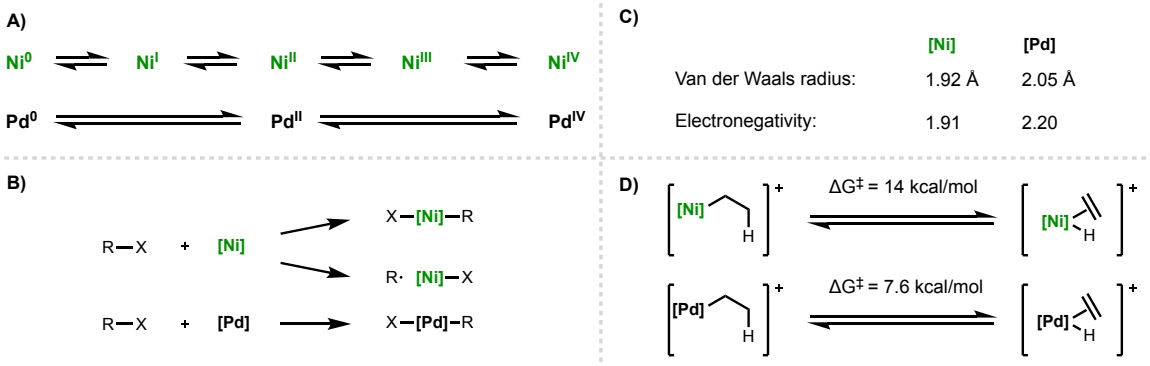


***Scheme 1.5.*** Differing physical properties of Ni vs Pd: A) oxidation states, B) oxidative addition, C) atomic radius and electronegativity, and D) β-hydride elimination.

### 1.4.2. Two-Component Ni-Catalyzed 1,2-Dicarbofunctionalization

In part due to the issues listed in section 1.2.3, much of the early work in Ni-catalyzed 1,2-DCF of alkenes focused on two-component reactions. For example, coupling partners with a tethered alkene, which easily engage in intramolecular cyclization with controlled regioselectivity, have been widely exploited to attain two-component 1,2-DCF. Also, two-component cyclizations using bifunctional coupling partners with alkenes were showcased by several research groups. However, much of the reported works have been focused on the enantioselective variants, which will be discussed in sections 1.5.2 and 1.5.3.

### 1.4.3. Three-Component Ni-Catalyzed 1,2-Dicarbofunctionalization

This section is organized based on the type of alkene employed: (1) acrylate-type substrates, (2) heteroatom-substituted alkenes, (3) styrenes, (4) strained alkenes, and (5) non-conjugated (and unstrained) alkenes (Scheme 1.6). Across the alkene types discussed,

different strategies are highlighted that have been leveraged to suppress β-hydride elimination and manipulate regioselectivity, noting that, in various cases, synergistic effects may also be present to enable the transformation.

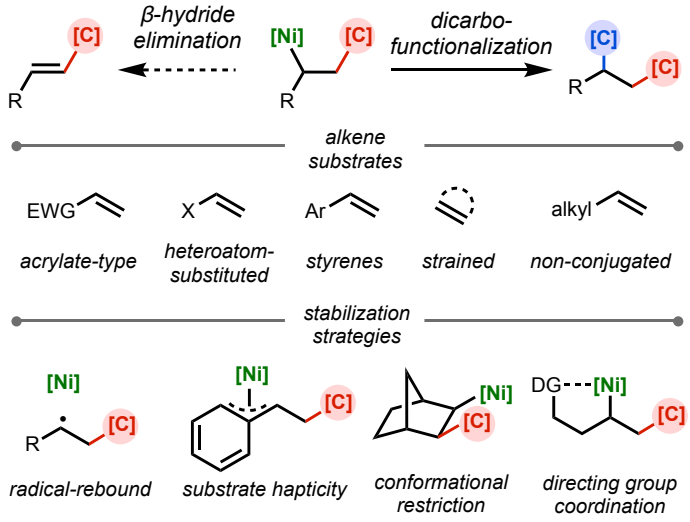


***Scheme 1.6.*** Alkene substrate classes and stabilization strategies of three component Ni-catalyzed 1,2-DCF.

Acrylate-based substrates can easily react in a Giese-type fashion with radical coupling partners typically leading to monocarbofunctionalized products. However, the *in situ* furnished secondary alkyl radical intermediates could be captured with a nickel catalyst, thus favoring 1,2-DCF. In 2016, Baran and colleagues exemplified the first examples of Ni-catalyzed three-component 1,2-DCF using benzyl acrylate substrates, redox-active esters (RAEs), and phenyl zinc halides as the nucleophilic coupling partner (Scheme 1.7A).[18] Similarly, in 2017, the Nevado group published a Ni-catalyzed reductive 1,2-arylalkylation protocol of various acrylate-type substrates with aryl iodides and tertiary alkyl iodides and under nickel/bipyridyl catalysis (Scheme 1.7B).[19] The key to the success of the transformation was using tetrakis(dimethylamino)ethylene (TDAE) which is a two-electron organic reductant unlike the conventional transitional metal solid reductants.

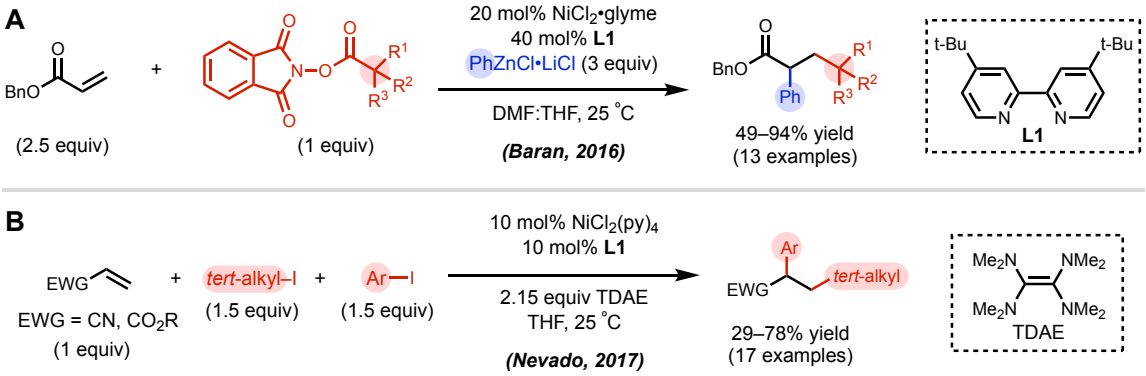


***Scheme 1.7.*** A/B) Ni-Catalyzed 1,2-DCF of acrylate-type substrates.

Alkenes with heteroatom-substitution possess sufficient polarization about the C=C thereby allowing addition by a carbogenic radical to be more facile setting the stage for 1,2-DCF. In 2016, the Zhang group demonstrated a 1,2-difluoroalkylarylation reaction of enamides using difluoroalkyl bromides and arylboronic acids as coupling partners (Scheme 1.8).[20] Mechanistic radical clock experiments provided evidence that supports the presence of a radical species and propose a potential directing effect from the oxygen atom of the carbonyl group. In 2019, the Zhang lab reported a complementary 1,2-difluoroalkylalkylation strategy using the same substrate type but with dialkyl zinc nucleophiles.[21]

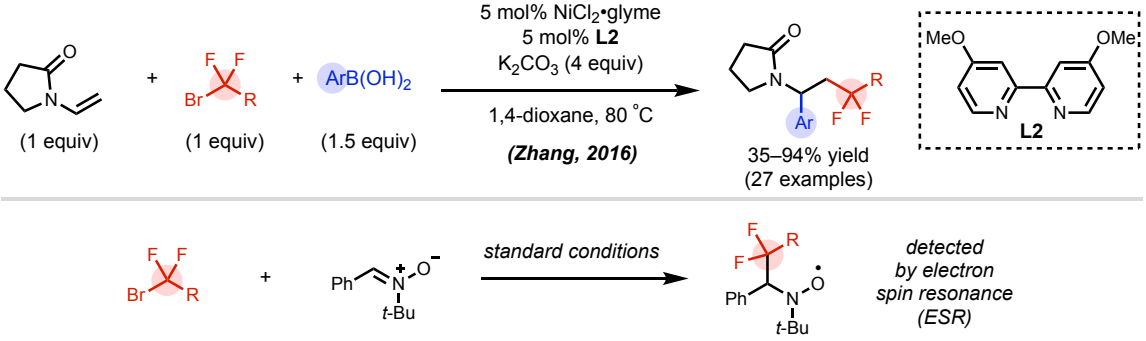


***Scheme 1.8.*** Ni-catalyzed 1,2-difluoroalkylarylation of enamides.

Styrenyl-based alkenes offer stabilization of nickel–alkyl intermediates because of the haptotropic shift provided by the benzylic position. This feature of styrenyl-based substrates enables excellent regioselectivity of the desired 1,2-dicarbofunctionalized products. In 2017, the Giri group reported a 1,2-diarylation of monosubstituted styrenes using imines as directing groups for further stabilization of the nickel alkyl species (Scheme 1.9A).[22] Subsequently, in 2018, the same lab published an analogous method toward the Ni-catalyzed 1,2-DCF of dimethylpyridylvinylsilane.[23] Only one year later, both the Giri and Brown groups reported 1,2-DCF transformations of vinyl arenes without the requisite of a directing group showing the beneficial nature of the styrene substrate (Scheme 1.9B/C).[24]

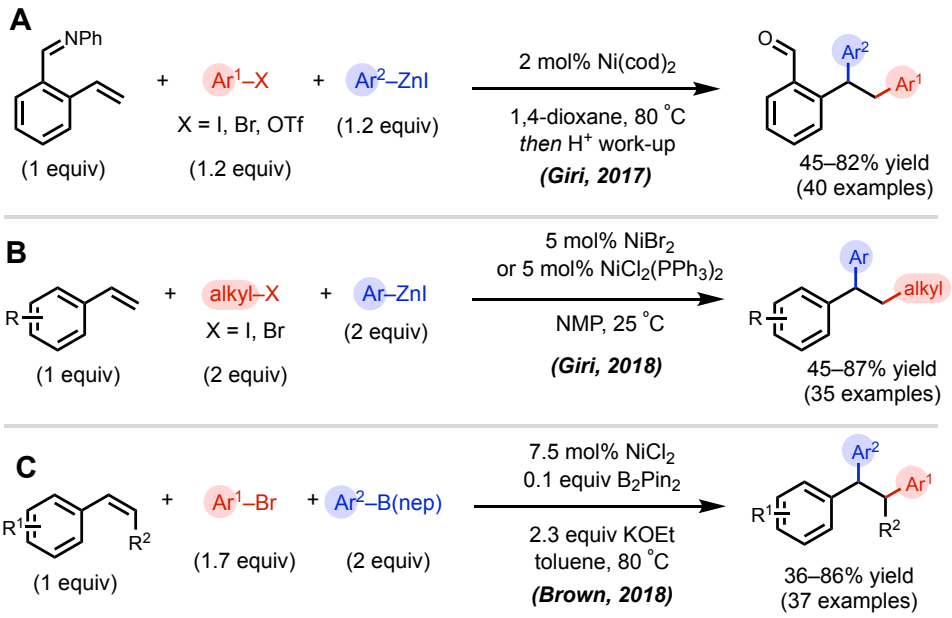


***Scheme 1.9.*** 1,2-Diarylation of A) styrenyl aldimines and B/C) vinyl arenes.

Strained alkenes, such as norbornene, have strain release as the driving force for migratory insertion or radical addition, which may lead to conformationally constrained nickel alkyl intermediates that are physically impeded to rotate about the C–C bond allowing β–H elimination to not occur. In light of these advantageous features, these alkene types are also good contenders in 1,2-DCF under nickel catalysis. In 2019, Stanley and colleagues published a *syn*-selective three-component 1,2-carboacylation method of norbornenes with *N*,*N*-substituted benzamide and tetraarylboron coupling partners (Scheme 1.10).[25]

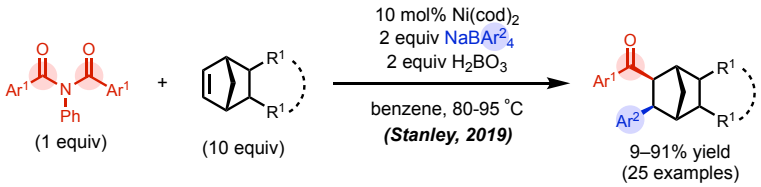


***Scheme 1.10.*** 1,2-Carboacylation of norbornenes.

With regard to unactivated alkenes, regioselective three-component 1,2-DCF becomes an arduous feat. Notwithstanding the importance of having non-conjugated alkenes in the 1,2-DCF toolkit, effectuating optimal reactivity is muddled by two factors: (1) increase in activation barrier for migratory insertion step and (2) β-hydride elimination may dominate in lieu of 1,2-DCF. While addressing these issues may seem unattainable, several research groups have made good progress in outlining ground rules for Ni-catalyzed 1,2-DCF of unactivated alkenes.

In 2017, the Engle lab employed a directing group method to obtain highly regio-, diastereo-, and *syn*-selective 1,2-arylalkylation of β,γ-unsaturated alkenyl carbonyls using a cleavable 8-aminoquinoline (AQ) auxiliary (Scheme 1.11A).[26] After the desired 1,2-DCF, the AQ auxiliary of the generated products could be removed via hydrolysis to

unmask the carboxylic acid. Using the same AQ auxiliary, the Engle group also published a 1,2-dialkylation using alkyl zinc nucleophiles and alkyl halide electrophiles exemplifying the first example of distinguishable 1,2-dialkylation of unactivated alkenes (Scheme 1.11B).[27] It is worth noting that the Lin and Yao groups used this AQ-directed strategy toward a reductive 1,2-dialkynylation of unactivated alkenes as well.[28]

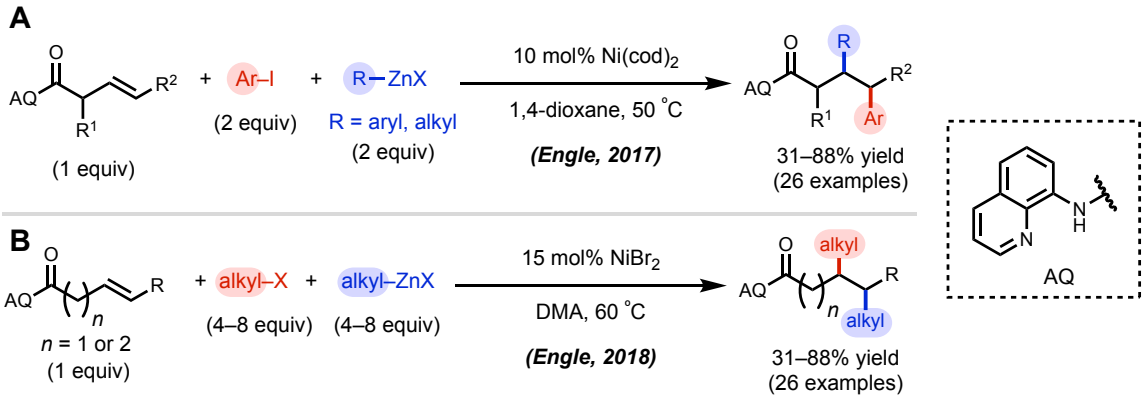


***Scheme 1.11.*** A) Ni-catalyzed 1,2-arylalkylation of β,γ-unsaturated carbonyls. B) Ni-catalyzed 1,2-dialkylation of β,γ- and γ,δ-unsaturated alkenyl carbonyls.

In 2018, the Zhao lab published several 1,2- and 1,3-DCF reactions of allyl amine substrates bearing the 2-aminopyrimidine auxiliary with alkynyl/alkenyl halide electrophiles and alkenyl/arylboronic acid nucleophiles (Scheme 1.12).[29] In the report, the regioselectivity of the transformation was determined based on the combination of electrophile and nucleophile; vinyl bromide electrophiles led to addition at the terminal position whereas alkynyl halides led to addition at the internal position.

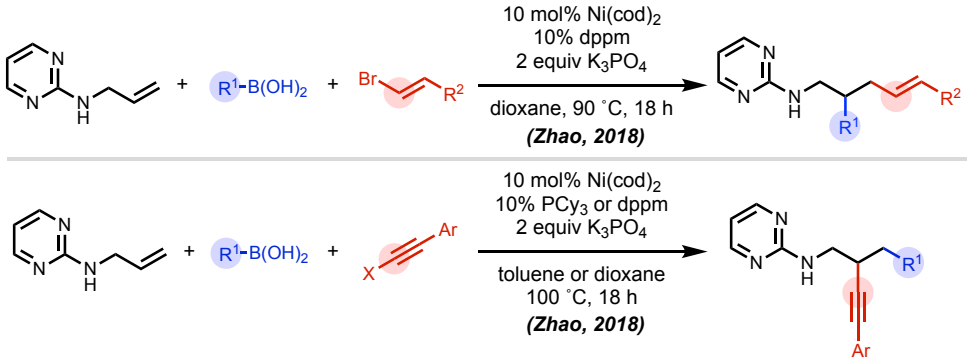


***Scheme 1.12.*** Regiodivergent Ni-catalyzed 1,2-DCF of allyl amines using pyrimidine directing groups.

The Giri group expanded their imine-directed diarylation of unactivated alkenes employing aryl zinc nucleophiles and aryl halide electrophiles. In their first attempts to synthesize the desired *γ*,*δ*-diarylated products, only unwanted Heck side product was obtained. With modification of the reaction conditions, they discovered that 1,3-DCF is possible under nickel/triphenylphosphite catalysis (Scheme 1.13A).[30] Thereafter, Giri and coworkers reported a complementary protocol to foster *γ*,*δ*-diarylketone products, this time with the use of low-valent nickel catalyst and $AgBF_4$ or CuI halide scavengers in lieu of an ancillary ligand (Scheme 1.13B).[31] In 2019, they reported a similar 1,3-DCF method but using weak cyanoesters directing groups with vinyl triflate electrophiles and diaryl zinc nucleophiles (Scheme 1.13C).[32]

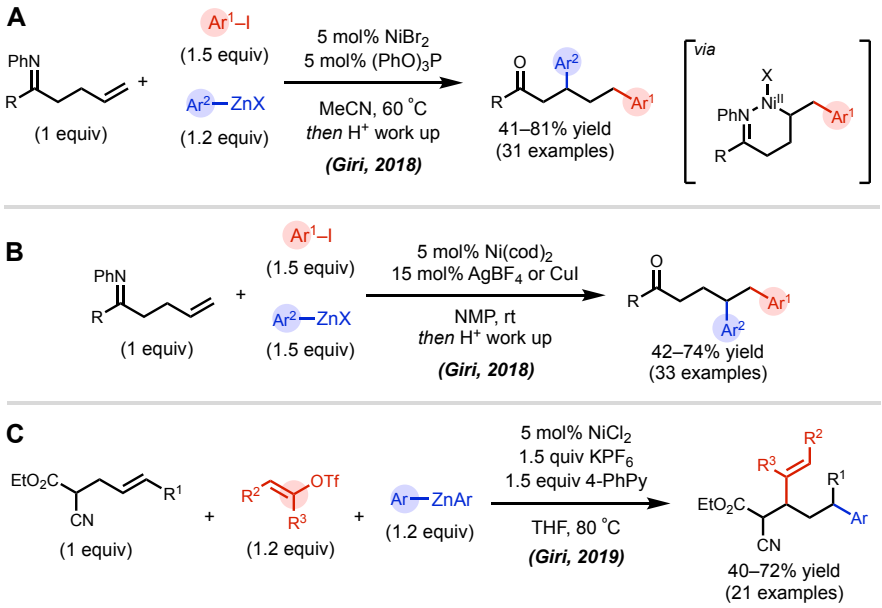


***Scheme 1.13.*** A/B) Ni-catalyzed imine-directed 1,3- and 1,2-DCF of γ,δ-unsaturated ketimines. C) Ni-catalyzed 1,3-DCF of γ,δ-unsaturated α-cyanoesters.

A robust radical addition method toward reacting allylic substrates with acyl chloride and perfluoroalkyl halide electrophiles in a reductive mode was effectuated by the Chu group in 2018 (Scheme 1.14).[33] The notable feature of the reaction, which merited its success, was the adequate placement of the carbonyl directing group in the substrate to provide sufficient stabilization of the 6-membered nickelacycle upon radical recombination.

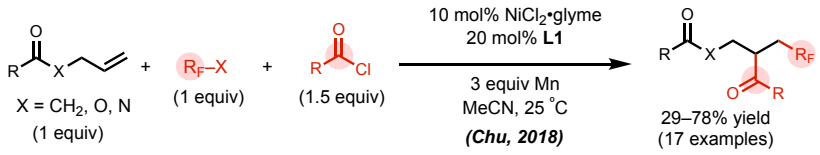


***Scheme 1.14.*** Ni-catalyzed reductive 1,2-perfluoroalkylacylation of allylic substrates.

Contemporaneously, in 2018, Engle and coworkers reported a 1,2-DCF protocol of β,γ- and γ,δ-unsaturated alkenyl amides having the amide functional group as the native

directing group in lieu of the AQ auxiliary (Scheme 1.15A).[34] The Engle group also published a method describing 1,2-allylmethylation of *N*-allyl heterocycles under nickel catalysis (Scheme 1.15B).[35] The use of a labile saccharin-derived native directing group enabled a Ni-catalyzed 1,2-DCF reaction that integrates an allyl electrophile without over functionalizing the resultant alkene. With the goal to extend the native-directed 1,2-DCF platform, Engle and colleagues also reported the employment of free carboxylic acids as competent native directing groups for Ni-catalyzed 1,2-diarylation and 1,2-arylalkenylation of unactivated alkenes with aryl iodide electrophiles and aryl/alkenylboronic ester nucleophiles (Scheme 1.15C).[36]

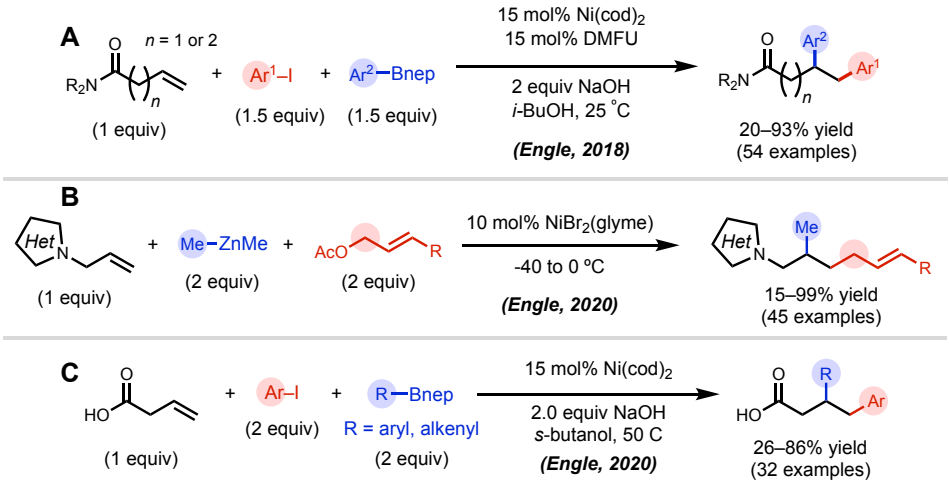


***Scheme 1.15.*** A) Ni-catalyzed 1,2-diarylation of alkenyl amides. B) Ni-catalyzed 1,2-allylmethylation of *N*-allyl heterocycles. C) Ni-catalyzed 1,2-diarylation of alkenyl carboxylates.

The last strategy discussed in this section revolves around Ni-catalyzed 1,2-DCF of alkenes with the usage of a co-catalytic photosensitizer. In 2019, the Chu lab published a regioselective 1,2-alkylarylation of unactivated alkenes with heteroaryl iodide electrophiles and tertiary alkyl oxalate nucleophiles under synergistic photoredox/nickel catalysis (Scheme 1.16A).[37] Complementarily, under a similar photocatalytic paradigm,

the Nevado group achieved 1,2-alkylarylation of unactivated alkenes with aryl iodide electrophiles and alkylsilicon nucleophiles (Scheme 1.16B).[38a] It is important to note recent work done by Macmillan showing 1,2-DCF of alkenes via a triple radical sorting modality.[38b,c] Dialkylated and arylalkylated products could be furnished in moderate to good yields from unactivated alkenes, alkyl electrophiles/aryl bromides, and alkyl radical reagents under photoredox/nickel catalysis. Such outer-sphere mechanism gives the methodologies an edge over the mainly discussed inner-sphere developments in that, for instance, C($sp^3$)–C($sp^3$) quaternary centers could be more easily accessed.

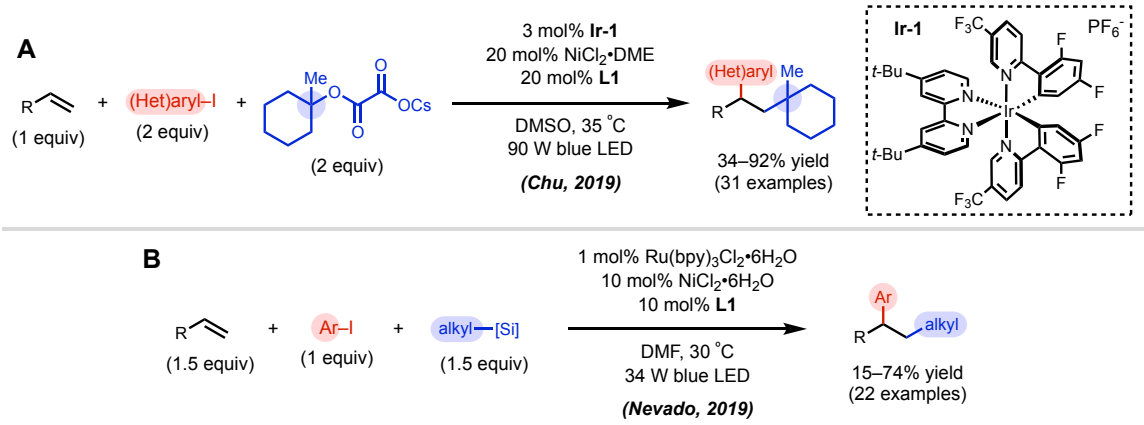


***Scheme 1.16.*** Photocatalytic 1,2-arylalkylation of unactivated alkenes.

The efflux of developments discussed in this section in three-component nickel-catalyzed 1,2-DCF of alkenes has allowed for the progression of a wide array of elegant methods toward achieving a general platform for universal alkene 1,2-DCF. While strong directing groups enable this type of reactivity, we anticipate that more synthetically relevant functional groups in combination with novel ligand scaffolds will continue to bridge the gap in this chemical space. Furthermore, this may lead to an upsurge in achieving asymmetry upon 1,2-DCF of alkenes. Still in its infancy, progress in asymmetric nickel- and palladium catalyzed 1,2-DCF of alkenes will be discussed in the next section.

## 1.5. ASYMMETRIC NICKEL- AND PALLADIUM-CATALYZED 1,2-DICARBOFUNCTIONALIZATION OF ALKENES

### 1.5.1. Background

Drug molecules in the pharmaceutical sector have become more structurally complex in the present-day, possessing a larger number of carbogenic stereocenters, which gives rise to synthetic difficulties. There is thus an urgent need for novel methods in asymmetric synthesis that may address the aforementioned demand.[39] Knowing that cross-couplings methods are the dominant way to furnish $C(sp^2)$–$C(sp^3)$ and $C(sp^3)$–$C(sp^3)$ bonds, it is apparent that asymmetric catalysis is the path for rapid build-up of molecular complexity.[40] The ultimate goal of catalysis investigations is selectivity control, and achieving high amounts of both diastereo- and enantioselectivity allows for the synthesis of molecules with desired three-dimensionality, which may serve various functions.

1,2-Dicarbofunctionalization (1,2-DCF) is an excellent platform to render asymmetric since the outcome of the transformation is the furnishing of two contiguous $C(sp^3)$–C centers.[8] In section 1.4, the discussion revolved around the non-stereoselective examples of Ni-catalyzed 1,2-DCF of alkenes, which is important per se, but enantioselective Ni-catalyzed 1,2-DCF offers an elevated characteristic for forming multiple $C(sp^3)$–C stereocenters in a single step (Scheme 1.17); however, actualizing this approach has deemed a very challenging feat.

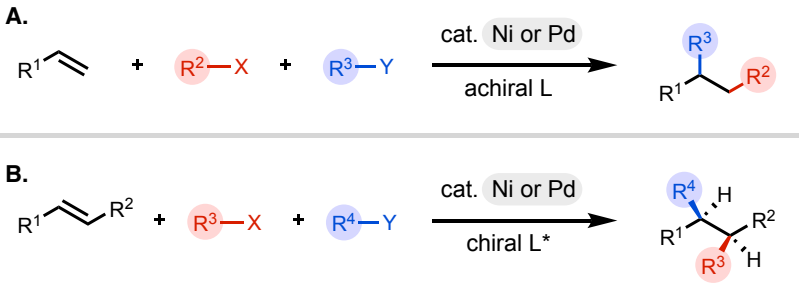


***Scheme 1.17.*** General scheme of non-stereoselective and asymmetric Ni- and Pd-catalyzed 1,2-DCF of alkenes.

This section describes progress in enantioselective Ni- and Pd-catalyzed 1,2-DCF of alkenes. Since these two transition metals represent a fair amount of the recently published works, comparison between them is edifying. Nevertheless, it is worth noting that there are other reports on closed-shell 1,2-DCF of alkenes with other metals, such as with Cu,[41] Rh,[42] and Co.[43] The section is categorized by the amount of reaction components be it either two- (intramolecular) or three-component (intermolecular) and by the mechanism of attaining enantioselectivity.

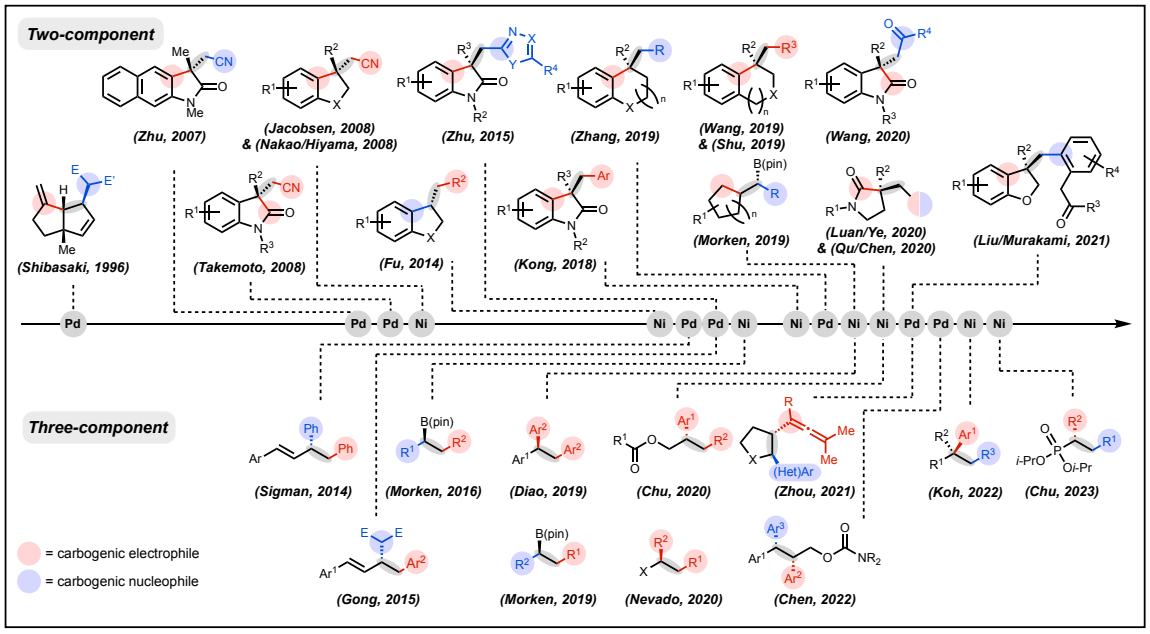


***Figure 1.2.*** Timeline (1996–2023) of Ni- and Pd-catalyzed 1,2-DCF of alkenes.

In the early 2010s, enantioselective Ni- and Pd-catalyzed 1,2-DCF of alkenes gained significant traction. Most of the research dealt with two-component approaches, since enantioinduction arising in the C–C bond-forming migratory insertion step is plausible due to a 5- or 6-membered cyclic transition state that is conformationally constrained (Scheme 1.18). Discovery and optimization of the three-component version has been elusive until lately. Since 2019, a few three-component protocols based on radical addition/capture mechanisms have been published, whereby enantioinduction occurs upon radical capture of the chiral Ni catalyst and subsequent reductive elimination sets the irreversible enantioenriched carbon center. Surprisingly, in 2022, enantioselective three-component 1,2-DCF of alkenes through an aryl/alkenyl nickel/palladium migratory insertion was exemplified for the first time in the chemical literature.

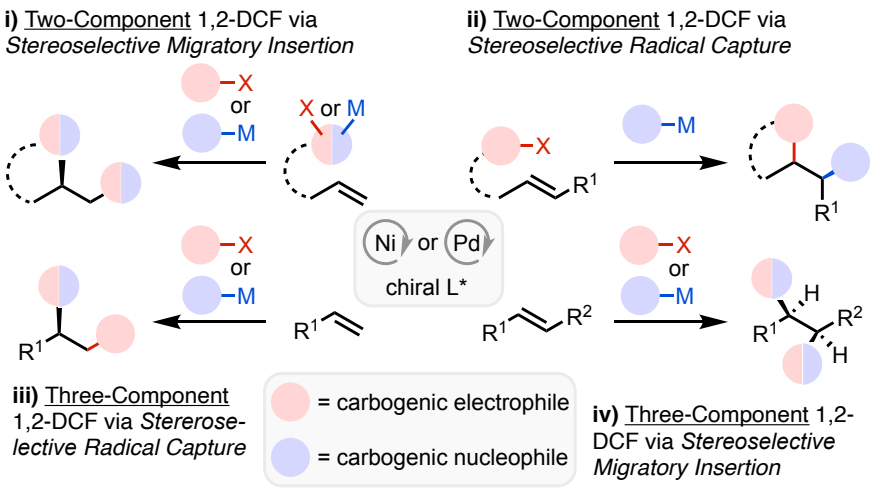


***Scheme 1.18.*** Component type and mechanisms of enantioinduction in Ni- and Pd-catalyzed 1,2-DCF of alkenes.

### 1.5.2. Two-Component Enantioselective 1,2-Dicarbofunctionalization of Alkenes via Migratory Insertion

The two-component enantioselective 1,2-DCF of alkenes comes from enantioselective Mizoroki–Heck reaction, which leverages migratory insertion as a key elementary step in achieving optimal enantioselectivity.[44] The earliest report of enantioselective two-component 1,2-DCF was showcased in 1996 by the Shibasaki lab, who used a cyclic diene starting material tethered to a vinyl triflate to allow cyclative enantioselective migratory insertion and subsequent nucleophilic substitution (Scheme 1.19).[45]

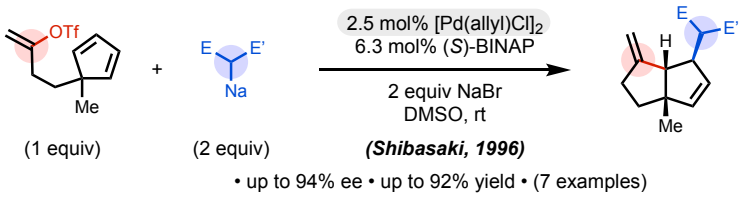


***Scheme 1.19.*** Pd-catalyzed 1,2-DCF of cyclopentadiene-tethered alkenyl triflates.

Since this work, a fair amount of alkene functionalizations, including hydroarylations, have been reported that exploit enantioselective two-component migratory insertion of arylmetal catalysts into tethered alkenes.[46] Furthermore, four works of two-component enantioselective 1,2-carbocyanation were communicated. The two former ones were carried out under Pd catalysis, and the two latter ones under Ni/Lewis acid cooperative catalysis (Scheme 1.20).[47] In 2007, the Zhu lab disclosed the 1,2-carboarylation protocol of acrylamides bearing an aryl-iodide under Pd/(*S*)-DIFLUOROPHOS catalysis.[47a] The next year, the Takemoto lab showcased enantioselective 1,2-cyanoamidation of styrenes linked with a cyanoformamide functional group under Pd/chiral phosphoramidite (**L3**) catalysis.[47b] Both the Jacobsen and

Nakao/Hiyama labs published 1,2-carbocyanation reactions of alkenes linked with benzonitriles under Ni/Lewis acid/chiral phosphine synergistic catalysis.[47c, 47d]

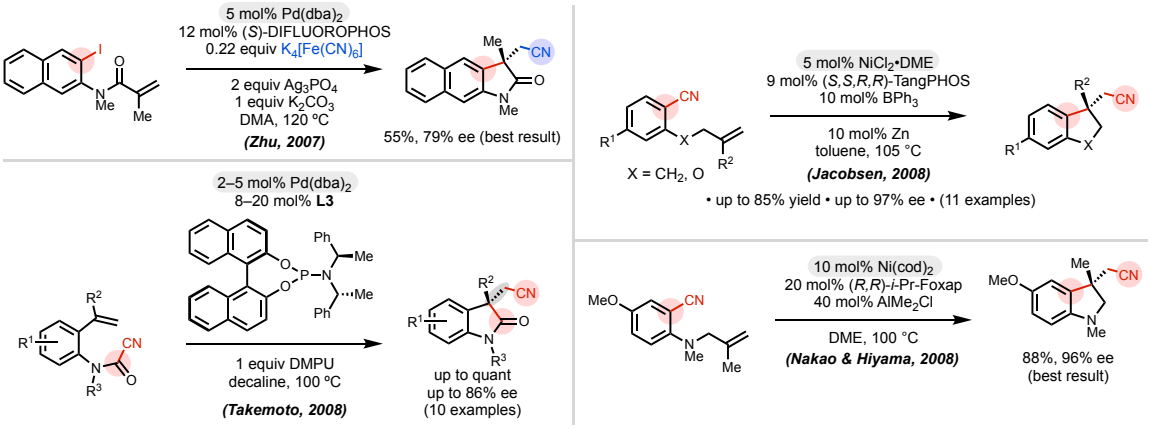


***Scheme 1.20.*** Ni-catalyzed two-component enantioselective 1,2-carbocyanation of alkenes linked with electrophiles.

A seminal report was produced by the Fu group in 2014 (Scheme 1.21),[48] whose lab demonstrated that, under Ni/chiral diamine (**L4**) catalysis, arylborane nucleophiles with a linked alkene can first undergo transmetalation and then engage in enantioselective two-component cyclization. The end sequence involves oxidative addition of the alkyl bromide electrophile and lastly reductive elimination to afford the desired 1,2-dicarbofunctionalized products.

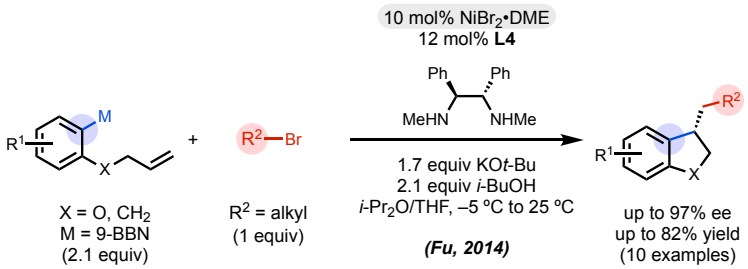


***Scheme 1.21.*** Ni-catalyzed two-component enantioselective 1,2-DCF of alkenes linked with arylboranes.

In 2015, the Zhu lab published an enantioselective 1,2-DCF of acrylamides tethered to an aryl triflate electrophile under Pd/phosphinooxazoline (PHOS, **L5**) catalysis (Scheme 1.22).[49]

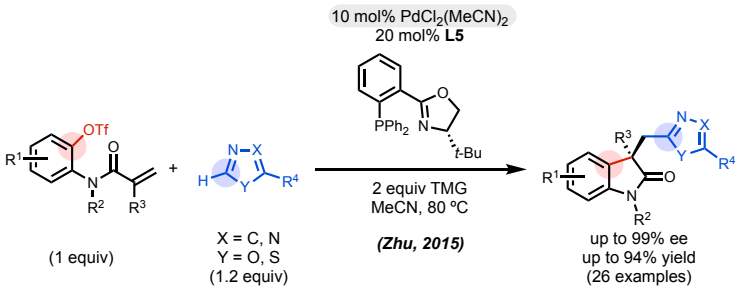


***Scheme 1.22.*** Pd-catalyzed two-component enantioselective 1,2-DCF of acrylamides possessing a tethered aryltriflate.

Based on the previously mentioned reports, several two-component 1,2-DCF have been carried out utilizing various combinations of coupling partners and chiral ligands under Pd or Ni catalysis. These transformations generally have a shared reaction pathway of oxidative addition and enantiodetermining cyclative migratory insertion of the substrate with a linked alkene and aryl(pseudo)halide electrophiles. Exploitation of the putative alkylmetal species can be done by using a plethora of nucleophilic trapping reagents (Scheme 1.23). For instance, isocyanates,[50] carbon monoxide,[51] alkenes,[52] aryl/alkylboronic acids,[53] and alkynes[54] have been published as viable coupling partners upon 1,2-DCF reactions, each having different operating mechanisms. Modularity in this alkylmetal capturing step comes from the multifaceted alkyl–Pd/Ni intermediate. Also, a handful of enantioselective 1,2-DCF reactions using atypical carbogenic nucleophiles, such as cyclobutenols (via β-carbon elimination)[55] or internal arenes (via C–H activation), have been disclosed.[56]

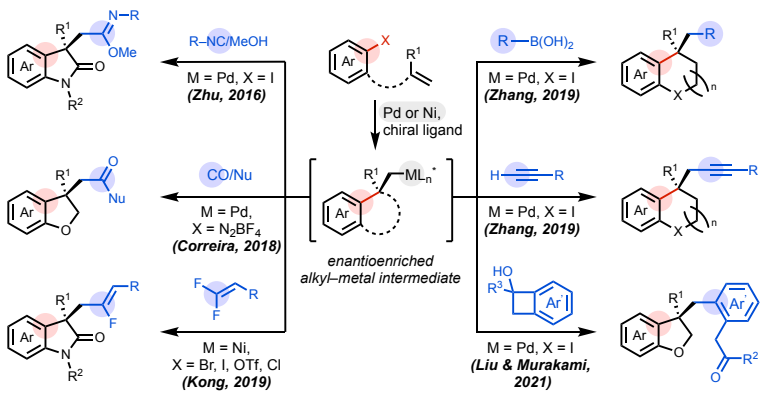


***Scheme 1.23.*** Redox-neutral two-component enantioselective 1,2-DCFs of aryl-(pseudo) halide tethered alkenes.

Reductive 1,2-DCF reactions that involve a nickel catalyst and a reductant are another important category of the enantioselective variant. Contrary to the classical redox-neutral platform that requires an electrophile and a nucleophile, the reductive platform utilizes two different electrophiles to be coupled. Nickel has an edge over palladium due to its accessibility to other oxidation states via single-electron transfer events,[57] and as such, single-electron reductants like Zn and Mn are usually employed in Ni-catalyzed reductive 1,2-DCF reactions.

Indeed, several Ni-catalyzed enantioselective reductive 1,2-DCF reactions of alkenes with tethered aryl-halides have been successfully coupled with aryl bromides,[58] alkyl bromides,[59] alkenyl triflates,[60] alkenyl bromides,[61] and benzyl chlorides[62] by various research labs (Scheme 1.24). In 2023, a mechanochemical approach for the enantioselective reductive paradigm was published by Morrill and Browne but with modest enantioselectivity.[63]

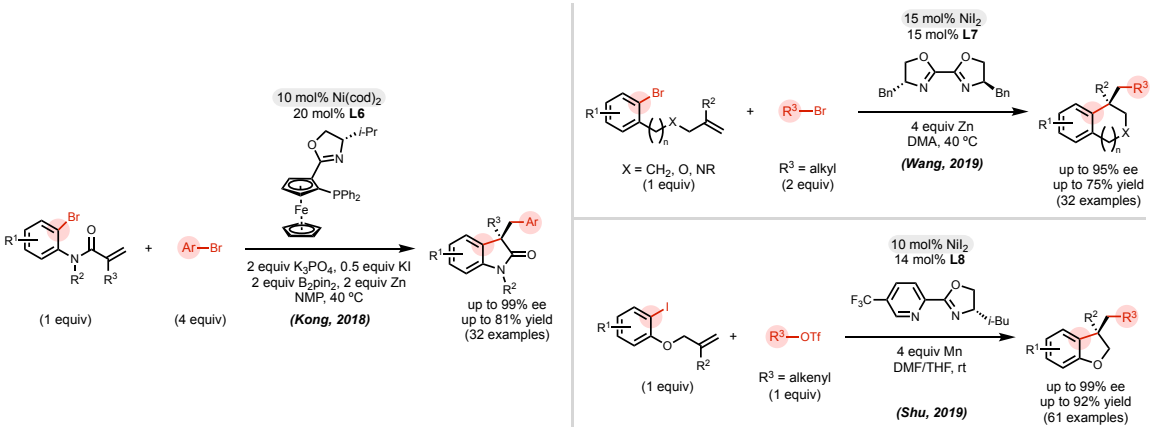


***Scheme 1.24.*** Ni-catalyzed two-component enantioselective reductive 1,2-DCF of alkenes.

Recent efforts in the asymmetric field have used alkene linked with carbamoyl halides as competent substrates under Ni catalysis (Scheme 1.25). For example, the Wang lab showcased that carbamoyl chlorides linked with a styrene may engage in oxidative addition and enantioselective cyclative migratory insertion to furnish alkyl–Ni intermediates that can be trapped by photogenerated acyl radicals.[64] In addition, both reductive and redox-neutral 1,2-DCF reactions of alkenes linked with carbamoyl halides were showcased, affording chiral γ-lactam products, by the Qu and Chen labs,[65] and the Ye lab,[66] respectively.

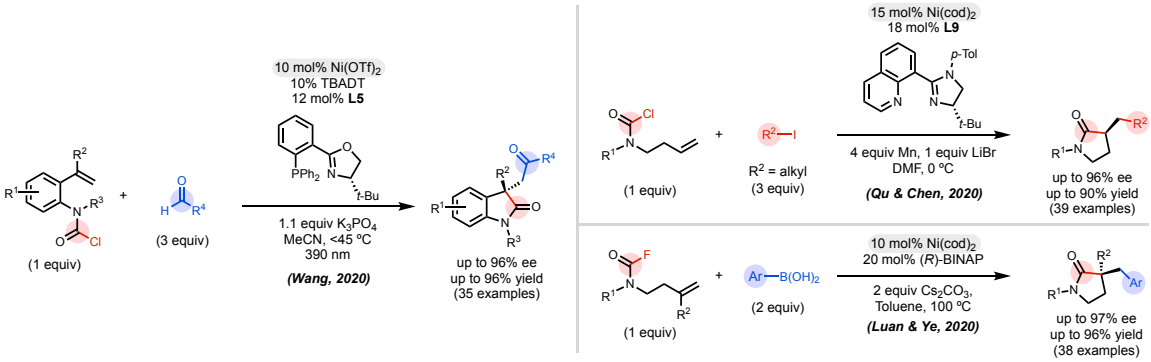


***Scheme 1.25.*** Ni-catalyzed two-component enantioselective 1,2-DCF of alkenes linked with carbamoyl halides.

### 1.5.3. Two-Component Enantioselective 1,2-Dicarbofunctionalization of Alkenes via Radical Capture

Radical-based, two-component, enantioselective 1,2-DCF is scarce, and only one report has been published by the Morken group in 2019. The work leverages alkenes that possess both alkenylboronic ester nucleophiles and alkyl iodide electrophiles under nickel/chiral 1,2-diamine catalysis (Scheme 1.26).[67] The mechanism initiates with the alkyl iodide turning into an alkyl radical via halide abstraction. The alkyl radical intermediate may then undergo exo-selective two-component cyclization onto the alkene forming a five or six-membered ring having a stable α-boryl radical species. Radical recombination with the aryl/alkylNi catalyst, followed by reductive elimination, affords the enantioenriched 1,2-dicarbofunctionalized product.

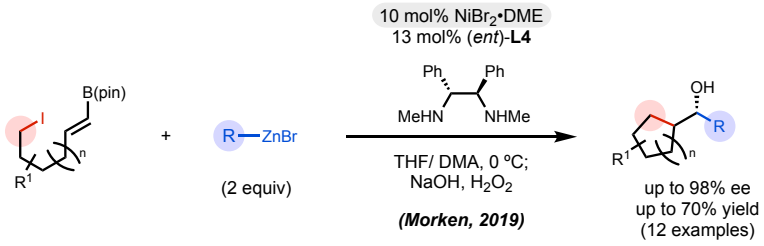


***Scheme 1.26.*** Ni-catalyzed two-component enantioselective 1,2-DCF via radical capture.

### 1.5.4. Three-Component Enantioselective 1,2-Dicarbofunctionalization of Alkenes via Radical Capture

While much progress has been made in two-component 1,2-DCF under Pd and Ni catalysis, efforts on the analogous three-component version has been held back due to lack of good stereocontrol, production of many side products, and high activation barriers of higher ordered alkene classes, such as 1,2-disubstituted alkenes. Without the advantage of having either the Ni/Pd–alkyl or carbogenic radical species linked to the substrate (i.e. two-

component), effectuating enantioselective migratory insertion or radical capture steps becomes more difficult.

Early works in Ni-catalyzed three-component enantioselective 1,2-DCF of alkenes in the latter part of the 2010s revolved around protocols with an enantioselective radical capture approach. This method is derived from previously discussed Ni-catalyzed nonstereoselective radical-based 1,2-DCF reactions, which deal with carbogenic radical addition into an alkene then radical capture with the nickel catalyst. Introduction of a chiral ligand would allow for the key radical capture process to occur in an enantioselective manner. In proof-of-concept work in 2016, the Zhang lab showcased a sole example of enantioselective 1,2-DCF with enantiodetermining radical capture, obtaining 18% ee when a chiral diamine ligand was employed in the 1,2-difluoroalkylation-arylation transformation.[68]

The first report of an optimized three-component enantioselective 1,2-DCF of alkenes was exemplified by Diao and colleagues in 2019. The authors disclosed a reductive enantioselective 1,2-homodiarylation of styrenes with aryl bromides electrophiles under nickel/chiral biOx catalysis achieving high product yields and enantioselectivities (Scheme 1.27).[69a]

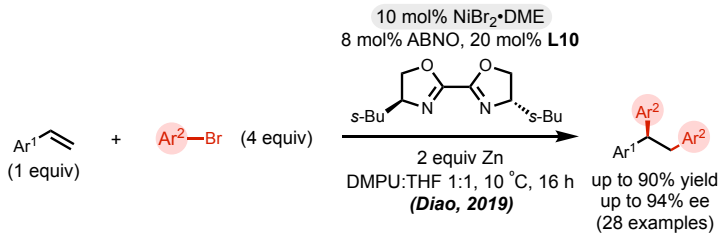


***Scheme 1.27.*** Ni-catalyzed three-component enantioselective 1,2-homodiarylation of styrenes.

Concurrently, the Morken lab published a 1,2-DCF protocol of vinylboronic acid pinacol esters with alkyl iodides electrophiles and alkyl/aryl zinc nucleophiles utilizing a nickel/chiral diamine (**L4**) catalyst system (Scheme 1.28).[67] Enantioenriched secondary alcohols could then be generated in good yields and high enantioselectivities after oxidative workup.

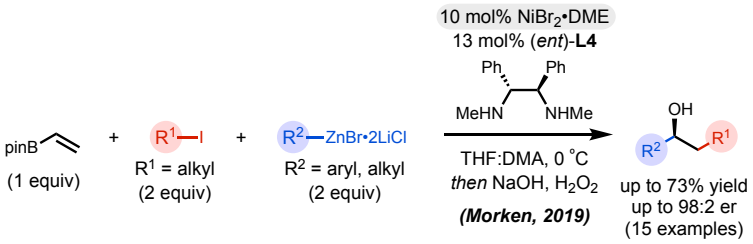


***Scheme 1.28.*** Enantioselective three-component 1,2-DCF of vinylboronic esters.

The first example of a three-component enantioselective 1,2-DCF of unactivated alkenes was disclosed by Chu and colleagues in 2020. The strategy joins allylic esters with aryl and alkyl halide electrophiles under nickel/chiral biOx catalysis (Scheme 1.29A).[70] The Nevado group published a similar reductive protocol but for the three-component enantioselective 1,2-DCF of enamides under nickel/biOx catalysis and using tetrakis(dimethylamino)ethylene (TDAE) organic reductant (Scheme 1.29B).[71] In addition to these works, the Zhang lab also showcased a reductive enantioselective three-component 1,2-DCF of 3,3,3-trifluoropropene with a comparable catalytic platform.[72]

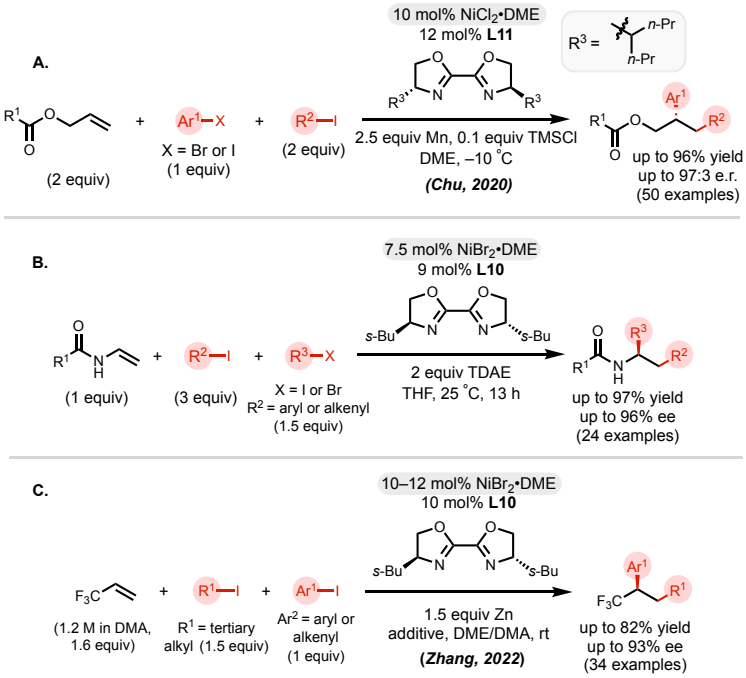


***Scheme 1.29.*** A) Enantioselective three-component 1,2-DCF of allylic esters. B) Enantioselective three-component reductive 1,2-DCF of vinyl amides. C) Enantioselective three-component reductive 1,2-DCF of 3,3,3-trifluoropropene.

Chu and Gutierrez disclosed an enantioselective three-component 1,2-DCF of vinyl phosphonates with aryl/alkenyl bromide electrophiles and alkyl trifluoroborate nucleophiles under metallaphotoredox catalytic conditions (Scheme 1.30).[73]

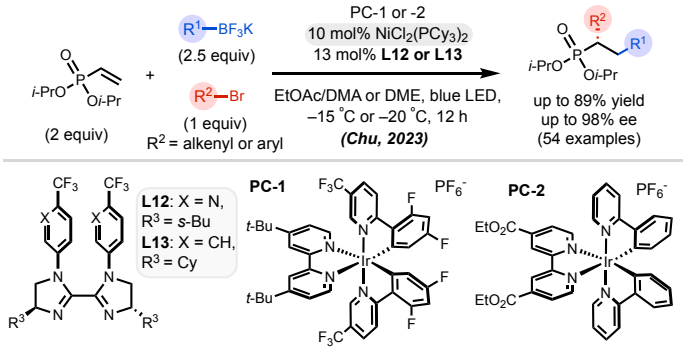


***Scheme 1.30.*** A) Enantioselective, three-component metallaphotoredox catalyzed 1,2-DCF of vinyl phosphonates.

### 1.5.5. Three-Component Enantioselective 1,2-Dicarbofunctionalization of Alkenes via Migratory Insertion

As mentioned in the last section, three-component Ni- and Pd-catalyzed 1,2-DCF of alkenes via enantioselective migratory insertion is cumbersome. In this mechanistic paradigm, both the absolute and relative stereochemical outcome of the arylmetal addition must be well guided. It is worth noting that, even though closed shell migratory insertion is *syn*-selective, the diastereoselectivity can nonetheless be lost due to other secondary pathways.[74] One privilege that migratory-insertion-based protocols have is the ability to furnish two adjacent carbon centers in a single synthetic step. Much of the early reports has been predominantly surrounded by Pd catalysis; only in recent times, such as in late 2022 and early 2023, did the first Ni-catalyzed methods develop.

In 2014, the Sigman group published a Pd-catalyzed 1,2-diarylation of 1,3-dienes with aryldiazonium tetrafluoroborate electrophiles and aryl boronic acid nucleophiles (Scheme 1.31A).[75] In this piece, the authors leveraged a (*R*)-(−)-α-phellandrene-derived chiral ligand (**L14**) to generate 1,2-diarylated products with moderate enantioselectivity albeit in low yields. The subsequent year, the Gong lab disclosed an enantioselective 1,2-DCF of the same 1,3-diene substrates but under Pd/chiral phosphoramidite (**L15**) catalysis with aryl iodide electrophiles and enolate nucleophiles (Scheme 1.31B).[76] Not until a few years later, the Zhao lab reported an enantioselective Pd-catalyzed 1,2-diarylation of aryl iodide electrophiles and aryl boronic acid nucleophiles with unactivated alkenes possessing the 8-aminoquinoline (AQ) directing auxiliary (Scheme 1.31C).[77] The group published a sole enantioselective example with the utility of a chiral PyrOx ligand (**L16**), where 1,2-diarylated product was furnished in moderate yield and enantioselectivity.

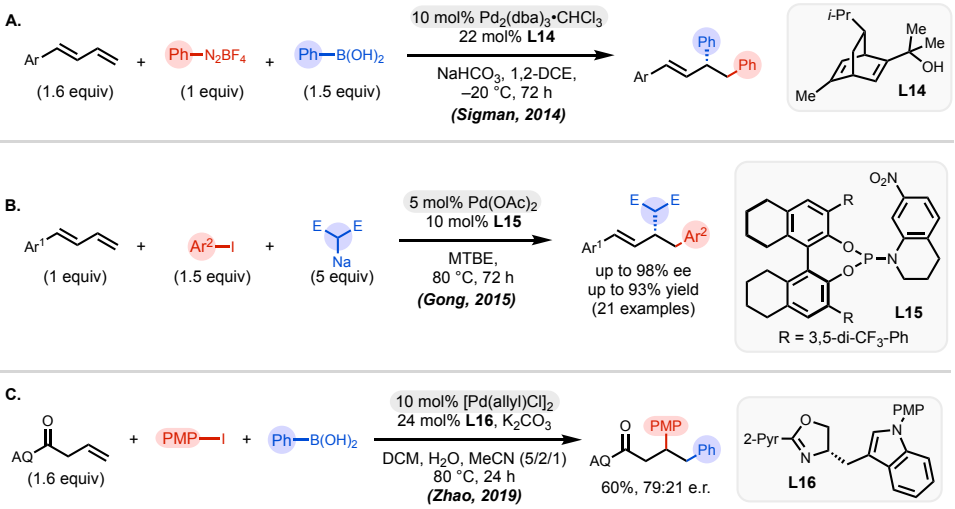


***Scheme 1.31.*** A) Enantioselective three-component Pd-catalyzed 1,2-diarylation of 1,3-dienes. B) Enantioselective three-component Pd-catalyzed 1,2-diarylation of 1,3-dienes. C) Enantioselective three-component Pd-Catalyzed 1,2-diarylation of unactivated alkenes with AQ auxiliary.

Important efforts by Chen and colleagues in 2022 demonstrated an enantioselective 1,2-diarylation of internal styrenes with aryldiazonium trifluoroborate electrophiles and aryl boronic acid nucleophiles under a Pd/biOx catalytic regime (Scheme 1.32).[78] Excellent yields and enantioselectivity of the 1,2-diarylated product could be furnished under the developed reaction.

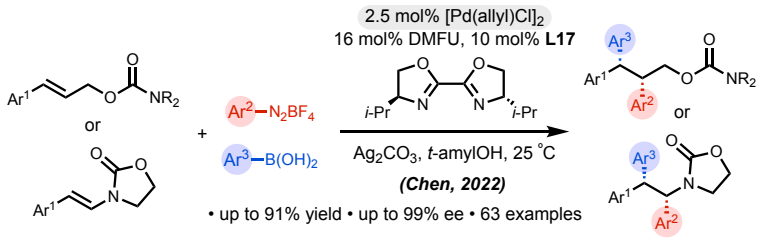


***Scheme 1.32.*** Enantioselective Pd-catalyzed 1,2-DCF of activated alkenes via enantiodetermining migratory insertion.

Both the Shi and Koh labs reported a three-component Ni-catalyzed 1,2-DCF of activated alkenes where asymmetric arylnickel migratory insertion may occur without the requisite of a directing group (Scheme 1.33).[79] In this work, aryl triflate electrophiles and

carbogenic Grignard nucleophiles were successfully implemented upon several activated alkenes under low valent nickel/chiral NHC catalysis.

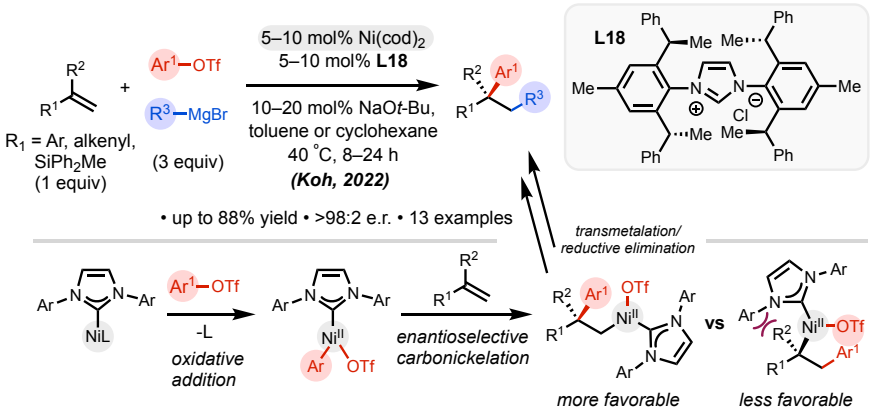


***Scheme 1.33.*** Enantioselective three-component Ni-catalyzed 1,2-diarylation of activated alkenes via enantiodetermining migratory insertion.

Last year, a reductive enantioselective three-component 1,2-homodiarylation of unactivated alkenes fostered by the AQ directing auxiliary was published by Chen and colleagues (Scheme 1.34).[80] This feat was accomplished by utilizing aryl iodide electrophiles under nickel/*i*-Pr-PHOX (**L19**) or nickel/*s*-Bu-PHOX (**L20**) catalytic regimes.

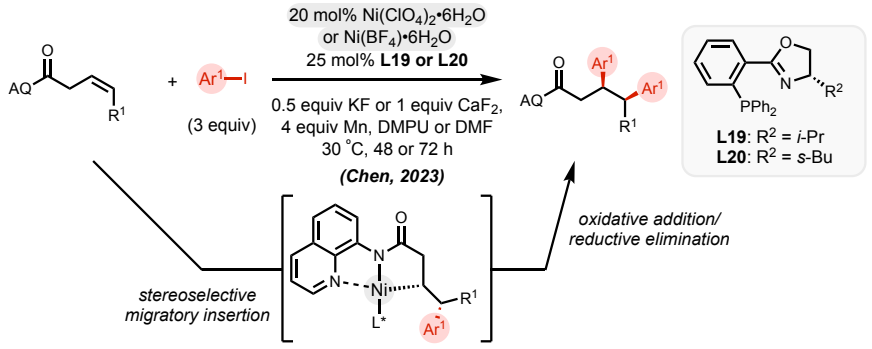


***Scheme 1.34.*** Enantioselective three-component Ni-catalyzed reductive 1,2-diarylation of unactivated alkenes with AQ auxiliary.

### 1.5.6. Miscellaneous Mechanisms

Although this introduction largely focuses on discussing mechanisms for enantioinduction such as radical capture and migratory insertion, other miscellaneous mechanisms, such as enantioselective metallate rearrangement and Wacker-type 1,2-DCF have also been showcased in the chemical literature.

In 2016, the Morken group published an enantioselective three-component 1,2-DCF of lithium vinylboronate esters with aryl/alkenyl triflate electrophiles under a Pd/MandyPhos catalytic system (Scheme 21).[81] The organoboronates nucleophiles were first synthesized *in situ* either by combining vinylboronic esters with alkenyl/aryl lithiums or alkenyl/arylboronic esters with vinyl lithium. Enantioenriched 1,2-dicarbofunctionalized secondary alcohols could subsequently be generated in excellent yields and enantioselectivity upon reaction with NaOH and $H_2O_2$.

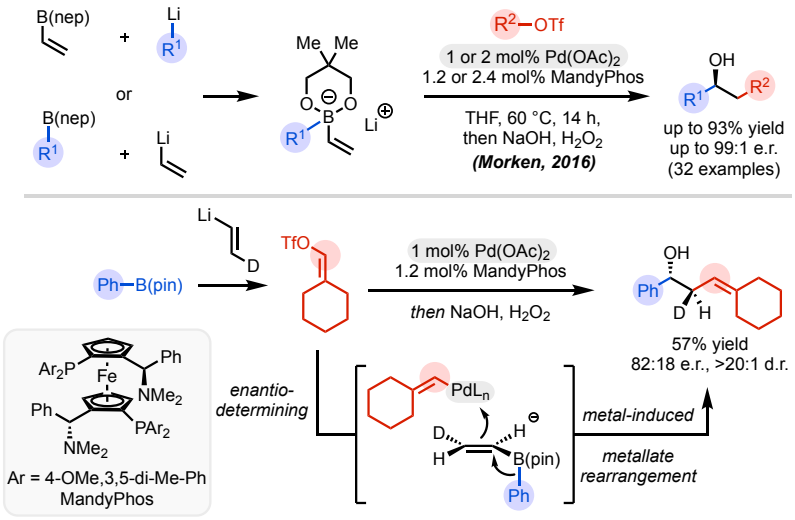


***Scheme 1.35.*** Enantioselective three-component Pd-catalyzed 1,2-DCF of vinylboronic esters via enantiodetermining metallate rearrangement.

In 2021, the Zhou lab showcased an enantioselective Wacker-type 1,2-DCF of cyclic alkenes with alkyne and heteroarene coupling partners under a (**L21**)$PdCl_2$ catalysis

platform (Scheme 1.36).[82] The enantioenriched 1,2-dicarbofunctionalized products possess adjacent C($sp^3$)–heteroaryl and C($sp^3$)–allenyl bonds that are *trans* to each other as confirmed by single-crystal X-ray diffraction, which suggests that enantiodetermining step is likely Wacker-type *anti*-carbopalladation.

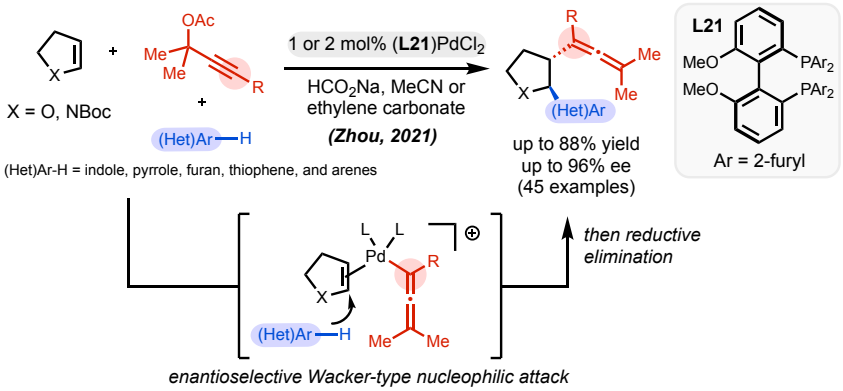


***Scheme 1.36.*** Enantioselective three-component Pd-catalyzed 1,2-DCF of vinylboronic esters via enantiodetermining metallate rearrangement.

In summary, these literature precedents lay the foundation of the central hypotheses formed throughout part I of this Thesis, namely that there remains a scarcity in using weak directing groups, dicarbofunctionalizing multisubstituted alkenes, and developing asymmetric versions. In Chapter 3, we showcase the successful implementation of ketone-directed 1,2-DCF of unactivated alkenes using organoboronic ester nucleophiles in lieu of organozinc nucleophiles and without the need of an *in situ* formed imine directing group. In Chapter 4, we discovered that sulfonamides are strong native directing groups in 1,2-DCF of unactivated alkenes, such that even multisubstituted alkenes are competent substrates. Finally, in Chapter 5, we report the first enantioselective three-component Ni-catalyzed 1,2-DCF of unactivated alkenes via enantiodetermining migratory insertion facilitated by a bulky sulfonamide directing group and nickel/chiral biOx catalysis.

## 1.6. REFERENCES

(1) (a) Johnsson Seechurn, C. C. C.; Kitching, M. O.; Colacot, T. J.; Snieckus, V. Palladium-Catalyzed Cross-Coupling: A Historical Contextual Perspective to the 2010 Nobel Prize. *Angew*. *Chem*. *Int*. *Ed*. **2012**, *51*, 5062–5085. (b) Ananikov, V. P. Nickel: The "Spirited Horse" of Transition Metal Catalysis. *ACS Catal*. **2015**, *5*, 1964–1971. (c) Wade, L.G. *Organic Chemistry*, 6th ed.; Pearson Prentice Hall, 2006.

(2) (a) Dewar, M. A Review of π Complex Theory. *Bull. Soc. Chim. Fr* **1951**, 1 8, C79.

(b) Chatt, J.; Duncanson, L. A. Olefin Coordination Compounds. Part III. Infra-Red Spectra and Structure: Attempted Preparation of Acetylene Complexes. *J. Chem. Soc.* **1953**, 2939–2947. (c) Chatt, J.; Duncanson, L. A.; Venanzi, L. M. Directing Effects in Inorganic Substitution Reactions. Part I. A Hypothesis to Explain the Trans-Effect. *J. Chem. Soc.* **1955**, 4456-4460.

(3) Kolb, H. C.; VanNieuwenhze, M. S.; Sharpless, K. B. Catalytic Asymmetric Dihydroxylation. *Chem. Rev.* **1994**, *94*, 2483–2547.

(4) (a) Chemler, S. R.; Bovino, M. T. Catalytic Aminohalogenation of Alkenes and Alkynes. *ACS Catal.* **2013**, *3*, 1076–1091. (b) Schultz, D. M.; Wolfe, J. P. Recent Developments in Palladium-Catalyzed Alkene Aminoarylation Reactions for the Synthesis of Nitrogen Heterocycles. *Synthesis* **2012**, *44*, 351–361. (c) Luo, Y.-C.; Xu, C.; Zhang, X. Nickel-Catalyzed Dicarbofunctionalization of Alkenes. *Chin. J. Chem.* **2020**, *38*, 1371–1394.

(5) (a) Taylor, R. J. K. Organocopper Conjugate Addition-Enolate Trapping Reactions. *Synthesis* **1985**, 364–392. (b) Ihara, M.; Fukumoto, K. Syntheses of Polycyclic Natural

Products Employing the Intramolecular Double Michael Reaction. *Angew. Chem. Int. Ed.* **1993**, *32*, 1010–1022.

(6) Miyaura, N.; Suzuki, A. Palladium-Catalyzed Cross-Coupling Reactions of Organoboron Compounds. *Chem*. *Rev*., **1995**, *95*, 2457–2483.

(7) Johansson Seechurn, C. C. C.; Kitching, M. O.; Colacot, T. J.; Snieckus, V. *Angew*. *Chem*., *Int*. *Ed*., **2012**, *51*, 5062–5085.

(8) (a) Derosa, J.; Tran, V. T.; van der Puyl, V. A.; Engle, K. M. Carbon–Carbon π-Bonds as Conjunctive Reagents in Cross-Coupling. *Aldrichimica Acta* **2018**, *51*, 21–32; (b) Giri, R.; KC, S. Strategies toward Dicarbofunctionalization of Unactivated Olefins by Combined Heck Carbometalation and Cross-Coupling. *J*. *Org*. *Chem*. **2018**, *83*, 3013–3022; (c) Zhang, J.-S.; Liu, L.; Chen, T.; Han, L.-B. Transition-Metal-Catalyzed Three-Component Difunctionalizations of Alkenes. *Chem*. *Asian J*. **2018**, *13*, 2277–2291. (d) Tu, H.-Y.; Zhu, S.; Qing, F.-L.; Chu, L. Recent Advances in Nickel-Catalyzed Three-Component Difunctionalization of Unactivated Alkenes. *Synthesis* **2020**, *52*, 1346–1356. (e) Badir, S. O.; Molander, G. A. Developments in Photoredox/Nickel Dual-Catalyzed 1,2-Difunctionalizations. *Chem* **2020**, *6*, 1327– 1339. (f) Qi, X.; Diao, T. Nickel-Catalyzed Dicarbofunctionalization of Alkenes. *ACS Catal.* **2020**, *10*, 8542–8556. (g) Lee, B. C.; Liu, C.- F.; Lin, L. Q. H.; Yap, K. Z.; Song, N.; Ko, C. H. M.; Chan, P. H.; Koh, M. N-Heterocyclic Carbenes as Privileged Ligands for Nickel-Catalysed Alkene Functionalisation J. *Chem*. *Soc*. *Rev*. **2023**, *52*, 2946.

(9) Derosa, J.; Apolinar, O.; Kang, T.; Tran; V. T.; Engle, K. M. Recent Developments in Nickel-Catalyzed Intermolecular Dicarbofunctionalization of Alkenes. *Chem*. *Sci*. **2020**, *11*, 4287–4296.

(10) (a) Catellani, M.; Chiusoli, G. P. One-Pot Palladium-Catalyzed Synthesis of 2,3-Disubstituted Bicyclo[2.2.1]heptanes and Bicyclo[2.2.1]hept-5-enes. *Tetrahedron Lett*. **1982**, *23*, 4517. (b) Catellani, M.; Chiusoli, G. P.; Giroldini, W.; Salerno, G. New Transition Metal-Catalyzed C–C Coupling Reactions Initiated by C–X Bond Cleavage and Terminated by H-Transfer. *J. Organomet. Chem*. **1980**, *199*, C21. (c) Catellani, M.; Chiusoli, G. P. Competitive Processes in Palladium-Catalyzed C–C Bond Formation. *J. Organomet. Chem*. **1982**, *233*, C21. (d) Catellani, M.; Chiusoli, G. P.; Sgarabotto, P. Palladium-Catalyzed Syntheses of Condensed Cyclopentanes. The Crystal and Molecular Structure of 3-Benzylidenpentacyclo[$9.2.1.^{5,8}.1^{1,11}.0^{2,10}.0^{4,9}$]-pentadecane *J. Organomet. Chem*. **1982**, *240*, 311.

(11) Ananikov, V. P. Nickel: The "Spirited Horse" of Transition Metal Catalysis. *ACS Catal*. **2015**, *5*, 1964–1971.

(12) (a) Lin, C.-Y.; Power, P.P. Complexes of Ni(I): a ''Rare'' Oxidation State of Growing Importance. *Chem. Soc. Rev*. **2017**, *46*, 5347–5399. (b) Zheng, B.; Tang, F.; Luo, J.; Schultz, J. W.; Rath, N. P.; Mirica, L. M. Organometallic Nickel(III) Complexes Relevant to Cross-Coupling and Carbon–Heteroatom Bond Formation Reactions. *J. Am. Chem. Soc*. **2014**, *136*, 6499–6504. (c) Camasso, N.M.; Sanford, M.S. Design, Synthesis, and Carbon–Heteroatom Coupling Reactions of Organometallic Nickel(IV) Complexes. *Science* **2015**, *347*, 1218–1220. (d) Roy, L.E.; Jakubikova, E.; Guthrie, M. G.; Batista, E. R. Calculation of One-Electron Redox Potentials Revisited. Is it Possible to Calculate Accurate Potentials with Density Functional Methods? *J. Phys. Chem. A* **2009**, *113*, 6745–6750.

(13) Diccianni, J.B.; Katigbak, J.; Hu, C.; Diao, T. Mechanistic Characterization of (Xantphos)Ni(I)-Mediated Alkyl Bromide Activation: Oxidative Addition, Electron Transfer, or Halogen-Atom Abstraction. *J. Am. Chem. Soc.* **2019**, *141*, 1788–1796.

(14) Batsanov, S.S. Van der Waals Radii of Elements. *Inorg. Mater.* **2001**, *37*, 871–885.

(15) Mann, J.B.; Meek, T. L.; Knight, E. T.; Capitani, J. F.; Allen, L. C. Configuration Energies of the d-Block Elements. *J. Am. Chem. Soc.* **2000**, *122*, 5132– 5137.

(16) (a) Leatherman, M.D.; Svejda, S. A.; Johnson, L. K.; Brookhart, M. Mechanistic Studies of Nickel(II) Alkyl Agostic Cations and Alkyl Ethylene Complexes: Investigations of Chain Propagation and Isomerization in (α-Diimine)Ni(II)-Catalyzed Ethylene Polymerization. *J. Am. Chem. Soc.* **2003**, *125*, 3068–3081. (b) Xu, H.W.; White, P. B.; Hu, C.; Diao, T. Structure and Isotope Effects of the β-H Agostic (α-Diimine)Nickel Cation as a Polymerization Intermediate. *Angew. Chem. Int. Ed.* **2017**, *56*, 1535–1538 (c) Xu, H.W.; Hu, C. T.; Wang, X.; Diao, T. Structural Characterization of β-Agostic Bonds in Pd-Catalyzed Polymerization. *Organometallics* **2017**, *36*, 4099–4102.

(17) (a) Yaroshevsky, A. A. Abundances of Chemical Elements in the Earth's Crust. *Geochem. Int.* **2006**, *44*, 48−55. (b) Chirik, P. J.; Engle, K. M.; Simmons, E. M.; Wisniewski, S. R. Collaboration as a Key to Advance Capabilities for Earth-Abundant Metal Catalysis, *Org. Process Res. Dev.* **2023**, *27*, 1160–1184.

(18) Qin, T.; Cornella, J.; Li, C.; Malins, L. R.; Edwards, J. T.; Kawamura, S.; Maxwell, B. D.; Eastgate, M. D.; Baran, P. S. A General Alkyl-Alkyl Cross-Coupling Enabled by Redox-Active Esters and Alkylzinc Reagents *Science*, **2016**, *352*, 801–805.

(19) García-Domínguez, A.; Li; Z.; Nevado, C. Nickel-Catalyzed Reductive Dicarbofunctionalization of Alkenes. *J. Am. Chem. Soc.* **2017**, *139*, 6835–6838.

(20) Shu, W.; García-Domínguez, A.; Quiróz, M. T.; Mondal, R.; Cárdenas, D. J.; Nevado, C. Ni-Catalyzed Reductive Dicarbofunctionalization of Nonactivated Alkenes: Scope and Mechanistic Insights. *J. Am. Chem. Soc.* **2019**, *141*, 13812–13821.

(21) Gu, J.-W.; Min, Q.-Q.; Yu, L.-C.; Zhang, X. Tandem Difluoroalkylation-Arylation of Enamides Catalyzed by Nickel. *Angew. Chem. Int. Ed.* **2016**, *55*, 12270–12274.

(22) Shrestha, B.; Basnet, P.; Dhungana, R. K.; KC, S.; Thapa, S.; Sears, J. M.; Giri, R. Ni-Catalyzed Regioselective 1,2-Dicarbofunctionalization of Olefins by Intercepting Heck Intermediates as Imine-Stabilized Transient Metallacycles. *J. Am. Chem. Soc.* **2017**, *139*, 10653–10656.

(23) Thapa, S.; Dhungana, R. K.; Magar, R. T.; Shrestha, B.; KC, S.; Giri, R. Ni-Catalysed Regioselective 1,2-Diarylation of Unactivated Olefins by Stabilizing Heck Intermediates as Pyridylsilyl-Coordinated Transient Metallacycles. *Chem. Sci.* **2018**, *9*, 904–909.

(24) (a) KC, S.; Dhungana, R. K.; Shrestha, B.; Thapa, S.; Khanal, N.; Basnet, P.; Lebrun, R. W.; Giri, R. Ni-Catalyzed Regioselective Alkylarylation of Vinylarenes via $C(sp^3)$–$C(sp^3)$/$C(sp^3)$–$C(sp^2)$ Bond Formation and Mechanistic Studies. *J. Am. Chem. Soc.* **2018**, *140*, 9801–9805. (b) Gao, P.; Chen, L.-A.; Brown, M. K. Nickel-Catalyzed Stereoselective Diarylation of Alkenylarenes. *J. Am. Chem. Soc.* **2018**, *140*, 10653–10657.

(25) Kadam, A. A.; Metz, T. L.; Qian, Y.; Stanley, L. M. Ni-Catalyzed Three-Component Alkene Carboacylation Initiated by Amide C–N Bond Activation. *ACS Catal.* **2019**, *9*, 5651–5656.

(26) Derosa, J.; Tran, V. T.; Boulous, M. N.; Chen, J. S.; Engle, K. M. Nickel-Catalyzed β,γ-Dicarbofunctionalization of Alkenyl Carbonyl Compounds via Conjunctive Cross-Coupling. *J. Am. Chem. Soc.* **2017**, *139*, 10657–10660.

(27) Derosa, J.; van der Puyl, V. A.; Tran, V. T.; Liu, M.; Engle, K. M. Directed Nickel-Catalyzed 1,2-Dialkylation of Alkenyl Carbonyl Compounds *Chem*. *Sci*. **2018**, *9*, 5278–5283.

(28) Pan, R.; Shi, C.; Zhang, D.; Tian, Y.; Guo, S.; Yao, H.; Lin, A. Nickel-Catalyzed Reductive 1,2-Dialkynylation of Alkenes Bearing an 8-Aminoquinoline Directing Group. *Org*. *Lett*. **2019**, *21*, 8915–8920.

(29) Li, W.; Boon, J. K.; Zhao, Y. Nickel-Catalyzed Difunctionalization of Allyl Moieties Using Organoboronic Acids and Halides with Divergent Regioselectivities. *Chem. Sci.* **2018**, *9*, 600–607.

(30) Basnet, P.; Dhungana, R. K.; Thapa, S.; Shrestha, B.; KC, S.; Sears, J. M.; Giri, R. Ni-Catalyzed Regioselective β,δ-Diarylation of Unactivated Olefins in Ketimines via Ligand-Enabled Contraction of Transient Nickellacycles: Rapid Access to Remotely Diarylated Ketones. *J*. *Am*. *Chem*. *Soc*. **2018**, *140*, 7782–7786.

(31) Basnet, P.; KC, S.; Dhungana, R. K.; Shrestha, B.; Boyle, T. J.; Giri, R. Synergistic Bimetallic Ni/Ag and Ni/Cu Catalysis for Regioselective γ,δ-Diarylation of Alkenyl Ketimines: Addressing β-H Elimination by in Situ Generation of Cationic Ni(II) Catalysts. *J*. *Am*. *Chem*. *Soc*. **2018**, *140*, 15586–15590.

(32) Dhungana, R. K.; KC, S.; Basnet, P.; Aryal, V.; Chesley, L. J.; Giri, R. Ni(I)-Catalyzed β,δ-Vinylarylation of γ,δ-Alkenyl α-Cyanocarboxylic Esters via Contraction of Transient Nickellacycles. *ACS Catal*. **2019**, *9*, 10887–10893.

(33) Zhao, X.; Tu, H.-Y.; Guo, L.; Zhu, S.; Qing, F.-L.; Chu, L. Intermolecular Selective Carboacylation of Alkenes via Nickel-Catalyzed Reductive Radical Relay. *Nat*. *Commun*. **2018**, *9*, 3488.

(34) Derosa, J.; Kleinmans, R.; Tran, V. T.; Karunananda, M. K.; Wisniewski, S. R.; Eastgate, M. D.; Engle, K. M. Nickel-Catalyzed 1,2-Diarylation of Simple Alkenyl Amides. *J. Am. Chem. Soc.* **2018**, *140*, 17878–17883.

(35) Tran, V. T.; Li, Z.-Q.; Gallagher, T. J.; Derosa, J.; Liu, P.; Engle, K. M. Integrating Allyl Electrophiles into Nickel-Catalyzed Conjunctive Cross-Coupling. *Angew. Chem. Int. Ed.* **2020**, *59*, 7029–7034.

(36) Derosa, J.; Kang, T.; Tran, V. T.; Wisniewski, S. R.; Karunananda, M. K.; Jankins, T. C.; Xu, K. L.; Engle, K. M. Nickel-Catalyzed 1,2-Diarylation of Alkenyl Carboxylates: A Gateway to 1,2,3-Trifunctionalized Building Blocks. *Angew. Chem. Int. Ed.* **2020**, *59*, 1201–1205.

(37) Guo, L.; Tu, H.-Y.; Zhu, S.; Chu, L. Selective, Intermolecular Alkylarylation of Alkenes via Photoredox/Nickel Dual Catalysis. *Org. Lett.* **2019**, *21*, 4771–4776.

(38) (a) García-Domínguez, A.; Mondal, R.; Nevado, C. Dual Photoredox/Nickel-Catalyzed Three-Component Carbofunctionalization of Alkenes. *Angew. Chem. Int. Ed.* **2019**, *58*, 12286–12290. (b) Wang, J. Z. Lyon, W. L.; MacMillan, D. W. C. Alkene Dialkylation by Triple Radial Sorting. *Nature* **2024**, 628, 104–109. (c) Wang, J. Z. Mao, E.; Nguyen, J. A.; Lyon, W. L.; MacMillan, D. W. C. Triple Radical Sorting: Aryl-Alkylation of Alkenes. *J. Am. Chem. Soc.* **2024**, *146*, 15693–15700.

(39) (a) Lovering, F.; Bikker, J.; Humblet, C. Escape from Flatland: Increasing Saturation as an Approach to Improving Clinical Success. *J. Med. Chem.* **2009**, *52*, 6752. (b) Lovering, F. Med. Escape from Flatland 2: Complexity and Promiscuity. *Chem. Commun.* **2013**, *4*, 515–519. (c) Li, J.; Eastgate, M. D. Current Complexity: a Tool for Assessing the Complexity of Organic Molecules. *Org. Biomol. Chem.* **2015**, *13*, 7164–7176. (d) Eastgate,

M. D.; Schmidt, M. A.; Fandrick, K. R. On the Design of Complex Drug Candidate Syntheses in the Pharmaceutical Industry. *Nat Rev Chem* **2017**, *1*, 0016. (e) Caille, S.; Cui, S.; Faul, M. M.; Mennen, S. M.; Tedrow, J. S.; Walker, S. D. Molecular Complexity as a Driver for Chemical Process Innovation in the Pharmaceutical Industry. *J. Org. Chem.* **2019**, *84*, 4583. (f) Beaver, M. G.; Caille, S.; Farrell, R. P.; Rötheli, A. R.; Smith, A. G.; Tedrow, J. S.; Thiel, O. R. Building Complexity and Achieving Selectivity through Catalysis–Case Studies from the Pharmaceutical Pipeline. *Synlett* **2021**, *32*, 457.

(40) (a) Hayashi, T.; Yamasaki, K. *Chem. Rev.* **2003**, *103*, 2829. (b) Trost, B. M.; Van Vranken, D. L. Asymmetric Transition Metal-Catalyzed Allylic Alkylations. *Chem. Rev.* **1996**, *96*, 395. (c) Kranthikumar, R. Recent Advances in C(sp3)–C(sp3) Cross-Coupling Chemistry: A Dominant Performance of Nickel Catalysts. *Organometallics* **2022**, *41*, 667. (d) Cherney, A. H.; Kadunce, N. T.; Reisman, S. E. Enantioselective and Enantiospecific Transition-Metal-Catalyzed Cross-Coupling Reactions of Organometallic Reagents to Construct C–C Bonds. *Chem. Rev.* **2015**, *115*, 9587.

(41) (a) Li, Z.-L.; Fang, G.-C.; Gu, Q.-S.; Liu, X.-Y. Recent Advances in Copper-Catalysed Radical-Involved Asymmetric 1,2-Difunctionalization of Alkenes. *Chem. Soc. Rev.* **2020**, *49*, 32. (b) You, W.; Brown, M. K. *J. Am. Chem. Soc.* **2015**, *137*, 14578.

(42) (a) Shintani, R.; Okamoto, K.; Otomaru, Y.; Ueyama, K.; Hayashi, T. Catalytic Asymmetric Arylative Cyclization of Alkynals: Phosphine-Free Rhodium/Diene Complexes as Efficient Catalysts. *J. Am. Chem. Soc.* **2005**, *127*, 54. (d) Miura, T.; Sasaki, T.; Nakazawa, H.; Murakami, M. Ketone Synthesis by Intramolecular Acylation of Organorhodium(I) with Ester. *J. Am. Chem. Soc.* **2005**, *127*, 1390. (e) Xu, T.; Ko, H. M.;

Savage, N. A.; Dong, G. Highly Enantioselective Rh-Catalyzed Carboacylation of Olefins: Efficient Syntheses of Chiral Poly-Fused Rings. *J. Am. Chem. Soc*. **2012**, *134*, 20005.

(43) Herraiz, A. G.; Cramer, N. Cobalt(III)-Catalyzed Diastereo- and Enantioselective Three-Component C–H Functionalization. *ACS Catal*. **2021**, *11*, 11938.

(44) (a) Sato, Y.; Sodeoka, M.; Shibasaki, M. Catalytic Asymmetric Carbon-Carbon Bond Formation: Asymmetric Synthesis of cis-Decalin Derivatives by Palladium-Catalyzed Cyclization of Prochiral Alkenyl Iodides *J. Org. Chem*. **1989**, *54*, 4738. (b) Carpenter, N. E.; Kucera, D. J.; Overman, L. E. Palladium-Catalyzed Polyene Cyclizations of Trienyl Triflates. *J. Org. Chem*. **1989**, *54*, 5846. (c) Dounay, A. B.; Overman, L. E. The Asymmetric Intramolecular Heck Reaction in Natural Product Total Synthesis. *Chem. Rev*. **2003**, *103*, 2945.

(45) Ohshima, T.; Kagechika, K.; Adachi, M.; Sodeoka, M.; Shibasaki, M. Asymmetric Heck Reaction−Carbanion Capture Process. Catalytic Asymmetric Total Synthesis of (−)-$\Delta^{9(12)}$-Capnellene. *J. Am. Chem. Soc*. **1996**, *118*, 7108.

(46) Diaz, P.; Gendre, F.; Stella, L.; Charpentier, B. New Synthetic Retinoids Obtained by Palladium-Catalyzed Tandem Cyclisation-Hydride Capture Process. *Tetrahedron* **1998**, *54*, 4579. (b) Yue, G.; Lei, K.; Hirao, H.; Zhou, J. Palladium-Catalyzed Asymmetric Reductive Heck Reaction of Aryl Halides. *Angew. Chem. Int. Ed*. **2015**, *54*, 6531.

(47) (a) Pinto, A.; Jia, Y.; Neuville, L.; Zhu, J. Palladium-Catalyzed Enantioselective Domino Heck–Cyanation Sequence: Development and Application to the Total Synthesis of Esermethole and Physostigmine. *Chem. Eur. J*. **2007**, *13*, 961. (b) Yasui, Y.; Kamisaki, H.; Takemoto, Y. Enantioselective Synthesis of 3,3-Disubstituted Oxindoles through Pd-Catalyzed Cyanoamidation. *Org. Lett*. **2008**, *10*, 3303. (c) Watson, M. P.; Jacobsen, E. N.

Asymmetric Intramolecular Arylcyanation of Unactivated Olefins via C−CN Bond Activation. *J. Am. Chem. Soc.* **2008**, *130*, 12594. (d) Nakao, Y.; Ebata, S.; Yada, A.; Hiyama, T.; Ikawa, M.; Ogoshi, S. Intramolecular Arylcyanation of Alkenes Catalyzed by Nickel/$AlMe_2Cl$. *J. Am. Chem. Soc.* **2008**, *130*, 12874.

(48) Cong, H.; Fu, G. C. Catalytic Enantioselective Cyclization/Cross-Coupling with Alkyl Electrophiles *J. Am. Chem. Soc.* **2014**, *136*, 3788−3791.

(49) Kong, W.; Wang, Q.; Zhu, J. Palladium-Catalyzed Enantioselective Domino Heck/Intermolecular C–H Bond Functionalization: Development and Application to the Synthesis of (+)-Esermethole. *J. Am. Chem. Soc.* **2015**, *137*, 16028.

(50) Kong, W.; Wang, Q.; Zhu, J. Synthesis of Diversely Functionalized Oxindoles Enabled by Migratory Insertion of Isocyanide to a Transient σ-Alkylpalladium(II) Complex. *Angew. Chem. Int. Ed.* **2016**, *55*, 9714.

(51) Carmona, R. C.; Köster, O. D.; Correia, C. R. D. Chiral N,N Ligands Enabling Palladium-Catalyzed Enantioselective Intramolecular Heck–Matsuda Carbonylation Reactions by Sequential Migratory and CO Insertions. *Angew. Chem. Int. Ed.* **2018**, *57*, 12067.

(52) Ma, T.; Chen, Y.; Li, Y.; Ping, Y.; Kong, W. Nickel-Catalyzed Enantioselective Reductive Aryl Fluoroalkenylation of Alkenes. *ACS Catal.* **2019**, *9*, 9127−9133.

(53) (a) Zhang, Z.-M.; Xu, B.; Wu, L.; Wu, Y.; Qian, Y.; Zhou, L.; Liu, Y.; Zhang, J. Enantioselective Dicarbofunctionalization of Unactivated Alkenes by Palladium-Catalyzed Tandem Heck/Suzuki Coupling Reaction. *Angew. Chem. Int. Ed.* **2019**, *58*, 14653. (b) Ju, B.; Chen, S.; Kong, W. Enantioselective Palladium-Catalyzed Diarylation of Unactivated Alkenes. *Chem. Commun.* **2019**, *55*, 14311. (c) Chen, Q.; Li, S.; Xie, X.;

Guo, H.; Yang, J.; Zhang, J. Pd-Catalyzed Enantioselective Dicarbofunctionalization of Alkene to Access Disubstituted Dihydroisoquinolinone. *Org*. *Lett*. **2021**, *23*, 4099. (d) Ma, Z.; Sun, L.; Zhou, J. S. Catalytic Enantioselective Domino Alkenylation-Alkynylation of Alkenes: Stereoselective Synthesis of 5–7 Membered Azacycles and Carbocycles *Sci*. *China*: *Chem*. **2023**, *66*, 1701.

(54) (a) Zhou, L.; Li, S.; Xu, B.; Ji, D.; Wu, L.; Liu, Y.; Zhang, Z.-M.; Zhang, J. Enantioselective Difunctionalization of Alkenes by a Palladium-Catalyzed Heck/Sonogashira Sequence. *Angew*. *Chem*. *Int*. *Ed*. **2020**, *59*, 2769. (b) Liu, R.-R.; Wang, Y.-G.; Li, Y.-L.; Huang, B.-B.; Liang, R.-X.; Jia, Y.-X. Enantioselective Dearomative Difunctionalization of Indoles by Palladium-Catalyzed Heck/Sonogashira Sequence. *Angew*. *Chem*. *Int*. *Ed*. **2017**, *56*, 7475. (c) Wu, Y.; Xu, B.; Zhao, G.; Pan, Z.; Zhang, Z.-M.; Zhang, J. Palladium/Xu-Phos Catalyzed Enantioselective Tandem Heck/Cacchi Reaction of Unactivated Alkenes. *Chin*. *J*. *Chem*. **2021**, *39*, 3255.

(55) (a) Liu, L.; Cheng, F.; Meng, C.; Zhang, A.-A.; Zhang, M.; Xu, K.; Ishida, N.; Murakami, M. Pd-Catalyzed Ring-Closing/Ring-Opening Cross Coupling Reactions: Enantioselective Diarylation of Unactivated Olefins. *ACS Catal*. **2021**, *11*, 8942. (b) Cao, K.; Zhang, Z.-M.; Zhang, J.; Chen, F. Palladium-Catalyzed Asymmetric Cross-Coupling Reactions of Cyclobutanols and Unactivated Olefins. *Org*. *Lett*. **2021**, *23*, 9520.

(56) (a) Ping, Y.; Li, Y.; Zhu, J.; Kong, W. Construction of Quaternary Stereocenters by Palladium-Catalyzed Carbopalladation-Initiated Cascade Reactions. *Angew*. *Chem*. *Int*. *Ed*. **2019**, *58*, 1562. (b) Xu, B.; Ji, D.; Wu, L.; Zhou, L.; Liu, Y.; Zhang, Z.-M.; Zhang, J. Palladium/Xu-Phos-Catalyzed Enantioselective Cascade Heck/Remote C($sp^2$)–H Alkylation Reaction. *Chem* **2022**, *8*, 836.

(57) Diccianni, J.; Lin, Q.; Diao, T. Mechanisms of Nickel-Catalyzed Coupling Reactions and Applications in Alkene Functionalization. *Acc*. *Chem*. *Res*. **2020**, *53*, 906.

(58) Wang, K.; Ding, Z.; Zhou, Z.; Kong, W. Ni-Catalyzed Enantioselective Reductive Diarylation of Activated Alkenes by Domino Cyclization/Cross-Coupling. *J*. *Am*. *Chem*. *Soc*. **2018**, *140*, 12364−12368.

(59) Jin, Y.; Wang, C. Nickel-Catalyzed Asymmetric Reductive Arylalkylation of Unactivated Alkenes. *Angew*. *Chem*., *Int*. *Ed*. **2019**, *58*, 6722−6726.

(60) Tian, Z.-X.; Qiao, J.-B.; Xu, G.-L.; Pang, X.; Qi, L.; Ma, W.-Y.; Zhao, Z.-Z.; Duan, J.; Du, Y.-F.; Su, P.; Liu, X.-Y.; Shu, X.-Z. Highly Enantioselective Cross-Electrophile Aryl-Alkenylation of Unactivated Alkenes *J*. *Am*. *Chem*. *Soc*. **2019**, *141*, 7637−7643.

(61) Li, Y.; Ding, Z.; Lei, A.; Kong, W. Ni-Catalyzed Enantioselective Reductive Aryl-Alkenylation of Alkenes: Application to the Synthesis of (+)-Physovenine and (+)-Physostigmine. *Org*. *Chem*. *Front*. **2019**, *6*, 3305−3309.

(62) Jin, Y.; Yang, H.; Wang, C. Nickel-Catalyzed Asymmetric Reductive Arylbenzylation of Unactivated Alkenes *Org*. *Lett*. **2020**, *22*, 2724−2729.

(63) Williams, M. T.; Morrill, L. C.; Browne, D. C. Nickel-Catalyzed Intramolecular Alkene Difunctionalization by Ball-Milling. *Adv*. *Synth*. *Catal*. **2023**, *365*, 1477.

(64) (a) Fan, P.; Lan, Y.; Zhang, C.; Wang, C. Nickel/Photo-Cocatalyzed Asymmetric Acyl-Carbamoylation of Alkenes *J*. *Am*. *Chem*. *Soc*. **2020**, *142*, 2180−2186. (b) Lan, Y.; Wang, C. Nickel-Catalyzed Enantioselective Reductive Carbo-Acylation of Alkenes. *Commun*. *Chem*. **2020**, *3*, 45.

(65) (a) Wu, X.; Qu, J.; Chen, Y. Quinim: A New Ligand Scaffold Enables Nickel-Catalyzed Enantioselective Synthesis of α-Alkylated γ-Lactam. *J*. *Am*. *Chem*. *Soc*. **2020**,

*142*, 15654. (b) Wu, X.; Luan, B.; Zhao, W.; He, F.; Wu, X.-Y.; Qu, J.; Chen, Y. Catalytic Desymmetric Dicarbofunctionalization of Unactivated Alkenes. *Angew*. *Chem*. *Int*. *Ed*. **2022**, *61*, e202111598.

(66) Li, Y.; Zhang, F.-P.; Wang, R.-H.; Qi, S.-L.; Luan, Y.-X.; Ye, M. Carbamoyl Fluoride-Enabled Enantioselective Ni-Catalyzed Carbocarbamoylation of Unactivated Alkenes. *J*. *Am*. *Chem*. *Soc*. **2020**, *142*, 19844.

(67) Chierchia, M.; Xu, P.; Lovinger, G. J.; Morken, J. P. Enantioselective Radical Addition/Cross-Coupling of Organozinc Reagents, Alkyl Iodides, and Alkenyl Boron Reagents *Angew*. *Chem*., *Int*. *Ed*. **2019**, *58*, 14245−14249.

(68) Gu, J.-W.; Min, Q.-Q.; Yu, L.-C.; Zhang, X. Tandem Difluoroalkylation-Arylation of Enamides Catalyzed by Nickel. *Angew*. *Chem*. *Int*. *Ed*. **2016**, *55*, 12270.

(69) Anthony, D.; Lin, Q.; Baudet, J.; Diao, T. Nickel-Catalyzed Asymmetric Reductive Diarylation of Vinylarenes. *Angew*. *Chem*., *Int*. *Ed*. **2019**, *58*, 3198–3202. (b) Lin, Q.; Spielvogel, E. H.; Diao, T. Carbon-Centered Radical Capture at Nickel(II) Complexes: Spectroscopic Evidence, Rates, and Selectivity. *Chem* **2023**, *9*, 1295.

(70) Tu, H.-Y.; Wang, F.; Huo, L.; Li, Y.; Zhu, S.; Zhao, X.; Li, H.; Qing, F.-L.; Chu, L. Enantioselective Three-Component Fluoroalkylarylation of Unactivated Olefins through Nickel-Catalyzed Cross-Electrophile Coupling. *J*. *Am*. *Chem*. *Soc*. **2020**, *142*, 9604–9611.

(71) Wei, X.; Shu, W.; García-Domínguez, A.; Merino, E.; Nevado, C. Asymmetric Ni-Catalyzed Radical Relayed Reductive Coupling. *J*. *Am*. *Chem*. *Soc*. **2020**, *142*, 13515–13522.

(72) Li, Y.-Z.; Rao, N.; An, L.; Wan, X.-L.; Zhang, Y.; Zhang, X. Enantioselective Nickel-Catalyzed Dicarbofunctionalization of 3,3,3-Trifluoropropene. *Nat*. *Commun*. **2022**, *13*, 5539.

(73) (a) Li, X.; Yuan, M.; Chen, F.; Huang, Z.; Qing, F.-L.; Gutierrez, O.; Chu, L. Three-Component Enantioselective Alkenylation of Organophosphonates via Nickel Metallaphotoredox Catalysis. *Chem* **2023**, *9*, 154. (b) Guo, L.; Yuan, M.; Zhang, Y.; Wang, F.; Zhu, S.; Gutierrez, O.; Chu, L. General Method for Enantioselective Three-Component Carboarylation of Alkenes Enabled by Visible-Light Dual Photoredox/Nickel Catalysis. *J*. *Am*. *Chem*. *Soc*. **2020**, *142*, 20390.

(74) (a) Kang, T.; Kim, N.; Cheng, P. T.; Zhang, H.; Foo, K.; Engle, K. M. Nickel-Catalyzed 1,2-Carboamination of Alkenyl Alcohols. *J*. *Am*. *Chem*. *Soc*. **2021**, *143*, 13962. (b) Kang, T.; González, J. M.; Li, Z.-Q.; Foo, K.; Cheng, P. T. W.; Engle, K. M. Alkene Difunctionalization Directed by Free Amines: Diamine Synthesis via Nickel-Catalyzed 1,2-Carboamination. *ACS Catal*. **2022**, *12*, 3890. (c) Li, Z.-Q.; Cao, Y.; Kang, T.; Engle, K. M. Electrophilic Sulfur Reagent Design Enables Directed syn-Carbosulfenylation of Unactivated Alkenes. *J*. *Am*. *Chem*. *Soc*. **2022**, *144*, 7189.

(75) Stokes, B. J.; Liao, L.; de Andrade, A. M.; Wang, Q.; Sigman, M. S. A Palladium-Catalyzed Three-Component-Coupling Strategy for the Differential Vicinal Diarylation of Terminal 1,3-Dienes. *Org*. *Lett*. **2014**, *16*, 4666.

(76) Wu, X.; Lin, H.-C.; Li, M.-L.; Li, L.-L.; Han, Z.-Y.; Gong, L.-Z. Enantioselective 1,2-Difunctionalization of Dienes Enabled by Chiral Palladium Complex-Catalyzed Cascade Arylation/Allylic Alkylation Reaction. *J*. *Am*. *Chem*. *Soc*. **2015**, *137*, 13476.

(77) Zhang, Y.; Chen, G.; Zhao, D., Three-Component Vicinal-Diarylation of Alkenes via Direct Transmetalation of Arylboronic Acids. *Chem. Sci.* **2019**, *10*, 7952–7957.

(78) Xi, Y.; Huang, W.; Wang, C.; Ding, H.; Xia, T.; Wu, L.; Fang, K.; Qu, J.; Chen, Y. Catalytic Asymmetric Diarylation of Internal Acyclic Styrenes and Enamides. *J. Am. Chem. Soc.* **2022**, *144*, 8389.

(79) Liu, C.-F.; Wang, Z.-C.; Luo, X.; Lu, J.; Ko, C. H. M.; Shi, S.-L.; Koh, M. J. Synthesis of Tri- and Tetrasubstituted Stereocentres by Nickel-Catalysed Enantioselective Olefin Cross-Couplings. *Nat. Catal.* **2022**, *5*, 934.

(80) Dong, Z.; Tang, Q.; Xu, C.; Chen, L.; Ji, H.; Zhou, S.; Song, L.; Chen, L.-A. Directed Asymmetric Nickel-Catalyzed Reductive 1,2-Diarylation of Electronically Unactivated Alkenes. *Angew. Chem. Int. Ed.* **2023**, *62*, e202218286.

(81) Zhang, L.; Lovinger, G. J.; Edelstein, E. K.; Szymaniak, A. A.; Chierchia, M. P.; Morken, J. P. Catalytic Conjunctive Cross-Coupling Enabled by Metal-Induced Metallate Rearrangement. *Science* **2016**, *351*, 70.

(82) Teng, S.; Chi, Y. R.; Zhou, J. S. Enantioselective Three-Component Coupling of Heteroarenes, Cycloalkenes and Propargylic Acetates. *Angew. Chem. Int. Ed.* **2021**, *60*, 4491.

# CHAPTER 2

## EXPERIMENTAL METHODS

## 2.1. CHROMATOGRAPHIC TECHNIQUES

### 2.1.1. Silica Gel Column Chromatography

Flash column chromatography was manually carried out by utilizing silica gel from SILICYCLE in 40–63 micron size particles and glass columns obtained from Chemglass.

### 2.1.2. Preparative Thin Layer Chromatography

Preparative Thin-Layer Chromatography (PTLC) plates were procured from MilliporeSigma as 1,000 micron or 500-micron size particles and carried out using glass chambers obtained from Sigma-Aldrich.

### 2.1.3. Supercritical Fluid Chromatography

Enantiomeric ratio (e.r.) was determined on a Waters UPC$^2$ system using commercially available chiral columns.

## 2.2. SPECTROSCOPIC AND ANALYTICAL TECHNIQUES

### 2.2.1. NMR Spectroscopy

$^1$H, $^{13}$C and $^{19}$F NMR spectra were recorded with Bruker AV-400, DPX-500 and AV-600 instruments. NMR spectra were internally referenced to $SiMe_4$ or solvent signals. The following abbreviations (or combinations thereof) were used to explain multiplicities: b = broad, s = singlet, d = doublet, t = triplet, q = quartet, p = pentet, hept = heptet and m = multiplet.

### 2.2.2. High Resolution Mass Spectroscopy

High-resolution mass spectra (HRMS) for new compounds were recorded on an Agilent LC/MSD TOF mass spectrometer.

### 2.2.3. X-Ray Crystallography

The single-crystal X-ray diffraction studies were carried out on a Bruker X8-ApexII CCD diffractometer (**3.5**, **4.1**) equipped with Mo $K_\alpha$ radiation ($\lambda$ = 0.7107 Å), Bruker Microstar X8 APEX II CCD diffractometer (**3.5**, **4.29**) equipped with Cu $K_\alpha$ radiation ($\lambda$ = 1.54178), or a Bruker Smart APEX II CCD diffractometer (**4.51**, **5.10**, **5.66**) equipped with Cu $K_\alpha$ radiation ($\lambda$ =1.54178 Å).

The data were integrated using the Bruker SAINT Software program and scaled using the SADABS software program. Solution by direct methods (SHELXT) produced a complete phasing model consistent with the proposed structure.

All nonhydrogen atoms were refined anisotropically by full-matrix least-squares (SHELXL-2014). All carbon-bonded hydrogen atoms were placed using a riding model. Their positions were constrained relative to their parent atom using the appropriate HFIX command in SHELXL-2014.

Crystallographic studies were carried out by Prof. Arnold L. Rheingold, Dr. Milan Gembicky, Dr. Han Nguyen, and Dr. Jake Bailey.

## 2.3. COMPUTATIONAL METHODS

**Computational details for Chapter 3:** All calculations were performed with Gaussian 09.[1] The B3LYP density functional and LANL2DZ basis set were used in

geometry optimizations. Single-point energies were calculated with M06 and a mixed basis set of SDD for Ni and I and 6-311+G(d,p) for other atoms. Solvation energy corrections were calculated using the SMD model.[2] In accordance with the experimental conditions, *i*-BuOH (ε = 16.8) was used as solvent in the single point calculations. To confirm the nature of the stationary points, vibrational frequency calculations were performed for all optimized structures. All optimized transition state structures have only one imaginary (negative) frequency, and all minima (reactants, products, and intermediates) have no imaginary frequencies. The imaginary frequencies of all transition states are provided in the "Cartesian Coordinates and Energies of the Optimized Structures" section below. The reported Gibbs free energies and enthalpies include zero-point vibrational energies and thermal corrections at 298 K.

**Computational details for Chapter 5:** Density functional theory (DFT) calculations were carried out using the *Gaussian 16* program[3] on Pitt CRC and XSEDE[4] supercomputers. Geometries of all stationary points were fully optimized using the dispersion-corrected[5] B3LYP-D3(BJ) functional[6] with the SDD basis set for nickel[7] and iodine[8] and the 6-31G(d) basis set for other atoms. Vibrational frequency calculations at the same level of theory of the geometry optimization were performed to confirm if each structure is a local minimum or a transition state. Gibbs free energies were calculated at 263.15 K using quasi-harmonic approximations with the Grimme's approach[9] using GoodVibes package,[10] with a cut-off vibrational frequency of 100 $cm^{-1}$ in entropy calculations. Single point energy calculations were carried out using the M06 functional[11] with the SDD basis set for palladium and iodine and the 6-311+G(d,p) basis set for other

atoms. Solvation energy corrections were calculated using the SMD solvation model[12] in single point energy calculations.

## 2.4. REFERENCES

(1) Gaussian 09, Revision D.01, Frisch, M. J.; Trucks, G. W.; Schlegel, H. B.; Scuseria, G. E.; Robb, M. A.; Cheeseman, J. R.; Scalmani, G.; Barone, V.; Mennucci, B.; Petersson, G. A.; Nakatsuji, H.; Caricato, M.; Li, X.; Hratchian, H. P.; Izmaylov, A. F.; Bloino, J.;Zheng, G.; Sonnenberg, J. L.; Hada, M.; Ehara, M.; Toyota, K.; Fukuda, R.; Hasegawa, J.; Ishida, M.; Nakajima, T.; Honda, Y.; Kitao, O.; Nakai, H.; Vreven, T.; Montgomery, J. A.; Peralta, J. E., Jr.; Ogliaro, F.; Bearpark, M.; Heyd, J. J.; Brothers, E.; Kudin, K. N.; Staroverov, V. N.; Kobayashi, R.; Normand, J.; Raghavachari, K.; Rendell, A.; Burant, J. C.; Iyengar, S. S.; Tomasi, J.; Cossi, M.; Rega, N.; Millam, J. M.; Klene, M.; Knox, J. E.; Cross, J. B.; Bakken, V.; Adamo, C.; Jaramillo, J.; Gomperts,R.; Stratmann, R. E.; Yazyev, O.; Austin, A. J.; Cammi, R.; Pomelli, C.; Ochterski, J. W.; Martin, R. L.; Morokuma, K.; Zakrzewski, V. G.; Voth, G. A.; Salvador, P.; Dannenberg, J. J.; Dapprich, S.; Daniels, A. D.; Farkas, Ö.; Foresman, J. B.; Ortiz, J. V.; Cioslowski, J. and Fox, D. J. Gaussian, Inc., Wallingford CT, 2009.

(2) Marenich, A. V.; Cramer, C. J.; Truhlar, D. G. “Universal Solvation Model Based on Solute Electron Density and on a Continuum Model of the Solvent Defined by the Bulk Dielectric Constant and Atomic Surface Tensions.” *J. Phys. Chem. B*, **2009**, *113*, 6378–6396.

(3) Frisch, M. J.; Trucks, G. W.; Schlegel, H. B.; Scuseria, G. E.; Robb, M. A.; Cheeseman, J. R.; Scalmani, G.; Barone, V.; Petersson, G. A.; Nakatsuji, H.; Li, X.; Caricato, M.; Marenich, A. V.; Bloino, J.; Janesko, B. G.; Gomperts, R.; Mennucci, B.; Hratchian, H. P.; Ortiz, J. V.; Izmaylov, A. F.; Sonnenberg, J. L.; Williams; Ding, F.; Lipparini, F.; Egidi, F.; Goings, J.; Peng, B.; Petrone, A.; Henderson, T.; Ranasinghe, D.; Zakrzewski, V. G.; Gao, J.; Rega, N.; Zheng, G.; Liang, W.; Hada, M.; Ehara, M.; Toyota, K.; Fukuda, R.; Hasegawa, J.; Ishida, M.; Nakajima, T.; Honda, Y.; Kitao, O.; Nakai, H.; Vreven, T.; Throssell, K.; Montgomery Jr., J. A.; Peralta, J. E.; Ogliaro, F.; Bearpark, M. J.; Heyd, J. J.; Brothers, E. N.; Kudin, K. N.; Staroverov, V. N.; Keith, T. A.; Kobayashi, R.; Normand, J.; Raghavachari, K.; Rendell, A. P.; Burant, J. C.; Iyengar, S. S.; Tomasi, J.; Cossi, M.; Millam, J. M.; Klene, M.; Adamo, C.; Cammi, R.; Ochterski, J. W.; Martin, R. L.; Morokuma, K.; Farkas, O.; Foresman, J. B.; Fox, D. J., *Gaussian 16 Rev. C.01*, Wallingford, CT, **2016**.

(4) Towns, J.; Cockerill, T.; Dahan, M.; Foster, I.; Gaither, K.; Grimshaw, A.; Hazlewood, V.; Lathrop, S.; Lifka, D.; Peterson, G. D.; Roskies, R.; Scott, J. R.; Wilkins-Diehr, N. *Comput. Sci. Eng.* **2014,** *16*, 62–74.

(5) (a) Grimme, S.; Ehrlich, S.; Goerigk, L. Effect of the Damping Function in Dispersion Corrected Density Functional Theory. *J. Comput. Chem.* **2011**, *32*, 1456–1465. (b) Grimme, S.; Antony, J.; Ehrlich, S.; Krieg, H. A Consistent and Accurate Ab Initio Parametrization of Density Functional Dispersion Correction (DFT-D) for the 94 Elements H-Pu. *J. Chem. Phys.* **2010**, *132*, 154104.

(6) (a) Becke, A. D. Density-functional Thermochemistry. III. The Role of Exact Exchange. *J. Chem. Phys.* **1993**, *98*, 5648–5652. (b) Lee, C.; Yang, W.; Parr, R. G.

Development of the Colle-Salvetti Correlation-Energy Formula into a Functional of the Electron Density. *Phys. Rev. B* **1988**, *37*, 785–789.

(7) Dolg, M.; Wedig, U.; Stoll, H.; Preuss, H. Energy-adjusted Ab Initio Pseudopotentials for The First Row Transition Elements. *J. Chem*. *Phys*. **1987**, *86*, 866–872.

(8) Bergner, A.; Dolg, M.; Küchle, W.; Stoll, H.; Preuß, H. Ab Initio Energy-Adjusted Pseudopotentials for Elements of Groups 13–17. *Mol. Phys.* **1993**, *80*, 1431–1441.

(9) Grimme, S. Supramolecular Binding Thermodynamics by Dispersion-Corrected Density Functional Theory. *Chem. Eur. J.* **2012**, *18*, 9955–9964.

(10) Luchini, G.; Alegre-Requena, J. V.; Funes-Ardoiz, I.; Paton, R. S. GoodVibes: Automated Thermochemistry for Heterogeneous Computational Chemistry Data. *F1000Res.* **2020**, *9*, 291. *Version 3.0.2.*

(11) Zhao, Y.; Truhlar, D. G. The M06 Suite of Density Functionals for Main Group Thermochemistry, Thermochemical Kinetics, Noncovalent Interactions, Excited States, and Transition Elements: Two New Functionals and Systematic Testing of Four M06-Class Functionals and 12 Other Functionals. *Theor. Chem. Acc.* **2008**, *120*, 215–241.

(12) Marenich, A. V.; Cramer, C. J.; Truhlar, D. G. Universal Solvation Model Based on Solute Electron Density and on a Continuum Model of the Solvent Defined by the Bulk Dielectric Constant and Atomic Surface Tensions. *J. Phys. Chem. B* **2009**, *113*, 6378–6396.

# CHAPTER 3

## NICKEL-CATALYZED 1,2-DIARYLATION OF ALKENYL KETONES: A COMPARATIVE STUDY OF CARBONYL-DIRECTED REACTION SYSTEMS

Adapted with permission from:

Kleinmans, R.; Apolinar, O.; Derosa, J.; Karunananda, M. K.; Li, Z.-Q.; Tran, V. T.; Wisniewski, S. R.; Engle, K. M. *Org*. *Lett*. **2021**, *23*, 5311–5316.

Copyright © 2021 American Chemical Society

## 3.1. INTRODUCTION

The catalytic incorporation of two carbogenic coupling partners across an alkene using a transition metal, also termed conjunctive cross-coupling, has lately been found as a powerful method for the construction of complex molecules.[1] Normally, this family of reactions involve an initial 1,2-migratory insertion step and have typically required conjugated alkene substrates for optimal control of reactivity and selectivity.[2] In an effort to improve this synthetic limitation, our group and others have used directing groups to allow for facile Ni-catalyzed 1,2-dicarbofunctionalization of non-conjugated alkenes.[3] This strategy was initially carried out by using N($sp^2$)-containing directing auxiliaries, which require at minimum two synthetic steps for installation and removal, depreciating from the practicality of the method (Figure 3.1A).[3a–d] Our group previously showed the employment of amide and carboxylate native directing groups in nickel-catalyzed 1,2-diarylation of alkenes (Figure 3.1B).[3e,g] Given the importance of ketone functional groups in synthesis,[4,5] we desired to further extend this regioselective 1,2-diarylation reaction to starting materials containing native ketone functional groups, which may presumably bind the nickel center via an O($sp^2$) atom.[6]

Nevertheless, we were cognizant of two potential challenges: 1) the diminished Lewis basicity of the carbonyl oxygen lone pair compared to amides and carboxylates, which may decrease productive binding to the nickel center in the migratory insertion step, and 2) elevated acidity of the α-protons, which may produce unwanted isomerization of the alkene starting material. In several previous studies, Giri and coworkers have found that pre-furnished ketimines can adequately engage in conjunctive cross-coupling[7a,b] and that the corresponding dicarbofunctionalized products can be

hydrolyzed back to the ketones. However, this method is limited to γ,δ-unsaturated enone starting materials, presumably because of the acidic α-protons that lead to isomerization in the presence of organozinc reagents, highlighting the arduousness of this type of transformation. Thus, herein, we showcase a selective 1,2-diarylation of alkenyl ketones effectuated by discreetly tuned reaction conditions that minimize alkene isomerization side reaction (Scheme 3.1B).

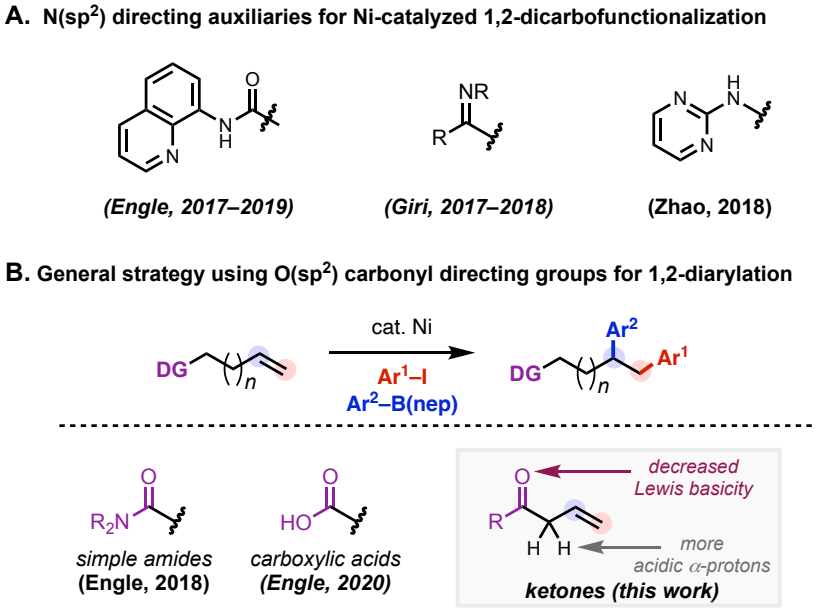


***Figure 3.1.*** Background and synopsis of work.

## 3.2. RESULTS AND DISCUSSION

### 3.2.1. Reaction Optimization

To begin our study, we selected 1-(4-methoxyphenyl)but-3-en-1-one as our standard aryl ketone substrate, with 4-iodotoluene (*p*-Tol–I) and phenylboronic acid neopentyl glycol ester (PhB(nep)) (nep = neopentyl glycolato) as the respective electrophile and nucleophile coupling partners, and $Ni(cod)_2$ as the precatalyst along with dimethyl fumarate (DMFU) ligand (Table 3.1).[8] After substantial optimization and

refining of reaction conditions to reduce isomerization, we were able to arrive at conditions that gave 83% combined yield of the two plausible regioisomers in 10:1 r.r., with the major product having the electrophile incorporated distal to the directing group (entry 1). Such observed regioselectivity is in line with that observed for our laboratory's previous systems. We found the use of NaOMe base as a stock solution to be key for high yields, presumably due to the poor dissolution of solid base in isobutanol solvent (entry 6).[9] Furthermore, under our previously reported reaction conditions for alkenyl amide substrates, which uses solid NaOH, the 1,2-diarylated product(s) could be observed in only 8% yield (entry 2). We found that the absence of $Ni(cod)_2$ precatalyst led to formation of isomerized side product in higher quantities (entry 3), whereas lowering the catalyst loading mainly led to a drastic drop in product yield (entry 11). Surprisingly, the reaction resulted in good yield without an DMFU ligand or with 1,3-bis(2,6-di-isopropylphenyl)imidazolidine-2-ylidene (SIPr) instead of DMFU, but with SIPr lower regioselectivity was obtained (entries 4 and 5). Lowering the coupling partner loading lowered the product yield approximately by half (entry 7). Both phenylboronic acid and the corresponding pinacol ester nucleophiles were found to be low-yielding and in the latter case gave elevated levels of isomerized side product (entries 8 and 9). 4-Bromotoluene electrophile was found to be unreactive upon subjection to the reaction conditions (entry 10). Fascinatingly, $NiBr_2$•glyme precatalyst was a viable Ni(II) source, giving the desired 1,2-diarylated products in 32% combined yield (entry 12). Other nickel precatalysts such as $NiCl_2$, $Ni(acac)_2$, and Ni(cod)(DQ) (DQ = duroquinone) were found to not be effective (entries 13 and 15). The Ni(cod)(DMFU) precatalyst that contains pre-

ligated DMFU ligand furnished the desired products in 75% yield which did not give an edge compared to $Ni(cod)_2$ (entry 14).

***Table 3.1.*** Reaction optimization table.[a]

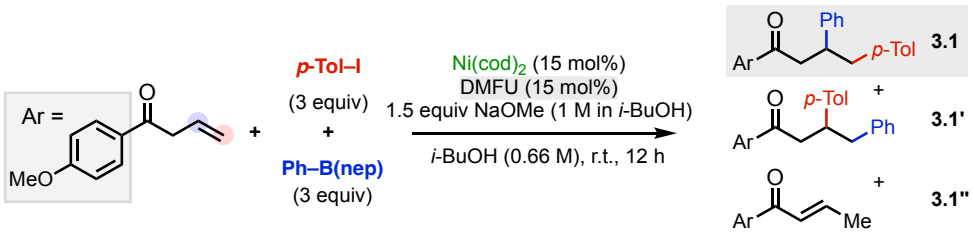


| entry | deviation from standard conditions | %yield[b] | **3.1**:**3.1'** | %yield **3.1''** |
|---|---|---|---|---|
| 1 | none | 83 (77) | 10:1 | 9 |
| 2 | conditions from alkenyl amide diarylation (Ref. 3e)[c] | 8 | -- | -- |
| 3 | no $Ni(cod)_2$ | n.d. | -- | 47 |
| 4 | no Ligand | 79 | 8:1 | -- |
| 5 | SIPr instead of DMFU | 59 | 5:1 | 2 |
| 6 | 1.5 equiv NaOMe (solid) | 63 | 8:1 | -- |
| 7 | 1.5 eq. of PhB(nep) and *p*-Tol–I instead of 3.0 equiv | 40 | 10:1 | 27 |
| 8 | $PhB(OH)_2$ instead of PhB(nep) | 29 | -- | -- |
| 9 | PhB(pin) instead of PhB(nep) | 17 | -- | 31 |
| 10 | *p*-Tol–Br instead of *p*-Tol–I | 8 | -- | 25 |
| 11 | 5 mol% $Ni(cod)_2$ instead of 15 mol% | 43 | 9:1 | 29 |
| 12 | $NiBr_2$•glyme instead of $Ni(cod)_2$ | 32 | 6:1 | 35 |
| 13 | $NiCl_2$ or $Ni(acac)_2$ instead of $Ni(cod)_2$ | n.d. | -- | -- |
| 14 | Ni(cod)(DMFU) instead of $Ni(cod)_2$ | 75 | 10:1 | 11 |
| 15 | Ni(cod)(DQ) instead of $Ni(cod)_2$ | n.d. | -- | 42 |

[a]Reactions were performed on a 0.1 mmol scale. Percentages represent $^1$H NMR yields using $CH_2Br_2$ as internal standard; n.d. = not detected. Percentages in parentheses represent isolated yields. Combined yield of **3.1** and **3.1'**. [c]Reaction conditions: 15 mol% $Ni(cod)_2$, 15 mol% DMFU, 1.5 equiv ArI, 1.5 equiv ArB(nep), 2 equiv NaOH, 0.1 M *i*-BuOH, at r.t.

### 3.2.2. Comparison of Other Carbonyl-Directed Reaction Systems

At this phase of the work, we decided to compare the optimized conditions in each of our previously reported carbonyl-directed 1,2-diarylation reactions. We were interested to further our knowledge of the impact of subtle changes to reaction conditions across different substrate classes (Table 3.2). In general, $Ni(cod)_2$ precatalyst and

alcoholic solvents were vital for generating high yields. Additionally, the predominant reactivity of ArB(nep) nucleophiles is a shared feature, emphasizing its unique role in nickel catalysis.[10] Testing the optimized reaction conditions for several 1,2-diarylation reactions upon alkenyl amide, carboxylate, and ketone substrates, showed that choice of ligand, base, alcohol solvent, and temperature, are important variables in successfully extending this methodology to distinct carbonyl-based substrate classes. For instance, the alkenyl amide substrate needs DMFU as a ligand to boost the product yield, whereas DMFU has only a minute effect with ketone substrates; ancillary ligand had no positive impact in the carboxylate system. A plausible explanation for the modest effect of DMFU in the alkenyl ketone system is that the isomerized starting material may act as an electron-deficient olefin ligand, making the DMFU ligand somewhat redundant. This notion is supported by DFT (Scheme 3.S10) and by the observation that γ,δ-unsaturated ketone substrate (**3.52** → **3.43**), under the optimized reaction conditions, is very low-yielding without the use of DMFU (9% yield, Scheme 3.S8). As mentioned in the previous section, less Lewis basic alkenyl ketones benefited from the employment of a NaOMe stock solution instead of mere solid NaOMe. It is worth noting that both the alkenyl amide and ketone substrates work well with *i*-BuOH solvent, whereas *s*-BuOH is crucial to the alkenyl carboxylate substrate. Curiously, alkenyl carboxylates are not efficacious substrates at room temperature, which is optimal for other classes, perhaps because of the higher temperatures needed to diminish inhibitory carboxylate binding to the nickel metal center. Altogether, these findings portray the subtleties of reaction optimization across these carbonyl-based systems, which gives end users insights as to what variables to maneuver.

***Table 3.2.*** Comparison of 1,2-diarylation conditions.[a]

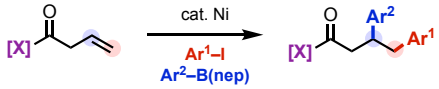


| *1,2-diarylation conditions* | **A** (Ref. 3e) | **B** (Ref. 3g) | **C** (as above) |
|---|---|---|---|
| **Ligand:** | 15 mol% DMFU | No Ligand | 15 mol% DMFU |
| **Base:** | 2.0 equiv NaOH | 2.0 equiv NaOH | 1.5 equiv NaOMe |
| **Solvent:** | *i*-BuOH | *s*-BuOH | *i*-BuOH |
| **Temperature:** | r.t. | 50 °C | r.t. |
| **Concentration:** | 0.1 M | 0.1 M | 0.66 M |
| **Coupling Partners:** | 1.5 equiv | 2.0 equiv | 3.0 equiv |
| [X] = 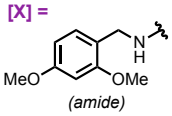 *(amide)* | 92%[b] | 29% | 79% |
|  *(carboxylic acid)* | 15%[c] | 81%[c] | <10% |
| 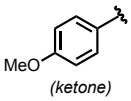 *(ketone)* | <10% | <10% | 83% |
| ***color legend*** = | <20% | 20–60% | 60–99% |

[a]Percentages represent $^1$H NMR yields using $CH_2Br_2$ as internal standard. [b]Yield taken from Ref 3e. [c]Yield taken from Ref 3g.

### 3.2.3. Substrate Scope

With optimal reaction conditions in hand, we turned to the electrophile scope using PhB(nep) as the model nucleophilic coupling partner (Table 3.3). It is worth noting that minimal isomerization is observed for most examples (≤10%), and there is no clear relationship between the amount of isomerized side product and the yield of the desired 1,2-diarylated product. Aryl iodide electrophiles with electron-donating substituents on the *para*- and *meta*-positions gave the desired 1,2-diarylated products in good to excellent yields with moderate to excellent regioselectivity (**3.1**–**3.5**, **3.9**, **3.10**, **3.12**, **3.13**, **3.15**). Electrophiles with substitution on the *ortho*-position afforded the desired product in good to excellent yields with excellent regioselectivity (**3.11**, **3.16**). Electron-withdrawing substituents on the *para*- and *meta*-positions of aryl iodides resulted in diminished

reactivity giving the desired products in moderate yields with excellent regioselectivity (**3.6**, **3.7**, **3.12, 3.14**). Particularly, aryl iodides containing –NHAc and –Ac groups were tolerated, allowing for potential downstream synthetic modification (**3.8**, **3.14**). In general, for sterically similar electrophiles, the regioisomeric ratio tends to be lowest for electron-rich aryl iodides and highest for electron-deficient aryl iodides. We found that various heteroaryl iodide electrophile coupling partners were incompetent under the reaction conditions (Table 3.S2).

***Table 3.3.*** Electrophile scope.[a]

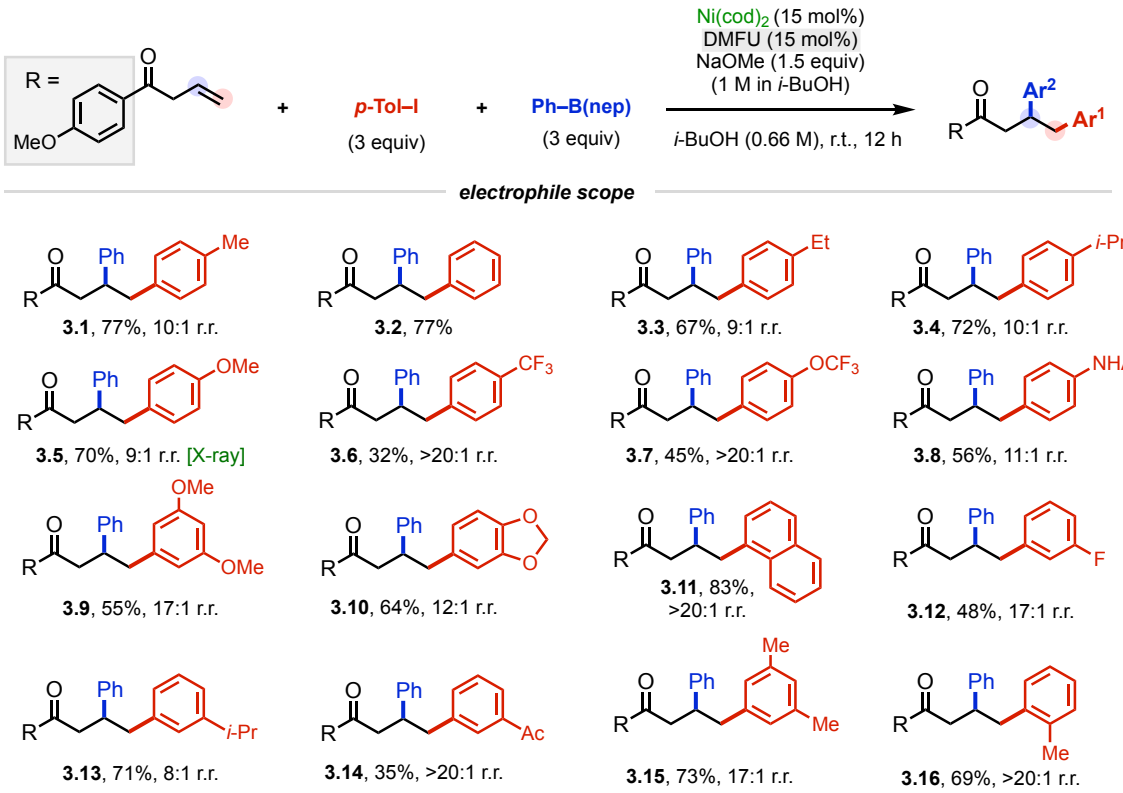


[a]Reactions performed on a 0.1 mmol scale. Percentages represent combined isolated yields regioisomers.

Subsequently, we explored the nucleophile scope of the reaction, using iodobenzene as the model electrophile coupling partner (Table 3.4). Typically, a wide array of electron-rich and electron-deficient ArylB(nep) nucleophiles reacted well under the optimized conditions, affording the desired 1,2-diarylated products in moderate to excellent yields and regioselectivities (**3.17**–**3.26**). Specifically, ArylB(nep) nucleophiles containing tethered alcohols, –Cl, and –Ac groups were compatible in the reaction giving desired products in moderate to good yields with moderate to excellent regioselectivity (**3.19**, **3.21**, **3.25**). We also found that heteroaryl nucleophiles were not tolerated in the optimized reaction conditions (Table 3.S3).

***Table 3.4.*** Nucleophile scope.[a]

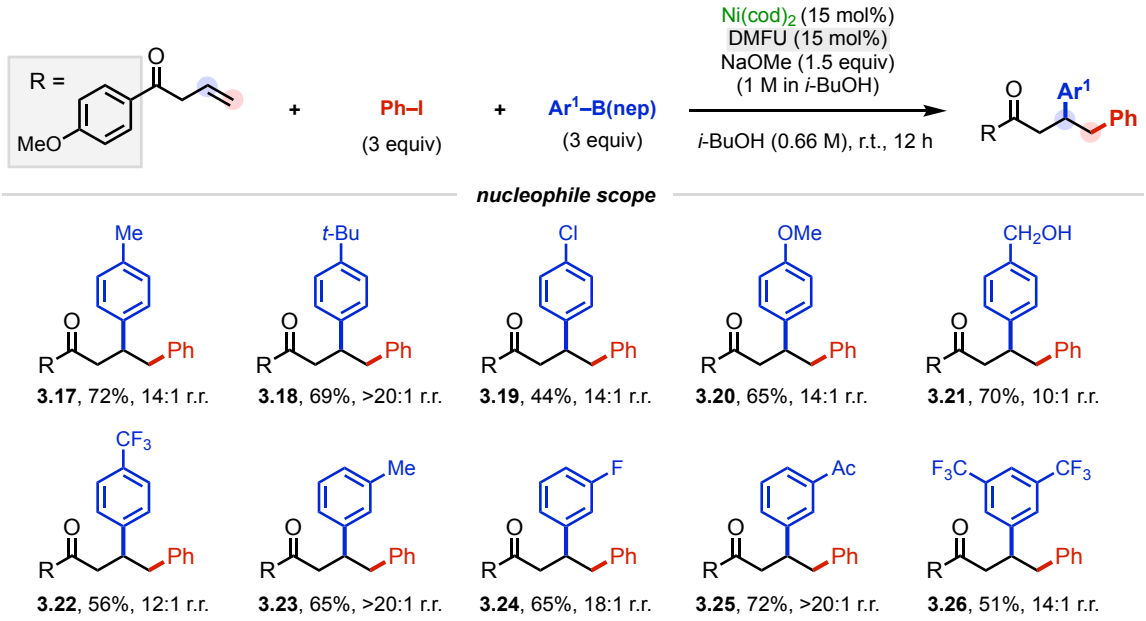


[a]Reactions performed on a 0.1 mmol scale. Percentages represent combined isolated yields of regioisomers. Reactions were performed in *i*-BuOH (0.5 M).

Then, we examined the ketone and alkene scope along with limitations of this method by testing other alkenyl ketones substrates (Table 3.5). Considering the facile and

modular synthesis of allyl ketones via a Barbier allylation/oxidation sequence, we thought that this method could be used as a powerful tool for rapid construction of 1,2-diarylated ketones. To our delight, across several different alkenyl ketones, moderate to excellent yields with moderate to good regioselectivity were forged (**3.27**–**3.42**). Aryl ketones with electron-donating substituents were demonstrated to be competent directing groups, while those with electron-withdrawing substituents led to lower yields (**3.27**–**3.36**) with the exception of product **3.31**. Heteroaryl ketones were found to be good contenders upon reaction (**3.37** and **3.38**), and a conjugated ketone was also viable showcasing excellent chemoselectivity (**3.39**). Finally, alkyl ketone substrates were suitable in the reaction giving the desired 1,2-diarylated products in moderate to good yields with good regioselectivity (**3.40**–**3.42**). We then tested the scope with respect to the alkenyl chain of the ketone substrate. Gratifyingly, both γ,δ-unsaturated enone and α-methyl ketone were competent substrates in the optimized 1,2-diarylation reaction (**3.43**, **3.44**). It is important to note that a δ,ε-unsaturated enone, a γ,δ-unsaturated enal, and a 1,2-disubstituted alkenyl ketone were found to be ineffective substrates (Table 3.S4). Lastly, aryl ketones with an electron-withdrawing group on the *para*-position, namely *p*-Cl and *p*-$CF_3$, gave uncharacterized side products, thus complicating separation, but $^1$H NMR yields are shown to exemplify reactivity trends across the entire electronic series.

***Table 3.5.*** Ketone and alkene scope.[a]

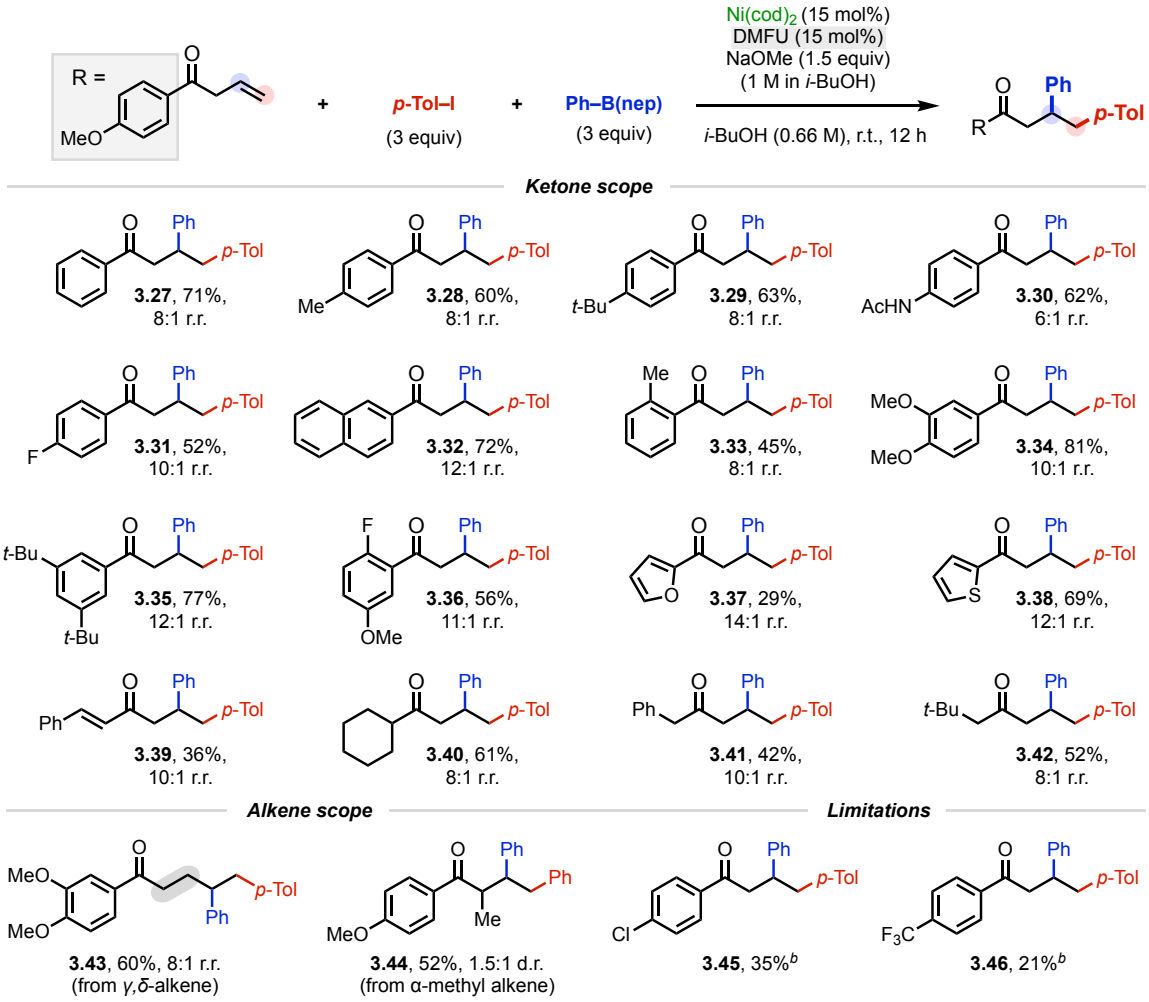


[a]Reactions performed on a 0.1 mmol scale. Percentages represent combined isolated yields of regioisomers. [b]Percentages represent $^1$H NMR yields using $CH_2Br_2$ as internal standard.

### 3.2.4. Product Diversification

To exemplify the usefulness of this method, we treated representative ketone product **3.5** to an array of diversification reactions (Scheme 3.1). Conventional functional group interconversions were conducted to give an assortment of synthetically useful products (**3.47–3.51**). A classical Baeyer–Villiger oxidation reaction afforded the corresponding aryl ester in good yield (**3.47**). On the other hand, ketone **3.5** could be

transformed into an amide via a Beckmann rearrangement in a high yield (**3.48**) or to an alkene via a Wittig olefination (**3.49**). The carbonyl group of ketone **3.5** could also be completely removed with $LiAlH_4$ and $AlCl_3$ reducing conditions to give **3.50** in good yield; whilst partial reduction of the ketone to the secondary alcohol was possible with $NaBH_4$ in moderate yield, but with no diastereoselectivity (**3.51**).

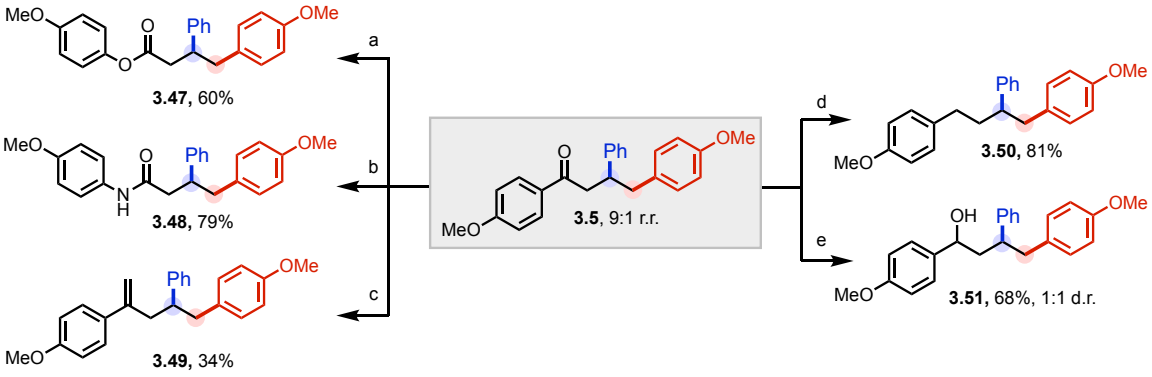


***Scheme 3.1.*** Diversification of a representative product. (a) *m*CPBA, TFA, anhydrous DCM, r.t. (b) $H_2NOH$•HCl, TFA, 70 ˚C. (c) $Ph_3PCH_2Br$, *n*-BuLi, THF, 70 ˚C. (d) $LiAlH_4$, $AlCl_3$, $Et_2O$/DCM, r.t. (e) $NaBH_4$, THF, reflux.

### 3.2.5. Mechanistic Experiments

To shed light into the mechanistic features of this ketone-directed 1,2-diarylation of unactivated alkenes, we focused on the binding mode of the ketone directing group to the nickel metal center. Under basic conditions, the alkenyl ketone could in essence bind to the catalyst via the oxygen atom in either its neutral ketone (L-type) or anionic enolate (X-type) forms (Scheme 3.2A).[7c] To test this, we initially ran control experiments. Since, under the reaction conditions, we observed isomerization of the alkenyl ketones to form α,β-unsaturated enones (such as **3.1''**), we suspected whether these side products were productive intermediates. In a predominant enolate mechanism, α,β-unsaturated enones

may still participate in β,γ-diarylation since the dienolate could form under the basic conditions. Contrarily, in the neutral ketone mechanism, the α,β-unsaturated enones would not be competent substrates. When we treated independently synthesized **3.1''** to the standard conditions, only unreacted α,β-unsaturated enone was observed (Scheme 3.2B). We then examined an alkenyl ketone (**3.52**), which possesses a *gem*-dimethyl group in lieu of the enolizable α-protons, and, under optimized reaction conditions we isolated 31% yield of desired 1,2-diarylated product **3.53** (Scheme 3.2C). We ascribe the low yield in this example to steric bulk provided by the *gem*-dimethyl group. Using $d_4$-methanol under otherwise standard conditions, we found that 19% deuterium incorporation at the α-position occurred in the 1,2-diarylated product. This experiment is inconsistent with an enolate pathway since ≥50% deuterium incorporation would be expected (Scheme 3.S11).

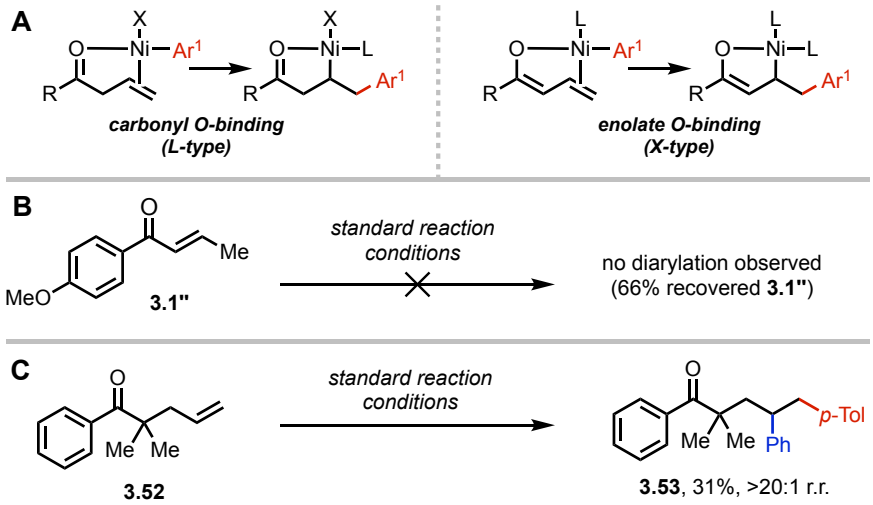


***Scheme 3.2.*** Mechanistic experiments.

Based on previous reports[3e] and Hammett data, the migratory insertion step was seen as a likely contender for the rate determining step. Thus, to further shed light into

the predominant directing group coordination mode, we resorted to density functional theory (DFT) and calculated probable migratory insertion transitions states (Scheme 3.3). This investigation demonstrated that the neutral ketone form (**TS1**, $\Delta G^{\ddagger}$ = 14.9 kcal/mol) is lower in energy when compared to both the neutral (**TS2**, $\Delta G^{\ddagger}$ = 18.1 kcal/mol) and anionic enolate forms (**TS3**, $\Delta G^{\ddagger}$ = 16.9 kcal/mol). It is important to note that both **TS4** and **TS5** with L = DMFU and L = COD, respectively, were computed to be higher in energy than **TS2** (Scheme 3.S9). Altogether, both experimental and computational data are in line with a mechanism with the neutral carbonyl directing group (L-type) as the preferred pathway.

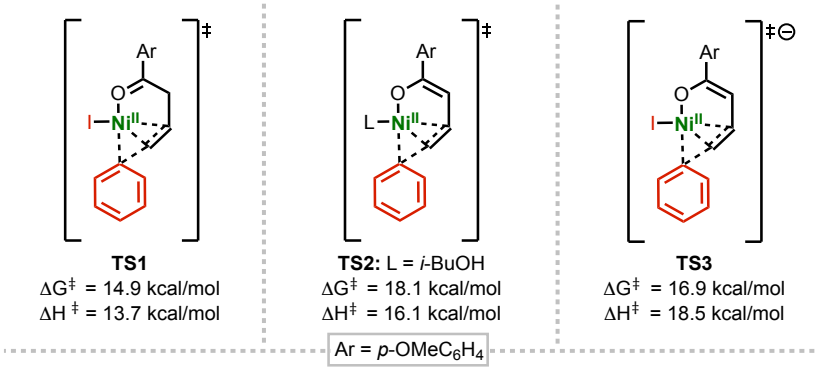


***Scheme 3.3.*** DFT calculations upon several migratory insertion transition states.

Lastly, we explored the effects of changing the electronic properties of the aryl iodide electrophile, arylboronate nucleophile, and aryl ketone components on the reaction rate (Table 3.6). Mirroring our previous observations using alkenyl amides,[3e] we found a negligible impact of the electronic properties of arylB(nep) on the initial rate, whereas electron-neutral and -rich aryl iodides electrophiles reacted faster than electron-poor aryl iodides ($\rho$ = –1.3). This trend aims to an elementary step as the rate determining step where the catalyst and electrophile aryl group are both involved; however, such finding is

the opposite trend that would be expected if oxidative addition were rate determining. Therefore, the data are in line with migratory insertion as the rate determining step. With regards to the aryl ketone electronic properties, we found a faster rate for electron-deficient aryl ketones even though these substrates are low-yielding ($\rho$ = 0.19). A plausible rationale for this dichotomy is that electron-poor ketones lead to off-cycle processes (e.g., isomerization) more readily, despite being faster for the productive catalytic reaction. On the catalytic cycle, bolstered reaction rate with more electron-poor carbonyl groups could reflect elevated electronic bias of the alkene *via* inductive effects as shown in the $^{13}C$ resonances of the alkenyl carbon atoms of various substrates (Table 3.S5). Another explanation that cannot be ruled out at this time is that the ketone directing group dissociates during migratory insertion and plausibly recoordinates to prevent β-H elimination allowing the 1,2-diarylation reaction to occur.

***Table 3.6.*** Initial rate trends.

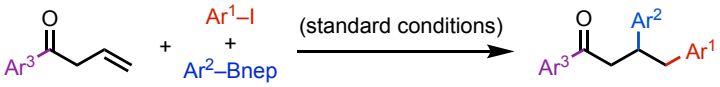


| | | *p*-OMe | *p*-Me | *p*-H | *p*-Cl | *p*-$CF_3$ |
|---|---|---|---|---|---|---|
| σ value | | –0.27 | –0.17 | 0.00 | 0.23 | 0.54 |
| **$Ar^1$–I** | ($v_{rel}$) | 3.2 | 2.5 | 1.0 | 0.4 | 0.3 |
| with Ph–B(nep) + *p*-OMePh‡ | | | | | | |
| **$Ar^2$–B(nep)** | ($v_{rel}$) | 0.7 | 1.6 | 1.0 | 1.0 | 0.8 |
| with Ph–I + *p*-OMePh‡ | | | | | | |
| **$Ar^3$‡** | ($v_{rel}$) | 0.8 | 0.9 | 1.0 | 1.1 | 1.2 |
| with Ph–I + Ph–B(nep) | | | | | | |

## 3.3. CONCLUSION

In summary, we have shown that ketones can be directly used to facilitate nickel-catalyzed 1,2-diarylation of unactivated alkenes.[11] The generated products can be further exploited using classical synthetic strategies to afford an array of valuable building blocks. Mechanistic investigations support a carbonyl binding mode of the ketone (L-type) instead of an enolate binding mode (X-type), while Hammett studies point to migratory insertion as the rate determining step. We envision that the addition of ketones as native directing groups to the growing toolkit of 1,2-dicarbofunctionalization reactions will aid the versatility of this class of transformations in the long run.

## 3.4. EXPERIMENTAL

### 3.4.1. General Information

Unless otherwise noted, all materials were used as received from commercial sources without further purification. All aryl iodides, aryl boronic acids, and solvents were purchased from Aldrich, Alfa Aesar, Oakwood, Combi-Blocks, and Lancaster. $Ni(cod)_2$ was purchased from Strem. In air- or moisture-sensitive reactions, anhydrous solvents from MilliporeSigma or from a Grubbs-type solvent purification system were used.

### 3.4.2. Arylboronic Acid Neopentylglycol Ester Synthesis

***Table 3.S1.*** Aryl boronic acid neopentylglycol esters **3.S1–3.S11**.

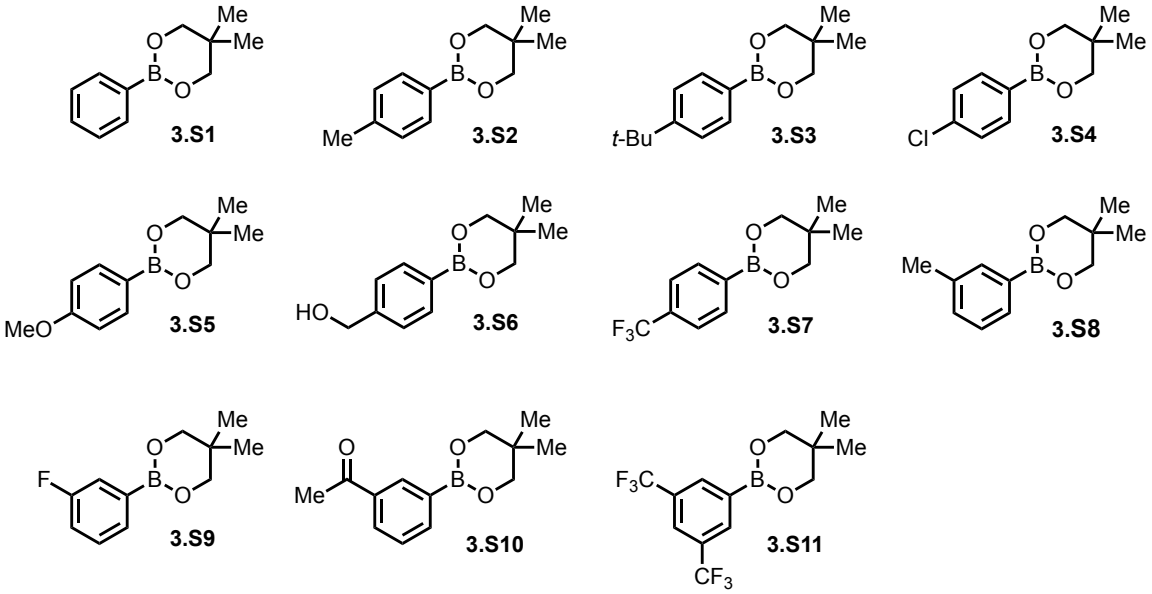


Compounds **3.S1–3.S11** were prepared according to literature procedures.[12,13]

### 3.4.3. Alkenyl Ketone Substrate Synthesis

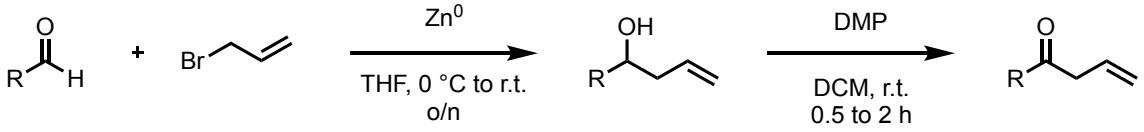


***Scheme 3.S2.*** Synthesis of alkenyl ketone substrates using a classical Barbier allylation with subsequent Dess–Martin oxidation.[14,15]

**General Procedure for Ketone Synthesis:**

The homoallylic alcohols were prepared according to a literature procedure.[14] The products were stored in a refrigerator at 0 °C to prevent isomerization.[15] The reported yields correspond to the yields of the oxidation step from the crude homoallylic alcohols.

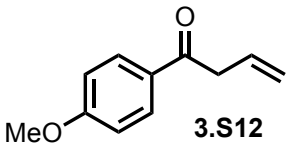


3.S12

**1-(4-Methoxyphenyl)but-3-en-1-one (3.S12)**: Purification by silica gel column chromatography (4% EtOAc/hexane) gave the product as a white solid (1.21 g, 6.88 mmol, 46% yield). **$^1$H NMR** (400 MHz, $CDCl_3$) $\delta$ 7.95 (d, $J$ = 8.7 Hz, 2H), 6.94 (d, $J$ = 8.7 Hz, 2H), 6.08 (ddt, $J$ = 17.0, 10.5, 6.7 Hz, 1H), 5.28–5.14 (m, 2H), 3.87 (s, 3H), 3.71 (d, $J$ = 7.7 Hz, 2H); **$^{13}$C NMR** (126 MHz, $CDCl_3$) δ 196.6, 163.6, 131.5, 130.6, 129.6, 118. 4, 113.8, 55.5, 43.2; **HRMS** (ESI-TOF) Calc'd for $C_{11}H_{13}O_2^+$ $[M+H]^+$ 177.0916, found 177.0916.

### 3.4.4. General Procedure for Nickel-Catalyzed 1,2-Diarylation of Alkenyl Ketones

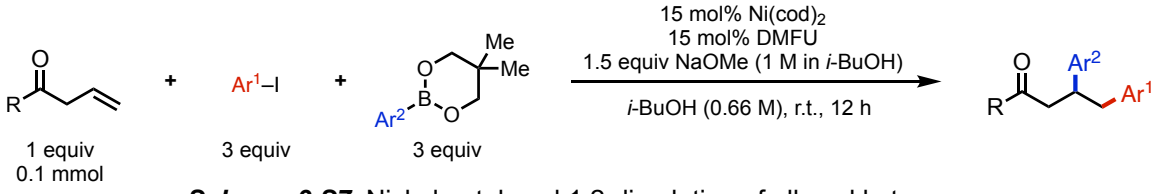


***Scheme 3.S7.*** Nickel-catalyzed 1,2-diarylation of alkenyl ketones.

**General 1,2-Diarylation Procedure:** To an oven-dried 8-mL dram vial equipped with a Teflon-coated magnetic stir bar were added the alkene substrate (0.1 mmol, 1.0 equiv), the appropriate aryl iodide electrophile (0.3 mmol, 3.0 equiv), the appropriate aryl boronic acid neopentylglycol ester (0.3 mmol, 3.0 equiv), and dimethyl fumarate (2.2 mg, 0.015 mmol, 15 mol%). The vial was sealed with a septum cap, which was pierced by a 20-gauge needle and introduced into an argon-filled glovebox antechamber. Once transferred inside the glovebox, $Ni(cod)_2$ (4.2 mg, 0.015 mmol, 15 mol%) was added followed directly by an aliquot of a stock solution of NaOMe in anhydrous *iso*-butanol (0.15 mL, 1.0 M, 1.5 equiv). The vial was sealed with a new screw-top septum cap,

removed from the glovebox, and stirred at room temperature for 12 h. After this time, the reaction mixture was diluted with EtOAc (4 mL), washed with sat. aq. $NaHCO_3$ (10 mL). The organic layer was separated, and the aqueous layer was extracted with EtOAc (2 × 4 mL). The combined organic layers were filtered through Celite, and the filtrate was concentrated *in vacuo* to leave a yellow residue, which afforded the product after preparative thin-layer chromatography (PTLC).

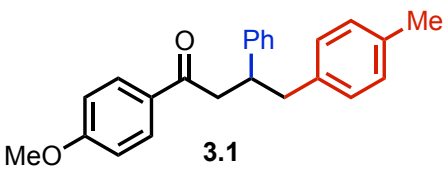

**3.1**

**1-(4-Methoxyphenyl)-3-phenyl-4-(*p*-tolyl)butan-1-one (3.1):** Purification by PTLC (1st run: 5% EtOAc in hexane, 2nd run: 15% EtOAc in hexane) gave the product as a colorless solid (26.4 mg, 77% yield, 10:1 r.r.). **$^1$H NMR** (600 MHz, $CDCl_3$) $\delta$ 7.85–7.81 (m, 2H), 7.25–7.21 (m, 2H), 7.19–7.16 (m, 2H), 7.16–7.13 (m, 1H), 7.01 (d, $J$ = 7.8 Hz, 2H), 6.96 (d, $J$ = 8.0 Hz, 2H), 6.90–6.85 (m, 2H), 3.85 (s, 3H), 3.63 (p, $J$ = 7.3 Hz, 1H), 3.29–3.18 (m, 2H), 2.94 (dq, $J$ = 13.0, 6.6 Hz, 2H), 2.27 (s, 3H); **$^{13}$C NMR** (101 MHz, $CDCl_3$) $\delta$ 197.5, 163.4, 144.5, 136.8, 135.5, 130.4, 130.4, 129.2, 128.9, 128.4, 127.8, 126.4, 113.7, 55.5, 43.9, 43.3, 42.6, 21.1; **HRMS** (ESI-TOF) Calc'd for $C_{24}H_{25}O_2^+$ $[M+H]^+$ 345.1855, found 345.1860.

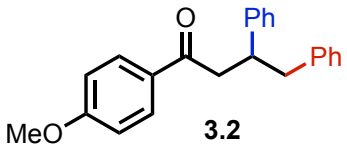

**3.2**

**1-(4-Methoxyphenyl)-3,4-diphenylbutan-1-one (3.2):** Purification by PTLC (2 runs in 100% toluene) gave the product as a white solid (25.4 mg, 77% yield). **$^1$H NMR** (400 MHz, $CDCl_3$) $\delta$ 7.83 (d, $J$ = 8.8 Hz, 2H), 7.26–7.10 (m, 8H), 7.06 (d, $J$ = 7.0 Hz, 2H), 6.87 (d, $J$ = 8.8 Hz, 2H), 3.83 (s, 3H), 3.65 (p, $J$ = 7.1 Hz, 1H), 3.33–3.17 (m, 2H),

3.04–2.90 (m, 2H); **$^{13}$C NMR** (101 MHz, $CDCl_3$) $\delta$ 197.5, 163.5, 144.4, 140.0, 130.4, 130.4, 129.4, 128.4, 128.3, 127.8, 126.5, 126.2, 113.8, 55.6, 43.9, 43.3, 43.1; **HRMS** (ESI-TOF) Calc'd for $C_{23}H_{23}O_2^+$ $[M+H]^+$ 331.1698, found 331.1685.

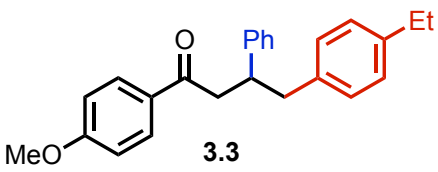

**3.3**

**4-(4-Ethylphenyl)-1-(4-methoxyphenyl)-3-phenylbutan-1-one** (**3.3**): Purification by PTLC (3 runs 5% EtOAc/hexane) gave the product as a colorless solid (24.0 mg, 67% yield, 9:1 r.r.). **$^1$H NMR** (600 MHz, $CDCl_3$) $\delta$ 7.83–7.80 (m, 2H), 7.24 (t, $J$ = 7.6 Hz, 2H), 7.21–7.17 (m, 2H), 7.17–7.13 (m, 1H), 7.04 (d, $J$ = 8.0 Hz, 2H), 6.99 (d, $J$ = 8.1 Hz, 2H), 6.89–6.85 (m, 2H), 3.85 (s, 3H), 3.64 (p, $J$ = 7.3 Hz, 1H), 3.26 (dd, $J$ = 16.4, 7.7 Hz, 1H), 3.21 (dd, $J$ = 16.4, 6.3 Hz, 1H), 2.94 (d, $J$ = 7.4 Hz, 2H), 2.58 (q, $J$ = 7.6 Hz, 2H), 1.19 (t, $J$ = 7.6 Hz, 3H); **$^{13}$C NMR** (101 MHz, $CDCl_3$) $\delta$ 197.6, 163.4, 144.6, 142.0, 137.2, 130.5, 130.4, 129.3, 128.4, 127.8, 127.8, 126.4, 113.7, 55.6, 43.9, 43.3, 42.7, 28.6, 15.7; **HRMS** (ESI-TOF) Calc'd for $C_{25}H_{27}O_2^+$ $[M+H]^+$ 359.2011, found 359.2019.

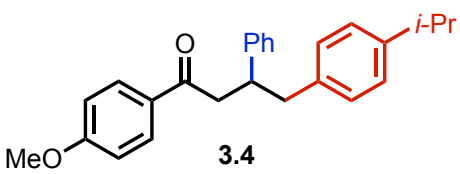

**3.4**

**4-(4-*iso*-Propylphenyl)-1-(4-methoxyphenyl)-3-phenylbutan-1-one** (**3.4**): Purification by PTLC (3 runs 5% EtOAc/hexane) gave the product as a colorless solid (27.0 mg, 72% yield, 10:1 r.r.). **$^1$H NMR** (600 MHz, $CDCl_3$) $\delta$ 7.83–7.79 (m, 2H), 7.24 (dd, $J$ = 8.0, 7.0 Hz, 2H), 7.21–7.19 (m, 2H), 7.15 (ddt, $J$ = 7.2, 5.2, 1.5 Hz, 1H), 7.07 (d, $J$ = 8.0 Hz, 2H), 7.01 (d, $J$ = 8.1 Hz, 2H), 6.88–6.85 (m, 2H), 3.84 (s, 3H), 3.64 (p, $J$ = 7.4 Hz, 1H), 3.29–3.18 (m, 2H), 2.98–2.90 (m, 2H), 2.84 (hept, $J$ = 6.8 Hz,

1H), 1.21 (dd, $J$ = 6.9, 0.8 Hz, 6H); **$^{13}$C NMR** (101 MHz, $CDCl_3$) $\delta$ 197.6, 163.4, 146.7, 144.7, 137.3, 130.5, 130.4, 129.3, 128.4, 127.8, 126.4, 126.3, 113.7, 55.6, 43.9, 43.3, 42.7, 33.8, 24.2; **HRMS** (ESI-TOF) Calc'd for $C_{26}H_{29}O_2^+$ $[M+H]^+$ 373.2168, found 373.2175.

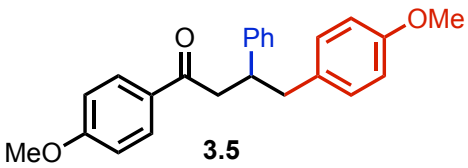

**3.5**

**1,4-Bis(4-methoxyphenyl)-3-phenylbutan-1-one (3.5):** Purification by PTLC (5% EtOAc/hexane) gave the product as a colorless solid (25.2 mg, 70% yield, 9:1 r.r.). **$^1$H NMR** (600 MHz, $CDCl_3$) $\delta$ 7.85–7.82 (m, 2H), 7.23 (dd, $J$ = 8.1, 7.0 Hz, 2H), 7.18–7.14 (m, 3H), 6.98–6.95 (m, 2H), 6.89–6.86 (m, 2H), 6.75–6.72 (m, 2H), 3.85 (s, 3H), 3.75 (s, 3H), 3.61 (p, $J$ = 7.1 Hz, 1H), 3.28–3.19 (m, 2H), 2.96–2.86 (m, 2H); **$^{13}$C NMR** (126 MHz, $CDCl_3$) $\delta$ 197.6, 163.5, 158.0, 144.5, 132.1, 130.5, 130.4, 130.3, 128.4, 127.8, 126.4, 113.7, 113.7, 55.6, 55.3, 43.9, 43.5, 42.2; **HRMS** (ESI-TOF) Calc'd for $C_{24}H_{25}O_3^+$ $[M+H]^+$ 361.1804, found 361.1810; **X-ray** (single-crystal) Colorless needle crystals of X-ray diffraction quality were obtained by slow evaporation of a saturated solution of **3.5** in $Et_2O$.[16]

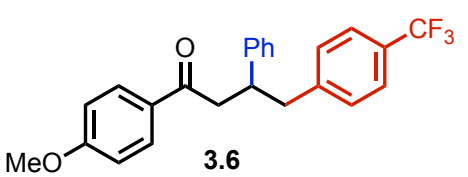

**3.6**

**1-(4-Methoxyphenyl)-3-phenyl-4-(4-(trifluoromethyl)phenyl) butan-1-one (3.6):** Purification by sequential PTLCs (plate 1: 1$^{st}$ run 15% EtOAc/hexane, 2$^{nd}$ run 5% EtOAc/hexane; plate 2: 100% toluene) gave the product as a colorless solid (12.7 mg, 32% yield, >20:1 r.r.). **$^1$H NMR** (600 MHz, $CDCl_3$) $\delta$ 7.89–7.85 (m, 2H), 7.42 (d, $J$ = 7.9 Hz, 2H), 7.26–7.22 (m, 2H), 7.18–7.11 (m, 5H), 6.92–6.89

(m, 2H), 3.86 (s, 3H), 3.66 (dt, $J$ = 14.3, 6.8 Hz, 1H), 3.33–3.22 (m, 2H), 3.11 (dd, $J$ = 13.5, 6.0 Hz, 1H), 2.95 (dd, $J$ = 13.5, 8.7 Hz, 1H); **$^{13}$C NMR** (151 MHz, $CDCl_3$) δ 197.1, 163.5, 144.1 (q, $J$ = 1.7 Hz), 143.6, 130.3, 130.2, 129.6, 128.5, 128.1 (d, $J$ = 26.5 Hz), 127.7, 126.6, 125.0 (q, $J$ = 3.8 Hz), 124.3 (d, $J$ = 271.5 Hz), 113.7, 55.5, 44.0, 42.9, 42.5; **$^{19}$F NMR** (376 MHz, $CDCl_3$) $\delta$ −62.6; **HRMS** (ESI-TOF) Calc'd for $C_{24}H_{22}F_3O_2^+$ $[M+H]^+$ 399.1572, found 399.1577.

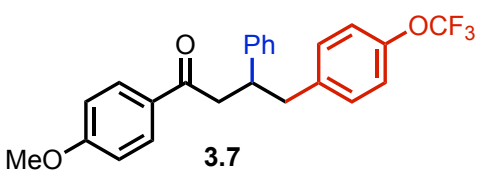

**3.7**

**1-(4-Methoxyphenyl)-3-phenyl-4-(4-(trifluoromethoxy)phenyl) butan-1-one (3.7):** Purification by sequential PTLCs (plate 1: 1$^{st}$ run 15% EtOAc/hexane, 2$^{nd}$ run 5% EtOAc/hexane; plate 2: 100% toluene) gave the product as a colorless solid (18.7 mg, 45% yield, >20:1 r.r.). **$^{1}$H NMR** (600 MHz, $CDCl_3$) $\delta$ 7.88–7.82 (m, 2H), 7.24 (dd, $J$ = 8.2, 6.9 Hz, 2H), 7.18–7.13 (m, 3H), 7.05–7.00 (m, 4H), 6.91–6.88 (m, 2H), 3.86 (s, 3H), 3.65–3.59 (m, 1H), 3.32–3.21 (m, 2H), 3.04 (dd, $J$ = 13.6, 6.3 Hz, 1H), 2.90 (dd, $J$ = 13.6, 8.4 Hz, 1H); **$^{13}$C NMR** (150 MHz, $CDCl_3$) $\delta$ 197.3, 163.6, 147.7 (q, $J$ = 1.6 Hz), 143.9, 138.8, 130.6, 130.4, 130.3, 128.6, 127.8, 126.7, 120.7, 120.6 (q, $J$ = 256.6 Hz), 113.8, 55.6, 44.0, 43.2, 42.2; **$^{19}$F NMR** (376 MHz, $CDCl_3$) $\delta$ −58.1; **HRMS** (ESI-TOF) Calc'd for $C_{24}H_{22}F_3O_3^+$ $[M+H]^+$ 415.1521, found 415.1512.

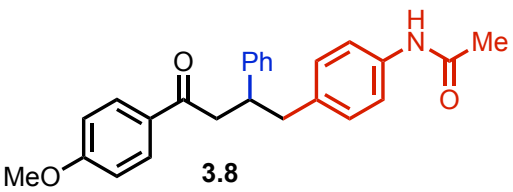

**3.8**

***N*-(4-(4-(4-Methoxyphenyl)-4-oxo-2-phenylbutyl)phenyl) acetamide (3.8):** Purification by PTLC (5 runs 40%

EtOAc/hexane) gave the product as a colorless solid (21.9 mg, 56% yield, 11:1 r.r.). **$^1$H NMR** (600 MHz, $CDCl_3$) $\delta$ 7.84 (d, $J$ = 8.9 Hz, 2H), 7.32 (d, $J$ = 8.4 Hz, 2H), 7.22 (dd, $J$ = 8.3, 6.9 Hz, 2H), 7.15 (dd, $J$ = 7.7, 1.0 Hz, 3H), 7.06 (d, $J$ = 2.9 Hz, 1H), 7.00 (d, $J$ = 8.4 Hz, 2H), 6.90–6.86 (m, 2H), 3.85 (s, 3H), 3.62 (p, $J$ = 7.1 Hz, 1H), 3.24 (qd, $J$ = 16.5, 7.1 Hz, 2H), 2.97 (dd, $J$ = 13.6, 6.7 Hz, 1H), 2.89 (dd, $J$ = 13.6, 8.0 Hz, 1H), 2.14 (s, 3H); **$^{13}$C NMR** (101 MHz, $CDCl_3$) $\delta$ 197.5, 168.2, 163.4, 144.1, 136.0, 135.9, 130.3, 130.2, 129.8, 128.4, 127.7, 126.4, 119.6, 113.7, 55.5, 43.8, 43.2, 42.3, 24.6; **HRMS** (ESI-TOF) Calc'd for $C_{25}H_{26}NO_3^+$ $[M+H]^+$ 388.1913, found 388.1911.

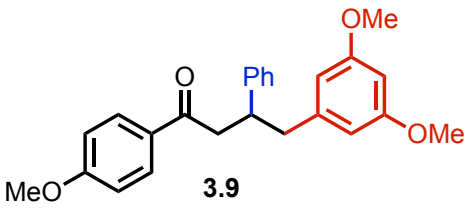

**3.9**

**4-(3,5-Dimethoxyphenyl)-1-(4-methoxyphenyl)-3-phenylbutan-1-one (3.9):** Purification by PTLC (3 runs 10% EtOAc/hexane) gave the product as a white foam (21.5 mg, 55% yield, 17:1 r.r.). **$^1$H NMR** (600 MHz, $CDCl_3$) δ 7.86–7.82 (m, 2H), 7.24 (dd, $J$ = 7.9, 7.0 Hz, 2H), 7.20–7.18 (m, 2H), 7.17–7.13 (m, 1H), 6.90–6.86 (m, 2H), 6.25 (t, $J$ = 2.3 Hz, 1H), 6.21 (d, $J$ = 2.3 Hz, 2H), 3.85 (s, 3H), 3.68 (s, 6H), 3.65 (p, $J$ = 7.2 Hz, 1H), 3.25 (qd, $J$ = 16.5, 7.0 Hz, 2H), 2.96–2.87 (m, 2H); **$^{13}$C NMR** (101 MHz, $CDCl_3$) $\delta$ 197.5, 163.5, 160.6, 144.4, 142.3, 130.4, 128.5, 127.8, 126.5, 113.8, 107.4, 98.5, 55.6, 55.3, 43.8, 43.4, 43.0; **HRMS** (ESI-TOF) Calc'd for $C_{25}H_{27}O_4^+$ $[M+H]^+$ 391.1909, found 391.1909.

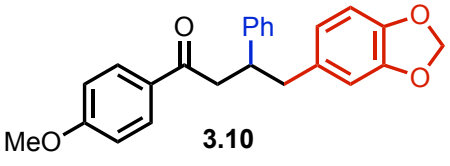

**3.10**

**4-(Benzo[*d*][1,3]dioxol-5-yl)-1-(4-methoxyphenyl)-3-phenylbutan-1-one (3.10):** Purification by PTLC (3 runs 5% EtOAc/hexane)

gave the product as a colorless solid (23.9 mg, 64% yield, 12:1 r.r.). **$^1$H NMR** (600 MHz, $CDCl_3$) $\delta$ 7.86–7.82 (m, 2H), 7.26–7.22 (m, 2H), 7.18–7.15 (m, 3H), 6.90–6.87 (m, 2H), 6.63 (d, $J$ = 7.8 Hz, 1H), 6.56 (d, $J$ = 1.7 Hz, 1H), 6.50 (dd, $J$ = 7.9, 1.7 Hz, 1H), 5.88 (s, 2H), 3.85 (s, 3H), 3.59 (p, $J$ = 7.2 Hz, 1H), 3.29–3.14 (m, 2H), 2.98–2.82 (m, 2H); **$^{13}$C NMR** (101 MHz, $CDCl_3$) $\delta$ 197.5, 163.5, 147.5, 145.9, 144.3, 133.9, 130.4, 130.4, 128.5, 127.8, 126.5, 122.3, 113.8, 109.7, 108.0, 100.8, 55.6, 43.9, 43.5, 42.8; **HRMS** (ESI-TOF) Calc'd for $C_{24}H_{23}O_4^+$ $[M+H]^+$ 375.1596, found 375.1593.

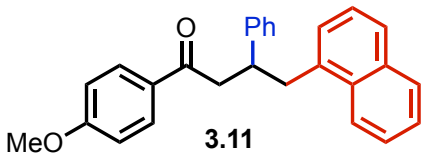

**3.11**

**1-(4-Methoxyphenyl)-4-(naphthalen-1-yl)-3-phenylbutan-1-one** (**3.11**): Purification by sequential PTLCs (plate 1: 3 runs 5% EtOAc/hexane; plate 2: 100% toluene) gave the product as a white foam (31.7 mg, 83% yield, >20:1 r.r.). **$^1$H NMR** (600 MHz, $CDCl_3$) $\delta$ 8.24 (d, $J$ = 9.1 Hz, 1H), 7.85–7.81 (m, 3H), 7.66 (d, $J$ = 8.2 Hz, 1H), 7.54 (ddd, $J$ = 8.3, 6.7, 1.4 Hz, 1H), 7.47 (ddd, $J$ = 8.0, 6.8, 1.2 Hz, 1H), 7.22 (dt, $J$ = 7.6, 6.7 Hz, 3H), 7.17–7.13 (m, 3H), 7.04–7.00 (m, 1H), 6.88–6.84 (m, 2H), 3.84 (m 4H), 3.57 (dd, $J$ = 13.8, 7.0 Hz, 1H), 3.40–3.31 (m, 2H), 3.27 (dd, $J$ = 13.8, 8.0 Hz, 1H); **$^{13}$C NMR** (101 MHz, $CDCl_3$) $\delta$ 197.6, 163.5, 144.6, 136.1, 134.0, 132.3, 130.4, 130.4, 128.8, 128.5, 127.7, 127.7, 127.0, 126.5, 126.1, 125.6, 125.2, 124.3, 113.8, 55.6, 44.5, 42.3, 40.5; **HRMS** (ESI-TOF) Calc'd for $C_{27}H_{25}O_2^+$ $[M+H]^+$ 381.1855, found 381.1851.

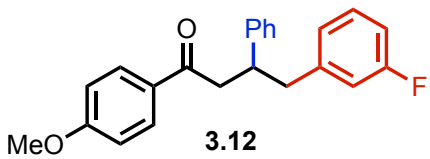

**3.12**

**4-(3-Fluorophenyl)-1-(4-methoxyphenyl)-3-phenylbutan-1-one** (**3.12**): Purification by sequential PTLCs (plate 1: 3 runs 5% EtOAc/hexane; plate 2: 2

runs 100% toluene) gave the product as a white foam (16.8 mg, 48% yield, 17:1 r.r.). **$^{1}$H NMR** (600 MHz, $CDCl_3$) $\delta$ 7.88–7.83 (m, 2H), 7.25–7.22 (m, 2H), 7.18–7.13 (m, 4H), 6.91–6.87 (m, 2H), 6.84–6.80 (m, 2H), 6.75 (dt, $J$ = 10.0, 2.1 Hz, 1H), 3.85 (s, 3H), 3.64 (dq, $J$ = 8.4, 6.8 Hz, 1H), 3.33–3.19 (m, 2H), 3.03 (dd, $J$ = 13.5, 6.5 Hz, 1H), 2.90 (dd, $J$ = 13.5, 8.4 Hz, 1H); **$^{13}$C NMR** (126 MHz, $CDCl_3$) $\delta$ 197.3, 163.6, 162.8 (d, $J$ = 245.3 Hz), 143.9, 142.6, 130.4, 130.4, 129.6 (d, $J$ = 8.2 Hz), 128.5, 127.8, 126.6, 125.0 (d, $J$ = 2.4 Hz), 116.2 (d, $J$ = 20.9 Hz), 113.8, 113.0 (d, $J$ = 21.0 Hz), 55.6, 44.0, 43.1, 42.7 (d, $J$ = 1.6 Hz); **$^{19}$F NMR** (376 MHz, $CDCl_3$) $\delta$ −114.2; **HRMS** (ESI-TOF) Calc'd for $C_{23}H_{22}FO_2^+$ $[M+H]^+$ 349.1604, found 349.1612.

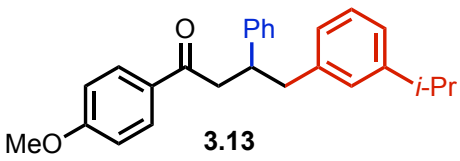

**3.13**

**4-(3-*iso*-Propylphenyl)-1-(4-methoxyphenyl)-3-phenylbutan-1-one** (**3.13**): Purification by PTLC (3 runs 5% EtOAc/hexane) gave the product as a colorless solid (26.5 mg, 71% yield, 8:1 r.r.). **$^{1}$H NMR** (600 MHz, $CDCl_3$) $\delta$ 7.85–7.81 (m, 2H), 7.25–7.21 (m, 2H), 7.17–7.14 (m, 3H), 7.12 (d, $J$ = 7.6 Hz, 1H), 7.02–6.99 (m, 1H), 6.90 (dt, $J$ = 7.3, 1.3 Hz, 1H), 6.89–6.86 (m, 2H), 6.83 (t, $J$ = 1.8 Hz, 1H), 3.85 (s, 3H), 3.63 (p, $J$ = 7.2 Hz, 1H), 3.30–3.21 (m, 2H), 3.00–2.90 (m, 2H), 2.78 (p, $J$ = 6.9 Hz, 1H), 1.15 (dd, $J$ = 6.9, 5.2 Hz, 6H); **$^{13}$C NMR** (101 MHz, $CDCl_3$) $\delta$ 197.6, 163.4, 148.7, 144.4, 139.8, 130.5, 130.4, 128.4, 128.2, 127.8, 127.7, 126.9, 126.4, 124.2, 113.8, 55.6, 43.8, 43.3, 43.3, 34.1, 24.1, 24.0; **HRMS** (ESI-TOF) Calc'd for $C_{26}H_{29}O_2^+$ $[M+H]^+$ 373.2168, found 373.2167.

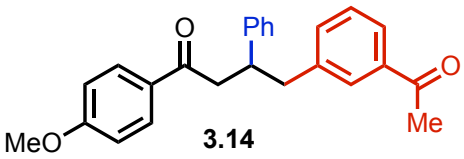


**3.14**

**4-(4-Acetylphenyl)-1-(4-methoxyphenyl)-3-phenylbutan-1-one (3.14):** Purification using sequential PTLCs (plate 1: 30% EtOAc/hexane; plate 2: 3 runs 10% EtOAc/hexane) gave the product as a white foam (12.9 mg, 35% yield, >20:1 r.r.). **$^1$H NMR** (600 MHz, $CDCl_3$) $\delta$ 7.88–7.85 (m, 2H), 7.73 (dt, $J$ = 7.5, 1.6 Hz, 1H), 7.54 (t, $J$ = 1.8 Hz, 1H), 7.28 (t, $J$ = 7.6 Hz, 1H), 7.26–7.22 (m, 3H), 7.15 (tt, $J$ = 8.1, 1.3 Hz, 3H), 6.91–6.88 (m, 2H), 3.86 (s, 3H), 3.67 (dq, $J$ = 8.5, 6.7 Hz, 1H), 3.32 (dd, $J$ = 16.6, 6.7 Hz, 1H), 3.25 (dd, $J$ = 16.6, 7.2 Hz, 1H), 3.11 (dd, $J$ = 13.5, 6.3 Hz, 1H), 2.97 (dd, $J$ = 13.5, 8.6 Hz, 1H), 2.47 (s, 3H); **$^{13}$C NMR** (101 MHz, $CDCl_3$) $\delta$ 198.4, 197.3, 163.6, 143.8, 140.5, 137.0, 134.2, 130.4, 130.3, 129.4, 128.6, 128.5, 127.9, 126.7, 126.2, 113.8, 55.6, 44.0, 43.2, 42.8, 26.7; **HRMS** (ESI-TOF) Calc'd for $C_{25}H_{25}O_3^+$ $[M+H]^+$ 373.1804, found 373.1808.

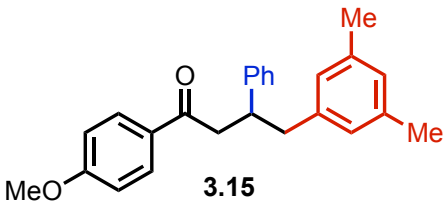


**3.15**

**4-(3,5-Dimethylphenyl)-1-(4-methoxyphenyl)-3-phenylbutan-1-one (3.15)**: Purification by PTLC (3 runs 5% EtOAc/hexane) gave the product as a colorless solid (26.3 mg, 73% yield, 17:1 r.r.). **$^1$H NMR** (600 MHz, $CDCl_3$) $\delta$ 7.84–7.80 (m, 2H), 7.26–7.22 (m, 2H), 7.21–7.18 (m, 2H), 7.17–7.13 (m, 1H), 6.89–6.85 (m, 2H), 6.80–6.78 (m, 1H), 6.72–6.70 (m, 2H), 3.85 (s, 3H), 3.64 (p, $J$ = 7.4 Hz, 1H), 3.22 (qd, $J$ = 16.4, 7.0 Hz, 2H), 2.92–2.84 (m, 2H), 2.23 (d, $J$ = 0.7 Hz, 6H); **$^{13}$C NMR** (101 MHz, $CDCl_3$) $\delta$ 197.7, 163.4, 144.7, 139.9, 137.7, 130.5, 130.4, 128.4, 127.8, 127.8, 127.3, 126.4, 113.7, 55.6, 43.7, 43.2, 43.1, 21.4; **HRMS** (ESI-TOF) Calc'd for $C_{25}H_{27}O_2^+$ $[M+H]^+$ 359.2011, found 359.2016.

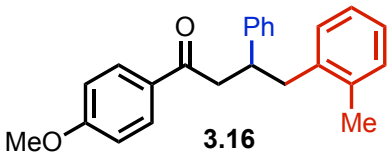


**3.16**

**1-(4-Methoxyphenyl)-3-phenyl-4-(*o*-tolyl)butan-1-one** (**3.16**): Purification by PTLC (2 runs 5% EtOAc/hexane) gave the product as a colorless solid (23.9 mg, 69% yield, >20:1 r.r.). **$^1$H NMR** (600 MHz, $CDCl_3$) $\delta$ 7.85–7.82 (m, 2H), 7.23 (td, $J$ = 7.3, 1.4 Hz, 2H), 7.18–7.15 (m, 3H), 7.10–7.08 (m, 1H), 7.06 (td, $J$ = 7.3, 1.5 Hz, 1H), 7.01 (td, $J$ = 7.3, 1.6 Hz, 1H), 6.95 (dd, $J$ = 7.6, 1.5 Hz, 1H), 6.90–6.87 (m, 2H), 3.85 (s, 3H), 3.62 (p, $J$ = 7.3 Hz, 1H), 3.30 (qd, $J$ = 16.4, 6.9 Hz, 2H), 3.02 (dd, $J$ = 13.7, 7.3 Hz, 1H), 2.89 (dd, $J$ = 13.7, 7.7 Hz, 1H), 2.25 (s, 3H); **$^{13}$C NMR** (150 MHz, $CDCl_3$) $\delta$ 197.5, 163.5, 144.6, 138.2, 136.6, 130.4, 130.3, 130.3, 128.5, 127.7, 126.5, 126.3, 125.7, 113.8, 55.6, 43.9, 42.2, 40.7, 19.6; **HRMS** (ESI-TOF) Calc'd for $C_{24}H_{25}O_2^+$ $[M+H]^+$ 345.1855, found 345.1855.

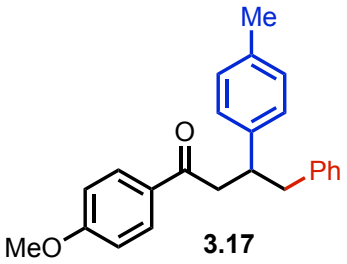


**3.17**

**1-(4-Methoxyphenyl)-4-phenyl-3-(*p*-tolyl)butan-1-one** (**3.17**)**:** Purification by PTLC (3 runs 5% EtOAc/hexane) gave the product as a white foam (24.9 mg, 72% yield, 14:1 r.r.). **$^1$H NMR** (600 MHz, $CDCl_3$) δ 7.84–7.81 (m, 2H), 7.23–7.18 (m, 2H), 7.16–7.12 (m, 1H), 7.10–7.02 (m, 6H), 6.89–6.86 (m, 2H), 3.85 (s, 3H), 3.62 (p, $J$ = 7.3 Hz, 1H), 3.27–3.17 (m, 2H), 2.95 (qd, $J$ = 13.5, 7.4 Hz, 2H), 2.28 (s, 3H); **$^{13}$C NMR** (101 MHz, $CDCl_3$) $\delta$ 197.6, 163.4, 141.3, 140.2, 135.9, 130.4, 130.4, 129.4, 129.2, 128.3, 127.6, 126.1, 113.7, 55.6, 44.0, 43.2, 42.9, 21.2; **HRMS** (ESI-TOF) Calc'd for $C_{24}H_{25}O_2^+$ $[M+H]^+$ 345.1855, found 345.1855.

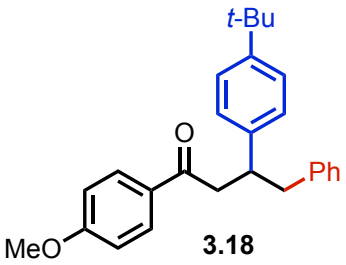


**3.18**

**3-(4-(*tert*-Butyl)phenyl)-1-(4-methoxyphenyl)-4-phenylbutan-1-one (3.18):** Purification by PTLC (3 runs 5% EtOAc/hexane) gave the product as a colorless solid (26.5 mg, 69% yield, >20:1 r.r.). **$^1$H NMR** (600 MHz, $CDCl_3$) $\delta$ 7.84–7.79 (m, 2H), 7.24 (d, $J$ = 1.5 Hz, 2H), 7.23–7.19 (m, 2H), 7.18–7.13 (m, 1H), 7.11 (ddd, $J$ = 11.6, 7.6, 1.7 Hz, 4H), 6.89–6.84 (m, 2H), 3.84 (s, 3H), 3.63 (p, $J$ = 7.2 Hz, 1H), 3.29–3.15 (m, 2H), 2.96 (dd, $J$ = 7.4, 1.7 Hz, 2H), 1.27 (s, 9H); **$^{13}$C NMR** (101 MHz, $CDCl_3$) $\delta$ 197.7, 163.4, 149.1, 141.4, 140.3, 130.5, 130.4, 129.5, 128.3, 127.3, 126.1, 125.3, 113.7, 55.6, 43.9, 43.1, 42.7, 34.5, 31.5; **HRMS** (ESI-TOF) Calc'd for $C_{27}H_{31}O_2^+$ $[M+H]^+$ 387.2324, found 387.2327.

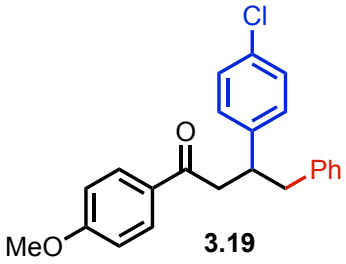


**3.19**

**3-(4-Chlorophenyl)-1-(4-methoxyphenyl)-4-phenylbutan-1-one (3.19):** Purification using sequential PTLCs (plate 1: 3 runs 5% EtOAc/hexane; plate 2: 100% toluene) gave the product as a white solid (16.1 mg, 44% yield, 14:1 r.r.). **$^1$H NMR** (600 MHz, $CDCl_3$) $\delta$ 7.85–7.82 (m, 2H), 7.23–7.18 (m, 4H), 7.17–7.13 (m, 1H), 7.11–7.08 (m, 2H), 7.07–7.03 (m, 2H), 6.90–6.87 (m, 2H), 3.85 (s, 3H), 3.64 (p, $J$ = 7.2 Hz, 1H), 3.28–3.19 (m, 2H), 2.99 (dd, $J$ = 13.5, 6.9 Hz, 1H), 2.89 (dd, $J$ = 13.6, 8.0 Hz, 1H); **$^{13}$C NMR** (101 MHz, $CDCl_3$) $\delta$ 197.2, 163.6, 142.8, 139.6, 132.1, 130.4, 130.3, 129.4, 129.2, 128.6, 128.4, 126.3, 113.8, 55.6, 43.8, 43.1, 42.7; **HRMS** (ESI-TOF) Calc'd for $C_{23}H_{22}ClO_2^+$ $[M+H]^+$ 365.1308, found 365.1314.

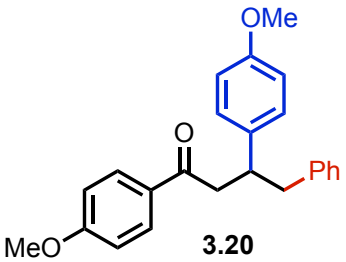


**3.20**

**1,3-Bis(4-methoxyphenyl)-4-phenylbutan-1-one (3.20):** Purification by PTLC (5% EtOAc/hexane) gave the product as a colorless solid (23.4 mg, 65% yield, 14:1 r.r.). **$^1$H NMR** (600 MHz, $CDCl_3$) $\delta$ 7.85–7.81 (m, 2H), 7.22–7.18 (m, 2H), 7.16–7.12 (m, 1H), 7.10–7.07 (m, 2H), 7.07–7.05 (m, 2H), 6.89–6.86 (m, 2H), 6.79–6.76 (m, 2H), 3.85 (s, 3H), 3.75 (s, 3H), 3.60 (p, $J$ = 7.2 Hz, 1H), 3.26–3.16 (m, 2H), 2.97 (dd, $J$ = 13.5, 7.0 Hz, 1H), 2.91 (dd, $J$ = 13.4, 7.8 Hz, 1H); **$^{13}$C NMR** (101 MHz, $CDCl_3$) $\delta$ 197.7, 163.4, 158.1, 140.1, 136.4, 130.4, 130.4, 129.4, 128.7, 128.3, 126.1, 113.8, 113.8, 55.6, 55.3, 44.2, 43.3, 42.6; **HRMS** (ESI-TOF) Calc'd for $C_{24}H_{25}O_3^+$ $[M+H]^+$ 361.1804, found 361.1798.

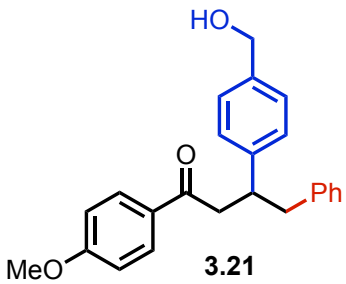


**3.21**

**3-(4-(Hydroxymethyl)phenyl)-1-(4-methoxyphenyl)-4-phenylbutan-1-one (3.21):** Purification by PTLC (30% EtOAc/hexane) gave the product as a colorless solid (25.4 mg, 70% yield, 10:1 r.r.). **$^1$H NMR** (600 MHz, $CDCl_3$) δ 7.84–7.81 (m, 2H), 7.25–7.21 (m, 2H), 7.21–7.19 (m, 2H), 7.19–7.17 (m, 2H), 7.17–7.13 (m, 1H), 7.09–7.07 (m, 2H), 6.89–6.86 (m, 2H), 4.63 (d, $J$ = 4.8 Hz, 2H), 3.85 (s, 3H), 3.70–3.63 (m, 1H), 3.25 (qd, $J$ = 16.5, 7.0 Hz, 2H), 3.02–2.91 (m, 2H), 1.26 (s, 1H); **$^{13}$C NMR** (126 MHz, $CDCl_3$) $\delta$ 197.5, 163.5, 143.9, 139.9, 139.0, 130.4, 130.3, 129.4, 128.3, 128.0, 127.2, 126.2, 113.8, 65.3, 55.6, 43.9, 43.1, 43.0; **HRMS** (ESI-TOF) Calc'd for $C_{24}H_{25}O_3^+$ $[M+H]^+$ 361.1804, found 361.1803.

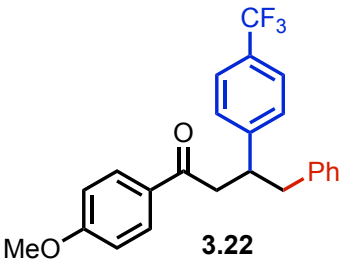


**3.22**

**1-(4-Methoxyphenyl)-4-phenyl-3-(4-(trifluoromethyl)phenyl)butan-1-one** (**3.22**)**:** Purification by sequential PTLCs (plate 1: 2 runs 5% EtOAc/hexane; plate 2: 100% toluene) gave the product as a colorless solid (22.3 mg, 56% yield, 12:1 r.r.). **$^1$H NMR** (600 MHz, $CDCl_3$) $\delta$ 7.85–7.82 (m, 2H), 7.48 (d, $J$ = 8.0 Hz, 2H), 7.28 (d, $J$ = 8.1 Hz, 2H), 7.24–7.20 (m, 2H), 7.18–7.14 (m, 1H), 7.08–7.04 (m, 2H), 6.90–6.87 (m, 2H), 3.85 (s, 3H), 3.74 (p, $J$ = 7.3 Hz, 1H), 3.33–3.24 (m, 2H), 3.02 (dd, $J$ = 13.6, 7.1 Hz, 1H), 2.93 (dd, $J$ = 13.6, 7.9 Hz, 1H); **$^{13}$C NMR** (126 MHz,$CDCl_3$) $\delta$ 196.9, 163.7, 148.5, 139.4, 130.4, 130.2, 129.3, 128.8 (q, $J$ = 32.1 Hz), 128.5, 128.2, 126.5, 125.4 (q, $J$ = 3.9 Hz), 124.33 (q, $J$ = 260.3 Hz), 113.9, 55.6, 43.5, 43.1, 42.9; **$^{19}$F NMR** (376 MHz, $CDCl_3$) $\delta$ −62.6; **HRMS** (ESI-TOF) Calc'd for $C_{24}H_{22}F_3O_2^+$ $[M+H]^+$ 399.1572, found 399.1574.

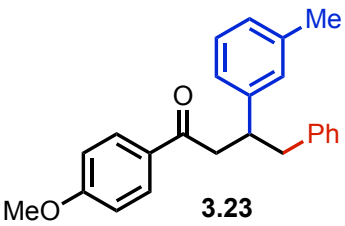


**3.23**

**1-(4-Methoxyphenyl)-4-phenyl-3-(*m*-tolyl)butan-1-one** (**3.23**)**:** Purification by PTLC (3 runs 5% EtOAc/hexane) gave the product as a white foam (22.4 mg, 65% yield, >20:1 r.r.). **$^1$H NMR** (600 MHz, $CDCl_3$) δ 7.85–7.81 (m, 2H), 7.22–7.19 (m, 2H), 7.16–7.11 (m, 2H), 7.09–7.06 (m, 2H), 6.99 (d, $J$ = 1.7 Hz, 1H), 6.98–6.95 (m, 2H), 6.89–6.86 (m, 2H), 3.85 (s, 3H), 3.61 (p, $J$ = 7.2 Hz, 1H), 3.29–3.17 (m, 2H), 2.99–2.91 (m, 2H), 2.28 (s, 3H); **$^{13}$C NMR** (126 MHz, $CDCl_3$) $\delta$ 197.6, 163.4, 144.4, 140.1, 137.9, 130.5, 130.4, 129.4, 128.6, 128.3, 128.3, 127.2, 126.2, 124.7, 113.7, 55.6, 43.9, 43.2, 43.1, 21.6; **HRMS** (ESI-TOF) Calc'd for $C_{24}H_{25}O_2^+$ $[M+H]^+$ 345.1855, found 345.1859.

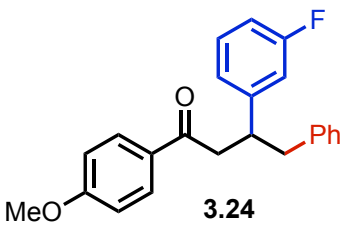


**3.24**

**3-(3-Fluorophenyl)-1-(4-methoxyphenyl)-4-phenylbutan-1-one (3.24):** Purification by sequential PTLCs (plate 1: 3 runs 5% EtOAc/hexane; plate 2: 100% toluene) gave the product as a white foam (22.5 mg, 65% yield, 18:1 r.r.). **$^1$H NMR** (600 MHz, $CDCl_3$) $\delta$ 7.86–7.82 (m, 2H), 7.23–7.19 (m, 2H), 7.19–7.13 (m, 2H), 7.08–7.05 (m, 2H), 6.94 (dt, $J$ = 7.7, 1.4 Hz, 1H), 6.90–6.86 (m, 3H), 6.84 (tdd, $J$ = 8.5, 2.6, 1.0 Hz, 1H), 3.85 (s, 3H), 3.67 (p, $J$ = 7.2 Hz, 1H), 3.24 (qd, $J$ = 16.7, 7.0 Hz, 2H), 3.00 (dd, $J$ = 13.6, 7.0 Hz, 1H), 2.91 (dd, $J$ = 13.5, 7.9 Hz, 1H); **$^{13}$C NMR** (101 MHz, $CDCl_3$) $\delta$ 197.1, 163.6, 162.9 (d, $J$ = 245.3 Hz), 147.1 (d, $J$ = 6.9 Hz), 139.6, 130.4, 130.3, 129.8 (d, $J$ = 8.3 Hz), 129.3, 128.4, 126.3, 123.6 (d, $J$ = 2.7 Hz), 114.6 (d, $J$ = 21.1 Hz), 113.8, 113.4 (d, $J$ = 21.0 Hz), 55.6, 43.7, 43.0, 43.0; **$^{19}$F NMR** (376 MHz, $CDCl_3$) $\delta$ −113.7; **HRMS** (ESI-TOF) Calc'd for $C_{23}H_{22}FO_2^+$ $[M+H]^+$ 349.1604, found 349.1604.

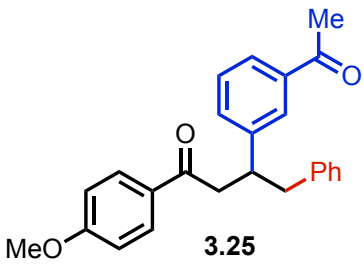


**3.25**

**3-(3-Acetylphenyl)-1-(4-methoxyphenyl)-4-phenylbutan-1-one (3.25):** Purification by PTLC (toluene:$Et_2O$:DCM = 8:1:1) the product was obtained as a white foam (27.0 mg, 72% yield, >20:1 r.r.). **$^1$H NMR** (600 MHz, $CDCl_3$) $\delta$ 7.86–7.83 (m, 2H), 7.78 (t, $J$ = 1.8 Hz, 1H), 7.74 (dt, $J$ = 7.7, 1.5 Hz, 1H), 7.37 (dt, $J$ = 7.6, 1.5 Hz, 1H), 7.32 (t, $J$ = 7.6 Hz, 1H), 7.20 (dd, $J$ = 8.1, 6.7 Hz, 2H), 7.17–7.13 (m, 1H), 7.07–7.04 (m, 2H), 6.90–6.87 (m, 2H), 3.85 (s, 3H), 3.74 (p, $J$ = 7.3 Hz, 1H), 3.36–3.25 (m, 2H), 3.04 (dd, $J$ = 13.5, 7.1 Hz, 1H), 2.93 (dd, $J$ = 13.5, 8.0 Hz, 1H), 2.54 (s, 3H); **$^{13}$C NMR** (101 MHz, $CDCl_3$) $\delta$ 198.4, 197.1, 163.6, 145.0, 139.6, 137.2, 133.0, 130.4, 130.2, 129.4, 128.6, 128.4, 127.3, 126.8, 126.3, 113.8, 55.6, 43.6,

43.1, 43.1, 26.8; **HRMS** (ESI-TOF) Calc'd for $C_{25}H_{25}O_3^+$ $[M+H]^+$ 373.1804, found 373.1805.

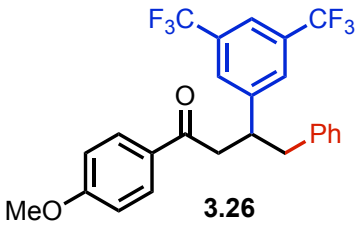

**3.26**

**3-(3,5-Bis(trifluoromethyl)phenyl)-1-(4-methoxyphenyl)-4-phenylbutan-1-one (3.26):** Purification by sequential PTLCs (plate 1: 3 runs 5% EtOAc/hexane; plate 2: 100% toluene) gave the product as a colorless solid (23.7 mg, 51% yield, 14:1 r.r.). **$^1$H NMR** (600 MHz, $CDCl_3$) $\delta$ 7.87–7.84 (m, 2H), 7.67 (s, 1H), 7.58 (s, 2H), 7.23 (td, $J$ = 7.4, 1.0 Hz, 2H), 7.19–7.16 (m, 1H), 7.04–7.01 (m, 2H), 6.92–6.89 (m, 2H), 3.86 (s, 3H), 3.82 (q, $J$ = 7.2 Hz, 1H), 3.37–3.28 (m, 2H), 3.06 (dd, $J$ = 13.5, 7.1 Hz, 1H), 2.91 (dd, $J$ = 13.6, 7.9 Hz, 1H); **$^{13}$C NMR** (150 MHz, $CDCl_3$) $\delta$ 196.3, 163.8, 147.0, 138.6, 131.5 (q, $J$ = 33.0 Hz), 130.3, 130.0, 129.3, 128.6, 128.1 (bq, $J$ = 3.9 Hz), 126.8, 123.5 (q, $J$ = 272.8 Hz), 120.6 (hept, $J$ = 3.9, 3.5 Hz), 114.0, 55.6, 43.1, 42.9, 42.9; **$^{19}$F NMR** (376 MHz, $CDCl_3$) $\delta$ −63.0; **HRMS** (ESI-TOF) Calc'd for $C_{25}H_{21}F_6O_2^+$ $[M+H]^+$ 467.1446, found 467.1438.

*Alkenyl Ketone Scope*

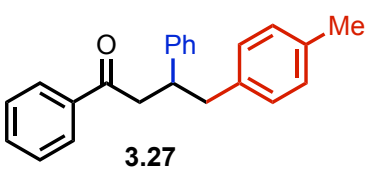

**3.27**

**1,3-Diphenyl-4-(*p*-tolyl)butan-1-one (3.27):** Purification by PTLC (2 runs 5% EtOAc/hexane) the product was obtained as a colorless solid (22.3 mg, 71% yield, 8:1 r.r.). **$^1$H NMR** (600 MHz, $CDCl_3$) $\delta$ 7.83 (dd, $J$ = 8.4, 1.3 Hz, 2H), 7.51 (ddt, $J$ = 8.6, 7.2, 1.3 Hz, 1H), 7.43–7.38 (m, 2H), 7.26–7.22 (m, 2H), 7.21–7.17 (m, 2H), 7.15 (ddt, $J$ = 8.6, 6.7, 1.4 Hz, 1H), 7.01 (d, $J$ = 7.6 Hz, 2H), 6.96 (d, $J$ = 8.0 Hz, 2H), 3.65 (p, $J$ = 7.3 Hz,

1H), 3.35–3.22 (m, 2H), 2.94 (d, $J$ = 7.5 Hz, 2H), 2.28 (s, 3H); **$^{13}$C NMR** (101 MHz, $CDCl_3$) $\delta$ 199.1, 144.4, 137.3, 136.8, 135.6, 133.0, 129.3, 129.0, 128.6, 128.5, 128.1, 127.8, 126.5, 44.2, 43.2, 42.7, 21.2; **HRMS** (ESI-TOF) Calc'd for $C_{23}H_{23}O^+$ $[M+H]^+$ 315.1749, found 315.1754.

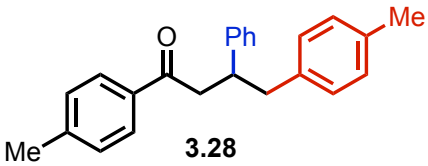

**3.28**

**3-Phenyl-1,4-di-*p*-tolylbutan-1-one (3.28):** Purification by PTLC (100% toluene) the product was obtained as a colorless solid (19.7 mg, 60% yield, 8:1 r.r.). **$^1$H NMR** (600 MHz, $CDCl_3$) $\delta$ 7.74 (d, $J$ = 8.3 Hz, 2H), 7.25–7.21 (m, 2H), 7.21–7.16 (m, 4H), 7.15 (ddt, $J$ = 7.2, 5.3, 1.4 Hz, 1H), 7.01 (d, $J$ = 7.6 Hz, 2H), 6.96 (d, $J$ = 8.0 Hz, 2H), 3.63 (p, $J$ = 7.3 Hz, 1H), 3.26 (qd, $J$ = 16.6, 6.9 Hz, 2H), 2.98–2.88 (m, 2H), 2.38 (s, 3H), 2.27 (s, 3H); **$^{13}$C NMR** (101 MHz, $CDCl_3$) $\delta$ 198.7, 144.5, 143.8, 136.9, 135.6, 134.9, 129.3, 129.3, 129.0, 128.4, 128.3, 127.8, 126.4, 44.1, 43.2, 42.7, 21.7, 21.2; **HRMS** (ESI-TOF) Calc'd for $C_{24}H_{25}O^+$ $[M+H]^+$ 329.1905, found 329.1902.

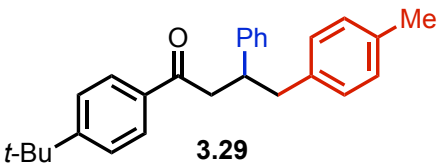

**3.29**

**1-(4-(*tert*-Butyl)phenyl)-3-phenyl-4-(*p*-tolyl)butan-1-one (3.29):** Purification by PTLC (100% toluene) the product was obtained as a colorless solid (23.2 mg, 63% yield, 8:1 r.r.). **$^1$H NMR** (600 MHz, $CDCl_3$) $\delta$ 7.81–7.78 (m, 2H), 7.44–7.40 (m, 2H), 7.24 (dd, $J$ = 8.0, 7.1 Hz, 2H), 7.20–7.17 (m, 2H), 7.17–7.13 (m, 1H), 7.01 (d, $J$ = 8.0 Hz, 2H), 6.96 (d, $J$ = 8.0 Hz, 2H), 3.65 (p, $J$ = 7.3 Hz, 1H), 3.33–3.21 (m, 2H), 2.97–2.89 (m, 2H), 2.27 (s, 3H), 1.32 (s, 9H); **$^{13}$C NMR** (101 MHz, $CDCl_3$) $\delta$ 198.7, 156.7, 144.5, 136.9, 135.6, 134.8, 129.3, 129.0, 128.4, 128.1, 127.8, 126.4, 125.6, 44.2,

43.1, 42.7, 35.2, 31.2, 21.2; **HRMS** (ESI-TOF) Calc'd for $C_{27}H_{31}O^+$ $[M+H]^+$ 371.2375, found 371.2373.

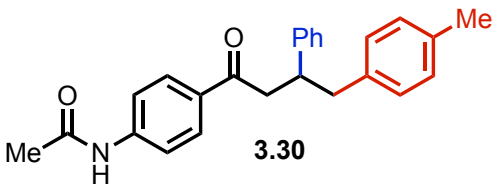

**3.30**

***N*-(4-(3-Phenyl-4-(*p*-tolyl)butanoyl)phenyl)acetamide (3.30):** Purification by PTLC (40% EtOAc/hexane) the product was obtained as a colorless solid (23.0 mg, 62% yield, 6:1 r.r.). **$^1$H NMR** (600 MHz, $CDCl_3$) $\delta$ 7.84–7.79 (m, 2H), 7.54 (d, $J$ = 8.3 Hz, 2H), 7.24 (d, $J$ = 1.8 Hz, 1H), 7.23 (dd, $J$ = 6.8, 1.4 Hz, 2H), 7.19–7.16 (m, 2H), 7.16–7.13 (m, 1H), 7.01 (d, $J$ = 7.7 Hz, 2H), 6.96 (d, $J$ = 7.9 Hz, 2H), 3.62 (p, $J$ = 7.4 Hz, 1H), 3.31–3.18 (m, 2H), 2.93 (d, $J$ = 7.5 Hz, 2H), 2.28 (s, 3H), 2.20 (s, 3H); **$^{13}$C NMR** (101 MHz, $CDCl_3$) $\delta$ 198.1, 144.3, 142.3, 136.8, 135.7, 129.5, 129.2, 129.0, 128.5, 128.3, 127.7, 127.5, 126.5, 118.9, 44.0, 43.4, 42.7, 24.8, 21.1; **HRMS** (ESI-TOF) Calc'd for $C_{25}H_{26}NO_2^+$ $[M+H]^+$ 372.1964, found 372.1966.

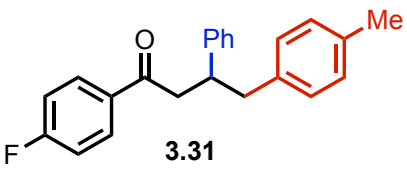

**3.31**

**1-(4-Fluorophenyl)-3-phenyl-4-(*p*-tolyl)butan-1-one (3.31):** Purification by PTLC (100% toluene) the product was obtained as a white foam (17.1 mg, 52% yield, 10:1 r.r.). **$^1$H NMR** (600 MHz, $CDCl_3$) $\delta$ 7.86–7.82 (m, 2H), 7.24 (dd, $J$ = 7.9, 7.0 Hz, 2H), 7.19–7.14 (m, 3H), 7.08–7.04 (m, 2H), 7.02 (d, $J$ = 7.8 Hz, 2H), 6.97 (d, $J$ = 8.0 Hz, 2H), 3.65–3.59 (m, 1H), 3.30–3.19 (m, 2H), 2.94 (d, $J$ = 7.1 Hz, 2H), 2.28 (s, 3H); **$^{13}$C NMR** (101 MHz, $CDCl_3$) $\delta$ 197.5, 144.3, 136.7, 135.7, 133.8 (d, $J$ = 3.0 Hz), 130.8, 130.7, 129.3, 128.1 (d, $J$ = 76.7 Hz), 127.8, 126.6, 115.8, 115.6, 44.1, 43.3, 42.7, 21.2;

**$^{19}$F NMR** (376 MHz, $CDCl_3$) $\delta$ −105.8; **HRMS** (ESI-TOF) Calc'd for $C_{23}H_{22}FO^+$ $[M+H]^+$ 333.1655, found 333.1655.

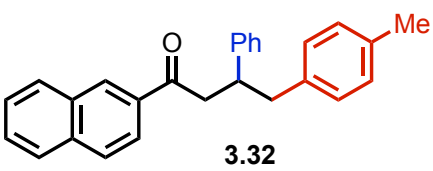


**3.32**

**1-(Naphthalen-2-yl)-3-phenyl-4-(*p*-tolyl)butan-1-one (3.32):** Purification by PTLC (100% toluene) the product was obtained as a colorless solid (26.2 mg, 72% yield, 12:1 r.r.). **$^1$H NMR** (600 MHz, $CDCl_3$) $\delta$ 8.30 (s, 1H), 7.90 (td, $J$ = 8.8, 1.5 Hz, 2H), 7.86–7.82 (m, 2H), 7.58 (ddd, $J$ = 8.2, 6.8, 1.4 Hz, 1H), 7.53 (ddd, $J$ = 8.1, 6.8, 1.3 Hz, 1H), 7.25 (d, $J$ = 7.0 Hz, 2H), 7.23–7.21 (m, 2H), 7.16 (ddt, $J$ = 7.0, 4.9, 1.6 Hz, 1H), 7.04 (d, $J$ = 7.8 Hz, 2H), 7.00 (d, $J$ = 8.1 Hz, 2H), 3.70 (p, $J$ = 7.2 Hz, 1H), 3.42 (dd, $J$ = 7.0, 2.1 Hz, 2H), 2.99 (d, $J$ = 7.5 Hz, 2H), 2.29 (s, 3H); **$^{13}$C NMR** (101 MHz, $CDCl_3$) $\delta$ 199.1, 144.4, 136.9, 135.7, 135.6, 134.6, 132.6, 129.8, 129.6, 129.3, 129.1, 128.5, 128.5, 128.4, 127.9, 127.8, 126.8, 126.5, 124.0, 44.3, 43.5, 42.7, 21.2; **HRMS** (ESI-TOF) Calc'd for $C_{27}H_{25}O^+$ $[M+H]^+$ 365.1905, found 365.1908.

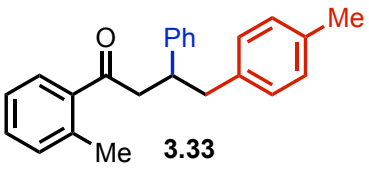


**3.33**

**3-Phenyl-1-(*o*-tolyl)-4-(*p*-tolyl)butan-1-one (3.33):** Purification by PTLC (100% toluene) the product was obtained as a white foam (14.9 mg, 45% yield, 8:1 r.r.). **$^1$H NMR** (600 MHz, $CDCl_3$) $\delta$ 7.39 (dd, $J$ = 7.7, 1.4 Hz, 1H), 7.30 (td, $J$ = 7.5, 1.4 Hz, 1H), 7.25–7.21 (m, 2H), 7.20–7.17 (m, 1H), 7.17–7.12 (m, 4H), 7.03 (d, $J$ = 7.6 Hz, 2H), 6.96 (d, $J$ = 8.0 Hz, 2H), 3.57 (p, $J$ = 7.5 Hz, 1H), 3.24–3.15 (m, 2H), 2.91 (qd, $J$ = 13.5, 7.4 Hz, 2H), 2.29 (s, 3H), 2.20 (s, 3H); **$^{13}$C NMR** (126 MHz, $CDCl_3$) $\delta$ 203.8, 144.1, 138.7, 137.9, 136.8, 135.7, 131.9, 131.0, 129.2, 129.1, 128.5, 128.1, 127.8, 126.5, 125.6,

47.4, 43.6, 42.9, 21.2, 20.8; **HRMS** (ESI-TOF) Calc'd for $C_{24}H_{25}O^+$ $[M+H]^+$ 329.1905, found 329.1913.

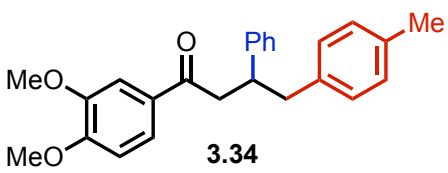


**3.34**

**1-(3,4-Dimethoxyphenyl)-3-phenyl-4-(*p*-tolyl)butan-1-one (3.34):** Purification by PTLC (2 runs 20% EtOAc/hexane) gave the product as white foam (30.5 mg, 81% yield, 10:1 r.r.). **$^1$H NMR** (600 MHz, $CDCl_3$) $\delta$ 7.47 (dd, $J$ = 8.3, 2.0 Hz, 1H), 7.40 (d, $J$ = 2.0 Hz, 1H), 7.26–7.22 (m, 2H), 7.20–7.17 (m, 2H), 7.17–7.14 (m, 1H), 7.02 (d, $J$ = 7.8 Hz, 2H), 6.97 (d, $J$ = 8.0 Hz, 2H), 6.83 (d, $J$ = 8.4 Hz, 1H), 3.93 (s, 3H), 3.88 (s, 3H), 3.63 (p, $J$ = 7.3 Hz, 1H), 3.30–3.20 (m, 2H), 2.98–2.90 (m, 2H), 2.28 (s, 3H); **$^{13}$C NMR** (101 MHz, $CDCl_3$) $\delta$ 197.7, 153.2, 149.0, 144.5, 136.9, 135.6, 130.6, 129.3, 129.0, 128.4, 127.8, 126.4, 122.7, 110.3, 110.0, 56.2, 56.0, 43.8, 43.5, 42.7, 21.1; **HRMS** (ESI-TOF) Calc'd for $C_{25}H_{27}O_3^+$ $[M+H]^+$ 375.1960, found 375.1962.

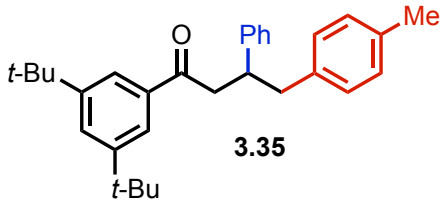


**3.35**

**1-(3,5-Di-*tert*-butylphenyl)-3-phenyl-4-(*p*-tolyl)butan-1-one (3.35):** Purification by PTLC (100% toluene) the product was obtained as a white foam (32.7 mg, 77% yield, 12:1 r.r.). **$^1$H NMR** (600 MHz, $CDCl_3$) $\delta$ 7.67 (d, $J$ = 1.8 Hz, 2H), 7.59 (t, $J$ = 1.8 Hz, 1H), 7.25–7.23 (m, 2H), 7.21–7.18 (m, 2H), 7.15 (ddt, $J$ = 8.6, 6.8, 1.4 Hz, 1H), 7.01 (d, $J$ = 7.8 Hz, 2H), 6.97 (d, $J$ = 8.0 Hz, 2H), 3.63 (p, $J$ = 7.1 Hz, 1H), 3.29 (d, $J$ = 7.0 Hz, 2H), 3.00–2.90 (m, 2H), 2.27 (s, 3H), 1.32 (s, 18H); **$^{13}$C NMR** (126 MHz, $CDCl_3$) $\delta$ 200.0, 151.2, 144.5, 137.1, 137.0, 135.6, 129.3, 129.0, 128.5, 127.9,

127.2, 126.5, 122.4, 44.7, 43.6, 42.6, 35.1, 31.5, 21.2; **HRMS** (ESI-TOF) Calc'd for $C_{31}H_{39}O^+$ $[M+H]^+$ 427.3001, found 427.3002.

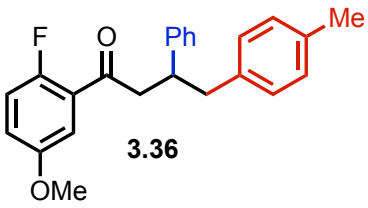


**3.36**

**1-(2-Fluoro-5-methoxyphenyl)-3-phenyl-4-(*p*-tolyl)butan-1-one (3.36):** Purification by sequential PTLCs (plate 1: 100% toluene; plate 2: 3 runs 5% EtOAc/hexane) the product was obtained as a white foam (20.1 mg, 56% yield, 11:1 r.r.). **$^1$H NMR** (600 MHz, $CDCl_3$) $\delta$ 7.24 (dd, $J$ = 8.1, 7.1 Hz, 2H), 7.19–7.13 (m, 3H), 7.12–7.09 (m, 1H), 7.02–6.98 (m, 4H), 6.95 (d, $J$ = 8.0 Hz, 2H), 3.75 (s, 3H), 3.64–3.58 (m, 1H), 3.36 (ddd, $J$ = 17.6, 7.9, 3.0 Hz, 1H), 3.29 (ddd, $J$ = 17.5, 6.2, 2.9 Hz, 1H), 2.91 (d, $J$ = 7.5 Hz, 2H), 2.27 (s, 3H); **$^{13}$C NMR** (150 MHz, $CDCl_3$) $\delta$ 197.3 (d, $J$ = 4.4 Hz), 156.4 (d, $J$ = 247.0 Hz), 155.8 (d, $J$ = 1.4 Hz), 144.4, 136.8, 135.6, 129.3, 129.0, 128.4, 127.8, 126.4, 121.4 (d, $J$ = 8.8 Hz), 117.6 (d, $J$ = 26.3 Hz), 112.9 (d, $J$ = 2.8 Hz), 56.0, 49.3 (d, $J$ = 7.6 Hz), 43.1 (d, $J$ = 1.6 Hz), 42.9, 21.2; **$^{19}$F NMR** (376 MHz, $CDCl_3$) $\delta$ −119.9; **HRMS** (ESI-TOF) Calc'd for $C_{24}H_{24}FO_2^+$ $[M+H]^+$ 363.1760, found 363.1761.

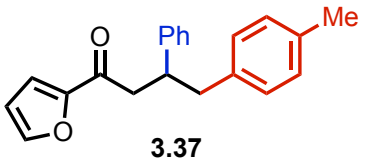


**3.37**

**1-(Furan-2-yl)-3-phenyl-4-(*p*-tolyl)butan-1-one (3.37):** Purification by PTLC (100% toluene) the product was obtained as a slightly green solid (8.7 mg, 29% yield, 14:1 r.r.). **$^1$H NMR** (600 MHz, $CDCl_3$) $\delta$ 7.51 (dd, $J$ = 1.7, 0.8 Hz, 1H), 7.25–7.21 (m, 2H), 7.19–7.17 (m, 2H), 7.16–7.13 (m, 1H), 7.04 (dd, $J$ = 3.6, 0.8 Hz, 1H), 7.01 (d, $J$ = 7.7 Hz, 2H), 6.95 (d, $J$ = 8.0 Hz, 2H), 6.46 (dd, $J$ = 3.5, 1.7 Hz, 1H), 3.66–3.59 (m, 1H), 3.18 (dd, $J$ = 16.1, 8.0 Hz, 1H), 3.10 (dd, $J$ = 16.1, 6.4 Hz, 1H), 2.93 (d, $J$ = 7.5 Hz, 2H), 2.27 (s,

3H); **$^{13}$C NMR** (101 MHz, $CDCl_3$) $\delta$ 188.1, 153.0, 146.1, 143.9, 136.6, 135.5, 129.1, 128.9, 128.3, 127.7, 126.4, 116.9, 112.1, 44.0, 43.0, 42.5, 21.0; **HRMS** (ESI-TOF) Calc'd for $C_{21}H_{21}O_2^+$ $[M+H]^+$ 305.1542, found 305.1546.

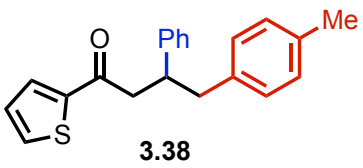


**3.38**

**3-Phenyl-1-(thiophen-2-yl)-4-(*p*-tolyl)butan-1-one (3.38):** Purification by PTLC (100% toluene) the product was obtained as a slightly greenish solid (22.2 mg, 69% yield, 12:1 r.r.). **$^1$H NMR** (600 MHz, $CDCl_3$) $\delta$ 7.59–7.56 (m, 2H), 7.25–7.22 (m, 2H), 7.20–7.17 (m, 2H), 7.17–7.13 (m, 1H), 7.06 (dd, $J$ = 4.9, 3.8 Hz, 1H), 7.01 (d, $J$ = 7.8 Hz, 2H), 6.96 (d, $J$ = 8.0 Hz, 2H), 3.63 (p, $J$ = 7.3 Hz, 1H), 3.26–3.16 (m, 2H), 2.99–2.91 (m, 2H), 2.27 (s, 3H); **$^{13}$C NMR** (126 MHz, $CDCl_3$) $\delta$ 191.8, 144.6, 144.0, 136.6, 135.6, 133.5, 131.7, 129.2, 128.9, 128.4, 128.0, 127.7, 126.4, 45.0, 43.4, 42.4, 21.0; **HRMS** (ESI-TOF) Calc'd for $C_{21}H_{21}OS^+$ $[M+H]^+$ 321.1313, found 321.1320.

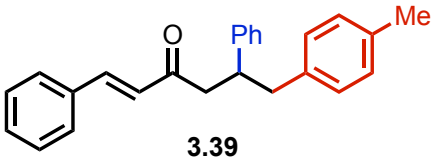


**3.39**

**(*E*)-1,5-Diphenyl-6-(*p*-tolyl)hex-1-en-3-one (3.39):** Purification by PTLC (100% toluene) the product was obtained as a colorless solid (12.3 mg, 36% yield, 10:1 r.r.). **$^1$H NMR** (600 MHz, $CDCl_3$) $\delta$ 7.47–7.44 (m, 2H), 7.39–7.35 (m, 4H), 7.26–7.24 (m, 2H), 7.20–7.18 (m, 2H), 7.18–7.14 (m, 1H), 7.04–7.01 (m, 2H), 6.97 (d, $J$ = 8.0 Hz, 2H), 6.60 (d, $J$ = 16.1 Hz, 1H), 3.55 (p, $J$ = 7.4 Hz, 1H), 3.02–2.88 (m, 4H), 2.28 (s, 3H); **$^{13}$C NMR** (150 MHz, $CDCl_3$) $\delta$ 199.1, 144.3, 142.5, 136.8, 135.7, 134.6, 130.5, 129.3, 129.0, 129.0, 128.5, 128.4, 127.8, 126.5, 126.5, 46.7, 43.5, 42.7, 21.2; **HRMS** (ESI-TOF) Calc'd for $C_{25}H_{25}O^+$ $[M+H]^+$ 341.1905, found 341.1910.

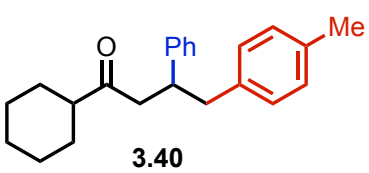


**3.40**

**1-Cyclohexyl-3-phenyl-4-(*p*-tolyl)butan-1-one (3.40):** Purification by PTLC (100% toluene) the product was obtained as a white foam (19.7 mg, 61% yield, 8:1 r.r.). **$^1$H NMR** (600 MHz, $CDCl_3$) $\delta$ 7.23 (dd, $J$ = 8.1, 6.8 Hz, 2H), 7.17–7.14 (m, 1H), 7.14–7.11 (m, 2H), 7.00 (d, $J$ = 7.6 Hz, 2H), 6.93 (d, $J$ = 8.0 Hz, 2H), 3.49–3.43 (m, 1H), 2.83 (dd, $J$ = 7.6, 1.8 Hz, 2H), 2.79 (dd, $J$ = 16.7, 7.8 Hz, 1H), 2.70 (dd, $J$ = 16.7, 6.3 Hz, 1H), 2.27 (s, 3H), 2.14 (tt, $J$ = 11.1, 3.3 Hz, 1H), 1.73–1.64 (m, 4H), 1.27–1.07 (m, 6H); **$^{13}$C NMR** (101 MHz, $CDCl_3$) $\delta$ 212.9, 144.5, 136.9, 135.6, 129.2, 128.9, 128.4, 127.8, 126.4, 51.4, 46.5, 42.7, 42.6, 28.2, 28.2, 26.0, 25.8, 25.7, 21.1; **HRMS** (ESI-TOF) Calc'd for $C_{23}H_{29}O^+$ $[M+H]^+$ 321.2218, found 321.2223.

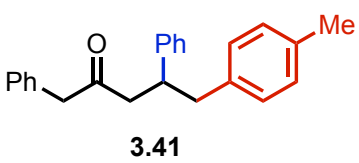


**3.41**

**1,4-Diphenyl-5-(*p*-tolyl)pentan-2-one (3.41)**: Purification by PTLC (100% toluene) the product was obtained as a white foam (13.8 mg, 42% yield, 10:1 r.r.). **$^1$H NMR** (600 MHz, $CDCl_3$) δ 7.27–7.20 (m, 5H), 7.18–7.14 (m, 1H), 7.09–7.06 (m, 2H), 6.99 (d, $J$ = 7.8 Hz, 4H), 6.88 (d, $J$ = 8.0 Hz, 2H), 3.48 (s, 2H), 3.43 (qd, $J$ = 7.6, 4.3 Hz, 1H), 2.85–2.76 (m, 3H), 2.72 (dd, $J$ = 16.4, 6.2 Hz, 1H), 2.27 (s, 3H); **$^{13}$C NMR** (101 MHz, $CDCl_3$) $\delta$ 207.2, 144.0, 136.6, 135.7, 134.0, 129.5, 129.2, 129.0, 128.8, 128.5, 127.7, 127.0, 126.5, 50.9, 47.5, 43.1, 42.6, 21.2; **HRMS** (ESI-TOF) Calc'd for $C_{24}H_{25}O^+$ $[M+H]^+$ 329.1905, found 329.1903.

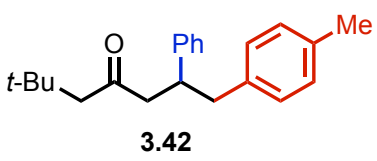


3.42

**6,6-Dimethyl-2-phenyl-1-(*p*-tolyl)heptan-4-one (3.42):** Purification by PTLC (100% toluene) the product was obtained as a colorless oil (16.0 mg, 52% yield, 8:1 r.r.). **$^1$H NMR** (600 MHz, $CDCl_3$) $\delta$ 7.26–7.22 (m, 2H), 7.17–7.15 (m, 1H), 7.14 (dt, $J$ = 8.0, 1.2 Hz, 2H), 7.01 (d, $J$ = 7.8 Hz, 2H), 6.93 (d, $J$ = 8.0 Hz, 2H), 3.48–3.39 (m, 1H), 2.83 (d, $J$ = 7.6 Hz, 2H), 2.69 (qd, $J$ = 16.6, 7.1 Hz, 2H), 2.27 (s, 3H), 2.16–2.08 (m, 2H), 0.87 (s, 9H); **$^{13}$C NMR** (101 MHz, $CDCl_3$) $\delta$ 209.7, 144.4, 136.8, 135.6, 129.2, 129.0, 128.4, 127.8, 126.4, 55.8, 50.7, 43.0, 42.6, 31.0, 29.7, 21.2; **HRMS** (ESI-TOF) Calc'd for $C_{22}H_{29}O^+$ $[M+H]^+$ 309.2218, found 309.2225.

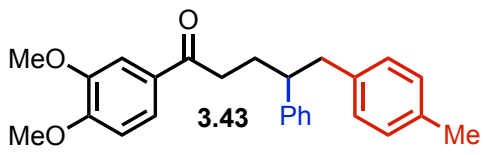


3.43

**1-(3,4-Dimethoxyphenyl)-4-phenyl-5-(*p*-tolyl)pentan-1-one (3.43):** Purification by sequential PTLCs (plate 1: 2 runs 20% EtOAc/hexane; plate 2: toluene:DCM:$Et_2O$ = 8:1:1) gave the product as white foam (23.5 mg, 60% yield, 8:1 r.r.). **$^1$H NMR** (600 MHz, $CDCl_3$) $\delta$ 7.40 (d, $J$ = 2.0 Hz, 1H), 7.34 (dd, $J$ = 8.4, 2.0 Hz, 1H), 7.28 (t, $J$ = 7.6 Hz, 2H), 7.21–7.17 (m, 1H), 7.17–7.14 (m, 2H), 7.01 (d, $J$ = 7.5 Hz, 2H), 6.94 (d, $J$ = 8.0 Hz, 2H), 6.78 (d, $J$ = 8.5 Hz, 1H), 3.91 (s, 3H), 3.88 (s, 3H), 2.93–2.87 (m, 3H), 2.71 (ddd, $J$ = 9.0, 6.5, 2.4 Hz, 2H), 2.27 (s, 3H), 2.20–2.13 (m, 1H), 2.00 (dtdd, $J$ = 14.4, 10.2, 7.1, 4.0 Hz, 1H); **$^{13}$C NMR** (101 MHz, $CDCl_3$) $\delta$ 199.1, 153.2, 149.0, 144.5, 137.3, 135.4, 130.3, 129.1, 128.9, 128.6, 128.0, 126.5, 122.7, 110.2, 110.0, 56.1, 56.1, 47.7, 43.7, 36.3, 30.4, 21.1; **HRMS** (ESI-TOF) Calc'd for $C_{26}H_{29}O_3^+$ $[M+H]^+$ 389.2117, found 389.2119.

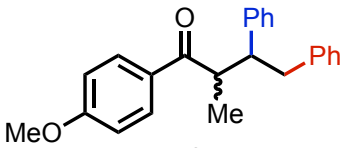


**3.44**

**1-(4-methoxyphenyl)-2-methyl-3-phenyl-4-(*p*-tolyl)butan-1-one (3.44):** Purification by sequential PTLCs (plate 1: 3 runs 20% EtOAc in hexane, plate 2: 5% EtOAc in hexane) gave the separated diastereomers as colorless oils (diastereomer 1: 11.1 mg, diastereomer 2: 6.8 mg, 52% yield, 1.5:1 d.r. from crude). *(±)-Diastereomer 1 (3.44'):* **$^1$H NMR** (600 MHz, $CDCl_3$) δ 7.80 (d, *J* = 8.9 Hz, 2H), 7.09 (dd, *J* = 8.5, 6.8 Hz, 4H), 7.05 (d, *J* = 7.8 Hz, 3H), 7.04–6.99 (m, 1H), 6.89 (d, *J* = 6.7 Hz, 2H), 6.86 (d, *J* = 8.9 Hz, 2H), 3.88–3.84 (m, 1H), 3.83 (s, 3H), 3.38 (ddd, *J* = 11.7, 8.2, 3.9 Hz, 1H), 3.21 (dd, *J* = 13.7, 3.9 Hz, 1H), 2.87 (dd, *J* = 13.6, 11.1 Hz, 1H), 1.37 (d, *J* = 6.9 Hz, 3H); **$^{13}$C NMR** (151 MHz, $CDCl_3$) δ 202.2, 163.2, 142.8, 140.1, 130.4, 129.9, 129.2, 128.4, 128.0, 127.9, 126.2, 125.7, 113.7, 55.4, 49.9, 45.8, 38.0, 15.4; **HRMS** (ESI-TOF) Calc'd for $C_{24}H_{25}O_2^+$ $[M+H]^+$ 345.1855, found 345.1849. *(±)-Diastereomer 2 (3.44''):* **$^1$H NMR** (600 MHz, $CDCl_3$) δ 7.99–7.95 (m, 2H), 7.23 (td, *J* = 7.3, 1.3 Hz, 2H), 7.18–7.14 (m, 1H), 7.13–7.09 (m, 2H), 7.07 (ddt, *J* = 7.9, 6.1, 1.3 Hz, 3H), 6.98–6.95 (m, 2H), 6.92–6.89 (m, 2H), 3.89 (s, 3H), 3.79 (dq, *J* = 9.4, 6.9 Hz, 1H), 3.37 (td, *J* = 9.7, 4.5 Hz, 1H), 2.96 (dd, *J* = 13.2, 4.5 Hz, 1H), 2.75 (dd, *J* = 13.2, 10.0 Hz, 1H), 0.94 (d, *J* = 6.9 Hz, 3H); **$^{13}$C NMR** (151 MHz, $CDCl_3$) δ 202.7, 163.5, 141.8, 140.1, 130.6, 130.19, 129.2, 128.7, 128.2, 127.9, 126.4, 125.8, 113.9, 55.5, 51.0, 45.0, 41.3, 16.6; **HRMS** (ESI-TOF) Calc'd for $C_{24}H_{25}O_2^+$ $[M+H]^+$ 345.1855, found 345.1852.

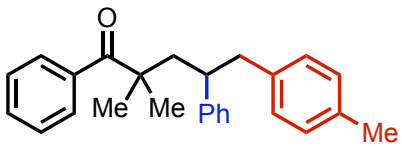


**3.53**

**2,2-Dimethyl-1,4-diphenyl-5-(*p*-tolyl)pentan-1-one (3.53):** Purification by sequential PTLCs (plate 1: 1 runs 20% EtOAc/hexane; plate 2: 10 runs 100%

hexanes) gave the product as colorless oil (11.2 mg, 31% yield, >20:1 r.r.). **$^1$H NMR** (600 MHz, $CDCl_3$) δ 7.56 (d, *J* = 8.1 Hz, 3H), 7.45–7.41 (m, 2H), 7.34 (t, *J* = 7.6 Hz, 2H), 7.30–7.26 (m, 1H), 7.23 (s, 2H), 7.14 (d, *J* = 7.6 Hz, 2H), 7.00 (d, *J* = 7.8 Hz, 2H), 3.06–3.00 (m, 1H), 2.90 (qd, *J* = 13.4, 7.5 Hz, 2H), 2.46–2.43 (m, 5H), 1.34 (s, 3H), 1.25 (s, 3H); **$^{13}$C NMR** (150 MHz, $CDCl_3$) *δ* 208.3, 145.4, 138.6, 137.1, 135.3, 130.6, 129.1, 128.8, 128.2, 128.1, 127.9, 127.8, 126.1, 47.9, 45.6, 45.2, 27.4, 26.8, 21.9, 21.0; **HRMS** (ESI-TOF) Calc'd for $C_{26}H_{29}O^+$ $[M+H]^+$ 357.2218, found 357.2222.

### 3.4.5. Unsuccessful/Low-Yielding Examples

***Table 3.S2.*** Unsuccessful/low-yielding heteroaryl iodides.

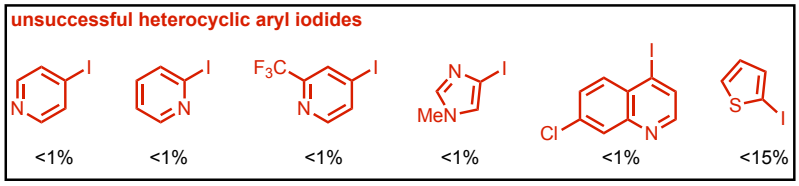


*NMR-yields

***Table 3.S3.*** Unsuccessful/low-yielding arylboronic acid neopentyl glycol esters.

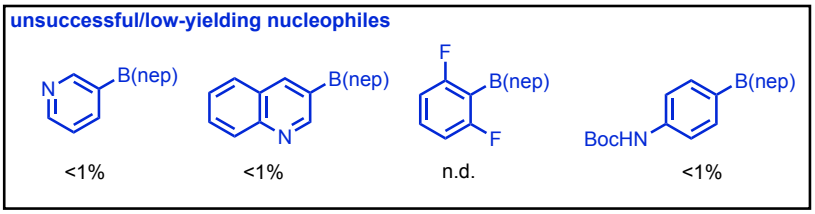


*NMR-yields

***Table 3.S4.*** Unsuccessful/low-yielding alkenyl ketones.

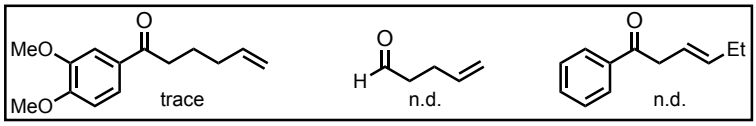

### 3.4.6. Control Experiment with γ,δ-Unsaturated Ketone

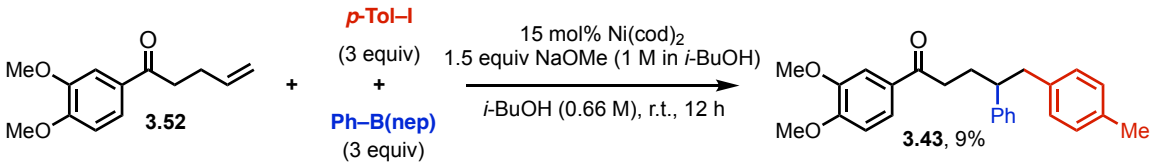


***Scheme 3.S8.*** Low-yielding 1,2-diarylation of γ,δ-unsaturated ketone in the absence of DMFU.

### 3.4.7. Proposed Catalytic Cycle

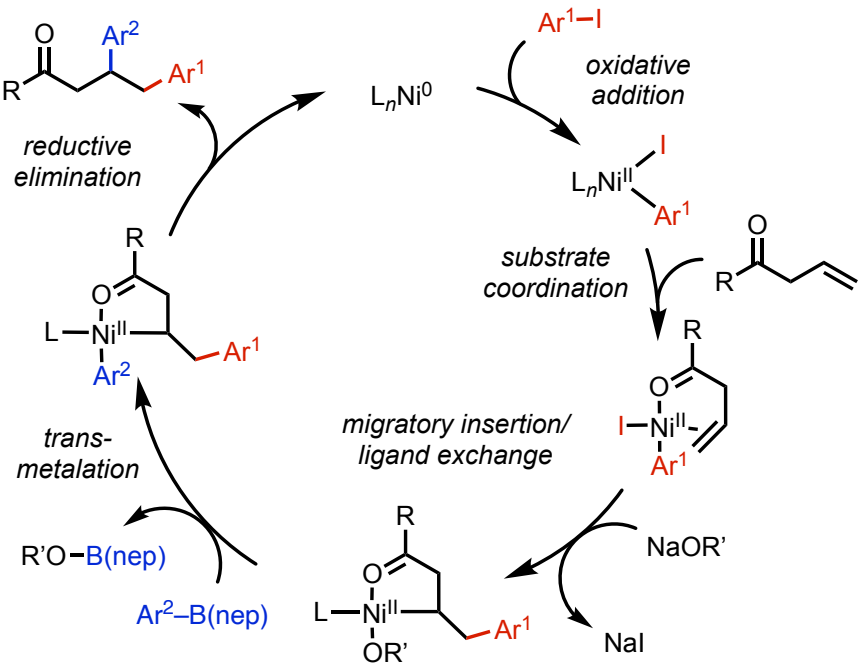


***Figure 3.S6.*** Proposed mechanism.

### 3.4.8. $^{1}$H NMR and $^{13}$C NMR Resonances of Ketone Substrates

***Table 3.S5.*** NMR resonances (ppm) of alkenes illustrating inductive effects.

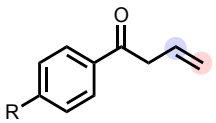


| | R = OMe | R = Me | R = H | R = Cl | R = $CF_3$ |
|---|---|---|---|---|---|
| $^{1}$H NMR (400 MHz) | 6.08, 5.28–5.14 | 6.09, 5.24–5.16 | 6.10, 5.28–5.17 | 6.07, 5.27–5.18 | 6.08, 5.33–5.18 |
| $^{13}$C NMR (126 MHz) | 131.5, 118.4 | 131.3, 118.6 | 131.1, 118.7 | 130.7, 119.0 | 130.3, 119.3 |

### 3.4.9. Deuterium Incorporation Experiment

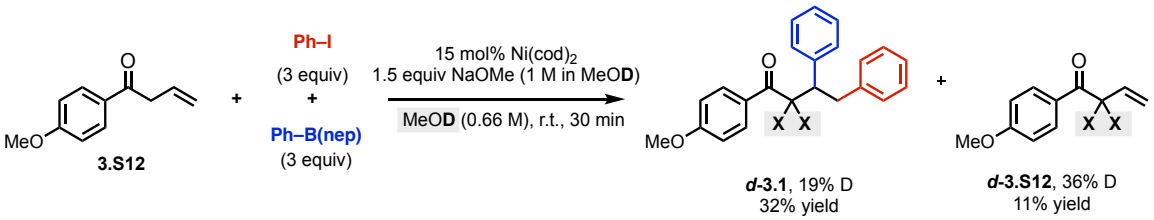


***Scheme 3.S9.*** Mechanistic experiment with deuterated alcohol solvent. Compounds ***d*-3.1** and ***d*-3.S12** were isolated together, and the yield was determined from the combined mass and $^1$H NMR analysis of the mixture.

Following slightly modified *general 1,2-diarylation procedure*, the reaction was performed with methanol-$d_4$. Deuterium incorporation was determined by $^1$H NMR (600 MHz, $CDCl_3$, relaxation delay d1=10 s) with the integration of the benzyl methylene signal (m, 2H) as internal standard for the product analysis; the integration of the terminal alkene signal (m, 2H) as internal standard for the starting material analysis.

## 3.5. REFERENCES

(1) For reviews, see: (a) Giri, R.; KC, S. Strategies toward Dicarbofunctionalization of Unactivated Olefins by Combined Heck Carbometalation and Cross-Coupling. *J. Org. Chem*. **2018**, *83*, 3013–3022; (b) Derosa, J.; Apolinar, O.; Kang, T.; Tran, V. T.; Engle, K. M. Recent Developments in Nickel-Catalyzed Intermolecular Dicarbofunctionalization of Alkenes. *Chem. Sci.* **2020**, *11*, 4287–4296; (c) Tu, H.-Y.; Zhu, S.; Qing, F.-L.; Chu, L. Recent Advances in Nickel-Catalyzed Three-Component Difunctionalization of Unactivated Alkenes. *Synthesis* **2020**, *52*, 1346–1356; (d) Badir, S. O.; Molander, G. A. Developments in Photoredox/Nickel Dual-Catalyzed 1,2-Difunctionalizations. *Chem* **2020**, *6*, 1327–1339; (e) Qi, X.; Diao, T. Nickel-Catalyzed Dicarbofunctionalization of Alkenes. *ACS Catal.* **2020**, *10*, 8542–8556.

(2) (a) Catellani, M.; Chiusoli, G. P.; Concari, S. A New Palladium Catalyzed Synthesis of *cis*,*exo*-2,3-Diarylsubstituted Bicyclo[2.2.1]heptanes or Bicyclo[2.2.1]hept-2-enes. *Tetrahedron* **1989**, *45*, 5263–5268; (b) Stokes, B. J.; Liao, L.; de Andrade, A. M.; Wang, Q.; Sigman, M. S. A Palladium-Catalyzed Three-Component-Coupling Strategy for the Differential Vicinal Diarylation of Terminal 1,3-Dienes. *Org. Lett.* **2014**, *16*, 4666–4669; (c) Kuang, Z.; Yang, K.; Song, Q. Pd-Catalyzed 1,2-Diarylation of Vinylarenes at Ambient Temperature. *Org. Chem. Front.* **2017**, *4*, 1224–1228; (d) Shrestha, B.; Basnet, P.; Dhungana, R. K.; KC, S.; Thapa, S.; Sears, J. M.; Giri, R. Ni-Catalyzed Regioselective 1,2-Dicarbofunctionalization of Olefins by Intercepting Heck Intermediates as Imine-Stabilized Transient Metallacycles. *J. Am. Chem. Soc.* **2017**, *139*, 10653–10656; (e) Gao, P.; Chen, L.-A.; Brown, M. K. Nickel-Catalyzed Stereoselective Diarylation of Alkenylarenes. *J. Am. Chem. Soc.* **2018**, *140*, 10653–10657.

(3) (a) Derosa, J.; Tran, V. T.; Boulous, M. N.; Chen, J. S.; Engle, K. M. Nickel-Catalyzed β,γ-Dicarbofunctionalization of Alkenyl Carbonyl Compounds via Conjunctive Cross-Coupling. *J. Am. Chem. Soc.* **2017**, *139*, 10657–10660; (b) Li, W.; Boon, J. K.; Zhao, Y. Nickel-Catalyzed Difunctionalization of Allyl Moieties using Organoboronic Acids and Halides with Divergent Regioselectivities. *Chem. Sci.* **2018**, *9*, 600–607; (c) Thapa, S.; Dhungana, R. K.; Magar, R. T.; Shrestha, B.; KC, S.; Giri, R. Ni-Catalysed Regioselective 1,2-Diarylation of Unactivated Olefins by Stabilizing Heck Intermediates as Pyridylsilyl-Coordinated Transient Metallacycles. *Chem. Sci.* **2018**, *9*, 904–909; (d) Derosa, J.; van der Puyl, V. A.; Tran, V. T.; Liu, M.; Engle, K. M. Directed Nickel-Catalyzed 1,2-Dialkylation of Alkenyl Carbonyl Compounds. *Chem. Sci.* **2018**, *9*, 5278–5283; (e) Derosa, J.; Kleinmans, R.; Tran, V. T.; Karunananda, M. K.; Wisniewski, S. R.;

Eastgate, M. D.; Engle, K. M. Nickel-Catalyzed 1,2-Diarylation of Simple Alkenyl Amides. *J. Am. Chem. Soc.* **2018**, *140*, 17878–17883; (f) Tran, V. T.; Li, Z.-Q.; Gallagher, T. J.; Derosa, J.; Liu, P.; Engle, K. M. Integrating Allyl Electrophiles into Nickel-Catalyzed Conjunctive Cross-Coupling. *Angew. Chem., Int. Ed.* **2020**, *59*, 7029–7034; (g) Derosa, J.; Kang, T.; Tran, V. T.; Wisniewski, S. R.; Karunananda, M. K.; Jankins, T. C.; Xu, K. L.; Engle, K. M. Nickel-Catalyzed 1,2-Diarylation of Alkenyl Carboxylates: A Gateway to 1,2,3-Trifunctionalized Building Blocks. *Angew. Chem., Int. Ed.* **2020**, *59*, 1201–1205. For related work involving sulfonamide coordination, see: (h) Apolinar, O.; Tran, V. T.; Kim, N.; Schmidt, M. A.; Derosa, J.; Engle, K. M. Sulfonamide Directivity Enables Ni-Catalyzed 1,2-Diarylation of Diverse Alkenyl Amines. *ACS Catal.* **2020**, *10*, 14234–14239.

(4) For examples of carbonyl-directed two-component C–C cross-couplings, see (Pd): (a) Sandrock, D. L.; Jean-Gérard, L.; Chen, C.; Dreher, S. D.; Molander, G. A. Stereospecific Cross-Coupling of Secondary Alkyl β-Trifluoroboratoamides. *J. Am. Chem. Soc.* **2010**, *132*, 17108–17110; (Ni): (b) Wilsily, A.; Tramutola, F.; Owston, N. A.; Fu, G. C. New Directing Groups for Metal-Catalyzed Asymmetric Carbon–Carbon Bond-Forming Processes: Stereoconvergent Alkyl–Alkyl Suzuki Cross-Couplings of Unactivated Electrophiles. *J. Am. Chem. Soc.* **2012**, *134*, 5794–5797.

(5) Huang, Z.; Lim, H. N.; Mo, F.; Young, M. C.; Dong, G. Transition Metal-Catalyzed Ketone-Directed or Mediated C–H Functionalization. *Chem. Soc. Rev.* **2015**, *44*, 7764–7786.

(6) For representative examples of radical-based, nickel-catalyzed, carbonyl-directed 1,2-dicarbofunctionalization of alkenes, see: (a) Gu, J.-W.; Min, Q.-Q.; Yu, L.-C.; Zhang, X.

Tandem Difluoroalkylation-Arylation of Enamides Catalyzed by Nickel. *Angew. Chem., Int. Ed.* **2016**, *55*, 12270–12274; (b) García-Domínguez, A.; Li, Z.; Nevado, C. Nickel-Catalyzed Reductive Dicarbofunctionalization of Alkenes. *J. Am. Chem. Soc.* **2017**, *139*, 6835−6838; (c) Zhao, X.; Tu, H.-Y.; Guo, L.; Zhu, S.; Qing, F.-L.; Chu, L. Intermolecular Selective Carboacylation of Alkenes via Nickel-Catalyzed Reductive Radical Relay. *Nat. Commun.* **2018**, *9*, 3488; (d) Xu, C.; Yang, Z.-F.; An, L.; Zhang, X. Nickel-Catalyzed Difluoroalkylation–Alkylation of Enamides. *ACS Catal.* **2019**, *9*, 8224–8229; (e) Yang, Z.-F.; Xu, C.; Zheng, X.; Zhang, X. Nickel-Catalyzed Carbodifunctionalization of *N*-Vinylamides Enables Access to γ-Amino Acids. *Chem. Commun.* **2020**, *56*, 2642–2645; (f) Wei, X.; Shu, W.; García-Domínguez, A.; Merino, E.; Nevado, C. Asymmetric Ni-Catalyzed Radical Relayed Reductive Coupling. *J. Am. Chem. Soc.* **2020**, *142*, 13515–13522; (g) Tu, H.-Y.; Wang, F.; Huo, L.; Li, Y.; Zhu, S.; Zhao, X.; Li, H.; Qing, F.-L.; Chu, L. Enantioselective Three-Component Fluoroalkylarylation of Unactivated Olefins through Nickel-Catalyzed Cross-Electrophile Coupling. *J. Am. Chem. Soc.* **2020**, *142*, 9604–9611. For related work involving copper catalysis, see: (h) Zhou, S.; Zhang, G.; Fu, L.; Chen, P.; Li, Y.; Liu, G. Copper-Catalyzed Asymmetric Cyanation of Alkenes via Carbonyl-Assisted Coupling of Alkyl-Substituted Carbon-Centered Radicals. *Org. Lett.* **2020**, *22*, 6299–6303.

(7) (a) Basnet, P.; Dhungana, R. K.; Thapa, S.; Shrestha, B.; KC, S.; Sears, J. M.; Giri, R. Ni-Catalyzed Regioselective β,δ-Diarylation of Unactivated Olefins in Ketimines via Ligand-Enabled Contraction of Transient Nickellacycles: Rapid Access to Remotely Diarylated Ketones. *J. Am. Chem. Soc.* **2018**, *140*, 7782–7786; (b) Basnet, P.; KC, S.; Dhungana, R. K.; Shrestha, B.; Boyle, T. J.; Giri, R. Synergistic Bimetallic Ni/Ag and

Ni/Cu Catalysis for Regioselective γ,δ-Diarylation of Alkenyl Ketimines: Addressing β-H Elimination by in Situ Generation of Cationic Ni(II) Catalysts. *J. Am. Chem. Soc.* **2018**, *140*, 15586–15590; (c) Dhungana, R. K.; KC, S.; Basnet, P.; Aryal, V.; Chesley, L. J.; Giri, R. Ni(I)-Catalyzed β,δ-Vinylarylation of γ,δ-Alkenyl α-Cyanocarboxylic Esters via Contraction of Transient Nickellacycles. *ACS Catal*. **2019**, *9*, 10887–10893.

(8) For examples of electron-deficient olefin ligands in nickel-catalysis, see Refs. 3e,h and the following: (a) Jensen, A. E.; Knochel, P. Nickel-Catalyzed Cross-Coupling between Functionalized Primary or Secondary Alkylzinc Halides and Primary Alkyl Halides. *J. Org. Chem.* **2002**, *67*, 79−85; (b) Estrada, J. G.; Williams, W. L.; Ting, S. I.; Doyle, A. G. Role of Electron-Deficient Olefin Ligands in a Ni-Catalyzed Aziridine Cross-Coupling to Generate Quaternary Carbons. *J. Am. Chem. Soc.* **2020**, *142*, 8928–8937; (c) Kim, N.; Tran, V. T.; Apolinar, O.; Wisniewski, S. R.; Eastgate, M. D. Ni(COD)(DMFU): A Heteroleptic 16-Electron Precatalyst for 1,2-Diarylation of Alkenes. *Synlett* **2021**, *32*, 157–1574.

(9) Wethman, R.; Derosa, J.; Tran, V. T.; Kang, T.; Apolinar, O.; Abraham, A.; Kleinmans, R.; Wisniewski, S. R.; Coombs, J. R.; Engle, K. M. An Under-Appreciated Source of Reproducibility Issues in Cross-Coupling: Solid-State Decomposition of Primary Sodium Alkoxides in Air. *ACS Catal.* **2021**, *11*, 502–508.

(10) For previous reports describing the superior performance of ArB(nep) nucleophiles in nickel-catalyzed cross-coupling, see: (a) Shimasaki, T.; Konno, Y.; Tobisu, M.; Chatani, N. Nickel-Catalyzed Cross-Coupling Reaction of Alkenyl Methyl Ethers with Aryl Boronic Esters. *Org. Lett.* **2009**, *11*, 4890–4892; (b) Martin-Montero, R.;

Krolikowski, T.; Zarate, C.; Manzano, R.; Martin, R. Stereospecific Nickel-Catalyzed Borylation of Secondary Benzyl Pivalates. *Synlett* **2017**, *28*, 2604–2608.

(11) A previous version of this paper was deposited on a preprint server: Kleinmans, R.; Apolinar, O.; Derosa, J.; Karunananda, M. K.; Li, Z.-Q.; Tran, V. T.; Wisniewski, S. R.; Engle, K. M. Nickel-Catalyzed 1,2-Diarylation of Alkenyl Ketones: A Comparative Study of Carbonyl-Directed Reaction Systems, *ChemRxiv* **2021**, DOI: 10.26434/chemrxiv.14150174.

(12) Makida, Y.; Marelli, E.; Slawin, A. M. Z.; Nolan, S. P. "Nickel-Catalysed Carboxylation of Organoboronates." *Chem. Commun.* **2014**, *50*, 8010–8013.

(13) Koseki, Y.; Kitazawa, K.; Miyake, M.; Kochi T.; Kakiuchi, F. "Ruthenium-Catalyzed Ortho C–H Arylation of Aromatic Nitriles with Arylboronates and Observation of Partial Para Arylation." *J. Org. Chem.* **2017**, *82*, 6503–6510.

(14) Zhu, L.; Yu, H.; Xu, Z.; Jiang, X.; Lin, L.; Wang, R. "Copper-Catalyzed Oxyazidation of Unactivated Alkenes: A Facile Synthesis of Isoxazolines Featuring an Azido Substituent." *Org. Lett.* **2014**, *16*, 1562–1565.

(15) Zhuo, L.-G.; Yao, Z. K.; Yu, Z.-X. "Synthesis of *Z*-Alkenes from Rh(I)-Catalyzed Olefin Isomerization of β,γ-Unsaturated Ketones." *Org. Lett.* **2013**, *15*, 4634–4637.

(16) CCDC 1957926 (**3.5**) contains the supplementary crystallographic data for this paper. These data can be obtained free of charge from The Cambridge Crystallographic Data Centre *via* www.ccdc.cam.ac.uk/data_request/cif.

## 3.6. CONTRIBUTIONS

The following individuals directly contributed to the work described in this Chapter: Omar Apolinar, Roman Kleinmans, Joseph Derosa, Malkanthi K. Karunananda, Zi-Qi Li, Van T. Tran, Steven R. Wisniewski, and Prof. Keary M. Engle. O.A., R.K., J.D., and K.M.E. conceived the project. Preliminary reaction optimization was performed by R.K. and final reaction optimization was carried out by O.A. Substrate synthesis was effectuated by O.A., R.K., J.D., Z.-Q.L., and V.T.T. Product isolation and characterization was carried out by O.A. and R.K. Mechanistic experiments were carried out by O.A. (experimental), J.D. (experimental), M.K.K. (computational), and S.R.W from BMS (kinetics). The Chapter was adapted with permission from a published manuscript, which was written by O.A., R.K., J.D., and K.M.E.

# CHAPTER 4

## SULFONAMIDE DIRECTIVITY ENABLES NICKEL-CATALYZED 1,2-DIARYLATION OF DIVERSE ALKENYL AMINES

Adapted with permission from:

Apolinar, O.; Tran, V. T.; Kim, N.; Schmidt, M. A.; Derosa, J.; Engle, K. M. *ACS Catal.* **2020**, *10*, 14234–14239.

Copyright © 2020 American Chemical Society.

## 4.1. INTRODUCTION

The construction of contiguous C–C bonds through 1,2-dicarbofunctionalization of alkenes, also known as conjunctive cross-coupling, has flourished into a buzzing area of catalysis that exploits the unique reactivity of transition metals, including Pd, Ni, Co, Cu, and Fe.[1a-b] In this reaction paradigm, base metal nickel provides distinctive advantages compared to other transition metals, such as precious metal palladium, by having a higher disposition toward oxidative addition and 1,2-migratory insertion elementary steps while simultaneously being more resilient towards β-hydride elimination.[1c] 1,2-Dicarbofunctionalization of alkenyl amines, wherein a stabilized amine directs the nickel catalyst in the catalytic cycle without concomitant catalyst poisoning, is an attractive approach not only for selectivity control, but for rapid entry to highly functionalized alkyl amine product libraries. In 2016 and 2017, Zhang[2a] and Giri[2d] reported 2-(fluoroalkyl)arylation and 1,2-diarylation of electronically activated enamides and ortho-vinyl aniline derivatives, respectively (Scheme 1). Thereafter, Zhao and coworkers reported the use of an irremovable pyrimidyl directing group that enables the 1,2-dicarbofunctionalization of non-conjugated terminal alkenes presumably via a Ni–N($sp^2$) coordination mode.[2e] Our group has successfully achieved 1,2-diarylation and 1,2-allylmethylation of alkenyl amides and *N*-allyl heterocycles by leveraging native directing effects.[3a-b] It is important to note that Ni-catalyzed 1,2-dicarbofunctionalization reactions of other classes of unactivated alkenes have been demonstrated by other research groups via different mechanistic modalities.[4] This progress notwithstanding, major limitations remain in this area of study. To date, current methods are incompatible with homoallyl, bis-homoallyl amines, and internal alkenyl amine substrates.

Furthermore, the directing groups used in earlier reports are synthetically limiting in that they cannot be removed for further functionalization. The goal of the present investigation was to pinpoint an amine-based, native directing group capable of facilitating 1,2-diarylation of distal, highly substituted alkenes. Then, such 1,2-diarylated products could engage in downstream *N*-functionalization chemistry, allowing alkenyl amines to act as linchpins in modular synthesis. To this end, we disclose the elucidation of sulfonamides as exclusively efficacious and versatile[5,6] directing groups in 1,2-diarylation of unactivated alkenes under nickel/dimethyl fumarate (DMFU) catalysis.[7]

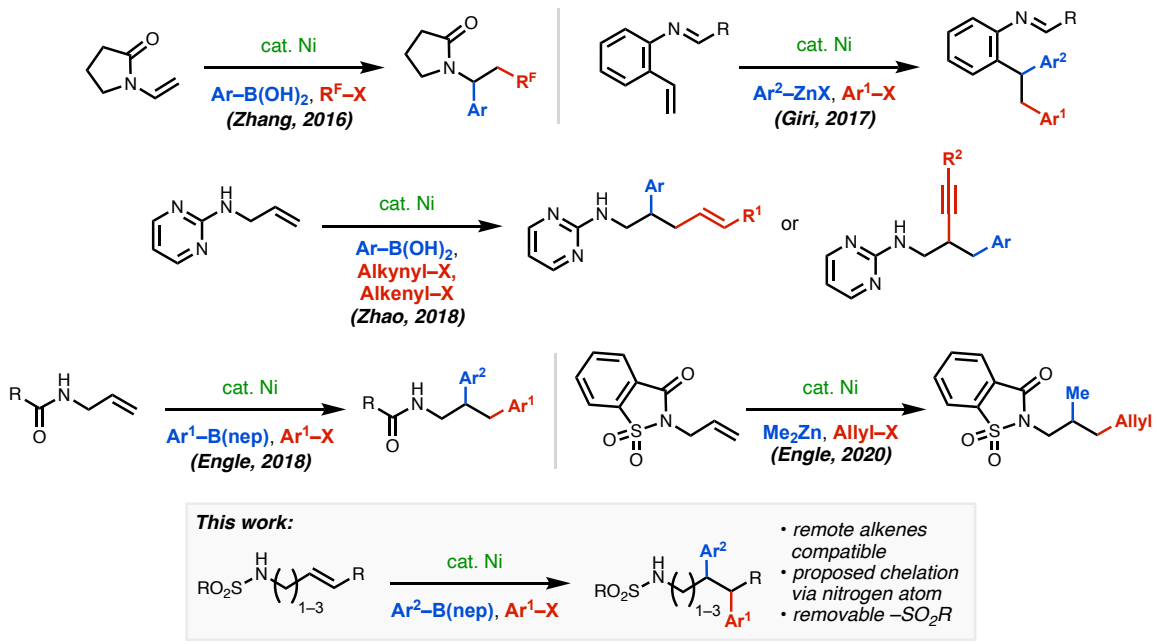


***Scheme 4.1.*** Previous reports and synopsis of new findings.

## 4.2. RESULTS AND DISCUSSION

### 4.2.1. Reaction Optimization

To initiate this investigation, we used iodobenzene (PhI) and 4-tolylboronic acid neopentyl glycol ester (*p*-TolB(nep)) as model coupling partners and surveyed various homoallyl amine substrates bearing viable native directing groups under $Ni(cod)_2$/DMFU

catalytic conditions (Table 4.1.).[2e,3a-b] We found that benzoylsulfonyl, phthaloyl, pyrimidyl, 2-picolinoyl, and diphenylphosphinic protecting groups did not effectuate the desired 1,2-diarylation reaction.[8] Carbonyl-based groups that were previously found to be efficacious, namely Boc-, Piv-, and Bz-, were incompetent with a more distal alkene motif. Then, we turned to sulfonyl-based protecting groups[6] with the aim that the nickel catalyst may bind the sulfonamide through nitrogen atom since the N–H would be more acidic. The triflyl-protected homoallyl amine gave the desired 1,2-diarylated product, but in low yield. Gratifyingly, switching to an aryl sulfonyl group provided 1,2-diarylated product **4.2** in excellent yield and regioselectivity, and the desired structural connectivity was confirmed by single-crystal X-ray diffraction. While other aryl sulfonamide native directing groups were similarly efficacious, the 4-(trifluoromethyl)-phenyl group provided a convenient $^{19}F$ NMR marker for reaction analysis of regioisomers, and thus was employed for most of this work. Without the use of DMFU ligand and utilization of aryl boronic acid and pinacol ester resulted in lower yields, highlighting the significance of electron-deficient olefin (EDO) DMFU ligand in facilitating reductive elimination and importance of the neopentyl glycol ester (nep) moiety (Entries 1–3).[7] Unfortunately, bromobenzene electrophile was found to be unreactive, and other nickel precatalysts, such as Ni(cod)(DQ), $NiCl_2$, $Ni(acac)_2$, and $NiBr_2$•glyme, were inactive upon subjection to the reaction conditions (Entries 4–5). Under our previously reported reaction conditions for 1,2-diarylation of alkenyl amide starting materials, diminished yield was observed (Entry 6). No 1,2-diarylation was obtained under previously published conditions for alkenyl carboxylate substrates (Entry 7).[3a,4i] Excellent yields were also obtained when lower catalyst loading or equivalents of coupling partners and base were

used with the model alkenyl sulfonamide substrate (Entry 8–9); however, other alkenyl sulfonamide substrates required higher loading and equivalents to obtain higher yields.

***Table 4.1.*** Optimization of 1,2-diarylation reaction.[a]

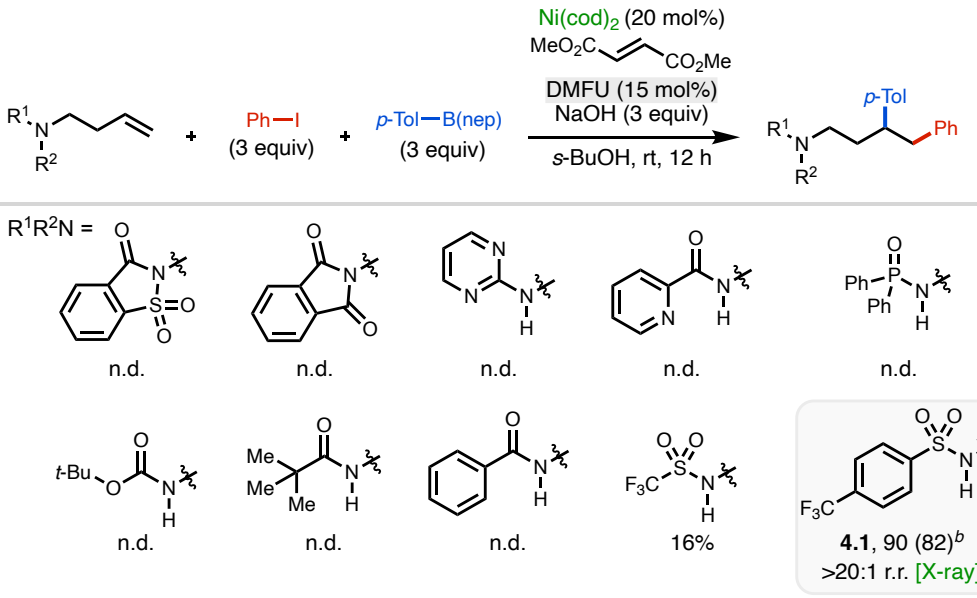


| entry | deviation from standard conditions | %Yield **4.1**[c] |
|---|---|---|
| 1 | no ligand | 30 |
| 2 | *p*-tol-B(OH)$_2$ instead of *p*-tol-B(nep) | 54 |
| 3 | *p*-tol-B(pin) instead of *p*-tol-B(nep) | 50 |
| 4 | Ph-Br instead of Ph-I | n.d. |
| 5 | Ni(cod)(DQ), NiCl$_2$, Ni(acac)$_2$, or NiBr$_2$•glyme instead of Ni(cod)$_2$ | n.d. |
| 6 | conditions from alkenyl amide diarylation[d] | 60 |
| 7 | conditions from alkenyl carboxylate diarylation[e] | n.d. |
| 8 | 10 mol% Ni(cod)$_2$ instead of 20 mol% | 90 |
| 9 | 1.5 equiv of PhI, *p*-tolB(nep), NaOH instead of 3 equiv | 90 |

[a]Reaction conditions: alkene SM (0.1 mmol), *s*-BuOH (0.2 M). [b]Values in parentheses are isolated yields. [c]Percentage yield by $^1$H NMR using $CH_2Br_2$ as the internal standard; n.d. = not detected. [d]Reaction conditions: 15 mol% Ni(cod)$_2$, 15 mol% dimethylfumarate, 1.5 equiv ArI, 1.5 equiv ArB(nep), 2 equiv NaOH, *i*-BuOH (0.2 M) at r.t. [e]Reaction conditions: 15 mol% Ni(cod)$_2$, 2 equiv ArI, 2 equiv ArB(nep), 2 equiv NaOH, *s*-BuOH (0.1 M) at 50 °C.

### 4.2.2. Substrate Scope

With optimized reaction conditions in hand, we turned to the exploration of the electrophile and nucleophile aryl coupling partner scope (Table 4.2.). Electrophiles with strong or weak electron-withdrawing groups at the *para* position afforded the highest product yields (**4.2–4.3**, **4.9**), whereas the product yield decreased moving towards electron-neutral and -donating groups (**4.5–4.6**, **4.13**). It is important to note that a scaled-up reaction was feasible, which furnished product **4.2** in an excellent yield (1 mmol, 0.48 g isolated). To our surprise, electrophiles with electron-withdrawing groups on the *meta* position gave no desired 1,2-diarylated product. On the other hand, electrophiles with electron-neutral and -donating groups on the *meta* position gave 1,2-diarylation in excellent yields (**4.7**, **4.14**). Electrophiles with *ortho*-substituted electron-withdrawing or donating groups had little negative effect on the product yield (**4.4**, **4.8**, **4.10**). To our delight, heterocyclic aryl iodides were also tolerated upon subjection to reaction conditions. Weakly electron-deficient 2-fluoro-4-iodopyridine electrophile gave a good yield (**4.11**), while more electron-deficient 4-iodo-2-(trifluoromethyl)pyridine gave a moderate yield (**4.12**). With regard to the nucleophile scope, no apparent trend was observed as was the case in the electrophile scope. Nucleophiles with electron-withdrawing and weakly electron-donating groups on the *para* position gave high yields (**4.15–4.16**, **4.20**). Aryl boronic esters with electron-donating groups on the *para* position gave good to excellent yields (**4.19**, **4.23**) except for the nucleophile with the Boc-protected amine substituent, which afforded product in a moderate yield (**4.22**). Lastly, nucleophiles with electron withdrawing groups on the *meta* and *ortho* positions (**4.17, 4.18, 4.21, 4.24**) afforded 1,2-diarylated products in moderate to excellent yields.

***Table 4.2.*** Electrophile and nucleophile scope.[a]

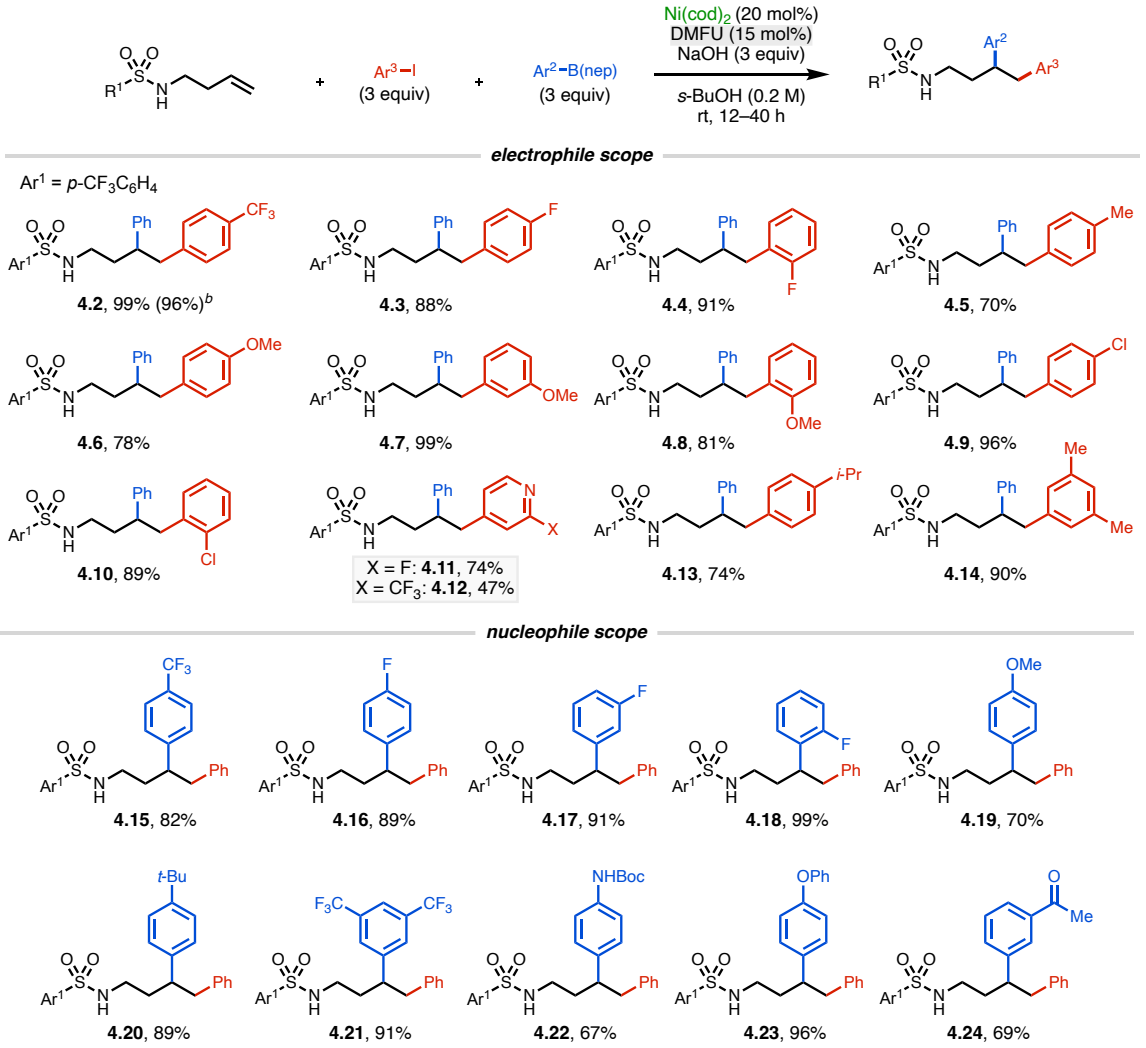


[a]Reactions performed on 0.1 mmol scale. [b]Reactions performed on 1 mmol scale. Percentages represent isolated yields.

Next, we examined the sulfonamide scope where we first varied the *para*-substitution of the aryl sulfonyl group and observed good to excellent yields (**4.25**–**4.27**, Table 4.3.). Gratifyingly, mesyl (Ms) protected homoallyl amine substrate was tolerated under the reaction conditions giving 1,2-diarylated product in a good yield (**4.28**). However, 1,2-diarylated product was not detected when a nosyl protecting group was used, which we attribute to the potential inhibitory effect of nitro groups on low valent Ni

species.[9] We then examined substituted alkene substrates that are typically not viable in Ni-catalyzed 1,2-diarylation reactions. 1,2-disubstituted (*Z*)- and (*E*)-alkenes were well tolerated under the optimized reaction conditions. Two 1,2-disubstituted (*Z*)-alkenes gave 1,2-diarylated products (**4.29**, **4.30**) in good yields and as single diastereomers, which was confirmed by single-crystal X-ray diffraction. Various 1,2-disubstituted (*E*)-alkenes were successfully 1,2-diarylated in good yields as well (**4.31–4.33**). Additionally, several 1,1-disubstituted alkenes were found to give the desired 1,2-diarylated products in low to moderately good yields (**4.34–4.36**). 1,2-diarylated product **4.37** was furnished in a mighty 40% yield with excellent diastereoselectivity from a trisubstituted (*E*)-alkene. Alkenyl sulfonamides with substitution at the α- or β-positions gave no conversion towards the desired 1,2-diarylated product. A homoprenyl trisubstituted alkenyl sulfonamide substrate deemed ineffective in giving the 1,2-diarylated product, instead the hydroarylated byproduct is mainly generated presumably via protodemetalation of the $Ni^{II}$(alkyl)(sulfonamido) intermediate. Lastly, a tetrasubstituted alkenyl sulfonamide substrate was completely inert to the reaction conditions.

***Table 4.3.*** Sulfonamide and alkene scope.[a]

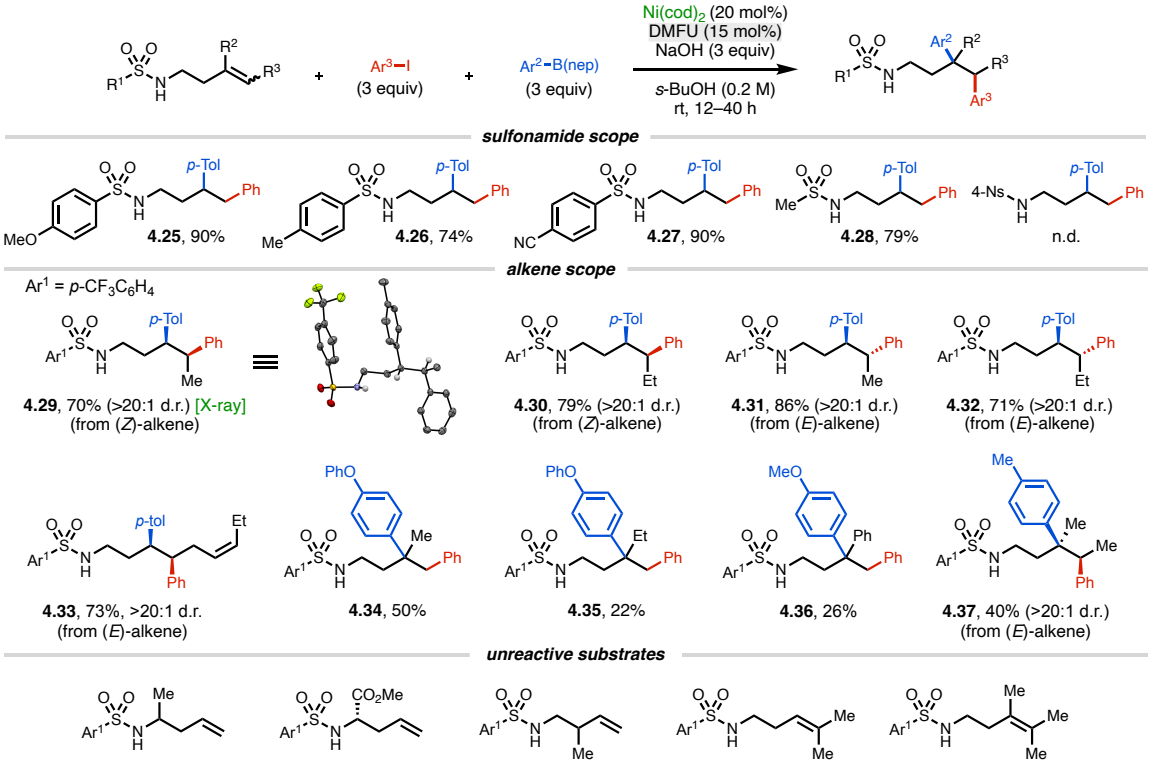


[a]Reactions performed on 0.1 mmol scale. Percentages represent isolated yields.

### 4.2.3. Control Experiments

To test whether N–H moiety is important in the transformation, a series of control experiments were performed, where homoallyl aryl sulfonate **4.38** and *N*-methylated sulfonamides **4.39** and **4.40** were subjected to the reaction conditions, which gave no 1,2-diarylated product formation (Scheme 4.2.). This observation also indicates that the neutral oxygen atoms of the sulfonamide functional group are unlikely to be involved in directing nickel.

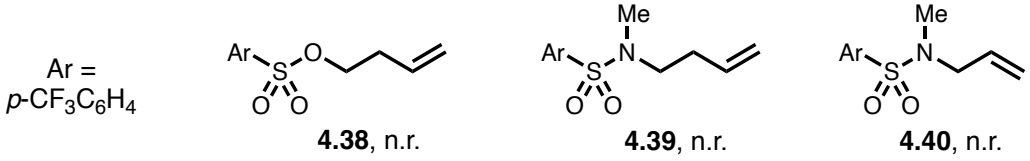


***Figure 4.1.*** Control experiments upon 1,2-diarylation reaction.

### 4.2.4. Tether Length Effects

Although we were fortunate in developing a remote alkene 1,2-diarylation reaction, we were interested about the impact of alkene distance on reactivity and regioselectivity (Table 4.4). We initiated this part of the study by examining the electrophile and nucleophile scopes for the aryl sulfonyl protected allyl and bis-homoallyl amines. In particular, we focused on investigating the electronic effects of the coupling partners. For the protected allyl amine substrate, electron-deficient electrophiles gave low yields but good regioselectivity (**4.41–4.42**) while electron-neutral and donating electrophiles gave higher yields albeit with lower regioselectivity (**4.43–4.44**). With regard to the protected bis-homoallyl amine substrate, electron-deficient and electron-donating electrophiles gave moderate to good yields accompanied with excellent regioselectivity (**4.45–4.48**). In terms of the nucleophile scope, for the protected allyl amine starting material, electron-deficient arylboronic esters gave the 1,2-diarylated product in good yields and excellent regioselectivity (**4.49–4.50**), whereas electron-neutral and electron-donating arylboronic esters gave diminished yields and regioselectivity (**4.51–4.52**). Across all the tested nucleophiles, moderate to excellent yields and excellent regioselectivity were obtained with the protected bis-homoallyl amine substrate (**4.53–4.56**). Elongation of the alkenyl chain to aryl sulfonyl protected bis,bis-homoallyl amine gave no desired 1,2-diarylated product. We envision that these alkenyl sulfonamide substrates likely proceed through 4–6-membered *N*-bound nickelacycles,[7c–d] where a 7-membered nickelacycle is thermodynamically unfavorable. The intermediacy of 6–8-membered O-bound (X-type) nickelacycles cannot be ruled out; however, it is less likely since tertiary sulfonamides are unreactive in this reaction

system. This, in turn, is the opposite trend to our previous report[3a] in which tertiary amides were viable substrates via O-bound intermediates which were supported by experimental and computational data.

***Table 4.4.*** Tether length effects on 1,2-diarylation.

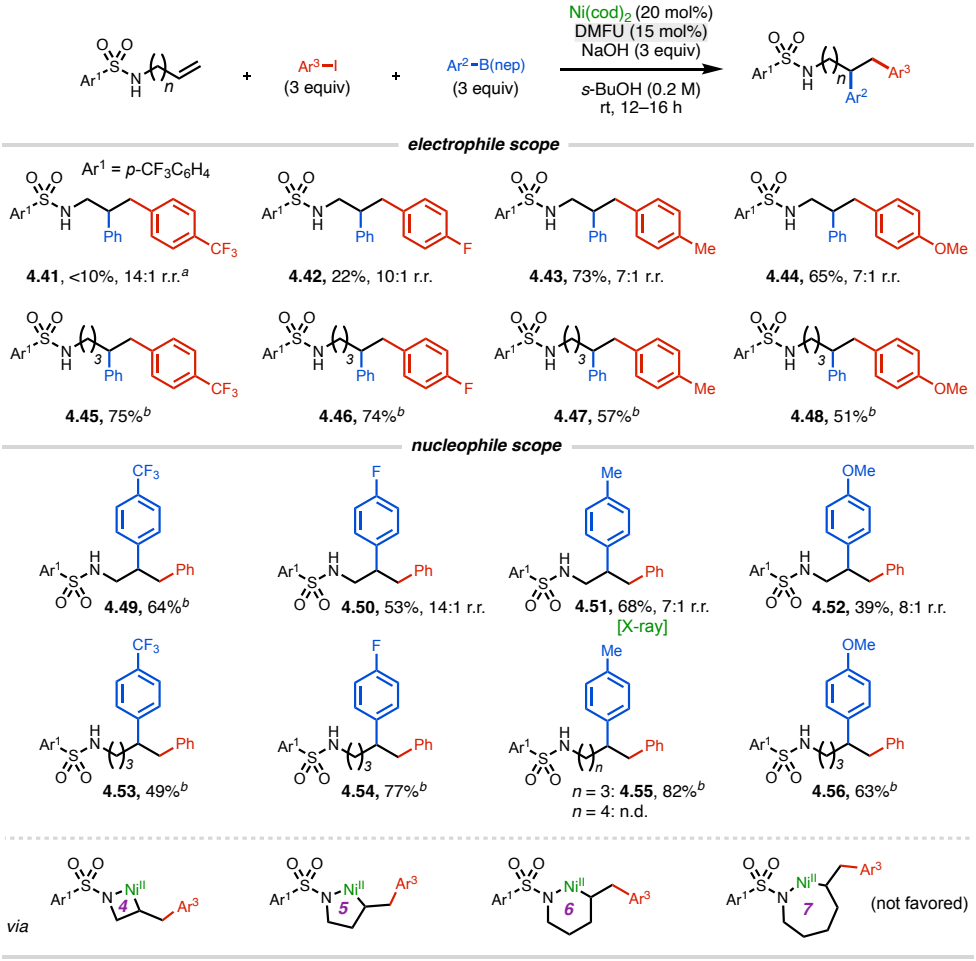


[a]Percentage yield by $^1$H NMR using $CH_2Br_2$ as the internal standard. [b]Product isolated as a single regioisomer (>20:1).

### 4.2.5. Proposed Catalytic Cycle

We envision this reaction proceeds via the key N–Ni coordination mode,[10] and the general catalytic cycle likely follows a similar pathway as that described of our previous

native directed 1,2-diarylation reactions (Figure 4.1.).[3a,4i] The catalytic cycle likely starts with nickel oxidatively adding into the aryl–iodide bond of the electrophile, followed by alkene coordination of the alkenyl sulfonamide substrate. Then, migratory insertion follows with the formation of the putative $Ni^{II}$(alkyl)(sulfonamido) metallacycle. Next, transmetalation[11] gives a $Ni^{II}$(alkyl)(aryl) species, which undergoes facile reductive elimination with the aid of DMFU to give the 1,2-diarylated product.[7c–e] It could also be plausible that this catalytic cycle may also function with the sulfonamide directing group as an L-type ligand donor upon migratory insertion; thus this alternative mechanism cannot be ruled out at this time.

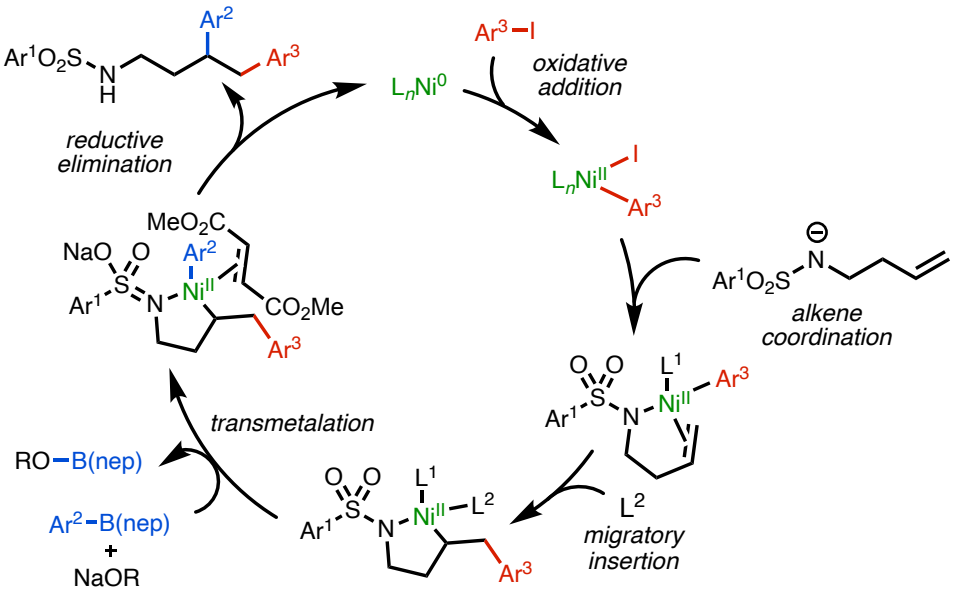


***Figure 4.2.*** Proposed catalytic cycle having directing group with X-type coordination upon migratory insertion. $L^1$ and $L^2$ represent neutral donors including DMFU, alkene substrate, solvent, etc.

### 4.2.6. Diversification of Representative Products

We then foresaw that this reaction could have an application in organic synthesis as a linchpin technology where the 1,2-diarylated products could be *N*-functionalized

followed by subsequent mild deprotection to form highly functionalized amines that would otherwise be cumbersome to synthesize. The 4-cyano-phenyl sulfonyl (4-Cs) protecting group was, therefore, appealing due to its precedented ease of removal by use of 1-dodecanethiol in comparison to the nosyl protecting group; hence, it was utilized in our scale-up and diversification efforts.[5] Thus, we synthesized 1,2-diarylated product **4.57** in a very good yield on a 1 mmol scale (Scheme 4.2.). This compound was then subjected to a series of *N*-functionalization reactions, namely Mitsunobu coupling, propargylation, benzylation, $S_NAr$, and Boc protection reactions, which furnished a diverse set of *N*-functionalized products in moderate to good yields (**4.58–4.62**). Next, mild treatment with 1-dodecanethiol and DBU led to the deprotection of the aryl sulfonyl group generating dialkyl, alkyl propargyl, alkyl benzyl, alkyl aryl, and alkyl Boc-protected amines ranging from low to excellent yields (**4.63–4.67**).

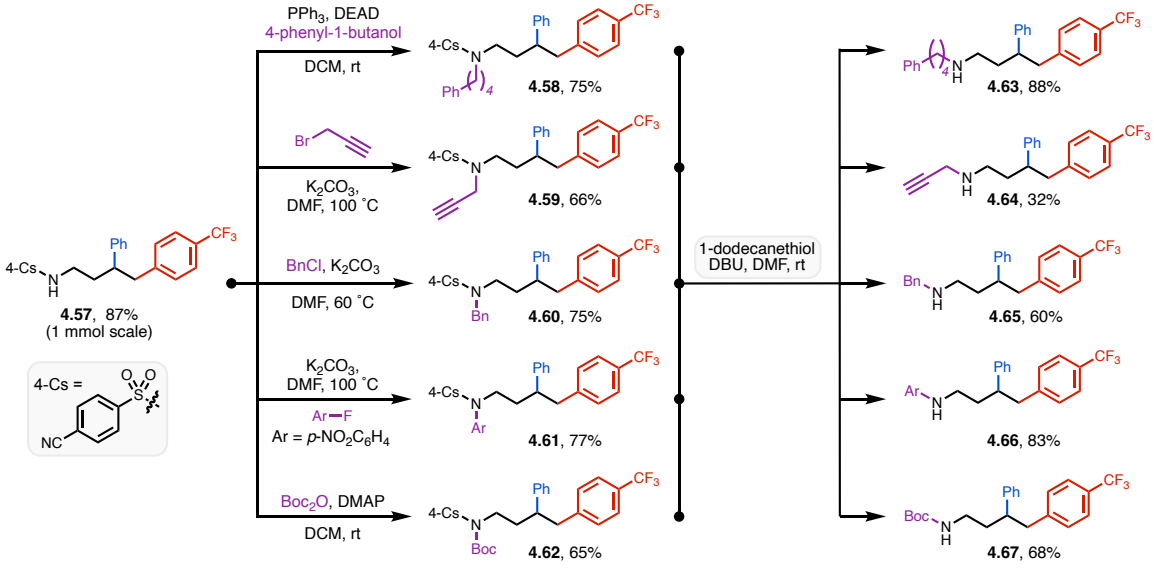


***Scheme 4.2.*** Diversification of 1,2-diarylated products as a linchpin technology. Percentages represent isolated yields.

Finally, a violet-light-initiated Hofmann–Löffler–Freytag (HLF) cyclization of 1,2-diarylated product **4.27** gave 4-Cs-protected pyrrolidine **4.68** in good yield and with a *trans* configuration (Scheme 4.3.).[12]

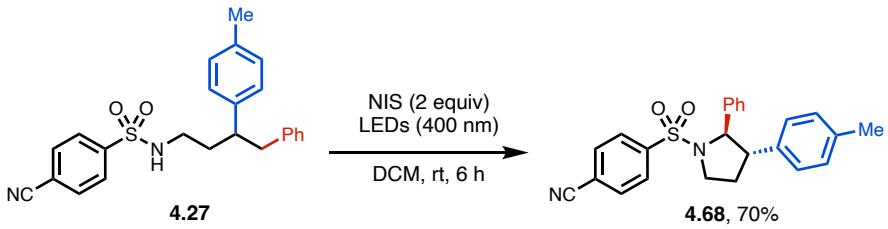


**4.27** **4.68**, 70%

***Scheme 4.3.*** HLF cyclization of a representative product.

## 4.3. CONCLUSION

In summary, a Ni-catalyzed 1,2-diarylation of alkenyl sulfonamides with aryl iodides and aryl boronic esters under a Ni/DMFU catalytic system was developed. This study tolerates a plethora of electronically varied aryl coupling partners. Electronic differentiation on the *para*-position of the aryl sulfonyl group is indiscriminate of its directing capabilities apart from nosyl substitution. For the first time, 1,1- and 1,2-disubstituted alkenes are viable substrates, affording the desired products in moderate to good yields with excellent regio- and diastereoselectivity. A series of control experiments showed that the N–H moiety of the sulfonamide is essential in the reaction. Elongation or shortening of the alkenyl chain length was found to tolerate 1,2-diarylation with aryl sulfonyl protected allyl and bis-homoallyl amines. Lastly, this method may be used as a linchpin technology where alkenyl sulfonamides could undergo 1,2-diarylation, followed by *N*-functionalization, and then mild deprotection to obtain trifunctionalized secondary amines allowing leeway for synthesis of complex amine libraries.

## 4.4. EXPERIMENTAL

### 4.4.1. General Information

Unless otherwise noted, all materials were used as received from commercial sources without further purification. All aryl iodides, aryl boronic acids, and solvents were purchased from Aldrich, Alfa Aesar, Oakwood, and Combi-Blocks. $Ni(cod)_2$ was purchased from Strem. Loftek LED flood lights were used for photochemical experiments. In air- or moisture-sensitive reactions, anhydrous solvents from MilliporeSigma or from a Grubbs-type solvent purification system were used.

### 4.4.2. Arylboronic Acid Neopentylglycol Ester Synthesis

***Table 4.S1.*** Aryl boronic acid neopentylglycol esters (**4.S1–4.S12)** used in this investigation.

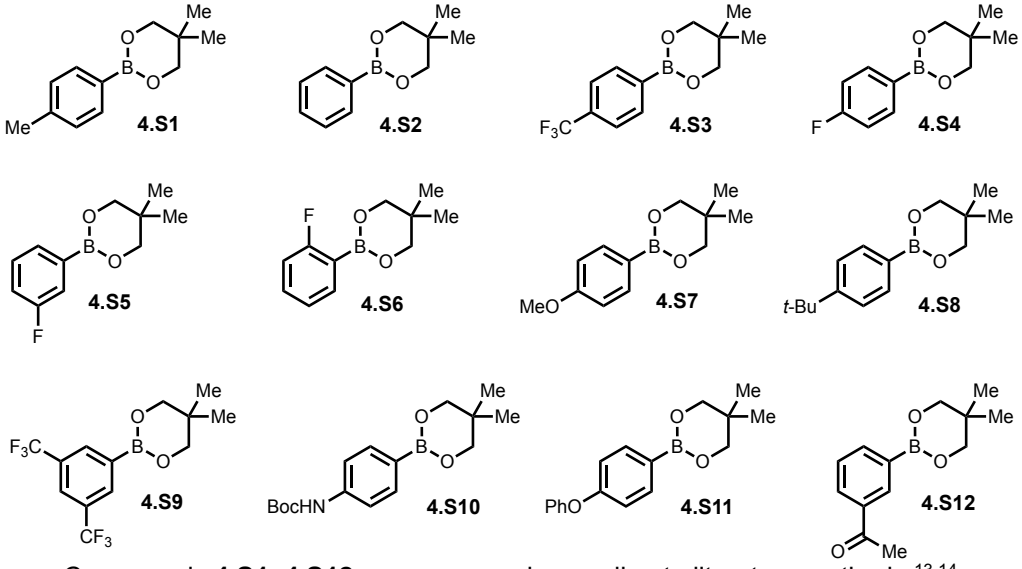


Compounds **4.S1–4.S12** were prepared according to literature methods.[13,14]

### 4.4.3. Alkenyl Sulfonamide and Miscellaneous Substrate Synthesis

***Table 4.S2.*** Starting materials used in this study: alkenyl sulfonamides **4.S13**, **4.S14**, **4.S15,** and **4.S16**; alkenyl sulfonates **4.S17–4.S26**; and alkenyl amine **4.S27**. Failed or low yielding alkenyl amine starting materials include **4.S28–S35**.

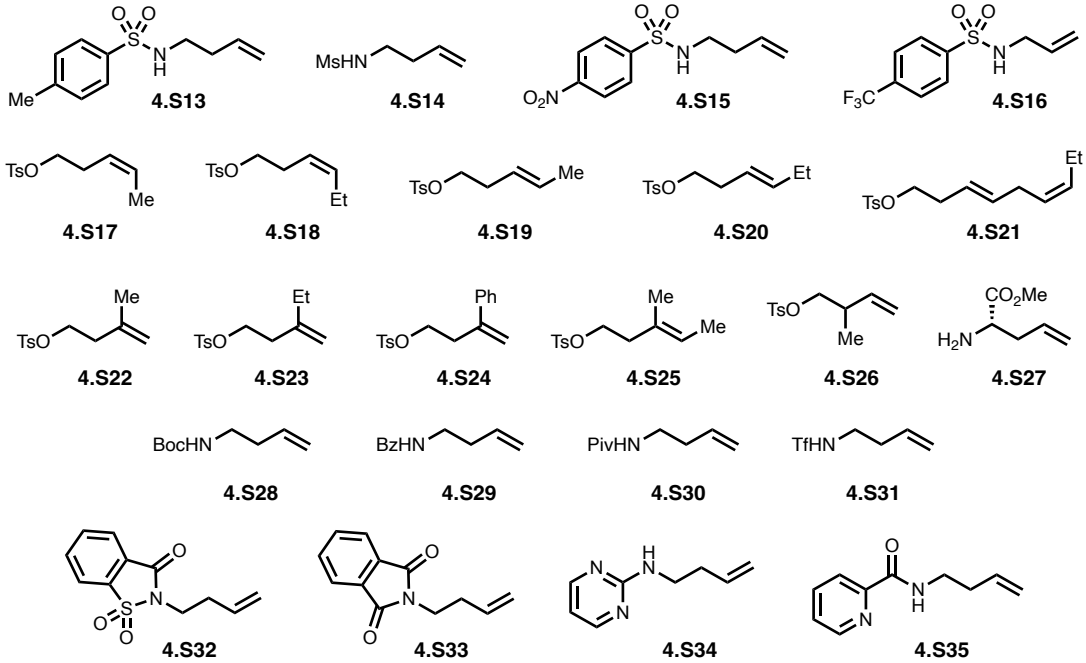


Compounds **4.S13** and **4.S14**,[15] **4.S13**,[16] **4.S13**,[17] **4.S17–S26**,[18] **4.S27**,[19] **4.S28**,[20] **4.S29**,[21] **4.S30**,[22], **4.S31**,[123] **4.S32**–**4.S33**,[24] **4.S34**,[2e] and **4.S35**[25] were prepared according to literature methods.

**A/B**

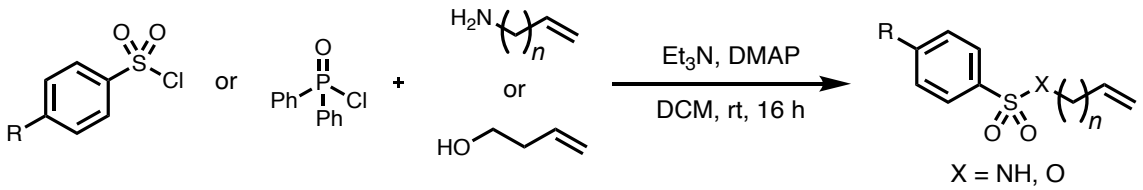


***Scheme 4.S1.*** Synthesis of alkenyl sulfonamides **4.S36**, **4.S37**, **4.S38**, **4.S39**, **4.38**, and **4.S40**. These compounds were synthesized using adapted versions of literature procedures describing the preparation of similar compounds.[15,17]

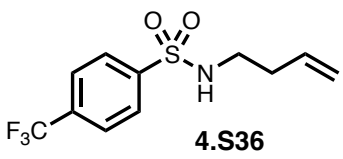


***N*-(but-3-en-1-yl)-4-(trifluoromethyl)benzenesulfonamide (4.S36):** Purification using silica gel column chromatography (20% EtOAc in Hexanes) gave the product

as a white solid (995 mg, 71% yield). Characterization data match those reported in the literature.[26]

### 4.4.4. General Procedure for Ni-Catalyzed 1,2-Diarylation of Alkenyl Sulfonamides

**General Procedure:** To a 1-dram (4 mL) vial equipped with a Teflon-coated magnetic stir bar were added the alkene substrate (0.1 mmol), the appropriate aryl boronic acid neopentylglycol ester (0.3 mmol), the appropriate aryl iodide electrophile (0.3 mmol), and dimethyl fumarate (15 mol%). The vial was then equipped with a septum cap, which was pierced by a 20-gauge needle and introduced into an argon-filled glovebox antechamber. Once transferred inside the glovebox, anhydrous NaOH (0.3 mmol), $Ni(cod)_2$ (20 mol%), and anhydrous sec-butanol (0.5 mL) were added. After stirring for 30 sec, the vial was sealed with a screw-top cap, removed from the glovebox, and left to stir at room temperature for 12 h. After this time, the reaction mixture was diluted with EtOAc (1 mL), poured into test tube filled with sat. aq. $NaHCO_3$ (10 mL), rinsed with EtOAc (1 mL), and extracted with EtOAc (3 × 1 mL). The organic layers were combined, and the solvent was removed *in vacuo* to leave a yellow residue, which afforded pure product after preparative thin-layer chromatography (PTLC).

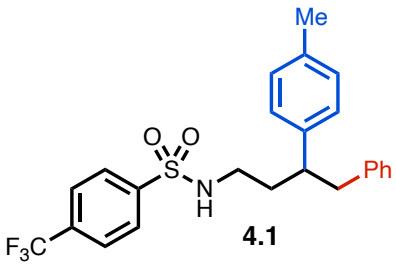

**4.1**

***N*-(4-phenyl-3-(*p*-tolyl)butyl)-4-(trifluoromethyl)benzenesulfonamide (4.1)**: Purification using PTLC (20% EtOAc in Hexanes) gave the product as a white solid (36.6 mg, 82% yield). **$^1$H NMR** (400 MHz, $CDCl_3$) δ 7.85–7.79 (m, 2H), 7.69 (d, $J$ = 8.3 Hz, 2H), 7.21–7.11 (m,

3H), 7.03 (d, $J$ = 7.8 Hz, 2H), 6.98 (d, $J$ = 6.4 Hz, 2H), 6.90 (d, $J$ = 8.0 Hz, 2H), 4.48 (t, $J$ = 6.0 Hz, 1H), 2.89–2.69 (m, 5H), 2.30 (s, 3H), 1.82 (dtd, $J$ = 13.5, 7.6, 3.7 Hz, 1H), 1.71 (dddd, $J$ = 13.5, 10.0, 7.4, 5.5 Hz, 1H); **$^{13}$C NMR** (150 MHz, $CDCl_3$) δ 143.45 (q, $J$ = 1.5 Hz), 140.11, 139.86, 136.26, 134.22 (q, $J$ = 33.1 Hz), 129.35, 129.07, 128.24, 127.51, 127.31, 126.18 (q, $J$ = 3.6 Hz), 126.11, 123.26 (q, $J$ = 272.5 Hz), 44.80, 43.75, 41.63, 34.93, 21.00; **HRMS** (ESI-TOF) Calc'd for $C_{24}H_{25}F_3NO_2S^+$ [M+H] 448.1558, found 448.1562; **$^{19}$F NMR** (376 MHz, $CDCl_3$) δ -63.30; **X-ray** (single-crystal) Colorless block crystals of X-ray diffraction quality were obtained by vapor diffusion of pentane to a saturated solution of **4.1** in benzene (CCDC 2011491).[27]

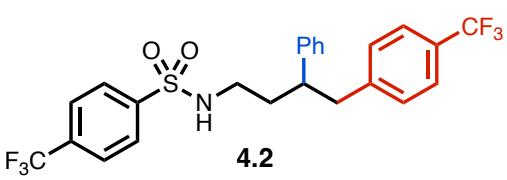


**4.2**

***N*-(3-phenyl-4-(4-(trifluoromethyl)phenyl)butyl)-4-(trifluoromethyl)benzenesulfonamide** (**4.2**): Purification using PTLC (20% EtOAc in Hexanes) gave the product as a yellow oil (49.4 mg, 99% yield). Additionally, on larger scale, purification using silica gel column chromatography (20% EtOAc in Hexanes) gave the product as a yellow solid (479 mg, 96% yield). **$^{1}$H NMR** (400 MHz, $CDCl_3$) δ 7.84 (d, $J$ = 8.2 Hz, 2H), 7.70 (d, $J$ = 8.3 Hz, 2H), 7.41 (d, $J$ = 8.0 Hz, 2H), 7.20 (pt, $J$ = 7.4, 1.8 Hz, 3H), 7.04 (d, $J$ = 8.0 Hz, 2H), 6.98 (dd, $J$ = 7.9, 1.6 Hz, 2H), 4.69 (t, $J$ = 6.0 Hz, 1H), 2.91–2.72 (m, 5H), 1.94–1.75 (m, 2H); **$^{13}$C NMR** (150 MHz, $CDCl_3$) δ 143.76 (q, $J$ = 1.4 Hz), 143.32 (q, $J$ = 1.4 Hz), 142.31, 134.36 (q, $J$ = 33.0 Hz), 129.33, 128.78, 128.45 (q, $J$ = 31.5 Hz), 127.49 (d, $J$ = 2.2 Hz), 127.00, 126.25 (q, $J$ = 3.6 Hz), 125.15 (q, $J$ = 271.8 Hz), 125.11 (q, $J$ = 3.6 Hz), 124.11 (q, $J$ = 273.2 Hz), 115.47, 44.97, 43.35, 41.45, 35.30; **$^{19}$F NMR** (376 MHz,

$CDCl_3$) δ -62.59, -63.38; **HRMS** (ESI-TOF) Calc'd for $C_{24}H_{22}F_6NO_2S^+$ [M+H] 502.1275, found 502.1272.

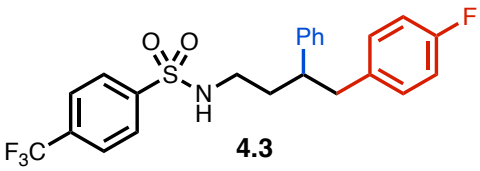


**4.3**

***N*-(4-(4-fluorophenyl)-3-phenylbutyl)-4-(trifluoromethyl)benzenesulfonamide (4.3)**: Purification using PTLC (20% EtOAc in Hexanes) gave the product as a white solid (39.6 mg, 88% yield). **$^1$H NMR** (400 MHz, $CDCl_3$) δ 7.84 (d, *J* = 8.2 Hz, 2H), 7.70 (d, *J* = 8.3 Hz, 2H), 7.25–7.15 (m, 3H), 7.00–6.95 (m, 2H), 6.91–6.81 (m, 4H), 4.61 (t, *J* = 6.1 Hz, 1H), 2.88–2.71 (m, 5H), 1.92–1.71 (m, 2H); **$^{13}$C NMR** (150 MHz, $CDCl_3$) δ 162.17, 160.55, 143.37 (q, *J* = 1.4 Hz), 142.75, 135.30 (d, *J* = 3.3 Hz), 134.30 (q, *J* = 33.2 Hz), 130.40 (d, *J* = 7.8 Hz), 128.68, 127.51 (d, *J* = 2.2 Hz), 126.83, 126.24 (q, *J* = 3.7 Hz), 123.23 (q, *J* = 272.8 Hz), 114.96 (d, *J* = 21.1 Hz), 45.34, 42.79, 41.53, 35.10; **$^{19}$F NMR** (376 MHz, $CDCl_3$) δ -63.34, -117.31; **HRMS** (ESI-TOF) Calc'd for $C_{23}H_{22}F_4NO_2S^+$ [M+H] 452.1307, found 452.1315.

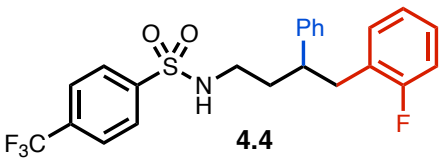


**4.4**

***N*-(4-(2-fluorophenyl)-3-phenylbutyl)-4-(trifluoromethyl)benzenesulfonamide (4.4)**: Purification using PTLC (20% EtOAc in Hexanes) gave the product as a white solid (41.1 mg, 91% yield). **$^1$H NMR** (400 MHz, $CDCl_3$) δ 7.83 (d, *J* = 7.9 Hz, 2H), 7.70 (d, *J* = 8.2 Hz, 2H), 7.24–7.08 (m, 4H), 7.04–6.98 (m, 2H), 6.91 (dddd, *J* = 15.8, 11.2, 7.8, 1.6 Hz, 3H), 4.60 (s, 1H), 2.92–2.72 (m, 5H), 1.82 (dddd, *J* = 13.0, 7.8, 6.1, 1.9 Hz, 2H); **$^{13}$C NMR** (150 MHz, $CDCl_3$) δ 161.94, 160.32, 143.44 (q, *J* = 1.4 Hz), 142.85, 134.25 (q, *J* = 33.0 Hz), 131.38 (d, *J* = 5.0 Hz), 128.67, 127.98 (d, *J*

= 8.2 Hz), 127.45 (d, *J* = 15.5 Hz), 126.85, 126.54 (d, *J* = 15.5 Hz), 126.22 (q, *J* = 3.9 Hz), 123.80 (d, *J* = 3.7 Hz), 123.25 (q, *J* = 273.0 Hz), 115.18 (d, *J* = 22.2 Hz), 43.96, 41.57, 36.68 (d, *J* = 1.6 Hz), 34.87; **$^{19}$F NMR** (376 MHz, $CDCl_3$) δ -63.31, -118.44; **HRMS** (ESI-TOF) Calc'd for $C_{23}H_{22}F_4NO_2S^+$ [M+H] 452.1307, found 452.1310.

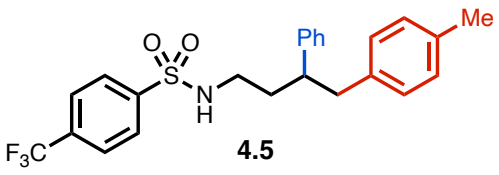


**4.5**

***N*-(3-phenyl-4-(*p*-tolyl)butyl)-4-(trifluoromethyl)benzenesulfonamide (4.5)**: Purification using PTLC (20% EtOAc in Hexanes) gave the product as a white solid (31 mg, 70% yield). **$^{1}$H NMR** (400 MHz, $CDCl_3$) δ 7.81 (d, *J* = 8.2 Hz, 2H), 7.69 (d, *J* = 8.3 Hz, 2H), 7.26–7.16 (m, 3H), 7.03–6.96 (m, 4H), 6.86 (d, *J* = 8.0 Hz, 2H), 4.50 (t, *J* = 5.6 Hz, 1H), 2.87–2.68 (m, 5H), 2.27 (s, 3H), 1.84 (dtd, *J* = 13.8, 7.7, 3.7 Hz, 1H), 1.73 (dddd, *J* = 13.5, 9.9, 7.5, 5.5 Hz, 1H); **$^{13}$C NMR** (150 MHz, $CDCl_3$) δ 143.43 (q, *J* = 1.4 Hz), 143.37, 136.60, 135.62, 134.12 (q, *J* = 32.5 Hz), 128.95, 128.94, 128.67, 127.51, 127.49, 126.72, 126.20 (q, *J* = 3.8 Hz), 123.26 (q, *J* = 272.9 Hz), 45.29, 43.22, 41.62, 34.90, 21.00; **$^{19}$F NMR** (376 MHz, $CDCl_3$) δ -63.31; **HRMS** (ESI-TOF) Calc'd for $C_{24}H_{25}F_3NO_2S^+$ [M+H] 448.1558, found 448.1556.

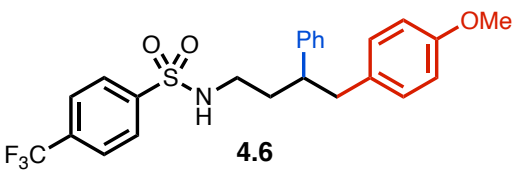


**4.6**

***N*-(4-(4-methoxyphenyl)-3-phenylbutyl)-4-(trifluoromethyl)benzenesulfonamide (4.6)**: Purification using PTLC (20% Acetone in Hexanes) gave the product as a colorless oil (35.8 mg, 78% yield). **$^{1}$H NMR** (400 MHz, $CDCl_3$) δ 7.82 (d, *J* = 8.2 Hz, 2H), 7.69 (d, *J* = 8.2 Hz, 2H), 7.24–7.14 (m, 3H), 7.02–

6.97 (m, 2H), 6.90–6.85 (m, 2H), 6.75–6.69 (m, 2H), 4.60 (t, $J$ = 6.0 Hz, 1H), 3.74 (s, 3H), 2.87–2.67 (m, 5H), 1.90–1.79 (m, 1H), 1.74 (dtd, $J$ = 9.9, 8.4, 8.0, 5.9 Hz, 1H); **$^{13}$C NMR** (150 MHz, $CDCl_3$) δ 157.94, 143.42 (q, $J$ = 1.6 Hz), 143.31, 134.21 (q, $J$ = 33.2 Hz), 131.78, 129.99, 128.63, 127.53, 127.51, 126.69, 126.21 (q, $J$ = 3.6 Hz), 123.27 (q, $J$ = 272.6 Hz), 113.62, 55.18, 45.40, 42.75, 41.61, 34.93; **$^{19}$F NMR** (376 MHz, $CDCl_3$) δ -63.31; **HRMS** (ESI-TOF) Calc'd for $C_{24}H_{25}F_3NO_3S^+$ [M+H] 464.1507, found 464.1502.

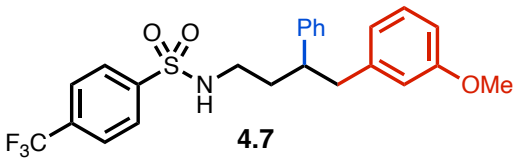

**4.7**

***N*-(4-(3-methoxyphenyl)-3-phenylbutyl)-4-(trifluoromethyl)benzenesulfonamide (4.7)**: Purification using PTLC (20% EtOAc in Hexanes) gave the product as a colorless oil (46 mg, 99% yield). **$^{1}$H NMR** (400 MHz, $CDCl_3$) δ 7.81 (d, $J$ = 8.3 Hz, 2H), 7.69 (d, $J$ = 7.9 Hz, 2H), 7.25 – 7.15 (m, 3H), 7.10 (t, $J$ = 7.9 Hz, 1H), 7.04 – 6.98 (m, 2H), 6.69 (ddd, $J$ = 8.2, 2.6, 0.9 Hz, 1H), 6.58 (dt, $J$ = 7.5, 1.3 Hz, 1H), 6.50 (dd, $J$ = 2.6, 1.6 Hz, 1H), 4.53 (t, $J$ = 6.0 Hz, 1H), 3.70 (s, 3H), 2.88 – 2.70 (m, 5H), 1.86 (dtd, $J$ = 13.9, 7.7, 3.7 Hz, 1H), 1.75 (dddd, $J$ = 13.4, 9.9, 7.4, 5.5 Hz, 1H); **$^{13}$C NMR** (150 MHz, $CDCl_3$) δ 159.45, 143.40 (q, $J$ = 1.4 Hz), 143.22, 141.32, 134.23 (q, $J$ = 33.0 Hz), 129.21, 128.68, 127.50, 126.77, 126.22 (q, $J$ = 3.8 Hz), 123.26 (q, $J$ = 272.5 Hz), 121.47, 114.78, 111.54, 55.09, 45.12, 43.68, 41.59, 34.97; **$^{19}$F NMR** (376 MHz, $CDCl_3$) δ -63.31; **HRMS** (ESI-TOF) Calc'd for $C_{24}H_{25}F_3NO_3S^+$ [M+H] 464.1507, found 464.1516.

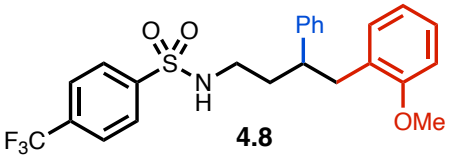

**4.8**

***N*-(4-(2-methoxyphenyl)-3-phenylbutyl)-4-(trifluoromethyl)benzenesulfonamide (4.8)**:

Purification using PTLC (20% Acetone in Hexanes) gave the product as a colorless oil (37.3 mg, 81% yield). **$^{1}$H NMR** (400 MHz, $CDCl_3$) δ 7.82 (d, *J* = 8.0 Hz, 2H), 7.69 (d, *J* = 8.2 Hz, 2H), 7.24–7.10 (m, 4H), 7.03–6.97 (m, 2H), 6.81 (ddd, *J* = 8.2, 2.9, 1.4 Hz, 2H), 6.74 (td, *J* = 7.3, 1.1 Hz, 1H), 4.62 (t, *J* = 6.1 Hz, 1H), 3.78 (s, 3H), 2.91–2.71 (m, 5H), 1.87–1.70 (m, 2H); **$^{13}$C NMR** (150 MHz, $CDCl_3$) δ 157.43, 143.92, 143.54 (q, *J* = 1.4 Hz), 134.17 (q, *J* = 32.4 Hz), 130.86, 128.49, 128.14, 127.50, 127.48, 127.46, 126.54, 126.20 (q, *J* = 3.9 Hz), 123.28 (q, *J* = 272.6 Hz), 110.32, 55.29, 43.42, 41.68, 37.65, 34.68; **$^{19}$F NMR** (376 MHz, $CDCl_3$) δ -63.30; **HRMS** (ESI-TOF) Calc'd for $C_{24}H_{25}F_3NO_3S^+$ [M+H] 464.1507, found 464.1501.

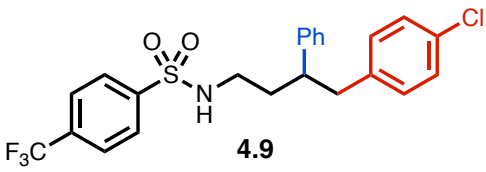


**4.9**

***N*-(4-(4-chlorophenyl)-3-phenylbutyl)-4-(trifluoromethyl)benzenesulfonamide (4.9)**: Purification using PTLC (20% EtOAc in Hexanes) gave the product as a white solid (44.8 mg, 96% yield). **$^{1}$H NMR** (400 MHz, $CDCl_3$) δ 7.83 (d, *J* = 8.2 Hz, 2H), 7.70 (d, *J* = 8.2 Hz, 2H), 7.24–7.15 (m, 3H), 7.14–7.10 (m, 2H), 7.00–6.94 (m, 2H), 6.86 (d, *J* = 8.4 Hz, 2H), 4.66 (s, 1H), 2.79 (p, *J* = 5.7, 5.1 Hz, 5H), 1.92–1.72 (m, 2H); **$^{13}$C NMR** (150 MHz, $CDCl_3$) δ 143.35, 142.60, 138.12, 134.32 (q, *J* = 33.0 Hz), 131.87, 130.38, 128.72, 128.31, 127.50, 126.89, 126.25 (q, *J* = 3.6 Hz), 123.23 (q, *J* = 273.3 Hz), 45.13, 42.93, 41.50, 35.17; **$^{19}$F NMR** (376 MHz, $CDCl_3$) δ -63.32; **HRMS** (ESI-TOF) Calc'd for $C_{23}H_{22}ClF_3NO_2S^+$ [M+H] 468.1012, found 468.1015.

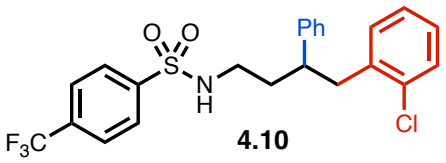


**4.10**

***N*-(4-(2-chlorophenyl)-3-phenylbutyl)-4-(trifluoromethyl)benzenesulfonamide (4.10)**: Purification using PTLC (20% EtOAc in Hexanes) gave the product as a colorless oil (43.7 mg, 89% yield). **$^{1}$H NMR** (400 MHz, $CDCl_3$) δ 7.83 (d, *J* = 8.2 Hz, 2H), 7.69 (d, *J* = 8.3 Hz, 2H), 7.28 (dd, *J* = 7.9, 1.4 Hz, 1H), 7.25–7.16 (m, 3H), 7.08 (td, *J* = 7.7, 1.8 Hz, 1H), 7.01 (dtd, *J* = 7.5, 3.4, 2.6, 1.4 Hz, 3H), 6.85 (dd, *J* = 7.5, 1.8 Hz, 1H), 4.60 (d, *J* = 5.9 Hz, 1H), 3.01–2.74 (m, 5H), 1.84 (q, *J* = 7.1 Hz, 2H); **$^{13}$C NMR** (150 MHz, $CDCl_3$) δ 143.45 (q, *J* = 1.4 Hz), 142.87, 137.28, 134.25 (q, *J* = 33.3 Hz), 134.05, 131.40, 129.51, 128.69, 127.72, 127.50, 127.42, 126.86, 126.49, 126.22 (q, *J* = 3.6 Hz), 123.25 (q, *J* = 273.3 Hz), 43.31, 41.62, 41.27, 34.78; **$^{19}$F NMR** (376 MHz, $CDCl_3$) δ -63.30; **HRMS** (ESI-TOF) Calc'd for $C_{23}H_{22}ClF_3NO_2S^+$ [M+H] 468.1012, found 468.1009.

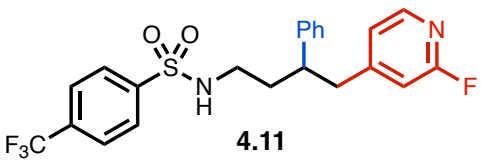


**4.11**

***N*-(3-phenyl-4-(2-(fluoromethyl)pyridin-4-yl)butyl)-4-(trifluoromethyl)benzenesulfonamide (4.11)**: Purification using PTLC (20% Acetone in Hexanes) gave the product as a white solid (33.3 mg, 74% yield). **$^{1}$H NMR** (400 MHz, $CDCl_3$) δ 7.98 (d, *J* = 5.2 Hz, 1H), 7.86 (d, *J* = 8.1 Hz, 2H), 7.75–7.69 (m, 2H), 7.26–7.17 (m, 3H), 6.99 (dd, *J* = 7.9, 1.6 Hz, 2H), 6.76 (dt, *J* = 5.2, 1.7 Hz, 1H), 6.50 (s, 1H), 4.97 (t, *J* = 6.1 Hz, 1H), 2.96–2.74 (m, 5H), 1.99–1.79 (m, 2H); **$^{13}$C NMR** (150 MHz, $CDCl_3$) δ 171.28, 164.60, 163.02, 154.83 (d, *J* = 8.0 Hz), 147.14 (d, *J* = 15.0 Hz), 143.34 (d, *J* = 1.1 Hz), 134.36 (q, *J* = 33.0 Hz), 128.89, 127.45 (d, *J* = 10.2 Hz), 127.26, 126.27 (q, *J* = 3.8 Hz), 123.19 (q, *J* = 273.0 Hz), 122.18

(d, $J$ = 3.8 Hz), 109.76 (d, $J$ = 36.5 Hz), 44.12, 42.55 (d, $J$ = 2.8 Hz), 41.25, 35.60; **$^{19}$F NMR** (376 MHz, $CDCl_3$) δ -63.36, -69.31; **HRMS** (ESI-TOF) Calc'd for $C_{22}H_{21}F_4N_2O_2S^+$ [M+H] 453.1260, found 453.1253.

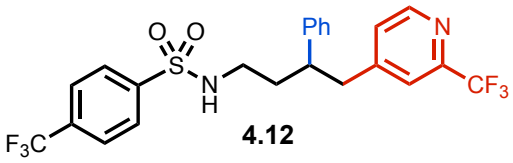


**4.12**

***N*-(3-phenyl-4-(2-(trifluoromethyl)pyridin-4 yl)butyl)-4-(trifluoromethyl)benzenesulfonamide (4.12)**: Purification using PTLC (20% Acetone in Hexanes) gave the product as a colorless oil (23.8 mg, 47% yield). **$^1$H NMR** (400 MHz, $CDCl_3$) δ 8.48 (d, $J$ = 5.0 Hz, 1H), 7.86 (d, $J$ = 8.2 Hz, 2H), 7.72 (d, $J$ = 8.2 Hz, 2H), 7.26–7.17 (m, 4H), 7.02 (dd, $J$ = 5.1, 1.6 Hz, 1H), 6.99–6.94 (m, 2H), 4.80 (s, 1H), 3.05–2.75 (m, 5H), 2.05–1.80 (m, 2H); **$^{13}$C NMR** (151 MHz, $CDCl_3$) δ 150.75, 149.69, 147.96 (q, $J$ = 34.3 Hz), 143.27 (q, $J$ = 1.7 Hz), 141.15, 134.41 (q, $J$ = 33.1 Hz), 128.94, 127.48, 127.45, 127.45, 127.38, 127.01, 126.28 (q, $J$ = 3.8 Hz), 123.17 (q, $J$ = 273.5 Hz), 121.48 (q, $J$ = 275 Hz), 121.12 (q, $J$ = 2.7 Hz), 44.28, 42.80, 41.24, 35.68; **$^{19}$F NMR** (376 MHz, $CDCl_3$) δ -65.80, -70.69; **HRMS** (ESI-TOF) Calc'd for $C_{23}H_{21}F_6N_2O_2S^+$ [M+H] 503.1228, found 503.1231.

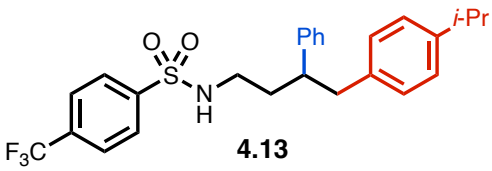


**4.13**

***N*-(4-(4-isopropylphenyl)-3-phenylbutyl)-4-(trifluoromethyl)benzenesulfonamide (4.13)**: Purification using PTLC (20% EtOAc in Hexanes) gave the product as a colorless oil (35.2 mg, 74% yield). **$^1$H NMR** (400 MHz, $CDCl_3$) δ 7.81 (d, $J$ = 9.0 Hz, 2H), 7.69 (d, $J$ = 8.4 Hz, 2H), 7.26–7.16 (m, 3H), 7.09–7.00 (m, 4H), 6.92 (d, $J$ = 8.1 Hz, 2H), 4.42 (t, $J$ = 6.0 Hz, 1H), 2.89–2.68 (m, 6H), 1.85

(dtd, $J$ = 13.7, 7.7, 3.9 Hz, 1H), 1.73 (dddd, $J$ = 13.5, 9.9, 7.4, 5.6 Hz, 1H), 1.21 (dd, $J$ = 6.9, 0.7 Hz, 6H); **$^{13}$C NMR** (150 MHz, $CDCl_3$) δ 146.71, 143.50, 143.42, 137.01, 134.24 (q, $J$ = 33.2 Hz), 128.97, 128.68, 127.52, 127.48, 126.73, 126.32, 126.21 (q, $J$ = 3.6 Hz), 123.26 (q, $J$ = 272.4 Hz), 45.22, 43.24, 41.63, 34.83, 33.66, 24.02; **$^{19}$F NMR** (376 MHz, $CDCl_3$) δ -63.31; **HRMS** (ESI-TOF) Calc'd for $C_{26}H_{29}F_3NO_2S^+$ [M+H] 476.1871, found 476.1863.

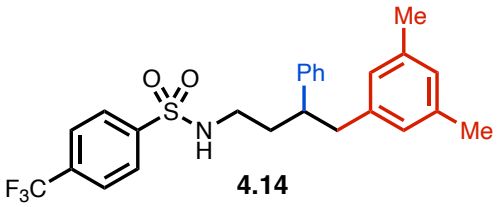

**4.14**

***N*-(4-(3,5-dimethylphenyl)-3-phenylbutyl)-4-(trifluoromethyl)benzenesulfonamide (4.14)**: Purification using PTLC (20% EtOAc in Hexanes) gave the product as a colorless oil (41.5 mg, 90% yield). **$^{1}$H NMR** (400 MHz, $CDCl_3$) δ 7.80 (d, $J$ = 8.3 Hz, 2H), 7.68 (d, $J$ = 8.3 Hz, 2H), 7.27–7.15 (m, 3H), 7.06–7.00 (m, 2H), 6.79 (s, 1H), 6.63 (s, 2H), 4.43 (t, $J$ = 6.0 Hz, 1H), 2.85–2.72 (m, 4H), 2.67 (qd, $J$ = 10.8, 10.2, 5.9 Hz, 1H), 2.23 (s, 6H), 1.83 (dtd, $J$ = 13.9, 7.7, 3.8 Hz, 1H), 1.72 (dddd, $J$ = 13.5, 10.2, 7.4, 5.6 Hz, 1H); **$^{13}$C NMR** (150 MHz, $CDCl_3$) δ 143.59, 143.39 (q, $J$ = 1.4 Hz), 139.65, 137.72, 134.22 (q, $J$ = 33.2 Hz), 128.67, 127.81, 127.51, 127.45, 126.96, 126.73, 126.18 (q, $J$ = 3.6 Hz), 123.26 (q, $J$ = 273.0 Hz), 45.20, 43.61, 41.66, 34.73, 21.23; **$^{19}$F NMR** (376 MHz, $CDCl_3$) δ -63.31; **HRMS** (ESI-TOF) Calc'd for $C_{25}H_{27}F_3NO_2S^+$ [M+H] 462.1715, found 462.1713.

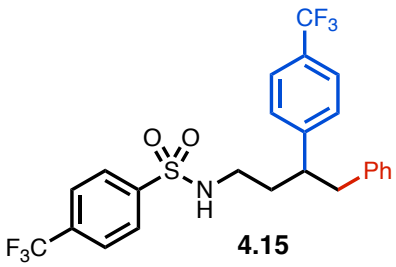

**4.15**

***N*-(4-phenyl-3-(4-(trifluoromethyl)phenyl)butyl)-4-(trifluoromethyl)benzenesulfonamide (4.15):** Purification using PTLC (20% EtOAc in Hexanes) gave

the product as a white solid (40.9 mg, 82% yield). **$^{1}$H NMR** (400 MHz, $CDCl_3$) δ 7.84 (dt, *J* = 8.1, 0.8 Hz, 2H), 7.71 (dt, *J* = 8.1, 0.7 Hz, 2H), 7.49 (d, *J* = 7.6 Hz, 2H), 7.23–7.11 (m, 5H), 6.98–6.93 (m, 2H), 4.54 (t, *J* = 6.0 Hz, 1H), 3.00–2.90 (m, 1H), 2.89–2.69 (m, 4H), 1.91 (dtd, *J* = 13.9, 7.8, 4.5 Hz, 1H), 1.81 (dddd, *J* = 14.0, 10.3, 7.5, 5.4 Hz, 1H); **$^{13}$C NMR** (150 MHz, $CDCl_3$) δ 147.40 (d, *J* = 1.1 Hz), 143.28 (d, *J* = 1.2 Hz), 139.03, 134.43 (q, *J* = 33.1 Hz), 129.01, 129.00 (q, *J* = 32.1 Hz), 128.36, 127.93, 127.49, 126.37, 126.29 (q, *J* = 3.7 Hz), 125.53 (q, *J* = 3.8 Hz), 124.13 (q, *J* = 272.0 Hz), 123.19 (q, *J* = 272.9 Hz), 44.83, 43.34, 41.28, 34.99; **$^{19}$F NMR** (400 MHz, $CDCl_3$) δ -62.67, -63.40; **HRMS** (ESI-TOF) Calc'd for $C_{24}H_{22}F_6NO_2S^+$ [M+H] 502.1275, found 502.1269.

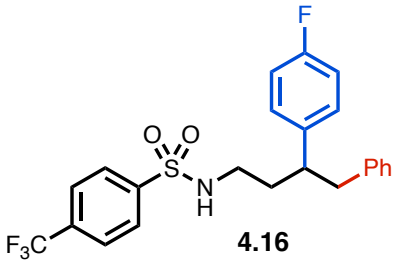


**4.16**

***N*-(3-(4-fluorophenyl)-4-phenylbutyl)-4-(trifluoromethyl)benzenesulfonamide (4.16):** Purification using PTLC (20% EtOAc in Hexanes) gave the product as a white solid (40.4 mg, 89% yield). **$^{1}$H NMR** (400 MHz, $CDCl_3$) δ 7.85 (d, *J* = 7.9 Hz, 2H), 7.71 (d, *J* = 8.3 Hz, 2H), 7.20–7.11 (m, 3H), 6.98–6.87 (m, 6H), 4.65 (s, 1H), 2.89–2.69 (m, 5H), 1.86 (dtd, *J* = 14.1, 7.7, 4.0 Hz, 1H), 1.79–1.68 (m, 1H); **$^{13}$C NMR** (150 MHz, $CDCl_3$) δ 162.34, 160.72, 143.39 (q, *J* = 1.4 Hz), 139.43, 138.74 (d, *J* = 3.3 Hz), 134.34 (q, *J* = 33.1 Hz), 129.05, 128.91 (d, *J* = 7.8 Hz), 128.26, 127.50, 126.27 (q, *J* = 3.7 Hz), 126.21, 123.23 (q, *J* = 273.1 Hz), 115.41 (d, *J* = 21.1 Hz), 44.34, 43.76, 41.43, 35.21; **$^{19}$F NMR** (376 MHz, $CDCl_3$) δ -63.33, -116.30; **HRMS** (ESI-TOF) Calc'd for $C_{23}H_{22}F_4NO_2S^+$ [M+H] 452.1307, found 452.1301.

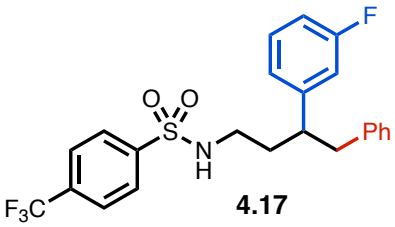


**4.17**

***N*-(3-(3-fluorophenyl)-4-phenylbutyl)-4-(trifluoromethyl)benzenesulfonamide (4.17):** Purification using PTLC (20% EtOAc in Hexanes) gave the product as a white solid (41.3 mg, 91% yield). **$^{1}$H NMR** (400 MHz, $CDCl_3$) δ 7.85 (d, *J* = 8.2 Hz, 2H), 7.71 (d, *J* = 8.2 Hz, 2H), 7.21–7.11 (m, 4H), 6.98–6.93 (m, 2H), 6.86 (td, *J* = 8.3, 2.4 Hz, 1H), 6.78 (dt, *J* = 7.7, 1.2 Hz, 1H), 6.71 (dt, *J* = 10.0, 2.1 Hz, 1H), 4.63 (t, *J* = 6.1 Hz, 1H), 2.90–2.70 (m, 5H), 1.86 (dtd, *J* = 14.1, 7.8, 3.9 Hz, 1H), 1.80–1.68 (m, 1H); **$^{13}$C NMR** (150 MHz, $CDCl_3$) δ 163.78, 162.15, 145.89 (d, *J* = 6.7 Hz), 143.34, 139.24, 134.36 (q, *J* = 32.9 Hz), 130.12 (d, *J* = 8.3 Hz), 129.01, 128.32, 127.49, 126.27 (dd, *J* = 6.5, 3.1 Hz), 123.32 (d, *J* = 2.8 Hz), 123.22 (q, *J* = 272.9 Hz), 114.22 (d, *J* = 21.0 Hz), 113.66 (d, *J* = 21.1 Hz), 44.93, 43.48, 41.42, 34.97; **$^{19}$F NMR** (376 MHz, $CDCl_3$) δ -63.35, -112.90; **HRMS** (ESI-TOF) Calc'd for $C_{23}H_{22}F_4NO_2S^+$ [M+H] 452.1307, found 452.1313.

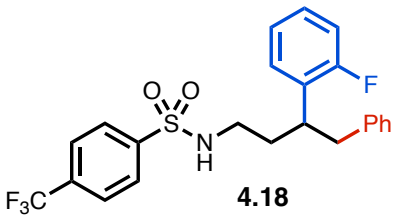


**4.18**

***N*-(3-(2-fluorophenyl)-4-phenylbutyl)-4-(trifluoromethyl)benzenesulfonamide (4.18):** Purification using PTLC (20% EtOAc in Hexanes) gave the product as a white solid (44.9 mg, 99% yield). **$^{1}$H NMR** (400 MHz, $CDCl_3$) δ 7.84 (d, *J* = 8.2 Hz, 2H), 7.70 (d, *J* = 8.3 Hz, 2H), 7.24–7.15 (m, 3H), 7.12 (td, *J* = 8.0, 6.1 Hz, 1H), 7.01–6.96 (m, 2H), 6.81 (td, *J* = 8.5, 2.6 Hz, 1H), 6.75–6.71 (m, 1H), 6.65 (dt, *J* = 9.9, 2.1 Hz, 1H), 4.69 (s, 1H), 2.88–2.71 (m, 5H), 1.91–1.72 (m, 2H); **$^{13}$C NMR** (150 MHz, $CDCl_3$) δ 163.49, 161.86, 143.36 (q, *J* = 1.4 Hz), 142.65, 142.25 (d, *J* = 7.2 Hz), 134.30 (q, *J* = 33.1 Hz), 129.61 (d, *J* = 8.3 Hz), 128.72,

127.48 (d, $J$ = 7.1 Hz), 126.90, 126.24 (q, $J$ = 3.8 Hz), 124.74 (d, $J$ = 2.7 Hz), 123.24 (q, $J$ = 272.9 Hz), 115.83 (d, $J$ = 21.0 Hz), 113.03 (d, $J$ = 21.0 Hz), 44.99, 43.31 (d, $J$ = 1.8 Hz), 41.49, 35.10; **$^{19}$F NMR** (376 MHz, $CDCl_3$) δ -63.33, -63.33, -113.92; **HRMS** (ESI-TOF) Calc'd for $C_{23}H_{22}F_4NO_2S^+$ [M+H] 452.1307, found 452.1308.

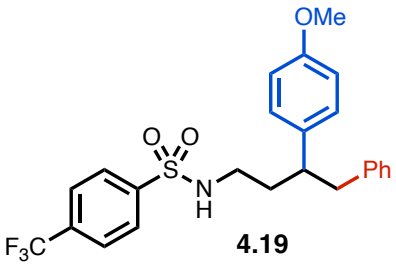


**4.19**

***N*-(3-(4-methoxyphenyl)-4-phenylbutyl)-4-(trifluoromethyl)benzenesulfonamide (4.19):** Purification using PTLC (20% EtOAc in Hexanes) gave the product as a white solid (32.5 mg, 70% yield). **$^1$H NMR** (400 MHz, $CDCl_3$) δ 7.83 (d, $J$ = 8.2 Hz, 2H), 7.70 (d, $J$ = 8.2 Hz, 2H), 7.21–7.10 (m, 3H), 6.98–6.94 (m, 2H), 6.92 (d, $J$ = 8.7 Hz, 2H), 6.76 (d, $J$ = 8.7 Hz, 2H), 4.56 (t, $J$ = 6.0 Hz, 1H), 3.76 (s, 3H), 2.87–2.70 (m, 5H), 1.87–1.77 (m, 1H), 1.70 (dddd, $J$ = 13.8, 10.1, 7.3, 5.5 Hz, 1H); **$^{13}$C NMR** (150 MHz, $CDCl_3$) δ 158.28, 143.48 (q, $J$ = 1.4 Hz), 139.84, 135.10, 134.22 (q, $J$ = 33.1 Hz), 129.08, 128.39, 128.22, 127.51, 126.21 (q, $J$ = 3.6 Hz), 126.09, 123.26 (q, $J$ = 273.1 Hz), 114.00, 55.20, 44.37, 43.87, 41.61, 35.13; **$^{19}$F NMR** (376 MHz, $CDCl_3$) δ -63.30; **HRMS** (ESI-TOF) Calc'd for $C_{24}H_{25}F_3NO_3S^+$ [M+H] 464.1507, found 464.1500.

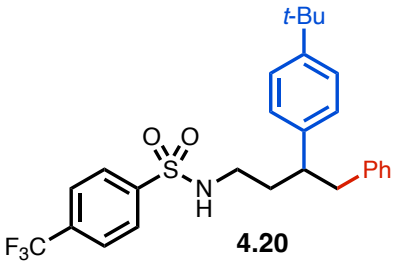


**4.20**

***N*-(3-(4-(*tert*-butyl)phenyl)-4-phenylbutyl)-4-(trifluoromethyl)benzenesulfonamide (4.20):** Purification using PTLC (20% EtOAc in Hexanes) gave the product as a white solid (43.8 mg, 89% yield). **$^1$H NMR** (400 MHz, $CDCl_3$) δ 7.81 (d, $J$ = 8.2 Hz, 2H), 7.69 (d, $J$ = 8.3 Hz, 2H), 7.26 (d, $J$ =

8.3 Hz, 2H), 7.23–7.12 (m, 3H), 7.02–6.98 (m, 2H), 6.96 (d, $J$ = 8.2 Hz, 2H), 4.44 (t, $J$ = 6.0 Hz, 1H), 2.91–2.85 (m, 1H), 2.85–2.68 (m, 4H), 1.84–1.64 (m, 2H), 1.30 (s, 9H); **$^{13}$C NMR** (150 MHz, $CDCl_3$) δ 149.66, 143.51 (q, $J$ = 1.3 Hz), 140.27, 139.96, 134.21 (q, $J$ = 33.1 Hz), 129.09, 128.27, 127.52, 127.02, 126.18 (q, $J$ = 3.6 Hz), 126.13, 125.55, 123.26 (q, $J$ = 273.0 Hz), 44.71 (d, $J$ = 1.8 Hz), 43.64, 41.70, 34.75, 34.42, 31.37; **$^{19}$F NMR** (376 MHz, $CDCl_3$) δ -63.27; **HRMS** (ESI-TOF) Calc'd for $C_{27}H_{31}F_3NO_2S^+$ [M+H] 490.2028, found 490.2027.

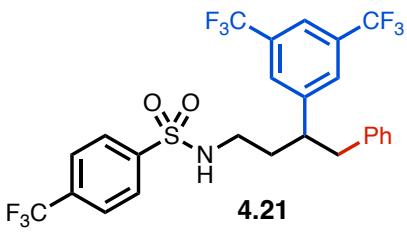


**4.21**

***N*-(3-(3,5-bis(trifluoromethyl)phenyl)-4-phenylbutyl)-4-(trifluoromethyl)benzenesulfonamide (4.21):** Purification using PTLC (20% EtOAc in Hexanes) gave the product as a colorless oil (52.1 mg, 91% yield). **$^{1}$H NMR** (400 MHz, $CDCl_3$) δ 7.87 (dt, $J$ = 8.1, 0.8 Hz, 2H), 7.74–7.68 (m, 3H), 7.47–7.44 (m, 2H), 7.22–7.15 (m, 3H), 6.94–6.89 (m, 2H), 4.88 (t, $J$ = 6.2 Hz, 1H), 3.09 (dtd, $J$ = 9.8, 7.4, 4.9 Hz, 1H), 2.94–2.72 (m, 4H), 1.97 (dtd, $J$ = 14.0, 7.7, 5.0 Hz, 1H), 1.86 (dddd, $J$ = 14.1, 9.9, 7.5, 5.6 Hz, 1H); **$^{13}$C NMR** (150 MHz, $CDCl_3$) δ 145.89, 143.19, 138.20, 134.55 (q, $J$ = 33.2 Hz), 131.73 (q, $J$ = 33.1 Hz), 128.98, 128.49, 127.85 (q, $J$ = 3.9 Hz), 127.45, 126.65, 126.35 (q, $J$ = 3.6 Hz), 123.23 (q, $J$ = 273.0 Hz), 123.14 (q, $J$ = 273.4 Hz) 44.62, 43.22, 41.13, 34.71; **$^{19}$F NMR** (376 MHz, $CDCl_3$) δ -63.10, -63.47; **HRMS** (ESI-TOF) Calc'd for $C_{25}H_{21}F_9NO_2S^+$ [M+H] 570.1149, found 570.1149.

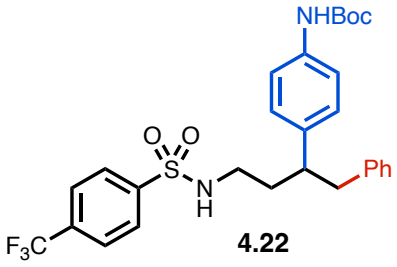


**4.22**

***tert*-butyl (4-(1-phenyl-4-((4-(trifluoromethyl)phenyl)sulfonamido)butan-2-yl)phenyl)carbamate (4.22):** Purification using PTLC (20% EtOAc in Hexanes) gave the product as a white solid (37 mg, 67% yield). **$^{1}$H NMR** (400 MHz, $CDCl_3$) δ 7.84–7.80 (m, 2H), 7.74–7.69 (m, 2H), 7.25–7.12 (m, 5H), 6.96 (ddd, *J* = 11.5, 7.4, 1.9 Hz, 4H), 6.41 (s, 1H), 4.20 (t, *J* = 6.1 Hz, 1H), 2.88–2.71 (m, 5H), 1.90–1.80 (m, 1H), 1.73 (td, *J* = 16.9, 15.7, 8.0 Hz, 1H), 1.52 (s, 9H); **$^{13}$C NMR** (150 MHz, $CDCl_3$) δ 152.88, 143.43 (q, *J* = 1.6 Hz), 139.71, 137.70, 136.90, 134.19 (q, *J* = 33.0 Hz), 129.07, 128.23, 128.00, 127.50, 126.23 (q, *J* = 3.9 Hz), 126.10, 123.27 (q, *J* = 273.6 Hz), 118.83, 80.58, 44.56, 43.71, 41.55, 35.09, 28.34; **$^{19}$F NMR** (376 MHz, $CDCl_3$) δ -63.28; **HRMS** (ESI-TOF) Calc'd for $C_{28}H_{32}F_3N_2O_4S^+$ [M+H] 549.2035, found 549.2024.

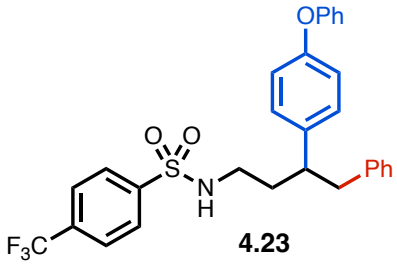


**4.23**

***N*-(3-(4-phenoxyphenyl)-4-phenylbutyl)-4-(trifluoromethyl)benzenesulfonamide (4.23):** Purification using PTLC (20% EtOAc in Hexanes) gave the product as a colorless oil (50.4 mg, 96% yield). **$^{1}$H NMR** (400 MHz, $CDCl_3$) δ 7.87–7.83 (m, 2H), 7.72–7.68 (m, 2H), 7.36–7.29 (m, 2H), 7.22–7.13 (m, 3H), 7.09 (td, *J* = 7.3, 1.1 Hz, 1H), 7.00–6.94 (m, 6H), 6.91–6.85 (m, 2H), 4.62 (t, *J* = 6.0 Hz, 1H), 2.90–2.72 (m, 5H), 1.84 (dtd, *J* = 15.4, 7.5, 4.6 Hz, 1H), 1.74 (dddd, *J* = 13.1, 9.3, 7.3, 5.3 Hz, 1H); **$^{13}$C NMR** (150 MHz, $CDCl_3$) δ 157.32, 155.84, 143.48, 139.69, 138.09, 134.31 (q, *J* = 33.0 Hz), 129.79, 129.12, 128.77, 128.26, 127.54, 126.28 (q, *J* = 3.8 Hz), 126.19, 123.27, 122.82 (q, *J* = 273.7 Hz), 119.12, 118.74, 44.54,

43.80, 41.62, 35.14; **$^{19}$F NMR** (376 MHz, $CDCl_3$) δ -63.26; **HRMS** (ESI-TOF) Calc'd for $C_{29}H_{27}F_3NO_3S^+$ [M+H] 526.1664, found 526.1666.

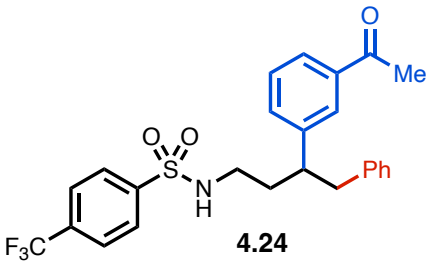

**4.24**

***N*-(3-(3-acetylphenyl)-4-phenylbutyl)-4-(trifluoromethyl)benzenesulfonamide (4.24):** The title compound was prepared from **4.S36** (28 mg, 0.1 mmol), 3-acetylphenyl boronic acid neopentyl glycol ester **4.S12** (70 mg, 0.3 mmol), and iodobenzene (61 mg, 0.3 mmol) according to General Procedure F. Purification using PTLC (20% EtOAc in Hexanes) gave the product as a colorless oil (32.9 mg, 69% yield). **$^1$H NMR** (400 MHz, $CDCl_3$) δ 7.84 (d, *J* = 8.2 Hz, 2H), 7.76 (dd, *J* = 7.7, 1.4 Hz, 1H), 7.72–7.66 (m, 3H), 7.33 (t, *J* = 7.6 Hz, 1H), 7.23 (dt, *J* = 7.7, 1.5 Hz, 1H), 7.21–7.11 (m, 3H), 6.98–6.93 (m, 2H), 4.76 (t, *J* = 6.1 Hz, 1H), 3.02–2.92 (m, 1H), 2.89–2.70 (m, 4H), 2.55 (s, 3H), 1.96–1.77 (m, 2H); **$^{13}$C NMR** (150 MHz, $CDCl_3$) δ 198.41, 143.43 (q, *J* = 1.4 Hz), 139.24, 137.33, 134.29 (q, *J* = 32.9 Hz), 132.50, 129.07, 128.87, 128.31, 127.47, 127.16, 127.07, 126.29, 126.27 (q, *J* = 3.8 Hz), 123.21 (q, *J* = 272.4 Hz), 44.91, 43.52, 41.44, 34.94, 26.70; **$^{19}$F NMR** (376 MHz, $CDCl_3$) δ -63.32; **HRMS** (ESI-TOF) Calc'd for $C_{25}H_{25}F_3NO_3S^+$ [M+H] 476.1507, found 476.1514.

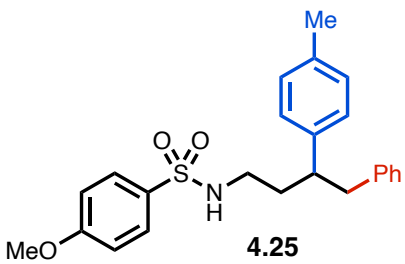

**4.25**

**4-methoxy-*N*-(4-phenyl-3-(*p*-tolyl)butyl)benzenesulfonamide (4.25)**: Purification using PTLC (20% EtOAc in Hexanes) gave the product as a colorless oil (36.9 mg, 90% yield). **$^1$H NMR** (400

MHz, $CDCl_3$) δ 7.65 (d, *J* = 8.9 Hz, 2H), 7.21–7.10 (m, 3H), 7.02 (d, *J* = 7.7 Hz, 2H), 6.97 (d, *J* = 6.6 Hz, 2H), 6.93–6.87 (m, 4H), 4.34 (t, *J* = 6.1 Hz, 1H), 3.84 (s, 3H), 2.86–2.65 (m, 5H), 2.29 (s, 3H), 1.85–1.75 (m, 1H), 1.70 (dqd, *J* = 10.1, 7.4, 5.4 Hz, 1H); **$^{13}$C NMR** (150 MHz, $CDCl_3$) δ 162.76, 140.34, 140.02, 136.01, 131.45, 129.26, 129.18, 129.12, 128.17, 127.42, 125.99, 114.15, 55.61, 44.77, 43.69, 41.48, 35.07, 21.05; **HRMS** (ESI-TOF) Calc'd for $C_{24}H_{28}NO_3S^+$ [M+H] 410.1790, found 410.1800.

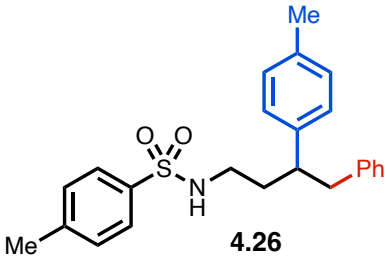


**4.26**

**4-methyl-*N*-(4-phenyl-3-(*p*-tolyl)butyl)benzenesulfonamide (4.26):** Purification using PTLC (20% Acetone in Hexanes) gave the product as a colorless oil (29 mg, 74% yield). **$^{1}$H NMR** (400 MHz, $CDCl_3$) δ 7.60 (d, *J* = 8.3 Hz, 2H), 7.24–7.20 (m, 2H), 7.20–7.09 (m, 3H), 7.02 (d, *J* = 7.6 Hz, 2H), 6.96 (d, *J* = 6.6 Hz, 2H), 6.89 (d, *J* = 8.0 Hz, 2H), 4.42 (t, *J* = 6.0 Hz, 1H), 2.85–2.65 (m, 5H), 2.40 (s, 3H), 2.29 (s, 3H), 1.80 (dddd, *J* = 15.3, 7.7, 3.9, 1.9 Hz, 1H), 1.71 (dddd, *J* = 11.6, 8.0, 5.7, 2.1 Hz, 1H); **$^{13}$C NMR** (150 MHz, $CDCl_3$) δ 143.23, 140.33, 140.02, 136.90, 136.01, 129.63, 129.26, 129.12, 128.17, 127.42, 125.98, 44.75, 43.68, 41.52, 35.12, 21.55, 21.06; **HRMS** (ESI-TOF) Calc'd for $C_{24}H_{28}NO_2S^+$ [M+H] 394.1841, found 394.1841.

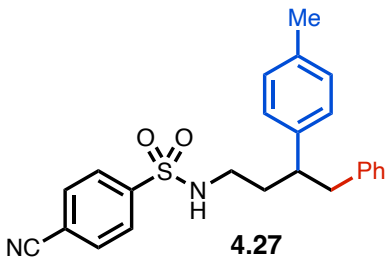


**4.27**

**4-cyano-*N*-(4-phenyl-3-(*p*-tolyl)butyl)benzenesulfonamide (4.27):** Purification using PTLC (20% EtOAc in Hexanes) gave the product as a colorless oil (37.6 mg, 90% yield). **$^{1}$H NMR** (400

MHz, $CDCl_3$) δ 7.78 (d, *J* = 8.6 Hz, 2H), 7.70 (d, *J* = 8.7 Hz, 2H), 7.23–7.13 (m, 3H), 7.05 (d, *J* = 7.6 Hz, 2H), 7.00–6.96 (m, 2H), 6.91 (d, *J* = 8.0 Hz, 2H), 4.47 (t, *J* = 6.0 Hz, 1H), 2.90–2.69 (m, 5H), 2.31 (s, 3H), 1.86–1.64 (m, 2H); **$^{13}$C NMR** (125 MHz, $CDCl_3$) δ 144.22, 140.08, 139.80, 136.34, 132.85, 129.40, 129.07, 128.28, 127.58, 127.30, 126.17, 117.37, 116.21, 44.81, 43.77, 41.69, 34.86, 21.06; **HRMS** (ESI-TOF) Calc'd for $C_{24}H_{25}N_2O_2S^+$ [M+H] 405.1637, found 405.1638.

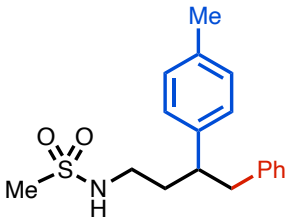

**4.28**

***N*-(4-phenyl-3-(*p*-tolyl)butyl)methanesulfonamide (4.28):** Purification using PTLC (20% Acetone in Hexanes) gave the product as a colorless oil (25.2 mg, 79% yield). **$^1$H NMR** (400 MHz, $CDCl_3$) δ 7.24–7.18 (m, 2H), 7.18–7.12 (m, 1H), 7.09 (d, *J* = 8.4 Hz, 2H), 7.07–6.99 (m, 4H), 4.18 (t, *J* = 6.1 Hz, 1H), 3.01–2.79 (m, 5H), 2.74 (s, 3H), 2.31 (s, 3H), 1.97–1.77 (m, 2H); **$^{13}$C NMR** (150 MHz, $CDCl_3$) δ 140.33, 140.02, 136.26, 129.40, 129.16, 128.26, 127.43, 126.11, 44.93, 43.89, 41.62, 40.08, 35.42, 21.06; **HRMS** (ESI-TOF) Calc'd for $C_{18}H_{24}NO_2S^+$ [M+H] 318.1528, found 318.1533.

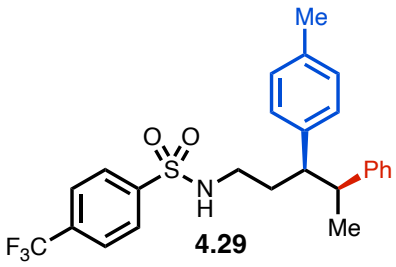

**4.29**

***N*-4-phenyl-3-(*p*-tolyl)pentyl)-4-(trifluoromethyl)benzenesulfonamide (4.29):** Purification using PTLC (20% EtOAc in Hexanes) gave the product as a white solid (32.2 mg, 70% yield). **$^1$H NMR** (400 MHz, $CDCl_3$) δ 7.74 (d, *J* = 8.1 Hz, 2H), 7.67 (d, *J* = 8.3 Hz, 2H), 7.30 (t, *J* = 7.3 Hz, 2H), 7.23 (d, *J* = 7.2 Hz, 1H), 7.15 (d, *J* = 7.4 Hz, 2H), 7.10 (d, *J* = 7.6 Hz, 2H), 6.97 (d, *J* = 7.7 Hz, 2H), 4.03 (s, 1H), 2.74 (p, *J* = 7.0 Hz, 1H), 2.69–2.52 (m, 3H), 2.34

(s, 3H), 1.50 (q, $J$ = 7.8, 7.0 Hz, 2H), 0.93 (d, $J$ = 6.9 Hz, 3H); **$^{13}$C NMR** (125 MHz, $CDCl_3$) δ 145.92, 143.44, 139.35, 136.35, 134.11 (q, $J$ = 33.0 Hz), 129.42, 128.60, 127.86, 127.46, 127.41, 126.40, 126.11 (q, $J$ = 3.8 Hz), 123.28 (q, $J$ = 272.8 Hz), 50.11, 46.32, 41.82, 34.28, 21.11, 21.02; **$^{19}$F NMR** (376 MHz, $CDCl_3$) δ -63.29; **HRMS** (ESI-TOF) Calc'd for $C_{25}H_{27}F_3NO_2S^+$ [M+H] 462.1715, found 462.1713; **X-ray** (single-crystal) Colorless block crystals of X-ray diffraction quality were obtained by vapor diffusion of hexane to a saturated solution of **4.29** in benzene (CCDC 2011492).[27]

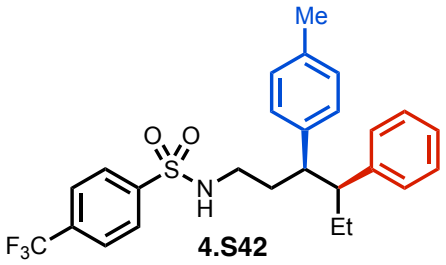

**4.S42**

***N*-4-phenyl-3-(*p*-tolyl)hexyl)-4-(trifluoromethyl)benzenesulfonamide (4.30):** Purification using PTLC (20% Acetone in Hexanes) gave the product as a colorless oil (37.4 mg, 79% yield). **$^{1}$H NMR** (600 MHz, $CDCl_3$) δ 7.74 (d, $J$ = 8.3 Hz, 2H), 7.66 (d, $J$ = 8.3 Hz, 2H), 7.28 (t, $J$ = 7.5 Hz, 2H), 7.23–7.19 (m, 1H), 7.13–7.06 (m, 4H), 6.97 (d, $J$ = 8.0 Hz, 2H), 4.27 (t, $J$ = 5.7 Hz, 1H), 2.66–2.54 (m, 3H), 2.50–2.44 (m, 1H), 2.33 (s, 3H), 1.44 (q, $J$ = 7.3 Hz, 2H), 1.36–1.28 (m, 1H), 1.28–1.21 (m, 1H), 0.48 (t, $J$ = 7.4 Hz, 3H); **$^{13}$C NMR** (150 MHz, $CDCl_3$) δ 143.63, 143.42 (q, $J$ = 1.2 Hz), 139.72, 136.29, 134.08 (q, $J$ = 32.8 Hz), 129.44, 128.50, 128.23, 127.85, 127.46, 126.39, 126.10 (q, $J$ = 3.6 Hz), 123.29 (q, $J$ = 272.6 Hz), 54.10, 49.17, 41.73, 34.35, 27.34, 21.02, 12.08; **$^{19}$F NMR** (376 MHz, $CDCl_3$) δ -65.71; **HRMS** (ESI-TOF) Calc'd for $C_{26}H_{27}F_3NO_2S^-$ [M-H] 474.1715, found 474.1719.

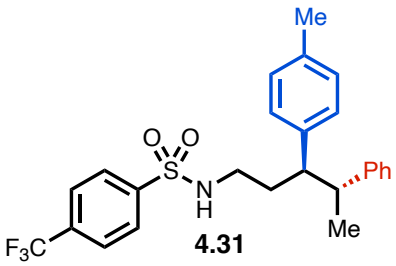

**4.31**

***N*-4-phenyl-3-(*p*-tolyl)pentyl)-4-(trifluoromethyl)benzenesulfonamide (4.31)**: Purification using PTLC (20% Acetone in Hexanes) gave the product as a colorless oil (39.6 mg, 86% yield). **$^1$H NMR** (400 MHz, $CDCl_3$) δ 7.83 (d, *J* = 8.2 Hz, 2H), 7.70 (d, *J* = 8.2 Hz, 2H), 7.17–7.07 (m, 3H), 6.95–6.86 (m, 4H), 6.69 (d, *J* = 8.0 Hz, 2H), 4.41 (t, *J* = 6.1 Hz, 1H), 2.97–2.77 (m, 2H), 2.76–2.65 (m, 2H), 2.24 (s, 3H), 1.98 (dtd, *J* = 13.6, 7.9, 3.8 Hz, 1H), 1.75 (dddd, *J* = 13.7, 12.1, 7.4, 5.0 Hz, 1H), 1.21 (d, *J* = 7.0 Hz, 3H); **$^{13}$C NMR** (150 MHz, $CDCl_3$) δ 144.62, 143.52 (q, *J* = 1.2 Hz), 138.11, 135.95, 134.22 (q, *J* = 33.1 Hz), 128.82, 128.30, 127.94, 127.84, 127.52, 126.16 (q, *J* = 3.8 Hz), 126.00, 123.25 (q, *J* = 272.6 Hz), 49.46, 45.45, 41.90, 32.07, 20.94, 18.42; **$^{19}$F NMR** (376 MHz, $CDCl_3$) δ -63.34; **HRMS** (ESI-TOF) Calc'd for $C_{25}H_{27}F_3NO_2S^+$ [M+H] 462.1715, found 462.1711.

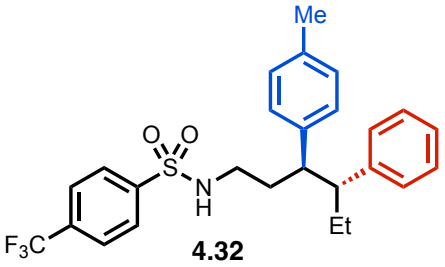

**4.32**

***N*-4-phenyl-3-(*p*-tolyl)hexyl)-4-(trifluoromethyl)benzenesulfonamide (4.32):** Purification using PTLC (20% Acetone in Hexanes) gave the product as a colorless oil (33.9 mg, 71% yield). **$^1$H NMR** (600 MHz, $CDCl_3$) δ 7.84 (d, *J* = 8.1 Hz, 2H), 7.70 (d, *J* = 8.3 Hz, 2H), 7.13–7.06 (m, 3H), 6.89 (d, *J* = 7.8 Hz, 2H), 6.79 (d, *J* = 6.7 Hz, 2H), 6.63 (d, *J* = 8.0 Hz, 2H), 4.60–4.56 (m, 1H), 2.82 (ddt, *J* = 13.0, 7.8, 5.2 Hz, 1H), 2.77 (ddd, *J* = 11.2, 6.9, 3.9 Hz, 1H), 2.71 (dtd, *J* = 13.1, 7.5, 5.5 Hz, 1H), 2.60 (ddd, *J* = 11.0, 6.9, 4.3 Hz, 1H), 2.23 (s, 3H), 2.05–1.97 (m, 1H), 1.78–1.66 (m, 2H), 1.49 (ddq, *J* = 14.5, 10.8, 7.2 Hz, 1H), 0.68 (t, *J* = 7.3 Hz, 3H); **$^{13}$C NMR** (150 MHz, $CDCl_3$) δ 143.54 (q, *J* = 1.7 Hz), 141.99,

137.79, 135.85, 134.22 (q, $J$ = 32.9 Hz), 128.98, 128.65, 128.56, 127.64, 127.53, 126.17 (q, $J$ = 3.6 Hz), 125.98, 123.26 (q, $J$ = 272.6 Hz), 53.36, 48.05, 41.85, 32.96, 25.55, 20.94, 12.25; **$^{19}$F NMR** (376 MHz, $CDCl_3$) δ -65.74; **HRMS** (ESI-TOF) Calc'd for $C_{26}H_{27}F_3NO_2S^-$ [M-H] 474.1715, found 474.1714.

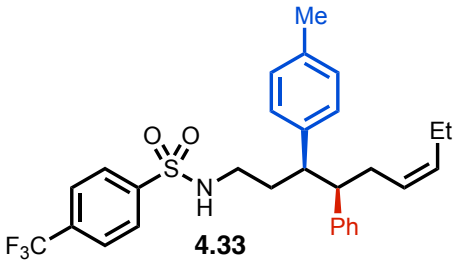

**4.33**

***N*-(*Z*)-4-phenyl-3-(*p*-tolyl)non-6-en-1-yl)-4-(trifluoromethyl)benzenesulfonamide (4.33):** Purification using PTLC (20% Acetone in Hexanes) gave the product as a colorless oil (37.6 mg, 73% yield). **$^1$H NMR** (600 MHz, $CDCl_3$) δ 7.84 (d, $J$ = 8.2 Hz, 2H), 7.70 (d, $J$ = 8.2 Hz, 2H), 7.14–7.08 (m, 3H), 6.91 (d, $J$ = 7.8 Hz, 2H), 6.80 (d, $J$ = 6.2 Hz, 2H), 6.61 (d, $J$ = 8.0 Hz, 2H), 5.31–5.24 (m, 1H), 5.14–5.07 (m, 1H), 4.42 (d, $J$ = 5.8 Hz, 1H), 2.83 (tdd, $J$ = 8.2, 5.9, 3.2 Hz, 2H), 2.78 (dt, $J$ = 9.4, 6.1 Hz, 1H), 2.72 (dt, $J$ = 12.9, 6.6 Hz, 1H), 2.43 (dddd, $J$ = 14.5, 7.2, 5.6, 1.6 Hz, 1H), 2.25 (s, 4H), 2.01 (dtd, $J$ = 13.7, 7.9, 3.9 Hz, 1H), 1.97–1.87 (m, 2H), 1.74 (dddd, $J$ = 13.7, 12.1, 7.4, 5.0 Hz, 1H), 0.86 (t, $J$ = 7.5 Hz, 3H); **$^{13}$C NMR** (150 MHz, $CDCl_3$) δ 143.52 (q, $J$ = 1.1 Hz), 141.75, 137.13, 136.05, 134.23 (q, $J$ = 33.2 Hz), 132.85, 129.04, 128.70, 128.67, 127.58, 127.52, 126.89, 126.16 (q, $J$ = 3.9 Hz), 126.15, 123.24 (q, $J$ = 273.0 Hz), 51.63, 47.40, 41.85, 33.16, 30.33, 20.96, 20.78, 14.09; **$^{19}$F NMR** (376 MHz, $CDCl_3$) δ -65.75; **HRMS** (ESI-TOF) Calc'd for $C_{29}H_{31}F_3NO_2S^-$ [M-H] 514.2028, found 514.2030.

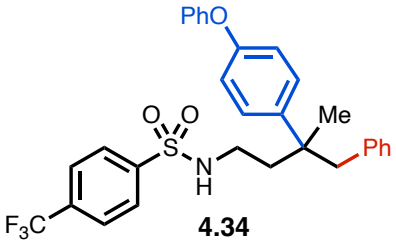


**4.34**

***N*-(3-methyl-3-(4-phenoxyphenyl)-4-phenylbutyl)-4-(trifluoromethyl)benzenesulfonamide (4.34):** Purification using PTLC (20% Acetone in Hexanes) gave the product as a colorless oil (27 mg, 50% yield). **$^1$H NMR** (600 MHz, $CDCl_3$) δ 7.87 (d, *J* = 8.2 Hz, 2H), 7.73 (d, *J* = 8.2 Hz, 2H), 7.35 (dd, *J* = 8.6, 7.3 Hz, 2H), 7.16–7.09 (m, 4H), 7.09–7.06 (m, 2H), 7.02–6.99 (m, 2H), 6.92 (d, *J* = 8.7 Hz, 2H), 6.73 (dd, *J* = 7.8, 1.8 Hz, 2H), 4.49–4.43 (m, 1H), 2.96–2.89 (m, 1H), 2.86 (d, *J* = 13.2 Hz, 1H), 2.77–2.70 (m, 2H), 2.13 (ddd, *J* = 13.5, 10.6, 5.3 Hz, 1H), 1.75 (ddd, *J* = 13.5, 10.5, 5.4 Hz, 1H), 1.20 (s, 3H); **$^{13}$C NMR** (150 MHz, $CDCl_3$) δ 157.30, 155.45, 143.59 (q, *J* = 1.2 Hz), 140.09, 137.32, 134.34 (q, *J* = 33.2 Hz), 130.50, 129.79, 127.85, 127.63, 127.53, 126.32, 126.25 (q, *J* = 3.7 Hz), 123.28, 123.23 (q, *J* = 272.8 Hz), 118.79, 118.68, 51.08, 41.83, 40.75, 39.73, 23.23; **$^{19}$F NMR** (376 MHz, $CDCl_3$) δ -63.28; **HRMS** (ESI-TOF) Calc'd for $C_{30}H_{29}F_3NO_3S^+$ [M+H] 540.1820, found 540.1827.

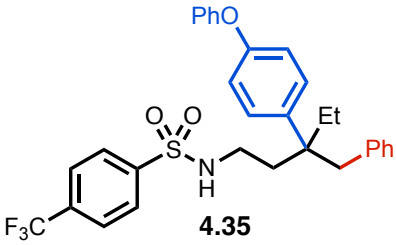


**4.35**

***N*-(3-benzyl-3-(4-phenoxyphenyl)pentyl)-4-(trifluoromethyl)benzenesulfonamide (4.35):** Purification using PTLC (20% EtOAc in Hexanes) gave the product as a colorless oil (12.1 mg, 22% yield). **$^1$H NMR** (600 MHz, $CDCl_3$) δ 7.91 (d, *J* = 8.2 Hz, 2H), 7.75 (d, *J* = 8.3 Hz, 2H), 7.35 (dd, *J* = 8.6, 7.3 Hz, 2H), 7.15–7.08 (m, 4H), 7.06 (d, *J* = 8.8 Hz, 2H), 7.00 (d, *J* = 7.5 Hz, 2H), 6.92 (d, *J* = 8.8 Hz, 2H), 6.65 (d, *J* = 6.7 Hz, 2H), 4.39 (s, 1H), 2.98–2.86 (m, 2H), 2.84 (s, 2H), 1.88 (ddd, *J* = 13.8, 10.8, 5.5 Hz, 1H), 1.82 (ddd, *J* = 13.7, 10.7, 5.6 Hz, 1H), 1.62 (q, *J* = 7.4 Hz, 2H), 0.84 (t, *J* = 7.4 Hz, 3H); **$^{13}$C NMR** (150 MHz, $CDCl_3$) δ 157.32,

155.29, 143.66 (q, $J$ = 1.6 Hz), 139.79, 137.34, 134.39 (q, $J$ = 33.2 Hz), 130.10, 129.77, 128.02, 127.74, 127.56, 126.30, 126.28 (q, $J$ = 3.9 Hz), 123.24, 123.22 (q, $J$ = 272.6 Hz), 118.77, 118.63, 44.34, 43.67, 39.29, 36.62, 28.08, 8.19; **HRMS** (ESI-TOF) Calc'd for $C_{31}H_{31}F_3NO_3S^+$ [M+H] 554.1977, found 554.1984.

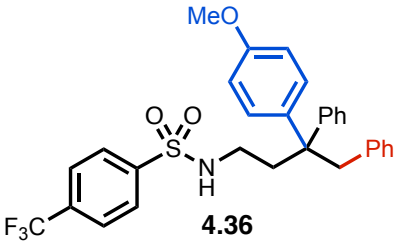

**4.36**

***N*-(3-(4-methoxyphenyl)-3,4-diphenylbutyl)-4-(trifluoromethyl)benzenesulfonamide (4.36):** Purification using mass-directed prep LC gave the product as a colorless oil (14.2 mg, 26% yield). **$^1$H NMR** (600 MHz, $CDCl_3$) δ 7.81 (d, $J$ = 8.2 Hz, 2H), 7.72 (d, $J$ = 8.2 Hz, 2H), 7.24–7.18 (m, 3H), 7.13–7.09 (m, 1H), 7.04–6.99 (m, 4H), 6.91 (d, $J$ = 8.8 Hz, 2H), 6.76 (d, $J$ = 8.8 Hz, 2H), 6.40 (d, $J$ = 6.7 Hz, 2H), 4.14 (t, $J$ = 6.1 Hz, 1H), 3.80 (s, 3H), 3.28 (d, $J$ = 2.2 Hz, 2H), 2.94–2.83 (m, 2H), 2.05 (t, $J$ = 7.8 Hz, 2H); **$^{13}$C NMR** (150 MHz, $CDCl_3$) δ 157.92, 146.95, 143.61 (q, $J$ = 1.4 Hz), 138.73, 136.88, 134.27 (q, $J$ = 33.1 Hz), 130.37, 129.03, 128.11, 127.97, 127.58, 127.54, 126.38, 126.36, 126.18 (q, $J$ = 3.6 Hz), 123.25 (q, $J$ = 272.9 Hz), 113.40, 55.24, 49.03, 44.46, 39.88, 36.94; **$^{19}$F NMR** (376 MHz, $CDCl_3$) δ -65.74; **HRMS** (ESI-TOF) Calc'd for $C_{30}H_{27}F_3NO_3S^-$ [M-H] 538.1664, found 538.1660.

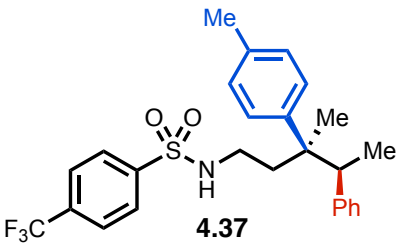

**4.37**

***N*-3-methyl-4-phenyl-3-(*p*-tolyl)pentyl)-4-(trifluoromethyl)benzenesulfonamide (4.37):** Purification using PTLC (20% Acetone in Hexanes) gave the product as a colorless oil (18.9 mg, 40% yield).

**$^{1}$H NMR** (600 MHz, $CDCl_3$) δ 7.86 (d, *J* = 8.1 Hz, 2H), 7.71 (d, *J* = 8.3 Hz, 2H), 7.12–7.07 (m, 3H), 7.02–6.98 (m, 2H), 6.86 (d, *J* = 8.2 Hz, 2H), 6.73 (d, *J* = 6.0 Hz, 2H), 4.36 (d, *J* = 5.8 Hz, 1H), 2.86 (dq, *J* = 14.4, 7.2, 6.5 Hz, 2H), 2.72–2.64 (m, 1H), 2.30 (s, 3H), 2.10 (ddd, *J* = 13.4, 10.9, 4.9 Hz, 1H), 1.77 (ddd, *J* = 13.5, 10.9, 5.5 Hz, 1H), 1.20 (s, 3H), 1.14 (d, *J* = 7.2 Hz, 3H); **$^{13}$C NMR** (150 MHz, $CDCl_3$) δ 143.66 (q, *J* = 1.7 Hz), 142.81, 140.73, 135.60, 134.25 (q, *J* = 33.1 Hz), 129.36, 128.55, 127.53, 127.21, 127.19, 126.18 (q, *J* = 4.0 Hz), 126.12, 123.35 (q, *J* = 273.3 Hz), 51.22, 43.26, 40.05, 38.95, 21.59, 20.85, 15.64; **$^{19}$F NMR** (376 MHz, $CDCl_3$) δ -65.75; **HRMS** (ESI-TOF) Calc'd for $C_{26}H_{28}F_3NO_2S^+$ [M+H] 448.1558, found 448.1562.

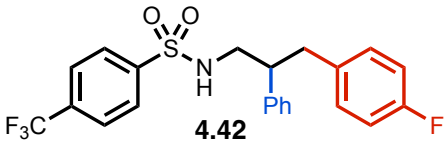


**4.42**

***N*-(3-(4-fluorophenyl)-2-phenylpropyl)-4-(trifluoromethyl)benzenesulfonamide (4.42):** Purification using mass-directed prep LC gave the product as a colorless oil (9.8 mg, 22% yield, 10:1 r.r.). **$^{1}$H NMR** (500 MHz, $CDCl_3$) δ 7.81 (d, *J* = 8.2 Hz, 2H), 7.73 (d, *J* = 8.2 Hz, 2H), 7.26–7.17 (m, 3H), 6.99–6.94 (m, 2H), 6.93–6.85 (m, 4H), 4.29 (dd, *J* = 7.9, 4.6 Hz, 1H), 3.32 (ddd, *J* = 12.9, 7.9, 4.8 Hz, 1H), 3.11 (ddd, *J* = 13.1, 8.8, 4.5 Hz, 1H), 2.95–2.77 (m, 3H); **$^{13}$C NMR** (150 MHz, $CDCl_3$) δ 161.51 (d, *J* = 244.6 Hz), 143.36 (q, *J* = 1.1 Hz), 140.18, 134.39 (d, *J* = 3.3 Hz), 134.37 (q, *J* = 32.6 Hz), 130.32 (d, *J* = 8.2 Hz), 129.03, 127.68, 127.54, 127.51, 126.26 (q, *J* = 3.8 Hz), 123.22 (q, *J* = 272.6 Hz), 115.20 (d, *J* = 21.0 Hz), 47.67, 47.43, 39.28 δ; **$^{19}$F NMR** (376 MHz, $CDCl_3$) δ -65.77, -119.21; **HRMS** (ESI-TOF) Calc'd for $C_{22}H_{18}F_4NO_2S^-$ [M-H] 436.0994, found 436.0999.

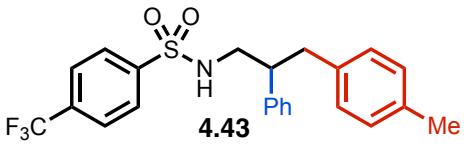


**4.43**

***N*-(2-phenyl-3-(*p*-tolyl)propyl)-4-(trifluoromethyl)benzenesulfonamide (4.43):** Purification using PTLC (20% EtOAc in Hexanes) gave the product as a white solid (31.5 mg, 73% yield, 7:1 r.r.). **$^1$H NMR** (400 MHz, $CDCl_3$) δ 7.77 (d, *J* = 8.2 Hz, 2H), 7.69 (d, *J* = 8.3 Hz, 2H), 7.27–7.15 (m, 3H), 7.06–6.95 (m, 4H), 6.85 (d, *J* = 8.0 Hz, 2H), 4.40 (dd, *J* = 7.7, 4.5 Hz, 1H), 3.30 (ddd, *J* = 12.7, 7.6, 5.0 Hz, 1H), 3.09 (ddd, *J* = 12.7, 9.1, 4.6 Hz, 1H), 2.90 (tdd, *J* = 8.9, 6.5, 4.9 Hz, 1H), 2.84–2.77 (m, 2H), 2.29 (s, 3H); **$^{13}$C NMR** (150 MHz, $CDCl_3$) δ 143.37 (q, *J* = 1.3 Hz), 140.81, 135.94, 135.67, 134.24 (q, *J* = 32.9 Hz), 129.12, 128.95, 128.79, 127.67, 127.53, 127.36, 126.21 (q, *J* = 3.7 Hz), 123.27 (q, *J* = 273.0 Hz), 47.45, 39.82, 21.01; **$^{19}$F NMR** (376 MHz, $CDCl_3$) δ -63.32; **HRMS** (ESI-TOF) Calc'd for $C_{23}H_{21}F_3NO_2S^-$ [M+H] 432.1245, found 432.1249.

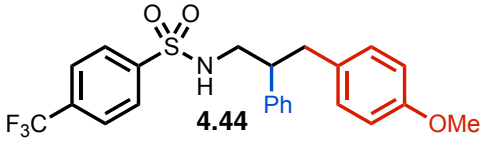


**4.44**

***N*-(3-(4-methoxyphenyl)-2-phenylpropyl)-4-(trifluoromethyl)benzenesulfonamide (4.44):** Purification using PTLC (20% EtOAc in Hexanes) gave the product as a white solid (29.3 mg, 65% yield, 7:1 r.r.). **$^1$H NMR** (400 MHz, $CDCl_3$) δ 7.78 (d, *J* = 8.4 Hz, 2H), 7.70 (d, *J* = 8.3 Hz, 2H), 7.27–7.15 (m, 3H), 6.98 (dd, *J* = 7.6, 1.8 Hz, 2H), 6.87 (d, *J* = 8.6 Hz, 2H), 6.74 (d, *J* = 8.6 Hz, 2H), 4.38 (dd, *J* = 7.6, 4.5 Hz, 1H), 3.76 (s, 3H), 3.31 (ddd, *J* = 12.7, 7.7, 4.9 Hz, 1H), 3.10 (ddd, *J* = 12.7, 9.1, 4.6 Hz, 1H), 2.93–2.84 (m, 1H), 2.79 (d, *J* = 7.4 Hz, 2H); **$^{13}$C NMR** (150 MHz, $CDCl_3$) δ 158.14, 143.38 (q, *J* = 1.2 Hz), 140.74, 134.24 (q, *J* = 33.2 Hz), 130.78, 129.88, 128.94, 127.70, 127.52, 127.35, 126.23 (q, *J* = 3.5 Hz), 123.26 (q, *J* = 272.6 Hz), 113.80, 55.21, 47.62, 47.42, 39.34; **$^{19}$F NMR**

(376 MHz, $CDCl_3$) δ -63.32; **HRMS** (ESI-TOF) Calc'd for $C_{23}H_{21}F_3NO_3S^-$ [M-H] 448.1194, found 448.1199.

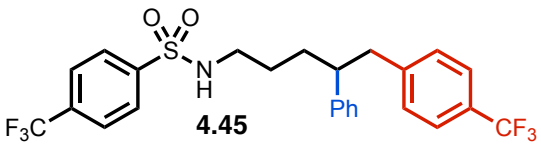


**4.45**

***N*-(4-phenyl-5-(4-(trifluoromethyl)phenyl)pentyl)-4-(trifluoromethyl)benzenesulfonamide (4.45):** Purification using PTLC (20% Acetone in Hexanes) gave the product as a colorless oil (38.8 mg, 75% yield). **$^1$H NMR** (600 MHz, $CDCl_3$) δ 7.90 (d, *J* = 8.1 Hz, 2H), 7.75–7.71 (m, 2H), 7.43 (d, *J* = 8.0 Hz, 2H), 7.25–7.21 (m, 2H), 7.19–7.16 (m, 1H), 7.06 (d, *J* = 8.0 Hz, 2H), 7.00 (d, *J* = 6.9 Hz, 2H), 4.49 (t, *J* = 5.9 Hz, 1H), 2.91–2.86 (m, 4H), 2.73 (dtd, *J* = 10.3, 7.4, 4.7 Hz, 1H), 1.70–1.56 (m, 3H), 1.36–1.23 (m, 3H); **$^{13}$C NMR** (150 MHz, $CDCl_3$) δ 144.24 (q, *J* = 1.1 Hz), 143.61 (q, *J* = 1.1 Hz), 143.30, 134.34 (q, *J* = 33.5 Hz), 129.33, 128.56, 128.31 (q, *J* = 32.1 Hz), 127.55, 127.47, 126.65, 126.28 (q, *J* = 3.8 Hz), 125.05 (q, *J* = 3.8 Hz), 124.29 (q, *J* = 272.0 Hz), 123.22 (q, *J* = 273.1 Hz), 47.41, 43.60, 43.20, 32.37, 27.70; **$^{19}$F NMR** (376 MHz, $CDCl_3$) δ -64.98, -65.76; **HRMS** (ESI-TOF) Calc'd for $C_{25}H_{23}F_6NO_2S^+$ [M+H] 514.1275, found 514.1271.

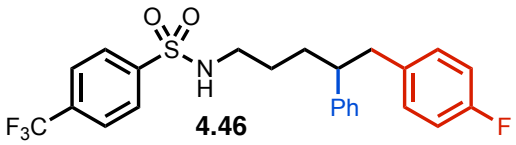


**4.46**

***N*-(5-(4-fluorophenyl)-4-phenylpentyl)-4-(trifluoromethyl)benzenesulfonamide (4.46):** Purification using PTLC (20% Acetone in Hexanes) gave the product as a colorless oil (34.5 mg, 74% yield). **$^1$H NMR** (600 MHz, $CDCl_3$) δ 7.90 (d, *J* = 7.8 Hz, 2H), 7.73 (d, *J* = 8.2 Hz, 2H), 7.23 (t, *J* = 7.4 Hz, 2H), 7.19–7.15 (m, 1H), 7.00 (d, *J* = 6.9 Hz, 2H), 6.90 (ddd, *J* = 8.4, 5.5, 2.5 Hz, 2H), 6.88–

6.84 (m, 2H), 4.43 (t, *J* = 6.0 Hz, 1H), 2.88 (ddt, *J* = 8.8, 6.9, 3.1 Hz, 2H), 2.79 (d, *J* = 7.4 Hz, 2H), 2.67 (dtd, *J* = 10.6, 7.3, 4.5 Hz, 1H), 1.65 (dddd, *J* = 13.5, 10.5, 6.1, 4.5 Hz, 1H), 1.61–1.53 (m, 1H), 1.34–1.21 (m, 2H); **$^{13}$C NMR** (150 MHz, $CDCl_3$) δ 161.30 (d, *J* = 243.8 Hz), 143.73, 143.64 (q, *J* = 1.7 Hz), 135.76 (d, *J* = 3.3 Hz), 134.31 (q, *J* = 32.6 Hz), 130.37 (d, *J* = 7.6 Hz), 128.48, 127.59, 127.48, 126.49, 126.27 (q, *J* = 3.6 Hz), 123.23 (q, *J* = 273.1 Hz), 114.89 (d, *J* = 21.1 Hz), 47.75, 43.24, 43.00, 32.19, 27.72; **$^{19}$F NMR** (376 MHz, $CDCl_3$) δ -65.75, -120.01; **HRMS** (ESI-TOF) Calc'd for $C_{24}H_{22}F_4NO_2S^-$ [M-H] 464.1307, found 464.1305.

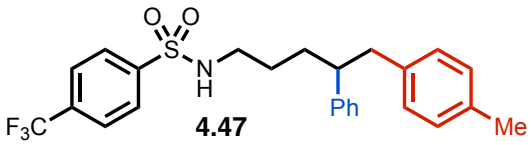


**4.47**

***N*-(4-phenyl-5-(*p*-tolyl)pentyl)-4-(trifluoromethyl)benzenesulfonamide (4.47):** Purification using PTLC (20% Acetone in Hexanes) gave the product as a colorless oil (26.3 mg, 57% yield). **$^{1}$H NMR** (600 MHz, $CDCl_3$) δ 7.88 (d, *J* = 8.0 Hz, 2H), 7.72 (d, *J* = 8.3 Hz, 2H), 7.23 (dd, *J* = 8.1, 6.8 Hz, 2H), 7.18–7.15 (m, 1H), 7.04 (d, *J* = 6.9 Hz, 2H), 7.01 (d, *J* = 7.7 Hz, 2H), 6.88 (d, *J* = 8.0 Hz, 2H), 4.47 (t, *J* = 6.1 Hz, 1H), 2.90–2.79 (m, 3H), 2.73 (dd, *J* = 13.4, 7.6 Hz, 1H), 2.68 (dtd, *J* = 14.7, 7.3, 4.2 Hz, 1H), 2.28 (s, 3H), 1.62 (dddd, *J* = 13.9, 10.4, 6.6, 4.3 Hz, 1H), 1.52 (dtd, *J* = 13.5, 9.9, 5.8 Hz, 1H), 1.28–1.21 (m, 2H); **$^{13}$C NMR** (150 MHz, $CDCl_3$) δ 144.37, 143.66 (q, *J* = 1.2 Hz), 137.10, 135.44, 134.27 (q, *J* = 33.2 Hz), 128.96, 128.88, 128.44, 127.58, 127.49, 126.36, 126.25 (q, *J* = 3.6 Hz), 123.26 (q, *J* = 273.1 Hz), 47.57, 43.26, 32.02, 27.66, 21.01; **$^{19}$F NMR** (376 MHz, $CDCl_3$) δ -65.73; **HRMS** (ESI-TOF) Calc'd for $C_{25}H_{25}F_3NO_2S^-$ [M-H] 460.1558, found 460.1550.

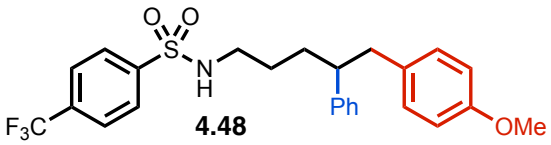


**4.48**

***N*-(5-(4-methoxyphenyl)-4-phenylpentyl)-4-(trifluoromethyl)benzenesulfonamide (4.48):** Purification using PTLC (20% Acetone in Hexanes) gave the product as a colorless oil (24.3 mg, 51% yield). **$^1$H NMR** (600 MHz, $CDCl_3$) δ 7.88 (d, *J* = 8.1 Hz, 2H), 7.72 (d, *J* = 8.2 Hz, 2H), 7.23 (t, *J* = 7.4 Hz, 2H), 7.18–7.15 (m, 1H), 7.02 (d, *J* = 6.8 Hz, 2H), 6.89 (d, *J* = 8.6 Hz, 2H), 6.74 (d, *J* = 8.6 Hz, 2H), 4.49–4.45 (m, 1H), 3.75 (s, 3H), 2.86 (dh, *J* = 11.2, 6.0 Hz, 2H), 2.79 (dd, *J* = 13.5, 7.3 Hz, 1H), 2.73 (dd, *J* = 13.6, 7.4 Hz, 1H), 2.66 (dtd, *J* = 14.7, 7.3, 4.3 Hz, 1H), 1.66–1.60 (m, 1H), 1.53 (dtd, *J* = 13.6, 9.5, 5.7 Hz, 1H), 1.29–1.22 (m, 2H); **$^{13}$C NMR** (150 MHz, $CDCl_3$) δ 157.84, 144.30, 143.66 (q, *J* = 1.6 Hz), 134.26 (q, *J* = 33.2 Hz), 132.26, 129.98, 128.43, 127.60, 127.49, 126.35, 126.25 (q, *J* = 3.7 Hz), 123.25 (q, *J* = 273.2 Hz), 113.56, 55.20, 47.75, 43.26, 42.93, 32.01, 27.68; **$^{19}$F NMR** (376 MHz, $CDCl_3$) δ -65.72; **HRMS** (ESI-TOF) Calc'd for $C_{25}H_{25}F_3NO_3S^-$ [M-H] 476.1507, found 476.1500.

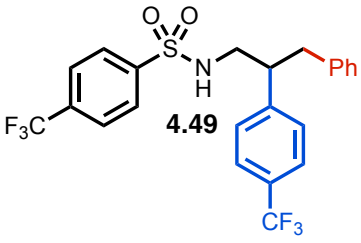


**4.49**

***N*-(3-phenyl-2-(4-(trifluoromethyl)phenyl)propyl)-4-(trifluoromethyl)benzenesulfonamide (4.49):** Purification using mass-directed prep LC gave the product as a white solid (31 mg, 64% yield). **$^1$H NMR** (600 MHz, $CDCl_3$) δ 7.79 (d, *J* = 8.0 Hz, 2H), 7.71 (d, *J* = 8.3 Hz, 2H), 7.50 (d, *J* = 8.0 Hz, 2H), 7.25–7.17 (m, 3H), 7.13 (d, *J* = 8.0 Hz, 2H), 6.97 (d, *J* = 6.5 Hz, 2H), 4.42 (dd, *J* = 7.3, 5.3 Hz, 1H), 3.34 (ddd, *J* = 12.7, 7.3, 5.1 Hz, 1H), 3.16 (ddd, *J* = 13.0, 9.1, 5.3 Hz, 1H), 3.08 (dtd, *J* = 9.0, 7.4, 5.0 Hz, 1H), 2.91 (dd, *J* = 13.8, 7.4 Hz, 1H), 2.85 (dd, *J* = 13.8, 7.5 Hz, 1H); **$^{13}$C NMR** (150 MHz, $CDCl_3$) δ 144.93 (q, *J* = 1.6 Hz), 143.26 (q, *J* = 1.6 Hz),

138.13, 134.48 (q, $J$ = 32.7 Hz), 128.87, 128.58, 128.12, 127.55 (q, $J$ = 32.6 Hz), 127.48, 126.69, 126.30 (q, $J$ = 3.5 Hz), 125.81 (q, $J$ = 3.8 Hz), 123.94 (q, $J$ = 272.0 Hz), 123.16 (q, $J$ = 273.1 Hz), 47.59, 47.37, 39.99; **$^{19}$F NMR** (376 MHz, $CDCl_3$) δ -65.22, -65.82; **HRMS** (ESI-TOF) Calc'd for $C_{23}H_{18}F_6NO_2S^-$ [M-H] 486.0962, found 486.0963.

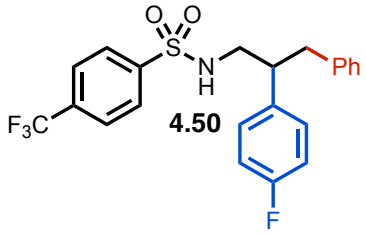


***N*-(2-(4-fluorophenyl)-3-phenylpropyl)-4-(trifluoromethyl)benzenesulfonamide (4.50):** Purification using mass-directed prep LC gave the product as a white solid (23 mg, 53% yield, 14:1 r.r.). **$^1$H NMR** (600 MHz, $CDCl_3$) δ 7.80 (d, $J$ = 8.3 Hz, 2H), 7.72 (d, $J$ = 8.2 Hz, 2H), 7.24–7.15 (m, 3H), 6.98–6.90 (m, 6H), 4.36 (dd, $J$ = 7.7, 4.8 Hz, 1H), 3.31 (ddd, $J$ = 12.8, 7.6, 5.1 Hz, 1H), 3.09 (ddd, $J$ = 12.9, 9.2, 4.9 Hz, 1H), 2.96 (dtd, $J$ = 9.1, 7.5, 5.1 Hz, 1H), 2.86 (dd, $J$ = 13.6, 7.4 Hz, 1H), 2.80 (dd, $J$ = 13.8, 7.6 Hz, 1H); **$^{13}$C NMR** (150 MHz, $CDCl_3$) δ 161.92 (d, $J$ = 246.4 Hz), 143.35 (q, $J$ = 1.3 Hz), 138.49, 136.26 (d, $J$ = 2.8 Hz), 134.39 (q, $J$ = 33.2 Hz), 129.16 (d, $J$ = 7.8 Hz), 128.90, 128.48, 127.50, 126.53, 126.27 (q, $J$ = 3.6 Hz), 123.20 (q, $J$ = 272.7 Hz), 115.82 (d, $J$ = 21.6 Hz), 47.58, 46.91, 40.35; **$^{19}$F NMR** (376 MHz, $CDCl_3$) δ -65.77, -117.58; **HRMS** (ESI-TOF) Calc'd for $C_{22}H_{18}F_4NO_2S^-$ [M-H] 436.0994, found 436.0989.

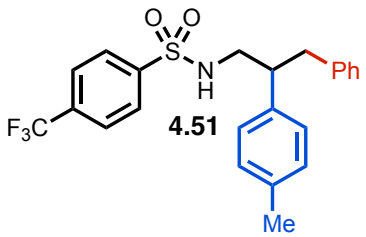


***N*-(3-phenyl-2-(*p*-tolyl)propyl)-4-(trifluoromethyl)benzenesulfonamide (4.51):** Purification using PTLC (20% Acetone in Hexanes) gave the product as a white solid (29.3 mg, 68% yield). **$^1$H**

**NMR** (400 MHz, $CDCl_3$) δ 7.77 (d, *J* = 8.2 Hz, 2H), 7.69 (d, *J* = 8.2 Hz, 2H), 7.24–7.13 (m, 3H), 7.04 (d, *J* = 7.4 Hz, 2H), 6.97 (d, *J* = 6.3 Hz, 2H), 6.87 (d, *J* = 8.1 Hz, 2H), 4.40 (dd, *J* = 7.8, 4.4 Hz, 1H), 3.29 (ddd, *J* = 12.6, 7.7, 4.7 Hz, 1H), 3.13–3.03 (m, 1H), 2.94–2.77 (m, 3H), 2.30 (s, 3H); **$^{13}$C NMR** (150 MHz, $CDCl_3$) δ 143.38 (d, *J* = 1.2 Hz), 138.95, 137.52, 137.02, 134.21 (q, *J* = 32.9 Hz), 129.64, 128.93, 127.53, 127.51, 126.40, 126.19 (q, *J* = 3.6 Hz), 123.28 (q, *J* = 273.1 Hz), 47.50, 46.97, 40.28, 21.00; **$^{19}$F NMR** (400 MHz, $CDCl_3$) δ -63.29; **HRMS** (ESI-TOF) Calc'd for $C_{23}H_{23}F_3NO_2S^+$ [M+H] 434.1402, found 434.1404. **X-ray** (single-crystal) Colorless block crystals of X-ray diffraction quality were obtained by vapor diffusion of hexane to a saturated solution of **4.51** in benzene (CCDC 2039700).[27]

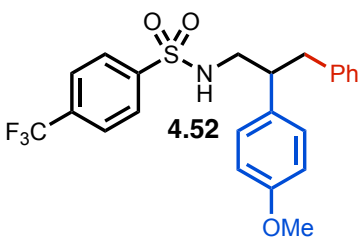

**4.52**

***N*-(2-(4-methoxyphenyl)-3-phenylpropyl)-4-(trifluoromethyl)benzenesulfonamide (4.52):** Purification using PTLC (20% EtOAc in Hexanes) gave the product as a white solid (18 mg, 39% yield, 8:1 r.r.). **$^{1}$H NMR** (400 MHz, $CDCl_3$) δ 7.85–7.79 (m, 2H), 7.69 (d, *J* = 8.3 Hz, 2H), 7.21–7.11 (m, 3H), 7.03 (d, *J* = 7.8 Hz, 2H), 6.98 (d, *J* = 6.4 Hz, 2H), 6.90 (d, *J* = 8.0 Hz, 2H), 4.48 (t, *J* = 6.0 Hz, 1H), 2.89–2.69 (m, 5H), 2.30 (s, 3H), 1.82 (dtd, *J* = 13.5, 7.6, 3.7 Hz, 1H), 1.71 (dddd, *J* = 13.5, 10.0, 7.4, 5.5 Hz, 1H); **$^{13}$C NMR** (150 MHz, $CDCl_3$) δ 158.80, 143.38 (q, *J* = 1.7 Hz), 138.90, 134.27 (q, *J* = 33.1 Hz), 132.37, 128.93, 128.63, 128.42, 127.53, 126.39, 126.22 (q, *J* = 3.7 Hz), 123.25 (q, *J* = 272.6 Hz), 114.35, 55.25, 47.58, 46.60, 40.42; **$^{19}$F NMR** (376 MHz, $CDCl_3$) δ -65.73; **HRMS** (ESI-TOF) Calc'd for $C_{23}H_{21}F_3NO_3S^-$ [M-H] 448.1194, found 448.1200.

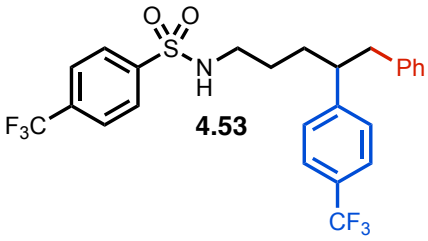


**4.53**

***N*-(5-phenyl-4-(4-(trifluoromethyl)phenyl)pentyl)-4-(trifluoromethyl)benzenesulfonamide (4.53):** Purification using mass-directed prep LC gave the product as a colorless oil (25.2 mg, 49% yield). **$^{1}$H NMR** (600 MHz, $CDCl_3$) δ 7.90 (d, *J* = 8.1 Hz, 2H), 7.74 (d, *J* = 8.2 Hz, 2H), 7.49 (d, *J* = 8.0 Hz, 2H), 7.22–7.19 (m, 2H), 7.18–7.13 (m, 3H), 6.97 (d, *J* = 6.8 Hz, 2H), 4.45 (t, *J* = 6.2 Hz, 1H), 2.91–2.86 (m, 2H), 2.86–2.79 (m, 3H), 1.75–1.67 (m, 1H), 1.64–1.55 (m, 2H), 1.28 (dddd, *J* = 21.3, 14.2, 8.6, 4.1 Hz, 3H); **$^{13}$C NMR** (150 MHz, $CDCl_3$) δ 148.31 (q, *J* = 1.4 Hz), 143.60 (q, *J* = 1.4 Hz), 139.47, 134.39 (q, *J* = 32.6 Hz), 129.01, 128.75 (q, *J* = 32.1 Hz), 128.31, 127.94, 127.48, 126.29 (q, *J* = 3.7 Hz), 126.24, 125.39 (q, *J* = 3.8 Hz), 124.20 (q, *J* = 272.5 Hz), 123.20 (q, *J* = 273.1 Hz), 47.52, 43.54, 43.15, 32.03, 27.69; **$^{19}$F NMR** (376 MHz, $CDCl_3$) δ -65.00, -65.79; **HRMS** (ESI-TOF) Calc'd for $C_{25}H_{22}F_6NO_2S^-$ [M-H] 514.1275, found 514.1279.

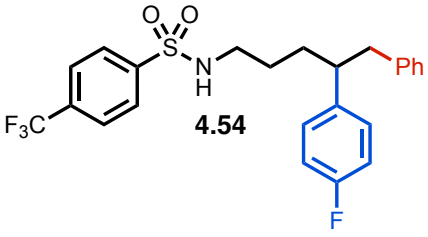


**4.54**

***N*-(4-(4-fluorophenyl)-5-phenylpentyl)-4-(trifluoromethyl)benzenesulfonamide (4.54):** Purification using PTLC (20% Acetone in Hexanes) gave the product as a colorless oil (35.7 mg, 77% yield). **$^{1}$H NMR** (600 MHz, $CDCl_3$) δ 7.90 (d, *J* = 8.2 Hz, 2H), 7.74 (d, *J* = 8.2 Hz, 2H), 7.21–7.17 (m, 2H), 7.16–7.12 (m, 1H), 6.98–6.94 (m, 4H), 6.93–6.88 (m, 2H), 4.55 (t, *J* = 6.1 Hz, 1H), 2.90–2.84 (m, 2H), 2.79 (dd, *J* = 7.4, 2.9 Hz, 2H), 2.71 (dtd, *J* = 10.1, 7.3, 4.4 Hz, 1H), 1.66 (dddd, *J* = 14.7, 13.6, 6.5, 3.2 Hz, 1H), 1.53 (dtd, *J* = 13.6, 10.0, 5.5 Hz, 1H), 1.33–1.21 (m, 3H); **$^{13}$C NMR** (150 MHz, $CDCl_3$) δ 161.40 (d, *J* = 244.3 Hz),

143.61 (q, $J$ = 1.3 Hz), 139.89, 139.68 (d, $J$ = 3.3 Hz), 134.35 (q, $J$ = 33.7 Hz), 129.05, 128.90 (d, $J$ = 7.8 Hz), 128.20, 127.49, 126.28 (q, $J$ = 3.8 Hz), 126.06, 123.22 (q, $J$ = 272.6 Hz), 115.20 (d, $J$ = 21.0 Hz), 46.90, 43.93, 43.20, 32.31, 27.68; **HRMS** (ESI-TOF) Calc'd for $C_{24}H_{22}F_3NO_2S^-$ [M-H] 448.1558, found 448.1562.

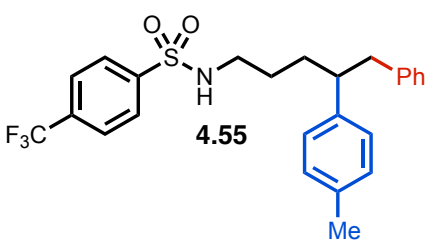


**4.55**

***N*-(5-phenyl-4-(*p*-tolyl)pentyl)-4-(trifluoromethyl)benzenesulfonamide (4.55):** Purification using PTLC (20% EtOAc in Hexanes) gave the product as a white solid (37.5 mg, 82% yield). **$^1$H NMR** (400 MHz, $CDCl_3$) δ 7.88 (d, $J$ = 8.2 Hz, 2H), 7.71 (d, $J$ = 8.2 Hz, 2H), 7.22–7.17 (m, 2H), 7.16–7.11 (m, 1H), 7.04 (d, $J$ = 7.8 Hz, 2H), 6.99 (d, $J$ = 6.7 Hz, 2H), 6.92 (d, $J$ = 8.0 Hz, 2H), 4.55 (t, $J$ = 6.1 Hz, 1H), 2.88–2.79 (m, 3H), 2.75 (dd, $J$ = 13.3, 7.5 Hz, 1H), 2.67 (dtd, $J$ = 10.1, 7.2, 4.3 Hz, 1H), 2.29 (s, 3H), 1.65–1.55 (m, 1H), 1.55–1.45 (m, 1H), 1.30–1.19 (m, 2H); **$^{13}$C NMR** (150 MHz, $CDCl_3$) δ 143.68 (q, $J$ = 1.5 Hz), 135.84, 134.26 (q, $J$ = 33.0 Hz), 129.15, 129.11, 128.17, 127.51, 126.25 (q, $J$ = 3.8 Hz), 125.95, 123.27 (q, $J$ = 273.6 Hz), 47.06, 43.92, 43.27, 32.09, 27.63, 21.01; **$^{19}$F NMR** (376 MHz, $CDCl_3$) δ -63.31; **HRMS** (ESI-TOF) Calc'd for $C_{25}H_{27}F_3NO_2S^+$ [M+H] 462.1715, found 462.1722.

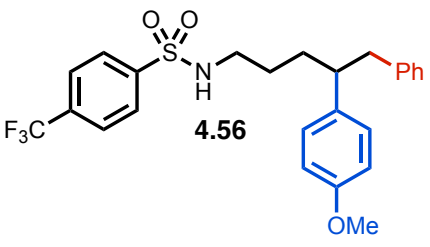


**4.56**

***N*-(4-(4-methoxyphenyl)-5-phenylpentyl)-4-(trifluoromethyl)benzenesulfonamide (4.56):** Purification using PTLC (20% Acetone in Hexanes) gave the product as a colorless oil (30.2 mg, 63%

yield). **$^{1}$H NMR** (600 MHz, $CDCl_3$) δ 7.89 (d, *J* = 8.2 Hz, 2H), 7.72 (d, *J* = 8.3 Hz, 2H), 7.19 (t, *J* = 7.3 Hz, 2H), 7.15–7.12 (m, 1H), 6.98 (d, *J* = 6.8 Hz, 2H), 6.94 (d, *J* = 8.6 Hz, 2H), 6.77 (d, *J* = 8.6 Hz, 2H), 4.53 (t, *J* = 6.1 Hz, 1H), 2.85 (qd, *J* = 6.8, 3.3 Hz, 2H), 2.83–2.73 (m, 2H), 2.66 (dtd, *J* = 14.8, 7.4, 4.4 Hz, 1H), 1.65–1.58 (m, 1H), 1.54–1.46 (m, 1H), 1.29–1.23 (m, 2H); **$^{13}$C NMR** (150 MHz, $CDCl_3$) δ 158.05, 143.65 (q, *J* = 1.1 Hz), 140.33, 136.16, 134.26 (q, *J* = 33.0 Hz), 129.11, 128.45, 128.15, 127.50, 126.25 (q, *J* = 3.8 Hz), 125.93, 123.26 (q, *J* = 272.6 Hz), 113.80, 55.19, 46.68, 44.04, 43.26, 32.27, 27.66; **$^{19}$F NMR** (376 MHz, $CDCl_3$) δ -65.72; **HRMS** (ESI-TOF) Calc'd for $C_{25}H_{25}F_3NO_3S^-$ [M-H] 476.1507, found 476.1501.

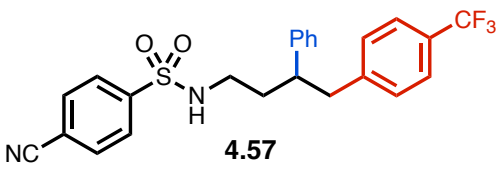


**4.57**

**4-cyano-*N*-(3-phenyl-4-(4-(trifluoromethyl)phenyl)butyl)benzenesulfonamide (4.57):** Purification using silica gel column chromatography (20% EtOAc in Hexanes) gave the product as a yellow solid (398 mg, 87% yield). **$^{1}$H NMR** (400 MHz, $CDCl_3$) δ 7.81 (d, *J* = 8.8 Hz, 2H), 7.73 (d, *J* = 8.8 Hz, 2H), 7.45 (d, *J* = 8.4 Hz, 2H), 7.29–7.19 (m, 3H), 7.07 (d, *J* = 7.9 Hz, 2H), 7.01 (d, *J* = 6.5 Hz, 2H), 4.32 (t, *J* = 6.1 Hz, 1H), 2.94–2.77 (m, 5H), 1.96–1.77 (m, 2H); **$^{13}$C NMR** (150 MHz, $CDCl_3$) δ 144.03, 143.80 (d, *J* = 1.6 Hz), 143.79, 142.34, 132.93, 129.38, 128.78, 128.38 (q, *J* = 32.3 Hz), 127.59, 127.50, 127.01, 126.98, 125.10 (q, *J* = 3.6 Hz), 124.28 (q, *J* = 271.5 Hz), 117.32, 116.28, 44.90, 43.32, 41.48, 35.27; **$^{19}$F NMR** (376 MHz, $CDCl_3$) δ -62.59; **HRMS** (ESI-TOF) Calc'd for $C_{24}H_{22}F_3N_2O_2S^+$ [M+H] 459.1354, found 459.1346.

### 4.4.5. Miscellaneous Experiments for Nickel-Catalyzed 1,2-Diarylation of Alkenes

***Table 4.S3.*** Effect of catalyst loading on product yield.[a]

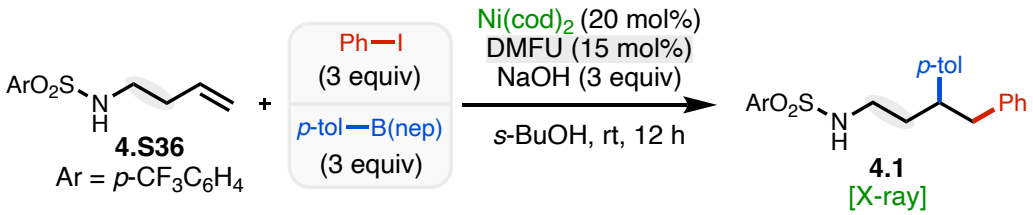


| entry | deviation from standard conditions | %Yield **4.1**[b] |
|---|---|---|
| 1 | none | 90 (82)[c] |
| 2 | 10 mol% $Ni(cod)_2$ | 90 |
| 3 | 5 mol% $Ni(cod)_2$ | 50 |
| 4 | 2.5 mol% $Ni(cod)_2$ | 22 |

[a]Reaction conditions: **4.S36** (0.1 mmol), *s*-BuOH (0.2 M). [b]Percentages represent $^1H$ NMR yields using $CH_2Br_2$ as the internal standard. [c]Values in parentheses are isolated yields.

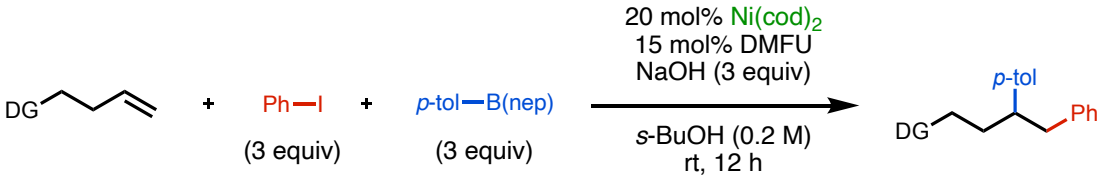


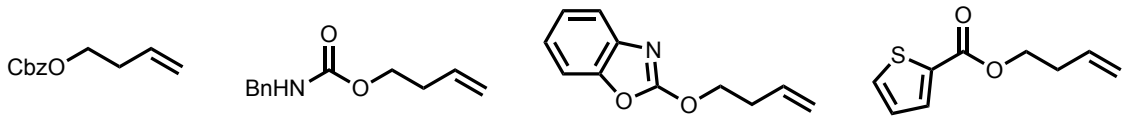


n.d. n.d. n.d. n.d.

***Scheme 4.S6.*** Attempts of 1,2-diarylation with O-containing directing groups.

## 4.5. REFERENCES

(1) For representative reviews on conjunctive cross-coupling, see: (a) Derosa, J.; Tran, V. T.; van der Puyl, V. A.; Engle, K. M. Carbon−Carbon π-Bonds as Conjunctive Reagents in Cross-Coupling. *Aldrichimica Acta* **2018**, *51*, 21−32. (b) Giri, R.; KC, S. Strategies toward Dicarbofunctionalization of Unactivated Olefins by Combined Heck Carbometalation and Cross-Coupling. *J. Org. Chem.* **2018**, *83*, 3013−3022. (c) Derosa, J.; Apolinar, O.; Kang, T.; Tran; V. T.; Engle, K. M. Recent Developments in Nickel-Catalyzed Intermolecular Dicarbofunctionalization of Alkenes. *Chem. Sci.* **2020**, *11*, 4287–4296. (d) Tu, H.-Y.; Zhu, S.; Qing, F.-L.; Chu, L. Recent Advances in Nickel-Catalyzed Three-Component Difunctionalization of Unactivated Alkenes. *Synthesis* **2020**, *52*, 1346–1356. (e) Badir, S. O.; Molander, G. A. Developments in Photoredox/Nickel Dual-Catalyzed 1,2-Difunctionalizations. *Chem* **2020**, *6*, 1327–1339. (f) Qi, X. ; Diao, T. Nickel-Catalyzed Dicarbofunctionalization of Alkenes. *ACS Catal.* **2020**, 10, 8542–8556.

(2) (a) Gu, J.-W.; Min, Q.-Q.; Yu, L.-C.; Zhang, X. Tandem Difluoroalkylation-Arylation of Enamides Catalyzed by Nickel. *Angew. Chem. Int. Ed.* **2016**, *55*, 12270–12274. (b) Xu, C.; Yang, Z.-F.; An, L.; Zhang, X. Nickel-Catalyzed Difluoroalkylation–Alkylation of Enamides. *ACS Catal.* **2019**, *9*, 8224–8229. (c) Yang, Z.-F.; Xu, C.; Zheng, X.; Zhang, X. Nickel-Catalyzed Carbodifunctionalization of N-Vinylamides Enables Access to γ-Amino Acids. *Chem. Commun.* **2020**, *56*, 2642–2645. (d) Shrestha, B.; Basnet, P.; Dhungana, R. K.; KC, S.; Thapa, S.; Sears, J. M.; Giri, R. Ni-Catalyzed Regioselective 1,2-Dicarbofunctionalization of Olefins by Intercepting Heck Intermediates as Imine-Stabilized Transient Metallacycles. *J. Am. Chem. Soc.* **2017**, *139*, 10653–10656. (e) Li,

W.; Boon, J. K.; Zhao, Y. Nickel-Catalyzed Difunctionalization of Allyl Moieties Using Organoboronic Acids and Halides with Divergent Regioselectivities. *Chem. Sci.* **2018**, *9*, 600–607. (f) Wei, X.; Shu, W.; García-Domínguez, A.; Merino, E.; Nevado, C. Asymmetric Ni-Catalyzed Radical Relayed Reductive Coupling. *J. Am. Chem. Soc.* **2020**, *142*, 13515–13522. (g) Xu, C.; Cheng, R.; Luo, Y.-C.; Wang, M.-K.; Zhang, X. *trans*-Selective Aryldifluoroalkylation of Endocyclic Enecarbamates and Enamides by Nickel Catalysis. *Angew. Chem. Int. Ed.* **2020**, *59*, 2–9.

(3) (a) Derosa, J.; Kleinmans, R.; Tran, V. T.; Karunananda, M. K.; Wisniewski, S. R.; Eastgate, M. D.; Engle, K. M. Nickel-Catalyzed 1,2-Diarylation of Simple Alkenyl Amides. *J. Am. Chem. Soc.* **2018**, *140*, 17878–17883. (b) Tran, V. T.; Li, Z.-Q.; Gallagher, T. J.; Derosa, J.; Liu, P.; Engle, K. M. Integrating Allyl Electrophiles into Nickel-Catalyzed Conjunctive Cross-Coupling. *Angew. Chem. Int. Ed.* **2020**, *59*, 7029–7034. (c) For an example of sulfonamide-directed $C(sp^3)$–$C(sp^3)$ cross-coupling, see: Wilsily, A.; Tramutola, F.; Owston, N. A.; Fu, G. C. New Directing Groups for Metal-Catalyzed Asymmetric Carbon–Carbon Bond-Forming Processes: Stereoconvergent Alkyl–Alkyl Suzuki Cross-Couplings of Unactivated Electrophiles. *J. Am. Chem. Soc.* **2012**, *134*, 5794–5797.

(4) (a) Derosa, J.; Tran, V. T.; Boulous, M. N.; Chen, J. S.; Engle, K. M. Nickel-Catalyzed β,γ-Dicarbofunctionalization of Alkenyl Carbonyl Compounds via Conjunctive Cross-Coupling. *J. Am. Chem. Soc.* **2017**, *139*, 10657–10660. (b) Derosa, J.; van der Puyl, V. A.; Tran, V. T.; Liu, M.; Engle, K. M. Directed Nickel-Catalyzed 1,2-Dialkylation of Alkenyl Carbonyl Compounds. *Chem. Sci.* **2018**, *9*, 5278–5283. (c) van der Puyl, V. A.; Derosa, J.; Engle, K. M. Directed, Nickel-Catalyzed Umpolung 1,2-

Carboamination of Alkenyl Carbonyl Compounds. *ACS Catal*. **2019**, *9*, 224–229. (d) Pan, R.; Shi, C.; Zhang, D.; Tian, Y.; Guo, S.; Yao, H.; Lin, A. Nickel-Catalyzed Reductive 1,2-Dialkynylation of Alkenes Bearing an 8-Aminoquinoline Directing Group. *Org*. *Lett*. **2019**, *21*, 8915–8920. (e) Basnet, P.; Dhungana, R. K.; Thapa, S.; Shrestha, B.; KC, S.; Sears, J. M.; Giri, R. Ni-Catalyzed Regioselective β,δ-Diarylation of Unactivated Olefins in Ketimines via Ligand-Enabled Contraction of Transient Nickellacycles: Rapid Access to Remotely Diarylated Ketones. *J*. *Am*. *Chem*. *Soc*. **2018**, *140*, 7782–7786. (f) Basnet, P.; KC, S.; Dhungana, R. K.; Shrestha, B.; Boyle, T. J.; Giri, R. Synergistic Bimetallic Ni/Ag and Ni/Cu Catalysis for Regioselective γ,δ-Diarylation of Alkenyl Ketimines: Addressing β-H Elimination by in Situ Generation of Cationic Ni(II) Catalysts. *J*. *Am*. *Chem*. *Soc*. **2018**, *140*, 15586–15590. (g) Dhungana, R. K.; KC, S.; Basnet, P.; Aryal, V.; Chesley, L. J.; Giri, R. Ni(I)-Catalyzed β,δ-Vinylarylation of γ,δ-Alkenyl α-Cyanocarboxylic Esters via Contraction of Transient Nickellacycles. *ACS Catal*. **2019**, *9*, 10887–10893. (h) Zhao, X.; Tu, H.-Y.; Guo, L.; Zhu, S.; Qing, F.-L.; Chu, L. Intermolecular Selective Carboacylation of Alkenes via Nickel-Catalyzed Reductive Radical Relay. *Nat*. *Commun*. **2018**, *9*, 3488. (i) Derosa, J.; Kang, T.; Tran, V. T.; Wisniewski, S. R.; Karunananda, M. K.; Jankins, T. C.; Xu, K. L.; Engle, K. M. Nickel-Catalyzed 1,2-Diarylation of Alkenyl Carboxylates: A Gateway to 1,2,3-Trifunctionalized Building Blocks. *Angew*. *Chem*. *Int*. *Ed*. **2020**, *59*, 1201–1205. (j) Guo, L.; Tu, H.-Y.; Zhu, S.; Chu, L. Selective, Intermolecular Alkylarylation of Alkenes via Photoredox/Nickel Dual Catalysis. *Org*. *Lett*. **2019**, *21*, 4771–4776. (k) García-Domínguez, A.; Mondal, R.; Nevado, C. Dual Photoredox/Nickel-Catalyzed Three-Component Carbofunctionalization of Alkenes. *Angew*. *Chem*. *Int*. *Ed*. **2019**, *58*,

12286–12290. (l) Yang, T.; Chen, X.; Rao, W.; Koh, M. J. Broadly Applicable Directed Catalytic Reductive Difunctionalization of Alkenyl Carbonyl Compounds. *Chem* **2020**, *6*, 738–751. (m) Tu, H.-Y.; Wang, F.; Huo, L.; Li, Y.; Zhu, S.; Zhao, X.; Li, H.; Qing, F.-L.; Chu, L. Enantioselective Three-Component Fluoroalkylarylation of Unactivated Olefins through Nickel-Catalyzed Cross-Electrophile Coupling. *J. Am. Chem. Soc.* **2020**, *142*, 9604–9611.

(5) (a) Schmidt, M. A.; Stokes, R. W.; Davies, M. L.; Roberts, F. 4-Cyanobenzenesulfonamides: Amine Synthesis and Protecting Strategy to Compliment the Nosyl Group. *J. Org. Chem.* **2017**, *82*, 4550−4560. (b) Kan, T.; Fukuyama, T. Ns Strategies: A Highly Versatile Synthetic Method for Amines. *Chem. Commun.* **2004**, 353–359.

(6) For representative reviews on use of sulfonyl groups in organic synthesis, see: (a) Jarowicki, K.; Kocienski, P. Protecting groups. *J. Chem. Soc., Perkin Trans. 1.* **1998**, 4005–4037. (b) Wilden, J. D. The Sulfonamide Motif as a Synthetic Tool. *J. Chem. Res.* **2010**, *34*, 541–548.

(7) For examples of electron-deficient olefins as ligands in transition metal catalysis, see: (a) Johnson, J. B.; Rovis, T. More than Bystanders: The Effect of Olefins on Transition-Metal-Catalyzed Cross-Coupling Reactions. *Angew. Chem. Int. Ed.* **2008**, *47*, 840−871. (b) Jensen, A. E.; Knochel, P. Nickel-Catalyzed Cross-Coupling between Functionalized Primary or Secondary Alkylzinc Halides and Primary Alkyl Halides. *J. Org. Chem.* **2002**, *67*, 79−85. (c) Huang, C.-Y.; Doyle, A. G. Electron-Deficient Olefin Ligands Enable Generation of Quaternary Carbons by Ni-Catalyzed Cross-Coupling. *J. Am. Chem. Soc.* **2015,** *137*, 5638−5641. (d) Estrada, J. G.; Williams, W. L.; Ting, S. l.;

Doyle, A. G. Role of Electron-Deficient Olefin Ligands in a Ni-Catalyzed Aziridine Cross-Coupling to Generate Quaternary Carbons. *J. Am. Chem. Soc.* **2020**, *142*, 8928–8937. (e) Lin, L. B.; Clough, C. R.; Hillhouse G. L. Interactions of Aziridines with Nickel Complexes: Oxidative-Addition and Reductive-Elimination Reactions that Break and Make C−N Bonds. *J. Am. Chem. Soc.* **2002**, *124*, 2890–2891.

(8) See Scheme 4.S6. for other ineffective O-based protecting groups.

(9) Berman, R. S.; Kochi, J. K. Kinetics and Mechanism of Oxygen Atom Transfer from Nitro Compounds Mediated by Nickel(0) Complexes. *Inorg. Chem.* **1980**, *19*, 248–254.

(10) McGuire, R. T.; Simon, C. M.; Yadav, A. A.; Ferguson, M. J.; Stradiotto, M. Nickel-Catalyzed Cross-Coupling of Sulfonamides With (Hetero)aryl Chlorides. *Angew. Chem. Int. Ed.* **2020**, *59*, 8952–8956.

(11) Payard, P.-A.; Perego, L. A.; Ciofini, I.; Grimaud, L. Taming Nickel-Catalyzed Suzuki-Miyaura Coupling: A Mechanistic Focus on Boron-to-Nickel Transmetalation. *ACS. Catal.* **2018**, *8*, 4812–4823.

(12) O'Broin, C. Q.; Fernández, P.; Martínez, C.; Muñiz, K. *N*-Iodosuccinimide-Promoted Hofmann–Löffler Reactions of Sulfonimides under Visible Light. *Org. Lett.* **2016**, *18*, 436–439.

(13) Koseki, Y.; Kitazawa, K.; Miyake, M.; Kochi, T.; Kakiuchi, F. Ruthenium-Catalyzed Ortho C–H Arylation of Aromatic Nitriles with Arylboronates and Observation of Partial Para Arylation. *J. Org. Chem.* **2017**, *82*, 6503–6510.

(14) Makida, Y.; Marelli, E.; Slawin, A. M. Z.; Nolan, S. P. Nickel-Catalysed Carboxylation of Organoboronates. *Chem. Commun.* **2014**, *50*, 8010–8013.

(15) Carballo, R. M.; Valdomir, G.; Purino, M.; Martín, V. S.; Padrón. J. L. Broadening

the Synthetic Scope of the Iron(III)-Catalyzed Aza-Prins Cyclization. *Eur*. *J*. *Org*. *Chem*. **2010**, *2010*, 2304–2313.

(16) Durel, V.; Lalli, C.; Roisnel, T.; van de Weghe, P. Synergistic Effect of the $TiCl_4$/*p*-TsOH Promoter System on the Aza-Prins Cyclization. *J. Org. Chem.* **2016**, 81, 849–859.

(17) Hu, S.; Wang, D.; Liu, J.; Li, X. Rhodium(III)-Catalyzed Oxidative Olefination of N-Allyl Sulfonamides. *Org. Biomol. Chem.* **2013**, *11*, 2761–2765.

(18) (a) Dobbs, A. P.; Guisné, S. J. J.; Parker, R. J.; Skidmore, J.; Stephenson, R. A.; Hursthouse, M. B. A Detailed Investigation of the Aza-Prins Reaction. *Org. Biomol. Chem.* **2010**, *8*, 1064–1080. (b) Sultana, S.; Bondalapati, S.; Indukuri, K.; Gogoi, P.; Saha, P.; Saikia, A. K. Scandium(III) triflate catalyzed synthesis of primary homoallylic alcohols via carbonyl-ene reaction. *Tetrahedron Lett*. **2013**, *54*, 1576–1578. (c) Hou, A.; Lauterbach, L.; Dickschat, J. S. Enzymatic Synthesis of Methylated Terpene Analogues Using the Plasticity of Bacterial Terpene Synthases. *Chem*. *Eur*. *J*. **2020**, *26*, 2178–2182.

(19) Jiang, H.-J.; Liu, K.; Yu, J.; Zhang, L.; Gong, L.-Z. Switchable Stereoselectivity in Bromoaminocyclization of Olefins: Using Brønsted Acids of Anionic Chiral Cobalt(III) Complexes. *Angew. Chem. Int. Ed.* **2017**, *56*, 11931–11935.

(20) Battiti, F. O.; Newman, A. H.; Bonifazi, A. Exception That Proves the Rule: Investigation of Privileged Stereochemistry in Designing Dopamine $D_3R$ Bitopic Agonists. *ACS Med. Chem. Lett.* **2020**, DOI: 10.1021/acsmedchemlett.9b00660.

(21) Kobayashi, Y.; Inukai, S.; Kondo, N.; Watanabe, T.; Sugiyama, Y.; Hamamoto, H.; Shioiri, T.; Matsugi, M. A Medium Fluorous Grubbs–Hoveyda 2$^{nd}$ Generation Catalyst for Phase Transfer Catalysis of Ring Closing Metathesis Reactions. *Tetrahedron Lett*. **2015**, *56*, 1363–1366.

(22) Jacobsen, M. A.; Williard, P. G. Generation of 1-Azapentadienyl Anion from *N*-(*tert*-Butyldimethylsilyl)-3-buten-1-amine *J. Org. Chem.* **2002**, *67*, 3915–3918.

(23) Dow, M.; Marchetti, F.; Abrahams, K. A.; Vaz, L.; Besra, G. S.; Warriner, S.; Nelson, A. Modular Synthesis of Diverse Natural Product-Like Macrocycles: Discovery of Hits with Antimycobacterial Activity. *Chem*. *Eur*. *J*. **2017**, *13*, 7207–7211.

(24) Lu, M.-Z.; Chen, X.-R.; Xu, H.; Dai, H.-X.; Yu, J.-Q. Ligand-Enabled *ortho*-C–H Olefination of Phenylacetic Amides with Unactivated Alkenes. *Chem*. *Sci*. **2018**, *9*, 1311–1316.

(25) O'Duill, M. L.; Matsuura, R.; Wang, Y.; Turnbull, J. L.; Gurak, J. A., Jr.; Gao, D.-W.; Lu, G.; Liu, P.; Engle, K. M. Tridentate Directing Groups Stabilize 6-Membered Palladacycles in Catalytic Alkene Hydrofunctionalization. *J*. *Am*. *Chem*. *Soc*. **2017**, *139*, 15576–15579.

(26) Lucas, E. L.; Hewitt, K. A.; Chen, P.-P.; Castro, A. J.; Hong, X.; Jarvo, E. R. Engaging Sulfonamides: Intramolecular Cross-Electrophile Coupling Reaction of Sulfonamides with Alkyl Chlorides. *J. Org. Chem.* **2020**, *85*, 1775–1793.

(27) CCDC 2011491 (**4.1**), 2011492 (**4.29**), 2039700 (**4.51**) contain the supplementary crystallographic data. These data can be obtained free of charge from The Cambridge Crystallographic Data Centre via www.ccdc.cam.ac.uk/data_request/cif.

## 4.6. CONTRIBUTIONS

The following individuals directly contributed to the work described in this Chapter: Omar Apolinar, Van T. Tran, Nana Kim, Joseph Derosa, Michael A. Schmidt, and Prof. Keary M. Engle. O.A., J.D., and K.M.E. conceived the project. Reaction optimization was performed by O.A. and J.D. Substrate synthesis was effectuated by O.A., V.T.T., N.K., and J.D. Product isolation and characterization was carried out by O.A. Mechanistic experiments were carried out by O.A., and product diversification was carried out by O.A. and M.A.S. The Chapter was adapted with permission from a published manuscript, which was written by O.A. and K.M.E.

# CHAPTER 5

## THREE COMPONENT ASYMMETRIC NICKEL-CATALYZED 1,2-DICARBOFUNCTIONALIZATION OF UNACTIVATED ALKENES VIA STEREOSELECTIVE MIGRATORY INSERTION

Adapted with permission from:

Apolinar, O.; Kang, T.; Alturaifi, T. M.; Bedekar, P. G.; Rubel, C. Z.; Derosa, J.; Sanchez, B. B.; Wong, Q. N.; Sturgell, E. J.; Chen, J. S.; Wisniewski, S. R.; Liu, P.; Engle, K. M. *J. Am. Chem. Soc.* **2022**, *144*, 19337–19343.

Copyright © 2022 American Chemical Society.

## 5.1. INTRODUCTION

Over the few past decades, 1,2-dicarbofunctionalization of alkenes under transition metal catalysis has made significant advancements.[1a–d] The base metal nickel offers an edge in this reaction platform because of its resilience towards β-H elimination processes in comparison to palladium and the capability to undergo one- or two-electronic redox protocols.[1e] The end result of 1,2-dicarbofunctionalization is the formation of two adjacent C($sp^3$)–C bonds from an alkene substrate, making it a potentially vital method in stereoselective synthesis. However, fully three-component asymmetric Ni-catalyzed 1,2-dicarbofunctionalization of alkenes remains in its infancy, with existing works mainly restricted to radical processes with activated alkenes starting materials.[2a] Accordingly, by exploiting steric interactions between a bulky achiral directing group and a chiral hemilabile bioxazoline ligand during intermolecular migratory insertion, we showcase three-component, asymmetric 1,2-dicarbofunctionalization of unactivated alkenes via a closed-shell Ni(0)/Ni(II) mechanism.

Prior art in enantioselective, nickel-catalyzed 1,2-dicarbofunctionalization of alkenes has predominantly revolved around two-component couplings where stereoselectivity is determined upon cyclative migratory insertion or radical capture (Scheme 5.1A and 5.1B).[1f,2b,3-6] Additionally, Morken reported a three-component variant where acyclic secondary alcohols were furnished in high enantioselectivity (Scheme 5.1C).[2b] Other examples of three-component, asymmetric, nickel-catalyzed 1,2-dicarbofuncationalizations of alkenes typically follow reductive catalytic processes, which all function via a stereoselective radical capture pathway. The Diao,[2c] Chu,[2a] and Nevado[2d] groups have demonstrated that styrenes, enamides, and allylic esters are good contenders

for this asymmetric induction modality (Scheme 5.1C). Even though radical-based approaches are vital, they only allow the assembly of one stereocenter and are usually limited to activated alkenes. Opposed to a radical-based method, we strived to develop an enantioselective nickel-catalyzed 1,2-dicarbofunctionalization of unactivated alkenes, which would have an enantiodetermining *syn*-migratory insertion step that generates two chiral centers in one step. These efforts would complement recent efforts in the palladium catalysis arena.[7,8] Our group has reported several works exemplifying the usefulness of native directing groups for 1,2-dicarbofunctionalization of unactivated alkenes via a nonradical mechanism.[9] We envisioned that protected alkenyl amines would be good substrates for three-component asymmetric 1,2-dicarbofunctionalization of unactivated alkenes because of the strong σ-donation nitrogen has towards nickel and the ability for facile directing group (DG) steric modulation.[9d] Thus, we report the discovery of sterically bulky aryl sulfonamides as excellent directing groups in enantioselective 1,2-dicarbofunctionalization of unactivated alkenes under nickel/bioxazoline (biOx) catalysis though a key enantiodetermining migratory insertion step (Scheme 5.1D).

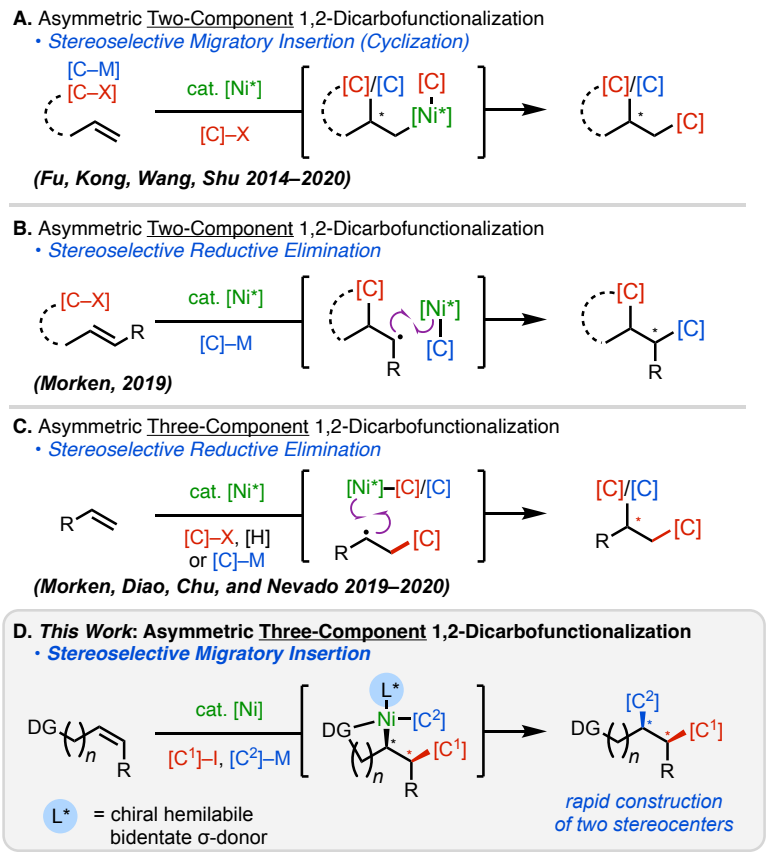


***Scheme 5.1.*** Precedents and synopsis of this work

## 5.2. RESULTS AND DISCUSSION

### 5.2.1. Reaction Optimization

Initially, we were curious to see the influence of (*S*)-benzyl biOx (Bn-biOx) ligand upon the optimized reaction conditions discussed in the previous chapter. Although we observed a low enantioselectivity of the 1,2-diarylated product (**5.2**), the result deemed an excellent entry point in that optimization may be feasible. We further pursued this study by electing 1-iodo-4-isopropoxybenzene and phenylboronic acid neopentyl glycol ester (PhB(nep)) as model electrophilic and nucleophilic coupling partners with Bn-biOx as the chiral ligand and surveyed a homoallyl amine substrate bearing various sulfonyl groups at a low temperature (Table 5.1). The investigation of the electronic series of *para*-substituted

arylsulfonyl groups afforded 1,2-diarylated product in low to excellent yields with moderate enantioselectivities (**5.3**–**5.6**). The benzylsulfonyl group gave the 1,2-diarylated product with slightly higher enantiomeric ratio (**5.7**). Sterically bulky arylsulfonyl groups possessing the 2,4,6-trisubstituted pattern such as mesityl gave the 1,2-diarylated product good enantioselectivity (**5.8**), and 2,4,6-tricyclohexylbenzene sulfonyl group afforded an increase in enantioselectivity but suffered in product yield (**5.9**). To our delight, the 2,4,6-triisopropylbenzene sulfonyl group (Tris or Trisyl) furnished the 1,2-diarylated product **5.10** in good yield with excellent enantio- and regioselectivity, and its absolute configuration as the (*S*)-enantiomer was affirmed by single-crystal X-ray diffraction.

***Table 5.1.*** Directing group optimization of asymmetric 1,2-diarylation reaction.[a]

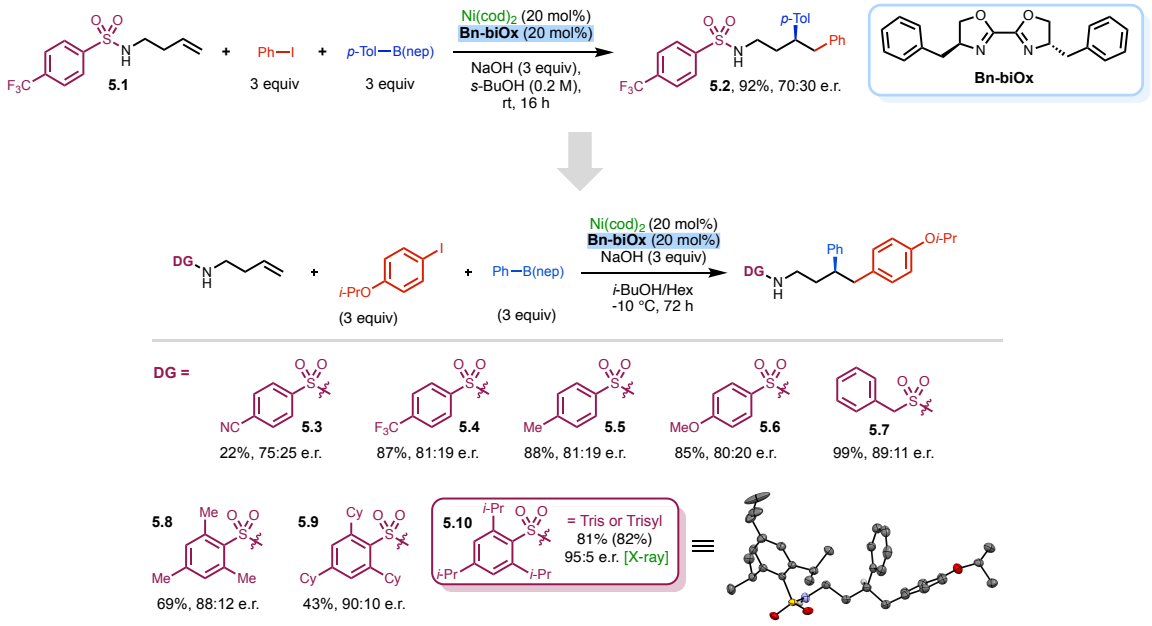


[a]Reaction conditions: SM (0.1 mmol), *i*-BuOH/hexane 1:1 (0.1 M) or *s*-BuOH (0.2 M). [b]Values in parentheses are isolated yields. [c]Percentage yield by $^1$H NMR using $CH_2Br_2$ as the internal standard; n.d. = not detected. nep = neopentylglycol.

Other chiral mono- and bisoxazoline ligands were also tested. The commonly used Bn-BOX (**5.11**), Bn-PyrOx (**5.13**), and Bn-MOX (**5.14**) ligands all gave 1,2-diarylated product in trace amounts, while Bn-PyBOX (**5.12**) ligand afforded the 1,2-diarylated product in low yield as a nearly racemic mixture. We turned towards examining other biOx

ligands and found those that were previously used in enantioselective nickel catalysis by Diao[2c] and Nevado[2d] gave 1,2-diarylated product in low yields with poor enantiomeric ratios, highlighting the significance of the benzyl group of the biOx ligand for this particular enantioselective reaction. The requirement of the benzyl motif is further demonstrated with analogues of Bn-biOx that afforded the 1,2-diarylated product with similar enantioselectivities but gave lower yields (**5.17**–**5.20**). Further structural modification was performed on the Bn-biOx ligand and we found that shortening of the benzyl chain length resulted in a low product yield as a nearly racemic mixture (**5.22**), meanwhile elongation led to a slightly elevated yield with good enantioselectivity (**5.21**). Implementation of a substituent on the methine or methylene positions of the Bn-biOx ligand led to the formation of the 1,2-diarylated product in low yields and as racemic mixtures (**5.23**–**5.24**). Other ligand archetypes were examined such as chiral electron-deficient olefin (EDO) ligands and a chiral diamine ligand, but Bn-biOx remained dominant in both product yield and enantioselectivity (**5.25**–**5.30**).

**Table 5.2.** Ligand optimization of asymmetric 1,2-diarylation reaction.[a]

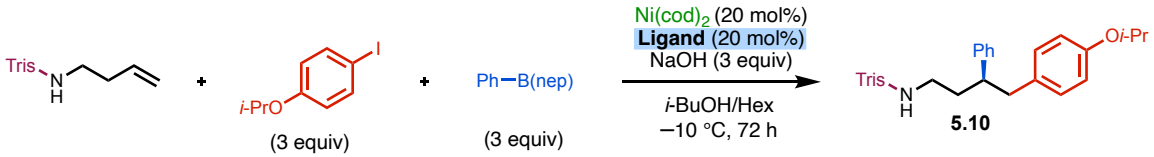


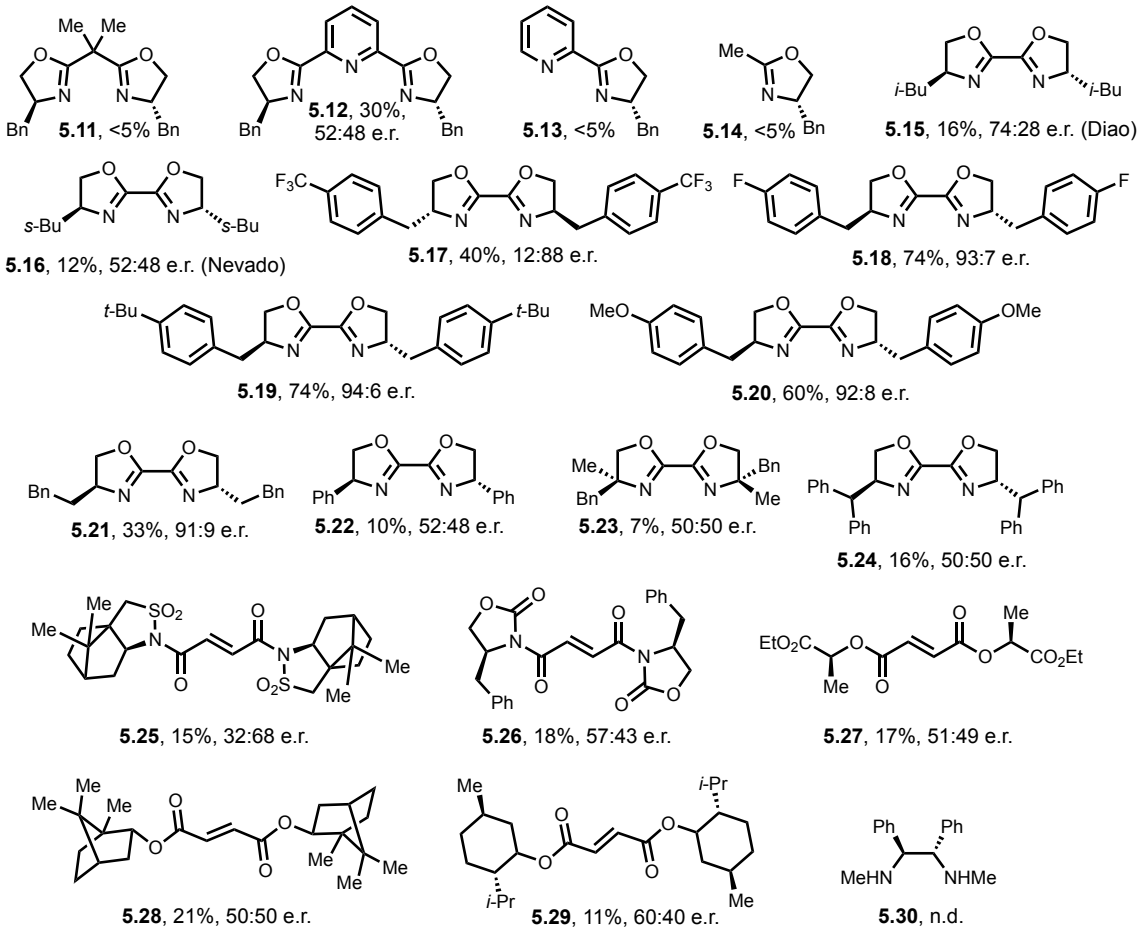


[a]Reaction conditions: SM (0.1 mmol), *i*-BuOH/hexane 1:1 (0.1 M). Percentage yield by $^1$H NMR using $CH_2Br_2$ as the internal standard; n.d. = not detected. nep = neopentylglycol.

In terms of the reaction conditions, we found that the absence of Bn-biOx ligand still gave the racemic product albeit in a 13% yield highlighting the existence of a background reaction even at low temperature (Table 5.3, Entry 1). Performing the reaction for a shorter time resulted in a lower product yield, but with the same excellent enantioselectivity (Entry 2). Lowering catalyst loading or coupling partners stoichiometry resulted in a lower yield, while high enantioselectivity was still achieved (Entry 3, 4). The

employment of arylboronic acid in lieu of the arylboronic ester resulted in a diminished yield, while good enantioselectivity was still observed (Entry 5). The 1-bromo-4-isopropoxybenzene electrophile and other nickel precatalysts, such as Ni(cod)(DQ), $NiCl_2$, $Ni(acac)_2$, and $NiBr_2$•glyme were found to be ineffective (Entry 6,7). Surprisingly, Ni(cod)(DMFU) precatalyst afforded 1,2-diarylated product in a low yield with good enantioselectivity (Entries 8). It is worth noting that one of the newly synthesized air-stable Ni(0) precatalysts from our group, Ni(cod)$TO^A$ ($TO^A$ = diethyl acenaphtho[1,2-c]thiophene-7,9-dicarboxylate 8-oxide), enabled the reaction to be conducted with moderate yield and good enantioselectivity without the use of an inert atmosphere glovebox (Table 5.3).[10]

**Table 5.3.** Deviation from optimized reaction conditions of asymmetric 1,2-diarylation reaction.[a]

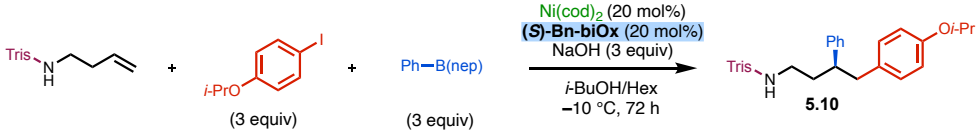


| entry | deviation from standard conditions | %Yield **5.10**[c] | e.r. |
|---|---|---|---|
| 1 | no ligand | 13 | 50:50 |
| 2 | 43 h instead of 72 h | 63 | 95:5 |
| 3 | 10 mol% $Ni(cod)_2$ instead of 20 mol% | 65 | 95:5 |
| 4 | 1.5 equiv of Ph–B(nep), $Ar^1$–I, NaOH instead of 3 equiv | 48 | 95:5 |
| 5 | Ph–$B(OH)_2$ instead of Ph–B(nep) | 60 | 91:9 |
| 6 | $Ar^1$–Br instead of Ph–I | n.d. | - - |
| 7 | Ni(cod)(DQ), $NiCl_2$, $Ni(acac)_2$, or $NiBr_2$•glyme instead of $Ni(cod)_2$ | n.d. | - - |
| 8 | Ni(cod)(DMFU) instead of $Ni(cod)_2$ | 33 | 91:9 |

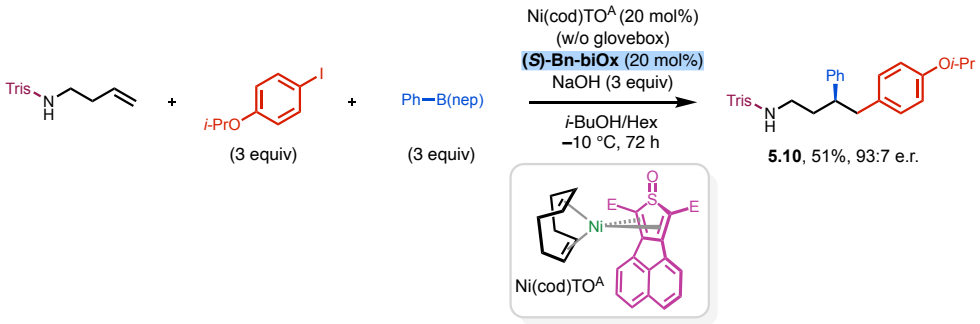


[a]Reaction conditions: SM (0.1 mmol), *i*-BuOH/hexane 1:1 (0.1 M). [b]Percentage yield by $^1H$ NMR using $CH_2Br_2$ as the internal standard; n.d. = not detected. nep = neopentylglycol.

### 5.2.2. Substrate Scope

Then, the electrophile and nucleophile coupling partner scope was investigated (Tables 5.4 and 5.5). With regards to the electrophile scope, in general, it was observed that electron-donating groups at the *para* position of the aryl iodide resulted in the highest enantioselectivities with varying yields (**5.10**, **5.31**–**5.33**, **5.39**, **5.44**–**5.46**). Diminished enantioselectivities and good to excellent product yields were obtained with electron-neutral and electron-withdrawing groups at the *para* position of the aryl iodides (**5.40**–**5.43**) ($\rho = -0.86$ at –10 °C and $\rho = -0.76$ at 0 °C).[11] Aryl iodides bearing electron-donating groups on the *ortho* and *meta* positions of the aryl iodides (**5.35**, **5.36**) gave 1,2-diarylated product in moderate to excellent yields, but enantioselectivity was lowered.

**Table 5.4.** Electrophile scope.[a]

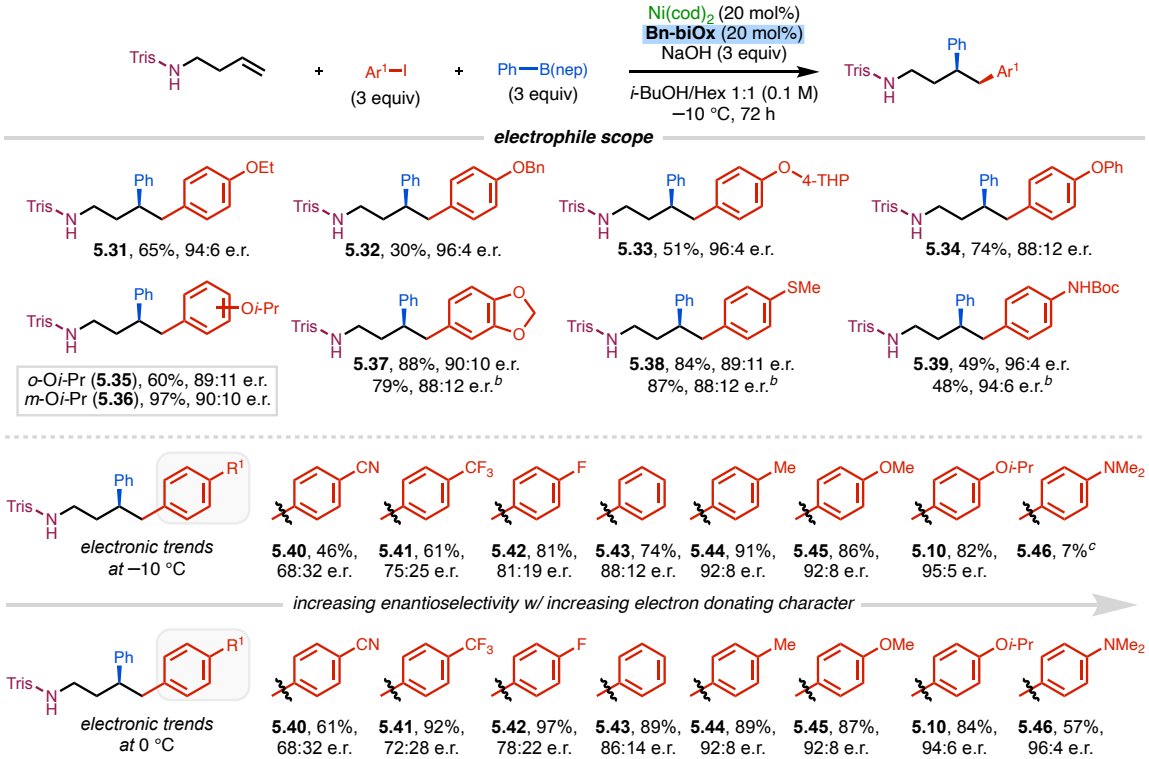


[a]Reactions performed on 0.1 mmol scale. [b]Reactions performed at 0 °C. [c]Enantiomeric ratio was not determined.

With regards to the nucleophile scope, varying the electronics of the *para* substituent on the arylboronic ester had no influence on the enantioselectivity ($\rho = 0.013$ at –10 °C).[12] We observed that electron-donating, -neutral or (weakly) -withdrawing substituents on the *para* position of the arylboronic esters (**5.47–5.51**, **5.53–5.55**) gave higher yields than in the case with 4-(trifluoromethyl)phenylboronic ester (**5.52**) presumably due its poor nucleophilicity. Both 3-thiophenyl- and 3-furanylboronic esters were accommodated upon subjection to the reaction conditions giving 1,2-arylheteroarylated products (**5.56**, **5.57**) with good enantioselectivities but in low to good yields. Arylboronic esters with *meta*- and *ortho*-substitution gave 1,2-diarylated products (**5.58**, **5.59**) in moderate yields with good enantioselectivities. We were also interested in surveying alkenylboronic ester nucleophiles because they have not previously been implemented in three-component enantioselective Ni-catalyzed 1,2-dicarbofunctionalization.[2] Employment of (*E*)-(4-methyl)styrylboronic acid neopentyl glycol ester led to the formation of the desired 1,2-dialkenylated product (**5.60**) in moderate yield and low enantioselectivity. Additionally, 1,2-arylalkenylated product (**5.61**) was also synthesized but in an excellent yield and with good enantioselectivity. Other (*E*)-alkenyl boronic ester nucleophiles for instance (*E*)-(3-phenylprop-1-en-1-yl)boronic ester and (*E*)-(3,3-dimethylbut-1-en-1-yl)boronic ester gave enantioenriched 1,2-arylalkenylated products (**5.62**, **5.63**) with good enantioselectivity but in low to good yields. Also, a 1,1-disubstituted boronic ester nucleophile, namely 1-phenylvinylboronic ester, was viable in the reaction conditions giving 1,2-arylalkenylated product (**5.64**) in moderate yield with good enantioselectivity. Lastly, cyclohexenylboronic ester was used to construct 1,2-arylalkenylated product (**5.65**) with good enantioselectivity but low yield.

**Table 5.5.** Nucleophile scope.[a]

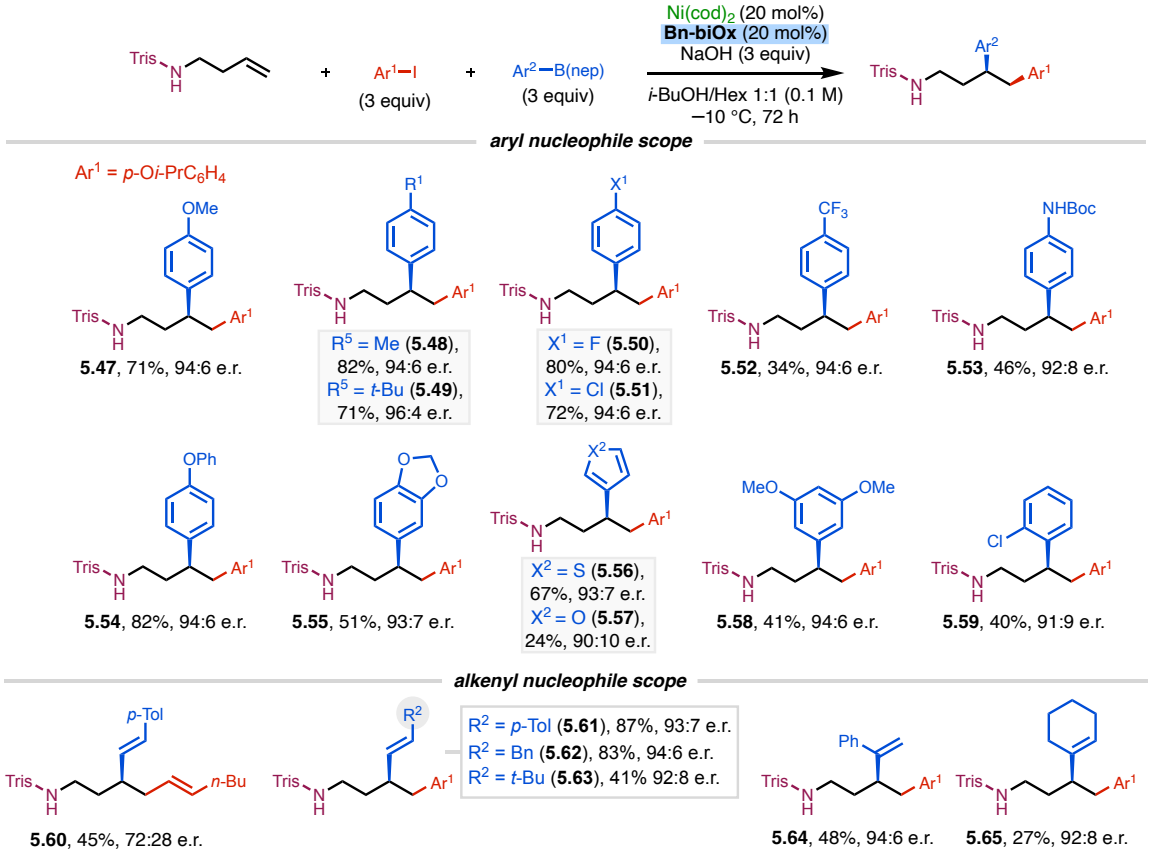


[a]Reactions performed on 0.1 mmol scale.

Next, we analyzed unactivated alkene starting materials that are usually challenging in 1,2-dicarbofunctionalization. Initially, we became aware that (*Z*)- and (*E*)-1,2-disubstituted alkenes bearing the trisyl group gave 1,2-diarylated product in very low yields under the optimized reaction conditions (Table 5.6). Switching to less sterically hindered sulfonyl directing group increased reactivity with both (*Z*)- and (*E*)-1,2-disubstituted alkenes, with 1,2-diarylated products (**5.66–5.69**) formed with excellent diastereoselectivity, albeit with moderate yields and enantiomeric ratios. Gratifingly, the major enantiomer of **5.66** was isolated via preparative chiral supercritical fluid chromatography (SFC), and its absolute stereochemistry was confirmed by single-crystal X-ray diffraction which is in line with a *syn*-insertion mechanism. Several 1,1-disubstituted

alkenes were found to be ineffective, and no reactivity was observed with alkenyl sulfonamides possessing substitution at the α- or β-positions. This demonstrates the sensitive nature of the putative alkyl nickelacycle intermediate to substitution along the carbon chain.

**Table 5.6.** Alkene scope and limitations.[a]

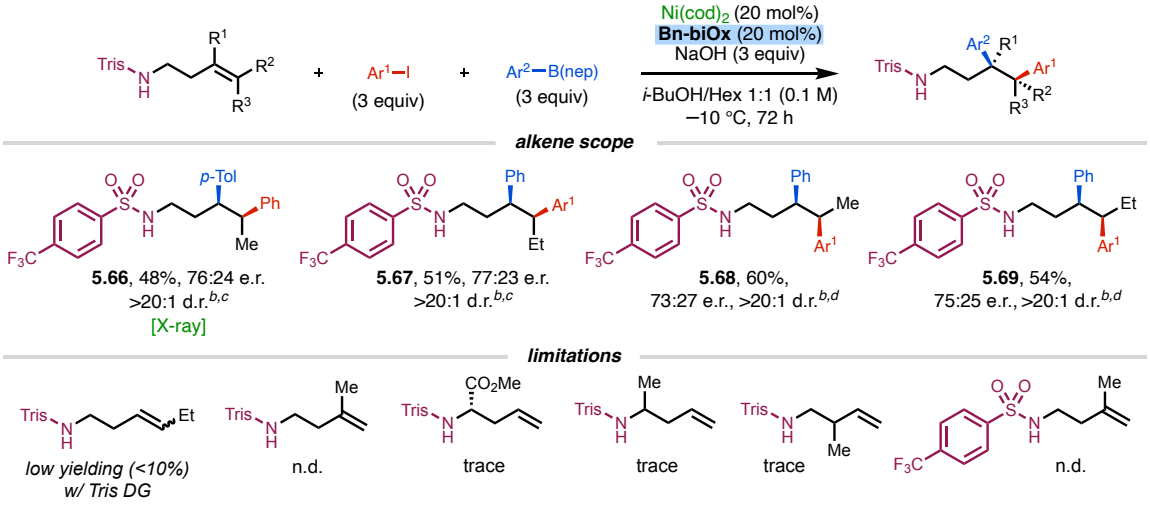


[a]Reactions performed on 0.1 mmol scale. [b]Reactions performed at 0 °C. [c]Product was synthesized from (*Z*)-alkene. [d]Product was synthesized from (*E*)-alkene.

### 5.2.3. Experimental Mechanistic Investigations

To evaluate the significance of the N–H motif of the trisyl directing group, control experiments were conducted of both trisyl sulfonate **5.70** and *N*-methylated trisyl homoallyl sulfonamide **5.71**, and, in both cases, no reaction occurred (Scheme 5.2A). We were also interested about the impact of alkene distance upon enantioselectivity. Both shortening of the alkenyl chain to trisyl allyl amine **5.72** or elongation of the alkenyl chain to either trisyl bis-homoallyl or trisyl bis,bis-homoallyl amines (**5.73, 5.74**) gave no 1,2-diarylated product (Scheme 5.2B). We think that the trisyl allyl amine substrate is unreactive because of the sterically encumbered 4–membered *N*-bound nickelacycle,

whereas the trisyl bis-homoallyl and trisyl bis,bis-homoallyl amine substrates would go through a less favorable 6- or 7-membered nickelacycle relative to the 5-membered nickelacycle with the trisyl homoallyl amine substrate.

To rule out whether the reaction operates via a radical intermediate, we performed a radical clock experiment with trisyl diene **5.75** and obtained exclusive 1,2-diarylation of one of the pendant alkenes in 20% yield with moderate diastereoselectivity (**5.76**) but at ambient temperature (Scheme 5.2C). The cyclized diarylated product was not observed, showcasing that this reaction does not proceed via an alkyl radical intermediate.

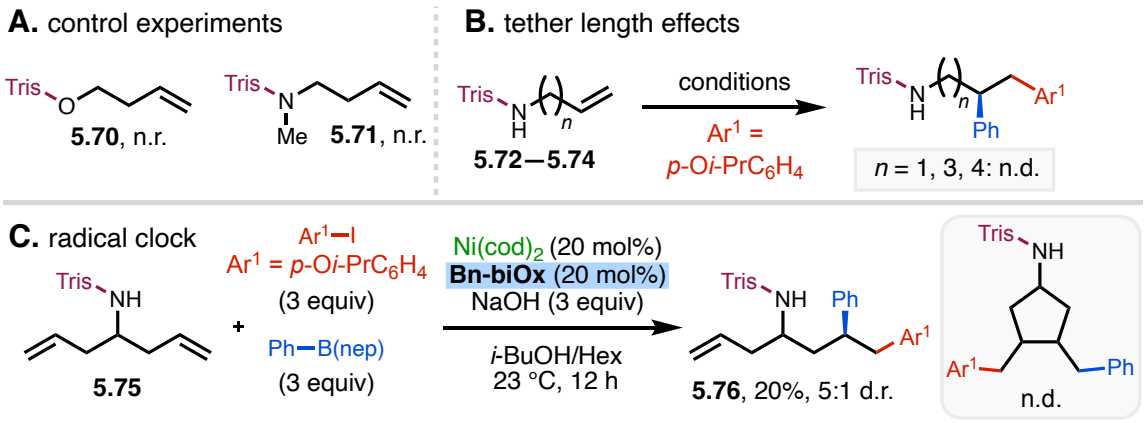


***Scheme 5.2.*** Mechanistic experiments of asymmetric 1,2-diarylation reaction.

### 5.2.4. Proposed Catalytic Cycle

The general catalytic cycle likely undergoes a mechanism like that in the previous chapter (Figure 5.1).[9e] One can envision that electron-rich $Ni^0$(Bn-biOx) complex may undergo oxidative addition into the C–I bond of the aryl iodide, followed by alkene substrate coordination. Subsequently, an enantioselective migratory insertion step follows forming a 5-membered $Ni^{II}$(Bn-biOx)(alkyl)(sulfonamido) metallacycle intermediate. Then, transmetalation with arylboronic ester nucleophile gave the $Ni^{II}$(Bn-

biOx)(alkyl)(aryl) species, which finally undergoes reductive elimination to afford the enantioenriched 1,2-dicarbofunctionalized product.[9c–e]

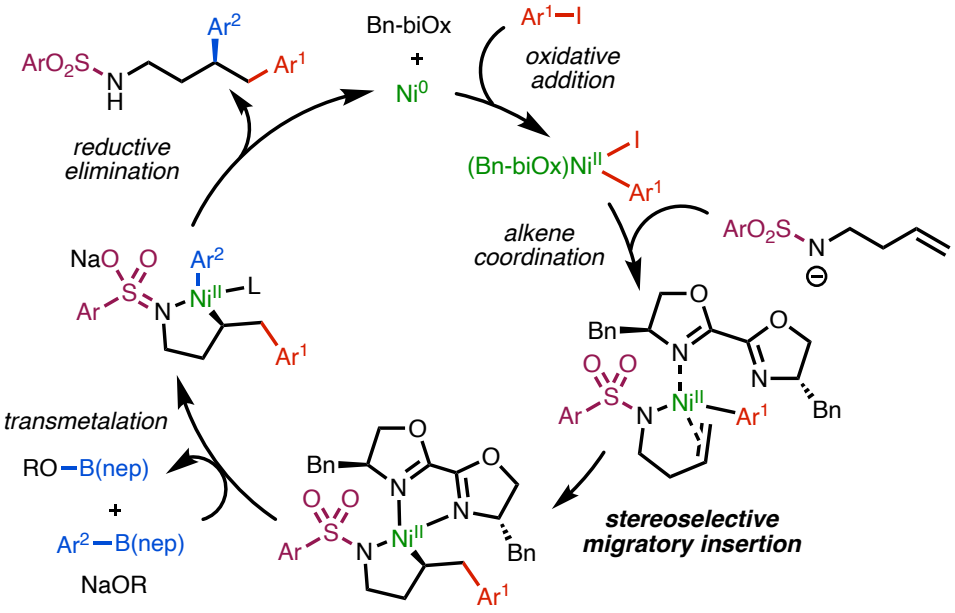


***Figure 5.1.*** Proposed catalytic cycle of asymmetric 1,2-diarylation reaction.

### 5.2.5. Additional Experiments

We then focused on establishing a protocol for the removal of the trisyl directing group to access highly enantioenriched 1,2-dicarbofunctionalized amines that would otherwise be difficult to construct. The standard 1,2-diarylated product **5.10** was furnished on larger scale in a good yield and with the same excellent enantioselectivity (Scheme 5.3A). Then, **5.10** was treated with Mg turnings, Ti(O*i*-Pr)$_4$, and TMSCl, leading to the removal of the trisyl group giving free amine **5.77** in a good yield with full preservation of the enantioselectivity.[13] Beyond alkenyl sulfonamides, we were keen to find a native carbonyl directing group that was viable in developed enantioselective 1,2-dicarbofunctionalization. Pleasingly, 3-butenoic acid was found to be a suitable substrate

which gave 1,2-diarylated product **5.79** with good enantioselectivity, albeit in a low product yield (Scheme 5.3B).

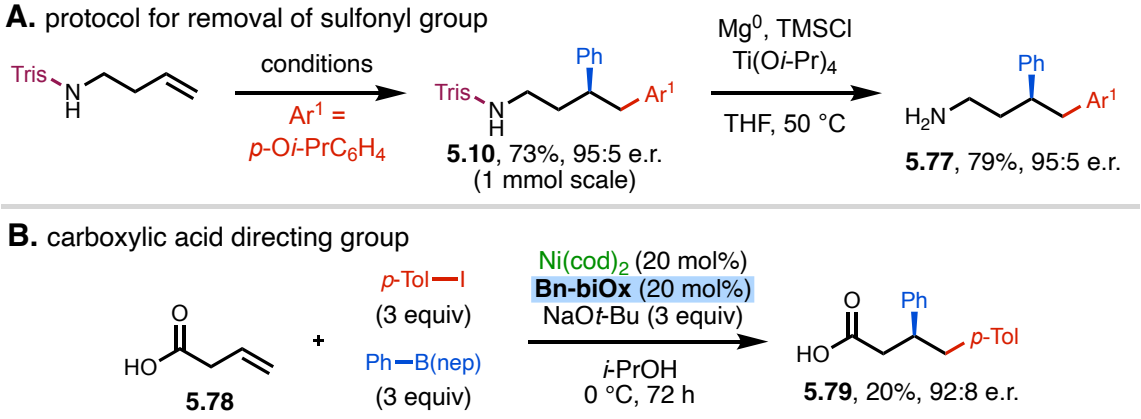


***Scheme 5.3.*** Additional experiments of asymmetric 1,2-diarylation reaction.

### 5.2.6. Computational Studies

To further inquire into the mechanism of the reaction and the role of the Bn-biOx ligand upon enantioinduction, we performed DFT calculations at the M06/SDD−6-311++G(d,p)/SMD(*i*-BuOH)//B3LYP-D3(BJ)/SDD−6-31+G(d,p) level of theory.[14] Due to the seemingly hemilabile nature of the Bn-biOx ligand[2d] and the flexibility of its benzyl arms, a careful conformational analysis was effectuated using a workflow which comprised of CREST/GFN2-xTB[15] conformational sampling plus DFT geometry optimizations of low-energy transition state conformers (refer to Figure 5.S4). Detailed in the computed reaction energy profile (Figure 5.2), the reaction commences with complex **5.81** which undergoes oxidative addition of phenyl iodide electrophile via **TS1** to afford $Ni^{II}$(Bn-biOx)(Ph)(I) intermediate **5.81** (refer to Figure 5.S9). Subsequently, salt metathesis occurs where the iodide anion is exchanged with the deprotonated sulfonamide substrate **5.10'** to form more stable $Ni^{II}$ intermediate **5.82**. Then, the alkene coordinates to the nickel center

to forge a π-alkene complex **5.83** which allows for migratory insertion via **TS2a** leading to the 5-membered nickelacycle **5.84**. Transmetalation with arylboronate ester **5.85** (**TS3**) then proceeds followed by reductive elimination (**TS4**) to afford product **5.43'**. The computed reaction energy profile gave support to several factors that would influence enantioinduction. The first is that, even though the migratory insertion step has a low kinetic barrier (5.6 kcal/mol with respect to **5.82**), it is exothermic and irreversible; thus, this step certainly governs the enantioselectivity. This calculation is in line with the experimental Hammett data that suggest the electronics of aryl group of the electrophile and not the nucleophile impacts the enantiodetermining step. Secondly, all of the Ni(II) intermediates and transition states possess square-planar geometry. That said, the Bn-biOx ligand coordinates to the Ni center in either mono- or bidentate fashion depending on the available coordination sites. This hemilability is in line with the experimental findings that more rigid, strongly coordinating BOX ligands are not efficacious in this reaction paradigm. It is also worth noting that isomers with dissociation of the sulfonamide directing group, in lieu of the oxazoline moiety, are less favorable. It was found that in the transmetalation transition state (**TS3**), the Bn-biOx ligand fully dissociates but then re-coordinates to the Ni center thereafter assisting in the reductive elimination step **TS4** (refer to Figure 5.S6, 5.S7, and 5.S8). The partial or full dissociation of the Bn-biOx ligand kinetically fosters key elementary steps from intermediates **5.82** and **5.84**.

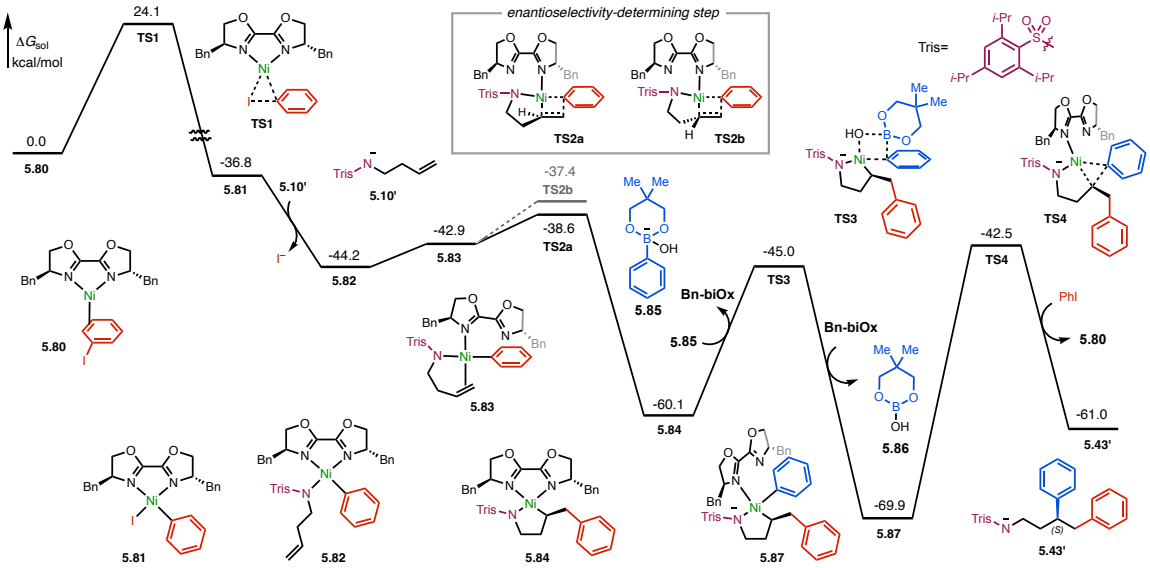


***Figure 5.2.*** Computed reaction energy profile of asymmetric 1,2-diarylation reaction.

Due to the monodentate coordination of the Bn-biOx ligand present during the enantiodetermining migratory insertion transition state, the mode of enantioinduction is unique from typical enantioselective migratory insertion processes involving $C_2$-symmetric chiral ligands.[16] Therefore, several low-energy conformers of the migratory insertion transition states were located (14 within 3.0 kcal/mol of the lowest-energy TS); and we found that the most stable transition states (**TS2a** and **TS2b**) leading to the *S* and *R* enantiomers have an activation free energy of 5.6 and 6.9 kcal/mol from **5.82**, respectively (Figure 5.3). The computed enantiomeric ratio from the Boltzmann averages of all migratory insertion TS conformers (refer to Table 5.S6) was determined to be 87:13 favoring the *S* enantiomer, which is in line with the experimental enantiomeric ratio being 88:12. In the more favored transition state, namely **TS2a**, the bulky trisyl group is oriented in a place less occupied by the (*S*)-Bn-biOx ligand, whereas greater steric clash between the trisyl group and the benzyl group of the coordinated moiety of the Bn-biOx ligand was found in the less favorable transition state **TS2b**. Furthermore, we found favorable C–H/π

interactions between the benzyl group of the dissociated arm of the Bn-biOx ligand and alkenyl group in **TS2a**, further showcasing the significance of the benzyl motif in governing the enantioselectivity. We were also interested in shedding light on influence of the enantioselectivity with an electron-deficient (*p*-CN)$C_6H_4I$ electrophile; hence, we pursued more computational investigations in this sector. In short, we elucidated the presence of stronger T-shaped π/π interactions between the electron-deficient aryl group of the electrophile and the benzyl group of the Bn-biOx ligand, which stabilizes a low-energy TS conformer leading to the minor enantiomeric product (refer to Figure 5.S5). This slightly lowers the predicted enantioselectivity which is in line with the obtained experimental data.

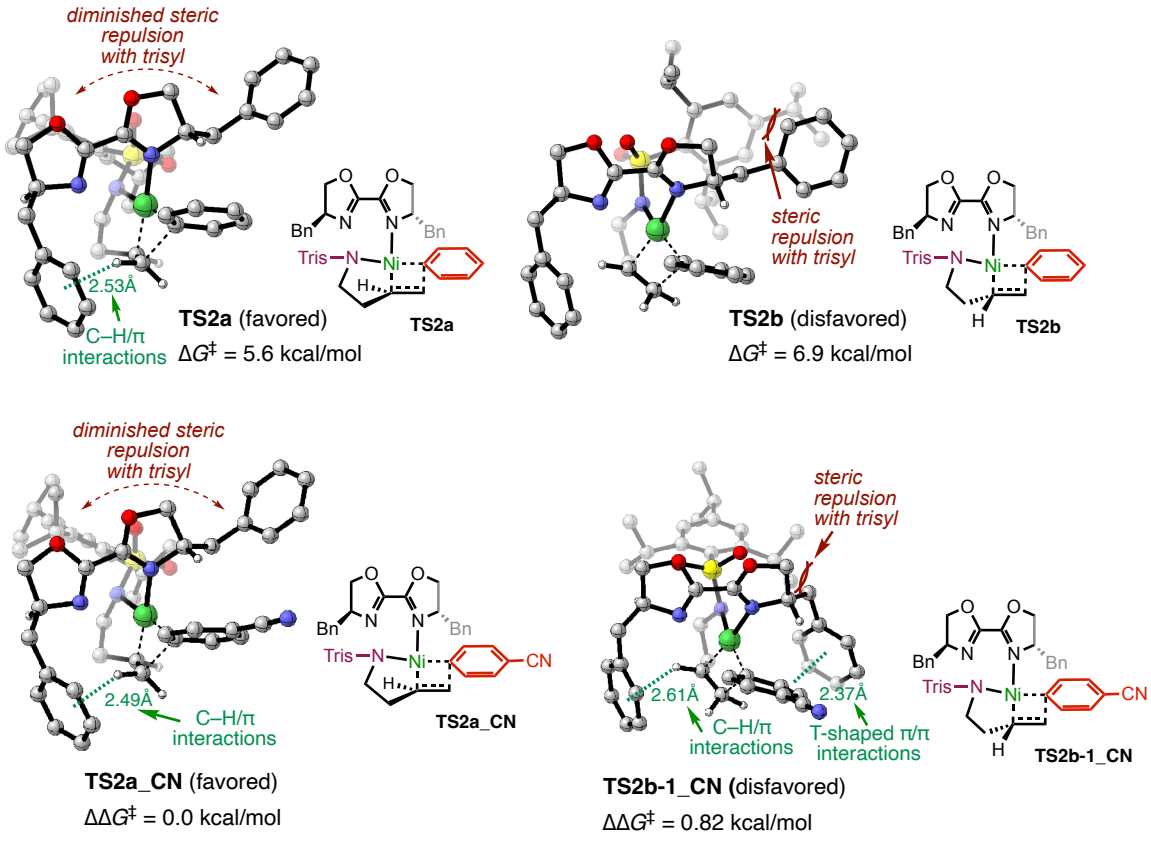


***Figure 5.3.*** Enantioselectivity-determining migratory insertion transition states.

## 5.3. CONCLUSION

Overall, a three-component, enantioselective, Ni-catalyzed 1,2-dicarbofunctionalization of trisyl alkenyl amines with aryl iodides and aryl/alkenylboronic esters was established. The described method accommodates a plethora of coupling partners where electron-donating electrophiles gave the highest enantioselectivities while either electron-rich or electron-poor nucleophiles are well tolerated. Alkenyl nucleophiles are also implemented in the developed reaction, which is important because of the lack of examples in three-component asymmetric Ni-catalyzed couplings. We managed to showcase that 1,2-disubstituted (*E*)- and (*Z*)-alkenes are viable under the optimized reaction conditions, giving the desired 1,2-diarylated products in moderate yields and enantioselectivities. A deprotection protocol of the trisyl group was identified which can be executed to give enantioenriched 1,2-diarylated free amines. Finally, computations revealed several aspects on the mechanism of enantioinduction and the key roles of the trisyl directing group and ligand, which will aid in future developments of enantioselective 1,2-dicarbofunctionalization as a tool in asymmetric synthesis.

## 5.4. EXPERIMENTAL

### 5.4.1. General Information

Unless otherwise noted, all materials were used as received from commercial sources without further purification. All aryl iodides, arylboronic acids, and solvents were purchased from MillporeSigma, Alfa Aesar, Oakwood, and Combi-Blocks. $Ni(cod)_2$ was purchased from Strem. In air- or moisture-sensitive reactions, anhydrous solvents from MilliporeSigma or from a Grubbs-type solvent purification system were used.

### 5.4.2. Arylboronic Acid Neopentylglycol Ester Synthesis

***Table 5.S1.*** Aryl/alkenylboronic acid neopentylglycol esters (**5.S1–5.S19**) used in this study.

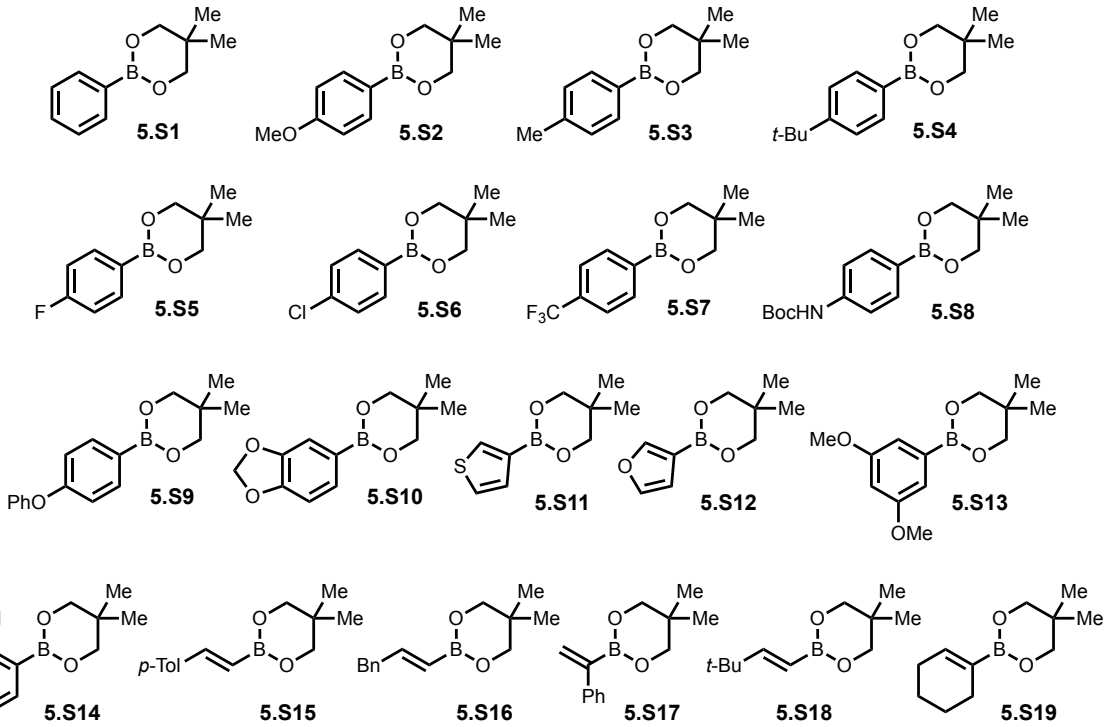


Compounds **5.S1–5.S19** were prepared according to literature methods.[17,18]

### 5.4.3. Ligand Synthesis

***Table 5.S2.*** Commercially procured chiral ligands (**5.11**, **5.12**, **Bn-biOx**, **5.29** and **5.30**) used in this study.

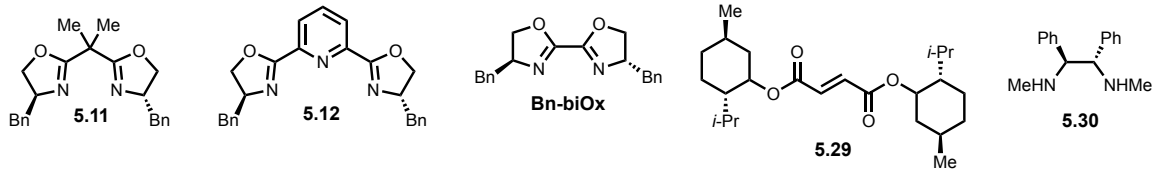


Ligands **5.11**, **5.12**, and **5.30** were purchased from ChemScene. **5.29** was purchased from Acros. (*S*)-**Bn-biOx** was purchased from MilliporeSigma, and (*R*)-**Bn-biOx** was purchased from Astatech.

***Table 5.S3.*** Known Chiral Ligands (**5.13**, **5.14**, **5.15**, **5.16**, **5.22**, and **5.24–5.28**).

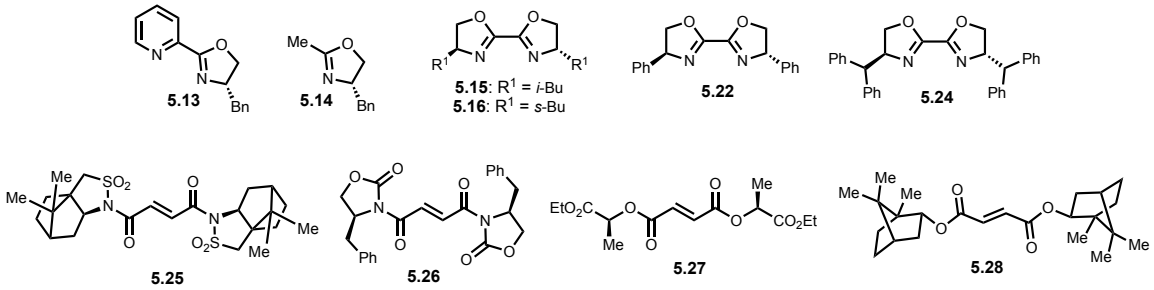


Ligands **5.13**,[19] **5.14**,[20] **5.15**,[2c] **5.16**,[2d] **5.22**,[21] and **5.24**,[2a] **5.25**,[22] **5.26**,[23] **5.27**,[24] and **5.28**[25] were prepared according to literature methods.

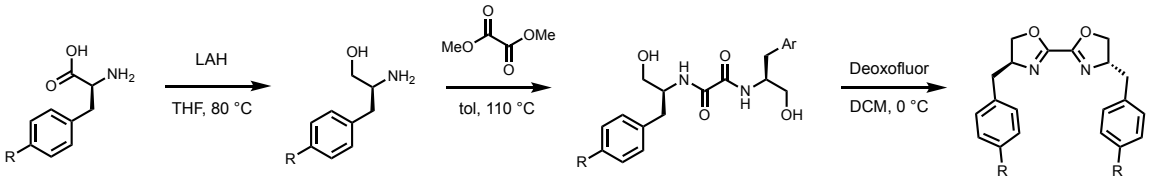


***Scheme 5.S1.*** Synthesis of BiOX ligands **5.17, 5.18, 5.19, 5.20**, **5.21** and **5.23**. These compounds were synthesized using adapted versions of literature procedures describing the preparation of similar compounds.[26,27]

## 5.4.4. Alkenyl Sulfonamide and Miscellaneous Substrate Synthesis

***Table 5.S4.*** Starting materials used in this study: alkenyl sulfonamides **5.1,** and **5.S20–5.S28**; sulfonyl chloride **5.S29**; alkenyl sulfonates **5.S30–5.S34** and **5.S36**; and alkenyl amine **5.S35**.

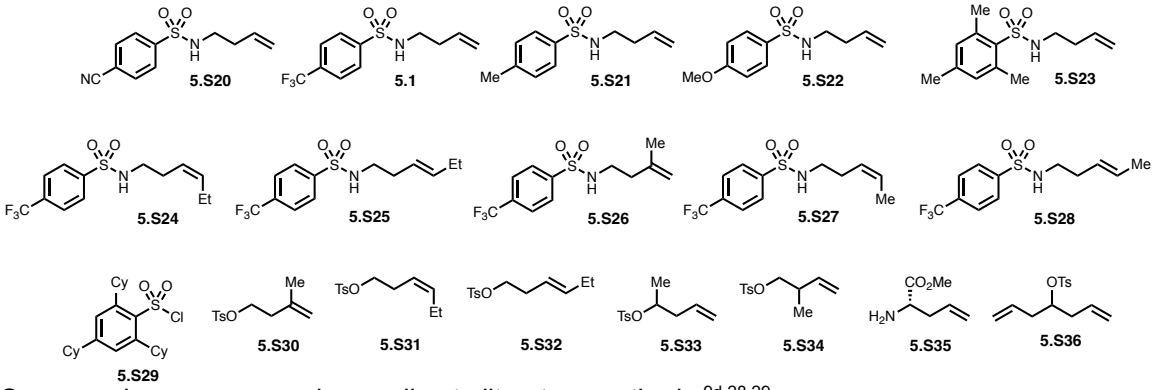


Compounds were prepared according to literature methods.[9d,28,29]

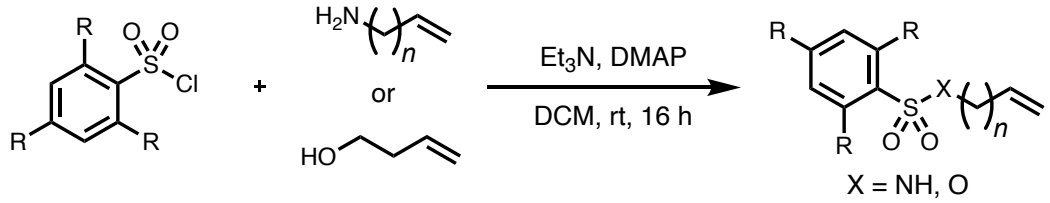


***Scheme 5.S2.*** Synthesis of alkenyl sulfonamides **1a**, **1f**, **1h**, **1p**, **1s**, and **1u**. These compounds were synthesized using adapted versions of literature procedures describing the preparation of similar compounds.[30,31]

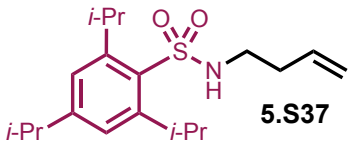


***N*-(but-3-en-1-yl)-2,4,6-triisopropylbenzenesulfonamide (5.S37):** Purification using silica gel column chromatography (20% Acetone in Hexanes) gave the product as a white solid (2.94 g, 87% yield). **$^{1}$H NMR** (400 MHz, $CDCl_3$) δ 7.16 (s, 2H), 5.74–5.59 (m, 1H), 5.14–5.05 (m, 2H), 4.34 (t, $J$ = 6.3 Hz, 1H), 4.15 (hept, $J$ = 6.8 Hz, 2H), 3.04 (q, $J$ = 6.5 Hz, 2H), 2.91 (h, $J$ = 6.6 Hz, 1H), 2.27 (q, $J$ = 6.4 Hz, 2H), 1.29–1.24 (m, 18H); **$^{13}$C NMR** (150 MHz, $CDCl_3$) δ 152.73, 150.32, 134.33, 132.14, 123.80, 118.32, 41.57, 34.14, 33.72, 29.63, 24.89, 23.59; **HRMS** (ESI-TOF) Calc'd for $C_{19}H_{32}NO_2S^+$ [M+H] 338.2154, found 338.2141.

### 5.4.5. Screens and Trends for Nickel-Catalyzed 1,2-Dicarbofunctionalization of Alkene

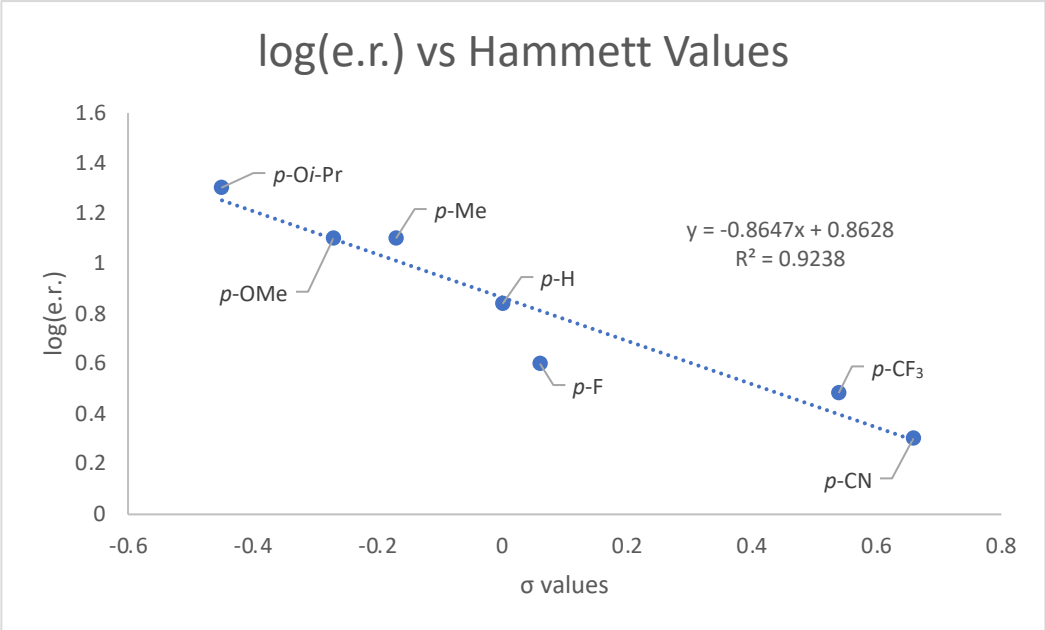


***Figure 5.S1.*** Plot of log(e.r.) vs Hammett values of electrophiles at –10 °C.

| $R^4$ = | σ values | e.r. | log(e.r.) |
|---|---|---|---|
| *p*-O*i*-Pr | -0.45 | 19 | 1.3 |
| *p*-OMe | -0.27 | 12 | 1.1 |
| *p*-Me | -0.17 | 12 | 1.1 |
| *p*-H | 0 | 7 | 0.84 |
| *p*-F | 0.06 | 4 | 0.60 |
| *p*-$CF_3$ | 0.54 | 3 | 0.48 |
| *p*-CN | 0.66 | 2 | 0.30 |

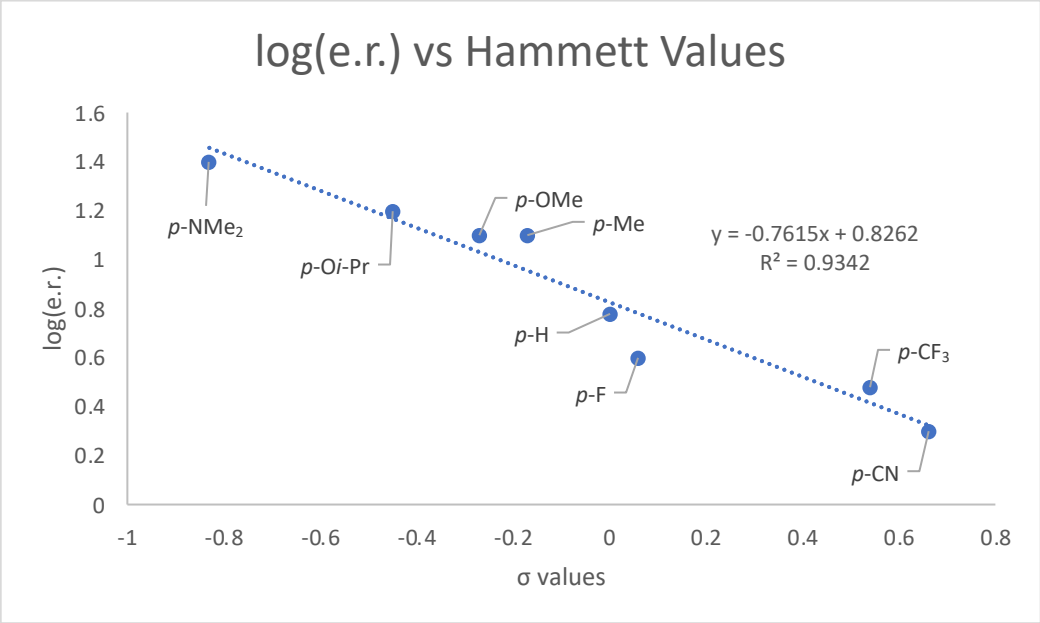


***Figure 5.S2.*** Plot of log(e.r.) vs Hammett values of electrophiles at 0 °C.

| $R^4$ = | σ values | e.r. | log(e.r.) |
|---|---|---|---|
| *p*-$NMe_2$ | -0.83 | 24 | 1.4 |
| *p*-O*i*-Pr | -0.45 | 16 | 1.2 |
| *p*-OMe | -0.27 | 12 | 1.1 |
| *p*-Me | -0.17 | 12 | 1.1 |
| *p*-H | 0 | 6 | 0.78 |
| *p*-F | 0.06 | 4 | 0.60 |
| *p*-$CF_3$ | 0.54 | 3 | 0.48 |
| *p*-CN | 0.66 | 2 | 0.30 |

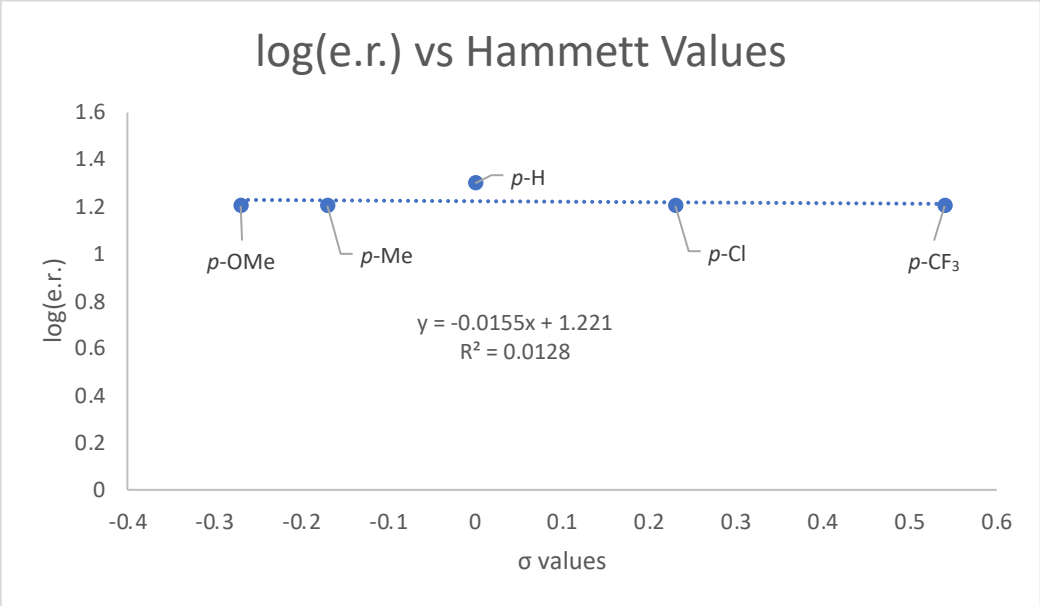


***Figure 5.S3.*** Plot of log(e.r.) vs Hammett values of nucleophiles at –10 °C.

| $R^4$ = | σ values | e.r. | log(e.r.) |
|---|---|---|---|
| *p*-OMe | -0.27 | 16 | 1.2 |
| *p*-Me | -0.17 | 16 | 1.2 |
| *p*-H | 0 | 19 | 1.3 |
| *p*-Cl | 0.23 | 16 | 1.2 |
| *p*-$CF_3$ | 0.54 | 16 | 1.2 |

***Table 5.S5.*** Low yielding electrophile and nucleophile examples.[a]

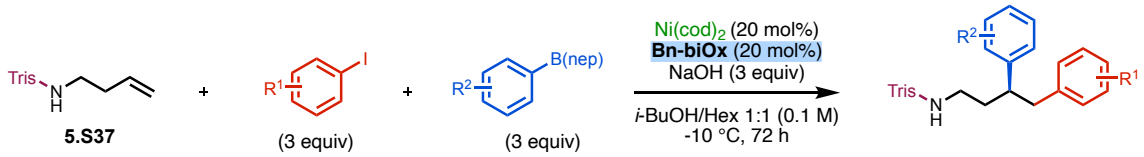


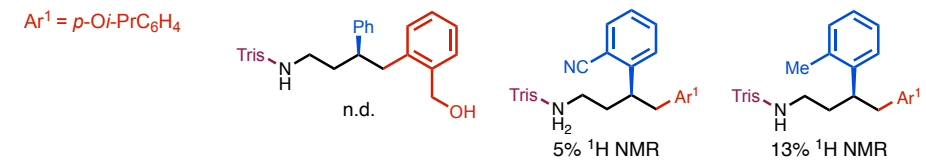


[a]Reaction conditions: **5.S37** (0.1 mmol). Percentages represent $^1$H NMR yields using $CH_2Br_2$ as the internal standard.

### 5.4.6. General Procedure for Nickel-Catalyzed 1,2-Dicarbofunctionalization of Alkenes

**General Procedure:** To an 8-mL round bottom glass tube equipped with a Teflon-coated magnetic stir bar, were added the alkene substrate (0.1 mmol), the appropriate arylboronic acid neopentylglycol ester (0.3 mmol), the appropriate aryl iodide electrophile (0.3 mmol), and (4*S*,4'*S*)-4,4'-dibenzyl-4,4',5,5'-tetrahydro-2,2'-bioxazole (**Bn-biOx**) (20 mol%). The tube was then equipped with a septum cap and introduced into an argon-filled glovebox antechamber. Once transferred inside the glovebox, anhydrous NaOH (0.3 mmol), anhydrous isobutanol (0.5 mL), and anhydrous hexanes were added (0.5 mL). The vial was allowed to pre-stir for 5 min at room temperature. After this time, $Ni(cod)_2$ (20 mol%) was added and the vial was removed from the glovebox, and was cooled while stirring to –10 °C in a Thermo Fisher Neslab CC 100 Immersion Cooler with an isopropanol bath for 72 h. After this time, the reaction mixture was quenched with sat. $NaHCO_3$ (1 mL); subsequently, sat. $NaHCO_3$ (4 mL) and EtOAc (1 mL) were added. The aqueous layer was further extracted with EtOAc (2 × 1 mL). Thereafter, the organic layers were combined, and the solvent was removed *in vacuo* to leave a yellow residue, which afforded pure product after preparative thin-layer chromatography (PTLC).

**General Procedure (without glovebox):** To an 8-mL round bottom glass tube equipped with a Teflon-coated magnetic stir bar, were added the alkene substrate (0.1 mmol), the appropriate arylboronic acid neopentylglycol ester (0.3 mmol), the appropriate aryl iodide electrophile (0.3 mmol), (4*S*,4'*S*)-4,4'-dibenzyl-4,4',5,5'-tetrahydro-2,2'-bioxazole (**Bn-biOx**) (20 mol%), anhydrous NaOH (0.3 mmol), anhydrous isobutanol (0.5 mL), and anhydrous hexanes (0.5 mL). The vial was sealed with a screw-top cap, evacuated

and backfilled with $N_2$, allowed to pre-stir for 5 min at room temperature. After this time, Ni(cod)TO[A] (20 mol%) was added. The vial was sealed with a screw-top cap, evacuated, backfilled with $N_2$, and was cooled while stirring to –10 °C in a Thermo Fisher Neslab CC 100 Immersion Cooler with an isopropanol bath for 72 h. After this time, the reaction mixture was quenched with sat. $NaHCO_3$ (1 mL); subsequently, sat. $NaHCO_3$ (4 mL) and EtOAc (1 mL) were added. The aqueous layer was further extracted with EtOAc (2 × 1 mL). Thereafter, the organic layers were combined, and the solvent was removed *in vacuo* to leave a yellow residue, which afforded pure product after preparative thin-layer chromatography (PTLC).

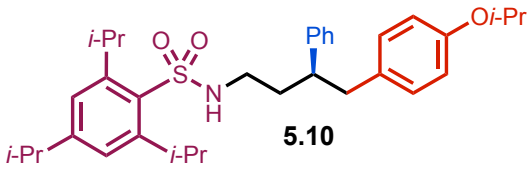


**5.10**

**(*S*)-*N*-(4-(4-isopropoxyphenyl)-3-phenylbutyl)-2,4,6-triisopropylbenzenesulfonamide (5.10)**: Purification using silica gel column chromatography (20% Acetone in Hexanes) gave the product as a white solid (45.3mg, 82% yield, 95:5 e.r.). Additionally, at 0 °C, purification using PTLC (20% Acetone in Hexanes) gave the product as a white solid (46.3 mg, 84% yield, 94:6 e.r.). Also, on larger scale, purification using silica gel column chromatography (20% Acetone in Hexanes) gave the product as a white solid 400 mg, 73% yield, 95:5 e.r.). **$^1$H NMR** (600 MHz, $CDCl_3$) δ 7.19 (t, $J$ = 7.3 Hz, 2H), 7.15–7.12 (m, 1H), 7.11 (s, 2H), 7.00–6.97 (m, 2H), 6.85 (d, $J$ = 8.6 Hz, 2H), 6.71 (d, $J$ = 8.6 Hz, 2H), 4.46 (hept, $J$ = 6.0 Hz, 1H), 4.13 (t, $J$ = 6.4 Hz, 1H), 4.02 (hept, $J$ = 6.8 Hz, 2H), 2.88 (p, $J$ = 6.9 Hz, 1H), 2.85–2.67 (m, 5H), 1.89–1.81 (m, 1H), 1.76 (dddd, $J$ = 13.3, 9.4, 7.9, 5.4 Hz, 1H), 1.30 (d, $J$ = 6.1 Hz, 6H), 1.24 (d, $J$ = 6.9 Hz, 6H), 1.17 (t, $J$ = 6.7 Hz, 12H); **$^{13}$C NMR** (150 MHz,

$CDCl_3$) δ 156.18, 152.59, 150.22, 143.56, 132.25, 131.78, 130.01, 128.52, 127.53, 126.50, 123.72, 115.66, 69.85, 45.52, 42.83, 41.13, 35.28, 34.13, 29.57, 24.86 (app-d), 23.60 (app-d), 22.09; **HRMS** (ESI-TOF) Calc'd for $C_{34}H_{48}NO_3S^+$ [M+H] 550.3355, found 550.3354; **X-ray** (single-crystal) Colorless block crystals of X-ray diffraction quality were obtained by recrystallization of **5.10** in hexanes (CCDC 2150217);[32] **SFC** (chiral column) The enantiomeric excess was determined by heart-cutting 2D LC-SFC.[33]

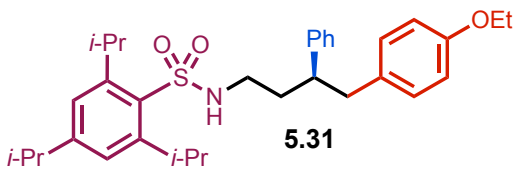

**5.31**

**(*S*)- *N*-(4-(4-ethoxyphenyl)-3-phenylbutyl)-2,4,6-triisopropylbenzenesulfonamide (5.31)**: Purification using PTLC (20% Acetone in Hexanes) gave the product as a white solid (34.8 mg, 65% yield, 94:6 e.r.). **$^1$H NMR** (600 MHz, $CDCl_3$) δ 7.19 (t, *J* = 7.3 Hz, 2H), 7.15 (q, *J* = 6.5 Hz, 1H), 7.11 (s, 2H), 7.01–6.94 (m, 2H), 6.85 (d, *J* = 8.6 Hz, 2H), 6.71 (d, *J* = 8.6 Hz, 2H), 4.08 (t, *J* = 6.3 Hz, 1H), 4.02 (hept, *J* = 6.7 Hz, 2H), 3.97 (q, *J* = 7.0 Hz, 2H), 2.88 (hept, *J* = 6.9 Hz, 1H), 2.85–2.68 (m, 5H), 1.89–1.81 (m, 1H), 1.81–1.72 (m, 1H), 1.38 (t, *J* = 7.0 Hz, 3H), 1.24 (d, *J* = 6.9 Hz, 6H), 1.17 (t, *J* = 6.4 Hz, 12H); **$^{13}$C NMR** (150 MHz, $CDCl_3$) δ 157.25, 152.58, 150.20, 143.51, 132.24, 131.75, 129.97, 128.51, 127.52, 126.50, 123.71, 114.15, 63.33, 45.53, 42.80, 41.12, 35.33, 34.12, 29.56, 24.84 (app-d), 23.59 (app-d), 14.88; **HRMS** (ESI-TOF) Calc'd for $C_{33}H_{46}NO_3S^+$ [M+H] 536.3198, found 536.3198.

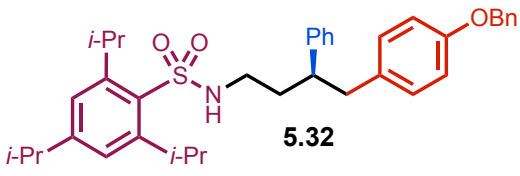

**5.32**

**(*S*)- *N*-(4-(4-(benzyloxy)phenyl)-3-phenylbutyl)-2,4,6-triisopropylbenzenesulfonamide (5.32)**:

Purification using PTLC (20% Acetone in Hexanes) gave the product as a white solid (17.9 mg, 30% yield, 96:4 e.r.). **$^1$H NMR** (600 MHz, $CDCl_3$) δ 7.41 (d, *J* = 6.8 Hz, 2H), 7.39–7.35 (m, 2H), 7.33–7.30 (m, 1H), 7.21–7.17 (m, 2H), 7.16–7.12 (m, 1H), 7.11 (s, 2H), 6.98 (d, *J* = 6.8 Hz, 2H), 6.86 (d, *J* = 8.6 Hz, 2H), 6.80 (d, *J* = 8.7 Hz, 2H), 5.00 (s, 2H), 4.11 (t, *J* = 6.4 Hz, 1H), 4.02 (hept, *J* = 6.8 Hz, 2H), 2.88 (hept, *J* = 6.9 Hz, 1H), 2.84–2.69 (m, 5H), 1.89–1.81 (m, 1H), 1.81–1.73 (m, 1H), 1.24 (d, *J* = 6.9 Hz, 6H), 1.17 (t, *J* = 6.5 Hz, 12H); **$^{13}$C NMR** (150 MHz, $CDCl_3$) δ 157.17, 152.60, 150.23, 143.48, 137.16, 132.26, 132.23, 130.04, 128.57, 128.54, 127.93, 127.54, 127.50, 126.53, 123.73, 114.56, 70.02, 45.52, 42.81, 41.12, 35.37, 34.13, 29.58, 24.86 (app-d), 23.61 (app-d); **HRMS** (ESI-TOF) Calc'd for $C_{38}H_{48}NO_3S^+$ [M+H] 598.3355, found 598.3356

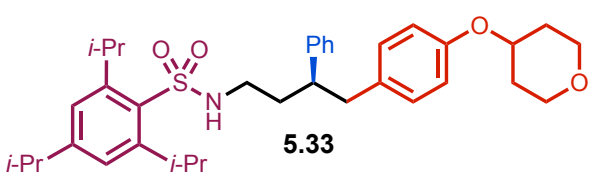


**5.33**

**(*S*)- 2,4,6-triisopropyl-*N*-(3-phenyl-4-(4-((tetrahydro-*2H*-pyran-4-yl)oxy)phenyl)butyl)benzenesulfonamide** (**5.33**): Purification using PTLC (20% Acetone in Hexanes) gave the product as a white solid (29.9 mg, 51% yield, 96:4 e.r.). **$^1$H NMR** (600 MHz, $CDCl_3$) δ 7.20 (t, *J* = 7.4 Hz, 2H), 7.14 (t, *J* = 7.3 Hz, 1H), 7.11 (s, 2H), 6.99 (d, *J* = 7.5 Hz, 2H), 6.86 (d, *J* = 8.4 Hz, 2H), 6.74 (d, *J* = 8.4 Hz, 2H), 4.40 (tt, *J* = 7.8, 3.8 Hz, 1H), 4.10 (t, *J* = 6.3 Hz, 1H), 4.02 (hept, *J* = 6.8 Hz, 2H), 3.99–3.92 (m, 2H), 3.55 (ddd, *J* = 11.6, 8.5, 3.1 Hz, 2H), 2.88 (hept, *J* = 6.8 Hz, 1H), 2.84–2.69 (m, 5H), 2.01–1.94 (m, 2H), 1.89–1.82 (m, 1H), 1.82–1.70 (m, 3H), 1.24 (d, *J* = 6.9 Hz, 6H), 1.17 (t, *J* = 6.1 Hz, 12H); **$^{13}$C NMR** (150 MHz, $CDCl_3$) 155.43, 152.59, 150.19, 143.45, 132.37, 132.21, 130.10, 128.52, 127.51, 126.52, 123.71, 115.93, 71.65, 65.16, 45.47, 42.80, 41.08, 35.34,

34.11, 31.86, 29.55, 24.84 (app-d), 23.58 (app-d); **HRMS** (ESI-TOF) Calc'd for $C_{36}H_{50}NO_4S^+$ [M+H] 592.3461, found 592.3464.

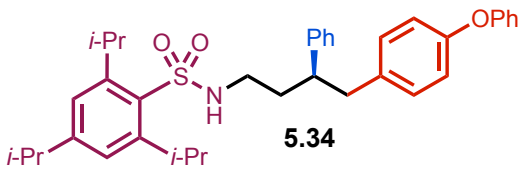


**5.34**

**(*S*)-2,4,6-triisopropyl-*N*-(4-(4-phenoxyphenyl)-3-phenylbutyl)benzenesulfonamide (5.34)**: Purification using PTLC (20% Acetone in Hexanes) gave the product as a white solid (43.1 mg, 74% yield, 88:12 e.r.). **$^1$H NMR** (600 MHz, $CDCl_3$) δ 7.31 (t, *J* = 7.8 Hz, 2H), 7.20 (t, *J* = 7.5 Hz, 2H), 7.18–7.13 (m, 1H), 7.12 (s, 2H), 7.07 (t, *J* = 7.8 Hz, 1H), 6.99 (d, *J* = 7.8 Hz, 2H), 6.95 (d, *J* = 8.5 Hz, 2H), 6.90 (d, *J* = 8.4 Hz, 2H), 6.82 (d, *J* = 8.3 Hz, 2H), 4.14 (t, *J* = 6.4 Hz, 1H), 4.03 (hept, *J* = 6.7 Hz, 2H), 2.92–2.73 (m, 6H), 1.93–1.85 (m, 1H), 1.85–1.75 (m, 1H), 1.24 (d, *J* = 6.9 Hz, 6H), 1.20–1.16 (m, 12H); **$^{13}$C NMR** (150 MHz, $CDCl_3$) δ 157.48, 155.30, 152.61, 150.21, 143.22, 134.80, 132.24, 130.28, 129.65, 128.54, 127.52, 126.60, 123.73, 122.98, 118.76, 118.55, 45.45, 42.93, 41.09, 35.41, 34.11, 29.56, 24.85 (app-d), 23.58 (app-d); **HRMS** (ESI-TOF) Calc'd for $C_{37}H_{46}NO_3S^+$ [M+H] 584.3198, found 584.3200.

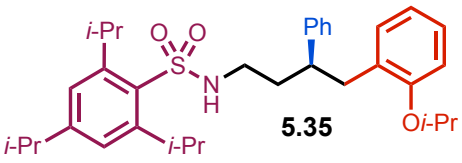


**5.35**

**(*S*)-*N*-(4-(2-isopropoxyphenyl)-3-phenylbutyl)-2,4,6-triisopropylbenzenesulfonamide (5.35)**: Purification using PTLC (20% Acetone in Hexanes) gave the product as a white solid (33 mg, 60% yield, 89:11 e.r.). **$^1$H NMR** (600 MHz, $CDCl_3$) δ 7.22–7.18 (m, 2H), 7.15–7.12 (m, 1H), 7.12–7.08 (m, 3H), 7.04 (s, 2H), 6.84 (dd, *J* = 7.4, 1.8 Hz, 1H), 6.81–6.78 (m, 1H), 6.72 (td, *J* = 7.4, 1.1 Hz, 1H), 4.54 (pd, *J* = 6.0,

0.7 Hz, 1H), 4.11 (t, *J* = 6.3 Hz, 1H), 4.02 (hept, *J* = 6.8 Hz, 2H), 2.89 (ddt, *J* = 20.8, 13.8, 7.2 Hz, 2H), 2.82–2.73 (m, 4H), 1.86–1.73 (m, 2H), 1.31 (dd, *J* = 6.0, 3.2 Hz, 6H), 1.24 (d, *J* = 6.9 Hz, 6H), 1.16 (dd, *J* = 6.8, 1.6 Hz, 12H); **$^{13}$C NMR** (150 MHz, $CDCl_3$) δ 155.70, 152.50, 150.23, 144.46, 132.25, 131.10, 129.20, 128.44, 127.41, 127.22, 126.34, 123.68, 119.79, 112.49, 69.52, 43.61, 41.40, 38.45, 35.25, 34.12, 29.54, 24.85, 23.60 (app-d), 22.23 (app-d); **HRMS** (ESI-TOF) Calc'd for $C_{34}H_{48}NO_3S^+$ [M+H] 550.3355, found 550.3354.

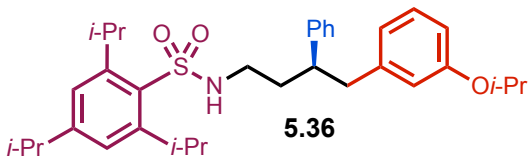


**5.36**

**(*S*)-*N*-(4-(3-isopropoxyphenyl)-3-phenylbutyl)-2,4,6-triisopropylbenzenesulfonamide (5.36)**: Purification using PTLC (20% Acetone in Hexanes) gave the product as a white solid (53.5 mg, 97% yield, 90:10 e.r.). **$^{1}$H NMR** (600 MHz, $CDCl_3$) δ 7.19 (t, *J* = 7.3 Hz, 2H), 7.15–7.11 (m, 1H), 7.11 (d, *J* = 0.5 Hz, 2H), 7.07 (dd, *J* = 8.2, 7.5 Hz, 1H), 7.00 (d, *J* = 6.9 Hz, 2H), 6.66 (ddd, *J* = 8.3, 2.6, 0.9 Hz, 1H), 6.55 (dt, *J* = 7.6, 1.1 Hz, 1H), 6.49 (dd, *J* = 2.5, 1.6 Hz, 1H), 4.41 (hept, *J* = 6.0 Hz, 1H), 4.18 (t, *J* = 6.4 Hz, 1H), 4.03 (p, *J* = 6.8 Hz, 2H), 2.89 (dq, *J* = 13.9, 6.9 Hz, 1H), 2.85–2.70 (m, 5H), 1.90–1.82 (m, 1H), 1.78 (dddd, *J* = 13.7, 10.2, 7.9, 5.3 Hz, 1H), 1.27 (d, *J* = 6.0 Hz, 3H), 1.24 (d, *J* = 6.8 Hz, 9H), 1.17 (t, *J* = 6.5 Hz, 12H); **$^{13}$C NMR** (151 MHz, $CDCl_3$) δ 157.75, 152.59, 150.24, 143.46, 141.42, 132.26, 129.13, 128.56, 127.51, 126.56, 123.73, 121.36, 116.83, 113.59, 69.72, 45.32, 43.76, 41.12, 35.47, 34.13, 29.57, 24.87 (d, *J* = 4.1 Hz), 23.61 (app-d), 22.09 (app-d); **HRMS** (ESI-TOF) Calc'd for $C_{34}H_{48}NO_3S^+$ [M+H] 550.3355, found 550.3356.

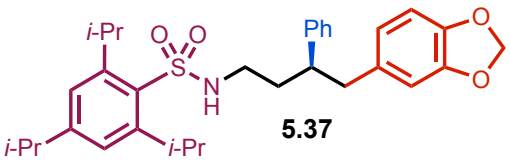


**5.37**

**(*S*)-*N*-(4-(benzo[*d*][1,3]dioxol-5-yl)-3-phenylbutyl)-2,4,6-triisopropylbenzenesulfonamide** (**5.37**): Purification using PTLC (20% Acetone in Hexanes) gave the product as a white solid (47.4 mg, 88% yield, 90:10 e.r.). The title compound was also prepared from **5.S37** (34 mg, 0.1 mmol), phenylboronic acid neopentyl glycol ester **5.S1** (57 mg, 0.3 mmol), and 5-iodobenzo[*d*][1,3]dioxole (74 mg, 0.3 mmol) according to General Procedure D, but at 0 °C with a reaction time of 48 h. Purification using PTLC (20% Acetone in Hexanes) gave the product as a white solid (42.4 mg, 79% yield, 88:12 e.r.). **$^1$H NMR** (600 MHz, $CDCl_3$) δ 7.20 (t, *J* = 7.3 Hz, 2H), 7.17–7.13 (m, 1H), 7.11 (s, 2H), 6.99 (d, *J* = 6.9 Hz, 2H), 6.62 (d, *J* = 7.9 Hz, 1H), 6.45 (d, *J* = 1.7 Hz, 1H), 6.41 (dd, *J* = 7.9, 1.7 Hz, 1H), 5.89 (s, 2H), 4.10 (t, *J* = 6.4 Hz, 1H), 4.02 (hept, *J* = 6.8 Hz, 2H), 2.88 (hept, *J* = 7.0 Hz, 1H), 2.84–2.67 (m, 5H), 1.90–1.81 (m, 1H), 1.80–1.72 (m, 1H), 1.24 (d, *J* = 6.9 Hz, 6H), 1.18 (dd, *J* = 6.8, 5.8 Hz, 12H); **$^{13}$C NMR** (150 MHz, $CDCl_3$) δ 152.61, 150.23, 147.40, 145.76, 143.31, 133.65, 132.29, 128.57, 127.50, 126.60, 123.74, 121.99, 109.41, 107.95, 100.75, 45.54, 43.40, 41.10, 35.41, 34.13, 29.57, 24.86 (app-d), 23.60 (app-d); **HRMS** (ESI-TOF) Calc'd for $C_{32}H_{42}NO_4S^+$ [M+H] 536.2835, found 536.2830.

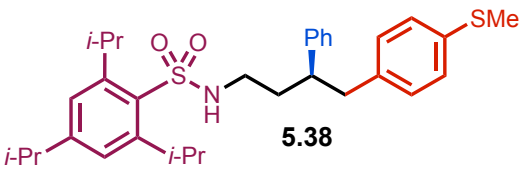


**5.38**

**(*S*)-2,4,6-triisopropyl-*N*-(4-(4-(methylthio)phenyl)-3-phenylbutyl)benzenesulfonamide** (**5.38**): Purification using PTLC (20% Acetone in Hexanes) gave the product as a white solid (45.2 mg, 84% yield, 89:11 e.r.). Additionally, at 0 °C, Purification using PTLC (20% Acetone

in Hexanes) gave the product as a white solid (46.8 mg, 87% yield, 88:12 e.r.). **$^1$H NMR** (600 MHz, $CDCl_3$) δ 7.21–7.17 (m, 2H), 7.15–7.12 (m, 1H), 7.11 (d, *J* = 0.5 Hz, 2H), 7.07 (d, *J* = 8.2 Hz, 2H), 6.98 (d, *J* = 6.8 Hz, 2H), 6.87 (d, *J* = 8.3 Hz, 2H), 4.20 (t, *J* = 6.4 Hz, 1H), 4.03 (p, *J* = 6.8 Hz, 2H), 2.88 (hept, *J* = 6.9 Hz, 1H), 2.85–2.71 (m, 5H), 2.43 (s, 3H), 1.86 (dddd, *J* = 13.9, 8.2, 7.2, 3.9 Hz, 1H), 1.82–1.74 (m, 1H), 1.24 (d, *J* = 6.9 Hz, 6H), 1.18 (dd, *J* = 6.8, 6.1 Hz, 12H); **$^{13}$C NMR** (150 MHz, $CDCl_3$) δ 152.62, 150.23, 143.21, 136.87, 135.64, 132.28, 129.62, 128.57, 127.54, 126.76, 126.60, 123.75, 45.29, 43.10, 41.07, 35.50, 34.13, 29.58, 24.87 (app-d), 23.62 (app-d), 16.13; **HRMS** (ESI-TOF) Calc'd for $C_{32}H_{44}NO_2S_2^+$ [M+H] 538.2813, found 538.2802.

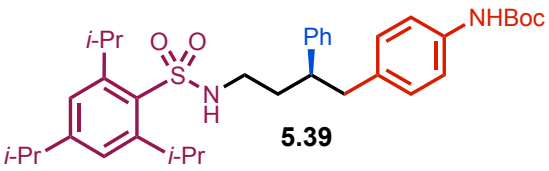


**5.39**

**(*S*)-*tert*-butyl (4-(2-phenyl-4-((2,4,6-triisopropylphenyl)sulfonamido)butyl)phenyl)carbamate** (**5.39**): Purification using PTLC (20% Acetone in Hexanes) gave the product as a white solid (29.6 mg, 49% yield, 96:4 e.r.). Additionally, at 0 °C, purification using PTLC (20% Acetone in Hexanes) gave the product as a white solid (21.9 mg, 36% yield, 94:6 e.r.). **$^1$H NMR** (600 MHz, $CDCl_3$) δ 7.20–7.14 (m, 4H), 7.14–7.11 (m, 1H), 7.11 (s, 2H), 6.97 (d, *J* = 6.9 Hz, 2H), 6.86 (d, *J* = 8.5 Hz, 2H), 6.40 (s, 1H), 4.16 (t, *J* = 6.4 Hz, 1H), 4.02 (hept, *J* = 6.8 Hz, 2H), 2.88 (hept, *J* = 6.9 Hz, 1H), 2.84–2.70 (m, 5H), 1.85 (dtd, *J* = 13.9, 7.4, 3.8 Hz, 1H), 1.81–1.74 (m, 1H), 1.50 (s, 9H), 1.24 (d, *J* = 6.9 Hz, 6H), 1.17 (t, *J* = 6.6 Hz, 12H); **$^{13}$C NMR** (150 MHz, $CDCl_3$) δ 152.80, 152.59, 150.22, 143.32, 136.36, 134.48, 132.26, 129.57, 128.53, 127.53, 126.54, 123.73, 118.38, 45.41, 42.98, 41.10, 35.45, 34.12, 29.57, 28.36, 24.87 (app-d),

23.61 (app-d); **HRMS** (ESI-TOF) Calc'd for $C_{36}H_{51}N_2O_4S^+$ [M+H] 607.3570, found 607.3580.

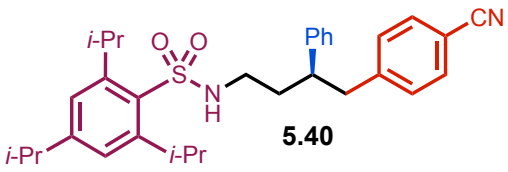


**5.40**

**(*S*)- *N*-(4-(4-cyanophenyl)-3-phenylbutyl)-2,4,6-triisopropylbenzenesulfonamide** (**5.40**): Purification using PTLC (20% Acetone in Hexanes) gave the product as a white solid (23.9 mg, 46% yield, 68:32 e.r.). Additionally, at 0 °C, purification using PTLC (20% Acetone in Hexanes) gave the product as a white solid (31.7 mg, 61% yield, 68:32 e.r.). **$^1$H NMR** (600 MHz, $CDCl_3$) δ 7.43 (d, *J* = 8.3 Hz, 2H), 7.22–7.17 (m, 2H), 7.17–7.13 (m, 1H), 7.12 (s, 2H), 7.00 (d, *J* = 8.3 Hz, 2H), 6.94 (d, *J* = 6.8 Hz, 2H), 4.23 (t, *J* = 6.4 Hz, 1H), 4.03 (hept, *J* = 6.8 Hz, 2H), 2.95–2.82 (m, 5H), 2.76 (dq, *J* = 13.9, 7.3 Hz, 1H), 1.95–1.82 (m, 2H), 1.24 (d, *J* = 6.9 Hz, 6H), 1.18 (dd, *J* = 6.8, 1.5 Hz, 12H); **$^{13}$C NMR** (150 MHz, $CDCl_3$) δ 152.74, 150.18, 145.48, 142.11, 132.20, 131.92, 129.84, 128.71, 127.49, 126.94, 123.78, 118.98, 109.94, 44.98, 43.67, 40.91, 35.91, 34.12, 29.59, 24.85, 23.59; **HRMS** (ESI-TOF) Calc'd for $C_{32}H_{41}N_2O_2S^+$ [M+H] 517.2889, found 517.2901.

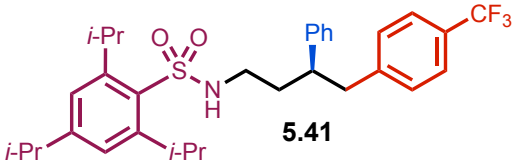


**5.41**

**(*S*)- 2,4,6-triisopropyl-*N*-(3-phenyl-4-(4-(trifluoromethyl)phenyl)butyl)benzenesulfonamide** (**5.41**): Purification using PTLC (20% Acetone in Hexanes) gave the product as a white solid (34.2 mg, 61% yield, 75:25 e.r.). Additionally, at 0 °C, purification using PTLC (20% Acetone in Hexanes) gave the product as a white solid (51.6 mg, 92% yield, 72:28 e.r.). **$^1$H NMR** (600 MHz, $CDCl_3$) δ

7.41 (d, $J$ = 8.0 Hz, 2H), 7.21–7.17 (m, 2H), 7.17–7.13 (m, 1H), 7.12 (s, 2H), 7.03 (d, $J$ = 7.9 Hz, 2H), 6.97 (d, $J$ = 6.8 Hz, 2H), 4.30 (t, $J$ = 6.4 Hz, 1H), 4.04 (hept, $J$ = 6.7 Hz, 2H), 2.92–2.81 (m, 5H), 2.76 (dq, $J$ = 14.0, 7.3 Hz, 1H), 1.92–1.80 (m, 2H), 1.24 (d, $J$ = 7.0 Hz, 6H), 1.18 (dd, $J$ = 6.9, 5.0 Hz, 12H); **$^{13}$C NMR** (150 MHz, $CDCl_3$) δ 152.69, 150.22, 143.94, 142.57, 129.37, 128.66, 128.35 (q, $J$ = 32.1 Hz), 127.51, 126.81, 125.04 (q, $J_{C-F}$ = 3.7 Hz), 124.28 (q, $J_{C-F}$ = 272.0 Hz), 123.76, 45.05, 43.39, 40.96, 35.70, 34.13, 29.58, 24.84 (app-d), 23.59 (app-d); **$^{19}$F NMR** (376 MHz, $CDCl_3$) δ –65.02; **HRMS** (ESI-TOF) Calc'd for $C_{32}H_{41}F_3NO_2S^+$ [M+H] 560.2810, found 560.2813.

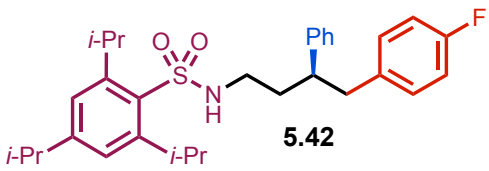


**5.42**

**(*S*)-** ***N*-(4-(4-fluorophenyl)-3-phenylbutyl)-2,4,6-triisopropylbenzenesulfonamide** (**5.42**): Purification using PTLC (20% Acetone in Hexanes) gave the product as a white solid (41.4 mg, 81% yield, 81:19 e.r.). Additionally, at 0 °C, purification using PTLC (20% Acetone in Hexanes) gave the product as a white solid (49.6 mg, 97% yield, 78:22 e.r.). **$^{1}$H NMR** (600 MHz, $CDCl_3$) δ 7.22–7.18 (m, 2H), 7.16–7.13 (m, 1H), 7.11 (s, 2H), 6.98–6.95 (m, 2H), 6.89–6.83 (m, 4H), 4.12 (t, $J$ = 6.4 Hz, 1H), 4.03 (hept, $J$ = 6.8 Hz, 2H), 2.93–2.71 (m, 7H), 1.86 (dtd, $J$ = 11.4, 7.5, 3.8 Hz, 1H), 1.83–1.76 (m, 1H), 1.24 (d, $J$ = 6.9 Hz, 6H), 1.18 (dd, $J$ = 6.8, 4.0 Hz, 12H); **$^{13}$C NMR** (150 MHz, $CDCl_3$) δ 161.34 (d, $J_{C-F}$ = 243.8 Hz), 152.64, 150.23, 143.00, 135.47 (d, $J_{C-F}$ = 3.2 Hz), 132.29, 130.43 (d, $J_{C-F}$ = 7.8 Hz), 128.57, 127.55, 126.64, 123.75, 114.87 (d, $J_{C-F}$ = 21.0 Hz), 45.43, 42.82, 41.05, 35.54, 34.13, 29.58, 24.86 (app-d), 23.60 (app-d); **$^{19}$F NMR** (376 MHz, $CDCl_3$) δ –119.94; **HRMS** (ESI-TOF) Calc'd for $C_{31}H_{41}FNO_2S^+$ [M+H] 510.2842, found 510.2849.

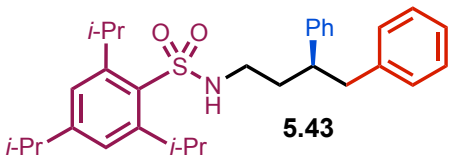


**5.43**

**(*S*)-** ***N*-(3,4-diphenylbutyl)-2,4,6-triisopropylbenzenesulfonamide** **(5.43)**: Purification using PTLC (20% Acetone in Hexanes) gave the product as a white solid (36.4 mg, 74% yield, 88:12 e.r.). Additionally, at 0 °C, purification using PTLC (20% Acetone in Hexanes) gave the product as a white solid (44 mg, 89% yield, 86:14 e.r.). **$^1$H NMR** (600 MHz, $CDCl_3$) δ 7.22–7.12 (m, 6H), 7.11 (s, 2H), 7.01–6.98 (m, 2H), 6.98–6.95 (m, 2H), 4.08 (t, $J$ = 5.9 Hz, 1H), 4.02 (hept, $J$ = 6.7 Hz, 2H), 2.91–2.71 (m, 6H), 1.89–1.82 (m, 1H), 1.82–1.75 (m, 1H), 1.24 (d, $J$ = 6.9 Hz, 6H), 1.17 (t, $J$ = 6.8 Hz, 12H); **$^{13}$C NMR** (150 MHz, $CDCl_3$) δ 152.60, 150.21, 143.38, 139.83, 132.23, 129.09, 128.55, 128.18, 127.50, 126.58, 126.06, 123.72, 45.35, 43.69, 41.10, 35.42, 34.12, 29.57, 24.85 (app-d), 23.60; **HRMS** (ESI-TOF) Calc'd for $C_{31}H_{42}NO_2S^+$ [M+H] 492.2936, found 492.2942.

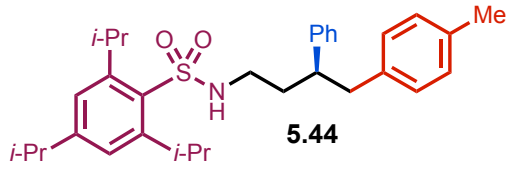


**5.44**

**(*S*)-** **2,4,6-triisopropyl-*N*-(3-phenyl-4-(*p*-tolyl)butyl)benzenesulfonamide** **(5.44)**: Purification using PTLC (20% Acetone in Hexanes) gave the product as a white solid (45.9 mg, 91% yield, 92:8 e.r.). Additionally, at 0 °C, purification using PTLC (20% Acetone in Hexanes) gave the product as a white solid (44.8 mg, 89% yield, 92:8 e.r.). **$^1$H NMR** (600 MHz, $CDCl_3$) δ 7.22–7.18 (m, 2H), 7.16–7.13 (m, 1H), 7.11 (s, 2H), 7.02–6.97 (m, 4H), 6.86 (d, $J$ = 8.0 Hz, 2H), 4.07 (t, $J$ = 6.3 Hz, 1H), 4.01 (p, $J$ = 6.8 Hz, 2H), 2.92–2.70 (m, 6H), 2.28 (s, 3H), 1.88–1.81 (m, 1H), 1.80–1.73 (m, 1H), 1.24 (d, $J$ = 6.9 Hz, 6H), 1.17 (dd, $J$ = 7.5, 6.8 Hz, 12H); **$^{13}$C NMR**

(150 MHz, $CDCl_3$) δ 152.58, 150.21, 143.58, 136.72, 135.50, 132.24, 128.95, 128.88, 128.54, 127.50, 126.53, 123.72, 45.38, 43.22, 41.11, 35.37, 34.13, 29.56, 24.84 (app-d), 23.59 (app-d), 21.00; **HRMS** (ESI-TOF) Calc'd for $C_{32}H_{44}NO_2S^+$ [M+H] 506.3093, found 506.3093.

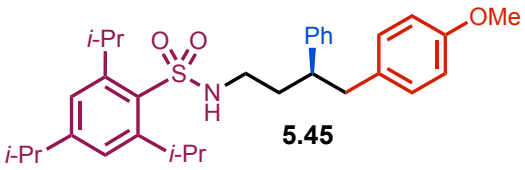


**5.45**

**(*S*)-2,4,6-triisopropyl-*N*-(4-(4-methoxyphenyl)-3-phenylbutyl)benzenesulfonamide (5.45)**: Purification using PTLC (20% Acetone in Hexanes) gave the product as a white solid (45 mg, 86% yield, 92:8 e.r). Additionally, at 0 °C purification using PTLC (20% Acetone in Hexanes) gave the product as a white solid (45.2 mg, 87% yield, 92:8 e.r.). **$^1$H NMR** (600 MHz, $CDCl_3$) δ 7.21–7.17 (m, 2H), 7.15–7.12 (m, 1H), 7.11 (d, $J$ = 0.6 Hz, 2H), 6.98 (d, $J$ = 6.8 Hz, 2H), 6.86 (d, $J$ = 8.6 Hz, 2H), 6.71 (d, $J$ = 8.6 Hz, 2H), 4.19 (t, $J$ = 6.3 Hz, 1H), 4.03 (hept, $J$ = 6.7 Hz, 2H), 3.74 (s, 3H), 2.88 (hept, $J$ = 6.9 Hz, 1H), 2.84–2.70 (m, 5H), 1.85 (dddd, $J$ = 13.6, 8.1, 7.1, 3.9 Hz, 1H), 1.77 (dddd, $J$ = 13.4, 9.4, 7.9, 5.4 Hz, 1H), 1.24 (d, $J$ = 7.0 Hz, 6H), 1.18 (t, $J$ = 6.6 Hz, 12H); **$^{13}$C NMR** (150 MHz, $CDCl_3$) δ 157.89, 152.60, 150.23, 143.50, 132.28, 131.92, 130.01, 128.53, 127.55, 126.51, 123.74, 113.58, 55.20, 45.53, 42.79, 41.12, 35.38, 34.14, 29.58, 24.87 (app-d), 23.62 (app-d); **HRMS** (ESI-TOF) Calc'd for $C_{32}H_{44}NO_3S^+$ [M+H] 522.3042, found 522.3044.

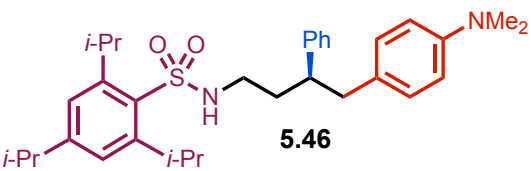


**5.46**

**(*S*)-*N*-(4-(4-(dimethylamino)phenyl)-3-phenylbutyl)-2,4,6-triisopropylbenzenesulfonamide (5.46)**:

Additionally, at 0 °C, purification using PTLC (20% Acetone in Hexanes) gave the product as a white solid (30.5 mg, 57% yield, 96:4 e.r.). **$^1$H NMR** (600 MHz, $CDCl_3$) δ 7.22–7.18 (m, 2H), 7.16–7.12 (m, 1H), 7.11 (s, 2H), 7.01 (d, *J* = 6.8 Hz, 2H), 6.85 (d, *J* = 8.6 Hz, 2H), 6.59 (d, *J* = 8.6 Hz, 2H), 4.09 (t, *J* = 6.4 Hz, 1H), 4.02 (hept, *J* = 6.8 Hz, 2H), 2.89 (s, 7H), 2.83–2.71 (m, 4H), 2.71–2.62 (m, 1H), 1.84 (dddd, *J* = 12.2, 11.1, 5.6, 3.0 Hz, 1H), 1.74 (dddd, *J* = 13.5, 9.9, 7.9, 5.4 Hz, 1H), 1.24 (d, *J* = 6.9 Hz, 6H), 1.19 – 1.15 (m, 12H); **$^{13}$C NMR** (150 MHz, $CDCl_3$) δ 152.54, 150.24, 149.12, 143.94, 132.27, 129.71, 128.50, 127.93, 127.54, 126.41, 123.71, 112.72, 45.59, 42.69, 41.17, 40.81, 35.22, 34.13, 29.57, 24.87 (app-d), 23.61 (app-d); **HRMS** (ESI-TOF) Calc'd for $C_{33}H_{47}N_2O_2S^+$ [M+H] 535.3358, found 535.3351.

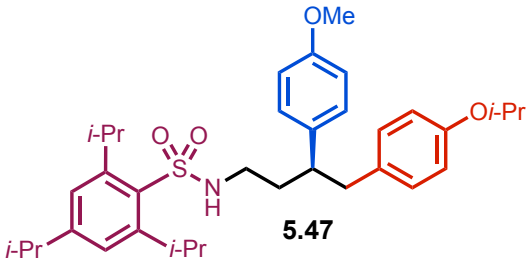


**5.47**

**(*S*)-*N*-(4-(4-isopropoxyphenyl)-3-(4-methoxyphenyl)butyl)-2,4,6-triisopropylbenzenesulfonamide (5.47):** Purification using PTLC (20% Acetone in Hexanes) gave the product as a white solid (41.2 mg, 71% yield, 94:6 e.r.). **$^1$H NMR** (600 MHz, $CDCl_3$) δ 7.11 (s, 2H), 6.89 (d, *J* = 8.5 Hz, 2H), 6.84 (d, *J* = 8.4 Hz, 2H), 6.74 (d, *J* = 8.5 Hz, 2H), 6.71 (d, *J* = 8.4 Hz, 2H), 4.47 (hept, *J* = 6.0 Hz, 1H), 4.10 (t, *J* = 6.4 Hz, 1H), 4.02 (h, *J* = 6.7 Hz, 2H), 3.76 (s, 3H), 2.88 (p, *J* = 6.9 Hz, 1H), 2.81 (dt, *J* = 13.2, 6.5 Hz, 1H), 2.78 – 2.65 (m, 4H), 1.82 (td, *J* = 7.5, 3.6 Hz, 1H), 1.72 (td, *J* = 13.9, 8.0 Hz, 1H), 1.30 (d, *J* = 6.1 Hz, 6H), 1.25 (d, *J* = 6.9 Hz, 6H), 1.18 (t, *J* = 6.4 Hz, 12H); **$^{13}$C NMR** (150 MHz, $CDCl_3$) δ 158.10, 156.13, 152.56, 150.20, 135.50, 132.28, 131.88, 130.01, 128.40, 123.71, 115.63, 113.89, 69.83, 55.20, 44.64, 42.99, 41.13, 35.45, 34.11, 29.56, 24.84 (app-

d), 23.59 (app-d), 22.08; **HRMS** (ESI-TOF) Calc'd for $C_{35}H_{50}NO_4S^+$ [M+H] 580.3461, found 580.3467.

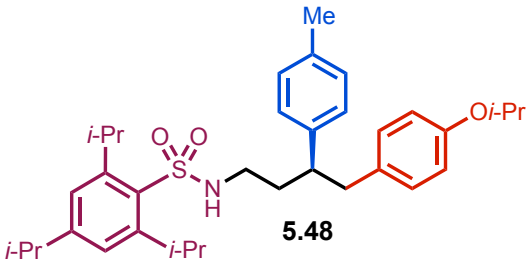


**5.48**

**(*S*)-** ***N*-(4-(4-isopropoxyphenyl)-3-(*p*-tolyl)butyl)-2,4,6-triisopropylbenzenesulfonamide (5.48):** Purification using PTLC (20% Acetone in Hexanes) gave the product as a white solid (46.1 mg, 82% yield, 94:6 e.r.). **$^1$H NMR** (600 MHz, $CDCl_3$) δ 7.11 (s, 2H), 7.00 (d, *J* = 7.7 Hz, 2H), 6.93–6.82 (m, 2H), 6.76–6.66 (m, 2H), 4.47 (hept, *J* = 6.1 Hz,1H), 4.12 (t, *J* = 6.4 Hz, 1H), 4.02 (hept, *J* = 6.8 Hz, 2H), 2.88 (hept, *J* = 6.8 Hz, 1H), 2.84–2.65 (m, 5H), 2.27 (s, 3H), 1.88–1.78 (m, 1H), 1.76–1.68 (m, 1H), 1.30 (d, *J* = 6.1 Hz, 6H), 1.25 (d, *J* = 7.0 Hz, 6H), 1.17 (t, *J* = 6.6 Hz, 12H); **$^{13}$C NMR** (150 MHz, $CDCl_3$) δ 156.14, 152.53, 150.21, 140.47, 135.89, 132.30, 131.92, 130.00, 129.19, 127.34, 123.69, 115.63, 69.82, 45.06, 42.86, 41.13, 35.30, 34.11, 29.55, 24.82 (app-d), 23.59, 22.09 (app-d), 20.98; **HRMS** (ESI-TOF) Calc'd for $C_{35}H_{50}NO_3S^+$ [M+H] 564.3511, found 564.3513.

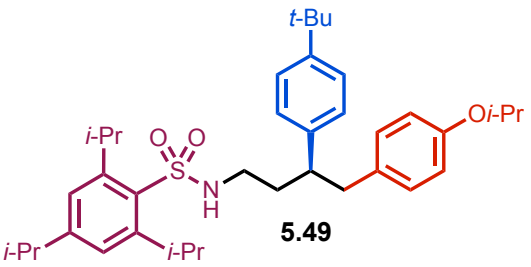


**5.49**

**(*S*)-** ***N*-(3-(4-(*tert*-butyl)phenyl)-4-(4-isopropoxyphenyl)butyl)-2,4,6-triisopropylbenzenesulfonamide (5.49):** Purification using PTLC (20% Acetone in Hexanes) gave the product as a white solid (43.3 mg, 71% yield, 96:4 e.r.). **$^1$H NMR** (600 MHz, $CDCl_3$) δ 7.21 (d, *J* = 8.3 Hz, 2H), 7.11 (s, 2H), 6.90 (dd, *J* = 15.8, 8.4 Hz, 4H), 6.73

(d, $J$ = 8.5 Hz, 2H), 4.48 (h, $J$ = 6.0 Hz, 1H), 4.02 (tq, $J$ = 13.5, 6.6 Hz, 3H), 2.88 (p, $J$ = 6.9 Hz, 1H), 2.81 (dt, $J$ = 13.1, 6.3 Hz, 2H), 2.77–2.63 (m, 3H), 1.84–1.76 (m, 1H), 1.75–1.67 (m, 1H), 1.31 (dd, $J$ = 6.0, 1.7 Hz, 6H), 1.27 (s, 9H), 1.25 (dd, $J$ = 6.9, 1.3 Hz, 6H), 1.16 (dd, $J$ = 10.4, 6.7 Hz, 12H); **$^{13}$C NMR** (150 MHz, $CDCl_3$) δ 156.18, 152.53, 150.26, 149.22, 140.57, 132.27, 132.03, 130.03, 127.04, 125.41, 123.71, 115.68, 69.86, 44.89, 42.81, 41.10, 35.00, 34.36, 34.13, 31.37, 29.55, 24.87 (app-d), 23.61 (app-d), 22.11 (app-d); **HRMS** (ESI-TOF) Calc'd for $C_{38}H_{56}NO_3S^+$ [M+H] 606.3981, found 606.3979.

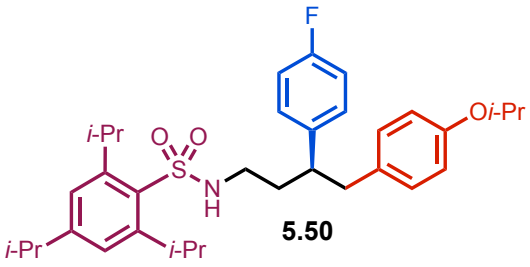


**5.50**

**(*S*)-*N*-(3-(4-fluorophenyl)-4-(4-isopropoxyphenyl)butyl)-2,4,6-triisopropylbenzenesulfonamide (5.50):** Purification using PTLC (20% Acetone in Hexanes) gave the product as a white solid (45.4 mg, 80% yield, 94:6 e.r.). **$^{1}$H NMR** (600 MHz, $CDCl_3$) δ 7.12 (s, 2H), 6.91 (ddt, $J$ = 8.3, 5.1, 2.5 Hz, 2H), 6.89–6.84 (m, 2H), 6.81 (d, $J$ = 8.6 Hz, 2H), 6.70 (d, $J$ = 8.6 Hz, 2H), 4.46 (hept, $J$ = 6.1 Hz, 1H), 4.24 (t, $J$ = 6.4 Hz, 1H), 4.03 (h, $J$ = 6.8 Hz, 2H), 2.89 (dq, $J$ = 13.9, 6.9 Hz, 1H), 2.83 – 2.68 (m, 5H), 1.86 (dddd, $J$ = 13.7, 8.3, 7.3, 4.3 Hz, 1H), 1.74 (dddd, $J$ = 13.6, 10.5, 7.9, 5.3 Hz, 1H), 1.29 (d, $J$ = 6.1 Hz, 6H), 1.25 (d, $J$ = 6.9 Hz, 6H), 1.18 (t, $J$ = 6.6 Hz, 12H); **$^{13}$C NMR** (150 MHz, $CDCl_3$) δ 161.45 (d, $J_{C-F}$ = 244.1 Hz), 156.22, 152.68, 150.23, 139.11 (d, $J_{C-F}$ = 3.3 Hz), 132.21, 131.46, 130.00, 128.94 (d, $J_{C-F}$ = 7.7 Hz), 123.75, 115.68, 115.24 (d, $J_{C-F}$ = 21.1 Hz), 69.86, 44.69, 42.92, 41.02, 35.49, 34.13, 29.57, 24.86, 24.84, 23.59, 22.09, 22.08; **$^{19}$F NMR** (471 MHz, $CDCl_3$) δ –116.90; **HRMS** (ESI-TOF) Calc'd for $C_{34}H_{47}FNO_3S^+$ [M+H] 568.3261, found 568.3257.

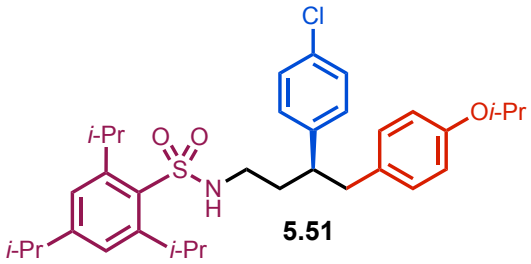


**5.51**

**(*S*)-** ***N*-(3-(4-chlorophenyl)-4-(4-isopropoxyphenyl)butyl)-2,4,6-triisopropylbenzenesulfonamide (5.51):** Purification using PTLC (20% Acetone in Hexanes) gave the product as a white solid (42 mg, 72% yield, 94:6 e.r.). **$^{1}$H NMR** (600 MHz, $CDCl_3$) δ 7.15 (s, 2H), 7.12 (s, 2H), 6.89 (d, *J* = 8.4 Hz, 2H), 6.81 (d, *J* = 8.6 Hz, 2H), 6.70 (d, *J* = 8.6 Hz, 2H), 4.46 (hept, *J* = 6.1 Hz, 1H), 4.25 (t, *J* = 6.4 Hz, 1H), 4.03 (hept, *J* = 6.8 Hz, 2H), 2.89 (hept, *J* = 6.8 Hz, 1H), 2.82–2.76 (m, 2H), 2.75–2.68 (m, 3H), 1.90–1.82 (m, 1H), 1.74 (dddd, *J* = 13.6, 10.4, 8.0, 5.3 Hz, 1H), 1.30 (d, *J* = 6.0 Hz, 6H), 1.25 (dd, *J* = 6.9, 0.9 Hz, 6H), 1.18 (t, *J* = 6.7 Hz, 12H); **$^{13}$C NMR** (150 MHz, $CDCl_3$) δ 156.26, 152.69, 150.23, 141.96, 132.20, 132.07, 131.30, 130.00, 128.94, 128.59, 123.77, 115.69, 69.86, 44.81, 42.71, 40.96, 35.39, 34.13, 29.58, 24.85 (app-d), 23.60, 22.08 (app-d); **HRMS** (ESI-TOF) Calc'd for $C_{34}H_{47}ClNO_3S^+$ [M+H] 584.2965, found 584.2968.

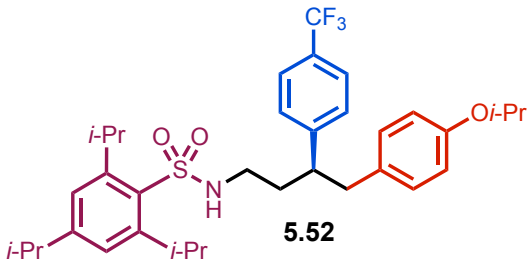


**5.52**

**(*S*)-** ***N*-(4-(4-isopropoxyphenyl)-3-(4-(trifluoromethyl)phenyl)butyl)-2,4,6-triisopropylbenzenesulfonamide (5.52):** Purification using PTLC (20% Acetone in Hexanes) gave the product as a white solid (21.0 mg, 34% yield, 94:6 e.r.). **$^{1}$H NMR** (600 MHz, $CDCl_3$) δ 7.44 (d, *J* = 8.0 Hz, 2H), 7.12 (s, 2H), 7.08 (d, *J* = 8.1 Hz, 2H), 6.88–6.77 (m, 2H), 6.77–6.63 (m, 2H), 4.47 (hept, *J* = 6.2 Hz, 1H), 4.16 (t, *J* = 6.4 Hz, 1H), 4.01 (hept, *J* = 6.8 Hz, 2H), 2.95–2.84 (m, 2H), 2.84–2.67 (m, 4H), 1.89 (ddt, *J* = 15.6, 7.7, 4.4

Hz, 1H), 1.86–1.74 (m, 1H), 1.30 (dd, $J$ = 6.1, 1.0 Hz, 6H), 1.24 (dd, $J$ = 6.9, 1.2 Hz, 6H), 1.16 (dd, $J$ = 9.3, 6.8 Hz, 12H); **$^{13}$C NMR** (150 MHz, $CDCl_3$) δ 156.48, 152.89, 150.35, 147.85, 132.24, 131.14, 130.10, 128.93 (q, $J_{C-F}$ = 32.5 Hz), 128.08, 126.27 (q, $J_{C-F}$ = 320.8 Hz), 125.55 (q, $J_{C-F}$ = 3.8 Hz), 123.92, 115.88, 70.00, 45.34, 42.69, 41.02, 35.36, 34.24, 29.71, 24.94 (app-d), 23.70 (app-d), 22.19; **$^{19}$F NMR** (471 MHz, $CDCl_3$) δ -62.70; **HRMS** (ESI-TOF) Calc'd for $C_{35}H_{47}F_3NO_3S^+$ [M+H] 618.3229, found 618.3229.

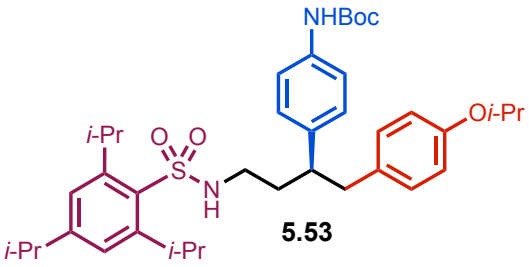


**5.53**

**(*S*)- *tert*-butyl (4-(1-(4-isopropoxyphenyl)-4-((2,4,6-triisopropylphenyl)sulfonamido)butan-2-yl)phenyl)carbamate (5.53):** Purification using PTLC (20% Acetone in Hexanes) gave the product as a white solid (30.9 mg, 46% yield, 92:8 e.r.). **$^1$H NMR** (600 MHz, $CDCl_3$) δ 7.20 (d, $J$ = 8.0 Hz, 2H), 7.12 (s, 2H), 6.91 (d, $J$ = 8.4 Hz, 2H), 6.83 (d, $J$ = 8.6 Hz, 2H), 6.69 (d, $J$ = 8.5 Hz, 2H), 6.42 (s, 1H), 4.46 (hept, $J$ = 6.1 Hz, 1H), 4.16 (t, $J$ = 6.3 Hz, 1H), 4.03 (hept, $J$ = 6.8 Hz, 2H), 2.88 (hept, $J$ = 6.4 Hz, 1H), 2.85–2.66 (m, 5H), 1.84 (ddt, $J$ = 16.7, 7.8, 3.5 Hz, 1H), 1.73 (ddt, $J$ = 13.7, 8.6, 4.5 Hz, 1H), 1.51 (s, 9H), 1.30 (d, $J$ = 6.1 Hz, 6H), 1.24 (d, $J$ = 6.9 Hz, 6H), 1.18 (dd, $J$ = 6.9, 4.2 Hz, 12H); **$^{13}$C NMR** (150 MHz, $CDCl_3$) δ 156.14, 152.75, 152.58, 150.19, 138.10, 136.72, 132.29, 131.76, 130.02, 128.03, 123.74, 118.60, 115.62, 69.82, 44.85, 42.83, 41.12, 35.45, 34.11, 29.57, 28.36, 24.86 (app-d), 23.59, 22.10 (app-d); **HRMS** (ESI-TOF) Calc'd for $C_{39}H_{57}N_2O_5S^+$ [M+H] 665.3988, found 665.3982.

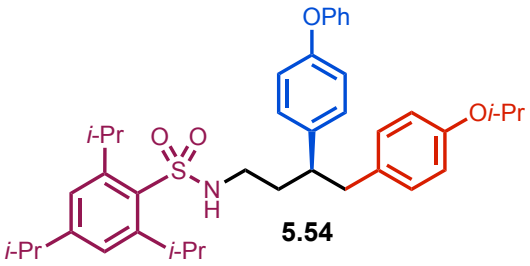


**5.54**

**(*S*)- *N*-(4-(4-isopropoxyphenyl)-3-(4-phenoxyphenyl)butyl)-2,4,6-triisopropylbenzenesulfonamide (5.54):** Purification using PTLC (20% Acetone in Hexanes) gave the product as a white solid (52.4 mg, 82% yield, 94:6 e.r.). **$^1$H NMR** (600 MHz, $CDCl_3$) δ 7.20 (d, *J* = 8.0 Hz, 2H), 7.12 (s, 2H), 6.91 (d, *J* = 8.4 Hz, 2H), 6.83 (d, *J* = 8.6 Hz, 2H), 6.69 (d, *J* = 8.5 Hz, 2H), 6.42 (s, 1H), 4.46 (hept, *J* = 6.1 Hz, 1H), 4.16 (t, *J* = 6.3 Hz, 1H), 4.03 (hept, *J* = 6.8 Hz, 2H), 2.88 (hept, *J* = 6.4 Hz, 1H), 2.85–2.66 (m, 5H), 1.84 (ddt, *J* = 16.7, 7.8, 3.5 Hz, 1H), 1.73 (ddt, *J* = 13.7, 8.6, 4.5 Hz, 1H), 1.51 (s, 9H), 1.30 (d, *J* = 6.1 Hz, 6H), 1.24 (d, *J* = 6.9 Hz, 6H), 1.18 (dd, *J* = 6.9, 4.2 Hz, 12H); **$^{13}$C NMR** (150 MHz, $CDCl_3$) δ 157.39, 156.20, 155.60, 152.66, 150.25, 138.43, 132.28, 131.70, 130.04, 129.71, 128.77, 123.76, 123.10, 119.02, 118.66, 115.67, 69.87, 44.83, 42.97, 41.12, 35.36, 34.13, 29.60, 24.90 (app-d), 23.61 (app-d), 22.10; **HRMS** (ESI-TOF) Calc'd for $C_{40}H_{52}NO_4S^+$ [M+H] 642.3617, found 642.3617.

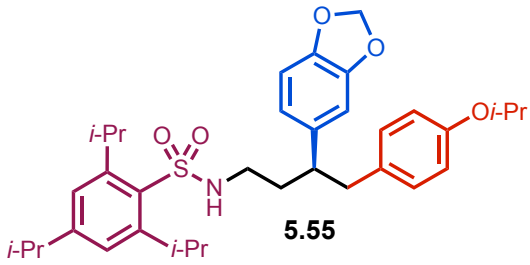


**5.55**

**(*S*)- *N*-(3-(benzo[*d*][1,3]dioxol-5-yl)-4-(4-isopropoxyphenyl)butyl)-2,4,6-triisopropylbenzenesulfonamide (5.55):** Purification using PTLC (20% Acetone in Hexanes) gave the product as a white solid (30.5 mg, 51% yield, 93:7 e.r.). **$^1$H NMR** (600 MHz, $CDCl_3$) δ 7.12 (s, 2H), 6.85 (d, *J* = 8.5 Hz, 2H), 6.71 (d, *J* = 8.5 Hz, 2H), 6.61 (d, *J* = 7.9 Hz, 1H), 6.52 (s, 1H), 6.40 (d, *J* = 7.9 Hz, 1H), 5.90 (d, *J* = 5.4 Hz, 2H), 4.47 (hept, *J* = 6.3 Hz, 1H), 4.12 (t, *J* = 6.4 Hz, 1H), 4.04 (hept, *J* = 6.7 Hz, 2H), 2.89 (p, *J* = 6.9 Hz,

1H), 2.86–2.78 (m, 1H), 2.78–2.64 (m, 4H), 1.85–1.76 (m, 1H), 1.68 (h, $J$ = 7.3 Hz, 1H), 1.31–1.28 (m, 6H), 1.25 (d, $J$ = 6.9 Hz, 6H), 1.19 (dd, $J$ = 6.8, 4.5 Hz, 12H); **$^{13}$C NMR** (150 MHz, $CDCl_3$) δ 156.18, 152.62, 150.22, 147.77, 146.02, 137.42, 132.26, 131.71, 129.99, 123.75, 120.79, 115.66, 108.17, 107.45, 100.83, 69.84, 45.29, 42.96, 41.10, 35.57, 34.13, 29.58, 24.85 (app-d), 23.59, 22.10; **HRMS** (ESI-TOF) Calc'd for $C_{35}H_{48}NO_5S^+$ [M+H] 594.3253, found 594.3258.

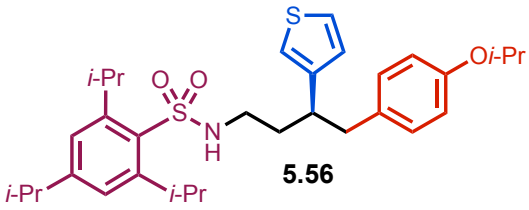


**5.56**

**(*S*)-*N*-(4-(4-isopropoxyphenyl)-3-(thiophen-3-yl)butyl)-2,4,6-triisopropylbenzenesulfonamide (5.56):** Purification using PTLC (20% Acetone in Hexanes) gave the product as a colorless oil (37.1 mg, 67% yield, 93:7 e.r.). **$^1$H NMR** (600 MHz, $CDCl_3$) δ 7.19 (dd, $J$ = 4.9, 2.9 Hz, 1H), 7.13 (s, 2H), 6.83 (d, $J$ = 8.6 Hz, 2H), 6.80 (dd, $J$ = 4.9, 1.3 Hz, 1H), 6.71 (d, $J$ = 8.6 Hz, 2H), 6.65 (dd, $J$ = 2.9, 1.3 Hz, 1H), 4.47 (hept, $J$ = 6.1 Hz, 1H), 4.18 (t, $J$ = 6.4 Hz, 1H), 4.06 (p, $J$ = 6.8 Hz, 2H), 2.95 (dtt, $J$ = 10.5, 7.4, 3.7 Hz, 1H), 2.92–2.84 (m, 2H), 2.77 (ddd, $J$ = 19.2, 14.1, 7.2 Hz, 2H), 2.69 (dd, $J$ = 13.6, 7.4 Hz, 1H), 1.83 (dtd, $J$ = 13.7, 7.7, 4.3 Hz, 1H), 1.75–1.67 (m, 1H), 1.30 (d, $J$ = 6.1 Hz, 6H), 1.25 (dd, $J$ = 6.9, 1.1 Hz, 6H), 1.20 (dd, $J$ = 7.6, 6.8 Hz, 12H); **$^{13}$C NMR** (150 MHz, $CDCl_3$) δ 156.23, 152.65, 150.28, 144.36, 132.25, 131.66, 129.98, 126.28, 125.81, 123.79, 123.76, 120.69, 115.65, 69.86, 42.45, 41.04, 40.63, 35.24, 34.15, 29.59, 24.89 (app-d), 23.63, 22.10 (app-d); **HRMS** (ESI-TOF) Calc'd for $C_{32}H_{46}NO_3S_2^+$ [M+H] 556.2919, found 556.2917.

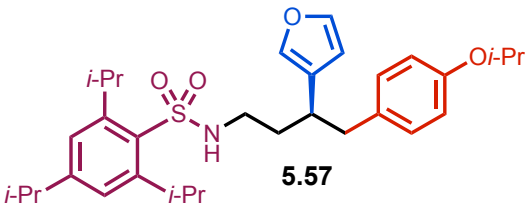


**5.57**

**(*S*)-*N*-(3-(furan-3-yl)-4-(4-isopropoxyphenyl)butyl)-2,4,6-triisopropylbenzenesulfonamide (5.57):** Purification using PTLC (20% Acetone in Hexanes) gave the product as a colorless oil (37.1 mg, 24% yield, 90:10 e.r.). **$^1$H NMR** (400 MHz, $CDCl_3$) δ 7.30 (t, *J* = 1.7 Hz, 1H), 7.14 (s, 2H), 6.90–6.85 (m, 3H), 6.73 (d, *J* = 8.6 Hz, 2H), 6.14 (dd, *J* = 1.9, 0.9 Hz, 1H), 4.48 (hept, *J* = 6.1 Hz, 1H), 4.16 (t, *J* = 6.4 Hz, 1H), 4.07 (hept, *J* = 6.8 Hz, 2H), 2.97–2.61 (m, 6H), 1.84–1.72 (m, 1H), 1.67–1.56 (m, 1H), 1.31 (d, *J* = 6.1 Hz, 6H), 1.25 (d, *J* = 6.9 Hz, 6H), 1.21 (dd, *J* = 6.8, 4.4 Hz, 12H); **$^{13}$C NMR** (150 MHz, $CDCl_3$) δ 156.25, 152.70, 150.28, 143.13, 139.19, 132.22, 131.58, 129.99, 126.79, 123.78, 115.64, 108.95, 69.85, 41.94, 40.95, 35.39, 34.76, 34.15, 29.60, 24.85 (app-d), 23.60, 22.10 (app-d); **HRMS** (ESI-TOF) Calc'd for $C_{32}H_{46}NO_4S^+$ [M+H] 540.3148, found 540.3147.

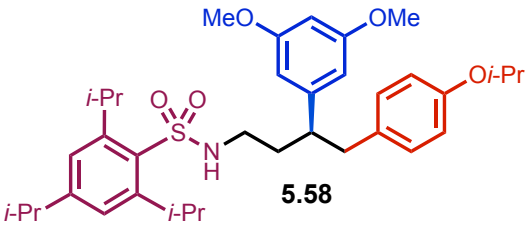


**5.58**

**(*S*)-*N*-(3-(3,5-dimethoxyphenyl)-4-(4-isopropoxyphenyl)butyl)-2,4,6-triisopropylbenzenesulfonamide (5.58):** Purification using PTLC (20% Acetone in Hexanes) gave the product as a colorless oil (25.0 mg, 41% yield, 94:6 e.r.). **$^1$H NMR** (600 MHz, $CDCl_3$) δ 7.11 (s, 2H), 6.90–6.86 (m, 2H), 6.75–6.70 (m, 2H), 6.26 (t, *J* = 2.2 Hz, 1H), 6.20 (d, *J* = 2.3 Hz, 2H), 4.47 (hept, *J* = 6.0 Hz, 1H), 4.15 (t, *J* = 6.4 Hz, 1H), 4.03 (hept, *J* = 6.7 Hz, 2H), 3.72 (s, 6H), 2.92–2.64 (m, 6H), 1.86–1.79 (m, 1H), 1.79–1.70 (m, 1H), 1.30 (d, *J* = 6.1 Hz, 6H), 1.24 (d, *J* = 6.9 Hz, 6H), 1.18 (d, *J* = 6.8 Hz, 12H); **$^{13}$C NMR** (150 MHz, $CDCl_3$) δ 160.80, 156.20, 152.55, 150.16, 146.14, 132.28, 131.76, 130.01,

123.71, 115.68, 105.66, 98.31, 69.85, 55.21, 45.85, 42.68, 41.15, 35.22, 34.10, 29.56, 24.80 (app-d), 23.55 (app-d), 22.08 (app-d); **HRMS** (ESI-TOF) Calc'd for $C_{36}H_{52}NO_5S^+$ [M+H] 610.3566, found 610.3585.

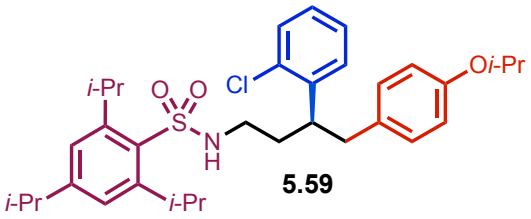


**5.59**

**(*S*)-*N*-(3-(2-chlorophenyl)-4-(4-isopropoxyphenyl)butyl)-2,4,6-triisopropylbenzenesulfonamide** (**5.59**): Purification using PTLC (20% Acetone in Hexanes) gave the product as a colorless oil (23.1 mg, 40% yield, 91:9 e.r.). **$^1$H NMR** (600 MHz, $CDCl_3$) δ 7.27 (dd, *J* = 8.0, 1.2 Hz, 1H), 7.21–7.05 (m, 3H), 7.10 (s, 2H), 6.93–6.88 (m, 2H), 6.74–6.70 (m, 2H), 4.47 (p, *J* = 6.1 Hz, 1H), 4.29–4.17 (m, 1H), 4.03 (hept, *J* = 6.7 Hz, 2H), 3.50–3.41 (m, 1H), 2.92–2.78 (m, 3H), 2.76–2.62 (m, 2H), 1.94–1.86 (m, 1H), 1.86–1.77 (m, 1H), 1.30 (d, *J* = 6.1 Hz, 6H), 1.24 (d, *J* = 6.9 Hz, 6H), 1.18 (d, *J* = 6.8 Hz, 12H); **$^{13}$C NMR** (150 MHz, $CDCl_3$) δ 156.29, 152.57, 150.18, 140.75, 134.19, 132.31, 131.20, 130.00, 129.67, 128.97, 127.55, 127.12, 123.70, 115.72, 69.86, 41.56, 40.89, 34.71, 34.11, 29.58, 24.86, 24.81, 23.58, 22.07; **HRMS** (ESI-TOF) Calc'd for $C_{34}H_{47}ClNO_3S^+$ [M+H] 584.2965, found 584.2973.

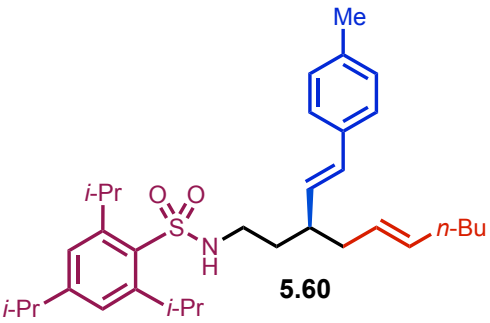


**5.60**

**2,4,6-triisopropyl-*N*-((*S*,*E*)-3-((*E*)-4-methylstyryl)dec-5-en-1-yl)benzenesulfonamide** (**5.60**): Purification using PTLC (10% Acetone in Hexanes) gave the product as a colorless oil (24.2 mg, 45% yield, 72:28 e.r.). **$^1$H NMR** (600 MHz, $CDCl_3$) δ 7.16 (d, *J* = 8.0 Hz, 2H), 7.14 (s, 2H), 7.08 (d,

$J$ = 8.0 Hz, 2H), 6.22 (d, $J$ = 15.8 Hz, 1H), 5.87–5.79 (m, 1H), 5.42–5.33 (m, 1H), 5.33–5.25 (m, 1H), 4.29 (t, $J$ = 6.3 Hz, 1H), 4.13 (hept, $J$ = 6.5 Hz, 2H), 3.06–2.83 (m, 3H), 2.32 (s, 3H), 2.23–2.18 (m, 1H), 2.05 (t, $J$ = 6.7 Hz, 2H), 1.94 (q, $J$ = 6.7 Hz, 2H), 1.68 (dtd, $J$ = 15.3, 7.7, 4.3 Hz, 1H), 1.52–1.43 (m, 1H), 1.29–1.25 (m, 4H), 1.24 (d, $J$ = 6.9 Hz, 6H), 1.23 (d, $J$ = 6.8 Hz, 12H), 0.85 (t, $J$ = 7.1 Hz, 3H); **$^{13}$C NMR** (150 MHz, $CDCl_3$) δ 152.59, 150.24, 136.89, 134.44, 132.86, 132.36, 132.22, 130.50, 129.13, 127.09, 125.96, 123.76, 41.12, 41.08, 38.67, 34.55, 34.10, 32.23, 31.67, 29.62, 24.87, 23.56 (app-d), 22.14, 21.14, 13.91; **HRMS** (ESI-TOF) Calc'd for $C_{34}H_{52}NO_2S^+$ [M+H] 538.3719, found 538.3726.

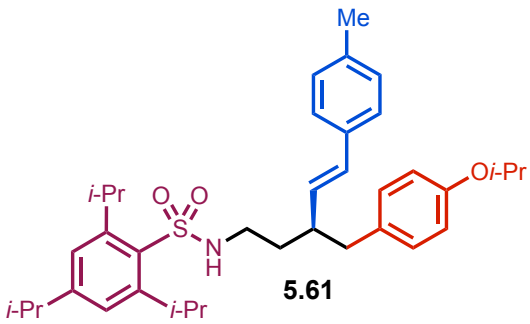


**5.61**

**(*S*)-(*E*)-*N*-(3-(4-isopropoxybenzyl)-5-(*p*-tolyl)pent-4-en-1-yl)-2,4,6-triisopropylbenzenesulfonamide (5.61):** Purification using PTLC (20% Acetone in Hexanes) gave the product as a white solid (51.1 mg, 87% yield, 93:7 e.r.). **$^{1}$H NMR** (600 MHz, $CDCl_3$) δ 7.13 (s, 2H), 7.12 (d, $J$ = 8.2 Hz, 2H), 7.07 (d, $J$ = 7.9 Hz, 2H), 6.97 (d, $J$ = 8.6 Hz, 2H), 6.76 (d, $J$ = 8.6 Hz, 2H), 6.16 (d, $J$ = 15.9 Hz, 1H), 5.85 (dd, $J$ = 15.8, 8.9 Hz, 1H), 4.48 (hept, $J$ = 6.0 Hz, 1H), 4.26 (t, $J$ = 6.2 Hz, 1H), 4.10 (hept, $J$ = 6.6 Hz, 2H), 3.02 (td, $J$ = 13.3, 5.8 Hz, 1H), 2.94 (dt, $J$ = 12.9, 7.0 Hz, 1H), 2.91–2.85 (m, 1H), 2.63 (dd, $J$ = 13.6, 7.1 Hz, 1H), 2.56 (dd, $J$ = 13.7, 6.9 Hz, 1H), 2.48–2.38 (m, 1H), 2.31 (s, 3H), 1.72–1.63 (m, 1H), 1.53–1.46 (m, 1H), 1.31 (dd, $J$ = 6.0, 1.5 Hz, 6H), 1.24 (d, $J$ = 6.9 Hz, 6H), 1.20 (dd, $J$ = 6.7, 4.5 Hz, 12H); **$^{13}$C NMR** (150 MHz, $CDCl_3$) δ 156.20, 152.57, 150.22, 136.92, 134.37, 132.36, 131.85, 131.43, 130.81, 130.19, 129.12, 125.98, 123.75, 115.69, 69.85, 42.75, 41.34, 41.16, 34.38,

34.09, 29.60, 24.85 (app-d), 23.56 (app-d), 22.10, 21.14; **HRMS** (ESI-TOF) Calc'd for $C_{37}H_{52}NO_3S^+$ [M+H] 590.3668, found 590.3676.

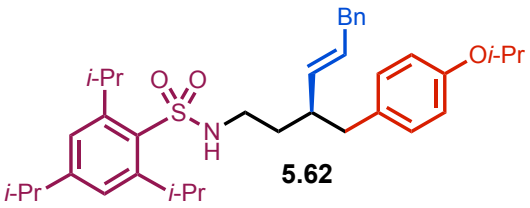


**5.62**

**(*S*)-(*E*)-*N*-(3-(4-isopropoxybenzyl)-6-phenylhex-4-en-1-yl)-2,4,6-triisopropylbenzenesulfonamide (5.62):** Purification using PTLC (20% Acetone in Hexanes) gave the product as a white solid (49 mg, 83% yield, 94:6 e.r.). **$^1$H NMR** (400 MHz, $CDCl_3$) δ 7.24–7.18 (m, 2H), 7.15 (d, *J* = 3.4 Hz, 3H), 6.96 (d, *J* = 6.8 Hz, 2H), 6.92 (d, *J* = 8.5 Hz, 2H), 6.74 (d, *J* = 8.5 Hz, 2H), 5.35 (dt, *J* = 15.3, 6.7 Hz, 1H), 5.16 (ddt, *J* = 15.3, 9.0, 1.4 Hz, 1H), 4.48 (hept, *J* = 6.1 Hz, 1H), 4.30 (t, *J* = 6.3 Hz, 1H), 4.14 (hept, *J* = 6.8 Hz, 2H), 3.22 (d, *J* = 6.6 Hz, 2H), 3.03 (ddt, *J* = 12.0, 8.4, 5.7 Hz, 1H), 2.90 (dq, *J* = 13.6, 7.0 Hz, 2H), 2.56–2.42 (m, 2H), 2.33–2.19 (m, 1H), 1.65–1.54 (m, 1H), 1.40 (dddd, *J* = 13.6, 10.0, 8.1, 5.5 Hz, 1H), 1.32 (d, *J* = 6.1 Hz, 6H), 1.24 (ddd, *J* = 6.8, 3.2, 1.0 Hz, 18H); **$^{13}$C NMR** (150 MHz, $CDCl_3$) δ 156.19, 152.64, 150.30, 140.30, 134.33, 132.39, 131.71, 130.45, 130.19, 128.46, 128.33, 125.91, 123.78, 115.64, 69.85, 42.59, 41.32, 41.25, 38.80, 34.44, 34.14, 29.62, 24.91, 23.62 (app-d), 22.16; **HRMS** (ESI-TOF) Calc'd for $C_{37}H_{52}NO_3S^+$ [M+H] 590.3668, found 590.3668.

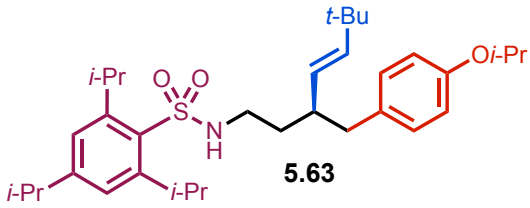


**5.63**

**(*S*)-(*E*)-*N*-(3-(4-isopropoxybenzyl)-6,6-dimethylhept-4-en-1-yl)-2,4,6-triisopropylbenzenesulfonamide (5.63):** Purification using PTLC (20% Ethyl Acetate in Hexanes) gave the product as a white solid (23.0 mg, 41% yield, 92:8 e.r.). **$^1$H NMR** (600 MHz, $CDCl_3$) δ 7.15 (s, 2H), 6.95–6.88 (m,

2H), 6.77–6.73 (m, 2H), 5.22 (d, $J$ = 15.6 Hz, 1H), 4.97 (dd, $J$ = 15.6, 8.9 Hz, 1H), 4.48 (hept, $J$ = 6.0 Hz, 1H), 4.24 (t, $J$ = 6.3 Hz, 2H), 4.13 (hept, $J$ = 6.7 Hz, 2H), 2.99–2.81 (m, 3H), 2.47 (d, $J$ = 7.2 Hz, 2H), 2.19–2.08 (m, 1H), 1.65–1.56 (m, 1H), 1.38–1.33 (m, 1H), 1.30 (dd, $J$ = 6.0, 2.9 Hz, 6H), 1.27–1.19 (m, 18H), 0.86 (s, 9H); **$^{13}$C NMR** (150 MHz, $CDCl_3$) δ 156.07, 152.60, 150.27, 143.15, 132.20, 131.91, 130.24, 127.17, 123.74, 115.66, 69.94, 42.81, 41.65, 41.34, 34.31, 34.13, 32.79, 29.58, 29.56, 24.90 (app-d), 23.59, 22.09 (app-d); **HRMS** (ESI-TOF) Calc'd for $C_{34}H_{54}NO_3S^+$ [M+H] 556.3824, found 556.3835.

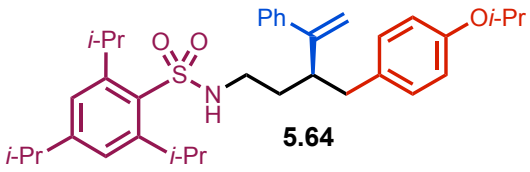


**5.64**

**(*S*)-*N*-(3-(4-isopropoxybenzyl)-4-phenylpent-4-en-1-yl)-2,4,6-triisopropylbenzenesulfonamide (5.64):** Purification using PTLC (20% Acetone in Hexanes) gave the product as a colorless oil (27.5 mg, 48% yield, 94:6 e.r.). **$^1$H NMR** (600 MHz, $CDCl_3$) δ 7.25–7.22 (m, 3H), 7.18–7.15 (m, 2H), 7.14 (s, 2H), 6.96 (d, $J$ = 8.6 Hz, 2H), 6.75 (d, $J$ = 8.6 Hz, 2H), 5.23 (d, $J$ = 0.8 Hz, 1H), 4.98 (d, $J$ = 0.9 Hz, 1H), 4.48 (hept, $J$ = 6.0 Hz, 1H), 4.14 (t, $J$ = 6.3 Hz, 1H), 4.08 (hept, $J$ = 6.7 Hz, 2H), 3.01 (ddt, $J$ = 12.3, 8.8, 6.0 Hz, 1H), 2.93–2.75 (m, 4H), 2.51 (dd, $J$ = 13.4, 7.7 Hz, 1H), 1.71–1.60 (m, 2H), 1.31 (d, $J$ = 6.1 Hz, 6H), 1.25 (d, $J$ = 6.9 Hz, 6H), 1.20 (dd, $J$ = 6.8, 3.3 Hz, 12H); **$^{13}$C NMR** (150 MHz, $CDCl_3$) δ 156.27, 152.63, 151.32, 150.28, 142.46, 132.19, 131.78, 130.06, 128.30, 127.38, 126.63, 123.75, 115.79, 113.45, 69.90, 43.86, 40.92, 40.49, 34.15, 33.43, 29.58, 24.86, 23.61, 22.10; **HRMS** (ESI-TOF) Calc'd for $C_{36}H_{50}NO_3S^+$ [M+H] 576.3511, found 576.3510.

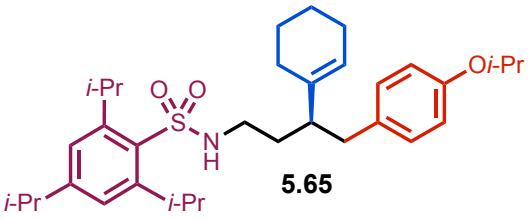


**5.65**

**(*S*)-*N*-(3-(cyclohex-1-en-1-yl)-4-(4-isopropoxyphenyl)butyl)-2,4,6-triisopropylbenzenesulfonamide (5.65):** Purification using PTLC (20% Ethyl Acetate in Hexanes) gave the product as a white solid (15.0 mg, 27% yield, 92:8 e.r.). **$^1$H NMR** (600 MHz, $CDCl_3$) δ 7.15 (s, 2H), 6.93 (d, *J* = 8.6 Hz, 2H), 6.75 (d, *J* = 8.6 Hz, 2H), 5.25–5.20 (m, 1H), 4.49 (hept, *J* = 6.1 Hz, 1H), 4.24 (t, *J* = 6.5 Hz, 1H), 4.12 (hept, *J* = 6.8 Hz, 2H), 2.95–2.84 (m, 2H), 2.84–2.77 (m, 1H), 2.55 (dd, *J* = 13.6, 7.3 Hz, 1H), 2.42 (dd, *J* = 13.7, 7.6 Hz, 1H), 2.16–2.08 (m, 1H), 1.89–1.77 (m, 3H), 1.77–1.68 (m, 1H), 1.55–1.41 (m, 6H), 1.31 (d, *J* = 6.1 Hz, 6H), 1.26–1.22 (m, 18H); **$^{13}$C NMR** (150 MHz, $CDCl_3$) δ 156.05, 152.60, 150.31, 138.17, 132.47, 132.19, 129.88, 123.82, 123.72, 115.66, 69.91, 47.51, 41.45, 39.75, 34.15, 31.90, 29.60, 25.17, 24.90 (app-d), 24.66, 23.61, 23.59, 22.78, 22.59, 22.11 (app-d); **HRMS** (ESI-TOF) Calc'd for $C_{34}H_{52}NO_3S^+$ [M+H] 554.3668, found 554.3665.

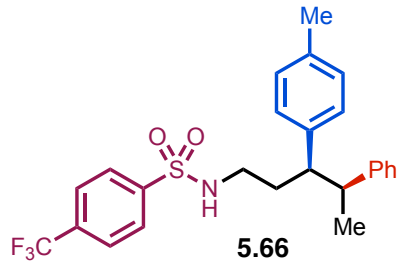


**5.66**

***N*-((3*R*,4*S*)-4-phenyl-3-(*p*-tolyl)pentyl)-4-(trifluoromethyl)benzenesulfonamide (5.66):** Purification using PTLC (20% Ethyl Acetate in Hexanes) gave the product as a colorless oil (22.1 mg, 48% yield, 76:24 e.r.). Spectral data match those previously reported.[9d] **Preparative SFC** The major enantiomer was separated on a Waters Prep SFC 150 AP using a Phenomenex CEL-1 column (5 um, 21x250 mm). The purification was run under isocratic conditions (8% IPA / CO2, 100 mL/min, 1600 psi backpressure) at 35 °C. Fractionation was triggered by mass

spec ($ESI^+$ on a Waters QDa, SIR channel m/z = 462.2). **X-ray** (single-crystal) Colorless crystals of X-ray diffraction quality were obtained by recrystallization of **5.66** in hexanes (CCDC 2201810).[32]

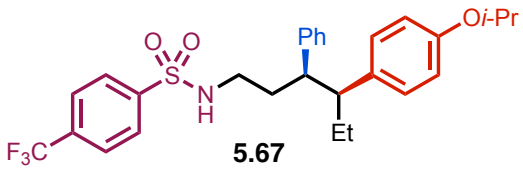


**5.67**

***N*-((3*R*,4*S*)-4-(4-isopropoxyphenyl)-3-phenylhexyl)-4-(trifluoromethyl)benzenesulfonamide (5.67):** Purification using silica gel column chromatography (20% Acetone in Hexanes) gave the product as a colorless oil (26.7 mg, 51% yield, 77:23 e.r.). **$^1$H NMR** (400 MHz, $CDCl_3$) δ 7.74 (d, *J* = 8.2 Hz, 2H), 7.67 (d, *J* = 8.3 Hz, 2H), 7.28 (td, *J* = 7.9, 1.5 Hz, 2H), 7.25–7.19 (m, 1H), 7.07 (d, *J* = 7.8 Hz, 2H), 7.01 (d, *J* = 8.3 Hz, 2H), 6.84 (d, *J* = 8.4 Hz, 2H), 4.54 (hept, *J* = 6.0 Hz, 1H), 4.08 (t, *J* = 6.0 Hz, 1H), 2.61 (dt, *J* = 12.3, 6.0 Hz, 3H), 2.45 (td, *J* = 10.6, 3.8 Hz, 1H), 1.49 (ddt, *J* = 20.4, 13.9, 7.6 Hz, 2H), 1.35 (d, *J* = 6.0 Hz, 6H), 1.33–1.15 (m, 2H), 0.50 (t, *J* = 7.3 Hz, 3H); **$^{13}$C NMR** (150 MHz, $CDCl_3$) δ 156.45, 143.38, 143.10, 135.16, 134.13 (q, $J_{C-F}$ = 32.9 Hz), 129.05, 128.74, 128.00, 127.46, 126.74, 126.12 (q, $J_{C-F}$ = 3.6 Hz), 123.26 (q, *J* = 272.9 Hz), 115.84, 69.87, 53.17, 49.87, 41.78, 34.36, 27.34, 22.16, 12.11; **HRMS** (ESI-TOF) Calc'd for $C_{28}H_{33}F_3NO_3S^+$ [M+H] 520.2133, found 520.2135.

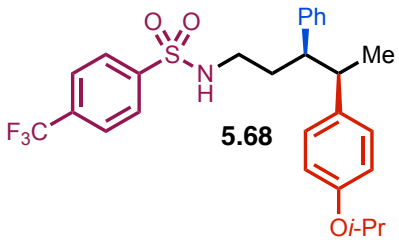


**5.68**

***N*-((3*R*,4*R*)-4-(4-isopropoxyphenyl)-3-phenylhexyl)-4-(trifluoromethyl)benzenesulfonamide (5.68):** Purification using PTLC (20% Acetone in Hexanes) gave the product as a colorless oil (30.4 mg, 60% yield, 73:27

e.r.). **$^1$H NMR** (600 MHz, $CDCl_3$) δ 7.84–7.80 (m, 2H), 7.73–7.68 (m, 2H), 7.15–7.08 (m, 3H), 6.80 (dd, *J* = 7.7, 1.8 Hz, 2H), 6.77 (d, *J* = 8.6 Hz, 2H), 6.66 (d, *J* = 8.7 Hz, 2H), 4.45 (hept, *J* = 6.1 Hz, 1H), 4.25 (t, *J* = 6.1 Hz, 1H), 2.89–2.79 (m, 2H), 2.75–2.65 (m, 2H), 1.99 (dtd, *J* = 13.5, 7.8, 3.7 Hz, 1H), 1.79 (dddd, *J* = 13.8, 12.1, 7.5, 5.0 Hz, 1H), 1.28 (dd, *J* = 6.1, 2.4 Hz, 6H), 1.20 (d, *J* = 7.1 Hz, 3H); **$^{13}$C NMR** (150 MHz, $CDCl_3$) δ 143.48, 141.31, 136.29, 134.24 (q, *J* = 32.5 Hz), 128.79, 128.53, 128.09, 127.49, 126.46, 126.18 (q, *J* = 3.8 Hz), 123.23 (q, *J* = 272.9 Hz), 115.30, 69.83, 50.13, 44.58, 41.94, 32.10, 22.06, 18.49; **$^{19}$F NMR** (376 MHz, $CDCl_3$) δ -65.78; **HRMS** (ESI-TOF) Calc'd for $C_{27}H_{31}F_3NO_3S^+$ [M+H] 506.1977, found 506.1975.

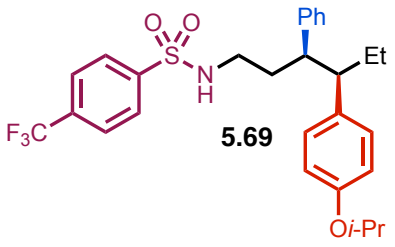


**5.69**

***N*-((3*R*,4*R*)-4-(4-isopropoxyphenyl)-3-phenylhexyl)-4-(trifluoromethyl)benzenesulfonamide (5.69):** Purification using PTLC (20% Acetone in Hexanes) gave the product as a colorless oil (29.8 mg, 54% yield, 75:25 e.r.). **$^1$H NMR** (600 MHz, $CDCl_3$) δ 7.85–7.80 (m, 2H), 7.73–7.68 (m, 2H), 7.12–7.07 (m, 3H), 6.76–6.71 (m, 2H), 6.68–6.63 (m, 4H), 4.45 (hept, *J* = 6.1 Hz, 1H), 4.32 (t, *J* = 6.1 Hz, 1H), 2.86–2.79 (m, 1H), 2.79–2.69 (m, 2H), 2.56 (ddd, *J* = 10.9, 6.7, 4.4 Hz, 1H), 2.01 (dtd, *J* = 13.8, 7.9, 4.0 Hz, 1H), 1.79–1.68 (m, 2H), 1.46 (ddq, *J* = 14.4, 10.7, 7.3 Hz, 1H), 1.28 (dd, *J* = 6.0, 1.9 Hz, 6H), 0.70 (t, *J* = 7.3 Hz, 3H); **$^{13}$C NMR** (150 MHz, $CDCl_3$) δ 156.09, 143.52, 140.98, 134.25 (q, $J_{C-F}$ = 33.0 Hz), 129.79, 128.79, 127.92, 127.50, 126.40, 126.19 (q, $J_{C-F}$ = 3.9 Hz), 123.23 (q, $J_{C-F}$ = 272.9 Hz), 115.15, 69.79, 52.52, 48.70, 41.90, 33.00, 25.63, 22.08, 12.30; **$^{19}$F NMR** (376 MHz, $CDCl_3$) δ -65.77; **HRMS** (ESI-TOF) Calc'd for $C_{28}H_{32}F_3NO_3S^+$ [M+H] 520.2133, found 520.2128.

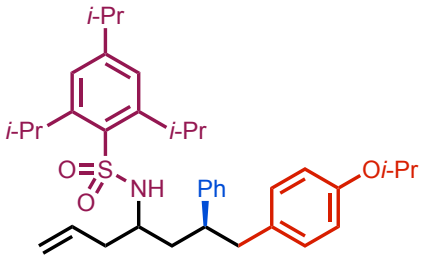


**5.76**

***N*-((6*S*)-7-(4-isopropoxyphenyl)-6-phenylhept-1-en-4-yl)-2,4,6-triisopropylbenzenesulfonamide (5.76):** Purification using PTLC (20% Acetone in Hexanes) gave the product as a colorless oil (11.6 mg, 20% yield, 5:1 d.r.). **$^1$H NMR** (600 MHz, $CDCl_3$) δ 7.14–7.09 (m, 5H), 6.83 (d, *J* = 8.6 Hz, 2H), 6.80–6.74 (m, 2H), 6.70 (d, *J* = 8.6 Hz, 2H), 5.52–5.42 (m, 1H), 5.00 (d, *J* = 10.3 Hz, 1H), 4.92 (dd, *J* = 17.1, 1.7 Hz, 1H), 4.48 (dp, *J* = 12.1, 6.0 Hz, 1H), 4.11 (d, *J* = 9.3 Hz, 1H), 4.02–3.90 (m, 2H), 3.14 (dd, *J* = 11.6, 6.8 Hz, 1H), 2.91 (dt, *J* = 13.8, 6.9 Hz, 1H), 2.72 (dd, *J* = 13.7, 7.2 Hz, 1H), 2.64 (dd, *J* = 13.7, 7.9 Hz, 1H), 2.20–2.14 (m, 1H), 2.11 (dt, *J* = 14.2, 7.8 Hz, 1H), 1.82 (ddd, *J* = 14.2, 11.0, 3.0 Hz, 1H), 1.60–1.55 (m, 1H), 1.31 (d, *J* = 6.0 Hz, 6H), 1.26 (dd, *J* = 7.0, 1.7 Hz, 7H), 1.21 (d, *J* = 6.7 Hz, 6H), 1.12 (d, *J* = 6.7 Hz, 6H); **$^{13}$C NMR** (150 MHz, $CDCl_3$) δ 156.11, 152.53, 149.96, 143.90, 138.23, 133.95, 133.18, 131.80, 130.05, 128.33, 127.80, 126.23, 123.79, 118.78, 118.27, 115.62, 69.85, 51.02, 43.92, 43.23, 40.50, 40.07, 34.17, 29.84, 24.95, 24.86, 23.67, 23.66, 22.11, 22.08, 21.92; **HRMS** (ESI-TOF) Calc'd for $C_{37}H_{52}NO_3S^+$ [M+H] 590.3668, found 590.3661.

## 5.5. REFERENCES

(1) For representative reviews on conjunctive cross-coupling, see: (a) Derosa, J.; Tran, V. T.; van der Puyl, V. A.; Engle, K. M. Carbon−Carbon π-Bonds as Conjunctive Reagents in Cross-Coupling. *Aldrichimica Acta* **2018**, *51*, 21−32. (b) Giri, R.; KC, S. Strategies toward Dicarbofunctionalization of Unactivated Olefins by Combined Heck Carbometalation and Cross-Coupling. *J. Org. Chem.* **2018**, *83*, 3013−3022. (c) Tu, H.-Y.; Zhu, S.; Qing, F.-L.; Chu, L. Recent Advances in Nickel-Catalyzed Three-Component Difunctionalization of Unactivated Alkenes. *Synthesis* **2020**, *52*, 1346–1356. (d) Badir, S. O.; Molander, G. A. Developments in Photoredox/Nickel Dual-Catalyzed 1,2-Difunctionalizations. *Chem* **2020**, *6*, 1327–1339. (e) Derosa, J.; Apolinar, O.; Kang, T.; Tran; V. T.; Engle, K. M. Recent Developments in Nickel-Catalyzed Intermolecular Dicarbofunctionalization of Alkenes. *Chem. Sci.* **2020**, *11*, 4287–4296. (f) Qi, X.; Diao, T. Nickel-Catalyzed Dicarbofunctionalization of Alkenes. *ACS Catal.* **2020**, *10*, 8542–8556.

(2) (a) Tu, H.-Y.; Wang, F.; Huo, L.; Li, Y.; Zhu, S.; Zhao, X.; Li, H.; Qing, F.-L.; Chu, L. Enantioselective Three-Component Fluoroalkylarylation of Unactivated Olefins through Nickel-Catalyzed Cross-Electrophile Coupling. *J. Am. Chem. Soc.* **2020**, *142*, 9604–9611. (b) Chierchia, M.; Xu, P.; Lovinger, G. J.; Morken, J. P. Enantioselective Radical Addition/Cross-Coupling of Organozinc Reagents, Alkyl Iodides, and Alkenyl Boron Reagents *Angew. Chem., Int. Ed.* **2019**, *58*, 14245−14249. (c) Anthony, D.; Lin, Q.; Baudet, J.; Diao, T. Nickel-Catalyzed Asymmetric Reductive Diarylation of Vinylarenes. *Angew. Chem., Int. Ed.* **2019**, *58*, 3198–3202. (d) Wei, X.; Shu, W.; García-Domínguez, A.; Merino, E.; Nevado, C. Asymmetric Ni-Catalyzed Radical Relayed Reductive Coupling. *J. Am. Chem. Soc.* **2020**, *142*, 13515–13522.

(3) Cong, H.; Fu, G. C. Catalytic Enantioselective Cyclization/Cross-Coupling with Alkyl Electrophiles *J. Am. Chem. Soc.* **2014**, *136*, 3788−3791.

(4) (a) Wang, K.; Ding, Z.; Zhou, Z.; Kong, W. Ni-Catalyzed Enantioselective Reductive Diarylation of Activated Alkenes by Domino Cyclization/Cross-Coupling. *J. Am. Chem. Soc.* **2018**, *140*, 12364−12368. (b) Li, Y.; Ding, Z.; Lei, A.; Kong, W. Ni-Catalyzed Enantioselective Reductive Aryl-Alkenylation of Alkenes: Application to the Synthesis of (+)-Physovenine and (+)-Physostigmine. *Org. Chem. Front.* **2019**, *6*, 3305−3309. (c) Ma, T.; Chen, Y.; Li, Y.; Ping, Y.; Kong, W. Nickel-Catalyzed Enantioselective Reductive Aryl Fluoroalkenylation of Alkenes. *ACS Catal.* **2019**, *9*, 9127−9133.

(5) (a) Jin, Y.; Wang, C. Nickel-Catalyzed Asymmetric Reductive Arylalkylation of Unactivated Alkenes. *Angew. Chem., Int. Ed.* **2019**, *58*, 6722−6726. (b) Fan, P.; Lan, Y.; Zhang, C.; Wang, C. Nickel/Photo-Cocatalyzed Asymmetric Acyl-Carbamoylation of Alkenes *J. Am. Chem. Soc.* **2020**, *142*, 2180−2186. (c) Jin, Y.; Yang, H.; Wang, C. Nickel-Catalyzed Asymmetric Reductive Arylbenzylation of Unactivated Alkenes *Org. Lett.* **2020**, *22*, 2724−2729. (d) Lan, Y.; Wang, C. Nickel-Catalyzed Enantioselective Reductive Carbo-Acylation of Alkenes. *Commun. Chem.* **2020**, *3*, 45.

(6) Tian, Z.-X.; Qiao, J.-B.; Xu, G.-L.; Pang, X.; Qi, L.; Ma, W.-Y.; Zhao, Z.-Z.; Duan, J.; Du, Y.-F.; Su, P.; Liu, X.-Y.; Shu, X.-Z. Highly Enantioselective Cross-Electrophile Aryl-Alkenylation of Unactivated Alkenes *J. Am. Chem. Soc.* **2019**, *141*, 7637−7643.

(7) Xi, Y.; Huang, W.; Wang, C.; Ding, H.; Xia, T.; Wu, L.; Fang, K.; Qu, J.; Chen, Y. Catalytic Asymmetric Diarylation of Internal Acyclic Styrenes and Enamides. *J. Am. Chem. Soc.* **2022**, *144*, 8389–8398.

(8) Zhang, Y.; Chen, G.; Zhao, D., Three-Component Vicinal-Diarylation of Alkenes via Direct Transmetalation of Arylboronic Acids. *Chem. Sci.* **2019**, *10*, 7952–7957 (one enantioselective example, 60% yield, 79:21 e.r.).

(9) (a) Derosa, J.; Kleinmans, R.; Tran, V. T.; Karunananda, M. K.; Wisniewski, S. R.; Eastgate, M. D.; Engle, K. M. Nickel-Catalyzed 1,2-Diarylation of Simple Alkenyl Amides. *J*. *Am*. *Chem*. *Soc*. **2018**, *140*, 17878–17883. (b) Derosa, J.; Kang, T.; Tran, V. T.; Wisniewski, S. R.; Karunananda, M. K.; Jankins, T. C.; Xu, K. L; Engle, K. M. Nickel-Catalyzed 1,2-Diarylation of Alkenyl Carboxylates A Gateway to 1,2,3-Trifunctionalized Building Blocks. *Angew*. *Chem*., *Int*. *Ed*. **2020**, *59*, 1201–1205. (c) Tran, V. T.; Li, Z.-Q.; Gallagher, T. J.; Derosa, J.; Liu, P.; Engle, K. M. Integrating Allyl Electrophiles into Nickel-Catalyzed Conjunctive Cross-Coupling. *Angew*. *Chem*., *Int*. *Ed*. **2020**, *59*, 7029–7034. (d) Apolinar, O.; Tran, V. T.; Kim, N.; Schmidt, M. A.; Derosa, J.; Engle, K. M. Sulfonamide Directivity Enables Ni-Catalyzed 1,2-Diarylation of Diverse Alkenyl Amines. *ACS Catal*. **2020**, *10*, 14234–14239. (e) Kleinmans, R.; Apolinar, O.; Derosa, J.; Karunananda, M. K.; Li, Z.-Q.; Tran, V. T.; Wisniewski, S. R.; Engle, K. M. Nickel-Catalyzed 1,2-Diarylation of Alkenyl Ketones: A Comparative Study of Carbonyl-Directed Reaction Systems. *Org*. *Lett*. **2021**, *23*, 5311–5316.

(10) Tran, V. T.; Kim, N.; Rubel, C. Z.; Wu, X.; Kang, T.; Jankins, T. C.; Li, Z.-Q.; Joannou, M. V.; Ayers, S.; Gembicky, M.; Bailey, J.; Sturgell, E. J.; Sanchez, B. B.; Chen, J. S.; Lin, S.; Eastgate, M. D.; Wisniewski, S. R.; Engle, K. M. Structurally Diverse Bench-Stable Nickel(0) Pre-Catalysts: A Practical Toolkit for In Situ Ligation Protocols, *Angew. Chem. Int. Ed.* **2023**, *62*, e202211794.

(11) See Figure 5.S1, and Figure 5.S2 in section 5.4.5.

(12) See Figure 5.S3 in section 5.4.5.

(13) Shohji, N; Kawaji, T.; Okamoto, S. Ti(O-*i*-Pr)$_4$/Me$_3$SiCl/Mg-Mediated Reductive Cleavage of Sulfonamides and Sulfonates to Amines and Alcohols. *Org*. *Lett*. **2011**, *13*, 2626–2629.

(14) For previous computational studies of asymmetric catalysis employing bisoxazoline ligands, see: (a) Lau, S. H.; Borden, M. A.; Steiman, T. J.; Wang, L. S.; Parasram, M.; Doyle, A. G. Ni/Photoredox-Catalyzed Enantioselective Cross-Electrophile Coupling of Styrene Oxides with Aryl Iodides. *J. Am. Chem. Soc.* **2021**, *143*, 15873–15881. (b) Werth, J.; Sigman, M. S. Linear Regression Model Development for Analysis of Asymmetric Copper-Bisoxazoline Catalysis. *ACS Catal.* **2021**, *11*, 3916–3922. (c) Li, Y.; Nie, W.; Chang, Z.; Wang, J.-W.; Lu, X.; Fu, Y. Cobalt-Catalysed Enantioselective C($sp^3$)–C($sp^3$) Coupling. *Nat. Catal.* **2021**, *4*, 901–911.

(15) (a) Pracht, P.; Bohle, F.; Grimme, S. Automated Exploration of the Low-Energy Chemical Space with Fast Quantum Chemical Methods. *Phys. Chem. Chem. Phys.* **2020**, *22*, 7169–7192. (b) Bannwarth, C.; Ehlert, S.; Grimme, S. GFN2-xTB–An Accurate and Broadly Parametrized Self-Consistent Tight-Binding Quantum Chemical Method with Multipole Electrostatics and Density-Dependent Dispersion Contributions. *J. Chem. Theory Comput.* **2019**, *15*, 1652–1671.

(16) (a) Lu, G.; Fang, C.; Xu, T.; Dong, G.; Liu, P. Computational Study of Rh-Catalyzed Carboacylation of Olefins: Ligand-Promoted Rhodacycle Isomerization Enables Regioselective C–C Bond Functionalization of Benzocyclobutenones. *J. Am. Chem. Soc.* **2015**, *137*, 8274–8283. (b) Shao, H.; Chakrabarty, S.; Qi, X.; Takacs, J. M.; Liu, P. Ligand Conformational Flexibility Enables Enantioselective Tertiary C–B Bond Formation in the

Phosphonate-Directed Catalytic Asymmetric Alkene Hydroboration. *J. Am. Chem. Soc.* **2021**, *143*, 4801–4808. (c) Dang, Y.; Qu, S.; Wang, Z.-X.; Wang, X. A Computational Mechanistic Study of an Unprecedented Heck-Type Relay Reaction: Insight into the Origins of Regio- and Enantioselectivities. *J. Am. Chem. Soc.* **2014**, *136*, 986–998.

(17) Koseki, Y.; Kitazawa, K.; Miyake, M.; Kochi, T.; Kakiuchi, F. Ruthenium-Catalyzed Ortho C–H Arylation of Aromatic Nitriles with Arylboronates and Observation of Partial Para Arylation. *J. Org. Chem.* **2017**, *82*, 6503–6510.

(18) Makida, Y.; Marelli, E.; Slawin, A. M. Z.; Nolan, S. P. Nickel-Catalysed Carboxylation of Organoboronates. *Chem. Commun.* **2014**, *50*, 8010–8013.

(19) Hallett, A. J.; O'Brien, T. M.; Carter, E.; Kariuki, B. M.; Murphy, D. M.; Ward, B. D. Copper(II) Complexes of Pyridine-Oxazoline (Pyox) Ligands: Coordination Chemistry, Ligand Stability, and Catalysis. *Inorg. Chim. Acta* **2016**, *441*, 86–94.

(20) Kamata, K.; Agata, I.; Meyers, A. I. An Efficient and Versatile Method for the Synthesis of Optically Active 2-Oxazolines: An Acid-Catalyzed Condensation of Ortho Esters with Amino Alcohols. *J. Org. Chem.* **1998**, *63*, 3113–3116.

(21) Qian, D.; Bera, S.; Hu, X. Chiral Alkyl Amine Synthesis via Catalytic Enantioselective Hydroalkylation of Enecarbamates. *J. Am. Chem. Soc.* **2021**, *143*, 1959–1967.

(22) Huang, C.-Y.; Doyle, A. G. Electron-Deficient Olefin Ligands Enable Generation of Quaternary Carbons by Ni-Catalyzed Cross-Coupling. *J. Am. Chem. Soc.* **2015**, *137*, 5638–5641.

(23) Martinelli, M. J. Asymmetric Diels–Alder Reactions with γ-Functionalized α,β-Unsaturated Chiral *N*-Acyloxazolidinones: Synthesis of (+)-S-145 *J. Org. Chem.* **1990**, *55*, 5065–5073.

(24) Becker, D. P.; Husa, R. K.; Moormann, A. E.; Villamil, C. I.; Flynn, D. L. Enantioselective Synthesis of Dual 5-$HT_4$ 5-$HT_3$ Serotonergic Azanoradamantane SC-52491. *Tetrahedron* **1999**, *55*, 11787–11802.

(25) Thunberg, L.; Allenmark, S. Asymmetric Cycloaddition Routes to Both Enantiomers of *trans*-9,10-Dihydro-9,10-ethanoanthracene-11,12-dicarboxylic acid. *Tetrahedron: Asymmetry* **2003**, *14*, 1317–1322.

(26) Denmark, S. E.; Stavenger, R. A.; Faucher, A.-M.; Edwards, J. P. Cyclopropanation with Diazomethane and Bis(oxazoline)palladium(II) Complexes. *J. Org. Chem.* **1997**, *62*, 3375–3389.

(27) Philipps, A. J.; Uto, Y.; Wipf, P.; Reno, M. J.; Williams, D. R. Synthesis of Functionalized Oxazolines and Oxazoles with DAST and Deoxo-Fluor. *Org. Lett.*, **2000**, *2*, 1165–1168.

(28) Torker, S.; Müller, A.; Chen, P. Building Stereoselectivity into a Chemoselective Ring-Opening Metathesis Polymerization Catalyst for Alternating Copolymerization. *Angew. Chem., Int. Ed.* **2010**, *49*, 3762–3766.

(29) Kim, D. S.; Lee, H. G. Formation of the Tertiary Sulfonamide C($sp^3$)-N Bond Using Alkyl Boronic Ester via Intramolecular and Intermolecular Copper-Catalyzed Oxidative Cross-Coupling. *J. Org. Chem.* **2021**, *86*, 17380–17394.

(30) Carballo, R. M.; Valdomir, G.; Purino, M.; Martín, V. S.; Padrón. J. L. Broadening the Synthetic Scope of the Iron(III)-Catalyzed Aza-Prins Cyclization. *Eur. J. Org. Chem.* **2010**, *2010*, 2304–2313.

(31) Hu, S.; Wang, D.; Liu, J.; Li, X. Rhodium(III)-Catalyzed Oxidative Olefination of *N*-Allyl Sulfonamides. *Org. Biomol. Chem.* **2013**, *11*, 2761–2765.

(32) CCDC 2150217 (**5.10**) and 2201810 (**5.66**) contain the supplementary crystallographic data for this paper. These data can be obtained free of charge from The Cambridge Crystallographic Data Centre via www.ccdc.cam.ac.uk/data_request/cif.

(33) Venkatramani, C. J.; Al-Sayah, M.; Li, G.; Goel, M.; Girotti, J.; Zang, L.; Wigman, L.; Yehl, P.; Chetwyn, N. Simultaneous Achiral-Chiral Analysis of Pharmaceutical Compounds Using Two-Dimensional Reversed Phase Liquid Chromatography-Supercritical Fluid Chromatography. *Talanta* **2016**, *148*, 548–555.

## 5.6. CONTRIBUTIONS

The following individuals directly contributed to the work described in this Chapter: Omar Apolinar, Taeho Kang, Turki M. Alturaifi, Pranali G. Bedekar, Camille Z. Rubel, Joseph Derosa, Brittany B. Sanchez, Quynh Nguyen Wong, Emily J. Sturgell, Jason S. Chen, Steven R. Wisniewski, Prof. Peng Liu, and Prof. Keary M. Engle. O.A., T.K., J.D., and K.M.E conceived the project. Reaction optimization was performed by O.A., T.K., and J.D. Product isolation and characterization was carried out by O.A., and T.K. Ligand synthesis was carried out by O.A., T.K., P.G.B., and C.Z.R. Computational studies were carried out by T.M.A., and P.L. SFC analysis and Preparative SFC was performed by B.B.S., Q.N.W., E.J.S., and J.S.C. The Chapter was adapted with permission from a published manuscript, which was written by O.A., T.K., T.M.A., P.L., and K.M.E., with input from P.G.B., C.Z.R., and S.R.W.

# CHAPTER 6

NEW VISTAS AND CONCLUSION

## 6.1. SUMMARY AND PERSPECTIVE

In Part I of this Thesis, we have presented our investigations revolving around the discovery and development of Ni-catalyzed 1,2-DCF reactions of unactivated alkenes. After a brief introduction to the field of transition-metal-catalyzed 1,2-dicarbofunctionalization of alkenes and the significance of the base metal nickel, we explored the maturation of the field from its origins (Catellani reaction) to its adolescence (non-stereoselective variants) and to its early adulthood, namely asymmetric 1,2-dicarbofunctionalization (Chapter 1). Then, we showcased the competence of ketones as native directing groups, despite their decreased Lewis basicity, for 1,2-DCF of unactivated alkenes (Chapter 3). Next, we presented the discovery and development of sulfonamides as effective native directing groups for 1,2-DCF of unactivated alkenes, and, for the first time, multisubstituted alkenes (Chapter 4). Lastly, following this work, the asymmetric variant was developed which features a stereoselective aryl/alkenylnickel migratory insertion step furnishing two contiguous enantioenriched carbon centers (Chapter 5).

The research investigations discussed in Chapters 3–5 have inspired other creative methods in the Engle lab. We have found other avenues for Ni-catalyzed 1,2-DCF of alkenes and have extended the use of alkenyl sulfonamide substrates to other types of 1,2-difunctionalization methods. We end Part I of the thesis by showcasing these findings.

## 6.2. NICKEL-CATALYZED HYDROARYLATION OF TRISUBSTITUTED ALKENES

During the course of the work discussed in Chapter 4, we found that a homoprenyl trisubstituted alkene is not a competent substrate in the desired 1,2-dicarbofunctionalization. However, unlike other alkenyl substrates that were unreactive, the outcome of the homoprenyl trisubstituted alkene was the generation of hydroarylated side product. This was intriguing since the other type of trisubstituted alkene was operative under the optimized reaction conditions. Progress towards development of this hydroarylation method as a preparatively useful tool is described here.

***Table 6.1.*** Preliminary screening of Ni-catalyzed hydroarylation reaction.

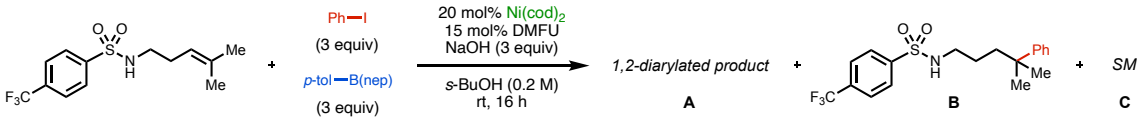


| entry | deviation from standard conditions | %Yield **A** | %Yield **B** | %Yield **C** |
|---|---|---|---|---|
| 1 | none | -- | 34 | 31 |
| 2 | 1.5 equiv of PhI | -- | 22 | 68 |
| 3 | NaOMe | -- | 61 | 31 |
| 4 | NaOEt | -- | 49 | 37 |
| 5 | EtOH | -- | 5 | 88 |
| 6 | *n*-PrOH | -- | 31 | 66 |
| 7 | *n*-BuOH | -- | 26 | 74 |
| 8 | i-BuOH | -- | 36 | 90 |
| 9 | *p*-tolB(OH)$_2$ | -- | 42 | 50 |

The initial result was found when *N*-(4-methylpent-3-en-1-yl)-4-(trifluoromethyl)benzenesulfonamide was reacted with phenyl iodide and *p*-tolylboronic ester coupling partners under Ni(cod)$_2$/DMFU catalysis (Table 6.1). With the aim to synthesize the desired 1,2-diarylated product (**A**), we obtained hydroarylated side product (**B**) in low yield. This occurs presumably via a protodemetalation process whereby the

alkylnickel intermediate is too sterically encumbered by the adjacent *gem*-dimethyl group to engage in transmetalation, leading instead to protonation by the alcoholic solvent. Compared to other hydroarylation methods in the literature, this catalytic transformation is unique in that aryl iodides are the aryl group source. From a practical perspective, aryl iodides are preferred to arylboronic acids due to aryl iodides being cheaper and available in greater structural diversity. Thus, screening was performed with the goal of increasing the yield of the hydroarylated side product. Lowering the amount of aryl iodide electrophile led to a lower yield of the hydroarylated product. Switching the base to NaOMe or NaOEt, increased the amount of hydroarylation. Other alcoholic solvents or switching to a *p*-tolylboronic acid nucleophile neither afforded 1,2-diarylation nor afforded substantial yield improvement of the hydroarylated side product. To our delight, we found that electron deficient olefin (EDO) ligand **5.25** facilitated the reaction, giving hydroarylated product in an excellent yield (Scheme 6.1). Control experiments and further refining of the reaction conditions may allow this reaction to be suitable as an addition to in the nickel catalysis toolkit. It is worth noting that the Engle lab has already disclosed a hydroarylation method of alkenyl sulfonamides with arylboronic acid nucleophiles in 2021 with different conditions compared to those used for 1,2-DCF.[1]

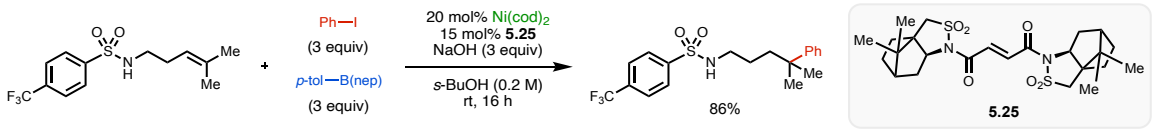


***Scheme 6.1.*** Preliminary screening of Ni-catalyzed hydroarylation reaction.

## 6.3. NICKEL-CATALYZED 1,2-ARYLALKYLATION OF UNACTIVATED ALKENES

We were also interested in developing a Ni-catalyzed 1,2-arylalkylation of unactivated alkenes leveraging the native sulfonamide directing group. The motivation for pursuing sulfonamide-directed 1,2-arylalkylation was to improve upon existing 1,2-arylalkylation methodology, which requires the synthetically restricting AQ bidentate directing auxiliary.[2] Thus, the investigation was carried out by using aryl iodide electrophiles and alkyl zinc reagents under the similar Ni/DMFU catalysis regime. In the event, the desired 1,2-arylalkylation product was observed by NMR and GC-MS, albeit in a low yield. The Heck side product was also obtained but in very low yields. Elevating the reaction temperature and in the absence of DMFU ligand led to a drop in the product yield; however, the amount of Heck side product remained the same. Although the envisioned transformation is indeed observed with alkyl zinc nucleophiles, from an operational perspective, alkyl zinc reagents are air-sensitive and pyrophoric. Switching to alkylboronic ester nucleophiles and achieving desired 1,2-DCF of unactivated alkenes would be a monumental step forward for the field. Recently, it was revealed that certain alkylboronic esters have aided in reductive elimination processes which could be a good avenue to pursue.[3]

***Table 6.2.*** Preliminary screening of Ni-catalyzed 1,2-arylalkylation reaction.

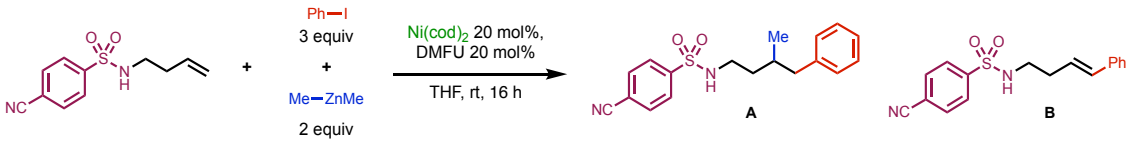


| entry | Deviation | %SM | %Yield A | %Yield B |
|---|---|---|---|---|
| 1 | rt | 20 | 34 | 12 |
| 2 | 50 °C | 16 | 20 | 14 |
| 3 | 50 °C no DMFU | 26 | 22 | 12 |

## 6.4. ADVANCEMENTS IN NICKEL-CATALYZED 1,2-DIFUNCTIONALIZATION OF UNACTIVATED ALKENES USING SULFONAMIDE DIRECTING GROUPS

The Engle lab has taken great interest the alkenyl sulfonamide system since it can be viewed as a second-generation model substrate with generality that rivals the venerable first-generation AQ-based substrate system. Thus, avenues in other sectors of 1,2-difunctionalization beyond 1,2-DCF, namely 1,2-carboamination and 1,2-carbosulfenylation, have been pursued with unactivated alkenyl sulfonamides. In 2021, our group disclosed two examples of Ni-catalyzed 1,2-carboamination of alkenyl sulfonamides.[4] The use of N–O electrophilic reagents with phenylboronic ester nucleophiles were successfully coupled to the alkene substrate affording the desired 1,2-carboaminated product in moderate yields. Thereafter, in 2022, a 1,2-carbosulfenylation protocol of various alkenyl sulfonamides was reported with N–S electrophilic reagents and arylboronic ester nucleophiles under nickel catalysis.[5] This method was also extended to incorporate aliphatic N–S electrophilic reagents and has been reported as a preprint.[3] It is important to note that the aforementioned works likely operate via $Ni^{I}/Ni^{III}$ catalytic cycles instead of the typical $Ni^{0}/Ni^{II}$ pathway. In 2023, another Ni-catalyzed 1,2-

carboamination strategy was disclosed this time via a hypothesized Ni-nitrenoid intermediate with tosyl azides and carbogenic zinc reagents.[6]

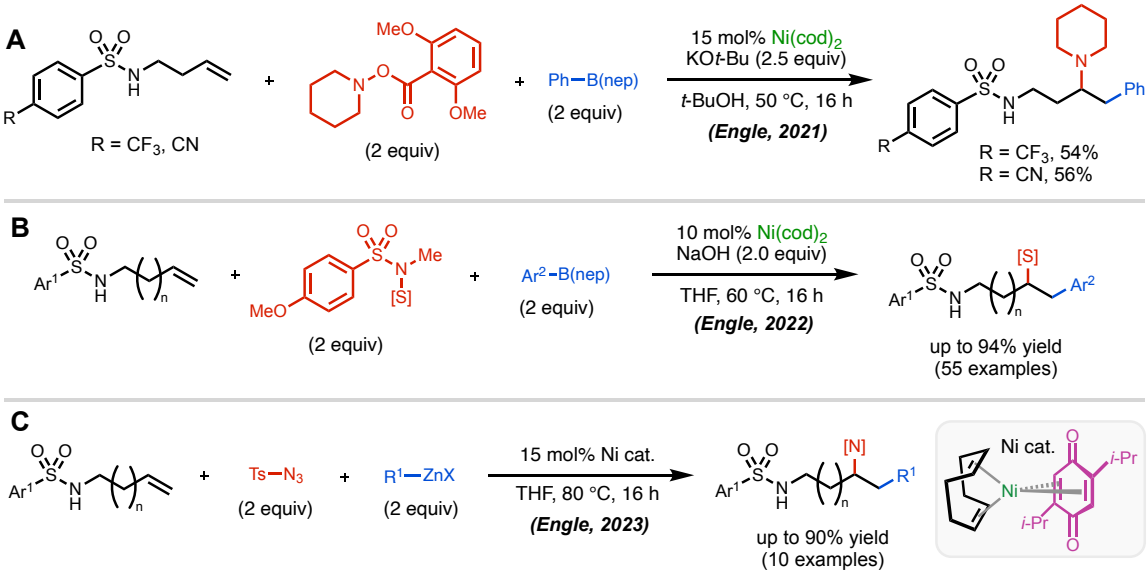


***Scheme 6.2.*** A) Ni-catalyzed 1,2-carboamination of alkenyl sulfonamides with N–O electrophiles. B) Ni-catalyzed 1,2-carbosulfenylation of alkenyl sulfonamides ([S] = aryl sulfenyl group). C) Ni-catalyzed 1,2-carboamination of alkenyl sulfonamides with sulfonyl azide reagents ([N] = sulfonamido group).

## 6.5. CONCLUSION

Since the first report of the discovery of sulfonamides as strong and effective native directing groups, other findings and several reports from the Engle lab have followed over the past 4 years. On top of the developments in 1,2-DCF, the alkenyl sulfonamide platform was found to enable hydroarylation with trisubstituted olefins. Furthermore, 1,2-arylalkylation could be achieved using arylboronic acids and alkyl zinc reagents showcasing that such transformation could be done with a monodentate native directing group. Advancements from the Engle lab in 1,2-carboamination (via migratory insertion and Ni-nitrenoid pathways) and 1,2-carbosulfenylation underscore the enabling nature of alkenyl sulfonamide substrates.

We foresee additional three-component couplings that use commonly encountered, native directing groups especially sulfonamides. Moreover, further enantioselective approaches would be of great impact not only to the 1,2-DCF subfield but 1,2-difunctionalization at large. To this end, more mechanistic investigations via reaction kinetics and characterization of organometallic intermediates would complement recent computational studies and may inspire future chiral ligand design. Progress in chiral ligand design may enable non-directed variants with unactivated alkenes.[7] Taken together these anticipated developments would constitute a toolkit for universal Ni-catalyzed enantioselective 1,2-difunctionalization of diverse alkenes, granting easy accessibility to various molecular structures required for myriad applications.

## 6.6. REFERENCES

(1) Li, Z.-Q.; Apolinar, O.; Deng, R.; Engle, K. M. Directed Markovnikov Hydroarylation and Hydroalkenylation of Alkenes Under Nickel Catalysis. *Chem. Sci.* **2021**, *12*, 11038–11044.

(2) Derosa, J.; Tran, V. T.; Boulous, M. N.; Chen, J. S.; Engle, K. M. Nickel-Catalyzed β,γ-Dicarbofunctionalization of Alkenyl Carbonyl Compounds via Conjunctive Cross-Coupling. *J. Am. Chem. Soc.* **2017**, *139*, 10657–10660.

(3) Li, Z.-Q.; Alturaifi, T. M.; Cao, Y.; Joannou, M. V.; Liu, P.; Engle, K. M. Hemilabile and Redox-Active Quinone Ligands Unlock $sp^3$-Rich Couplings in Nickel-Catalyzed Olefin Carbosulfenylation. *Angew. Chem. Int. Ed.* **2024**, *63*, e202411870.

(4) Kang, T.; Kim, N.; Cheng, P. T.; Zhang, H.; Foo, K.; Engle, K. M. Nickel-Catalyzed 1,2-Carboamination of Alkenyl Alcohols. *J. Am. Chem. Soc.* **2021**, *143*, 13962–13970.

(5) Li, Z.-Q.; Cao, Y.; Kang, T.; Engle, K. M. Electrophilic Sulfur Reagent Design Enables Directed *syn*-Carbosulfenylation of Unactivated Alkenes. *J. Am. Chem. Soc.* **2022**, *144*, 7189–7197.

(6) Hwang, Y.; Wisniewski, S. R.; Engle, K. M. Ligand-Enabled Carboamidation of Unactivated Alkenes through Enhanced Organonickel Electrophilicity. *J. Am. Chem. Soc.* **2023**, *145*, 25293–25303.

(7) Liu, C.-F.; Wang, Z.-C.; Luo, X.; Lu, J.; Ko, C. H. M.; Shi, S.-L.; Koh, M. J. Synthesis of Tri- and Tetrasubstituted Stereocentres by Nickel-Catalysed Enantioselective Olefin Cross-Couplings. *Nat*. *Catal*. **2022**, *5*, 934.

# PART II

SYNTHESIS AND REACTIVITY OF NUCLEOPHILIC CALCIUM FLUORIDE COMPLEXES WITH OXYGENIC LIGAND FRAMEWORKS

# CHAPTER 7

# INTRODUCTION

## 7.1. CONSPECTUS

Organofluorine compounds containing one or more C–F bonds are widely used as medicines, agrochemicals, materials and as $^{18}F$ imaging agents. For the past two centuries, the process to harness fluoride has exploited $H_2SO_4$ thereby generating large amounts of hazardous HF. Although such industrial processes have been standardized, safety concerns are a powerful driver for the development of new approaches.

Recently, we found a mechanochemical method that activates $CaF_2$ using $K_2HPO_4$ to generate Fluoromix in the solid state, which could then be used to directly fluorinate organic molecules, thereby avoiding the use of HF. However, there remains little progress in the fundamental understanding of Ca–F bonds at the molecular level due to the overwhelming stability of $CaF_2$ in terms of its physical properties in the context of wet chemistry. Such investigations are vital to furthering methodologies for enabling nucleophilicity from molecular Ca–F complexes in the solution phase. Thus, endeavors to synthesize well-defined molecular Ca–F complexes and explore their fluoride anion delivery have been undertaken. In Part II of this Thesis, we present our findings from the molecular main group side of this study. In this present chapter, we provide a brief introduction to calcium difluoride in terms of its physical properties and usage (Section 7.2). We then segue into the previously reported inorganic complexes featuring the Ca–F motif (Section 7.3). We conclude by discussing the current state of the art in solubilized well-defined Ca–F complexes (Section 7.4).

In Chapter 8, we discuss the experimental techniques that were used. In Chapter 9, we highlight our findings of well-defined Ca–F complexes stabilized with macrocyclic oxygenic ligand donors and the fluoride anion delivery performance, which was carried

out by the author in conjunction with several collaborators (see Acknowledgments) from August 2022 to September 2024 in the Aldridge laboratory at the University of Oxford. This research investigation has combined solid-state X-ray diffraction studies of Ca–F complexes and reactivity data. Through extensive experimentation into the synthesis of Ca–F complexes, we have determined the limitations of these efforts. This knowledge, in turn, has led to an enhancement in fluoride anion delivery compared to our previous report.[1] We conclude Part II by highlighting ongoing research efforts in the Aldridge and Gouverneur groups that are advancing this theme and offer a perspective on the future evolution of the field (Chapter 10).

## 7.2. CALCIUM DIFLUORIDE

### 7.2.1. Physical Properties

The naturally occurring inorganic salt, calcium difluoride ($CaF_2$), is a fluorite mineral also known as fluorspar. Commercial grade $CaF_2$ is a white solid that has a low concentration in water (0.2 nM at 20 °C) and other common organic solvents owing to its high lattice energy ($\Delta U_L$ = 2640 kJ mol$^{-1}$) and solubility product constant ($K_{SP}$ = 3.9 x 10$^{-11}$).[2] $CaF_2$ is known to be a fluorite, as it crystallizes in a cubic lattice, possessing full saturation about the calcium centers, in which eight fluoride anions are coordinated to each $Ca^{2+}$ cation, and each fluoride is coordinated to four calcium centers (Figure 7.1).[3] Gas phase predications have suggested that $CaF_2$ is bent (~145 °C) and not linear, possibly due to the fluorides interacting with the d-orbital of the calcium center, since this is also observed with strontium and barium.[4]

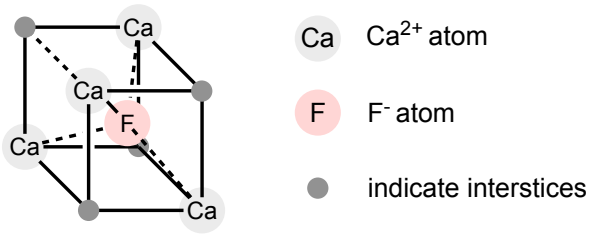


***Figure 7.1.*** Unit cell of $CaF_2$ from the fluoride anion perspective.

### 7.2.2. Applications

At this point in time, $CaF_2$ is the main source from which fluoride is harnessed in the form of hydrofluoric acid (HF). This highly reactive intermediate is used for the fluorination of compounds and materials that are vital to various sectors that affect our daily lives. The typical process by which $CaF_2$ is converted to HF is by treatment of $CaF_2$ with concentrated sulfuric acid ($H_2SO_4$) at 250 °C thereby generating $CaSO_4$ as the byproduct.[5] $CaF_2$ is also used in its own right as a coating for optical components since it has a high chemical stability in terms of temperature (melting point = 1418 °C) and reactivity. Other applications extend to window materials in the infrared (IR) and ultraviolet (UV) wavelength regions (0.18–8.0 μm), since $CaF_2$ is transparent and possesses a low-refractive index ($\eta_D$ = 1.4328).[2]

## 7.3. CLUSTER CALCIUM FLUORIDE COMPLEXES

### 7.3.1 Background and Motive

Work done by Agricola revolving around $CaF_2$ was known since 1529 but it has proved largely inaccessible to modern organometallic techniques owing to the unfavorable physical properties of $CaF_2$ in the context of wet chemistry.[6] Alternative sources that have been reported include the proposed formation of fleeting ArCaF and $MeCa_xF$ species, but

they have not been characterized via X-ray diffraction.[7] It is noteworthy to highlight innovation in producing a porous $CaF_2$ material that has been shown to fluorinate organohalides under catalytic conditions; however, such material is synthesized from commercial soda lime and anhydrous HF.[8] Although solid state structures of $CaF_2$ have been elucidated over the past century,[9] there has been a paucity in solubilized molecular complexes that contain a Ca–F bond and have been characterized by single crystal X-ray diffraction. Finding an entry point for $CaF_2$ in solution state chemistry would open the doors to dive deeper into the fundamental properties of the $CaF_2$ bonding motif. In addition, new insights would allow for more methods to be developed that may give easy access to the fluoride from $CaF_2$ thereby giving an alternative to current processes. Therefore, arriving at such desired solubilized calcium fluoride complexes was attractive, and seminal work reported in the 1990s was quintessential for this niche field to emerge.

### 7.3.2. Calcium Fluoride Complexes of Titanium

The first report of a complex bearing a Ca–F bond is that of Roesky and coworkers in 1995 (Scheme 7.1).[10] Inspired by their report in 1994,[11] in which [Cp*$TiF_3$] was reacted with sodium or magnesium metal generating titanium sodium (or magnesium) fluoride clusters, the Roesky group extended this approach to Ca/Hg alloy. Serving as the first soluble $CaF_2$-containing complex, they were able to synthesize $(Cp^*TiF_2)_6CaF_2(THF)_2$ and obtain pale green single crystals, which were suitable for X-ray diffraction. The X-ray crystal structure obtained showed a molecular species which possessed six $Ti^{III}$ centers with one sole Ca atom in the center of the cluster which was surrounded by eight F atoms (four long Ca–F bonds at 2.53 Å (2.446(2)–2.663(2) Å) and four short Ca–F bonds at 2.26 Å

(2.252(2)–2.272(2) Å) similar to the solid-state structure of $CaF_2$ but distorted. Nonetheless, this report launched the way forward in the pursuit of more solubilized calcium fluoride complexes.

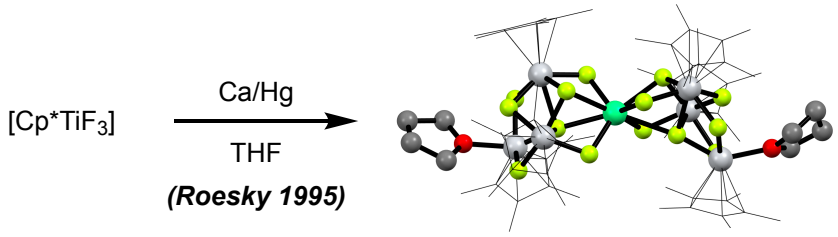


***Scheme 7.1.*** Synthesis of a titanium calcium fluoride cluster from [Cp*$TiF_3$] and Ca/Hg alloy.

Continuing the same theme, the Roesky group targeted an alternative route to arrive at a similar titanium/calcium fluoride complexes, but via the direct use of $CaF_2$. They found that no reaction occurred between [Cp*$TiF_3$] and $CaF_2$, but when $CaF_2$ was made *in situ* by the reaction of $Me_3SnF$ and $CaCl_2$, they were successful in generating $(Cp^*TiF_3)_4CaF_2$ or $((C_5Me_4Et)TiF_3)_4CaF_2$ when either [Cp*$TiF_3$] or [$(C_5Me_4Et)TiF_3$] was employed (Scheme 7.2).[12] The X-ray crystal structure of $(Cp^*TiF_3)_4CaF_2$ revealed the cluster to be similar to the previously reported $(Cp^*TiF_2)_6CaF_2(THF)_2$ in that the Ca atom is also in the center of the cluster and coordinated to eight F atoms. For this complex, the range of the Ca–F bond distances (four at 2.312(2) Å and four at 2.396(2) Å) was more comparable to those of $CaF_2$ (2.366 Å). Interestingly, when the authors attempted to crystallize $(Cp^*TiF_3)_4CaF_2$, they observed that a THF molecule does not tightly coordinate to the calcium center indicating that an open coordination site may be available. A year later, Roesky and coworkers reported the incorporation of hexamethylphosphoramide (HMPA) upon $(Cp^*TiF_3)_4CaF_2$ and $((C_5Me_4Et)TiF_3)_4CaF_2$ forging $(Cp^*TiF_3)_4CaF_2(HMPA)$ and $((C_5Me_4Et)TiF_3)_4CaF_2$ adducts characterized by X-ray crystallography and NMR spectroscopy.[13]

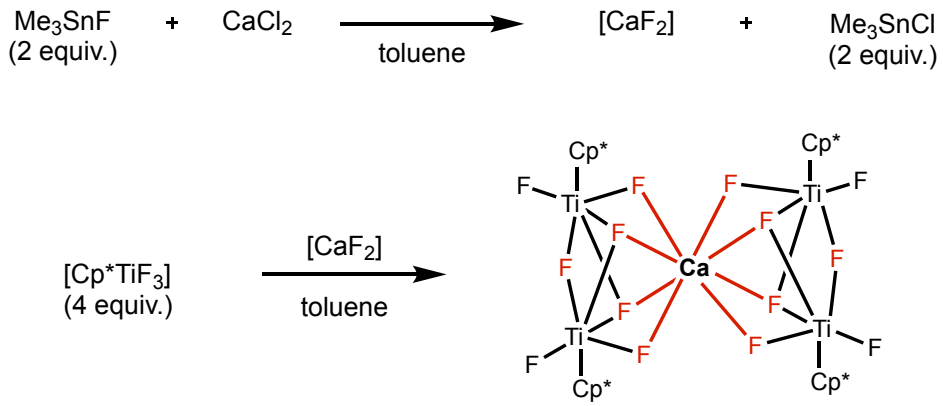


***Scheme 7.2.*** Synthesis of a titanium calcium fluoride cluster from [Cp*$TiF_3$] and *in situ* formed $CaF_2$.

### 7.3.3. Molecular Calcium Fluoride Cages

Although only one report exists, it is still worth highlighting that a molecular calcium fluoride cage has been disclosed in 2010 by Deacon and Junk.[14] Herein they treated calcium metal with $Hg(C_6F_5)_2$ and 2,4,6-trimethylphenol (HOMes) in DME at room temperature, which gave an arrested $CaF_2$ cage formulated as [$Ca_5(\mu_4\text{-}F)(\mu_3\text{-}F)(\mu\text{-}OMes)(OMes)(DME)_4$] (Figure 7.2). X-ray crystallography revealed the cage to bear four calcium atoms at the base of a square pyramid, meaning that the generated 'fluorite' motif is far off from being tetrahedral in geometry. Each of the Ca centers is capped with an aryloxide ligand along with a coordinating DME solvent molecule, and it is important to point out that the four Ca atoms at the square base are heptacoordinate and the apical Ca atom is pentacoordinate. Despite the structural differences from $CaF_2$, the cage possesses Ca–F bond lengths ranging from 2.237(2)–2.371(2) Å which is comparable to those found for $CaF_2$. $^{19}F$ NMR spectroscopy also supports the presence of both ($\mu_3$-F) and ($\mu_4$-F) bridging motifs which give signals at $\delta_F$ = -97.8 ppm and $\delta_F$ = -119.4 ppm.

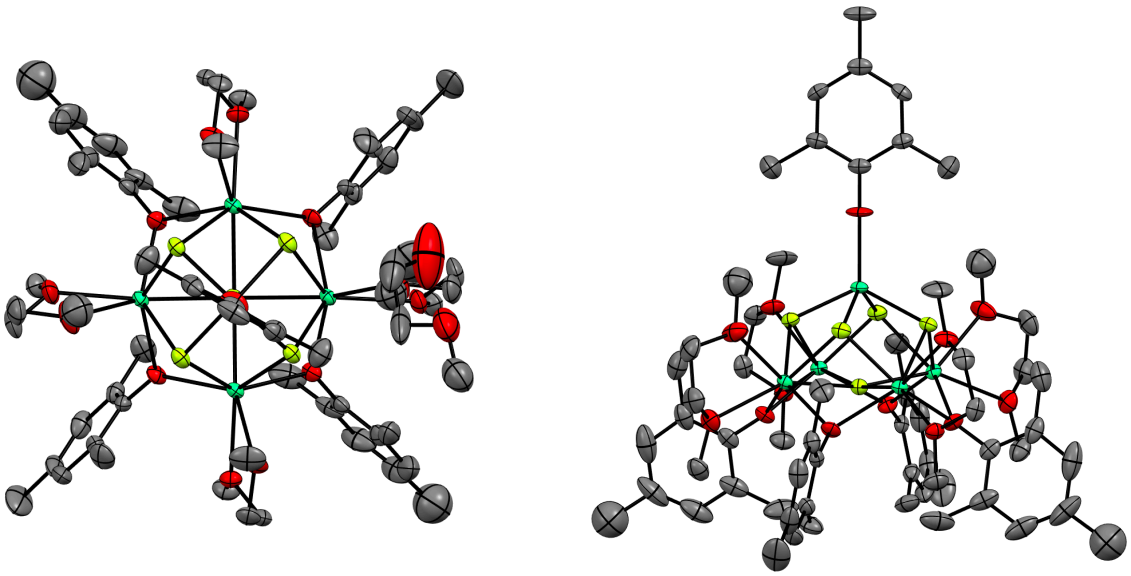

***Figure 7.2.*** X-ray structure of a fluoro(aryloxo)calcium molecular cage.

## 7.4. WELL-DEFINED MOLECULAR CALCIUM FLUORIDE COMPLEXES

### 7.4.1. β-Diketiminate-Supported Calcium Fluoride Complexes

Although the Roesky group trailblazed the first examples of solubilized complexes featuring a $CaF_2$ moiety, all of these initial reports displayed $CaF_2$ encased in an organometallic matrix. In 2007, with an aim of generating a more well-defined molecular equivalent to $CaF_2$, they reported success in synthesizing their target LCaF complex by leveraging the commonly employed β-diketiminate ligand (NacNac = CH{(CMe)(2,6-$i$Pr$_2$C$_6$H$_3$N)}$_2$) (Scheme 7.3).[15] The authors first synthesized the neutral precursor (NacNac)CaN(SiMe$_3$)$_2$(THF), which upon treatment with Me$_3$SnF, generated the desired complex {(NacNac)CaF(THF)}$_2$ ($\delta_F$ = –78 ppm). The solid-state structure revealed the complex to be a dimer, but possessing different structural properties to previous cases. In this case, each calcium center is five-coordinate with a distorted trigonal bypyramidal geometry in which the axial positions are occupied by THF and one of the fluorine atoms. It is also important to note that the complex bears the smallest average Ca–F bond length

at 2.180 Å (2.170(2)–2.189(2) Å) compared to the Ca–F bonds in the titanium complexes and $CaF_2$ (2.366 Å). Finally, the authors examined the potential for the complex to deposit $CaF_2$ as a coating, thereby providing an alternative to the existing methods. They were successful in coating a silicon surface as shown by scanning electron microscope (SEM) analysis.

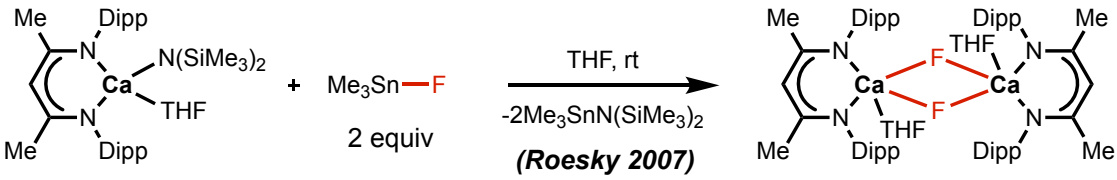


***Scheme 7.3.*** Synthesis of a NacNac-stabilized calcium fluoride complex via $Me_3SnF$.

Contemporaneously, the Barrett and Hill groups discovered an unsual reaction between a β-diketiminate ligand, which possessed a backbone trifluoromethyl group in lieu of the more common methyl group, and calcium iodide (Scheme 7.4).[16] Instead of the expected complexation in which only one NacNac ligand binds to a calcium center, two NacNac ligands bind to calcium each via one nitrogen and two C–F bonds. The X-ray crystal structure of this complex showed the unusual linear binding mode of the NacNac ligand with the calcium center being six-coordinate. The Ca–F bond lengths (2.489(3) Å and 2.468(2) Å) were found to be longer than in $CaF_2$ as expected since the C–F bonds were also found to be longer (1.328(5) Å average of uncoordinated ligand vs. 1.381(5) Å and 1.361(5) Å of the Ca–F complex). The authors also found that the complex decomposed without heating after 5 days, to form a dimeric calcium fluoride complex, as confirmed by single crystal X-ray diffraction and $^{19}F$ NMR spectroscopy ($\delta_F$ = –74.6 ppm vs. $\delta_F$ = –78.0 ppm (Roesky)). Although analogous to the structure that Roesky reported,

it was found not to be isostructural. Notably, the Ca–N bonds were determined to be longer than Roesky's complex, while the Ca–F bonds were found to be very close in length (2.168(2) Å vs 2.180(2) Å). The authors concluded by proposing a mechanism for the C–F bond activation in which the polarized C–F bond of the intermediate calcium fluoride complex was intramolecularly attacked by the uncoordinated imine thereby forging the dimeric calcium fluoride complex. Production of a heterocyclic product which was isolable and identified by NMR spectroscopy and single crystal X-ray diffraction, further supporting the proposed mechanism in action. It is also worth noting that the dehydrohalogenation of halobenzenes could be accomplished by reactions with a molecular calcium hydride complex also stabilized by a NacNac ligand, thereby generating a similar molecular calcium fluoride species to Roesky's example.[17]

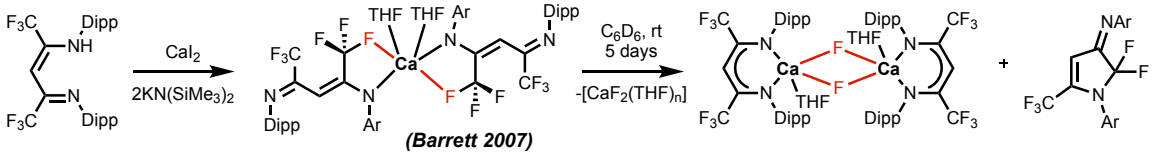


***Scheme 7.4.*** Synthesis of a NacNac-stabilized calcium fluoride complex via C–F bond activation.

### 7.4.2. TACD-Supported Calcium Fluoride Complexes

More than a decade later, the Okuda group found their way into well-defined calcium fluoride complexes, as they were pushing forward their molecular calcium hydride regime. With their platform, they reported a cationic calcium hydride complex which is supported by the NNNN-macrocycle known as 1,4,7,10-tetramethyl-1,4,7,10-tetraazacyclododecane (TACD).[18] Formulated as $[(Me_4TACD)_2Ca_2(\mu\text{-}H)_2(THF)][BAr_4]_2$ ($BAr_4$ = $B(C_6H_3\text{-}3,5\text{-}Me_2)_4$), the cationic complex effects the hydrodefluorination of fluorobenzene as determined by NMR spectroscopy to give a fluoride-containing product

characterized by a resonance at $\delta_F$ = –84 ppm (Scheme 7.5).[19] The structure of the dimeric cationic calcium fluoride product ([(Me$_4$TACD)$_2$Ca$_2$(μ-F)$_2$][BAr$_4$]$_2$) was confirmed by X-ray crystallography, which revealed the calcium center to be seven-coordinate with a pentagonal-bipyramidal geometry. The Ca–F bond lengths (2.1955(15) Å and 2.1876(13) Å) were comparable to those found by Roesky and Barrett showing that such feature may extend to other ligand frameworks.

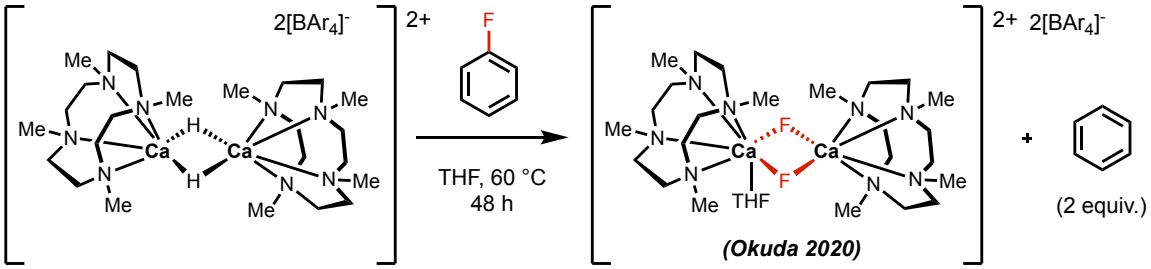


***Scheme 7.5.*** Synthesis of a TACD-stabilized calcium fluoride complex via C–F bond activation.

### 7.4.3. NON-Supported Calcium Fluoride Complexes

In 2024, the Aldridge group reported several calcium fluoride complexes stabilized by the 4,5-bis(2,6-diisopropylanilido)-2,7-di-tertbutyl-9,9-dimethylxanthene (NON) ligand (Scheme 7.6).[1] Knowing the coordinating properties of the NON ligand, anionic system [L$_n$(X)$_2$CaF]$^-$ was targeted in hopes to be leveraged for unprecedented fluoride anion delivery. The authors were successful in furnishing several [M][(NON)CaF$_n$] complexes from the well-established (NON)Ca(THF)$_2$ precursor (**i**) under various fluorination conditions. A dinuclear calcium monofluoride ([K(2.2.2-crypt)][{(NON)Ca(THF)}$_2$(μ$_2$-F)], **ii**, $\delta_F$ = -87.3 ppm) was generated by a KF/2.2.2-cryptand fluorinating combination which was characterized by X-ray diffraction and NMR spectroscopy. The complex has pentacoordinate calcium centers with a single bridging

fluoride such that the Ca–F–Ca motif is bent (166.9(1)°). With the employment of tetramethylammonium fluoride (TMAF), a dinuclear calcium difluoride complex could be generated ($[NMe_4]_2[\{(NON)Ca(\mu_2\text{-}F)\}_2]$, **iii**, $\delta_F$ = -70.4 ppm), which contains pentacoordinate calcium centers and two bridging fluorides as confirmed by the solid-state structure. Interestingly, when **i** was treated with a K(HMDS)/$Me_3SnF$ combination, a potassium bridged dinuclear calcium monofluoride (**iv**) was obtained which had shorter Ca–F bonds than previous calcium fluoride species (2.151(1) Å). Subsequent reaction with 18-crown-6 led to the formation of a mononuclear calcium monofluoride complex capped with a crown-sequestered $K^+$ cation ([K(18-crown-6)]FCa(THF)(NON)], **v**, $\delta_F$ = 90.5 ppm). Single crystal X-ray diffraction analysis showed that the complex had a very short Ca–F bond (2.085(8) Å) and a relatively moderate K···F interaction (2.472(9) Å). Finally, the authors demonstrated that fluoride anion delivery to small molecule electrophiles is plausible with the synthesized calcium fluoride complexes. A structure/activity trend was found whereby the rate of fluoride anion delivery increased as the fluoride anion became more sterically accessible. The mononuclear calcium monofluoride complex possessed the most facile reactivity.

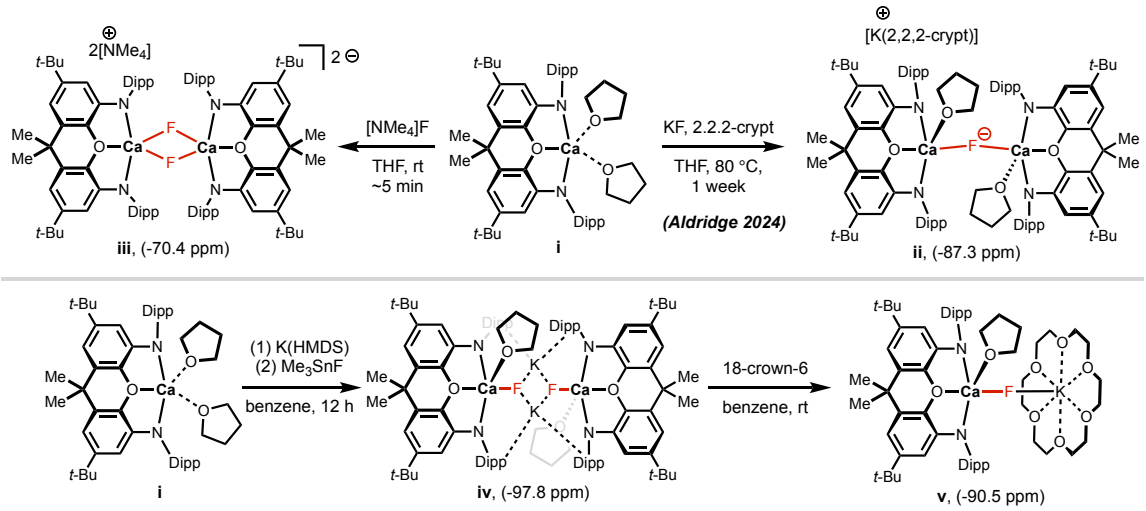


***Scheme 7.6.*** Synthesis of a NON-stabilized calcium fluoride complex via C–F bond activation.

### 7.4.4. Impetus for More Well-Defined Calcium Fluoride Complexes for Fluoride Anion Delivery

Based on these precedents, we foresaw the further potential for innovation with regards to ligand design in supporting well-defined calcium fluoride complexes and ultimately improving reactivity. The O-donor ligand framework was seen as attractive since calcium is known to be more oxophilic and tends to have higher coordination capacities with oxygen atoms. To this end, we sought to exploit a macrocyclic ligand that possesses strong O-donation while at the same time allows for formation of a Ca–F bond and the fluoride anion delivery therefrom. However, such ligands in the literature have not been well developed for this purpose, so innovation in synthesizing a pentadentate ligand would have to be essential to the success of said chemical investigation.

These aims have motivated the research showcased in Part II of this Thesis, and in Chapter 9, we disclose the first calcium fluoride complex supported by a TACN ligand, a complex that shows enhanced fluoride anion delivery capabilities over the NON

counterpart. With O-donor ligands as an entry point in molecular calcium fluoride chemistry, the Aldridge group is well situated to extend this study to other analogs of the TACN ligand or innovate on the ligand design front with other O-donating ligands. To provide the reader a sense of insight into this ongoing research paradigm, preliminary results with TACN analogs and the use of monodentate N-heterocyclic boryloxy (NHBO) ligand are discussed in Chapter 10.

## 7.5. REFERENCES

(1) Struijs, J.J.C.; Ellwanger, M. A.; Crumpton, A. E. Enabling Nucleophilic Reactivity in Molecular Calcium Fluoride Complexes. *Nat. Chem.* **2024**: https://doi.org/10.1038/s41557-024-01524-x.

(2) Ropp, J. C. Group 17 (H, F, Cl, Br, I) Alkaline Earth Compounds. In *Encyclopedia of the Alkaline Earths Compounds*; Elsevier, 2013.

(3) Miessler, G. L.; Tarr D. A. *Inorganic Chemistry* 3rd Ed; Pearson/Prentice Hall, 2004.

(4) (a) Bytheway, I.; Gillespie, R. J.; Tang, T. H.; Bader, R.F. Core Distortions and Geometries of the Difluorides and Dihydrides of Ca, Sr, and Ba. *Inorg. Chem.* **1995**, *34*, 2407–2414. (b) Seijo, L.; Barandiarán, Z.; Huzinaga, S. Ab initio model potential study of the equilibrium geometry of alkaline earth dihalides: $MX_2$ (M=Mg, Ca, Sr, Ba; X=F, Cl, Br, I). *J. Chem. Phys.* **1991**, 94, 3762.

(5) Holleman, A. F.; Wiberg, E. *Inorganic Chemistry*; Academic Press, 2001.

(6) Maple, T. G. *Gmelin Handbuch der Anorganische Chemie*; Springer, 1937.

(7) (a) Mochida, K.; Yamanishi, T.; A New Method for Preparation of Organocalcium Halides by Cocondensation of Calcium Vapor with Solvents. *J. Organomet. Chem.* **1987**,

*332*, 247. (b) Klabunde, K. J.; Whetten, A. Metal Cluster vs. Atom Reactivities. Calcium and Magnesium Vapor with Alkyl Halides and Methane. *J. Am. Chem. Soc.* **1986**, *108*, 6529.

(8) Quan, H.-D.; Tamura, M.; Gao, R.-X.; Sekiya, A. Preparation and Application of Porous Calcium Fluoride—A Novel Fluorinating Reagent and Support of Catalyst. *J. Fluor. Chem.* **2002**, *116*, 65–69.

(9) Miller, G. J. In *Encyclopedia of Inorganic Chemistry*; Wiley, 1994; Vol. 3, pp 1343.

(10) Liu, F.-Q.; Stalke, D.; Roesky, H. W. $(C_5Me_5)TiF_2$–A Versatile Building Block for Generating Large Soluble Dimetallic Aggregates. *Angew. Chem. Int. Ed. Engl.* **1995**, *34*, 1872– 1874.

(11) Liu, F.-Q; Kuhn, A.; Herbst-Irmer, R.; Stalke, D.; Roesky, H. W. Molecular Solids as Ligands in Organometallic Chemistry: $[Cp^*Ti_6Na_7F_{19}\cdot 2.5thf]$ ($Cp^* = C_5Me_5$) and $[Cp^*Ti_4Mg_2F_{12}\cdot 7thf]$, Links Between Ionic Solids and Organometallic Compound. *Angew. Int. Ed. Engl.* **1994**, *33*, 555–556.

(12) Pevec, A.; Demsar, A.; Gramlich, V.; Petricek, S.; Roesky, H. W. Reactions of Molecular $CaF_2$ with $[(C_5Me_5)TiF_3]$ and $[(C_5Me_4Et)TiF_3]$: Symbiosis between Ionic Solids and Organometallic Compounds. *J. Chem. Soc. Dalton Trans.* **1997**, 2215–2216.

(13) Demsar, A.; Pevec, A.; Petriček, S.; Golič, L.; Petrič, A.; Björgvinsson, M.; Roesky, H. W. Calcium Fluoride Incorporated in Soluble Organometallics: Adduct Formation and Solution Dynamics. *J. Chem. Soc. Dalton Trans.* **1998**, 4043–4048.

(14) Deacon, G. B.; Junk, P. C.; Moxey, G. J. Synthesis of Fluoro(aryloxo)alkaline Earth Metal Cages by C–F Bond Activation. *Dalton Trans.* **2010**, *39*, 5620–5622.

(15) Nembenna, S.; Roesky, H. W.; Nagendran, S.; Hofmeister, A.; Magull, J.; Wilbrandt, P.-J.; Hahn, M. A Well-Defined Hydrocarbon-Soluble Calcium Monofluoride, [{LCaF(thf)}$_2$]: The Application of Soluble Calcium Derivatives for Surface Coating *Angew. Chem. Int. Ed.* **2007**, *46*, 2512–2514.

(16) Barrett, A. G. M.; Crimmin, M. R.; Hill, M. S.; Hitchcock, P. B.; Procopiou, P. A. Trifluoromethyl Coordination and C–F Bond Activation at Calcium. *Angew. Chem. Int. Ed.* **2007**, *46*, 6339–6342.

(17) Wilson, A. S. S.; Hill, M. S.; Mahon, M. F.; Dinoi, C.; Maron, L. Dehydrohalogenation of Halobenzenes and C($sp^3$)-X (X = F, OPh) Bond Activation by a Molecular Calcium Hydride. *Tetrahedron* **2021**, *82*, 131931.

(18) (a) Schuhknecht, D.; Lhotzky, C.; Spaniol, T. P.; Maron, L.;Okuda, J. Calcium Hydride Cation $[CaH]^+$ Stabilized by an NNNN-type Macrocyclic Ligand: A Selective Catalyst for Olefin Hydro-genation. *Angew*. *Chem*., *Int*. *Ed*. **2017**, *56*, 12367−12371. (b) Leich, V.; Spaniol, T. P.; Maron, L.; Okuda, J. Molecular Calcium Hydride: Dicalcium Trihydride Cation Stabilized by a Neutral NNNN-Type Macrocyclic Ligand. *Angew*. *Chem*., *Int*. *Ed*. **2016**, *55*, 4794−4797.

(19) Schuhknecht, D.; Spaniol, T. P.; Yang, Y.; Maron, L.; Okuda, J. Reactivity of a Molecular Calcium Hydride Cation ($[CaH]^+$) Supported by an NNNN Macrocycle. *Inorg. Chem.* **2020**, *59*, 9406–9415.

# CHAPTER 8

EXPERIMENTAL TECHNIQUES

## 8.1. INERT ATMOSPHERE TECHNIQUES

Most of the experiments carried out in Part 2 of this thesis dealt with molecules that are sensitive to moisture. Thus, it was crucial that reactions were carried out under inert atmospheric conditions in lieu of the open air. The two common techniques used to work under an inert atmospheric environment are the Schenk line and the glove box.[1,2]

The use of a Schenk line has been found to be convenient for transformations that require air- and moisture-free conditions with low risk of oxidation or hydrolysis if performed properly.[3] To exclude oxygen and moisture the common practice was using an "evacuation and backfill" cycle, of alternating vacuum and argon gas, three times before conducting any manipulation steps. Transfer of solvent or liquids between Schlenk flasks was acheived by the utilizing stainless steel cannulae and purged syringes to exclude air and moisture.

Air- and moisture-sensitive solids were manipulated and stored in a nitrogen-filled glove box. Materials and reaction vessels were placed into the glove box via the antechamber to which the "evacuation and backfill" cycle method was used.

## 8.2. SPECTROSCOPIC AND ANALYTICAL TECHNIQUES

### 8.2.1. NMR Spectroscopy

$^{1}H$, $^{13}C$ and $^{19}F$ NMR spectra were recorded on either 400 MHz Bruker and 500 MHz Brucker Avance III spectrometers at ambient temperature and referenced internally to residual protio-solvent ($^{1}H$) or solvent ($^{13}C$) resonances and are reported relative to tetramethylsilane ($\delta$ = 0 ppm). $^{19}F$ resonances are referenced externally to $CFCl_3$. Chemical shifts are quoted in $\delta$ (ppm) and coupling constants in Hz.

### 8.2.2. Elemental Analysis

Elemental analyses were carried out at London Metropolitan University.

### 8.2.3. X-Ray Crystallography

All crystallographic data were collected on eitheran Oxford Diffraction/Agilent SuperNova diffractometer equipped with a 135 mm Atlas CCD area detector or a Rigaku XtaLAB Synergy-DW VHF instrument equipped with a PhotonJet-R dual wavelength rotating anode and HyPix-Arc 150° detector. Crystals were prepared with Paratone-N or perfluorinated oil, mounted on MiTeGen Micromount loops, and quench-cooled with an Oxford Cryosystems open flow $N_2$ cooling device.[4,5] Data processing involved the software CrysAlisPro: unit cell refinement, SCALE3 ABSPACK inter-frame scaling, merging equivalent reflections, and diffraction pattern processing. Structures were solved using SHELXT and refined with SHELXL in OLEX2.[6-8] Crystallographic studies were carried out by Job Strujis, Liam P. Griffin, Lewis Wales, and Agamemnon E. Crumpton.

## 8.3. REFERENCES

(1) Dodd; R. E.; Robinson, P. L. *Experimental inorganic chemistry: a guide to laboratory practice*, Elsevier Pub. Co, Amsterdam, **1954**.

(2) Errington, R. J. *Advanced practical inorganic and metalorganic chemistry*, Blackie Academic & Professional, London, **1997**.

(3) D. F. Shriver and M. A. Drezdzon, *The manipulation of air-sensitive compounds*, Wiley, New York, 2nd edn., **1986**.

(4) Cosier, J.; Glazer, A. M. A Nitrogen-Gas-Stream Cryostat for General X-ray Diffraction Studies *J. Appl. Cryst.* **1986**, *19*, 105.

(5) CrysAlisPro, Agilent Technologies, Version 1.171.39.46.

(6) Sheldrick, G. M. *SHELXT*–Integrated Space-Group and Crystal-Structure Determination. *Acta Crystallogr., Sect. A: Found. Adv.* **2015**, 71, 3.

(7) Sheldrick, G. M. Crystal Structure Refinement with *SHELXL*. *Acta Crystallogr., Sect. C: Struct. Chem.* **2015**, 71, 3.

(8) Dolomanov, O. V.; Bourhis, L. J.; Gildea, R. J.; Howard, J. A. K.; Puschmann, H. OLEX2: A Complete Structure Solution, Refinement and Analysis Program *J. Appl. Cryst.* **2009**, *42*, 339.

# CHAPTER 9

## ENHANCING NUCLEOPHILIC FLUORIDE ANION DELIVERY FROM TRIAZACYCLONONANE-SUPPORTED MOLECULAR CALCIUM FLUORIDE COMPLEXES

Adapted with permission from:

Apolinar, O.; Struijs, J. C.; Sarkar, D.; Gouverneur, V.; Aldridge, S. *Angew. Chem. Int. Ed.* **2024**, e202414790.

Copyright © 2024 Wiley.

## 9.1. INTRODUCTION

Organofluorine compounds are prevalent in our modern times mainly due to the beneficial properties they pose, which have impacted materials, agrochemicals, and pharmaceutical industries.[1,2] For over two centuries, the industrial process of harnessing fluoride from fluorspar has relied on the use of $H_2SO_4$ to generate large amounts of extremely corrosive and hazardous HF.[3-7] Recently, mechanochemical methods have been found to be an excellent approach for activating $CaF_2$, using $K_2HPO_4$ to generate Fluoromix in the solid state, which could then be directly used to synthesize fluorochemicals.[8] Such a novel process bypasses HF, disrupting the current paradigm of fluoride extraction. Notwithstanding such work, there still remains minor progress in the fundamental understanding of the nucleophilic reactivity of Ca–F bonds at the molecular level due to $CaF_2$ having a high lattice energy ($\Delta U_L$ = 2640 kJ mol$^{-1}$) and poor solubility in organic solvents.[9-13] Such investigations are vital to furthering methodologies for enabling nucleophilic delivery from molecular Ca–F complexes.

The presence of well-defined Ca–F complexes in the chemical literature is surprisingly lacking with few reports ranging from inorganic clusters to main group complexes.[14-24] Although structurally diverse, such cluster complexes display bridging Ca–F bond motifs, and exist in matrices or cages. By contrast, the molecular main group Ca–F complexes independently reported by Roesky and Barrett and Hill demonstrate solubility in hydrocarbon solvents and represented the first well-defined Ca–F complexes (Scheme 9.1). However, both types of complexes lack the exemplification of nucleophilic fluoride anion delivery. Recently, our group disclosed the synthesis and nucleophilicity of well-defined Ca–F-containing complexes featuring the 4,5-bis(2,6-diisopropylanilido)-2,7-di-

tertbutyl-9,9-dimethylxanthene (NON) ligand.[25] The reported complexes were demonstrably unique in being able to deliver fluoride to electrophilic reagents; a structure-activity relationship was found prescribing increased reaction rates as the nuclearity of the Ca–F moiety is reduced and the unit becomes less sterically crowded.

We wanted to pursue a complimentary investigation in synthesizing more stable well-defined Ca–F complexes based on O-donor ligand platforms and enhancing their respective fluoride anion delivery. In contrast to the diamido NON ligand, which is nearly flat and tridentate, we focused on ligand design that would possess three-dimensionality (for more proper geometric stability), O-ligation (as calcium is more oxophilic), and a higher available coordination number (leading to saturation of the Ca center diminishing aggregation). We were interested in the macrocyclic ligand families, notably 1,4,7-triazacyclononane (TACN) derived ligands, because of their capabilities for encapsulating metals such as Al and Ga allowing for subsequent fluorination and enabling applications which extend to $^{18}$F imaging.[26-27] Other closely related macrocyclic ligands such as crowns, azacrowns, or tetraxetan (DOTA), are not optimal in that they do not provide adequate X-type coordination modes, even though they have been shown to encapsulate Ca cations.[28] To our knowledge, there is only one structurally characterized tetranuclear (TACN)Ca complex,[29] and no known (TACN)Ca complexes containing a Ca–F bond. Thus, we disclose herein the synthesis of mononuclear (TACN)Ca and dinuclear (TACN)Ca fluoride complexes and the fluoride delivery capabilities thereof.

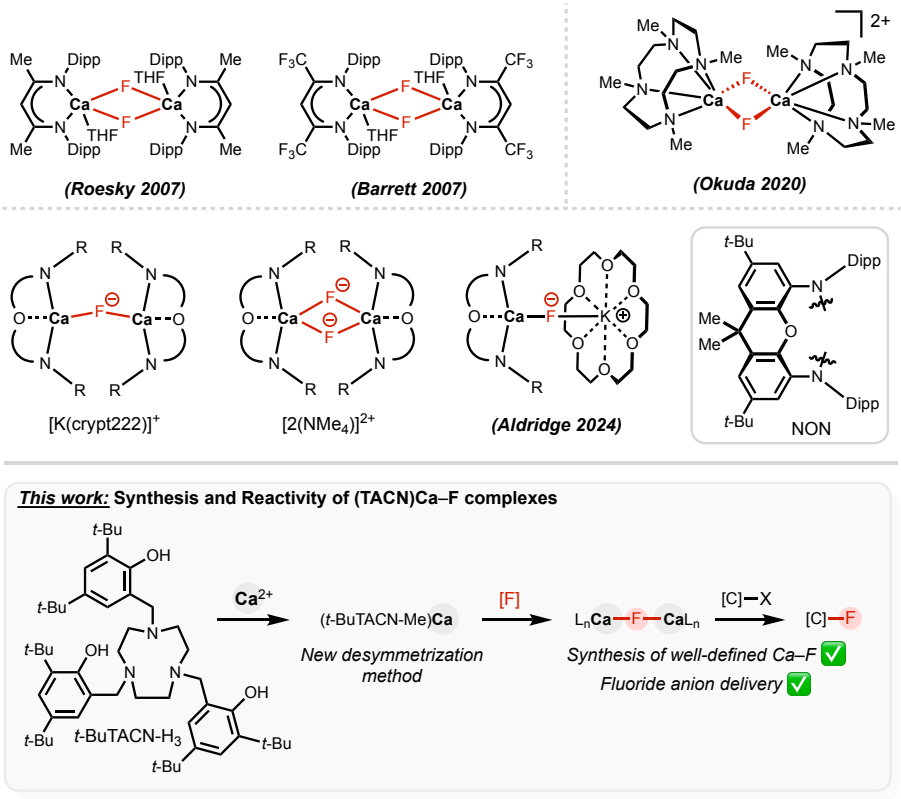


***Scheme 9.1.*** Precedents and synopsis of the disclosed work.

## 9.2. RESULTS AND DISCUSSION

### 9.2.1. Synthesis and Attempted Fluorination of [K(η$^6$-benzene)][(*t*-BuTACN)Ca] and (*t*-BuTACN-H)Ca

We began our investigation by first synthesizing the anionic and neutral (TACN)Ca complexes from a bulky $C_3$-symmetric phenolic TACN ligand and exploring the fluorination affinities of such complexes (Scheme 9.2). We reacted calcium in the form of $Ca(HMDS)_2(THF)_2$ with the bulky $C_3$-symmetric 1,4,7-tris(3,5-tert-butyl-2-hydroxybenzyl)-1,4,7-triazacyclononane (*t*-BuTACN-$H_3$) ligand **9.1** with the aid of an equivalent of KHMDS to furnish the anionic complex [K(η$^6$-benzene)][(*t*-BuTACN)Ca] **9.2** in moderate yield (47%). The six-coordinate anionic (TACN)Ca complex characterized by X-ray crystallography displays non-crystallographic $C_3$-symmetry, and sets of three

very similar Ca–O and Ca–N bonds (ranges: 2.236(1)-2.264(1) and 2.468(1)-2.487(1) Å, respectively). The $[K(\eta^6\text{-benzene})]^+$ counter-ion symmetrically crowns the central $CaO_3$ unit, with three K···O distances in the range 2.735(1)–2.761(1) Å, and a K···centroid separation of 3.257 Å. Additionally, we synthesized neutral complex (*t*-BuTACN-H)Ca **9.3**, albeit in lower yield (34%), by reacting $Ca(HMDS)_2(THF)_2$ and *t*-BuTACN-$H_3$ **9.1** in a 1:1 ratio in the absence of additional base. This neutral six-coordinate complex has a longer Ca–O(H) bond (2.381(9) Å) between the calcium center and the pendent protonated phenolic arm (cf. 2.186(1) and 2.271(1) Å for the other Ca–O distances).

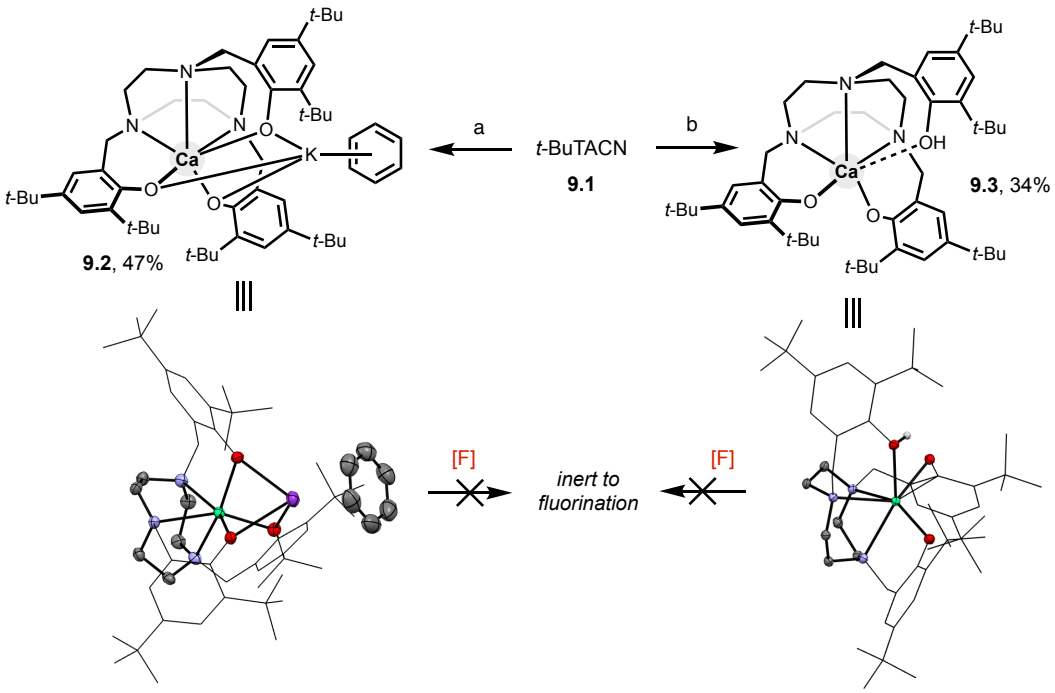


***Scheme 9.2.*** Synthesis and X-ray structures of anionic and neutral calcium complexes **9.2** and **9.3** (ellipsoids set at 50% probability level; H atoms omitted and arenes shown in wireframe format for clarity). (a) $Ca(HMDS)_2(THF)_2$, KHMDS, and $C_6D_6$. (b) $Ca(HMDS)_2(THF)_2$ and $C_6D_6$.

Unfortunately, complexes **9.2** and **9.3** were found to be inert to various fluorination conditions, such as KF/18-crown-6, trimethyltin fluoride ($Me_3SnF$), or tetramethylammonium fluoride (TMAF), each of which has been previously shown to offer

the possibility for introducing fluoride into the coordination sphere of calcium.[18,25] Presumably, the net charge derived from the (anionic) calcium-containing component of **9.2** makes the corresponding dianionic Ca–F-containing species synthetically inaccessible. Thus, little to no trace of a promising $^{19}$F NMR signal is obtained on subjecting anionic complex **9.2** to various fluorination protocols (Scheme 9.3). Alternatively, with [$NMe_4$]F simple cation metathesis is observed.

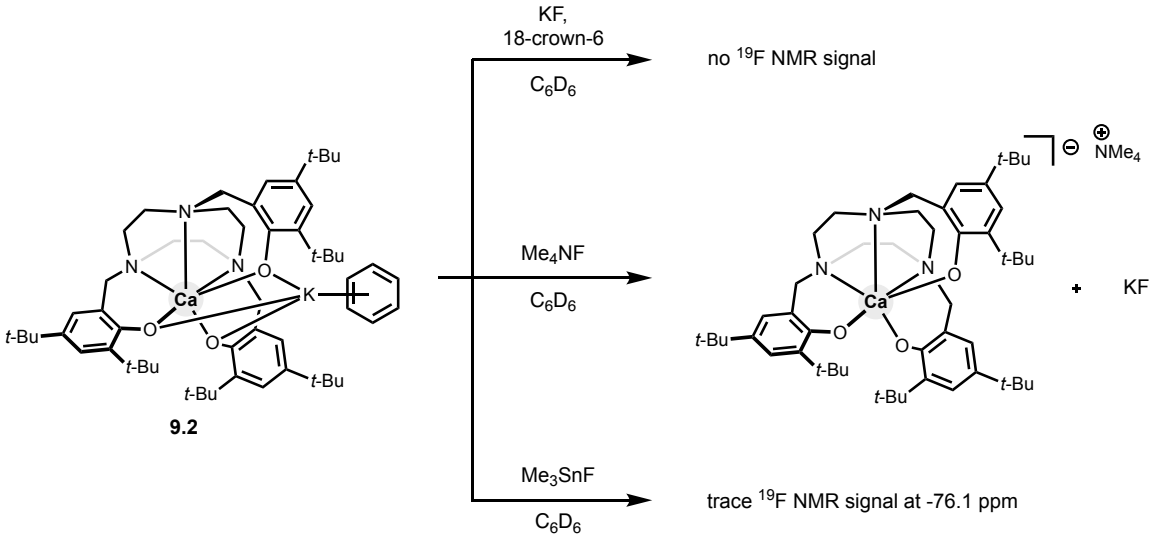


***Scheme 9.3.*** Unsuccessful fluorination attempts of complex **9.2**.

Neutral complex **9.3**, on the other hand, affords HF and protio-ligand in addition to other resultant species (i.e. metathesis or trace $^{19}$F NMR signal) under similar conditions (Scheme 9.4).

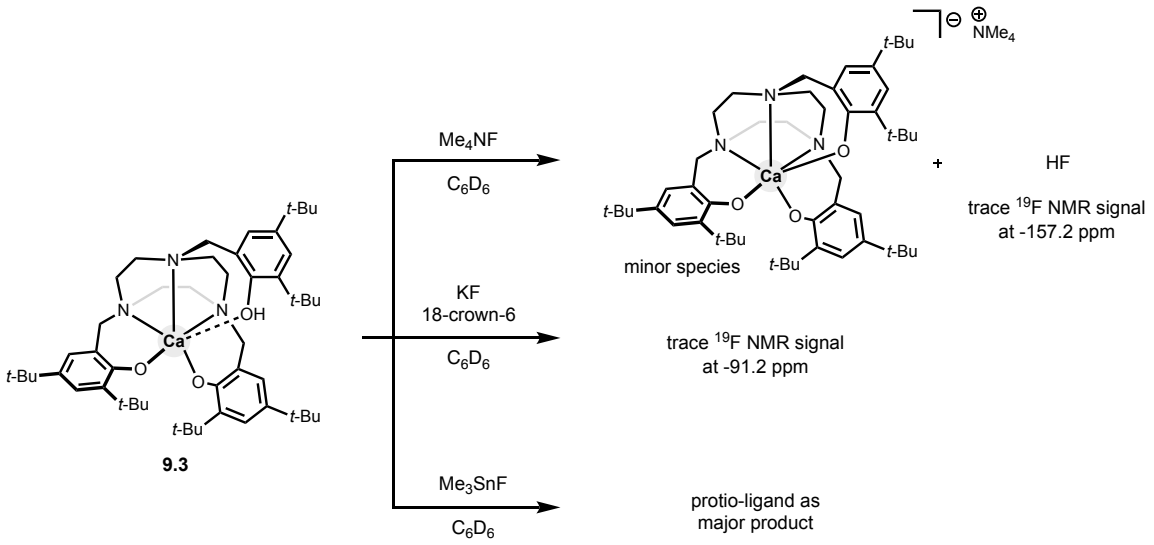


***Scheme 9.4.*** Unsuccessful fluorination attempts of complex **9.3**.

### 9.2.2. Synthesis and Initial Fluorination Attempt of (*t*-BuTACN-Me)Ca

We therefore turned our attention to desymmetrizing the *t*-BuTACN-$H_3$ ligand **9.1**, with the aim of generating an $L_3L'X_2$ framework, and to subsequently introduce calcium and obtain a neutral (TACN)Ca complex without having a pendent acidic Ar–OH bond. Upon examination of the precedented pathways for modulation of the $C_3$-symmetric phenolic TACN ligands, it is apparent that a paucity of methods exists for selective monofunctionalization, probably due to the selectivity issues that are inherent in stochastic methodologies. Instead, synthetic routes have been devised to monoalkylate one of the amine groups of the TACN backbone, thereby yielding pentadentate *N*,*N*,*N*,*O*,*O*-donor ligands.[30] We targeted an alternative approach in which [K($\eta^6$-benzene)][(*t*-BuTACN)Ca] **9.2** was to be desymmetrized by monoalkylation of one of the phenoxide arms. We opted for a methylation strategy given its limited steric requirements and importance in organic synthesis.[31] To our delight, we found that methylation of anionic complex **9.2** with iodomethane affords neutral complex (*t*-BuTACN-Me)Ca **9.4** in excellent yield without

overmethylation of the ligand scaffold (Scheme 9.5). Other functionalization strategies such as benzylation, tosylation and acylation were deemed to not be fruitful avenues. NMR spectroscopy strongly supports the formation of such a complex; the two aromatic signals of $C_3$-symmetric anionic complex **9.2** are split into six aromatic resonances, showcasing the full desymmetrization on formation of complex **9.4**. Furthermore, single crystal X-ray diffraction confirmed the structural integrity of complex **9.4**, with the single methylated O-donor giving rise to the longest Ca–O bond of the series of monomeric complexes **9.2-9.4** (2.407(4) Å, cf. 2.189(4) and 2.214(5) Å for the anionic phenoxide donors).

With neutral complex **9.4** in hand, we then evaluated its affinity for fluoride, given its likely higher fluorophilicity compared to the anionic precursor **9.2**. In our previous report, we generated $[L_n(X)_2CaF]^-$ systems featuring the NON ligand framework using a method first disclosed by Roesky et al., in which a calcium amido complex (either isolated or generated *in situ*) undergoes metathesis with $Me_3SnF$ to generate a Ca–F bond.[18] We envisioned that we could obtain a similar structural motif, but in our case, no reaction is observed when KHMDS alone is reacted with neutral complex **9.4**. The combination of KHMDS/2.2.2-cryptand does lead to the formation of a new species. However, NMR spectroscopy revealed the new complex to have $C_3$-symmetry and single crystal X-ray diffraction showed it to be anionic complex [K(2.2.2-crypt)] [(*t*-BuTACN)Ca] **9.5**, which was formed by aminative demethylation in excellent yield (93%).

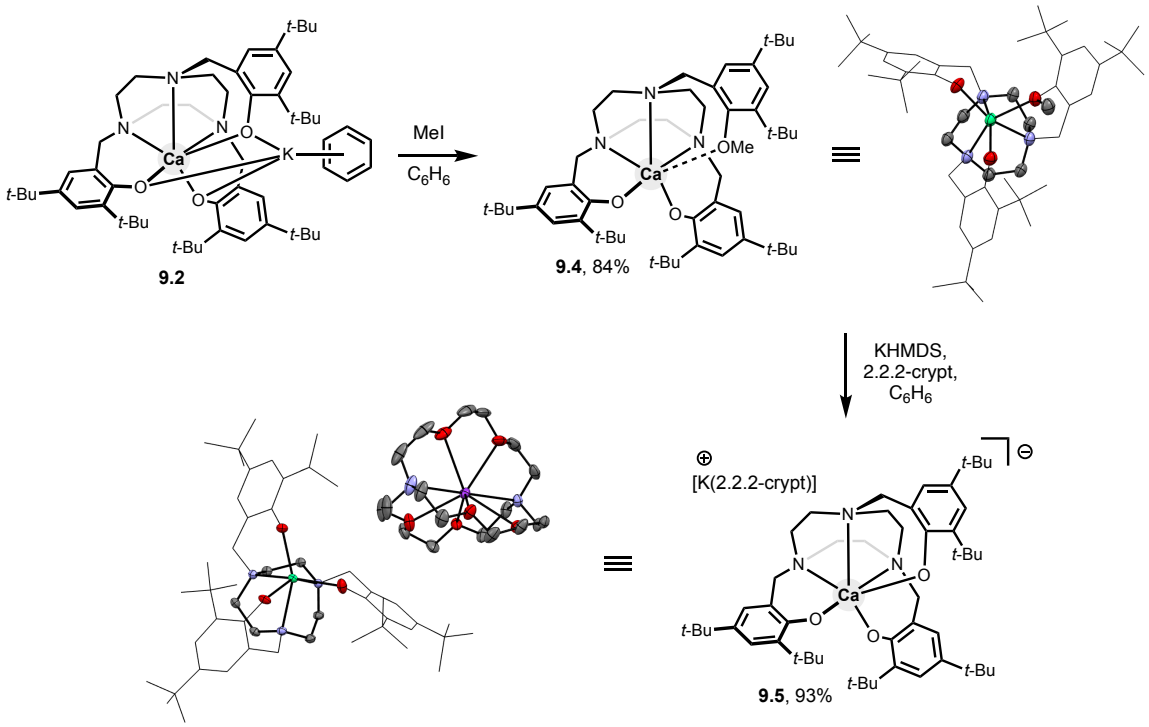


***Scheme 9.5.*** Synthesis and X-ray structures of Ca complexes **9.4** and **9.5** (ellipsoids set at 50% probability level; H atoms omitted and arenes shown in wireframe format for clarity).

### 9.2.3. Synthesis of [M][{(*t*-BuTACN-Me)Ca}$_2$F] Complexes

To avoid the potential for demethylation of neutral complex **9.4**, milder fluorination conditions were used. The KF/2.2.2-cryptand fluorination combination was first used, which was deemed successful upon sonication at 50 °C for 1 h on the basis of a major new fluorine-containing species with a $^{19}$F resonance at -89.4 ppm (THF-$d_8$). This signal is comparable to our previously reported dinuclear calcium monofluoride species [{(NON)Ca(THF)}$_2$(μ-F)]$^-$ (-87.3 ppm in THF-$d_8$; Scheme 9.1).[25] Single crystals were obtained by layering a concentrated solution of the new species in benzene with hexane and X-ray crystallography confirmed the fluorine-containing species to be dinuclear anionic calcium monofluoride complex [K(2.2.2-crypt)][{(t-BuTACN)Ca}$_2$F] **9.6** which was obtained in a low yield (31%) (Scheme 9.6). The solid state structure of **9.6** has a close-

to-linear Ca–F–Ca unit (165.87(4)°, Table 9.1) and statistically equal Ca–F bond lengths (2.176(9), 2.192(8) Å); these metrics are also very similar to those measured for [K(2.2.2-crypt)][{(NON)Ca(THF)}$_2$(μ-F)] (166.9(1)° and 2.182(1)/2.187(1) Å).

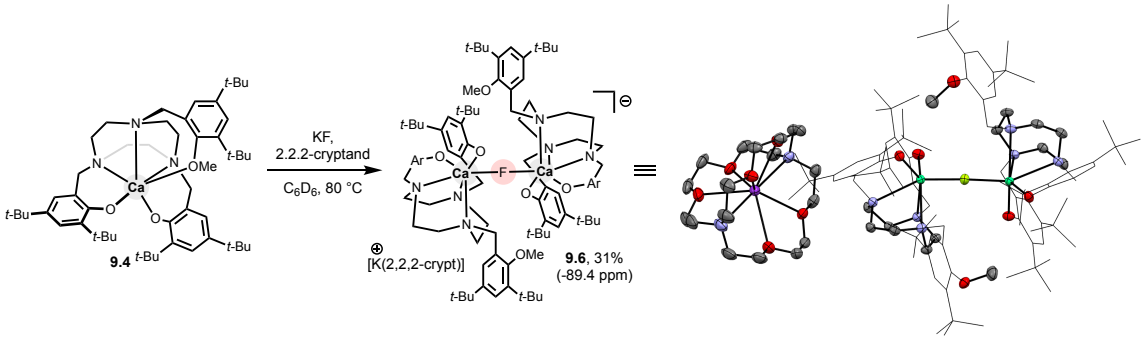


***Scheme 9.6.*** Synthesis and X-ray structures of Ca–F–Ca complex **9.6** (ellipsoids set at 50% probability level; H atoms omitted and arenes shown in wireframe format for clarity).

With a view to improving the yield of this or related calcium fluoride complexes, neutral complex **9.4** was also treated in two separate reactions with KF/18-crown-6 and TMAF (Scheme 9.7). These conditions gave structurally similar dinuclear anionic calcium monofluoride complexes [K(18-crown-6)][{(*t*-BuTACN-Me)Ca}$_2$F] **9.7** and [TMAF][{(t-BuTACN)Ca}$_2$F] **9.8** which were obtained in low (**9.7**, 23%) to moderate yields (**9.8**, 63%) respectively.

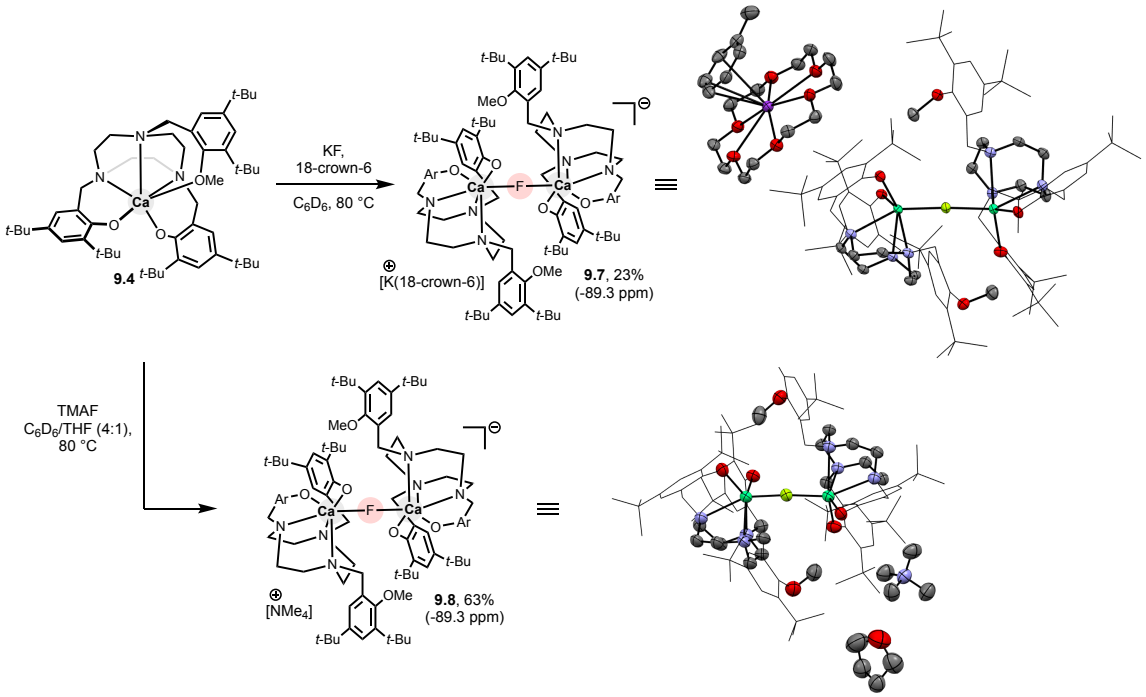


***Scheme 9.7.*** Synthesis and X-ray structures of Ca–F–Ca complex **9.6** (ellipsoids set at 50% probability level; H atoms omitted and arenes shown in wireframe format for clarity).

Both complexes possess identical $^{19}F$ resonances in THF-$d_8$ ($\delta_F$ = -89.3 ppm), and single crystals of both complexes suitable for X-ray crystallography could be grown from toluene or toluene/THF. The solid state structure of **9.8** resembles closely that of **9.6** (∠Ca–F–Ca = 160.78(1)° *d*(Ca–F) = 2.182(2), 2.174(2) Å), whereas the X-ray structure of complex **9.7** features a more linear Ca–F–Ca bonding motif (176.55(7)°) and longer Ca–F bonds (2.211(1), 2.213(1) Å), plausibly due to a relatively shallow potential energy surface for deformation of the Ca–F–Ca moiety.

***Table 9.1.*** Tabulated Ca–F–Ca bond angles and Ca–F bond lengths of complexes **9.6-9.8**.

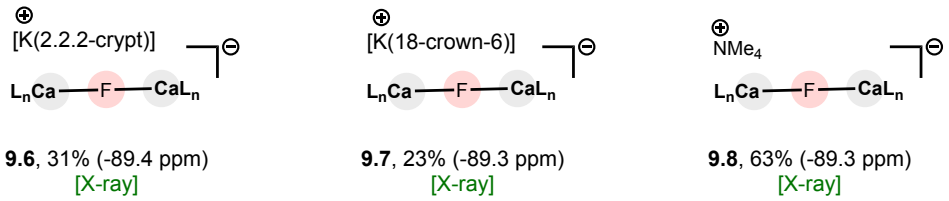


**9.6**, 31% (-89.4 ppm) [X-ray] | **9.7**, 23% (-89.3 ppm) [X-ray] | **9.8**, 63% (-89.3 ppm) [X-ray]

| complex | ∠Ca(1)–F–Ca(2) Bond Angle | Ca–F Bond Lengths (Å) |
|---|---|---|
| **9.6** | 165.87(4)° | 2.176(9), 2.192(8) |
| **9.7** | 176.55(7)° | 2.211(1), 2.213(1) |
| **9.8** | 160.78(1)° | 2.182(2), 2.174(2) |

### 9.2.4. Synthesis of [NMe$_4$][{(*t*-BuTACN-Me)CaF}$_2$]

With the clear observation that, under the one pot method, the formation of bridged complexes **9.6-9.8** with a 2:1 Ca:F ratio are favored, it appears that a second equivalent of neutral complex **9.4** will always act as a 'capping' entity across all fluorination conditions. We attribute this to the low local concentration of fluoride anion due to the poor solubility of KF and TMAF in benzene in comparison to that of neutral complex **9.4**. Nonetheless, we thought that it was plausible for TMAF to display a higher local fluoride anion concentration, via the use of a more polar solvent such as THF (accompanied with sonication). Therefore, a dilute solution of complex **9.4** in THF was added dropwise to a pre-sonicated and rapidly stirred THF-solution of TMAF (0.15 M) (Scheme 9.8). A new fluorine-containing species **9.9** was observed giving a $^{19}$F resonance at -82 ppm which differs spectroscopically from the dinuclear calcium monofluoride complexes **9.6-9.8** (-89.4 ppm for **9.6**, and -89.3 ppm for **9.7** & **9.8**). The downfield shift observed in the $^{19}$F NMR spectrum (compared to those measured for compounds **9.6-9.8** vs. **9.9**) is of the same sense as that determined between single and doubly fluoride-bridged NON-ligated calcium

fluoride complexes (e.g. $\delta_F$ = -87.3 and -70.4 for [K(2.2.2-crypt)][{(NON)Ca(THF)}$_2$(μ-F)] vs. [TMA]$_2$[{(NON)Ca}$_2$ (μ-F)$_2$], respectively; Scheme 9.1). The resulting complex, formulated as [TMA]$_2$[{(*t*-BuTACN-Me)Ca}$_2$(μ-F)$_2$] **9.9** was isolated in 52% yield, but at this point in time no single crystals suitable for X-ray diffraction have been obtained to fully elucidate its solid state structure. Thus, to gain more insight in terms of the structure *in situ*, we resorted to spectroscopic techniques. The $^1$H NMR spectrum of **9.9**, in line with the measured $^{19}$F chemical shift, is consistent with the presence of a 1:1 Ca:F ratio, on the basis of an equimolar ratio of the intensities of the [NMe$_4$]$^+$ and *t*-BuTACN resonances. Additionally, we performed diffusion-ordered spectroscopy (DOSY) $^{19}$F NMR measurements on both complexes **9.7** and **9.9** in THF-$d_8$ (Figures 9.S1 and 9.S2). The hydrodynamic radius obtained for complex **9.7** (10.7 Å) is comparable to that of complex **9.9** (9.3 Å) suggesting that the Ca–F complex **9.9** is dimeric at least in the solution state. Other isomeric forms of complex **9.9** are plausible and have not been ruled out, but the structure drawn closely resembles our previously reported dimeric Ca–F complex.[25,32]

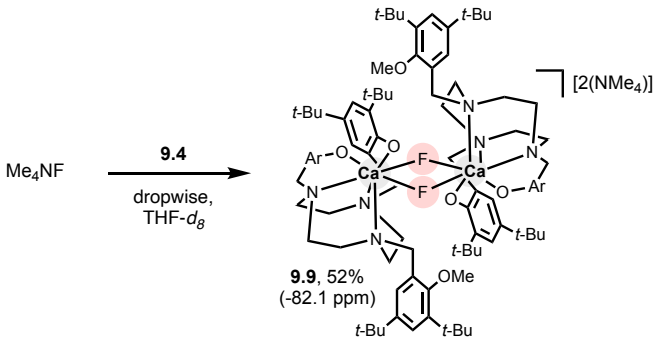


***Scheme 9.8.*** Synthesis of dinuclear calcium difluoride complex **9.9**.

### 9.2.5. Reactivity of of [K(2.2.2-crypt)][{(*t*-BuTACN-Me)Ca}$_2$F]

We were interested in evaluating the fluoride anion delivery performance of the newly synthesized [M][{(t-BuTACN)Ca}$_2$F] structural motif under mild conditions (room temperature, benzene solution). The study was carried out by using [K(2.2.2-crypt)][{(t-BuTACN)Ca}$_2$F] complex **9.6** because of its ease of synthesis and isolation compared to complexes **9.7** and **9.8**. Furthermore, we wanted to compare the capabilities of **9.6** in nucleophilic fluoride anion delivery to recently reported NON-bound systems. Thus, reacting complex **9.6** with 1-adamantanecarbonyl chloride in $C_6D_6$ at room temperature gave 1-adamantanecarbonyl fluoride ($\delta_F$ = 23.2 ppm, $^{19}$F NMR) in moderate yield (58%), representing a similar result as achieved with [K(2.2.2-crypt)][{(NON)Ca(THF)}$_2$(μ-F)] (Scheme 9.9). Triphenylcarbenium tetrakis(pentafluorophenyl)borate ([$Ph_3C$][$B(C_6F_5)_4$]) was also reacted with complex **9.6** in $C_6D_6$ at room temperature, which furnished the desired product bearing a quaternary C–F center ($\delta_F$ = -125.6 ppm, $^{19}$F NMR) also in moderate yield (54%). We were also curious to see if the reactivity could be expanded to construct other fluorine-heteroatom bonds, and so silicon- and sulfur-based electrophiles were also investigated. We treated complex **9.6** with chlorotriphenylsilane in $C_6D_6$ at room temperature which gave fluorotriphenylsilane ($\delta_F$ = -168.9 ppm, $^{19}$F NMR) in an excellent yield (92%), in contrast to [K(2.2.2-crypt)][{(NON)Ca(THF)}$_2$(μ-F)], which plateaus at a more moderate yield (62%) after ~15 min. Finally, we reacted tosyl chloride with complex **9.6** in $C_6D_6$ at room temperature to generate the corresponding tosyl fluoride ($\delta_F$ = 66.6 ppm, $^{19}$F NMR) in good/excellent yield after 30 min/72 h (68%/93%). The similar reaction with [K(2.2.2-crypt)][{(NON)Ca(THF)}$_2$(μ-F)] gives only 17% conversion to tosyl fluoride after 15 min, a figure which does not improve even after 24 h. It is important to

note that the latter example suffers in terms of product yield with the (NON)Ca system because of the side reactivity involving attack of the nitrogenic arms of the NON ligand. In the present case, the TACN ligand provides more support towards Ca center with its oxygenic arms suppressing side reactivity and thus enhancing fluoride anion delivery.

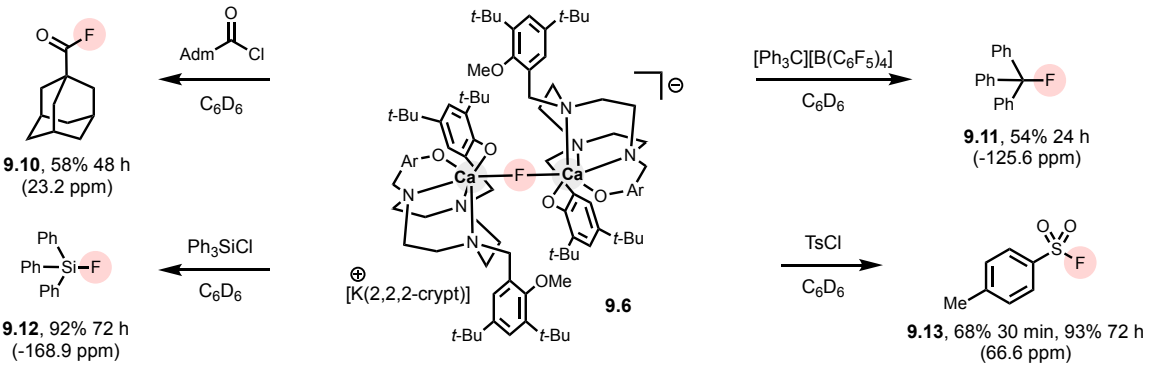


***Scheme 9.9***. Reactivity of Ca–F complex **9.6** with organic electrophiles. Percentage yield by $^{19}$F NMR using fluorobenzene as internal standard.

Consistently, all of the reactions of **9.6** carried out with electrophiles containing a chloride leaving group produce the same Ca-containing product, which we identify as [{(*t*-BuTACN-Me)Ca}$_2$(μ-Cl)]$^-$. The $^1$H NMR spectra obtained *in situ* for all of the aforementioned reactions align with that measured for a sample of [K(2.2.2-crypt)][{(*t*-BuTACN-Me)Ca}$_2$(μ-Cl)], which was independently synthesized by reacting complex **9.4** with excess KCl and 2.2.2-cryptand at 80 °C (Scheme 9.10).

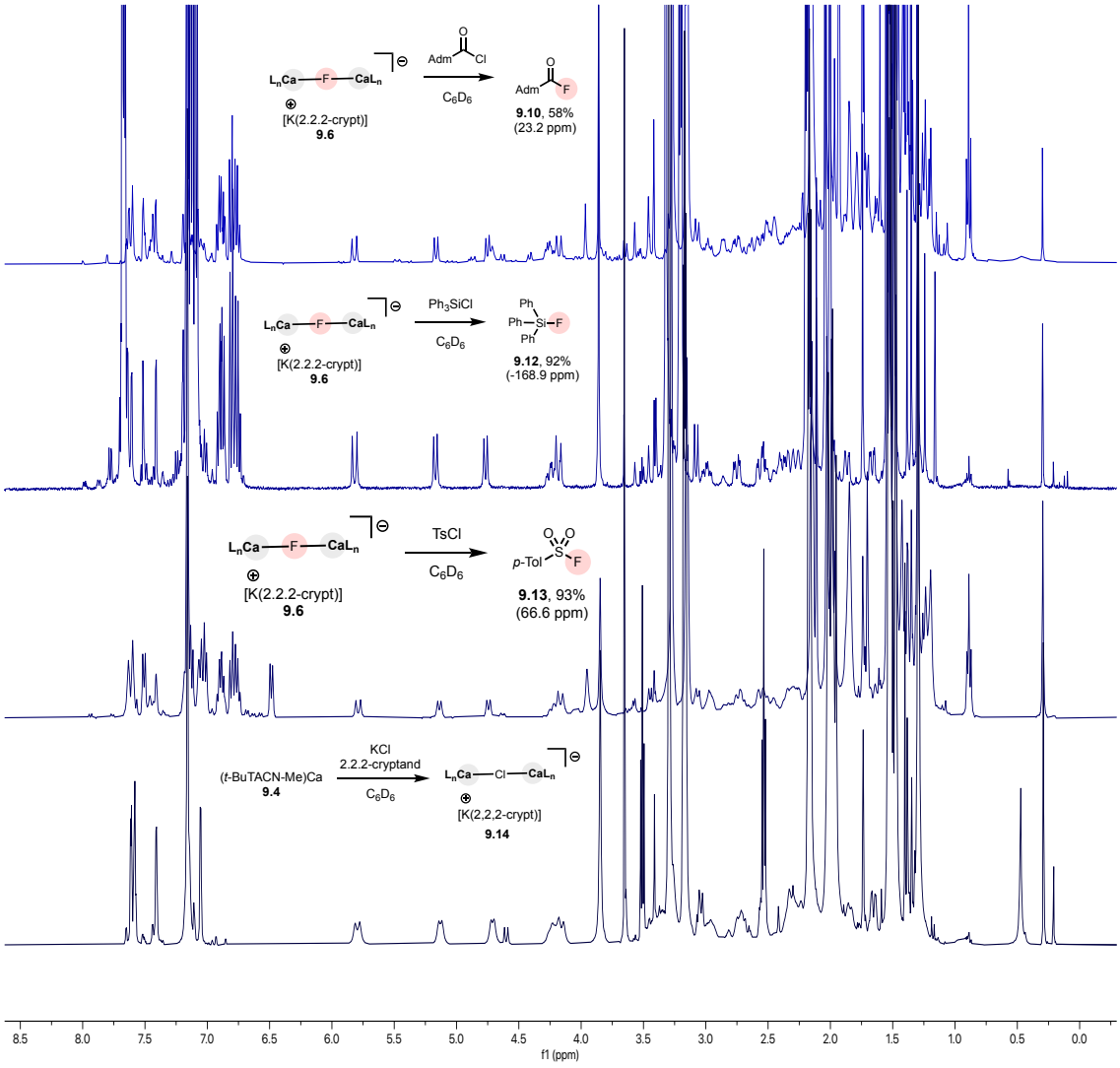


***Scheme 9.10.*** Stacked crude $^{1}$H NMR spectra of reactions with compound **9.6** and independent synthesis of [K(2.2.2-crypt)][{(*t*-BuTACN-Me)Ca}$_2$(μ-Cl)].

## 9.3. CONCLUSIONS

In summary, we have synthesized and obtained X-ray crystallographic data on the first monomeric neutral and anionic (*t*-BuTACN)Ca complexes **9.2-9.3**. Furthermore, we have developed a novel desymmetrization method that is viable with iodomethane as the methylating reagent, affording unsymmetrical $L_4X_2$-supported complex (*t*-BuTACN-Me)Ca, **9.4**. The complex possesses sufficient amount of fluorophilicity as exemplified by

fluoride coordination to the Ca center in either benzene or THF solution, to produce series of dinuclear anionic calcium monofluoride complexes **9.6-9.8**. A doubly bridged $Ca_2(\mu\text{-}F)_2$ complex **9.9** evidenced by $^{1}H$ and $^{19}F$ DOSY NMR experiments could be synthesized by strategically adding a dilute solution of complex **9.4** to a solution of TMAF. Lastly, we showed enhanced fluoride anion delivery in comparison to our previously reported (NON)Ca systems, especially towards the less reactive Si- and S-centered electrophiles. O-ligation from the TACN ligand appears to give higher yields of Si–F and S–F -containing products, because of less competitive side reactions, due to the less nucleophilic nature of the aryloxide X-donors. Furthermore, we demonstrated NMR spectroscopic evidence that there is clear exchange between the fluoride anion from the Ca–F–Ca unit and the chloride anion from chloride-containing electrophiles. We believe that these findings will inspire future work in developing further examples of well-defined soluble molecular Ca–F complexes, and thus push the frontiers of our fundamental understanding of the nucleophilicity of the Ca–F bond.

## 9.4. EXPERIMENTAL

### 9.4.1. General information

All manipulations were carried out using standard Schlenk line or dry-box techniques under an atmosphere of argon or dinitrogen. Solvents were degassed by sparging with argon and dried by passing through a column of the appropriate drying agent. Both $Me_3SnF$[33] and $Ca(HMDS)_2(THF)_2$[34] were prepared by the literature methods.

### 9.4.2. Ligand Synthesis

**Preparation of *t*-BuTACN ligand 9.1**

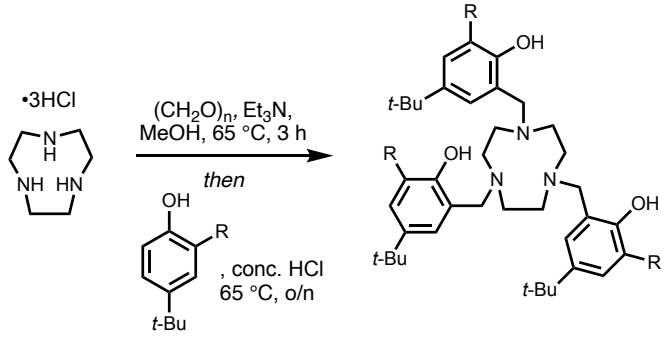


An adapted version of the literature procedure was used to synthesize the *t*-BuTACN-$H_3$ proteo-ligand **9.1**.[35] To a flame-dried Schlenk flask equipped with a stirrer bar was added 1,4,7-triazacyclononane (TACN)·3HCl (1.00 g, 4.19 mmol) and paraformaldehyde (660 mg, 22.0 mmol). MeOH (0.4 M) and $Et_3N$ (1.75 mL) were then added, and the reaction mixture stirred at 65 °C for 3 h. Thereafter, 2,4-di-*tert*-butylphenol (5.91 g, 25.2 mmol) was added to the clear orange solution, and several drops of conc. HCl were added. The reaction mixture was allowed to stirred overnight at 65 °C after which time a white precipitate emerged. The mother liquor was removed via filter cannula and the residual solid washed with MeCN (20 mL x 5). After drying under vacuum, the product was obtained as a white solid (2.72 g, 83% yield).

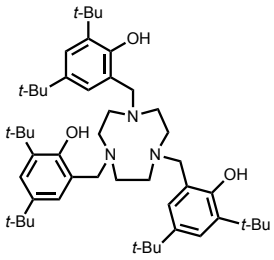


**1,4,7-tris(3,5-tert-butyl-2-hydroxybenzyl)-1,4,7-triazacyclononane (*t*-BuTACN-$H_3$), 9.1, 1: $^1$H NMR** (400 MHz, $CDCl_3$) δ 10.23 (br s, 3H, PhO*H*), 7.22 (d, *J* = 2.4 Hz, 3H, Ph*H*), 6.77 (d, *J* = 2.3 Hz, 3H, Ph*H*), 3.73 (s, 6H, NC$H_2$Ph), 2.84 (s, 12H,

NC$H_2$C$H_2$N), 1.43 (s, 27H, PhC(C$H_3$)$_3$), 1.25 (s, 27H, PhC(C$H_3$)$_3$); **$^{13}$C{$^1$H} NMR** (100 MHz, $CDCl_3$) δ 153.9, 141.0, 135.8, 123.9, 123.4, 121.6 (*Ph*), 63.6 (N*C*H$_2$Ph), 55.4 (N*C*H$_2$*C*H$_2$N), 35.0, 34.3 (Ph*C*(CH$_3$)$_3$), 31.8, 29.8 (PhC(*C*H$_3$)$_3$). Characterization data in $CDCl_3$ match those reported in the literature.[3] **$^1$H NMR** (400 MHz, $C_6D_6$) δ 10.43 (s, 3H), 7.51 (d, *J* = 2.4 Hz, 3H), 6.80 (d, *J* = 2.4 Hz, 3H), 3.32 (s, 6H), 2.43 (s, 12H), 1.73 (s, 27H), 1.34 (s, 27H). **$^{13}$C{$^1$H} NMR** (100 MHz, $C_6D_6$) δ 154.6, 141.1, 136.1, 124.0, 123.5, 122.2 (*Ph*), 63.8 (N*C*H$_2$Ph), 55.7 (N*C*H$_2$*C*H$_2$N), 35.3, 34.4 (Ph*C*(CH$_3$)$_3$), 32.0, 30.0 (PhC(*C*H$_3$)$_3$).

### 9.4.3. Preparation of [K(η$^6$-benzene)][(*t*-BuTACN)Ca]

To a flame-dried Schlenk flask equipped with a Teflon-coated magnetic stirrer bar was added **9.1** (500 mg, 0.64 mmol), Ca(HMDS)$_2$(THF)$_2$ (322 mg, 0.64 mmol), and K[HMDS] (127 mg, 0.64 mmol) in an nitrogen filled glovebox. 12.5 mL of dry benzene was added via cannula and the reaction stirred at 80 °C overnight. After this time, the reaction mixture was transferred to another Schlenk flask by filter cannula and the precipitate further extracted with benzene (10 mL x 2). The combined benzene filtrate was concentrated under reduced pressure to ~10 mL and allowed to stand at room temperature. After 1 d, colorless crystals were observed to form; the mother liquor was removed by decantation to afford pure complex **9.2** as colorless crystals (260 mg, 47%).

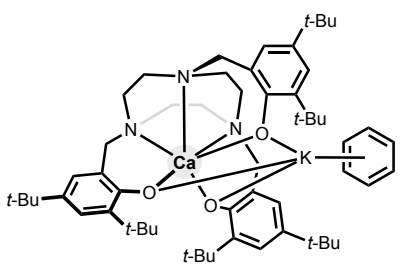


**$^1$H NMR** (400 MHz, $C_6D_6$) δ 7.56 (d, *J* = 2.7 Hz, 3H, Ph*H*), 6.99 (d, *J* = 2.6 Hz, 3H, Ph*H*), 3.96 (d, *J* = 11.1 Hz, 3H, NC*H*$_2$Ph), 2.78 (d, *J* = 11.1 Hz, 3H, NC*H*$_2$Ph), 2.44 (dd, *J* = 14.3, 4.1 Hz, 3H, NC*H*$_2$C*H*$_2$N), 2.19–1.95 (m,

6H, NC$H_2$C$H_2$N), 1.68 (d, $J$ = 2.9 Hz, 3H, NC$H_2$C$H_2$N), 1.64 (s, 27H, PhC(C$H_3$)$_3$), 1.47 (s, 27H, PhC(C$H_3$)$_3$); **$^{13}$C{$^1$H} NMR** (100 MHz, $C_6D_6$) δ 163.8, 134.2, 131.9, 126.4, 123.2, 122.8 (*Ph*), 61.3 (N*C*H$_2$Ph), 56.0, 45.9 (N*C*H$_2$*C*H$_2$N), 33.9, 32.9 (Ph*C*(CH$_3$)$_3$), 31.2, 29.2 (PhC(*C*H$_3$)$_3$). Anal. Calcd. [%] for $C_{57}H_{84}CaKN_3O_3$: C, 72.95; H, 9.02; N, 4.48. Found: C, 73.62; H, 9.26; N, 4.36.

### 9.4.4. Preparation of (*t*-BuTACN-H)Ca

To a flame-dried Schlenk flask equipped with a Teflon-coated magnetic stir bar was added **1** (500 mg, 0.64 mmol) and Ca(HMDS)$_2$(THF)$_2$ (322 mg, 0.64 mmol) in an nitrogen filled glovebox. 12.5 mL of dry benzene were added via cannula and the reaction stirred overnight in an oil bath at 80 °C. After this time, volatiles were removed under reduced pressure yielding a crude yellow oil. Purification by trituration with hot hexane (10 mL x 3) gave complex **2** as a white solid (176 mg, 34%).

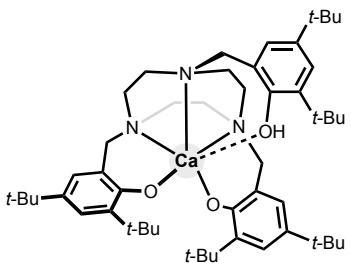


**$^1$H NMR** (400 MHz, $C_6D_6$) δ 7.55 (d, $J$ = 2.1 Hz, 3H, Ph*H*), 7.39 (br s, 1H, PhO*H*), 6.94 (d, $J$ = 2.3 Hz, 3H, Ph*H*), 3.96 (d, $J$ = 11.6 Hz, 3H, NC$H_2$Ph), 2.77 (d, $J$ = 11.6 Hz, 3H, NC$H_2$Ph), 2.30 (d, $J$ = 14.2 Hz, 3H, NC$H_2$C$H_2$N), 2.14 (d, $J$ = 13.3 Hz, 3H, NC$H_2$C$H_2$N), 2.06 (d, $J$ = 14.5 Hz, 3H, NC$H_2$C$H_2$N), 1.72 (d, $J$ = 2.0 Hz, 27H, PhC(C$H_3$)$_3$), 1.55 (d, $J$ = 11.0 Hz, 3H, NC$H_2$C$H_2$N), 1.40 (d, $J$ = 2.0 Hz, 27H, PhC(C$H_3$)$_3$); **$^{13}$C{$^1$H} NMR** (100 MHz, $C_6D_6$) δ 159.6, 136.8, 136.6, 126.5, 124.2, 123.7 (*Ph*), 62.8 (N*C*H$_2$Ph), 57.5, 47.2 (N*C*H$_2$*C*H$_2$N), 35.0, 33.9 (Ph*C*(CH$_3$)$_3$), 31.8, 30.3

($PhC(CH_3)_3$. Anal. Calcd. [%] for $C_{51}H_{79}CaN_3O_3$: C, 74.49; H, 9.68; N, 5.11. Found: C, 74.37; H, 9.81; N, 4.94.

### 9.4.5. Preparation of (*t*-BuTACN-Me)Ca

To a flame-dried Schlenk flask equipped with a Teflon-coated magnetic stir bar was added **2** (2.0 g, mmol) in a nitrogen-filled glovebox. 50 mL of dry benzene was added via cannula followed by 15 min of sonication and heating, causing the complex to partially dissolve. To the stirred solution was added dry iodomethane (0.6 mL, 4.5 equiv) via syringe and the reaction mixture stirred at 80 °C overnight. After this time, the reaction mixture was transferred into another Schlenk flask via filter cannula and volatiles were removed under reduced pressure yielding an off white solid in sufficient purity for subsequent reactions (1.5 g, 84%).

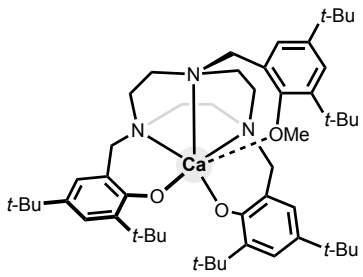


**$^1$H NMR** (400 MHz, $C_6D_6$) δ 7.65 (d, *J* = 2.7 Hz, 1H, Ph*H*), 7.60 (d, *J* = 2.7 Hz, 1H, Ph*H*), 7.47 (d, *J* = 2.5 Hz, 1H, Ph*H*), 7.05 (d, *J* = 2.7 Hz, 1H, Ph*H*), 7.03 (d, *J* = 2.7 Hz, 1H, Ph*H*), 6.75 (d, *J* = 2.5 Hz, 1H, Ph*H*), 4.14 (d, *J* = 12.1 Hz, 1H, $NCH_2Ph$), 4.03 (d, *J* = 11.6 Hz, 1H, $NCH_2Ph$), 3.96 (s, 3H, $PhOCH_3$), 3.82 (d, *J* = 10.9 Hz, 1H, $NCH_2Ph$), 2.96 (d, *J* = 12.2 Hz, 1H, $NCH_2Ph$), 2.80 (d, *J* = 10.9 Hz, 1H, $NCH_2Ph$), 2.72 (td, *J* = 12.6, 5.0 Hz, 1H, $NCH_2CH_2N$), 2.64–2.52 (m, 1H, $NCH_2Ph$; 1H, $NCH_2CH_2N$), 2.47 (dd, *J* = 14.8, 5.0 Hz, 1H, $NCH_2CH_2N$), 2.27 (td, *J* = 12.9, 5.1 Hz, 1H, $NCH_2CH_2N$), 2.13–1.90 (m, 3H, $NCH_2CH_2N$), 1.84 (d, *J* = 3.7 Hz, 18H, $PhC(CH_3)_3$), 1.79 (d, *J* = 4.8 Hz, 1H, $NCH_2CH_2N$), 1.60 (dd, *J* = 12.7, 3.7 Hz, 1H, $NCH_2CH_2N$), 1.48 (d, *J* = 6.0 Hz, 18H,

PhC(C$H_3$)$_3$), 1.42 (s, 9H, PhC(C$H_3$)$_3$), 1.39 (d, $J$ = 3.4 Hz, 1H, NC$H_2$C$H_2$N), 1.34 (d, $J$ = 6.9 Hz, 1H, NC$H_2$C$H_2$N), 1.19 (s, 9H, PhC(C$H_3$)$_3$), 1.07 (td, $J$ = 13.4, 5.2 Hz, 1H, NC$H_2$C$H_2$N); **$^{13}$C{$^1$H} NMR** (100 MHz, $C_6D_6$) δ 166.0, 165.9, 153.5, 148.5, 143.5, 137.1, 135.9, 132.6, 132.1, 131.0, 128.9, 127.2, 126.0, 124.2, 124.2, 123.9, 123.2 (*Ph*), 67.0 (PhOC$H_3$), 65.2, 64.6, 59.7 (NC$H_2$Ph), 57.8, 57.5, 57.5, 48.0, 47.6, 45.4 (NC$H_2$C$H_2$N), 36.3, 35.8, 35.7, 34.6, 34.1 (PhC(CH$_3$)$_3$), 32.9, 32.6, 32.5, 31.4, 30.6, 30.3 (PhC(CH$_3$)$_3$). Anal. Calcd. [%] for $C_{52}H_{81}CaN_3O_3$: C, 74.68; H, 9.76; N, 5.02. Found: C, 74.24; H, 9.90; N, 4.59.

### 9.4.6. Preparation of [K(2.2.2-cryptand)][(*t*-BuTACN)Ca]

To a J-Young NMR tube was added **9.4** (50.0 mg, 59.8 μmol), K[HMDS] (11.9 mg, 59.8 μmol), 2.2.2-cryptand (22.5 mg, 59.8 μmol), and $C_6D_6$ in a nitrogen filled glovebox. The NMR tube was placed in an 80 °C oil bath for ca. 12 h. After this time, $^1$H NMR spectroscopy revealed full consumption of the starting complex and the formation of a new symmetrical species. In a glovebox, the reaction mixture was filtered into a vial via syringe and layered with 1 mL of hexane. After 1 d, a white precipitate was observed to form, which after removal of the mother liquor and drying under reduced pressure afforded complex **9.5** as a white solid (69 mg, 93%).

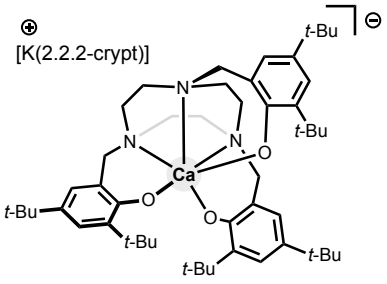


**$^1$H NMR** (400 MHz, THF-d$_8$) δ 7.00 (d, $J$ = 2.8 Hz, 3H, Ph*H*), 6.68 (d, $J$ = 2.7 Hz, 3H, Ph*H*), 4.04 (d, $J$ = 10.6 Hz, 3H, NC$H_2$Ph), 3.56 (s, 12H, OC$H_2$C$H_2$O-crypt), 3.54–3.49 (m, 12H, OC$H_2$-crypt), 2.71 (d, $J$ = 10.7 Hz, 3H,

NC$H_2$Ph), 2.67–2.56 (m, 3H, NC$H_2$C$H_2$N-TACN), 2.56–2.46 (m, 16H {(12H, NC$H_2$-crypt) + (4H, NC$H_2$C$H_2$N-TACN)}), 2.31 (td, $J$ = 12.5, 5.2 Hz, 3H, NC$H_2$C$H_2$N-TACN), 1.76 (d, $J$ = 3.3 Hz, 2H, NC$H_2$C$H_2$N-TACN), 1.48 (s, 27H, PhC(C$H_3$)$_3$), 1.22 (s, 27H, PhC(C$H_3$)$_3$); **$^{13}$C{$^1$H} NMR** (100 MHz, THF-d$_8$) δ 168.2, 135.8, 129.2, 126.9, 125.1, 123.0 (*Ph*), 71.5 (OC$H_2$C$H_2$O-crypt), 68.6 (OC$H_2$-crypt), 65.2 (NC$H_2$Ph), 59.2 (NC$H_2$C$H_2$N-TACN), 54.9 (NC$H_2$-crypt), 47.9 (NC$H_2$C$H_2$N-TACN), 36.1, 34.4 (PhC(CH$_3$)$_3$), 32.9, 31.05 (PhC(CH$_3$)$_3$). Anal. Calcd. [%] for $C_{72}H_{121}CaKN_5O_9$: C, 67.56; H, 9.53; N, 5.47. Found: C, 67.19; H, 8.94; N, 5.06.

### 9.4.7. Preparation of [M][{(*t*-BuTACN-Me)Ca}$_2$F] Complexes

**General Procedure:** To a J-Young NMR tube was added **9.4**, the appropriate fluorinating agent, and $C_6D_6$ or toluene-$d_8$. The reaction mixture was sonicated for 30 min then placed in an oil bath at 80 °C until major conversion was observed. After this time, the reaction solution was filtered into a vial and allowed to settle or layered with hexane for crystallization. The mother liquor was decanted off and the resulting crystals washed with the mother solvent to afford pure colorless crystalline material of **9.6-9.8**.

**[K(2.2.2-crypt)][{(*t*-BuTACN-Me)Ca}$_2$(μ-F)]**, **9.6**: Complex **9.6** was prepared from **9.4** (100 mg, 120 μmol), KF (17.4 mg, 299 μmol), 2.2.2-crypt (22.5 mg, 59.8 μmol), and $C_6D_6$ (0.5 mL) according to the General Procedure. Near full conversion was observed after 7 d, and the reaction mixture was filtered into a vial and layered with hexane. After 1 d, the mother liquor was removed, and the remaining crystalline material washed with hexane (0.3 mL x 3), to afford after drying, complex **9.6** as a colorless crystalline solid (39 mg,

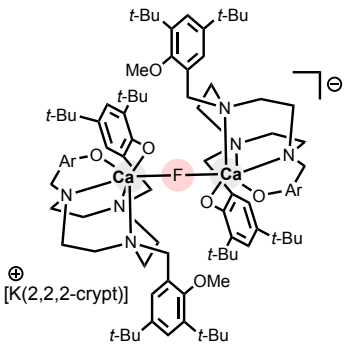


31%). Single crystals suitable for X-ray crystallography were obtained via the same crystallization method. **$^{1}$H NMR** (500 MHz, THF-$d_8$) δ 7.16 (d, $J$ = 2.5 Hz, 2H, Ph*H*), 7.04 (d, $J$ = 2.7 Hz, 2H, Ph*H*), 7.00 (d, $J$ = 2.7 Hz, 2H, Ph*H*), 6.87 (d, $J$ = 2.6 Hz, 2H, Ph*H*), 6.64 (d, $J$ = 2.8 Hz, 2H, Ph*H*), 6.62 (d, $J$ = 2.8 Hz, 2H, Ph*H*), 5.08 (d, $J$ = 14.8 Hz, 2H, NC$H_2$Ph), 4.45 (d, $J$ = 12.0 Hz, 2H, NC$H_2$Ph), 4.27 (s, 6H, PhOC$H_3$), 4.02 (d, $J$ = 10.3 Hz, 2H, NC$H_2$Ph), 3.97–3.82 (m, 4H, {(2H, NC$H_2$Ph) + (2H, NC$H_2$C$H_2$N)}), 3.58 (s, 12H, {(OC$H_2$C$H_2$O-crypt) + (overlap with THF-$d_8$ 3.58 peak)}, 3.53 (t, $J$ = 4.7 Hz, 14H, {(12H, OC$H_2$-crypt) + (2H, NC$H_2$C$H_2$N)}), 2.71 (d, $J$ = 11.9 Hz, 2H, NC$H_2$Ph), 2.66 (d, $J$ = 10.4 Hz, 2H, NC$H_2$Ph), 2.55 (t, $J$ = 4.7 Hz, 14H, {(12H, OC$H_2$-crypt) + (2H, NC$H_2$C$H_2$N)}), 2.52–2.43 (m, 4H, NC$H_2$C$H_2$N), 2.43–2.30 (m, 6H, NC$H_2$C$H_2$N), 2.05 (d, $J$ = 13.0 Hz, 2H, NC$H_2$C$H_2$N), 1.89 (q, $J$ = 10.5 Hz, 2H, NC$H_2$C$H_2$N), 1.71 (s, 2H, NC$H_2$C$H_2$N), 1.58 (s, 18H, PhC(C$H_3$)$_3$), 1.36 (s, 18H, PhC(C$H_3$)$_3$), 1.31 (d, $J$ = 10.2 Hz, 2H, NC$H_2$C$H_2$N), 1.24 (s, 18H, PhC(C$H_3$)$_3$), 1.22 (s, 18H, PhC(C$H_3$)$_3$), 1.21 (s, 18H, PhC(C$H_3$)$_3$), 1.17 (s, 18H, PhC(C$H_3$)$_3$). **$^{13}$C{$^{1}$H} NMR** (126 MHz, THF) δ 168.2, 167.7, 158.1, 144.5, 142.6, 135.8, 135.6, 132.0, 130.3, 129.7, 129.7, 127.7, 127.2, 125.7, 125.2, 123.3, 123.2, 122.7 (*Ph*), 71.5 (O*C*H$_2$*C*H$_2$O-crypt), 68.6 (OC$H_2$-crypt), 65.0 (PhO*C*H$_3$), 64.8, 64.3 (N*C*H$_2$Ph), 58.7, 57.5 (N*C*H$_2$*C*H$_2$N), 57.0 (N*C*H$_2$Ph), 54.9 (NC$H_2$-crypt + overlap with N*C*H$_2$*C*H$_2$N-TACN peak), 48.0, 47.3, 47.1 (N*C*H$_2$*C*H$_2$N), 36.4, 36.0, 36.0, 35.1, 34.4, 34.3 (Ph*C*(CH$_3$)$_3$), 32.9, 32.8, 32.3, 31.9, 31.6, 31.2 (PhC(*C*H$_3$)$_3$). **$^{19}$F{$^{1}$H} NMR** (377 MHz, THF) δ -89.4.

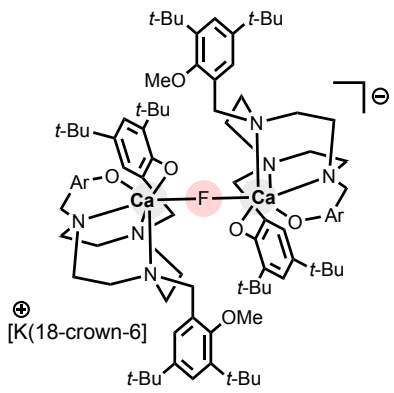


**[K(18-crown-6)][{(*t*-BuTACN-Me)Ca}$_2$(μ-F)], 9.7:** Complex **9.7** prepared from **9.4** (100 mg, 120 μmol), KF (17.4 mg, 299 μmol), 18-crown-6 (15.8 mg, 59.8 μmol), and toluene-$d_8$ (0.5 mL) according to the General Procedure. Near full conversion was observed after 21 d, and the reaction mixture was filtered into a vial and allowed to stand. After 1 d, the mother liquor was removed, and the remaining crystalline material was washed with toluene (0.3 mL x 3), to afford, after drying, complex **7** as a colorless crystalline solid (27 mg, 23%). Single crystals suitable for X-ray crystallography were obtained via the same crystallization method. **$^1$H NMR** (500 MHz, THF) δ 7.16 (d, *J* = 2.5 Hz, 2H, Ph*H*), 7.04 (d, *J* = 2.8 Hz, 2H, Ph*H*), 7.00 (d, *J* = 2.8 Hz, 2H, Ph*H*), 6.88 (d, *J* = 2.6 Hz, 2H, Ph*H*), 6.65 (d, *J* = 2.8 Hz, 2H, Ph*H*), 6.62 (d, *J* = 2.7 Hz, 2H, Ph*H*), 5.08 (d, *J* = 14.9 Hz, 2H, NC$H_2$Ph), 4.45 (d, *J* = 11.9 Hz, 2H, NC$H_2$Ph), 4.27 (s, 6H, PhOC$H_3$), 4.02 (d, *J* = 10.2 Hz, 2H, NC$H_2$Ph), 3.98–3.83 (m, 4H, {(2H, NC$H_2$Ph) + (2H, NC$H_2$C$H_2$N)}), 3.59 (s, 24H, {(OC$H_2$C$H_2$O-18-crown-6) + (overlap with THF-$d_8$ 3.58 peak)}), 3.55 (dd, *J* = 15.4, 4.4 Hz, 2H, NC$H_2$C$H_2$N), 2.71 (d, *J* = 11.8 Hz, 2H, NC$H_2$Ph), 2.67 (d, *J* = 10.3 Hz, 2H, NC$H_2$Ph), 2.63–2.53 (m, 2H, NC$H_2$C$H_2$N), 2.50 (dd, *J* = 14.8, 4.6 Hz, 4H, NC$H_2$C$H_2$N), 2.44–2.33 (m, 6H, NC$H_2$C$H_2$N), 2.05 (dd, *J* = 13.1, 3.2 Hz, 2H, NC$H_2$C$H_2$N), 1.89 (td, *J* = 11.6, 7.5 Hz, 2H, NC$H_2$C$H_2$N), 1.70 (d, *J* = 3.5 Hz, 2H, NC$H_2$C$H_2$N), 1.58 (s, 18H, PhC(C$H_3$)$_3$), 1.36 (s, 18H, PhC(C$H_3$)$_3$), 1.34 (d, *J* = 2.7 Hz, 2H, NC$H_2$C$H_2$N), 1.24 (s, 18H, PhC(C$H_3$)$_3$), 1.22 (s, 18H, PhC(C$H_3$)$_3$), 1.215 (s, 18H, PhC(C$H_3$)$_3$), 1.17 (s, 18H, PhC(C$H_3$)$_3$). **$^{13}$C{$^1$H} NMR** (126 MHz, THF) δ 168.2, 167.7, 158.1, 144.6, 142.6, 135.8, 135.6, 132.1, 130.2, 129.8, 129.7, 127.6, 127.2, 125.7, 125.2,

123.3, 123.2, 122.7 (*Ph*), 71.3 (O*C*H$_2$*C*H$_2$O-18-crown-6), 65.0 (PhO*C*H$_3$), 64.8 (N*C*H$_2$Ph), 64.3 (N*C*H$_2$Ph), 58.7 (N*C*H$_2$*C*H$_2$N), 57.5 (N*C*H$_2$*C*H$_2$N), 57.0 (N*C*H$_2$Ph), 55.0 (N*C*H$_2$*C*H$_2$N), 48.0 (N*C*H$_2$*C*H$_2$N), 47.3 (N*C*H$_2$*C*H$_2$N), 47.1 (N*C*H$_2$*C*H$_2$N), 36.4, 36.0, 36.0, 35.1, 34.4, 34.3 (Ph*C*(CH$_3$)$_3$), 32.9, 32.8, 32.3, 31.9, 31.6, 31.2 (PhC(*C*H$_3$)$_3$). **$^{19}$F{$^1$H} NMR** (377 MHz, THF) δ -89.3. Anal. Calcd. [%] for $C_{116}H_{186}Ca_2FKN_6O_{12}$: C, 69.84; H, 9.40; N, 4.21. Found: C, 70.08; H, 9.10; N, 3.96.

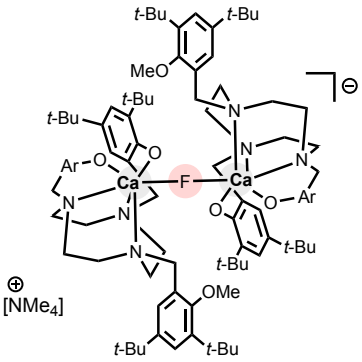


**[NMe$_4$][{(*t*-BuTACN-Me)Ca}$_2$(μ-F)] 9.8:** Complex **9.8** was prepared from **9.4** (50.0 mg, 59.8 μmol), TMAF (6.0 mg, 64 μmol) and $C_6D_6$/THF 4:1 solvent mixture (0.5 mL) according to the General Procedure. Near full conversion was observed after 12 h, and the reaction mixture was filtered into a vial and allowed to stand. After 1 d, the mother liquor was removed, the remaining crystalline material was washed with hexane (0.3 mL x 3), and after drying afforded complex **9.8** as a colorless crystalline solid (33 mg, 63%). Single crystals suitable for X-ray crystallography were obtained by slow cooling a reaction mixture of the same scale in a J-Young NMR tube, but with toluene-$d_8$/THF 4:1 as the crystallization solvent system. **$^1$H NMR** (500 MHz, THF) δ 7.17 (d, *J* = 2.5 Hz, 2H, *Ph*), 7.04 (d, *J* = 2.7 Hz, 2H, *Ph*), 7.02 (d, *J* = 2.7 Hz, 2H, *Ph*), 6.87 (d, *J* = 2.5 Hz, 2H, *Ph*), 6.65 (d, *J* = 2.7 Hz, 4H, *Ph*), 5.07 (d, *J* = 14.8 Hz, 2H, NC*H*$_2$Ph), 4.44 (d, *J* = 12.0 Hz, 2H, NC*H*$_2$Ph), 4.25 (s, 6H, PhOC*H*$_3$), 4.00 (d, *J* = 10.3 Hz, 2H, NC*H*$_2$Ph), 3.95–3.83 (m, 4H, {(2H, NC*H*$_2$Ph) + (2H, NC*H*$_2$C*H*$_2$N)}), 3.57–3.50 (m, 2H, NC*H*$_2$C*H*$_2$N), 3.00 (s, 12H, N(C*H*$_3$)$_4^+$, 2.71 (d, *J* = 11.9 Hz, 2H, NC*H*$_2$Ph), 2.68 (d, *J* = 10.3 Hz, 2H, NC*H*$_2$Ph), 2.58 (dd, *J* = 15.5, 11.9 Hz, 2H,

NC$H_2$C$H_2$N), 2.54–2.44 (m, 6H, NC$H_2$C$H_2$N), 2.40 (d, $J$ = 8.2 Hz, 4H, NC$H_2$C$H_2$N), 2.38–2.30 (m, 2H, NC$H_2$C$H_2$N), 2.09–2.00 (m, 2H, NC$H_2$C$H_2$N), 1.86 (q, $J$ = 11.6 Hz, 2H, NC$H_2$C$H_2$N), 1.58 (s, 18H, PhC(C$H_3$)$_3$), 1.36 (s, 20H, {18H, (PhC(C$H_3$)$_3$) + 2H, NC$H_2$C$H$}) , 1.24 (s, 18H, PhC(C$H_3$)$_3$), 1.22 (s, 18H, PhC(C$H_3$)$_3$), 1.21 (s, 18H, PhC(C$H_3$)$_3$), 1.17 (s, 18H, PhC(C$H_3$)$_3$). **$^{13}$C{$^1$H} NMR** (126 MHz, THF) δ 168.2, 167.7, 158.0, 144.6, 142.7, 135.9, 135.5, 132.0, 130.2, 130.0, 129.8, 127.7, 127.3, 125.7, 125.2, 123.4, 122.7 (*Ph*), 64.9 (PhO*C*H$_3$), 64.8 (N*C*H$_2$Ph), 64.2 (N*C*H$_2$Ph), 58.7 (N*C*H$_2$*C*H$_2$N), 57.5 (N*C*H$_2$*C*H$_2$N), 57.0 (N*C*H$_2$Ph), 55.9 (N(*C*H$_3$)$_4$), 55.0, 48.0, 47.3, 47.0 (N*C*H$_2$*C*H$_2$N), 36.4, 36.1, 36.0, 35.1, 34.4, 34.3 (Ph*C*(CH$_3$)$_3$), 32.9, 32.8, 32.3, 31.9, 31.6, 31.2 (PhC(*C*H$_3$)$_3$). **$^{19}$F{$^1$H} NMR** (377 MHz, THF) δ -89.3. Anal. Calcd. [%] for $C_{108}H_{174}Ca_2FN_7O_6$: C, 73.46; H, 9.93; N, 5.55. Found: C, 73.97; H, 9.74; N, 4.68.

### 9.4.8. Preparation of [NMe$_4$][{(*t*-BuTACN-Me)CaF}$_2$]

TMAF (22.3 mg, 239 μmol) was loaded into a flame-dried Schlenk flask equipped with a Teflon-coated magnetic stirrer bar in a nitrogen filled glovebox. 1.5 mL of dry THF was added via cannula, and the mixture sonicated at 40 °C for 1 h then stirred for a further 24 h. In a separate flame dried Schlenk flask **9.4** (100 mg, 120 μmol) was dissolved in 3.5 mL of THF and added dropwise to the TMAF solution at room temperature. After addition, the reaction mixture was stirred for an additional 30 min and a new fluoride-containing species was observed as the major product by $^1$H and $^{19}$F NMR measurements. The stirring of the reaction mixture was stopped and, when the precipitate had settled, was filtered by cannula into another Schlenk flask. Volatiles were removed

*in vacuo*, and the resulting solid washed with hexane (0.3 mL x 3), to afford, after drying, complex **9.9** as a white solid (58 mg, 52%).

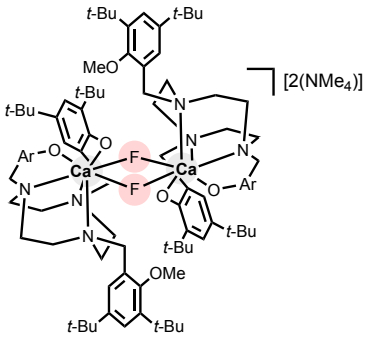


**$^{1}$H NMR** (400 MHz, $C_6D_6$) δ 7.62 (t, *J* = 2.3 Hz, 4H, *Ph*), 7.42 (d, *J* = 2.5 Hz, 2H, *Ph*), 7.15 (s, 4H, *Ph* + overlap with $C_6D_6$ 7.16 ppm peak), 7.06 (d, *J* = 2.7 Hz, 2H, *Ph*), 5.20 (d, *J* = 14.9 Hz, 2H, NC*H*$_2$Ph), 4.61 (d, *J* = 10.7 Hz, 2H, NC*H*$_2$Ph), 4.52 (d, *J* = 10.7 Hz, 2H, NC*H*$_2$Ph), 4.02 (d, *J* = 14.9 Hz, 2H, NC*H*$_2$Ph), 3.70–3.64 (m, 2H, NC*H*$_2$C*H*$_2$N), 3.61 (s, 6H, PhOC*H*$_3$), 3.26 (d, *J* = 10.8 Hz, 2H, NC*H*$_2$Ph), 3.16 (dd, *J* = 14.3, 3.1 Hz, 2H, NC*H*$_2$C*H*$_2$N), 2.99 (d, *J* = 10.7 Hz, 2H, NC*H*$_2$Ph), 2.65 (d, *J* = 11.7 Hz, 4H, NC*H*$_2$C*H*$_2$N), 2.54 (s, 24H, N(C*H*$_3$)$_4^+$), 2.51–2.47 (m, 2H, NC*H*$_2$C*H*$_2$N), 2.30–2.12 (m, 8H, NC*H*$_2$C*H*$_2$N), 2.07 (m, 2H, NC*H*$_2$C*H*$_2$N), 1.94 (s, 18H, PhC(C*H*$_3$)$_3$), 1.89 (s, 18H, PhC(C*H*$_3$)$_3$), 1.79 (s, 2H, NC*H*$_2$C*H*$_2$N), 1.68–1.63 (m, 2H, NC*H*$_2$C*H*$_2$N), 1.54 (s, 18H, PhC(C*H*$_3$)$_3$), 1.50 (s, 18H, PhC(C*H*$_3$)$_3$), 1.47 (s, 18H, PhC(C*H*$_3$)$_3$), 1.29 (s, 18H, PhC(C*H*$_3$)$_3$). **$^{13}$C{$^{1}$H} NMR** (100 MHz, $C_6D_6$) δ 167.4, 167.3, 157.4, 145.3, 142.4, 136.1, 134.5, 130.9, 130.8, 129.9, 129.3, 129.1, 127.5, 125.1, 124.5, 123.8, 123.5, 123.2 (*Ph*), 64.2, 63.4 (NCH$_2$Ph), 62.7 (PhOCH$_3$), 57.6, 56.2 (NCH$_2$CH$_2$N), 55.2 (N(CH$_3$)$_4^+$ + NCH$_2$CH$_2$N + NCH$_2$Ph), 47.8, 45.9 (NCH$_2$CH$_2$N), 36.0, 35.9, 35.4, 34.5, 34.1 (PhC(CH$_3$)$_3$), 32.7, 31.7, 31.5, 31.0 (PhC(CH$_3$)$_3$). **$^{19}$F{$^{1}$H} NMR** (377 MHz, $C_6D_6$) δ -82.1.

### 9.4.9. $^{19}$F DOSY NMR Spectra of Complexes 9.8 and 9.9

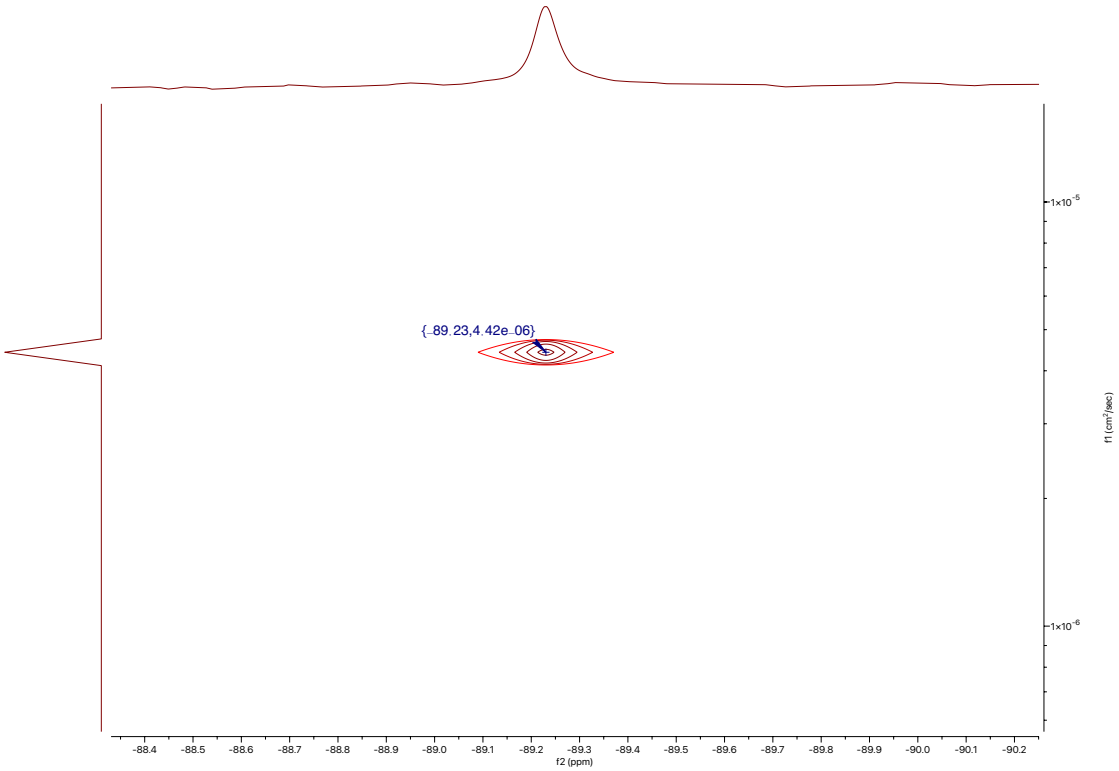


***Figure 9.S1.*** $^{19}$F DOSY NMR spectrum of complex **9.8** in THF-$d_8$.

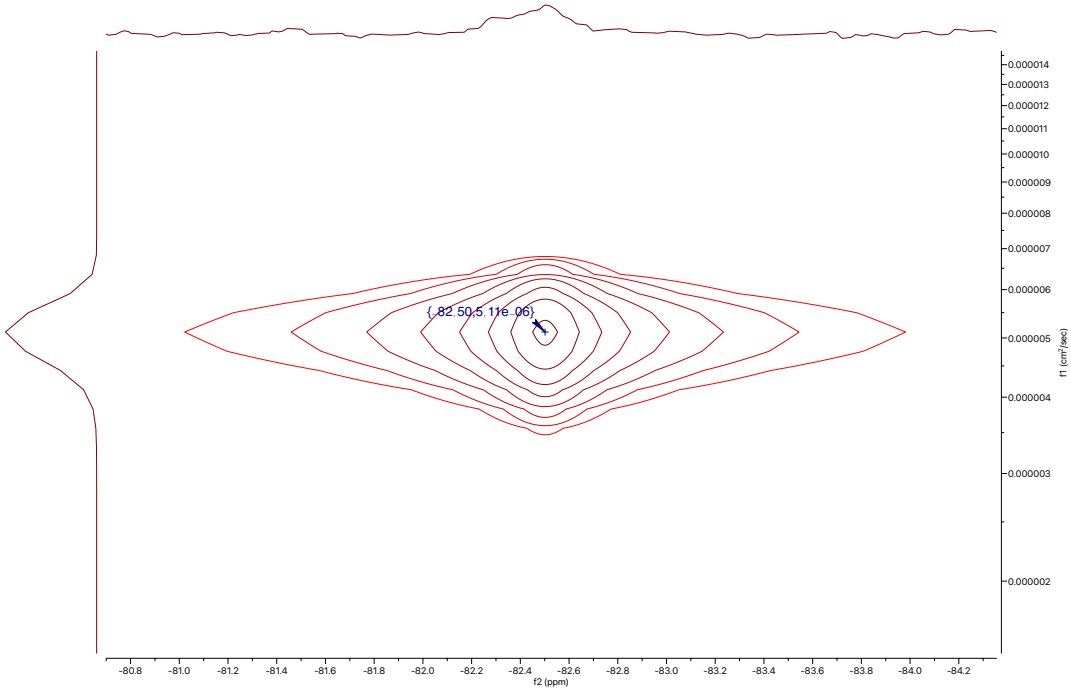


***Figure 9.S2.*** $^{19}$F DOSY NMR spectrum of compound **9.9** in THF-$d_8$.

### 9.4.10. Reactivity of [K(2.2.2-cryptand)][{(*t*-BuTACN-Me)Ca}$_2$F] 9.6 with Electrophiles

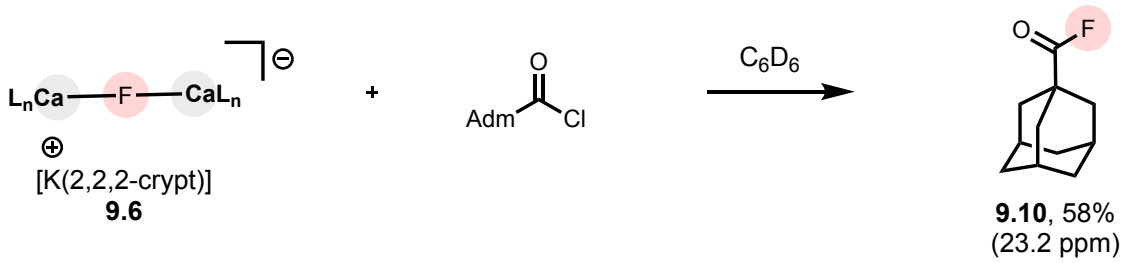


***Scheme 9.S1.*** Reaction of complex **9.6** with 1-adamantanecarbonyl chloride.

To a J-Young NMR tube were added **9.6** (10 mg, 4.9 µmol), 1-adamantanecarbonyl chloride (0.95 mg, 4.8 µmol), and $C_6D_6$ (0.5 mL) in a nitrogen filled glovebox. The NMR tube was inverted, and the reaction was monitored over several days by $^{19}$F NMR. After 48 h, a fluorobenzene internal standard (0.9 µL) was added and the NMR yield of compound **9.10** was determined to be 58% yield by $^{19}$F NMR spectroscopy.

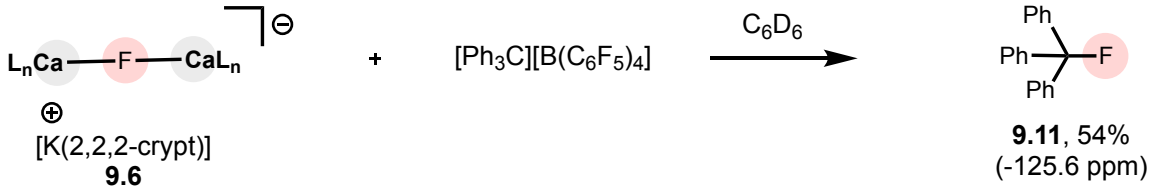


***Scheme 9.S2.*** Reaction of complex **9.6** with triphenylcarbenium tetrakis(pentafluorophenyl)borate.

To a J-Young NMR tube were added **9.6** (10 mg, 4.8 µmol), triphenylcarbenium tetrakis(pentafluorophenyl)borate (4.4 mg, 4.8 µmol), and $C_6D_6$ (0.5 mL) in a nitrogen filled glovebox. The NMR tube was inverted, and the reaction was monitored over 24 h by $^{19}$F NMR. After 24 h, a fluorobenzene internal standard (0.9 µL) was added and the NMR yield of compound **9.11** was determined to be 54% yield by $^{19}$F NMR spectroscopy.

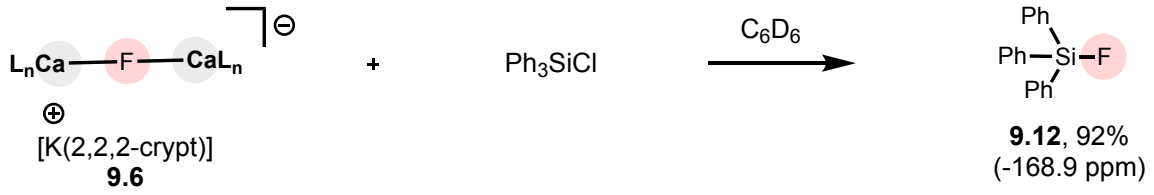


***Scheme 9.S3.*** Reaction of complex **9.6** with chlorotriphenylsilane.

To a J-Young NMR tube were added **9.6** (5 mg, 2.4 µmol), chlorotriphenylsilane (0.70 mg, 2.4 µmol), and $C_6D_6$ (0.5 mL) in a nitrogen filled glovebox. The NMR tube was inverted, and the reaction was monitored over 72 h by $^{19}F$ NMR. After 72 h, a fluorobenzene internal standard (0.9 µL) was added and the NMR yield of compound **9.12** was determined to be 92% yield by $^{19}F$ NMR spectroscopy.




***Scheme 9.S4.*** Reaction of complex **9.6** with tosyl chloride.

To a J-Young NMR tube were added **9.6** (15 mg, 7.2 µmol), tosyl chloride (1.4 mg, 7.2 µmol µmol), a fluorobenzene internal standard (0.9 µL), and $C_6D_6$ (0.5 mL) in a nitrogen filled glovebox. The NMR tube was inverted, and the reaction was monitored over 72 h by $^{19}F$ NMR. After 30 min, the NMR yield of compound **9.13** was determined to be 68% yield via $^{19}F$ NMR. After 72 h, the NMR yield of compound **9.13** was determined to be 93% yield by $^{19}F$ NMR spectroscopy.

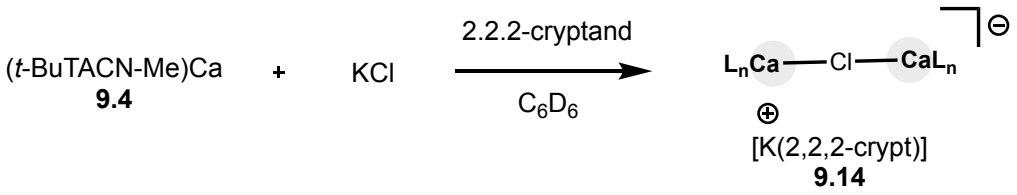


***Scheme 9.S5.*** Independent synthesis of complex **9.14** with KCl/2.2.2-cryptand combination.

To a J-Young NMR tube were added **9.4** (20 mg, 24 μmol), potassium chloride (8.9 mg, 120 μmol), 2.2.2-cryptand (9.0 mg, 24 μmol), and $C_6D_6$ (0.5 mL) in a nitrogen filled glovebox. The NMR tube was placed in an 80 °C oil bath and after 14 d, near complete formation of the [K(2.2.2-crypt)][{(*t*-BuTACN-Me)Ca}$_2$(μ-Cl)] **9.14** was observed. The stacked $^1$H NMR spectra of three of the reactivity entries match the spectrum of the independently synthesized complex as determined by the diagnostic benzylic and methoxy proton resonances (from the TACN backbone).

## 9.5. REFERENCES

(1) Groult, H.; Leroux, F.; Tressaud, A. *Modern Synthesis Processes and Reactivity of Fluorinated Compounds: Progress in Fluorine Science*, Elsevier, 2016.

(2) Britton, R.; Gouverneur, V.; Lin, J.-H.; Meanwell, M.; Ni, C.; Pupo, G.; Xiao, J.-C.; Hu, J. Contemporary Synthetic Strategies in Organofluorine Chemistry, *Nat. Rev. Methods Primer* **2021**, *1*, 1–22.

(3) Harsanyi, A.; Sandford, G. Organofluorine Chemistry: Applications, Sources and Sustainability, *Green Chem.* **2015**, *17*, 2081–2086.

(4) Siegemund, G.; Schwertfeger, W.; Feiring, A.; Smart, B.; Behr, F.; Vogel, H.; McKusick, B.; Kirsch, P. Fluorine Compounds, Organic. in *Ullmann's Encyclopedia of Industrial* Chemistry, Wiley, 2016; pp. 1–56.

(5) Scheele, C. W. Investigations of Fluorite and its Acid. *Kongl. Vetensk. Acad. Handl.* **1771**, *32*, 120–138.

(6) Aigueperse, J.; Mollard, P.; Devilliers, D.; Chemla, M.; Faron, R.; Romano, R.; Cuer, J. P. Fluorine Compounds, Inorganic. in *Ullmann's Encyclopedia of Industrial* Chemistry, Wiley, 2000.

(7) Horowitz, D. This Chemical Kills. Why Aren't Regulators Banning It? *The New York Times*, July 8, 2019.

(8) Patel, C.; André-Joyaux, E.; Leitch, J. A.; Martínez de Irujo-Labalde, X.; Ibba, F.; Strujis, J.; Ellwanger, M. A.; Paton, R.; Browne, D. L.; Pupo, G.; Aldridge, S.; Hayward, M. A.; Gourverneur V. Fluorochemicals from Fluorspar via a Phosphate-Enabled Mechanochemical Process that Bypasses HF. *Science* **2023**, *381*, 302–306.

(9) Haynes, W. M. *CRC Handbook of Chemistry and Physics*, CRC Press, 2014.

(10) Haupt, A. *Organic and Inorganic Fluorine Chemistry: Methods and Applications*, Walter de Gruyter GmbH & Co KG, 2021.

(11) Tarbutton, G.; Egan, E. P.; Frary, S. G. Phosphorus-Halogen Compounds from Phosphorus Pentoxide and Halides. Properties of Phosphorus Trifluoride and Phosphorus Oxyfluoride. *J. Am. Chem. Soc.* **1941**, *63*, 1782–1789.

(12) Jordan, R. K. Carbonyl Fluorination Process. US 4087 475 A, 1978.

(13) Liu, J.; Cai, Y.; Xiao, C.; Zhang, H.; Lv, F.; Luo, C.; Hu, Z.; Cao, Y.; Cao, B.; Yu, L. Synthesis of $LiPF_6$ Using $CaF_2$ as the Fluorinating Agent Directly: An Advanced Industrial Production Process Fully Harmonious to the Environments. *Ind. Eng. Chem. Res.* **2019**, *58*, 20491–20494.

(14) Quan, H.-D.; Tamura, M.; Gao, R.-X.; Sekiya, A. Preparation and Application of Porous Calcium Fluoride—A Novel Fluorinating Reagent and Support of Catalyst. *J. Fluor. Chem.* **2002**, *116*, 65–69.

(15) Liu, F.-Q.; Stalke, D.; Roesky, H. W. $(C_5Me_5)TiF_2$–A Versatile Building Block for Generating Large Soluble Dimetallic Aggregates. *Angew. Chem. Int. Ed. Engl.* **1995**, *34*, 1872– 1874.

(16) Pevec, A.; Demsar, A.; Gramlich, V.; Petricek, S.; Roesky, H. W. Reactions of Molecular $CaF_2$ with $[(C_5Me_5)TiF_3]$ and $[(C_5Me_4Et)TiF_3]$: Symbiosis between Ionic Solids and Organometallic Compounds. *J. Chem. Soc. Dalton Trans.* **1997**, 2215–2216.

(17) Demsar, A.; Pevec, A.; Petriček, S.; Golič, L.; Petrič, A.; Björgvinsson, M.; Roesky, H. W. Calcium Fluoride Incorporated in Soluble Organometallics: Adduct Formation and Solution Dynamics. *J. Chem. Soc. Dalton Trans.* **1998**, 4043–4048.

(18) Nembenna, S.; Roesky, H. W.; Nagendran, S.; Hofmeister, A.; Magull, J.; Wilbrandt, P.-J.; Hahn, M. A Well-Defined Hydrocarbon-Soluble Calcium Monofluoride, $[\{LCaF(thf)\}_2]$: The Application of Soluble Calcium Derivatives for Surface Coating *Angew. Chem. Int. Ed.* **2007**, *46*, 2512–2514.

(19) Barrett, A. G. M.; Crimmin, M. R.; Hill, M. S.; Hitchcock, P. B.; Procopiou, P. A. Trifluoromethyl Coordination and C–F Bond Activation at Calcium. *Angew. Chem. Int. Ed.* **2007**, *46*, 6339–6342.

(20) Deacon, G. B.; Junk, P. C.; Moxey, G. J. Synthesis of Fluoro(aryloxo)alkaline Earth Metal Cages by C–F Bond Activation. *Dalton Trans.* **2010**, *39*, 5620–5622.

(21) Keyzer, E. N.; Matthews, P. D.; Liu, Z.; Bond, A. D.; Grey, C. P.; Wright, D.S. Synthesis of $Ca(PF_6)_2$, Formed *via* Nitrosonium Oxidation of Calcium *Chem. Commun.* **2017**, *53*, 4573–4576.

(22) Schuhknecht, D.; Spaniol, T. P.; Yang, Y.; Maron, L.; Okuda, J. Reactivity of a Molecular Calcium Hydride Cation ($[CaH]^+$) Supported by an NNNN Macrocycle. *Inorg. Chem.* **2020**, *59*, 9406–9415.

(23) Wilson, A. S. S.; Hill, M. S.; Mahon, M. F.; Dinoi, C.; Maron, L. Dehydrohalogenation of Halobenzenes and C($sp^3$)-X (X = F, OPh) Bond Activation by a Molecular Calcium Hydride. *Tetrahedron* **2021**, *82*, 131931.

(24) Sheldon, D. J.; Crimmin, M. R. Repurposing of F-Gases: Challenges and Opportunities in Fluorine Chemistry. *Chem. Soc. Rev.* **2022**, *51*, 4977–4995.

(25) Struijs, J.J.C.; Ellwanger, M. A.; Crumpton, A. E. Enabling Nucleophilic Reactivity in Molecular Calcium Fluoride Complexes. *Nat. Chem.* **2024**, *16*, 1473–1480.

(26) Shetty, D.; Choi, S. Y.; Jeong, J. M.; Lee, J. Y.; Hoigebazar, L.; Lee, Y.-S.; Lee, D. S.; Chung, J.-K.; Lee, M. C. Stable Aluminium Fluoride Chelates with Triazacyclononane Derivatives Proved by X-ray Crystallography and $^{18}$F-Labeling Study. *Chem. Commun.* **2011**, *47*, 9732–9734.

(27) Bhalla, R.; Levason, W.; Luthra, S. K.; McRobbie, G.; Sanderson, G.; Reid, G. Radiofluorination of a Pre-formed Gallium(III) Aza-macrocyclic Complex: Towards Next-Generation Positron Emission Tomography (PET) Imaging Agents *Chem. Eur. J.* **2015**, *21*, 4688–4694.

(28) Trautnitz, M. F. K.; Haas, T.; Schubert, H.; Seitz, M. Unexpected Discovery of Calcium Cryptates with Exceptional Stability *Chem. Commun.* **2020**, *56*, 9874.

(29) Schuhknecht, D.; Spaniol, T. P.; Douair, I.; Maron, L.; Okuda, J. A Tetranuclear Calcium Hydride Cluster with a Highly Symmetric $[Ca_4H_6]^{2+}$ Core. *Chem*. *Commun*. **2019**, *55*, 14837–14839.

(30) Halfen, J. A.; Jazdzewski, B. A.; Mahapatra, S.; Berreau, L. M.; Wilkinson, E. C.; Que, L.; Tolman, W. B. Synthetic Models of the Inactive Copper(II)−Tyrosinate and Active Copper(II)−Tyrosyl Radical Forms of Galactose and Glyoxal Oxidases. *J*. *Am*. *Chem*. *Soc*. **1997**, *119*, 8217–8227.

(31) Schönherr H.; and Cernak, T. Profound Methyl Effects in Drug Discovery and a Call for New C–H Methylation Reactions. *Angew. Chem., Int. Ed.* **2013**, ***52***, 12256–12267.

(32) A. K. Katz, J. P. Glusker, S. A. Beebe, C. W. Bock, Calcium Ion Coordination: A Comparison with that of Beryllium, Magnesium, and Zinc. *J*. *Am*. *Chem*. *Soc*. **1996**, *118*, 5752–5763.

(33) Roesky, H. W.; Keller, K. Trimethyltin Fluoride: A New Fluorinating Reagent for the Preparation of Silicon Fluorides. *J. Fluor. Chem.* **1998**, *89*, 3–4.

(34) Panda, T. K.; Hrib, C. G.; Jones, P. G.; Jenter, J.; Roesky, P. W.; Tamm, M. Rare Earth and Alkaline Earth Metal Complexes with $Me_2Si$-Bridged Cyclopentadienyl-Imidazolin-2-Imine Ligands and Their Use as Constrained-Geometry Hydroamination Catalysts. *Eur. J. Inorg. Chem.* **2008**, 2008, 4270–4279.

(35) Adam, B.; Bill, E.; Bothe, E.; Goerdt, B.; Haselhorst, G.; Hildenbrand, K.; Sokolowski, A.; Steenken, S.; Weyhermüller, T.; Wieghardt, K. Phenoxyl Radical Complexes of Gallium, Scandium, Iron and Manganese. *Chem*. *Eur*. *J*. **1997**, *3*, 308–319.

## 9.6. CONTRIBUTIONS

The following individuals directly contributed to the work described in this Chapter: Omar Apolinar, Job J. C. Struijs, Debotra Sarkar, Prof. Véronique Gouverneur, and Prof. Simon Aldridge. O.A. and S.A. conceived the project. Ligand synthesis was done by O.A. Complexes were synthesized and spectroscopically characterized by O.A. and D.S. X-ray crystallography was mainly carried out by J.J.C.S. Supplementary X-ray crystallography was performed by Liam P. Griffin (L.P.G.), Lewis Wales (L.W.), and Agamemnon E. Crumpton (A.E.C). Reactivity studies of model calcium fluoride complexes were carried out by O.A. The Chapter was adapted with permission from a published manuscript, which was written by O.A., J.J.C.S., and D.S. with input from V.G., and S.A.

# CHAPTER 10

## FUTURE DIRECTIONS AND CONCLUSION

## 10.1. SUMMARY AND PERSPECTIVE

Part II of this Thesis has demonstrated an approach for the synthesis and reactivity of solubilized calcium fluoride complexes stabilized by O-donor ligand frameworks. Chapter 7 starts with background on the inorganic salt calcium difluoride, its physical properties, and role in the chemical industry. Then, the focus shifts to discussing inorganic calcium fluoride complexes, which are found as clusters or cages. Finally, the introduction ends with a section discussing the various solubilized well-defined molecular calcium fluoride complexes found in the chemical literature. Chapter 8 showcases the experimental methods used. Chapter 9 deals with our original research, in which 1,4,7-triazacyclononane-derived (TACN) ligands are leveraged for the synthesis and reactivity of dinuclear calcium mono- and difluoride complexes, supported by X-ray structural characterization and thorough NMR spectroscopic analysis. We think that these discoveries will facilitate future work in developing ligands that stabilize soluble molecular Ca–F complexes, and thus give further insight of our knowledge of the nucleophilicity of the Ca–F bond. Current work in the Aldridge and Gouverneur laboratories is focused on furthering the synthesis of more well-defined calcium fluoride complexes with O-donor ligands. Part II of this Thesis concludes by showcasing the preliminary results of these ongoing efforts.

## 10.2. LEVERAGING BULKY 1,4,7-TRIAZACYCLONONANE LIGANDS FOR MONOMERIC MOLECULAR CALCIUM FLUORIDE COMPLEXES

### 10.2.1. Synthesis of K[(*t*-BuAdmTACN)Ca]

In the previous chapter, we presented our success in synthesizing the monomeric complex [K($\eta^6$-benzene)][(*t*-BuTACN)Ca] **9.2** and being able to desymmetrize it by means of methylation, and then finally introduce fluoride into the newly generated neutral complex. However, we obtained solely dinuclear calcium monofluoride complexes **9.6-9.8** using the one-pot method, and under more carefully designed conditions, we synthesized a dinuclear calcium difluoride complex **9.9**. Experimentally, it was clear that the *tert*-butyl group was not bulky enough to prevent aggregation. It could also be speculated that the methylated phenoxide arm of the ligand is also culpable since it does not possess strong enough Lewis basicity to coordinate to the calcium center and prevent dinucleation. In view of this, we sought to increase the steric bulk of the phenoxide arms of the TACN ligand in the hope of accessing a monomeric calcium fluoride complex.

We were intrigued by reports from the Meyer group in 2004 and 2008, in which they used 1,4,7-tris(3-adamantyl-5-tert-butyl-2-hydroxybenzyl)-1,4,7-triazacyclononane (*t*-BuAdmTACN-$H_3$) to bind to uranium to allow for further reactivity of small organic molecules such as N-heterocyclic carbene (NHC) or diphenyldiazomethane (Scheme 10.1).[1,2] The authors disclose that such generated (*t*-BuAdmTACN)U complexes remain monomeric even after such reactions as determined by single crystal X-ray diffraction.

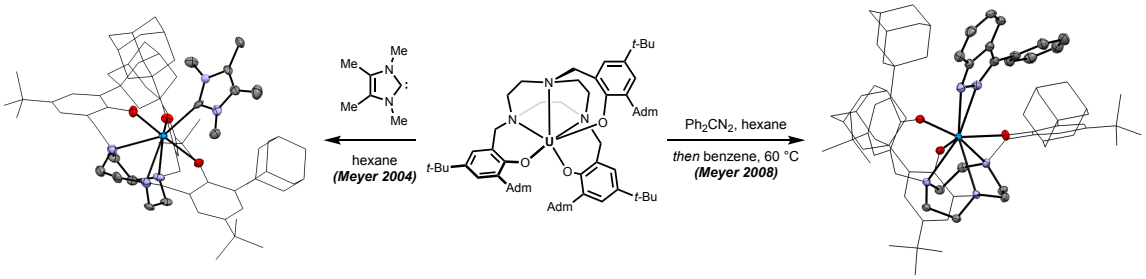


***Scheme 10.1.*** A uranium complex supported by (*t*-BuAdmTACN) and its reactivity thereof.

Inspired by these works, we elected *t*-BuAdmTACN as a promising TACN ligand to potentially afford a terminal calcium fluoride complex. We initiated the investigation by synthesizing the target (*t*-BuAdmTACN-$H_3$) protio-ligand **10.1** which was achieved by a classical Mannich reaction albeit in a low yield since the 1,4,7-triazacyclononane (TACN)·3HCl salt was used instead of 1,4,7-triazacyclononane (TACN-$H_3$) (Scheme 10.2). Next, we reacted ligand **10.1** with one equivalent of both $Ca(HMDS)_2(THF)_2$ and K[HMDS] in benzene which afforded K[(*t*-BuAdmTACN)Ca] **10.2** in a moderate yield (63%). Unlike complex **9.2**, the synthesized complex **10.2** did not crystallize out as a benzene solvate. In fact, at this point in time, no conditions have been found to obtain crystals suitable for X-ray crystallography.

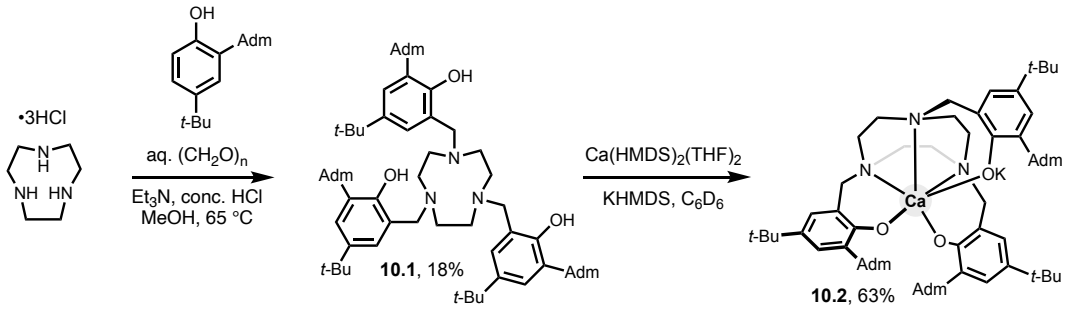


***Scheme 10.2.*** Synthesis of (*t*-BuAdmTACN) **10.1** and complex K[(*t*-BuAdmTACN)Ca] **10.2**.

### 10.2.2. Desymmetrization Attempts with K[(*t*-BuAdmTACN)Ca]

With complex **10.2** in hand, we next sought to desymmetrize it using the same methylation conditions used for complex **9.2**. To our surprise, the use of methyl iodide with complex **10.2** led to the formation of intractable product mixtures (Scheme 10.3). We employed other methylating reagents, such as methyl triflate and dimethyl sulfate, but to no avail. Treatment of complex **10.2** with other functionalizing reagents such as $Me_3SnF$ or 1-adamantanecarbonyl chloride favored the formation of the metathesis product whereas use of tosyl chloride gave no reaction. Gratifyingly, however, when trimethyloxonium tetrafluoroborate $[Me_3O][BF_4]$ was reacted with **10.2**, a new unsymmetrical species was observed, which we formulate as (*t*-BuAdmTACN-Me)Ca **10.3**. However, the formed complex is generated within a mixture of starting material and other unknown side products, plus the reaction with $[Me_3O][BF_4]$ is not easily reproducible due to its high reactivity profile. It is also worth noting that no conditions have also been found to grow crystals suitable for X-ray diffraction.

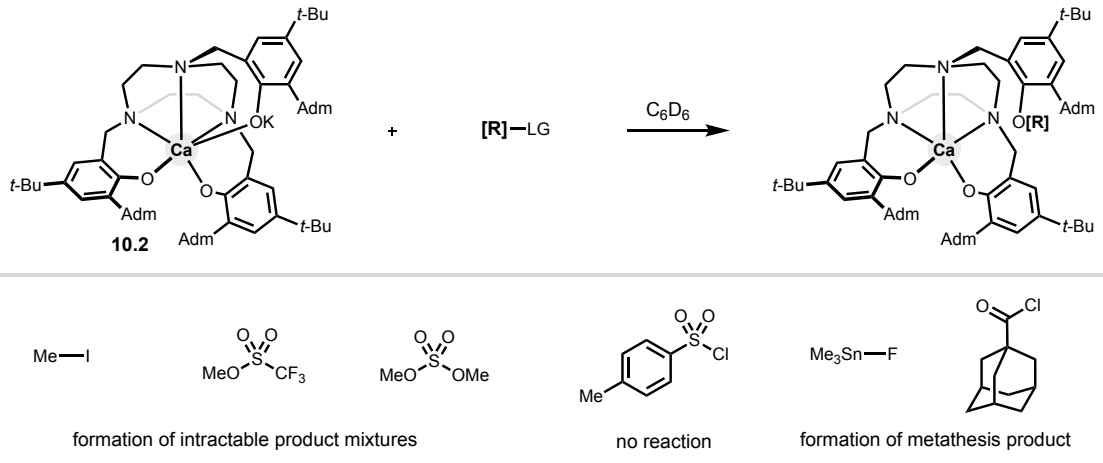


***Scheme 10.3.*** Desymmetrization attempts of complex K[(*t*-BuAdmTACN)Ca] **10.2**.

### 10.2.3. Fluorination Attempts with (*t*-BuAdmTACN-Me)Ca

Although we could only form desymmetrized complex **10.3** *in situ*, we went ahead in the hopes of successfully introducing a fluoride anion into the complex analogous to the work done by Meyer and colleagues. Therefore, complex **10.3** was subjected to the KF/2.2.2-cryptand fluorinating combination but this failed to give the desired monomeric calcium fluoride complex **10.4** (Scheme 10.4). Employment of the TMAF fluorinating reagent was deemed not to be effective either. We postulate that (*t*-BuAdmTACN-Me)Ca **10.3** possesses too much steric bulk or not enough fluorophilicity to take up fluoride. Current efforts in attempting to introduce fluoride are currently being carried out.

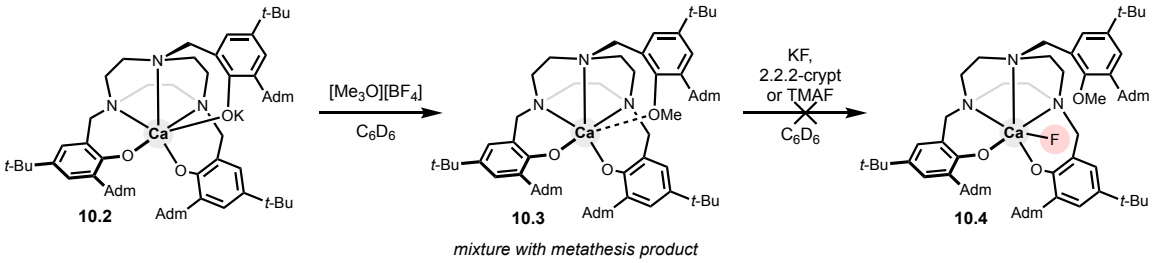


***Scheme 10.4.*** Telescoping fluorination experiment of complex (*t*-BuAdmTACN-Me)Ca **10.3**.

## 10.3. PROGRESS TOWARDS ACYCLIC MOLECULAR CALCIUM FLUORIDES USING AN O-DONOR BORYLOXY LIGAND

### 10.3.1. Synthesis of $Ca(OB(NDippCH)_2(THF)_2$

Based on the discussion revolving around solubilized molecular calcium fluoride complexes in the previous chapters, most of the work has been carried out with ligand frameworks that stabilize calcium in a cyclic fashion. This makes sense when one considers the high equilibrium constant favored for intramolecular binding ($K_{eq} \sim 10^5$ per

chelate ring) when compared to intermolecular binding at least for transition metals.[3] We were still interested in pursuing the synthesis of solubilized molecular calcium fluoride complexes using a monodentate O-donating ligand in hopes to furnish an acyclic variant. Recent work from our group leveraged N-heterocyclic boryloxy (NHBO) ligand to form acyclic group 13 anionic bis(boryloxy) complexes ([E(OB(NDippCH)$_2$]$^-$, E = Al, Ga, In), which were shown to exhibit excellent stability yet possess a reactive group 13 atom center (Scheme 10.5).[4,5]

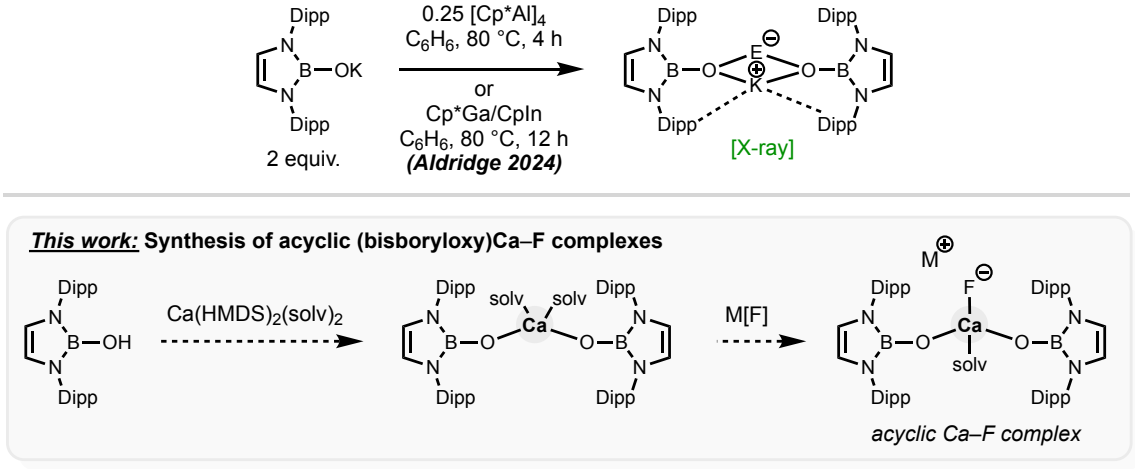


***Scheme 10.5.*** Precedents with N-heterocyclic boryloxy and synopsis of inspired work.

Inspired by this work, we elected HOB(NDippCH)$_2$ **10.5** as the O-donating ligand and reacted it with Ca(HMDS)$_2$(THF)$_2$ in equimolar amounts in benzene to afford Ca(OB(NDippCH)$_2$)$_2$(THF)$_2$ **10.6** in a good yield. The complex was easily isolable by trituration with hexanes and further crystallization could be achieved by leaving the mother liquor in a –35 °C freezer. Single crystals were obtained by slow evaporation from benzene. X-ray crystallography confirmed its structural integrity and revealed that the complex features a distorted tetrahedral geometry with identical Ca–O bond lengths provided by the boryloxy ligand.

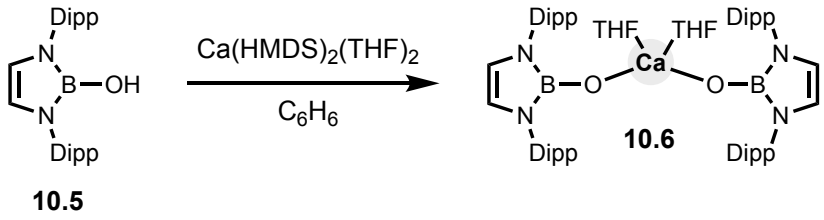


***Scheme 10.6***. Synthesis and structure of calcium complex **10.6**.

### 10.3.2. Fluorination Attempts of $Ca(OB(NDippCH)_2(THF)_2$

With neutral complex **10.6** in hand, we next attempted to subject it to previously used fluorination conditions given that the calcium center likely has a high fluorophilicity. We initially used the commonly employed KF/2.2.2-cryptand fluorinating combination, which upon reaction with complex **10.6**, no $^{19}F$ NMR signal was observed but $^{1}H$ NMR revealed the complex to be consumed. Colorless single crystals precipitated out of solution, which were suitable for X-ray crystallography and revealed the chemical structure to be [K(2.2.2-crypt)][$Ca(OB(NDippCH)_2)_3(THF)$] **10.7** as the major resulting species. This complex likely forms on the basis of the ability of the monodentate boryloxy ligand to migrate intermolecularly and draws on $CaF_2$ as a thermodynamic sink. Treatment of complex **10.6** with TMAF afforded a similar species ([$NMe_4$][$Ca(OB(NDippCH)_2)_3(THF)$] **10.8)** as determined by $^{1}H$ NMR spectroscopy from analysis of the integration of $[NMe_4]^+$ cation and boryloxy ligand backbone.

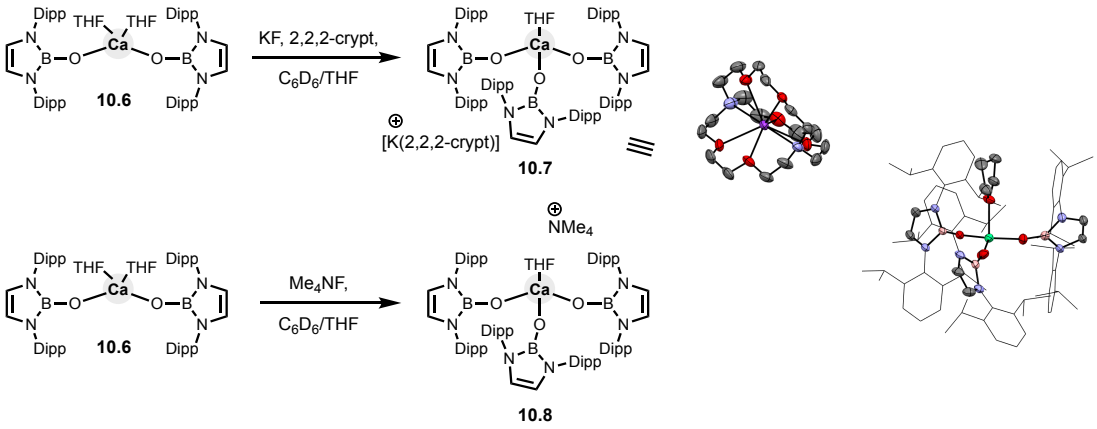


***Scheme 10.7***. Initial fluorination attempts of calcium complex **10.6**.

On the other hand, reaction with $Me_3SnF$ gave a $^{19}F$ NMR signal at -65.2 ppm, but $^{1}H$ NMR monitoring showed that another species was present that did not contain any fluoride. Single crystals were grown by slow evaporation of a concentrated solution in hexane, which were suitable for X-ray crystallography, but they were revealed to be the side product $Me_3SnOB(NDippCH)_2$ **10.10**. Thus, we postulate that the fluoride-containing species is likely be $\{(\mu\text{-}F)Ca(OB(NDippCH)_2)_2(THF)\}_2$ **10.9**. Such a dimeric complex is reasonable since it is analogous to the dimeric calcium fluoride complexes first synthesized by Roesky and Barrett and Hill but with the NacNac ligand system.[6,7] However, at this time, no conditions have been found to favor crystallization of complex **10.9** to give unequivocal structural determination. Current efforts on this front are currently continuing.

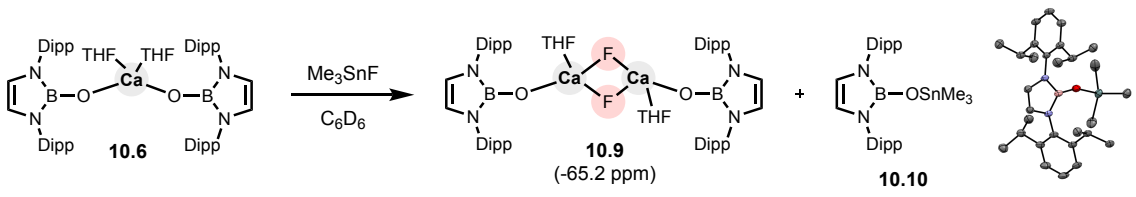


***Scheme 10.8***. Fluorination of calcium complex **10.6** with $Me_3SnF$.

## 10.4. CONCLUSIONS

Part II of this Thesis has reported on recent efforts towards understanding the nucleophilicity of the Ca–F bond from a solubilized calcium fluoride complex. Leveraging the TACN ligand, we were able to synthesize well-defined monomeric anionic and neutral TACN complexes that may further greatly impact group 2 chemistry as well. In addition, the newly developed desymmetrization method of the (*t*-BuTACN)Ca complex may also extend to other alkaline earth metals enabling chemistry that would otherwise not be plausible. Synthesis of the desymmetrized (*t*-BuTACN)Ca complex **9.4**, has allowed leeway for the generation of several dinuclear calcium mono- and difluoride complexes **9.6**-**9.9**, which exhibit intriguing structural properties as confirmed by X-ray crystallography and NMR spectroscopy. We found enhanced reactivity of a representative dinuclear calcium monofluoride complex (**9.6**) upon the use of electrophilic reagents compared to the corresponding variant with the NON ligand which showcases that oxygenic ligand frameworks are more stabilizing for calcium than amido-based ligands. Thus, calcium fluoride complexes with O-donor ligands are the way forward and may be applicable to other areas such as in mechanical activation of $CaF_2$. We were also able to observe direct exchange between the fluoride anion from the dinuclear calcium monofluoride complex and a chloride-containing electrophile indicating that nucleophilicity is not just possible but favored.

More recently, new projects have emerged whereby modification of the TACN ligand to a bulkier variant has been used in the hope of preventing aggregation and forge terminal molecular calcium fluoride species. Unfortunately, we fell short in achieving the goal since the introduced adamantyl substituent likely provides too much steric bulk

preventing the fluoride anion to bind to calcium. A less sterically bulky variant may be the road to pursue in this sector. We also strived to obtain an acyclic molecular calcium fluoride analogous to those previously reported. Thus far, we have been able to arrive at a dimeric calcium fluoride species with the N-heterocyclic boryloxy ligand as determined by NMR spectroscopy. Further work on structural characterization would greatly push this project forward and make an impact to the field as the first acyclic ligand-supported molecular calcium fluoride complex.

Moving forward, it is foreseen that this research program will continue to grow in expanding the repertoire of solubilized well-defined calcium fluoride complexes. It is apparent that the avenue should focus more on ligand design for optimal stability and reactivity. All of the discussed findings in Part II of this thesis and those that will come thereafter will greatly impact the way that we envision calcium fluoride chemistry and open new applications for fluoride delivery.

## 10.5. REFERENCES

(1) Nakai, H.; Hu, X.; Zakharov, L. N.; Rheingold, A. L.; Meyer, K. Synthesis and Characterization of N-Heterocyclic Carbene Complexes of Uranium(III). *Inorg. Chem.* **2004**, *43*, 855–857.

(2) Lam. O. P.; Feng, P. L.; Heinemann, F. W.; O'Connor, J. M.; Meyer, K. Charge-Separation in Uranium Diazomethane Complexes Leading to C−H Activation and Chemical Transformation *J. Am. Chem. Soc.* **2008**, *130*, 2806–2816.

(3) Crabtree, R. H. *The Organometallic Chemistry of the Transition Metals*; John Wiley & Sons, 2014.

(4) Sarkar, D.; Vasko, P.; Roper, A. F.; Crumpton, A. E.; Roy, M. M. D.; Griffin, L. P.; Bogle, C.; Aldridge S. Reversible [4 + 1] Cycloaddition of Arenes by a "Naked" Acyclic Aluminyl Compound *J. Am. Chem. Soc.* **2024**, *146*, 11792–11800.

(5) Sarkar, D.; Vasko, P.; Gluharev, T.; Griffin, L. P.; Bogle, C.; Struijs, J.; Tang, J.; Roper, A. F.; Crumpton, A. E.; Aldridge, S. Synthesis, Isolation, and Reactivity Studies of 'Naked' Acyclic Gallyl and Indyl Anions. *Angew. Chem. Int. Ed.* **2024**, *63*, e202407427.

(6) Nembenna, S.; Roesky, H. W.; Nagendran, S.; Hofmeister, A.; Magull, J.; Wilbrandt, P.-J.; Hahn, M. A Well-Defined Hydrocarbon-Soluble Calcium Monofluoride, [{LCaF(thf)}$_2$]: The Application of Soluble Calcium Derivatives for Surface Coating *Angew. Chem. Int. Ed.* **2007**, *46*, 2512–2514.

(7) Barrett, A. G. M.; Crimmin, M. R.; Hill, M. S.; Hitchcock, P. B.; Procopiou, P. A. Trifluoromethyl Coordination and C–F Bond Activation at Calcium. *Angew. Chem. Int. Ed.* **2007**, *46*, 6339–6342.

# APPENDIX I

X-RAY CRYSTALLOGRAPHY DATA

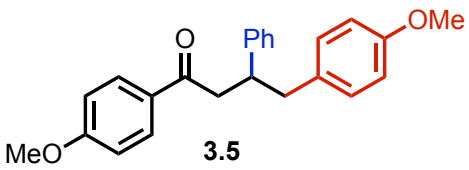


**3.5**

**1,4-Bis(4-methoxyphenyl)-3-phenylbutan-1-one (3.5):**

**X-ray** (single-crystal) Colorless needle crystals of X-ray diffraction quality were obtained by slow evaporation of a saturated solution of **3.5** in $Et_2O$.

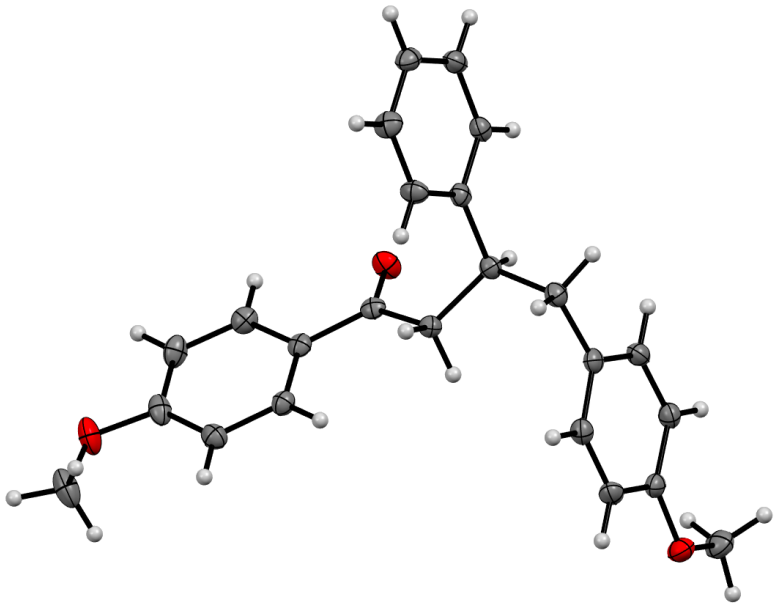

# Crystal Data

| | | |
|---|---|---|
| CCDC Number | 1957926 | |
| Empirical formula | $C_{24}H_{24}O_3$ | |
| Formula weight | 360.43 | |
| Temperature | 100.0 K | |
| Wavelength | 1.54184 Å | |
| Crystal system | Monoclinic | |
| Space group | P 21/c | |
| Unit cell dimensions | a = 21.21(2) Å | α = 90°. |
| | b = 5.590(5) Å | β = 103.88(3)°. |
| | c = 16.363(16) Å | γ = 90°. |
| Volume | 1883(3) $Å^3$ | |
| Z | 4 | |
| Density (calculated) | 1.271 $Mg/m^3$ | |
| Absorption coefficient | 0.655 $mm^{-1}$ | |
| F(000) | 768 | |
| Crystal size | 0.26 x 0.25 x 0.08 $mm^3$ | |
| Theta range for data collection | 2.146 to 68.478°. | |
| Index ranges | -25<=h<=25, -6<=k<=6, -15<=l<=19 | |

| | |
|---|---|
| Reflections collected | 10855 |
| Independent reflections | 3418 [R(int) = 0.0267] |
| Completeness to theta = 67.684° | 99.1 % |
| Absorption correction | Semi-empirical from equivalents |
| Max. and min. transmission | 0.7531 and 0.6764 |
| Refinement method | Full-matrix least-squares on $F^2$ |
| Data / restraints / parameters | 3418 / 0 / 246 |
| Goodness-of-fit on $F^2$ | 1.085 |
| Final R indices [I>2sigma(I)] | R1 = 0.0351, wR2 = 0.0933 |
| R indices (all data) | R1 = 0.0393, wR2 = 0.0969 |
| Extinction coefficient | n/a |
| Largest diff. peak and hole | 0.211 and -0.236 e.Å$^{-3}$ |

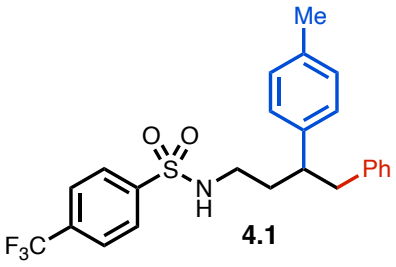


**4.1**

***N*-(4-phenyl-3-(*p*-tolyl)butyl)-4-(trifluoromethyl)benzenesulfonamide (4.1)**:

**X-ray** (single-crystal) Colorless block crystals of X-ray diffraction quality were obtained by vapor diffusion of pentane to a saturated solution of **4.1** in benzene.

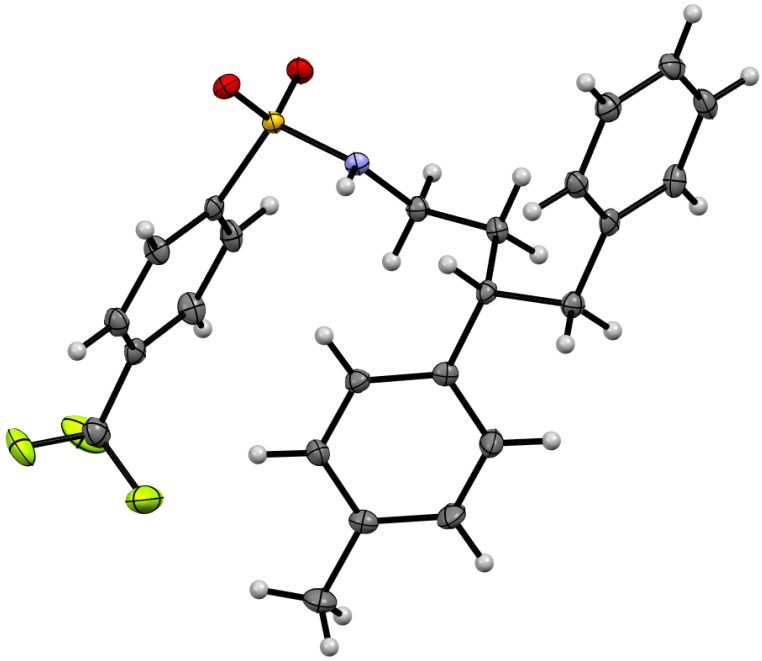

# Crystal Data

| | | |
|---|---|---|
| CCDC Number | 2011491 | |
| Empirical formula | $C_{24}H_{24}F_3NO_2S$ | |
| Formula weight | 447.50 | |
| Temperature | 100.0 K | |
| Wavelength | 0.71073 Å | |
| Crystal system | Monoclinic | |
| Space group | P 1 21/n 1 | |
| Unit cell dimensions | a = 16.6732(7) Å | α = 90°. |
| | b = 7.8057(3) Å | β = 103.9000(10)°. |
| | c = 16.9323(7) Å | γ = 90°. |
| Volume | 2139.14(15) $Å^3$ | |
| Z | 4 | |
| Density (calculated) | 1.390 $Mg/m^3$ | |
| Absorption coefficient | 0.199 $mm^{-1}$ | |
| F(000) | 936 | |
| Crystal size | 0.2 x 0.1 x 0.08 $mm^3$ | |
| Theta range for data collection | 2.889 to 25.683°. | |
| Index ranges | -20<=h<=12, -8<=k<=9, -19<=l<=20 | |
| Reflections collected | 12263 | |
| Independent reflections | 4067 [R(int) = 0.0298] | |
| Completeness to theta = 25.242° | 99.9 % | |
| Absorption correction | Analytical | |
| Max. and min. transmission | 0.7453 and 0.6625 | |
| Refinement method | Full-matrix least-squares on $F^2$ | |
| Data / restraints / parameters | 4067 / 0 / 284 | |
| Goodness-of-fit on $F^2$ | 1.027 | |
| Final R indices [I>2sigma(I)] | R1 = 0.0363, wR2 = 0.0842 | |
| R indices (all data) | R1 = 0.0494, wR2 = 0.0903 | |
| Extinction coefficient | n/a | |
| Largest diff. peak and hole | 0.294 and -0.415 $e.Å^{-3}$ | |

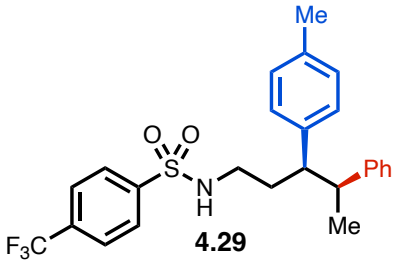

**4.29**

***N*-4-phenyl-3-(*p*-tolyl)pentyl)-4-(trifluoromethyl)benzenesulfonamide (4.29):**

**X-ray** (single-crystal) Colorless block crystals of X-ray diffraction quality were obtained by vapor diffusion of hexane to a saturated solution of **4.29** in benzene.

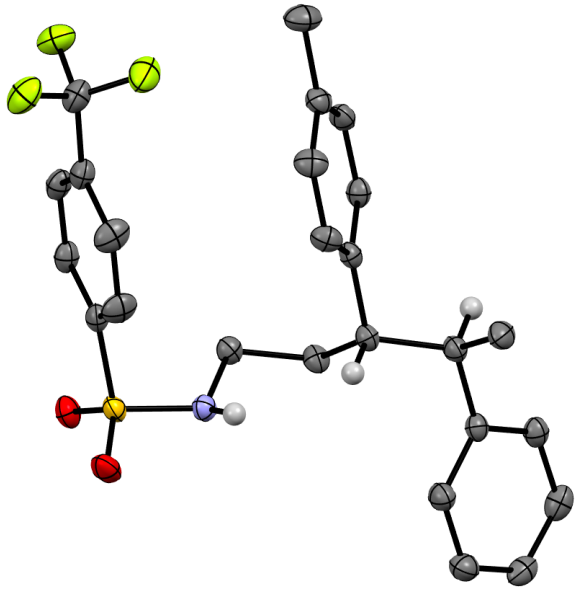

# Crystal Data

| | | |
|---|---|---|
| CCDC Number | 2011492 | |
| Empirical formula | $C_{25}H_{26}F_3NO_2S$ | |
| Formula weight | 461.53 | |
| Temperature | 100.0 K | |
| Wavelength | 1.54178 Å | |
| Crystal system | Monoclinic | |
| Space group | C 1 21/c 1 | |
| Unit cell dimensions | a = 28.1491(7) Å | α = 90°. |
| | b = 9.7037(3) Å | β = 123.7560(10)°. |
| | c = 19.9138(5) Å | γ = 90°. |
| Volume | 4522.4(2) $Å^3$ | |
| Z | 8 | |
| Density (calculated) | 1.356 $Mg/m^3$ | |
| Absorption coefficient | 1.682 $mm^{-1}$ | |
| F(000) | 1936 | |
| Crystal size | 0.175 x 0.15 x 0.12 $mm^3$ | |
| Crystal color, habit | colorless block | |
| Theta range for data collection | 3.777 to 69.496°. | |
| Index ranges | -33<=h<=33, -11<=k<=11, -24<=l<=21 | |
| Reflections collected | 32376 | |
| Independent reflections | 4121 [R(int) = 0.0375] | |
| Completeness to theta = 25.242° | 98.4 % | |
| Absorption correction | Semi-empirical from equivalents | |
| Max. and min. transmission | 0.7532 and 0.6812 | |
| Refinement method | Full-matrix least-squares on $F^2$ | |

| | |
|---|---|
| Data / restraints / parameters | 4121 / 1 / 294 |
| Goodness-of-fit on $F^2$ | 1.021 |
| Final R indices [I>2sigma(I)] | R1 = 0.0341, wR2 = 0.0858 |
| R indices (all data) | R1 = 0.0391, wR2 = 0.0898 |
| Largest diff. peak and hole | 0.475 and -0.425 e.Å$^{-3}$ |

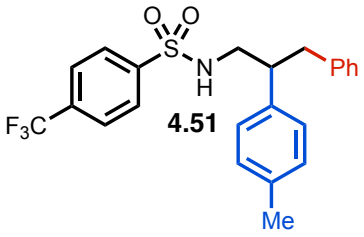


***N*-(3-phenyl-2-(*p*-tolyl)propyl)-4-(trifluoromethyl)benzenesulfonamide (4.51):**

**X-ray** (single-crystal) Colorless block crystals of X-ray diffraction quality were obtained by vapor diffusion of hexane to a saturated solution of **4.51** in benzene.

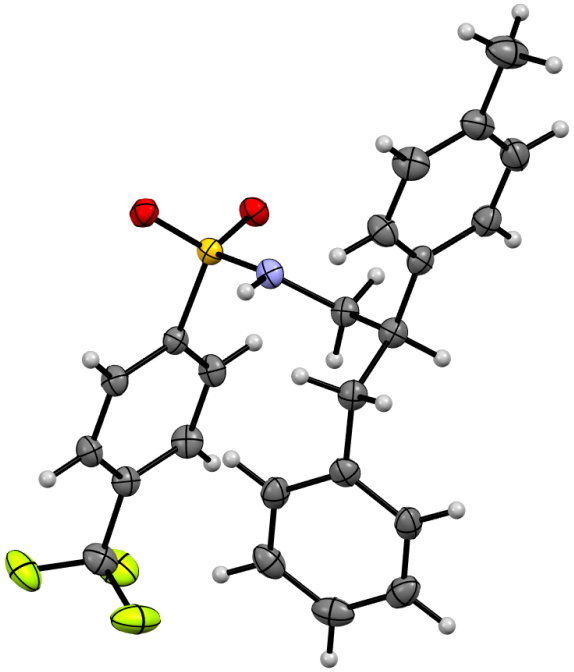

# Crystal Data

| | |
|---|---|
| CCDC Number | 2039700 |
| Empirical formula | $C_{23}H_{22}F_3NO_2S$ |
| Formula weight | 433.47 |
| Temperature | 100.0 K |
| Wavelength | 1.54178 Å |
| Crystal system | Triclinic |
| Space group | P-1 |

| | | |
|---|---|---|
| Unit cell dimensions | a = 9.6838(2) Å | α = 100.8930(10)°. |
| | b = 10.9311(2) Å | β = 102.7520(10)°. |
| | c = 11.3356(2) Å | γ = 115.0350(10)°. |
| Volume | 1004.78(3) $Å^3$ | |
| Z | 2 | |
| Density (calculated) | 1.433 $Mg/m^3$ | |
| Absorption coefficient | 1.857 $mm^{-1}$ | |
| F(000) | 452 | |
| Crystal size | 0.22 x 0.1 x 0.08 $mm^3$ | |
| Theta range for data collection | 4.220 to 70.268°. | |
| Index ranges | -11<=h<=11, -12<=k<=13, -13<=l<=13 | |
| Reflections collected | 6655 | |
| Independent reflections | 3672 [R(int) = 0.0148] | |
| Completeness to theta = 67.679° | 97.0 % | |
| Absorption correction | None | |
| Refinement method | Full-matrix least-squares on $F^2$ | |
| Data / restraints / parameters | 3672 / 0 / 275 | |
| Goodness-of-fit on $F^2$ | 1.059 | |
| Final R indices [I>2sigma(I)] | R1 = 0.0349, wR2 = 0.0947 | |
| R indices (all data) | R1 = 0.0368, wR2 = 0.0959 | |
| Extinction coefficient | n/a | |
| Largest diff. peak and hole | 0.425 and -0.382 $e.Å^{-3}$ | |

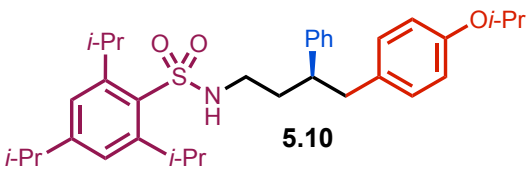


**5.10**

**(*S*)-*N*-(4-(4-isopropoxyphenyl)-3-phenylbutyl)-2,4,6-triisopropylbenzenesulfonamide (5.10):**

**X-ray** (single-crystal) Colorless crystals of X-ray diffraction quality were obtained by recrystallization of **5.10** in hexanes.

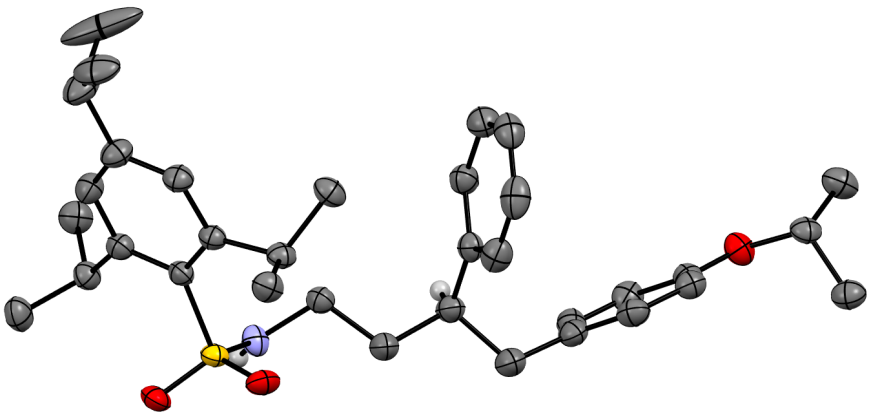

# Crystal Data

| | | |
|---|---|---|
| CCDC Number | 2150217 | |
| Empirical formula | $C_{34}H_{47}NO_3S$ | |
| Formula weight | 549.78 | |
| Temperature | 100.15 K | |
| Wavelength | 1.54178 Å | |
| Crystal system | Monoclinic | |
| Space group | P 1 21 1 | |
| Unit cell dimensions | a = 13.7427(10) Å | α = 90°. |
| | b = 6.1971(7) Å | β = 91.133(5)°. |
| | c = 18.8047(18) Å | γ = 90°. |
| Volume | 1601.2(3) $Å^3$ | |
| Z | 2 | |
| Density (calculated) | 1.140 $Mg/m^3$ | |
| Absorption coefficient | 1.142 $mm^{-1}$ | |
| F(000) | 596 | |
| Crystal size | 0.24 x 0.03 x 0.03 $mm^3$ | |
| Theta range for data collection | 2.350 to 70.522°. | |
| Index ranges | -16<=h<=16, -7<=k<=7, -22<=l<=21 | |
| Reflections collected | 19461 | |
| Independent reflections | 6006 [R(int) = 0.0620] | |
| Completeness to theta = 67.679° | 99.9 % | |
| Absorption correction | Semi-empirical from equivalents | |
| Max. and min. transmission | 0.7533 and 0.5524 | |
| Refinement method | Full-matrix least-squares on $F^2$ | |
| Data / restraints / parameters | 6006 / 1 / 360 | |
| Goodness-of-fit on $F^2$ | 1.035 | |
| Final R indices [I>2sigma(I)] | R1 = 0.0519, wR2 = 0.1300 | |
| R indices (all data) | R1 = 0.0629, wR2 = 0.1388 | |
| Absolute structure parameter | 0.00(2) | |
| Largest diff. peak and hole | 0.411 and -0.509 $e.Å^{-3}$ | |

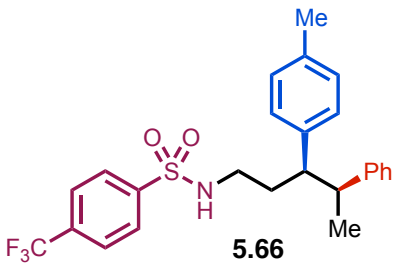

**5.66**

***N*-((3*R*,4*S*)-4-phenyl-3-(*p*-tolyl)pentyl)-4-(trifluoromethyl)benzenesulfonamide (5.66):**

**X-ray** (single-crystal) Colorless crystals of X-ray diffraction quality were obtained by recrystallization of **5.66** in hexanes.

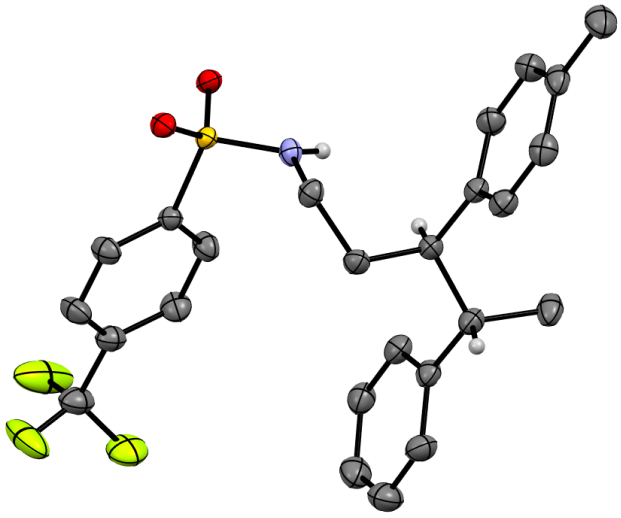

# Crystal Data

| | | |
|---|---|---|
| Identification code | Engle433 | |
| Empirical formula | $C_{25}H_{26}F_3NO_2S$ | |
| Molecular formula | $C_{25}H_{26}F_3NO_2S$ | |
| Formula weight | 461.53 | |
| Temperature | 100.15 K | |
| Wavelength | 1.54178 Å | |
| Crystal system | Triclinic | |
| Space group | P1 | |
| Unit cell dimensions | a = 10.6804(8) Å | α = 82.420(3)°. |
| | b = 14.9420(11) Å | β = 71.733(2)°. |
| | c = 16.4296(12) Å | γ = 72.379(3)°. |
| Volume | 2371.0(3) $Å^3$ | |
| Z | 4 | |
| Density (calculated) | 1.293 $Mg/m^3$ | |
| Absorption coefficient | 1.604 $mm^{-1}$ | |
| F(000) | 968 | |
| Crystal size | 0.24 x 0.125 x 0.1 $mm^3$ | |
| Crystal color, habit | colorless block | |
| Theta range for data collection | 2.835 to 70.277°. | |
| Index ranges | -13<=h<=13, -18<=k<=18, -20<=l<=20 | |
| Reflections collected | 97003 | |
| Independent reflections | 17266 [R(int) = 0.0397] | |
| Completeness to theta = 67.679° | 98.4% | |
| Absorption correction | Semi-empirical from equivalents | |
| Max. and min. transmission | 0.7533 and 0.6899 | |
| Refinement method | Full-matrix least-squares on $F^2$ | |
| Data / restraints / parameters | 17266 / 7 / 1173 | |

| | |
|---|---|
| Goodness-of-fit on $F^2$ | 1.026 |
| Final R indices [I>2sigma(I)] | R1 = 0.0293, wR2 = 0.0762 |
| R indices (all data) | R1 = 0.0303, wR2 = 0.0770 |
| Absolute structure parameter | 0.044(3) |
| Largest diff. peak and hole | 0.392 and -0.345 e.Å$^{-3}$ |

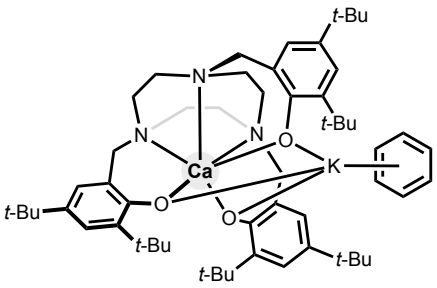


**[K(η$^6$-benzene)][(*t*-BuTACN)Ca] (9.2):**

**X-ray** (single-crystal) To a J-Young NMR tube was added **9.1** (20 mg, 25.50 µmol), Ca(HMDS)$_2$(THF)$_2$ (12.88 mg, 25.50 µmol), K[HMDS (5.09 mg, 25.50 µmol) and 0.5 mL of $C_6D_6$. The reaction was allowed to proceed at room temperature, and after 1 d, colorless crystals of complex **9.2** were obtained, which were suitable for X-ray crystallography.

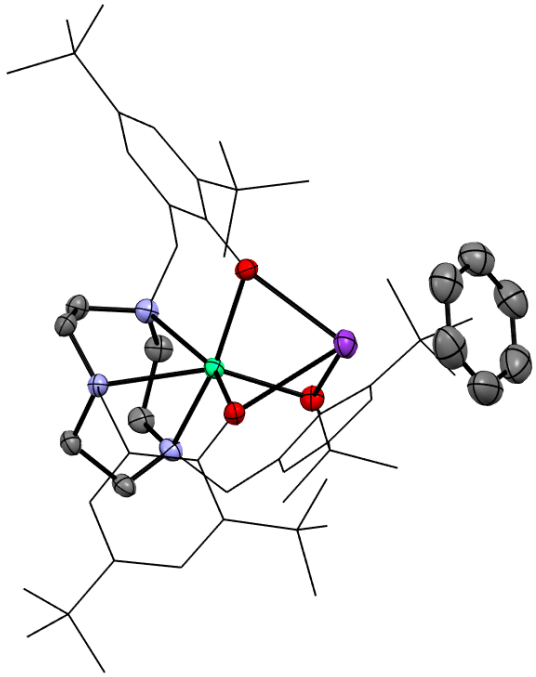

# Crystal Data

| | |
|---|---|
| CCDC Number | 2356741 |
| Empirical formula | $C_{63}H_{90}CaKN_3O_3$ |
| Formula weight | 1016.56 |
| Temperature/K | 150 (10) |
| Crystal system | monoclinic |
| Space group | $P2_1/n$ |

| | |
|---|---|
| a/Å | 19.8547(3) |
| b/Å | 15.1276(2) |
| c/Å | 19.8908(3) |
| α/° | 90 |
| β/° | 92.033(2) |
| γ/° | 90 |
| Volume/Å$^3$ | 5970.52(15) |
| Z | 4 |
| $\rho_{calc}$g/cm$^3$ | 1.131 |
| μ/mm$^{-1}$ | 1.866 |
| F(000) | 2208.0 |
| Crystal size/mm$^3$ | 0.25 × 0.25 × 0.1 |
| Radiation | Cu Kα (λ = 1.54184) |
| 2Θ range for data collection/° | 7.344 to 153.1 |
| Index ranges | -23 ≤ h ≤ 25, -15 ≤ k ≤ 19, -24 ≤ l ≤ 24 |
| Reflections collected | 66897 |
| Independent reflections | 12405 [$R_{int}$ = 0.0371, $R_{sigma}$ = 0.0248] |
| Data/restraints/parameters | 12405/185/704 |
| Goodness-of-fit on F$^2$ | 1.017 |
| Final R indexes [I>=2σ (I)] | $R_1$ = 0.0323, $wR_2$ = 0.0804 |
| Final R indexes [all data] | $R_1$ = 0.0407, $wR_2$ = 0.0866 |
| Largest diff. peak/hole / e Å$^{-3}$ | 0.305/-0.289 |

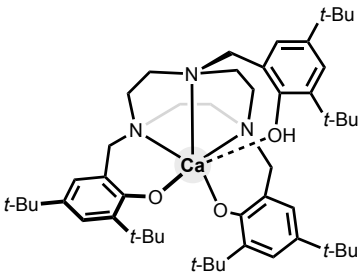


**(*t*-BuTACN-H)Ca (9.3):**

**X-ray** (single-crystal) To a J-Young NMR tube was added **9.1** (20 mg, 25.50 μmol), $Ca(HMDS)_2(THF)_2$ (12.88 mg, 25.50 μmol) and 0.5 mL of $C_6D_6$. The reaction was allowed to proceed until full conversion to **3** was observed by $^1$H NMR spectroscopy. After this time, volatiles were removed under reduced pressure yielding a crude yellow oil to which was added hexane, and the concentrated solution immediately placed in an oil bath at 80 °C. After 1 d, colorless crystals of **9.3** were obtained, which were suitable for X-ray crystallography.

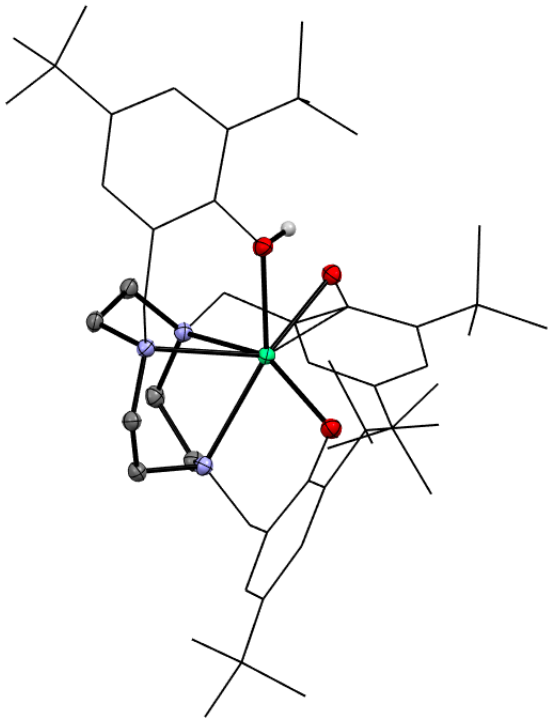

# Crystal Data

| | |
|---|---|
| CCDC Number | 2356742 |
| Empirical formula | $C_{51}H_{79}CaN_3O_3$ |
| Formula weight | 822.25 |
| Temperature/K | 100 (10) |
| Crystal system | monoclinic |
| Space group | $P2_1/n$ |
| a/Å | 16.89147 (14) |
| b/Å | 15.37922 (12) |
| c/Å | 19.54836 (17) |
| α/° | 90 |
| β/° | 101.8707 (9) |
| γ/° | 90 |
| Volume/Å$^3$ | 4969.63 (7) |
| Z | 4 |
| $\rho_{calc}$g/cm$^3$ | 1.099 |
| μ/mm$^{-1}$ | 0.168 |
| F(000) | 1800.0 |
| Crystal size/mm$^3$ | 0.25 × 0.24 × 0.15 |
| Radiation | Mo Kα (λ = 0.71073) |

| | |
|---|---|
| 2Θ range for data collection/° | 3.932 to 54.968 |
| Index ranges | $-21 \leq h \leq 21, -19 \leq k \leq 19, -25 \leq l \leq 25$ |
| Reflections collected | 159008 |
| Independent reflections | 11378 [$R_{int}$ = 0.0342, $R_{sigma}$ = 0.0136] |
| Data/restraints/parameters | 11378/360/545 |
| Goodness-of-fit on $F^2$ | 1.033 |
| Final R indexes [I>=2σ (I)] | $R_1$ = 0.0318, $wR_2$ = 0.0814 |
| Final R indexes [all data] | $R_1$ = 0.0372, $wR_2$ = 0.0853 |
| Largest diff. peak/hole / e $Å^{-3}$ | 0.335/-0.235 |

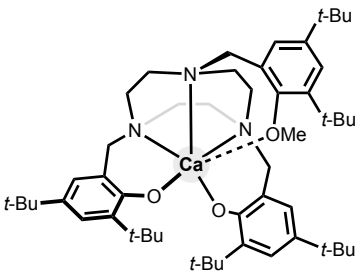


**(*t*-BuTACN-Me)Ca(OMe) (9.4):**

**X-ray** (single-crystal) Complex **9.4** (100 mg, 119.57 µmol) and 1 mL of toluene were loaded into a lambda tube. Slow evaporation over a period of 5 d led to the formation of colorless crystals of **9.4**, which were suitable for X-ray crystallography.

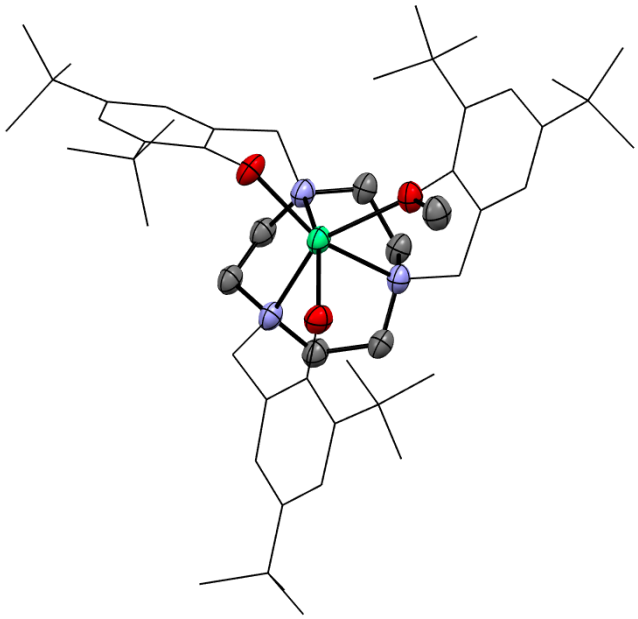

# Crystal Data

| | |
|---|---|
| CCDC Number | 2356743 |
| Empirical formula | $C_{59}H_{89}CaN_3O_3$ |
| Formula weight | 928.41 |
| Temperature/K | 100(10) |

| | |
|---|---|
| Crystal system | orthorhombic |
| Space group | *P*na2$_1$ |
| a/Å | 39.4007(6) |
| b/Å | 14.5413(2) |
| c/Å | 9.82760(10) |
| α/° | 90 |
| β/° | 90 |
| γ/° | 90 |
| Volume/Å$^3$ | 5630.60(13) |
| Z | 4 |
| $\rho_{calc}$g/cm$^3$ | 1.095 |
| μ/mm$^{-1}$ | 1.285 |
| F(000) | 2032.0 |
| Crystal size/mm$^3$ | 0.1 × 0.02 × 0.02 |
| Radiation | Cu Kα (λ = 1.54184) |
| 2Θ range for data collection/° | 4.486 to 177.588 |
| Index ranges | -48 ≤ h ≤ 49, -18 ≤ k ≤ 18, -12 ≤ l ≤ 12 |
| Reflections collected | 163824 |
| Independent reflections | 11101 [$R_{int}$ = 0.0935, $R_{sigma}$ = 0.0296] |
| Data/restraints/parameters | 11101/483/605 |
| Goodness-of-fit on F$^2$ | 1.042 |
| Final R indexes [I>=2σ (I)] | $R_1$ = 0.0772, w$R_2$ = 0.2075 |
| Final R indexes [all data] | $R_1$ = 0.0846, w$R_2$ = 0.2146 |
| Largest diff. peak/hole / e Å$^{-3}$ | 0.768/-0.394 |

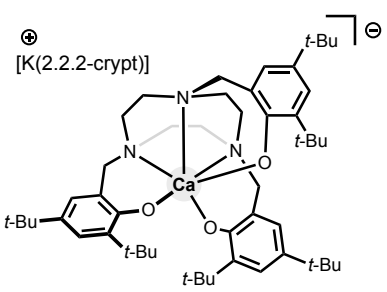


**[K(2.2.2-cryptand)][(*t*-BuTACN)Ca] (9.5):**

**X-ray** (single-crystal) To a J-Young NMR tube was added **9.5** (20 mg, 16.17 μmol) in a nitrogen filled glovebox; 0.5 mL of THF was added via syringe and the NMR tube placed in an oil bath at 80 °C until all of the solid had dissolved. The solvent was then removed under reduced pressure leaving a colorless oily residue. Inside the glovebox, 0.5 mL of toluene was added, and the resulting solution filtered into a vial by syringe. After 1 d, colorless crystals of complex **9.5** were obtained, which were suitable for X-ray crystallography.

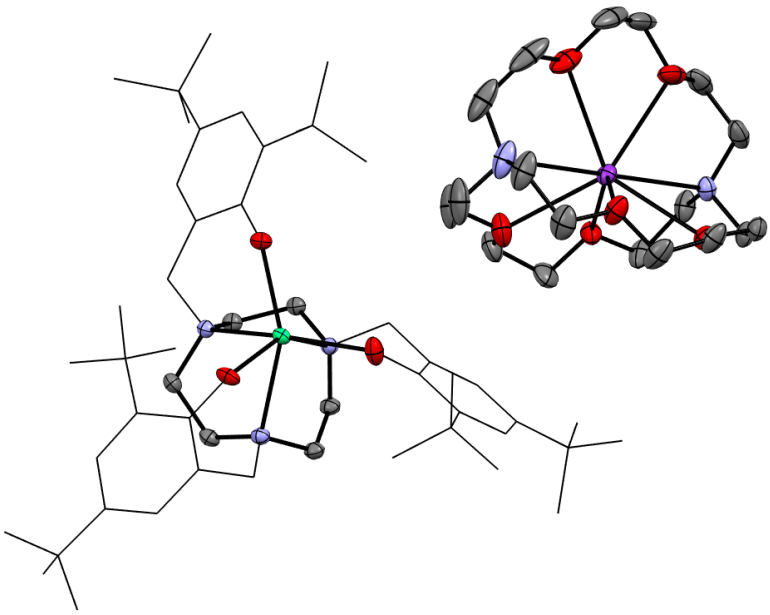

# Crystal Data

| | |
|---|---|
| CCDC Number | 2356736 |
| Empirical formula | $C_{76}H_{122}CaKN_5O_9$ |
| Formula weight | 1236.83 |
| Temperature/K | 100(10) |
| Crystal system | monoclinic |
| Space group | C2/c |
| a/Å | 23.32270(5) |
| b/Å | 16.20159(4) |
| c/Å | 42.30145(10) |
| α/° | 90 |
| β/° | 96.2766(2) |
| γ/° | 90 |
| Volume/Å$^3$ | 15888.41(6) |
| Z | 8 |
| $\rho_{calc}$g/cm$^3$ | 1.034 |
| μ/mm$^{-1}$ | 1.540 |
| F(000) | 5392.0 |
| Crystal size/mm$^3$ | 0.2 × 0.06 × 0.05 |
| Radiation | Cu Kα (λ = 1.54184) |
| 2Θ range for data collection/° | 6.656 to 151.798 |
| Index ranges | -29 ≤ h ≤ 29, -20 ≤ k ≤ 20, -52 ≤ l ≤ 46 |
| Reflections collected | 344516 |

| | |
|---|---|
| Independent reflections | 16336 [$R_{int}$ = 0.0258, $R_{sigma}$ = 0.0076] |
| Data/restraints/parameters | 16336/21/815 |
| Goodness-of-fit on $F^2$ | 1.021 |
| Final R indexes [I>=2σ (I)] | $R_1$ = 0.0347, $wR_2$ = 0.0869 |
| Final R indexes [all data] | $R_1$ = 0.0352, $wR_2$ = 0.0873 |
| Largest diff. peak/hole / e $Å^{-3}$ | 0.303/-0.262 |

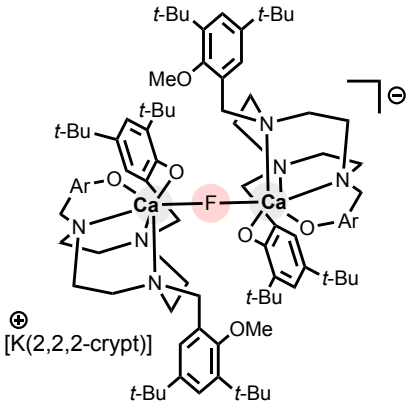


**[K(2.2.2-crypt)][{(*t*-BuTACN-Me)Ca}$_2$(μ-F)] (9.6):**

**X-ray** (single-crystal) The crude reaction mixture in benzene was filtered into a vial and layered with hexane. After 1 d, colorless crystals of complex **9.6** were obtained, which were suitable for X-ray crystallography.

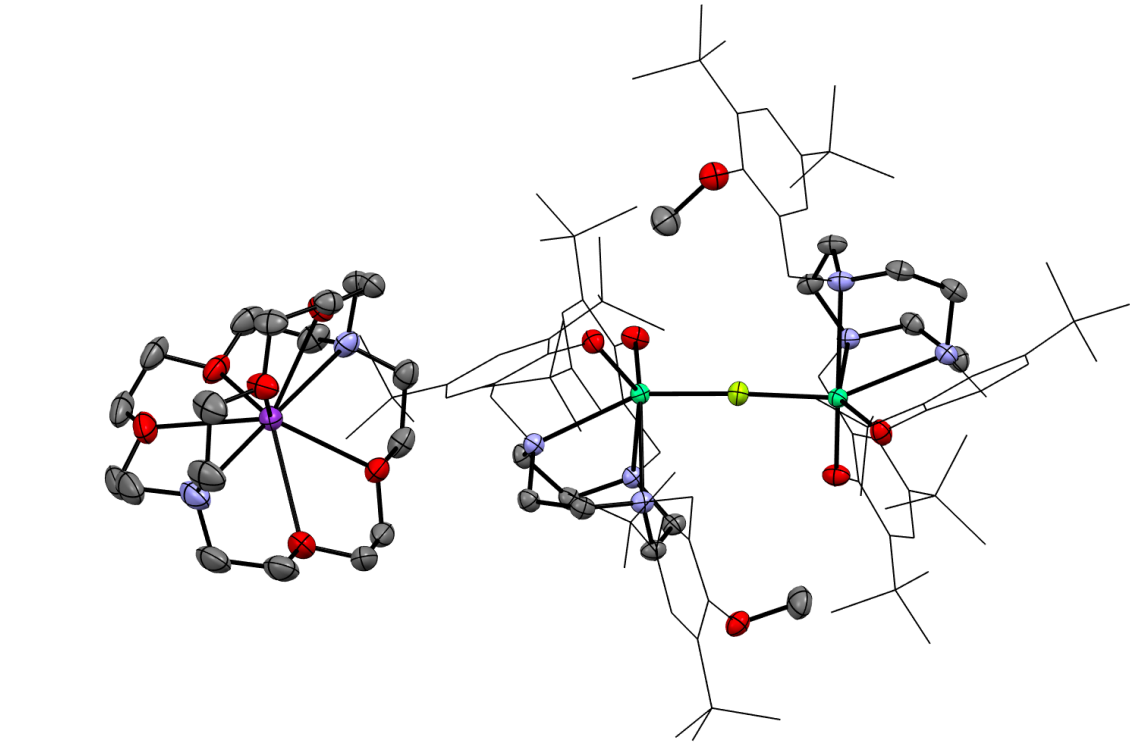

# Crystal Data

| | |
|---|---|
| CCDC Number | 2356737 |
| Empirical formula | $C_{161}H_{237}Ca_2FKN_8O_{12}$ |
| Formula weight | 2614.83 |
| Temperature/K | 150.01(10) |
| Crystal system | triclinic |
| Space group | $P\ \bar{1}$ |
| a/Å | 17.6508(2) |
| b/Å | 20.0851(3) |
| c/Å | 24.0778(3) |
| α/° | 96.9760(10) |
| β/° | 91.4070(10) |
| γ/° | 113.6790(10) |
| Volume/Å$^3$ | 7734.20(18) |
| Z | 2 |
| $\rho_{calc}$g/cm$^3$ | 1.123 |
| μ/mm$^{-1}$ | 1.349 |
| F(000) | 2846.0 |
| Crystal size/mm$^3$ | 0.1 × 0.08 × 0.05 |
| Radiation | Cu Kα (λ = 1.54184) |
| 2Θ range for data collection/° | 7.422 to 153.632 |
| Index ranges | -22 ≤ h ≤ 22, -25 ≤ k ≤ 24, -30 ≤ l ≤ 30 |
| Reflections collected | 166830 |
| Independent reflections | 32009 [$R_{int}$ = 0.0433, $R_{sigma}$ = 0.0264] |
| Data/restraints/parameters | 32009/1684/1905 |
| Goodness-of-fit on F$^2$ | 1.012 |
| Final R indexes [I>=2σ (I)] | $R_1$ = 0.0411, $wR_2$ = 0.1063 |
| Final R indexes [all data] | $R_1$ = 0.0535, $wR_2$ = 0.1158 |
| Largest diff. peak/hole / e Å$^{-3}$ | 0.346/-0.495 |

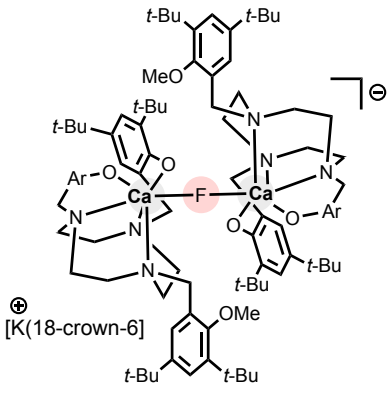


**[K(18-crown-6)][{(*t*-BuTACN-Me)Ca}$_2$(μ-F)] (9.7):**

**X-ray** (single-crystal) The crude reaction mixture in toluene was filtered into a vial and allowed to stand. After 1 d, colorless crystals of complex **9.7** were obtained, which were suitable for X-ray crystallography.

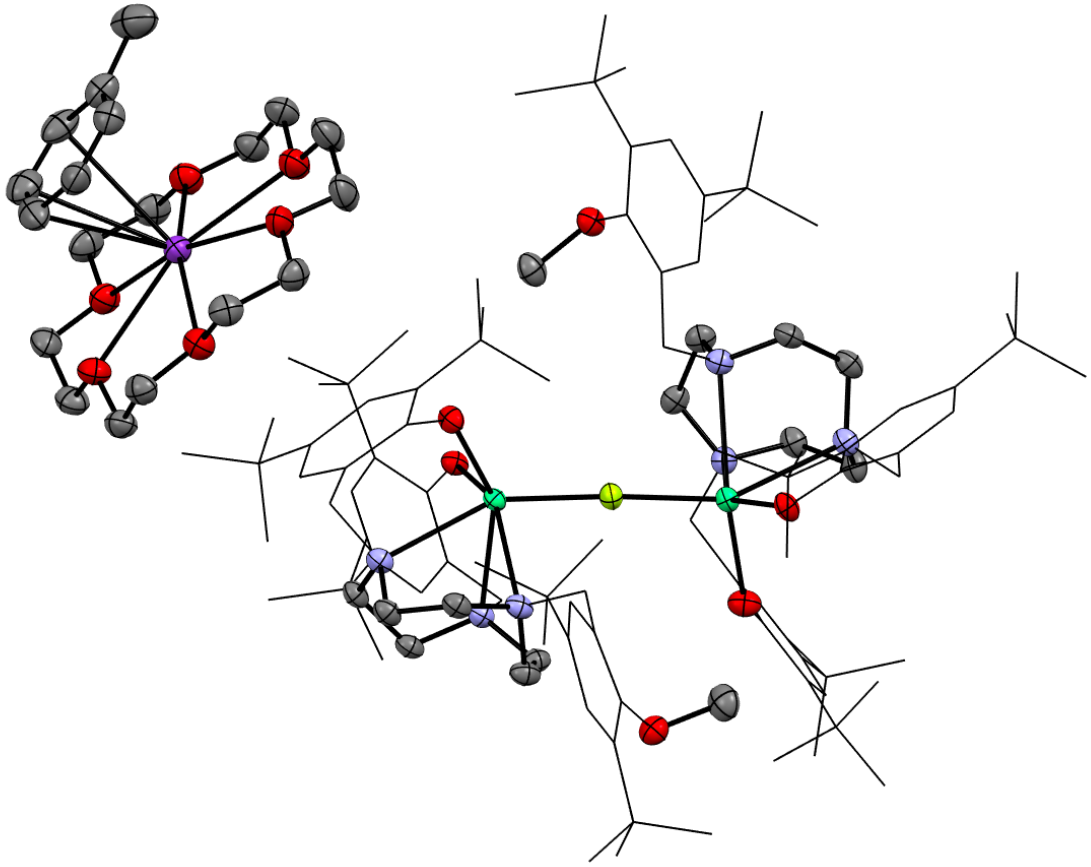

# Crystal Data

| | |
|---|---|
| CCDC Number | 2356738 |
| Empirical formula | $C_{158}H_{234}Ca_2FKN_6O_{12}$ |
| Formula weight | 2547.76 |
| Temperature/K | 100.00(10) |
| Crystal system | orthorhombic |
| Space group | $P2_12_12_1$ |
| a/Å | 15.49960(10) |
| b/Å | 28.53030(10) |
| c/Å | 33.74380(10) |
| α/° | 90 |
| β/° | 90 |
| γ/° | 90 |
| Volume/Å$^3$ | 14921.79(12) |
| Z | 4 |
| $\rho_{calc}$g/cm$^3$ | 1.134 |
| μ/mm$^{-1}$ | 1.382 |

| | |
|---|---|
| F(000) | 5552.0 |
| Crystal size/mm$^3$ | 0.06 × 0.05 × 0.04 |
| Radiation | Cu Kα (λ = 1.54184) |
| 2Θ range for data collection/° | 4.056 to 159.896 |
| Index ranges | -19 ≤ h ≤ 19, -28 ≤ k ≤ 35, -41 ≤ l ≤ 42 |
| Reflections collected | 133632 |
| Independent reflections | 30003 [$R_{int}$ = 0.0272, $R_{sigma}$ = 0.0224] |
| Data/restraints/parameters | 30003/648/1823 |
| Goodness-of-fit on F$^2$ | 1.043 |
| Final R indexes [I>=2σ (I)] | $R_1$ = 0.0345, $wR_2$ = 0.0959 |
| Final R indexes [all data] | $R_1$ = 0.0366, $wR_2$ = 0.0971 |
| Largest diff. peak/hole / e Å$^{-3}$ | 0.341/-0.348 |

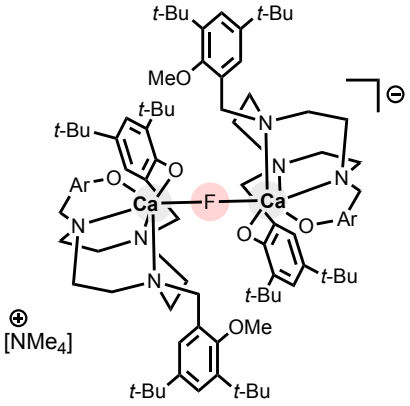


**[NMe$_4$][{(*t*-BuTACN)Ca}$_2$(μ-F)] (9.8):**

**X-ray** (single-crystal) Colorless crystals suitable for X-ray crystallography were obtained by slow cooling a crude reaction mixture in a J-Young NMR tube with toluene-$d_8$/THF 4:1 as the crystallizing solvent system.

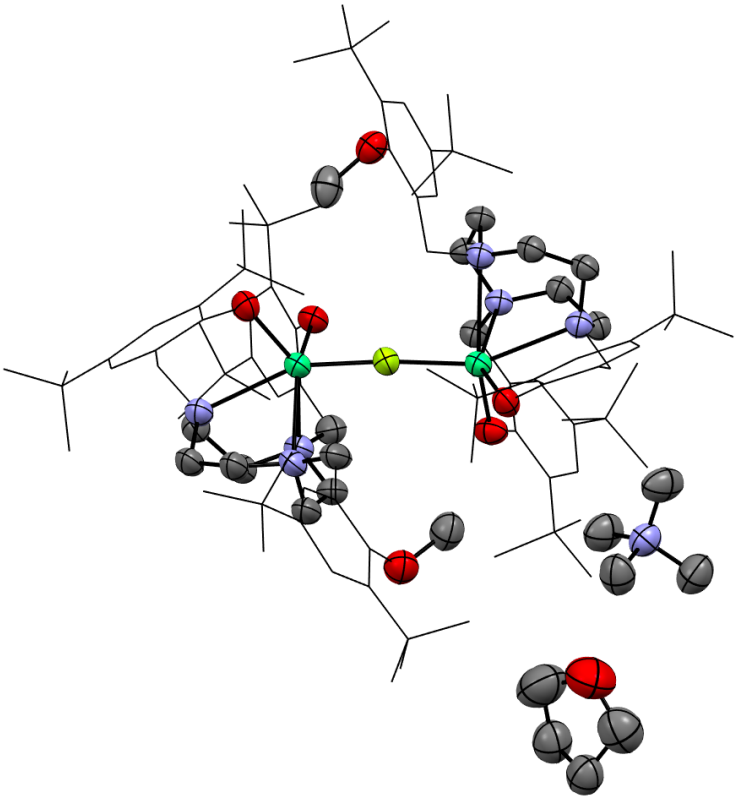

# Crystal Data

| | |
|---|---|
| CCDC Number | 2356739 |
| Empirical formula | $C_{150.5}H_{226}Ca_2FKN_7O_7$ |
| Formula weight | 2344.53 |
| Temperature/K | 100.00(10) |
| Crystal system | monoclinic |
| Space group | $P2_1/n$ |
| a/Å | 15.5878(2) |
| b/Å | 29.2064(3) |
| c/Å | 31.0854(5) |
| α/° | 90 |
| β/° | 98.9410(10) |
| γ/° | 90 |
| Volume/Å$^3$ | 13980.1(3) |
| Z | 4 |
| $\rho_{calc}$g/cm$^3$ | 0.873 |
| μ/mm$^{-1}$ | 1.048 |
| F(000) | 4032.0 |
| Crystal size/mm$^3$ | 0.29 × 0.04 × 0.02 |

| | |
|---|---|
| Radiation | Cu Kα (λ = 1.54184) |
| 2Θ range for data collection/° | 4.176 to 152.19 |
| Index ranges | $-19 \leq h \leq 19$, $-30 \leq k \leq 36$, $-38 \leq l \leq 38$ |
| Reflections collected | 233112 |
| Independent reflections | 28661 [$R_{int}$ = 0.0922, $R_{sigma}$ = 0.0424] |
| Data/restraints/parameters | 28661/282/1288 |
| Goodness-of-fit on $F^2$ | 1.068 |
| Final R indexes [I>=2σ (I)] | $R_1$ = 0.0990, $wR_2$ = 0.3004 |
| Final R indexes [all data] | $R_1$ = 0.1167, $wR_2$ = 0.3161 |
| Largest diff. peak/hole / e $Å^{-3}$ | 1.110/-0.557 |

# APPENDIX II

ADDITIONAL NMR DATA

# NMR Data for Chapter 3:

**General Procedure for Ketone Synthesis:**

The homoallylic alcohols were prepared according to a literature procedure.[1] To a 200-mL round bottom flask equipped with a Teflon-coated magnetic stir bar were added zinc dust (1.31 g, 20 mmol, 2.0 equiv) and dry THF (40 mL). Allyl bromide (1.7 mL, 20 mmol, 2.0 equiv) was added dropwise to the suspension at 0 °C and the mixture was stirred at this temperature for 15 min. The aldehyde (10 mmol, 1.0 equiv) was dissolved in dry THF (10 mL), and the solution was added dropwise to the reaction mixture. Subsequently, the reaction mixture was allowed to warm to room temperature and stir overnight. The reaction was quenched with sat. aq. $NH_4Cl$ (40 mL) at 0 °C and stirred until the precipitate turned colorless. The quenched reaction mixture was filtered, the organic layer was separated, and the aqueous layer was washed with EtOAc (3×). The combined organic layers were washed with brine, dried over $Na_2SO_4$ and the solvent was removed *in vacuo* to afford the crude product. The crude product was used without further purification in the next step.

In a 100-mL round bottom flask equipped with a Teflon-coated magnetic stir bar was dissolved the crude homoallyl alcohol (5.0 mmol, 1.0 equiv) in dry DCM (30 mL). DMP (2.76 g, 6.5 mmol, 1.3 equiv) was added portionwise to the stirring mixture at room temperature. The reaction mixture was stirred until the starting material was consumed (reaction monitored by TLC, approx. 0.5–2 h) and then quenched with water (10 mL). After stirring for an additional 30 min, the mixture was filtered, the organic layer was separated, and the aqueous layer was washed with DCM (3×). The combined organic layers were washed with brine, dried over $Na_2SO_4$ and concentrated *in vacuo*. Purification by

silica gel column chromatography afforded the alkenyl ketone product. The products were stored in a refrigerator at 0 °C to prevent isomerization.[2] The reported yields correspond to the yields of the oxidation step from the crude homoallylic alcohols.

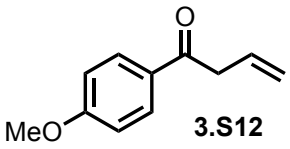

**3.S12**

**1-(4-Methoxyphenyl)but-3-en-1-one** (**3.S12**): The title compound was prepared from *p*-anisaldehyde (3.7 mL, 30 mmol) according to the *general procedure for ketone synthesis* on a three-times larger scale. Purification by silica gel column chromatography (4% EtOAc/hexane) gave the product as a white solid (1.21 g, 6.88 mmol, 46% yield). **$^1$H NMR** (400 MHz, $CDCl_3$) $\delta$ 7.95 (d, $J$ = 8.7 Hz, 2H), 6.94 (d, $J$ = 8.7 Hz, 2H), 6.08 (ddt, $J$ = 17.0, 10.5, 6.7 Hz, 1H), 5.28–5.14 (m, 2H), 3.87 (s, 3H), 3.71 (d, $J$ = 7.7 Hz, 2H); **$^{13}$C NMR** (126 MHz, $CDCl_3$) δ 196.6, 163.6, 131.5, 130.6, 129.6, 118. 4, 113.8, 55.5, 43.2; **HRMS** (ESI-TOF) Calc'd for $C_{11}H_{13}O_2^+$ $[M+H]^+$ 177.0916, found 177.0916.

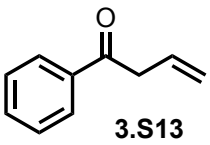

**3.S13**

**1-Phenylbut-3-en-1-one** (**3.S13**)**:** The title compound was prepared from benzaldehyde (1.0 mL, 10 mmol) according to the *general procedure for ketone synthesis*. Purification by silica gel column chromatography (1 to 3% EtOAc/hexane) gave the product as a colorless liquid (374 mg, 2.56 mmol, 51% yield). **$^1$H NMR** (400 MHz, $CDCl_3$) $\delta$ 8.00 (d, $J$ = 7.7 Hz, 2H), 7.60 (t, $J$ = 7.4 Hz, 1H), 7.50 (t, $J$ = 7.6 Hz, 2H), 6.10 (ddt, $J$ = 17.1, 10.4, 6.7 Hz, 1H), 5.28–5.17 (m, 2H), 3.79 (d, $J$ = 6.7 Hz, 2H); **$^{13}$C NMR** (126 MHz, $CDCl_3$) $\delta$ 198.0, 136.6, 133.2, 131.1, 128.6, 128.3, 118.7, 43.4; **HRMS** (ESI-TOF) Calc'd for $C_{10}H_{11}O^+$ $[M+H]^+$ 147.0810, found 147.0811.

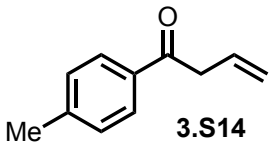

3.S14

**1-(*p*-Tolyl)but-3-en-1-one (3.S14):** The title compound was prepared from *p*-tolualdehyde (1.2 mL, 10 mmol) according to the *general procedure for ketone synthesis*. Purification by silica gel column chromatography (3% EtOAc/hexane) gave the product as a yellow liquid (687 mg, 4.29 mmol, 86% yield). **$^1$H NMR** (400 MHz, $CDCl_3$) $\delta$ 7.87 (d, $J$ = 8.2 Hz, 2H), 7.26 (d, $J$ = 8.0 Hz, 2H), 6.09 (ddt, $J$ = 17.1, 10.4, 6.7 Hz, 1H), 5.24–5.16 (m, 2H), 3.73 (d, $J$ = 6.7 Hz, 2H), 2.41 (s, 3H); **$^{13}$C NMR** (126 MHz, $CDCl_3$) $\delta$ 197.8, 144.0, 134.1, 131.3, 129.3, 128.5, 118.6, 43.4, 21.7; **HRMS** (ESI-TOF) Calc'd for $C_{11}H_{13}O^+$ $[M+H]^+$ 161.0966, found 161.0967.

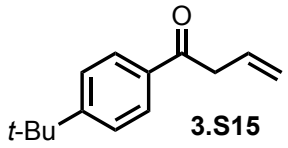

3.S15

**1-(4-(*tert*-Butyl)phenyl)but-3-en-1-one (3.S15):** The title compound was prepared from 4-(*tert*-butyl)benzaldehyde (1.7 mL, 10 mmol) according to the *general procedure for ketone synthesis*. Purification by silica gel column chromatography (5% EtOAc/hexane) gave the product as a colorless liquid (745 mg, 3.69 mmol, 74% yield). **$^1$H NMR** (400 MHz, $CDCl_3$) $\delta$ 7.91 (d, $J$ = 8.7 Hz, 2H), 7.48 (d, $J$ = 8.7 Hz, 2H), 6.09 (ddt, $J$ = 17.2, 10.6, 6.7 Hz, 1H), 5.25–5.22 (m, 1H), 5.22–5.18 (m, 1H), 3.74 (d, $J$ = 6.7 Hz, 2H), 1.34 (s, 9H); **$^{13}$C NMR** (126 MHz, $CDCl_3$) $\delta$ 197.7, 156.9, 134.0, 131.3, 128.3, 125.6, 118.6, 43.5, 35.2, 31.1; **HRMS** (ESI-TOF) Calc'd for $C_{14}H_{19}O^+$ $[M+H]^+$ 203.1436, found 203.1438.

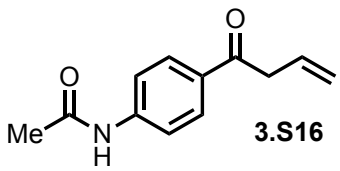

3.S16

***N*-(4-(But-3-enoyl)phenyl)acetamide (3.S16):** The title compound was prepared from 4-acetamidobenzaldehyde (1.63 g, 10 mmol) according to the *general procedure for*

*ketone synthesis*. Purification by silica gel column chromatography (20 to 40% EtOAc/hexane) gave the product as a brown solid (368 mg, 1.81 mmol, 36% yield). **$^1$H NMR** (400 MHz, $CDCl_3$) $\delta$ 7.95 (d, $J$ = 8.7 Hz, 2H), 7.62 (d, $J$ = 8.5 Hz, 2H), 7.40 (bs, 1H), 6.08 (ddt, $J$ = 16.9, 10.3, 6.8 Hz, 1H), 5.27–5.16 (m, 2H), 3.73 (d, $J$ = 6.7 Hz, 2H), 2.22 (s, 3H); **$^{13}$C NMR** (126 MHz, $CDCl_3$) $\delta$ 197.1, 168.8, 142.6, 132.3, 131.2, 129.9, 119.1, 118.9, 43.4, 24.9; **HRMS** (ESI-TOF) Calc'd for $C_{12}H_{14}NO_2^+$ $[M+H]^+$ 204.1025, found 204.1027.

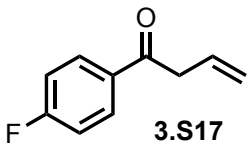

**3.S17**

**1-(4-Fluorophenyl)but-3-en-1-one** (**3.S17**)**:** The title compound was prepared from 4-fluorobenzaldehyde (1.1 mL, 10 mmol) according to the *general procedure for ketone synthesis*. Purification by silica gel column chromatography (3% EtOAc/hexane) gave the product as a colorless liquid (642 mg, 3.91 mmol, 78% yield). **$^1$H NMR** (400 MHz, $CDCl_3$) $\delta$ 8.00 (dd, $J$ = 8.5, 5.6 Hz, 2H), 7.14 (t, $J$ = 8.6 Hz, 2H), 6.07 (ddt, $J$ = 17.1, 10.5, 6.8 Hz, 1H), 5.28–5.17 (m, 2H), 3.74 (d, $J$ = 6.8 Hz, 2H); **$^{13}$C NMR** (126 MHz, $CDCl_3$) $\delta$ 196.5, 165.9 (d, $J$ = 254.8 Hz), 133.0 (d, $J$ = 2.9 Hz), 131.0 (d, $J$ = 9.4 Hz), 130.9, 119.0, 115.8 (d, $J$ = 21.9 Hz), 43.5; **$^{19}$F NMR** (376 MHz, $CDCl_3$) $\delta$ −105.3; **HRMS** (ESI-TOF) Calc'd for $C_{10}H_{10}FO^+$ $[M+H]^+$ 165.0716, found 165.0717.

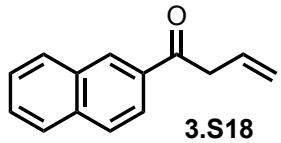

**3.S18**

**1-(Naphthalen-2-yl)but-3-en-1-one** (**3.S18**)**:** The title compound was prepared from 2-naphthaldehyde (1.56 g, 10 mmol) according to the *general procedure for ketone synthesis*. Purification by silica gel column chromatography (2 to 4% EtOAc/hexane) gave the product as a colorless liquid (440 mg,

2.24 mmol, 45% yield). **$^1$H NMR** (400 MHz, $CDCl_3$) $\delta$ 8.49 (s, 1H), 8.04 (dd, $J$ = 8.6, 1.7 Hz, 1H), 7.97 (d, $J$ = 8.0 Hz, 1H), 7.92–7.86 (m, 2H), 7.64–7.53 (m, 2H), 6.23–6.10 (m, 1H), 5.32–5.23 (m, 2H), 3.90 (d, $J$ = 6.7 Hz, 2H); **$^{13}$C NMR** (101 MHz, $CDCl_3$) $\delta$ 198.1, 135.8, 134.0, 132.6, 131.3, 130.1, 129.7, 128.7, 128.6, 127.9, 126.9, 124.1, 118.9, 43.7; **HRMS** (ESI-TOF) Calc'd for $C_{14}H_{13}O^+$ $[M+H]^+$ 197.0966, found 197.0967.

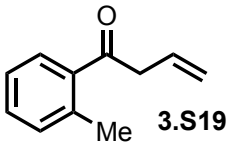

**3.S19**

**1-(*o*-Tolyl)but-3-en-1-one** (**3.S19**)**:** The title compound was prepared from *o*-tolualdehyde (1.1 mL, 10 mmol) according to the *general procedure for ketone synthesis*. Purification by silica gel column chromatography (5% EtOAc/hexane) gave the product as a colorless liquid (644 mg, 4.03 mmol, 81% yield). **$^1$H NMR** (400 MHz, $CDCl_3$) $\delta$ 7.66 (d, $J$ = 7.8 Hz, 1H), 7.40–7.35 (m, 1H), 7.29–7.23 (m, 2H), 6.04 (ddt, $J$ = 17.1, 10.3, 6.8 Hz, 1H), 5.24–5.16 (m, 2H), 3.69 (d, $J$ = 6.8 Hz, 2H), 2.50 (s, 3H); **$^{13}$C NMR** (126 MHz, $CDCl_3$) $\delta$ 202.0, 138.4, 137.5, 132.1, 131.5, 131.2, 128.7, 125.7, 118.7, 46.4, 21.4; **HRMS** (ESI-TOF) Calc'd for $C_{11}H_{13}O^+$ $[M+H]^+$ 161.0966, found 161.0965.

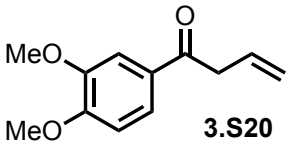

**3.S20**

**1-(3,4-Dimethoxyphenyl)but-3-en-1-one** (**3.S20**)**:** The title compound was prepared from 3,4-dimethoxybenzaldehyde (1.66 g, 10 mmol) according to the *general procedure for ketone synthesis*. Purification by silica gel column chromatography (10% EtOAc/hexane) gave the product as a colorless solid (612 mg, 2.97 mmol, 59% yield). **$^1$H NMR** (400 MHz, $CDCl_3$) $\delta$ 7.60 (dd, $J$ = 8.4, 2.0 Hz, 1H), 7.54 (d, $J$ = 2.0 Hz, 1H), 6.90 (d, $J$ = 8.4 Hz, 1H), 6.09 (ddt, $J$ = 17.4, 10.8, 6.8 Hz, 1H), 5.25–5.23 (m, 1H), 5.22–5.18 (m, 1H), 3.95 (s, 3H), 3.94

(s, 3H), 3.74–3.71 (m, 2H); **$^{13}$C NMR** (101 MHz, $CDCl_3$) $\delta$ 196.7, 153.4, 149.2, 131.6, 129.9, 123.1, 118.5, 110.4, 110.1, 56.2, 56.1, 43.2. The spectral data match reported data in the literature.[2]

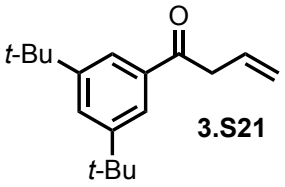


**1-(3,5-di-*tert*-Butylphenyl)but-3-en-1-one** (**3.S21**)**:** The title compound was prepared from 3,5-di-*tert*-butylbenzaldehyde (2.18 g, 10 mmol) according to the *general procedure for ketone synthesis*. Purification by silica gel column chromatography (2% EtOAc/hexane) gave the product as a yellow liquid (1.16 g, 4.50 mmol, 90% yield). **$^{1}$H NMR** (400 MHz, $CDCl_3$) $\delta$ 7.83 (s, 2H), 7.65 (s, 1H), 6.18–6.02 (m, 1H), 5.27–5.19 (m, 2H), 3.77 (d, $J$ = 6.8 Hz, 2H), 1.36 (s, 18H); **$^{13}$C NMR** (101 MHz, $CDCl_3$) $\delta$ 198.8, 151.3, 136.4, 131.6, 127.5, 122.7, 118.6, 44.0, 35.1, 31.5; **HRMS** (ESI-TOF) Calc'd for $C_{18}H_{27}O^+$ $[M+H]^+$ 259.2062, found 259.2066.

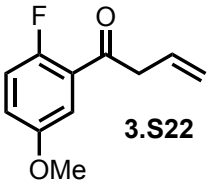


**1-(2-Fluoro-5-methoxyphenyl)but-3-en-1-one** (**3.S22**)**:** The title compound was prepared from 2-fluoro-5-methoxybenzaldehyde (1.2 mL, 10 mmol) according to the *general procedure for ketone synthesis*. Purification by silica gel column chromatography (1 to 3% EtOAc/hexane) gave the product as a colorless liquid (804 mg, 4.14 mmol, 83% yield). **$^{1}$H NMR** (400 MHz, $CDCl_3$) $\delta$ 7.36–7.30 (m, 1H), 7.08–7.03 (m, 2H), 6.08 (ddt, $J$ = 17.1, 10.5, 7.0 Hz, 1H), 5.24–5.16 (m, 2H), 3.82 (s, 3H), 3.78–3.73 (m, 2H); **$^{13}$C NMR** (101 MHz, $CDCl_3$) $\delta$ 196.05 (d, $J$ = 4.7 Hz), 156.5 (d, $J$ = 247.5 Hz), 155.82 (d, $J$ = 1.7 Hz), 130.7 (d, $J$ = 2.4 Hz), 125.3 (d, $J$ = 14.8 Hz), 121.5 (d, $J$ = 8.8 Hz), 118.7, 117.6 (d, $J$ = 26.4 Hz), 113.1 (d, $J$ = 3.0 Hz),

55.9, 48.0 (d, $J$ = 8.3 Hz); **$^{19}$F NMR** (376 MHz, $CDCl_3$) $\delta$ −119.8; **HRMS** (ESI-TOF) Calc'd for $C_{11}H_{12}FO_2^+$ $[M+H]^+$ 195.0821, found 195.0820.

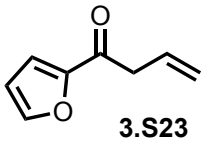

**3.S23**

**1-(Furan-2-yl)but-3-en-1-one** (**3.S23**)**:** The title compound was prepared from furfural (0.83 mL, 10 mmol) according to the *general procedure for ketone synthesis*. Purification by silica gel column chromatography (1 to 2% EtOAc/hexane) gave the product as a slightly yellow liquid (100 mg, 0.735 mmol, 15% yield). **$^1$H NMR** (400 MHz, $CDCl_3$) $\delta$ 7.61–7.57 (m, 1H), 7.22 (d, $J$ = 3.6 Hz, 1H), 6.54 (dd, $J$ = 3.5, 1.6 Hz, 1H), 6.11–5.98 (m, 1H), 5.27–5.23 (m, 1H), 5.23–5.20 (m, 1H), 3.61 (d, $J$ = 6.9 Hz, 2H); **$^{13}$C NMR** (126 MHz, $CDCl_3$) $\delta$ 187.0, 152.4, 146.6, 130.4, 119.1, 117.6, 112.4, 43.5. The spectral data match reported data in the literature.[3]

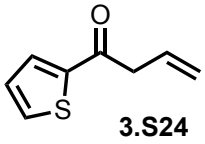

**3.S24**

**1-(Thiophen-2-yl)but-3-en-1-one** (**3.S24**)**:** The title compound was prepared from thiophene-2-carbaldehyde (0.93 mL, 10 mmol) according to the *general procedure for ketone synthesis*. Purification by silica gel column chromatography (2% EtOAc/hexane) gave the product as a slightly green liquid (258 mg, 1.70 mmol, 34% yield). **$^1$H NMR** (400 MHz, $CDCl_3$) $\delta$ 7.75 (d, $J$ = 3.8 Hz, 1H), 7.65 (d, $J$ = 5.0 Hz, 1H), 7.14 (t, $J$ = 4.3 Hz, 1H), 6.07 (ddt, $J$ = 16.9, 10.1, 6.8 Hz, 1H), 5.28–5.24 (m, 1H), 5.24–5.21 (m, 1H), 3.69 (d, $J$ = 6.8 Hz, 2H); **$^{13}$C NMR** (101 MHz, $CDCl_3$) $\delta$ 190.8, 143.8, 133.9, 132.3, 130.8, 128.2, 119.0, 44.3. The spectral data match reported data in the literature.[3]

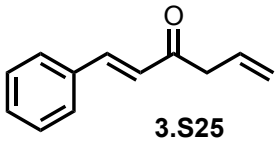

3.S25

**(*E*)-1-Phenylhexa-1,5-dien-3-one** (**3.S25**)**:** The title compound was prepared from cinnamaldehyde (1.3 mL, 10 mmol) according to the *general procedure for ketone synthesis*. Purification by silica gel column chromatography (2% EtOAc/hexane) gave the product as a slightly green liquid (365 mg, 2.12 mmol, 42% yield). **$^1$H NMR** (400 MHz, $CDCl_3$) $\delta$ 7.58 (d, $J$ = 16.2 Hz, 1H), 7.56–7.53 (m, 2H), 7.41–7.37 (m, 3H), 6.76 (d, $J$ = 16.2 Hz, 1H), 6.02 (ddt, $J$ = 17.2, 10.4, 6.9 Hz, 1H), 5.27–5.16 (m, 2H), 3.44 (d, $J$ = 6.9 Hz, 2H); **$^{13}$C NMR** (101 MHz, $CDCl_3$) $\delta$ 197.8, 143.2, 134.5, 131.0, 130.6, 129.0, 128.4, 125.5, 118.9, 45.9; **HRMS** (ESI-TOF) Calc'd for $C_{12}H_{13}O^+$ $[M+H]^+$ 173.0966, found 173.0968.

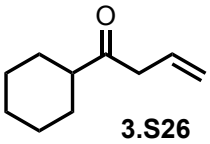

3.S26

**1-Cyclohexylbut-3-en-1-one** (**3.S26**)**:** The title compound was prepared from cyclohexane-carboxaldehyde (1.2 mL, 10 mmol) according to the *general procedure for ketone synthesis*. Purification by silica gel column chromatography (2% EtOAc/hexane) gave the product as a colorless liquid (365 mg, 2.40 mmol, 48% yield). **$^1$H NMR** (400 MHz, $CDCl_3$) $\delta$ 5.93 (ddt, $J$ = 17.2, 10.3, 6.9 Hz, 1H), 5.21–5.06 (m, 2H), 3.21 (d, $J$ = 7.9 Hz, 2H), 2.40 (tt, $J$ = 11.1, 3.4 Hz, 1H), 1.89–1.74 (m, 4H), 1.71–1.62 (m, 1H), 1.38–1.17 (m, 5H); **$^{13}$C NMR** (126 MHz, $CDCl_3$) $\delta$ 211.7, 131.0, 118.4, 50.4, 45.6, 28.4, 25.9, 25.7. The spectral data match reported data in the literature.[4]

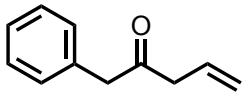

3.S27

**1-Phenylpent-4-en-2-one** (**3.S27**)**:** The title compound was prepared by allylation of phenylacetaldehyde (1.8 mL, 15 mmol) and subsequent oxidation on a 2.9 mmol scale according to the *general*

*procedure for ketone synthesis*. Purification by silica gel column chromatography (3% EtOAc/hexane) gave the product as a colorless liquid (376 mg, 2.35 mmol, 81% yield). **$^1$H NMR** (400 MHz, $CDCl_3$) $\delta$ 7.36–7.30 (m, 2H), 7.30–7.24 (m, 1H), 7.22–7.18 (m, 2H), 5.90 (ddt, $J$ = 17.2, 10.2, 6.9 Hz, 1H), 5.18 (dq, $J$ = 10.2, 1.4 Hz, 1H), 5.11 (dq, $J$ = 17.1, 1.5 Hz, 1H), 3.72 (s, 2H), 3.21 (dt, $J$ = 6.9, 1.4 Hz, 2H); **$^{13}$C NMR** (101 MHz, $CDCl_3$) $\delta$ 206.3, 134.0, 130.4, 129.5, 128.8, 127.1, 119.1, 49.6, 46.8; **HRMS** (ESI-TOF) Calc'd for $C_{11}H_{13}O^+$ $[M+H]^+$ 161.0966, found 161.0963.

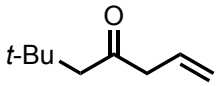

**3.S28**

**6,6-Dimethylhept-1-en-4-one** (**3.S28**)**:** The title compound was prepared by allylation of 3,3-dimethylbutanal (0.80 mL, 10 mmol) and subsequent oxidation on a 3.0 mmol scale according to the *general procedure for ketone synthesis.* Purification by silica gel column chromatography (2% $Et_2O$/hexane) gave the product as a colorless liquid (106 mg, 0.757 mmol, 25% yield). **$^1$H NMR** (500 MHz, $CDCl_3$) $\delta$ 5.91 (ddt, $J$ = 17.2, 10.2, 7.0 Hz, 1H), 5.19–5.15 (m, 1H), 5.14–5.08 (m, 1H), 3.18–3.13 (m, 2H), 2.33 (s, 2H), 1.02 (s, 9H); **$^{13}$C NMR** (126 MHz, $CDCl_3$) $\delta$ 208.6, 131.0, 118.7, 54.6, 49.9, 31.1, 29.9; **HRMS** (ESI-TOF) Calc'd for $C_9H_{17}O^+$ $[M+H]^+$ 141.1247, found 141.1238.

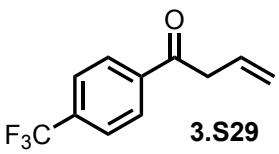

**3.S29**

**1-(4-(Trifluoromethyl)phenyl)but-3-en-1-one** (**3.S29**): The title compound was prepared from 4-(trifluoromethyl)benzaldehyde (1.4 mL, 10 mmol) according to the *general procedure for ketone synthesis*. Purification by silica gel column chromatography (3% EtOAc/hexane) gave the product as a colorless liquid (810 mg, 4.16 mmol, 83% yield). **$^1$H NMR** (400 MHz, $CDCl_3$)

$\delta$ 8.07 (d, $J$ = 8.1 Hz, 2H), 7.74 (d, $J$ = 8.2 Hz, 2H), 6.08 (ddt, $J$ = 17.0, 10.3, 6.7 Hz, 1H), 5.33–5.18 (m, 2H), 3.79 (d, $J$ = 6.7 Hz, 2H); **$^{13}$C NMR** (126 MHz, $CDCl_3$) δ 196.99, 139.18, 134.47 (q, $J$ = 32.6 Hz), 130.31, 128.62, 125.72 (q, $J$ = 3.9 Hz), 123.58 (q, $J$ = 272.8 Hz), 119.29, 43.64; **$^{19}$F NMR** (376 MHz, $CDCl_3$) $\delta$ −63.4. The spectral data match reported data in the literature.[5]

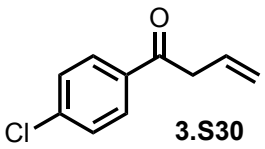

**3.S30**

**1-(4-Chlorophenyl)but-3-en-1-one** (**3.S30**)**:** The title compound was prepared from 4-chlorobenzaldehyde (703 mg, 5 mmol) according to the *general procedure for ketone synthesis*. Purification by silica gel column chromatography (10% EtOAc/hexane) gave the product as a white solid (450 mg, 3.21 mmol, 78% yield). **$^{1}$H NMR** (400 MHz, $CDCl_3$) $\delta$ 7.93–7.89 (m, 2H), 7.46–7.42 (m, 2H), 6.07 (ddt, $J$ = 17.0, 10.3, 6.7 Hz, 1H), 5.27–5.18 (m, 2H), 3.73 (dt, $J$ = 6.7, 1.4 Hz, 2H); **$^{13}$C NMR** (126 MHz, $CDCl_3$) $\delta$ 196.8, 139.6, 134.9, 130.7, 129.7, 129.0, 119.0, 43.4; **HRMS** (ESI-TOF) Calc'd for $C_{10}H_{10}ClO^+$ $[M+H]^+$ 181.0420, found 181.0424.

**1-(3,4-Dimethoxyphenyl)pent-4-en-1-one** (**3.S31**)**:**

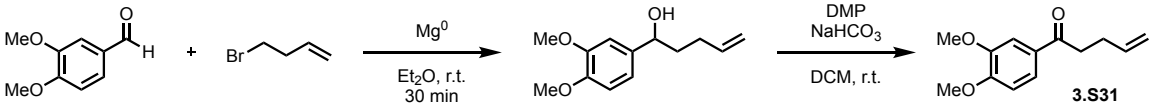


***Scheme 3.S3.*** Synthesis of the *γ*,*δ*-unsaturated ketone **3.S31**.[6]

Mg (875 mg, 36 mmol, 3.6 equiv) was stirred in an oven-dried 100-mL Schlenk tube at room temperature under nitrogen atmosphere for 1.5 h. Subsequently, the activated Mg

was covered with dry ether (25 mL). To this suspension was added dropwise a solution of 4-bromo-1-butene (1.7 mL, 17 mmol, 1.7 equiv) in dry ether (4 mL). The reaction mixture reached reflux temperature and was subsequently stirred for additional 30 min. The mixture was cooled to 0 °C, and a solution of 3,4-dimethoxybenzaldehyde (1.66 g, 10 mmol, 1.0 equiv) in dry THF (4 mL) was added dropwise. The reaction mixture was allowed to warm to room temperature and was then heated at reflux for 5 min in an oil bath. Subsequently, the reaction was cooled to 0 °C and quenched with sat. aq. $NH_4Cl$. The suspension was filtered, the organic layer was separated, and the aqueous layer was washed with EtOAc (3×). The combined organic layers were washed with brine, dried over $Na_2SO_4$, and concentrated *in vacuo*. Purification by silica gel column chromatography (15% EtOAc/hexane) afforded the alcohol product as a slightly yellow oil.[6]

To a 100-mL round bottom flask equipped with a Teflon-coated magnetic stir bar were added $NaHCO_3$ (739 mg, 8.8 mmol, 4.0 equiv), the alcohol from the previous step (495 mg, 2.2 mmol, 1.0 equiv), and dry DCM (15 mL). The mixture was stirred at room temperature, and DMP (1.31 g, 3.1 mmol, 1.4 equiv) was added portionwise. After full consumption of the starting material (reaction monitored by TLC) the reaction was quenched by adding water (4 mL) and stirred for additional 30 min. The precipitate was filtered off, the organic layer separated, and the aqueous layer was extracted with DCM (3× 5 mL). The combined organic layers were washed with brine, dried over $Na_2SO_4$ and concentrated *in vacuo*. Purification by silica gel column chromatography (15% EtOAc/hexane) gave the product as a colorless liquid (424 mg, 1.93 mmol, 88% yield, 62% yield over both steps).[2] The product was stored in a fridge to prevent isomerization.

**$^1$H NMR** (400 MHz, $CDCl_3$) $\delta$ 7.59 (d, $J$ = 8.4 Hz, 1H), 7.54 (s, 1H), 6.89 (d, $J$ = 8.4 Hz, 1H), 5.91 (ddt, $J$ = 16.8, 10.2, 6.6 Hz, 1H), 5.14–4.97 (m, 2H), 3.95 (s, 3H), 3.94 (s, 3H), 3.04 (t, $J$ = 7.4 Hz, 2H), 2.49 (q, $J$ = 7.0 Hz, 2H); **$^{13}$C NMR** (101 MHz, $CDCl_3$) $\delta$ 198.2, 153.3, 149.2, 137.6, 130.3, 122.8, 115.3, 110.2, 110.1, 56.2, 56.1, 37.4, 28.6; **HRMS** (ESI-TOF) Calc'd for $C_{13}H_{17}O_3^+$ $[M+H]^+$ 221.1178, found 221.1179.

**(±)-1-(4-methoxyphenyl)-2-methylbut-3-en-1-one** (**3.S32**):

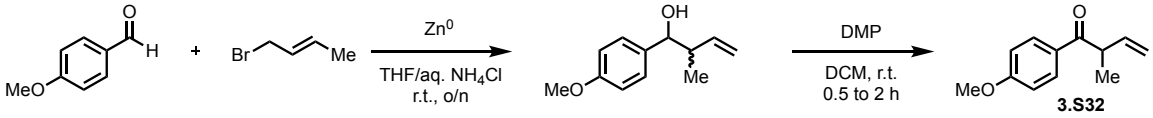


***Scheme 3.S4.*** Synthesis of α-methyl β,γ-unsaturated ketone **3.S32**.[6]

To a solution of *p*-anisaldehyde (1.2 mL, 10 mmol, 1.0 equiv.) in THF (25 mL) and sat. aq. $NH_4Cl$ (25 mL) were added crotyl bromide (1.6 mL, 15 mmol, 1.5 equiv.) and zinc dust (1.31 g, 20 mmol, 2.0 equiv.). The reaction mixture was stirred at room temperature overnight. The mixture was then filtered, the organic layer was separated, and the aqueous layer was washed with EtOAc (3×). The combined organic layers were washed with brine, dried over $Na_2SO_4$ and concentrated *in vacuo*. The crude product was used without further purification in the next step.[6]

The subsequent oxidation of the crude *α*-methyl homo allyl alcohol (960 mg, 5.0 mmol, 1.0 equiv.) to the ketone was carried out according to the *general procedure for ketone synthesis*.[2] Purification by sequential silica gel column chromatography (column 1:2 to 3% EtOAc in hexane, column 2: 100% toluene) afforded the product (440 mg, 2.31 mmol, 46% yield) as a colorless liquid. **$^1$H NMR** (400 MHz, $CDCl_3$) $\delta$ 7.97 (d, $J$ = 8.8 Hz, 2H), 6.94

(d, $J$ = 8.8 Hz, 2H), 5.99 (ddd, $J$ = 17.8, 10.3, 7.7 Hz, 1H), 5.21 – 5.08 (m, 2H), 4.13 (p, $J$ = 7.2 Hz, 1H), 3.87 (s, 3H), 1.32 (d, $J$ = 6.8 Hz, 3H); **$^{13}$C NMR** (101 MHz, $CDCl_3$) $\delta$ 199.9, 163.5, 138.7, 131.0, 129.4, 116.3, 113.9, 55.6, 45.3, 17.3; **HRMS** (ESI-TOF) Calc'd for $C_{12}H_{15}O_2^+$ $[M+H]^+$ 191.1072, found 191.1075.

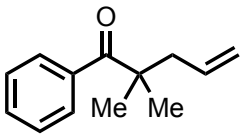


**3.52**

**2,2-Dimethyl-1-phenylpent-4-en-1-one** (**3.52**): The title compound was prepared according to a literature procedure.[7] **$^1$H NMR** (500 MHz, $CDCl_3$) $\delta$ 7.67 (d, $J$ = 7.0 Hz, 2H), 7.48 (t, $J$ = 7.4 Hz, 1H), 7.41 (d, $J$ = 7.1 Hz, 2H), 5.75 (ddt, $J$ = 17.5, 10.2, 7.3 Hz, 1H), 5.10–5.00 (m, 2H), 2.51 (d, $J$ = 7.3 Hz, 2H), 1.35 (s, 6H); **$^{13}$C NMR** (101 MHz, $CDCl_3$) $\delta$ 208.8, 134.1, 130.8, 128.1, 127.60, 118.1, 110.0, 47.7, 46.0, 25.8. The spectral data match reported data in the literature.[7]

**1-(3,4-Dimethoxyphenyl)hex-5-en-1-one** (**3.S33**)**:**

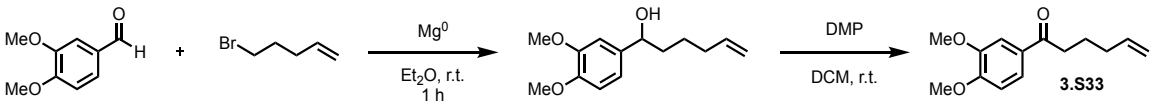


***Scheme 3.S5.*** Synthesis of the *δ,ε*-unsaturated ketone **3.S33**.[6]

Mg (875 mg, 36 mmol, 3.6 equiv) was stirred in an oven-dried 100-mL Schlenk tube at room temperature under nitrogen atmosphere covered with dry ether (25 mL). To this suspension was added dropwise a solution of 5-bromo-1-pentene (2.0 mL, 17 mmol, 1.7 equiv) in dry ether (4 mL). The reaction started to reflux and was subsequently stirred for an additional 30 min. Then, a solution of 3,4-dimethoxybenzaldehyde (1.66 g,

10 mmol, 1.0 equiv) in dry THF (4 mL) was added dropwise and allowed to react for 1 hour. After this time, the reaction was quenched with sat. aq. $NH_4Cl$. The suspension was filtered, the organic layer was separated, and the aqueous layer was washed with EtOAc (3×). The combined organic layers were washed with brine, dried over $Na_2SO_4$ and concentrated *in vacuo*. Purification by silica gel column chromatography (20% EtOAc/hexane) afforded the alcohol product as a slightly yellow oil.

To a 100-mL round bottom flask equipped with a Teflon-coated magnetic stir bar were added the alcohol (600 mg, 2.5 mmol, 1.0 equiv), and dry DCM (15 mL). The mixture was stirred at room temperature, and DMP (1.40 g, 3.3 mmol, 1.3 equiv) was added portionwise. After full consumption of the starting material (reaction monitored by TLC), the reaction was quenched by adding water (4 mL) and stirring for an additional 30 min. The precipitate was filtered off, the organic layer was separated, and the aqueous layer was extracted with DCM (3 × 5 mL). The combined organic layers were washed with brine, dried over $Na_2SO_4$, and concentrated *in vacuo*. Purification by silica gel column chromatography (20% EtOAc/hexane) gave the product as a colorless oil (478.5 mg, 2.04 mmol, 80% yield, 20% yield over two steps). The product was stored in a fridge to prevent isomerization. Characterization data match those reported in the literature.[8]

**1-(3,4-Dimethoxyphenyl)hex-5-en-1-one (3.S34):**

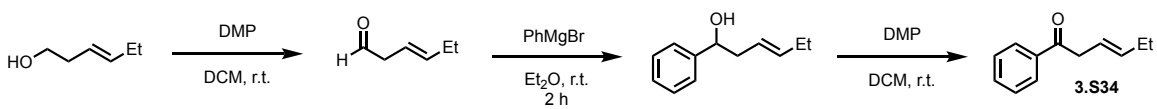


***Scheme 3.S6.*** Synthesis of the internal *β,γ*-unsaturated ketone **3.S34**.

To a 100-mL round bottom flask equipped with a Teflon-coated magnetic stir bar were added (*E*)-hex-3-en-1-ol (501 mg, 5.0 mmol, 1.0 equiv) and dry DCM (30 mL). The mixture was stirred at room temperature, and DMP (2.76 g, 6.5 mmol, 1.3 equiv) was added portionwise. After full consumption of the starting material (reaction monitored by TLC), the reaction was quenched by adding water (10 mL) and stirring for an additional 30 min. The precipitate was filtered off, the organic layer was separated, and the aqueous layer was extracted with DCM (3 × 5 mL). The combined organic layers were washed with brine, dried over $Na_2SO_4$, and concentrated *in vacuo*. The crude mixture was passed through a plug of silica gel and carried on to the next step without further purification.

To an oven-dried 100-mL Schlenk tube at room temperature under nitrogen atmosphere was added dry ether (11 mL). Then, phenyl magnesium bromide solution (7.5 mmol, 3 M in ether, 1.5 equiv) was added. Subsequently, a solution of the alkenyl aldehyde in dry ether (5 mL) was added dropwise and allowed to react for 2 h. After this time, the reaction was quenched with sat. aq. $NH_4Cl$. The suspension was filtered, the organic layer was separated, and the aqueous layer was washed with EtOAc (3×). The combined organic layers were washed with brine, dried over $Na_2SO_4$, and concentrated *in vacuo*. Purification by silica gel column chromatography (20% EtOAc/hexane) afforded the alcohol product as a slightly yellow oil.

To a 100-mL round bottom flask equipped with a Teflon-coated magnetic stir bar were added the alcohol (277 mg, 1.57 mmol, 1.0 equiv) and dry DCM (10 mL). The mixture was stirred at room temperature and DMP (867 mg, 2.0 mmol, 1.3 equiv) was added portionwise. After full consumption of the starting material (reaction control by TLC) the reaction was quenched by adding water (10 mL) and stirred for additional 30

min. The precipitate was filtered off, the organic layer separated, and the aqueous layer was extracted with DCM (3 × 5 mL). The combined organic layers were washed with brine, dried over $Na_2SO_4$ and concentrated *in vacuo*. Purification by silica gel column chromatography (20% EtOAc/hexane) gave the product as a colorless oil (96.5 mg, 0.55 mmol, 35% yield, 12% yield over the last two steps). The product was stored in a fridge to prevent isomerization. Characterization data match those reported in the literature.[9]

**Diversification of 1,2-Diarylated Product**

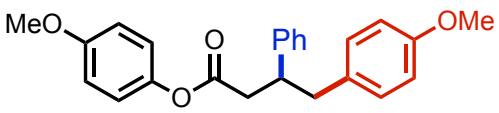


**3.47**

**4-Methoxyphenyl 4-(4-methoxyphenyl)-3-phenylbutanoate** (**3.47**): To a 1-dram (4 mL) vial equipped with a Teflon-coated magnetic stir bar were added ketone **3.5** (18 mg, 0.05 mmol, 1 equiv), *m*-CPBA (35 mg, 0.2 mmol, 4 equiv), TFA (7.7 µL, 0.1 mmol, 2 equiv), and dry DCM (1 mL). The reaction mixture was allowed to stir at rt for 48 h. After this time, the reaction was quenched with sat. aq. $NaHCO_3$, and extracted with DCM (3 × 1 mL). The combined organic layers were dried over $Na_2SO_4$, and the solvent was removed *in vacuo*. Purification using PTLC (5% EtOAc/hexane) gave the product as a colorless oil (11 mg, 60% yield). **$^1$H NMR** (400 MHz, $CDCl_3$) $\delta$ 7.33–7.27 (m, 2H), 7.25–7.19 (m, 3H), 7.00 (d, $J$ = 8.6 Hz, 2H), 6.81–6.76 (m, 4H), 6.67 (d, $J$ = 9.0 Hz, 2H), 3.77 (s, 3H), 3.75 (s, 3H), 3.46 (m, $J$ = 9.2, 7.3 Hz, 1H), 2.99–2.90 (m, 2H), 2.89–2.76 (m, 2H); **$^{13}$C NMR** (126 MHz, $CDCl_3$) $\delta$ 171.3, 158.1, 157.2, 144.0, 143.1, 131.4, 130.2, 128.5, 127.7, 126.6, 122.2, 114.4, 113.7, 55.6, 55.2, 44.5, 42.2, 40.2; **HRMS** (ESI-TOF) Calc'd for $C_{24}H_{25}O_4^+$ $[M+H]^+$ 377.1753, found 377.1747.

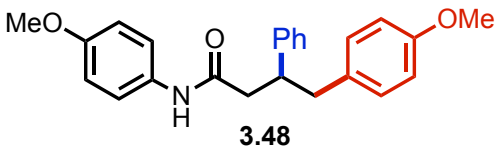


**3.48**

***N*,4-Bis(4-methoxyphenyl)-3-phenylbutanamide (3.48):** To a 1-dram (4 mL) vial equipped with a Teflon-coated magnetic stir bar were added ketone **3.5** (36 mg, 0.1 mmol, 1 equiv), hydroxylammonium chloride (21 mg, 0.3 mmol, 3 equiv), and TFA (0.4 mL). The reaction mixture was allowed to stir at 70 °C for 24 h in a heating block. After this time, the reaction was quenched with sat. aq. $NaHCO_3$, and extracted with DCM (3 × 1 mL). The combined organic layers were dried over $Na_2SO_4$, and the solvent was removed *in vacuo*. Purification using PTLC (10% EtOAc/hexane) gave the product as a white solid (30 mg, 79% yield). **$^1$H NMR** (500 MHz, $CDCl_3$) $\delta$ 7.26 (d, $J$ = 7.9 Hz, 2H), 7.22–7.14 (m, 3H), 7.13 (d, $J$ = 8.9 Hz, 2H), 6.96 (d, $J$ = 8.6 Hz, 2H), 6.87 (s, 1H), 6.75 (d, $J$ = 9.0 Hz, 2H), 6.73 (d, $J$ = 8.6 Hz, 2H), 3.73 (s, 6H), 3.48–3.40 (m, 1H), 2.98–2.87 (m, 2H), 2.67 (dd, $J$ = 14.3, 5.8 Hz, 1H), 2.55 (dd, $J$ = 14.3, 8.8 Hz, 1H); **$^{13}$C NMR** (126 MHz, $CDCl_3$) $\delta$ 169.8, 158.0, 156.4, 143.6, 130.2, 128.6, 127.7, 126.7, 122.0, 122.0, 114.0, 113.6, 55.5, 55.2, 44.7, 43.7, 41.8; **HRMS** (ESI-TOF) Calc'd for $C_{24}H_{26}NO_3^+$ $[M+H]^+$ 376.1913, found 376.1912.

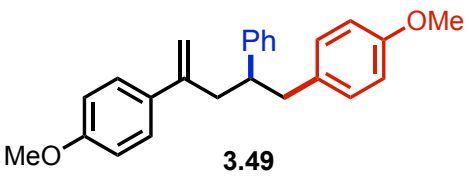


**3.49**

**4,4'-(2-Phenylpent-4-ene-1,4-diyl)bis(methoxybenzene) (3.49):** To a 2-dram (8 mL) vial equipped with a Teflon-coated magnetic stir bar were added methylphosphonium bromide (79 mg, 0.22 mmol, 1.1 equiv), and dry THF (0.25 mL). The solution was subjected to an ice bath, and then *n*-BuLi (0.1 mL, 2.5 M in hexanes, 1.2 equiv) was added dropwise. The reaction mixture was allowed to stir for

a 1 h at 0 °C. Lastly, ketone **3.5** (72 mg, 0.2 mmol, 2 equiv) dissolved in 0.1 mL of THF was added. The reaction mixture was allowed to warm to rt, then heated to 70 °C in a heating block and was stirred overnight. After this time, the reaction was quenched with sat. aq. $NH_4Cl$, and extracted with $Et_2O$ (3 × 1 mL). The combined organic layers were dried over $MgSO_4$, and the solvent was removed *in vacuo*. Purification using PTLC (5% EtOAc/hexane) gave the product as a white solid (24.3 mg, 34% yield). **$^1$H NMR** (400 MHz, $CDCl_3$) $\delta$ 7.23–7.13 (m, 5H), 7.00 (d, $J$ = 6.8 Hz, 2H), 6.83 (t, $J$ = 8.5 Hz, 4H), 6.70 (d, $J$ = 8.6 Hz, 2H), 5.08 (d, $J$ = 1.7 Hz, 1H), 4.80 (d, $J$ = 1.4 Hz, 1H), 3.81 (s, 3H), 3.74 (s, 3H), 2.94–2.83 (m, 3H), 2.82–2.76 (m, 1H), 2.71 (m, $J$ = 10.2, 7.1, 5.2 Hz, 1H); **$^{13}$C NMR** (126 MHz, $CDCl_3$) $\delta$ 159.0, 157.7, 146.1, 144.8, 133.4, 132.6, 130.1, 128.1, 127.9, 127.5, 126.0, 113.6, 113.4, 113.1, 55.3, 55.2, 46.2, 42.0, 41.7; **HRMS** (ESI-TOF) Calc'd for $C_{25}H_{27}O_2^+$ $[M+H]^+$ 359.2011, found 359.2003.

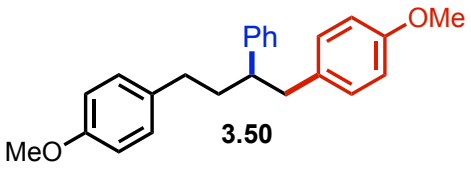

**3.50**

**4,4'-(2-Phenylbutane-1,4-diyl)bis(methoxybenzene) (3.50):** In a 1-dram (4 mL) vial equipped with a Teflon-coated magnetic stir bar $AlCl_3$ (17 mg, 0.13 mmol, 2.5 equiv) was dissolved in dry $Et_2O$ (0.2 mL). In another 1-dram (4 mL) vial equipped with a Teflon-coated magnetic stir bar was dissolved $LiAlH_4$ (4.7 mg, 0.13 mmol, 2.5 equiv) in dry $Et_2O$ (0.13 mL). The $LiAlH_4$ solution was added dropwise to the $AlCl_3$ solution. Then ketone **3.50** (18 mg, 0.05 mmol, 1 equiv) dissolved in 1 mL of DCM was added dropwise to the $LiAlH_4/AlCl_3$ mixture and allowed to stir at rt overnight. After this time, the reaction was quenched with water and 1 M HCl, and extracted with DCM (2 × 1 mL). The combined organic layers were washed with brine,

dried over $Na_2SO_4$, and the solvent was removed *in vacuo*. No further purification was needed affording the product as a colorless oil (13.8 mg, 81% yield). **$^1$H NMR** (400 MHz, $CDCl_3$) $\delta$ 7.27 (t, $J$ = 7.3 Hz, 2H), 7.21–7.15 (m, 1H), 7.11 (d, $J$ = 6.8 Hz, 2H), 6.96 (d, $J$ = 8.6 Hz, 2H), 6.89 (d, $J$ = 8.6 Hz, 2H), 6.77 (d, $J$ = 8.7 Hz, 2H), 6.72 (d, $J$ = 8.6 Hz, 2H), 3.77 (s, 3H), 3.75 (s, 3H), 2.86–2.74 (m, 3H), 2.47–2.28 (m, 2H), 2.02–1.83 (m, 2H); **$^{13}$C NMR** (126 MHz, $CDCl_3$) $\delta$ 157.7, 157.6, 144.9, 134.5, 132.6, 130.1, 129.2, 128.3, 127.9, 126.1, 113. 7, 113.4, 55.3, 55.2, 47.6, 43.0, 37.3, 32.8; **HRMS** (ESI-TOF) Calc'd for $C_{24}H_{27}O_2^+$ $[M+H]^+$ 347.2011, found 347.2015.

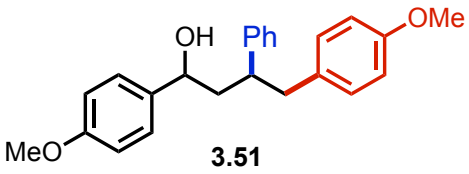

**3.51**

**1,4-Bis(4-methoxyphenyl)-3-phenylbutan-1-ol (3.51):** In a 1-dram (4 mL) vial equipped with a Teflon-coated magnetic stir bar was dissolved ketone **3.5** (18 mg, 0.05 mmol, 1 equiv) in dry THF (0.5 mL). Then $NaBH_4$ (1.9 mg, 0.05 mmol, 1 equiv) was added and the reaction was allowed to run for 72 h at 70 °C in a heating block. After this time, the reaction was quenched with water, and extracted with DCM (3 × 1 mL). The combined organic layers were dried over $Na_2SO_4$, and the solvent was removed *in vacuo*. Purification using PTLC (20% EtOAc/hexane) gave the product as a colorless oil (12.2 mg, 68% yield, 1:1 d.r.). **$^1$H NMR** (600 MHz, $CDCl_3$, both diastereomers) $\delta$ 7.30–7.26 (m, 3H), 7.21–7.17 (m, 2H), 7.17–7.14 (m, 2H), 7.14–7.11 (m, 2H), 7.08–7.04 (m, 5H), 6.91 (d, $J$ = 8.6 Hz, 2H), 6.85–6.80 (m, 7H), 6.72 (d, $J$ = 8.5 Hz, 2H), 6.70 (d, $J$ = 8.6 Hz, 2H), 4.38 (dd, $J$ = 8.5, 5.9 Hz, 1H), 4.32 (dd, $J$ = 10.2, 3.2 Hz, 1H), 3.81 (s, 3H), 3.77 (s, 3H), 3.75 (s, 6H), 3.18 (dtd, $J$ = 11.4, 7.5, 4.1 Hz, 1H), 2.84 (d, $J$ = 7.5 Hz, 2H), 2.82–2.75 (m, 2H), 2.60 (dtd, $J$ = 14.8, 7.8, 4.1 Hz, 1H), 2.21 (ddd, $J$ =

13.6, 10.1, 5.9 Hz, 1H), 2.13–2.05 (m, 2H), 1.91 (ddd, $J$ = 14.2, 11.0, 3.1 Hz, 1H), 1.60 (s, 2H); **$^{13}$C NMR** (150 MHz, $CDCl_3$, both diastereomers) $\delta$ 159.2, 158.9, 157.8, 157.7, 144.5, 144.3, 137.5, 136.0, 132.3, 132.1, 130.1, 130.1, 128.4, 128.0, 127.9, 127.7, 126.8, 126.3, 126.3, 113.8, 113.8, 113.5, 113.4, 72.7, 71.4, 60.4, 55.3, 55.2, 55.2, 45.0, 44.6, 44.6, 43.8, 43.2, 43.1; **HRMS** (ESI-TOF) Calc'd for $C_{24}H_{26}NaO_3^+$ $[M+Na]^+$ 385.1780, found 385.1776.

# NMR Data for Chapter 4:

**General Procedure A:** To a 100-mL round-bottom flask equipped with a Teflon-coated magnetic stir bar were added the alkenyl amine (5.0 mmol) and dry DCM (25 mL). The flask was placed in an ice bath, and triethylamine (15.0 mmol) and DMAP (25 mol%) were subsequently added. The reaction mixture was allowed to stir for at least 5 min. Lastly, the appropriate sulfonyl chloride (5.5 mmol) was added, and the reaction mixture was allowed to warm to room temperature and continue stirring for 16 h. After this time, the reaction mixture was transferred to a separatory funnel, washed with 1M HCl (100 mL), and was extracted with DCM (3 × 20 mL). The combined organic layers were then washed with brine (100 mL), dried over $Na_2SO_4$, and concentrated *in vacuo* to leave a white solid, which afforded pure product after silica gel column chromatography.

**General Procedure B (for small-scale synthesis):** To a 10-mL scintillation vial equipped with a Teflon-coated magnetic stir bar were added the alkenyl amine (1.0 mmol) and dry DCM (5 mL). The flask was placed in an ice bath, and triethylamine (3.0 mmol) and DMAP (25 mol%) were subsequently added. The reaction mixture was allowed to stir for at least

5 min. Lastly, the appropriate sulfonyl chloride (1.1 mmol) was added, and the reaction mixture was allowed to warm to room temperature and continue stirring for 16 h. After this time, the reaction mixture was transferred to a separatory funnel, washed with 1M HCl (5 mL), and extracted with DCM (3 × 1 mL). The combined organic layers were then washed with brine (5 mL), dried over $Na_2SO_4$, and concentrated *in vacuo* to leave a white solid, which afforded pure product after silica gel column chromatography.

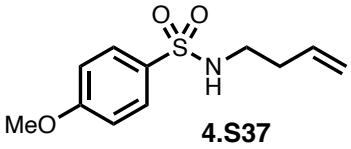

**4.S37**

**N-(but-3-en-1-yl)-4-methoxybenzenesulfonamide (4.S37):** The title compound was prepared from but-3-en-1-amine (71.1 mg, 1.0 mmol) and 4-methoxybenzenesulfonyl chloride (227 mg, 1.1 mmol), according to General Procedure B. Purification using silica gel column chromatography (20% EtOAc in Hexanes) gave the product as a colorless oil (190 g, 79% yield). Characterization data match those reported in the literature.[10]

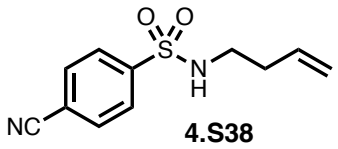

**4.S38**

***N*-(but-3-en-1-yl)-4-cyanobenzenesulfonamide (4.S38):** The title compound was prepared from but-3-en-1-amine (356 mg, 5.0 mmol) and 4-cyanobenzenesulfonyl chloride (1.10 g, 5.5 mmol), according to General Procedure A. Purification using silica gel column chromatography (30% EtOAc in Hexanes) gave the product as a white solid (695 mg, 59% yield). **$^1$H NMR** (400 MHz, $CDCl_3$) δ 7.98 (d, *J* = 8.7 Hz, 2H), 7.83 (d, *J* = 8.7 Hz, 2H), 5.62 (ddt, *J* = 17.1, 10.3, 6.9 Hz, 1H), 5.14–5.03 (m, 2H), 4.52 (t, *J* = 6.1 Hz, 1H), 3.09 (q, *J* = 6.4 Hz, 2H), 2.24 (qt, *J* = 6.6, 1.3 Hz, 2H); **$^{13}$C NMR** (150 MHz, $CDCl_3$) δ 144.42,

133.70, 133.00, 127.70, 118.64, 117.32, 116.42, 42.20, 33.70; **HRMS** (ESI-TOF) Calc'd for $C_{11}H_{13}N_2O_2S^+$ [M+H] 237.0698, found 237.0697.

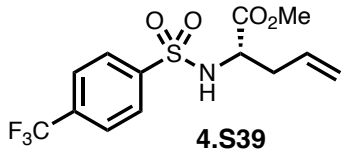

**4.S39**

**Methyl (*S*)-2-((4-(trifluoromethyl)phenyl)sulfonamido)pent-4-enoate (4.S39):** The title compound was prepared from methyl 2-aminopent-4-enoate **4.S27** (129 mg, 1.0 mmol) and 4-(trifluoromethyl)benzenesulfonyl chloride (269 mg, 1.1 mmol), according to General Procedure B. Purification using silica gel column chromatography (20% EtOAc in Hexanes) gave the product as a white solid (250 mg, 74% yield). **$^1$H NMR** (400 MHz, $CDCl_3$) δ 7.98 (d, *J* = 8.2 Hz, 2H), 7.78 (d, *J* = 8.3 Hz, 2H), 5.61 (ddt, *J* = 17.3, 10.2, 7.2 Hz, 1H), 5.21 (d, *J* = 9.0 Hz, 1H), 5.17–5.07 (m, 2H), 4.08 (dt, *J* = 9.0, 5.8 Hz, 1H), 3.54 (s, 3H), 2.53–2.47 (m, 2H); **$^{13}$C NMR** (150 MHz, $CDCl_3$) δ 171.05, 143.47 (q, *J* = 1.4 Hz), 134.58 (q, *J* = 32.9 Hz), 130.90, 127.77, 126.20 (q, *J* = 3.9 Hz), 123.18 (q, *J* = 273.0 Hz), 120.23, 55.29, 52.59, 37.54; **$^{19}$F NMR** (376 MHz, $CDCl_3$) δ -63.40; **HRMS** (ESI-TOF) Calc'd for $C_{13}H_{15}F_3NO_4S^+$ [M+H] 338.0674, found 338.0674.

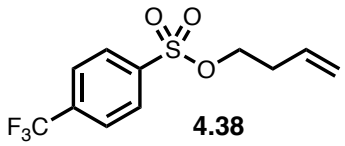

**4.38**

**But-3-en-1-yl 4-(trifluoromethyl)benzenesulfonate (4.38):** The title compound was prepared from but-3-en-1-ol (71.2 mg, 1.0 mmol) and 4-(trifluoromethyl)benzenesulfonyl chloride (269 mg, 1.1 mmol), according to General Procedure B. Purification using silica gel column chromatography (20% EtOAc in Hexanes) gave the product as a yellow oil (48 mg, 17% yield). **$^1$H NMR** (400 MHz, $CDCl_3$) δ 8.05 (d, *J* = 8.1 Hz, 2H), 7.85–7.81 (m, 2H), 5.67 (ddt, *J* = 16.4, 10.6,

6.7 Hz, 1H), 5.14–5.06 (m, 2H), 4.15 (t, $J$ = 6.7 Hz, 2H), 2.44 (qt, $J$ = 6.7, 1.3 Hz, 2H); **$^{13}$C NMR** (150 MHz, $CDCl_3$) δ 139.81 (q, $J$ = 1.7 Hz), 135.40 (q, $J$ = 33.2 Hz), 132.04, 128.45, 126.42 (q, $J$ = 3.8 Hz), 123.07 (q, $J$ = 272.8 Hz), 118.57, 70.28, 33.13; **$^{19}$F NMR** (376 MHz, $CDCl_3$) δ -63.52; **HRMS** (ESI-TOF) Calc'd for $C_{11}H_{12}F_3O_3S^+$ [M+H] 281.0459, found 281.0452.

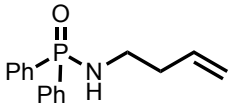

**4.S40**

***N*-(but-3-en-1-yl)-*P*,*P*-diphenylphosphinic amide (4.S40):** The title compound was prepared from but-3-en-1-amine (71.1 mg, 1.0 mmol) and diphenylphosphinic chloride (260 mg, 1.1 mmol), according to General Procedure B. Purification using silica gel column chromatography (20% Acetone in Hexanes) gave the product as a white solid (145 mg, 53% yield). **$^{1}$H NMR** (400 MHz, $CDCl_3$) δ 7.96–7.87 (m, 4H), 7.56–7.43 (m, 6H), 5.78 (ddt, $J$ = 17.1, 10.2, 6.9 Hz, 1H), 5.19–5.08 (m, 2H), 3.07 (dq, $J$ = 8.6, 6.7 Hz, 2H), 2.91 (d, $J$ = 6.6 Hz, 1H), 2.39–2.31 (m, 2H); **$^{13}$C NMR** (150 MHz, $CDCl_3$) δ 135.22, 132.98, 132.08 (d, $J$ = 9.4 Hz), 131.80 (d, $J$ = 2.8 Hz), 128.53 (d, $J$ = 12.2 Hz), 117.53 (d, $J$ = 1.7 Hz), 39.67 (d, $J$ = 1.7 Hz), 36.15 (d, $J$ = 7.6 Hz); **$^{31}$P NMR** (162 MHz, $CDCl_3$) δ 23.50; **HRMS** (ESI-TOF) Calc'd for $C_{16}H_{19}NOP^+$ [M+H] 272.1204, found 272.1207.

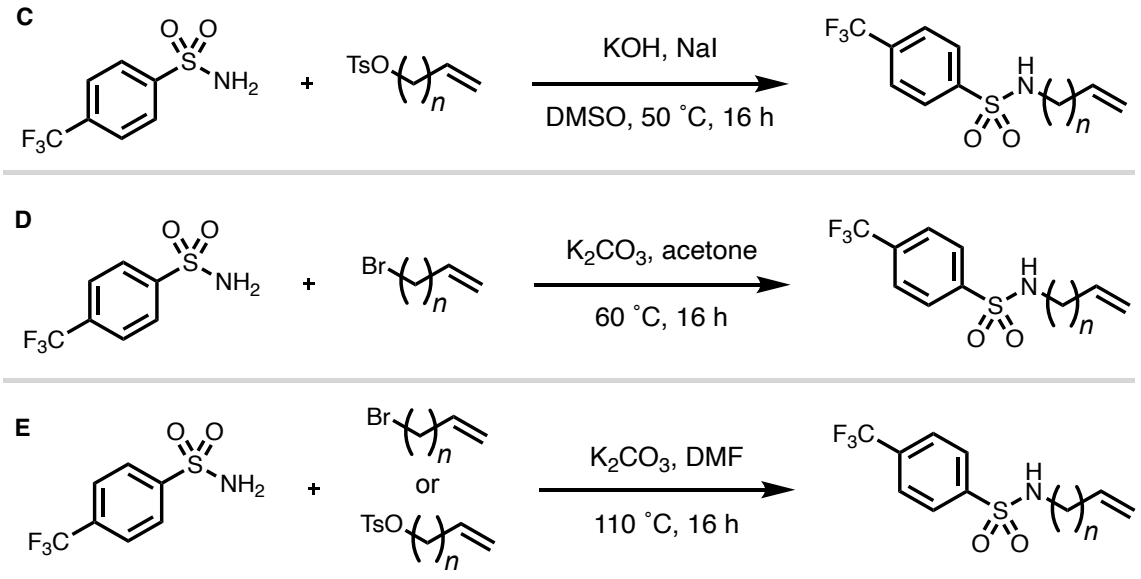


***Scheme 4.S2.*** Synthesis of alkenyl sulfonamides **4.S41–4.S43**, **4.S46**, **4.S47**, and **4.S49–4.S50**. These compounds were synthesized using adapted versions of literature procedures describing the preparation of similar compounds.[11]

**General Procedure C:** To a 4-mL dram vial equipped with a Teflon-coated magnetic stir bar were added 4-(trifluoromethyl)benzenesulfonamide (2.3 mmol), finely ground KOH powder (1.3 mmol), and DMSO (1.25 mL). The vial was placed on a heating block and allowed to stir at 50 °C for 2 h. After this time, the vial was cooled to room temperature, and a solution of the appropriate alkenyl tosylate (1.0 mmol) dissolved in DMSO (0.15 mL) was added dropwise, followed by addition of NaI (0.3 mmol) in a single portion. The reaction was allowed to continue at 50 °C for 16 h. After this time, water (10 mL) was added to the vial, and the reaction mixture was extracted with DCM (3 × 1 mL). The combined organic layers were then washed with 10% aqueous solution of NaOH (10 mL) and brine (10 mL) and dried over $MgSO_4$. The solvent was removed *in vacuo* to leave a white solid, which afforded pure product after silica gel column chromatography.

**General Procedure D:** To a 35-mL bomb flask equipped with a Teflon-coated magnetic stir bar were added 4-(trifluoromethyl)benzenesulfonamide (1 equiv), the appropriate alkenyl bromide (1.1 equiv), $K_2CO_3$ (2 equiv), and acetone (0.1 M). The flask was placed in an oil bath, and the reaction mixture was allowed to stir at 60 °C for 16 h. After this time, the reaction mixture was allowed to cool to room temperature and was then filtered over Celite, rinsing with EtOAc. The filtrate was concentrated *in vacuo* to leave a brown, which afforded pure product after silica gel column chromatography.

**General Procedure E:** To a 35-mL bomb flask equipped with a Teflon-coated magnetic stir bar were added 4-(trifluoromethyl)benzenesulfonamide (1.2 equiv), the appropriate alkenyl bromide (1 equiv), $K_2CO_3$ (2 equiv), and DMF (0.3 M). The flask was placed in an oil bath, and the reaction mixture was allowed to stir at 110 °C for 16 h. After this time, the reaction mixture was allowed to cool to room temperature. Then, water (10 mL) was added to the vial, and the reaction mixture was extracted with EtOAc (3 × 1 mL). The filtrate was concentrated *in vacuo* to leave a brown oil, which afforded pure product after silica gel column chromatography.

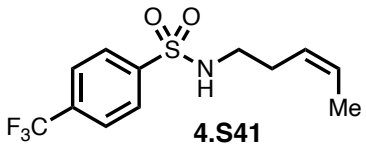

**4.S41**

**(*Z*)-*N*-(pent-3-en-1-yl)-4-(trifluoromethyl)benzenesulfonamide (4.S41):** The title compound was prepared from (*Z*)-pent-3-en-1-yl 4-methylbenzenesulfonate **4.S17** (240 mg, 1.0 mmol) and 4-(trifluoromethyl)benzenesulfonamide (518 mg, 2.3 mmol), according to General Procedure C. Purification using silica gel column chromatography (20% EtOAc in Hexanes) gave the

product as a white solid (50 mg, 17% yield). **$^1$H NMR** (400 MHz, $CDCl_3$) δ 7.99 (d, *J* = 8.2 Hz, 2H), 7.79 (d, *J* = 8.3 Hz, 2H), 5.66–5.55 (m, 1H), 5.21 (dtd, *J* = 10.9, 7.4, 1.9 Hz, 1H), 4.46 (t, *J* = 6.0 Hz, 1H), 3.04 (q, *J* = 6.5 Hz, 2H), 2.25 (q, *J* = 7.0 Hz, 2H), 1.60–1.56 (m, 3H); **$^{13}$C NMR** (150 MHz, $CDCl_3$) δ 143.67, 134.37 (q, *J* = 33.1 Hz), 128.10, 127.59, 126.30 (q, *J* = 3.8 Hz), 125.22, 123.27 (q, *J* = 272.4 Hz), 42.77, 27.07, 12.90; **$^{19}$F NMR** (376 MHz, $CDCl_3$) δ -63.36; **HRMS** (ESI-TOF) Calc'd for $C_{12}H_{15}F_3NO_2S^+$ [M+H] 294.0776, found 294.0776.

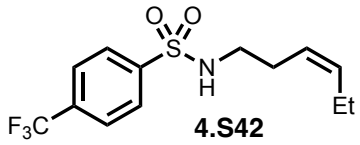

**4.S42**

**(*Z*)-*N*-(hex-3-en-1-yl)-4-(trifluoromethyl)benzenesulfonamide (4.S42):** The title compound was prepared from (*Z*)-hex-3-en-1-yl 4-methylbenzenesulfonate **4.S18** (1.27 g, 5.00 mmol) and 4-(trifluoromethyl)benzenesulfonamide (1.35 g, 6.00 mmol) $K_2CO_3$ (1.38 g, 10.0 mmol) and DMF (16.7 mL) according to General Procedure E. Purification using silica gel column chromatography (20% Acetone in Hexanes) gave the product as a white solid (869 mg, 57% yield). **$^1$H NMR** (400 MHz, $CDCl_3$) δ 7.99 (d, *J* = 8.1 Hz, 2H), 7.79 (d, *J* = 8.2 Hz, 2H), 5.56–5.48 (m, 1H), 5.18–5.10 (m, 1H), 4.49 (t, *J* = 6.0 Hz, 1H), 3.03 (td, *J* = 6.7, 6.1 Hz, 2H), 2.27–2.20 (m, 2H), 2.03–1.93 (m, 2H), 0.94 (t, *J* = 7.5 Hz, 3H); **$^{13}$C NMR** (150 MHz, $CDCl_3$) δ 143.67 (q, *J* = 1.1 Hz), 135.79, 134.37 (q, *J* = 33.2 Hz), 127.59, 126.30 (q, *J* = 3.6 Hz), 123.62, 123.24 (q, *J* = 272.6 Hz), 42.88, 27.34, 20.61, 14.13; **$^{19}$F NMR** (376 MHz, $CDCl_3$) δ -65.78; **HRMS** (ESI-TOF) Calc'd for $C_{13}H_{15}F_3NO_2S^-$ [M-H] 306.0776, found 306.0776.

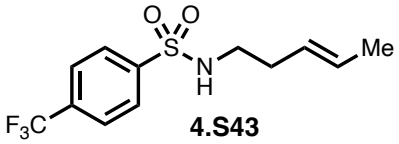

**4.S43**

**(*E*)-*N*-(pent-3-en-1-yl)-4-(trifluoromethyl)benzenesulfonamide (4.S43):** The title compound was prepared from (*E*)-pent-3-en-1-yl 4-methylbenzenesulfonate **4.S19** (240 mg, 1.0 mmol) and 4-(trifluoromethyl)benzenesulfonamide (518 mg, 2.3 mmol), according to General Procedure C. Purification using silica gel column chromatography (20% EtOAc in Hexanes) gave the product as a white solid (100 mg, 34% yield). **$^1$H NMR** (400 MHz, $CDCl_3$) δ 7.99 (d, *J* = 8.0 Hz, 2H), 7.79 (d, *J* = 8.2 Hz, 2H), 5.53–5.42 (m, 1H), 5.25–5.15 (m, 1H), 4.47 (t, *J* = 6.3 Hz, 1H), 3.03 (q, *J* = 6.4 Hz, 2H), 2.15 (q, *J* = 6.7 Hz, 2H), 1.63 (dt, *J* = 6.5, 1.4 Hz, 3H); **$^{13}$C NMR** (150 MHz, $CDCl_3$) δ 143.67 (q, *J* = 1.7 Hz), 134.29 (q, *J* = 33.1 Hz), 129.16, 127.60, 126.29, 126.25 (q, *J* = 3.9, 3.3 Hz), 123.25 (q, *J* = 273.5, 272.9 Hz), 42.76, 32.51, 17.87; **$^{19}$F NMR** (376 MHz, $CDCl_3$) δ -63.35; **HRMS** (ESI-TOF) Calc'd for $C_{12}H_{15}F_3NO_2S^+$ [M+H] 294.0776, found 294.0780.

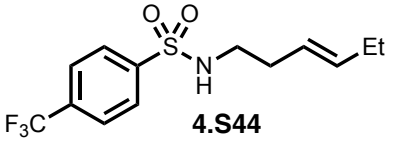

**4.S44**

**(*E*)-*N*-(hex-3-en-1-yl)-4-(trifluoromethyl)benzenesulfonamide (4.S44):** The title compound was prepared from (*E*)-hex-3-en-1-yl 4-methylbenzenesulfonate **4.S20** (1.27 g, 5.00 mmol) and 4-(trifluoromethyl)benzenesulfonamide (1.35 g, 6.00 mmol) $K_2CO_3$ (1.38 g, 10.0 mmol) and DMF (16.7 mL) according to General Procedure E. Purification using silica gel column chromatography (20% Acetone in Hexanes) gave the product as a white solid (856 mg, 56% yield). **$^1$H NMR** (400 MHz, $CDCl_3$) δ 7.99 (d, *J* = 8.1 Hz, 2H), 7.79 (d, *J* = 8.2 Hz, 2H), 5.50 (dtt, *J* = 15.3, 6.3, 1.4 Hz, 1H), 5.18 (dtt, *J* = 15.5, 7.0, 1.6 Hz, 1H), 4.52 (t, *J* = 5.9 Hz, 1H), 3.03 (td, *J* = 6.6, 5.9 Hz, 2H), 2.16 (tdt, *J* = 6.7, 5.5, 1.2 Hz, 2H), 1.98 (ttdd, *J* = 7.4, 6.3, 2.6, 1.2 Hz, 2H), 0.94 (t, *J* = 7.5 Hz, 3H); **$^{13}$C NMR** (150 MHz,

$CDCl_3$) δ 143.71 (q, *J* = 1.2 Hz), 136.40, 134.34 (q, *J* = 32.9 Hz), 127.59, 126.27 (q, *J* = 3.8 Hz), 123.95, 123.25 (q, *J* = 273.0 Hz), 42.74, 32.49, 25.49, 13.55; **$^{19}$F NMR** (376 MHz, $CDCl_3$) δ -65.77; **HRMS** (ESI-TOF) Calc'd for $C_{13}H_{15}F_3NO_2S^-$ [M-H] 306.0776, found 306.0771.

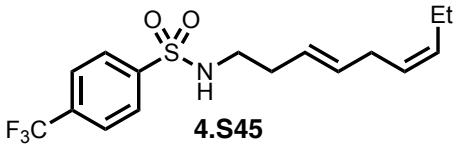

**4.S45**

***N*-((3*E*,6*Z*)-nona-3,6-dien-1-yl)-4-(trifluoromethyl)benzenesulfonamide (4.S45):** The title compound was prepared from (3*E*,6*Z*)-nona-3,6-dien-1-yl 4-methylbenzenesulfonate **4.S21** (1.27 g, 5.00 mmol) and 4-(trifluoromethyl)benzenesulfonamide (1.35 g, 6.00 mmol) $K_2CO_3$ (1.38 g, 10.0 mmol) and DMF (16.7 mL) according to General Procedure E. Purification using silica gel column chromatography (20% Acetone in Hexanes) gave the product as a yellow oil (588 mg, 34% yield). **$^1$H NMR** (400 MHz, $CDCl_3$) δ 7.99 (d, *J* = 8.2 Hz, 2H), 7.79 (d, *J* = 8.2 Hz, 2H), 5.50–5.39 (m, 2H), 5.31–5.18 (m, 2H), 4.48 (t, *J* = 5.9 Hz, 1H), 3.03 (q, *J* = 6.5 Hz, 2H), 2.74–2.67 (m, 2H), 2.21–2.13 (m, 2H), 2.07–1.96 (m, 2H), 0.96 (t, *J* = 7.5 Hz, 3H); **$^{13}$C NMR** (150 MHz, $CDCl_3$) δ 143.68 (q, *J* = 1.3 Hz), 134.39 (q, *J* = 33.0 Hz), 133.06, 132.88, 127.59, 126.30 (q, *J* = 3.8 Hz), 125.98, 125.28, 123.23 (q, *J* = 272.6 Hz), 42.61, 32.50, 30.18, 20.46, 14.24; **$^{19}$F NMR** (376 MHz, $CDCl_3$) δ -65.77; **HRMS** (ESI-TOF) Calc'd for $C_{16}H_{19}F_3NO_2S^-$ [M-H] 346.1089, found 346.1093.

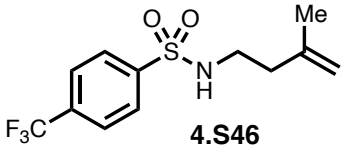

**4.S46**

***N*-(3-methylbut-3-en-1-yl)-4-(trifluoromethyl)benzenesulfonamide (4.S46):** The title compound was prepared from 3-methylbut-3-en-1-yl 4-

methylbenzenesulfonate **4.S22** (937.2 mg, 3.9 mmol) and 4-(trifluoromethyl)benzenesulfonamide (743.1 mg, 3.3 mmol), according to General Procedure C. Purification using silica gel column chromatography (20% EtOAc in Hexanes) gave the product as an off-white solid (194 mg, 22% yield). **$^1$H NMR** (600 MHz, $CDCl_3$) δ 8.01 (d, *J* = 7.9 Hz, 2H), 7.80 (d, *J* = 8.1 Hz, 2H), 4.82 (t, *J* = 1.6 Hz, 1H), 4.67 (dd, *J* = 1.9, 1.0 Hz, 1H), 4.63 (t, *J* = 5.8 Hz, 1H), 3.12 (td, *J* = 6.7, 5.8 Hz, 2H), 2.18 (td, *J* = 6.7, 1.2 Hz, 2H), 1.62 (s, 3H); **$^{13}$C NMR** (150 MHz, $CDCl_3$) δ 143.74, 141.29, 134.54 (q, *J* = 33.0 Hz), 127.73, 126.43 (q, *J* = 3.7 Hz), 123.36 (q, *J* = 272.6 Hz), 113.65, 40.69, 37.41, 21.82; **$^{19}$F NMR** (376 MHz, $CDCl_3$) δ -63.41; **HRMS** (ESI-TOF) Calc'd for $C_{12}H_{15}F_3NO_2S^+$ [M+H] 294.0776, found 294.0764.

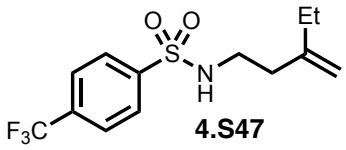

**4.S47**

***N*-(3-methylenepentyl)-4-(trifluoromethyl)benzenesulfonamid benzenesulfonamide** (**4.S47**): The title compound was prepared from 3-methylenepentyl 4-methylbenzenesulfonate **4.S23** (450 mg, 1.8 mmol) and 4-(trifluoromethyl)benzenesulfonamide (478 mg, 2.1 mmol), according to General Procedure E. Purification using silica gel column chromatography (20% diethyl ether in hexanes) gave the product as an white solid (341 mg, 63% yield). **$^1$H NMR** (600 MHz, $CDCl_3$) δ 7.99 (d, *J* = 8.2 Hz, 2H), 7.79 (d, *J* = 8.2 Hz, 2H), 4.83 (q, *J* = 1.6 Hz, 1H), 4.68 (q, *J* = 1.2 Hz, 1H), 4.52 (t, *J* = 6.0 Hz, 1H), 3.11 (td, *J* = 6.7, 5.8 Hz, 2H), 2.20 (ddd, *J* = 7.3, 6.2, 0.9 Hz, 2H), 1.89 (qt, *J* = 7.5, 1.2 Hz, 2H), 0.96 (t, *J* = 7.4 Hz, 3H); **$^{13}$C NMR** (150 MHz, CDCl3) δ 146.91, 143.79, 134.59 (q, *J* = 33.1 Hz), 127.77, 126.48 (q, *J* = 3.7 Hz), 123.41

(q, *J* = 272.8 Hz), 111.33, 40.93, 36.01, 28.25, 12.22. **$^{19}$F NMR** (376 MHz, CDCl3) δ –65.77. **HRMS** (ESI-TOF) Calc'd for $C_{13}H_{15}F_3NO_2S^-$ [M−H] 306.0776, found 306.0777.

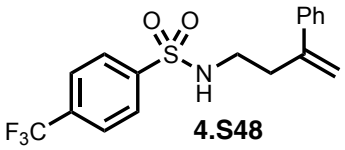

**4.S48**

***N*-(3-phenylbut-3-en-1-yl)-4-(trifluoromethyl)benzenesulfonamide** (**4.S48**): The title compound was prepared from 3-phenylbut-3-en-1-yl 4-methylbenzenesulfonate **4.S24** (1.5 g, 5.0 mmol) and 4-(trifluoromethyl)benzenesulfonamide (1.3 g, 6.0 mmol), according to General Procedure E. Purification using silica gel column chromatography (20% diethyl ether in hexanes) gave the product as an white solid (1.0 g, 59% yield). **$^{1}$H NMR** (600 MHz, $CDCl_3$) δ 7.87 (d, *J* = 8.5 Hz, 2H), 7.70 (d, *J* = 8.2 Hz, 2H), 7.31–7.20 (m, 5H), 5.36 (s, 1H), 5.07 (s, 1H), 4.47 (t, *J* = 5.9 Hz, 1H), 3.09 (q, *J* = 6.4 Hz, 2H), 2.71 (t, *J* = 6.7 Hz, 2H); **$^{13}$C NMR** (150 MHz, CDCl3) δ 144.27, 143.49, 139.23, 134.47 (q, *J* = 33.1 Hz), 128.78, 128.26, 127.65, 126.38 (q, *J* = 3.7 Hz), 123.39 (q, *J* = 272.5 Hz), 115.77, 41.39, 35.36. **$^{19}$F NMR** (376 MHz, CDCl3) δ –65.78. **HRMS** (ESI-TOF) Calc'd for $C_{17}H_{15}F_3NO_2S^-$ [M−H] 354.0776, found 354.0775.

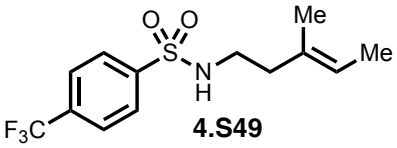

**4.S49**

**(*E*)-*N*-(3-methylpent-3-en-1-yl)-4-(trifluoromethyl)benzenesulfonamide (4.S49):** The title compound was prepared from (*E*)-3-methylpent-3-en-1-yl 4-methylbenzenesulfonate **4.S25** (1.27 g, 5.00 mmol) and 4-(trifluoromethyl)benzenesulfonamide (1.35 g, 6.00 mmol) $K_2CO_3$ (1.38 g, 10.0 mmol) and DMF (16.7 mL) according to General Procedure E. Purification using silica gel column

chromatography (20% Acetone in Hexanes) gave the product as a white solid (894 mg, 58% yield). **$^{1}$H NMR** (400 MHz, $CDCl_3$) δ 16.99 (d, *J* = 8.2 Hz, 2H), 16.79 (d, *J* = 8.1 Hz, 2H), 14.21 (dddq, *J* = 8.0, 6.7, 5.3, 1.3 Hz, 1H), 13.41 (t, *J* = 5.6 Hz, 1H), 12.10–12.04 (m, 2H), 11.13 (tt, *J* = 6.5, 1.1 Hz, 2H), 10.57 (dq, *J* = 6.6, 2.1, 1.6 Hz, 3H), 10.46 (p, *J* = 1.1 Hz, 3H); **$^{13}$C NMR** (150 MHz, $CDCl_3$) δ 143.63 (q, *J* = 1.5 Hz), 134.31 (q, *J* = 32.9 Hz), 131.13, 127.60, 126.24 (q, *J* = 3.6 Hz), 125.96, 123.25 (q, *J* = 273.1 Hz), 40.73, 39.00, 14.91, 13.40; **$^{19}$F NMR** (376 MHz, $CDCl_3$) δ -65.77; **HRMS** (ESI-TOF) Calc'd for $C_{13}H_{15}F_3NO_2S^-$ [M-H] 306.0776, found 306.0772.

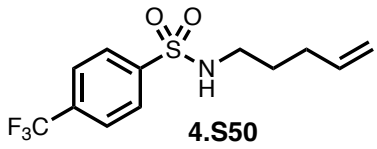

**4.S50**

***N*-(pent-4-en-1-yl)-4-(trifluoromethyl)benzenesulfonamide (4.S50):** The title compound was prepared from 4-(trifluoromethyl)benzenesulfonamide (1.13 g, 5.0 mmol), 5-bromopent-1-ene (820 mg, 5.5 mmol), $K_2CO_3$ (10 mmol) and acetone (5 mL) according to General Procedure D. Purification using silica gel column chromatography (20% EtOAc in Hexanes) gave the product as a white solid (584.5 mg, 40% yield). **$^{1}$H NMR** (400 MHz, $CDCl_3$) δ 7.99 (d, *J* = 8.0 Hz, 2H), 7.79 (d, *J* = 8.1 Hz, 2H), 5.77–5.65 (m, 1H), 5.02–4.94 (m, 2H), 4.44 (t, *J* = 6.4 Hz 1H), 3.06–2.98 (m, 2H), 2.07 (q, *J* = 7.1 Hz, 2H), 1.60 (p, *J* = 7.2 Hz, 2H); **$^{13}$C NMR** (150 MHz, $CDCl_3$) δ 143.66 (q, *J* = 1.4 Hz), 136.96, 134.39 (q, *J* = 33.1 Hz), 127.56, 126.32 (q, *J* = 3.6 Hz), 124.14 (q, *J* = 272.8 Hz), 115.83, 42.72, 30.56, 28.71; **$^{19}$F NMR** (376 MHz, $CDCl_3$) δ -63.37; **HRMS** (ESI-TOF) Calc'd for $C_{12}H_{15}F_3NO_2S^+$ [M+H] 294.0776, found 294.0776.

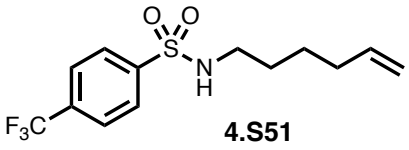


**4.S51**

***N*-(hex-5-en-1-yl)-4-(trifluoromethyl)benzenesulfonamide (4.S51):** The title compound was prepared from 4-(trifluoromethyl)benzenesulfonamide (349 mg, 1.55 mmol), 6-bromohex-1-ene (277 mg, 1.7 mmol), $K_2CO_3$ (3.1 mmol) and acetone (1.7 mL) according to General Procedure D. Purification using silica gel column chromatography (20% EtOAc in Hexanes) gave the product as a white solid (95 mg, 20% yield). **$^1$H NMR** (400 MHz, $CDCl_3$) δ 7.99 (d, *J* = 7.9 Hz, 2H), 7.79 (d, *J* = 8.2 Hz, 2H), 5.71 (ddt, *J* = 17.0, 10.2, 6.6 Hz, 1H), 5.00–4.91 (m, 2H), 4.40 (t, *J* = 6.1 Hz, 1H), 3.05–2.97 (m, 2H), 2.01 (q, *J* = 7.1 Hz, 2H), 1.53–1.45 (m, 2H), 1.42–1.32 (m, 2H); **$^{13}$C NMR** (150 MHz, $CDCl_3$) δ 143.65 (q, *J* = 1.5 Hz), 137.93, 134.34 (q, *J* = 33.1 Hz), 127.57, 126.30 (q, *J* = 3.5 Hz), 123.24 (q, *J* = 272.8 Hz), 115.00, 43.15, 32.99, 28.95, 25.61; **$^{19}$F NMR** (376 MHz, $CDCl_3$) δ -63.39; **HRMS** (ESI-TOF) Calc'd for $C_{13}H_{17}F_3NO_2S^+$ [M+H] 308.0932, found 308.0932.

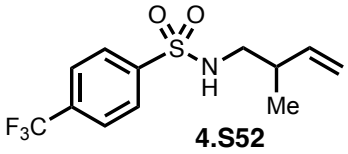


**4.S52**

***N*-(2-methylbut-3-en-1-yl)-4-(trifluoromethyl)benzenesulfonamide (4.S52):** The title compound was prepared from 4-(trifluoromethyl)benzenesulfonamide (270 mg, 1.20 mmol), 2-methylbut-3-en-1-yl 4-methylbenzenesulfonate **4.S26** (240 mg, 1.00 mmol), $K_2CO_3$ (276 mg, 2.00 mmol) and DMF (3 mL) according to General Procedure E. Purification using silica gel column chromatography (20% Acetone in Hexanes) gave the product as a white solid (92.2 mg, 31% yield). **$^1$H NMR** (400 MHz, $CDCl_3$) δ 8.01 (d, *J* = 8.1 Hz, 2H), 7.82 (d, *J* = 8.2 Hz, 2H), 5.55 (ddd, *J* = 17.1, 10.4, 7.8 Hz, 1H), 5.13–5.02 (m, 2H), 4.54–4.44 (m, 1H), 3.05

(ddd, *J* = 12.3, 7.6, 5.3 Hz, 1H), 2.81 (ddd, *J* = 12.3, 8.4, 4.7 Hz, 1H), 2.33 (dt, *J* = 14.0, 7.0 Hz, 1H), 1.02 (d, *J* = 6.8 Hz, 3H); **$^{13}$C NMR** (150 MHz, $CDCl_3$) δ 143.68 (q, *J* = 1.5 Hz), 139.96, 134.35 (q, *J* = 33.2 Hz), 127.57, 126.29 (q, *J* = 3.9 Hz), 123.24 (q, *J* = 272.8 Hz), 116.50, 48.05, 38.01, 17.33; **$^{19}$F NMR** (376 MHz, $CDCl_3$) δ -65.76; **HRMS** (ESI-TOF) Calc'd for $C_{12}H_{15}F_3NO_2S^+$ [M+H] 294.0776, found 294.0786.

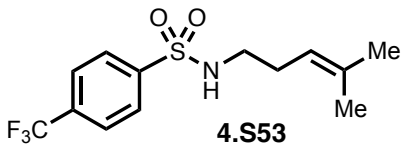

**4.S53**

***N*-(4-methylpent-3-en-1-yl)-4-(trifluoromethyl)benzenesulfonamide (4.S53):** The title compound was prepared from 4-(trifluoromethyl)benzenesulfonamide (1.22 g, 5.41 mmol), 5-bromo-2-methylpent-2-ene (735 mg, 4.51 mmol), $K_2CO_3$ (1.25 g, 9.02 mmol) and DMF (3 mL) according to General Procedure E. Purification using silica gel column chromatography (20% Acetone in Hexanes) gave the product as a white solid (639.2 mg, 46% yield). **$^{1}$H NMR** (400 MHz, $CDCl_3$) δ 8.02 (d, *J* = 8.1 Hz, 2H), 7.82 (d, *J* = 8.2 Hz, 2H), 4.95 (ddq, *J* = 8.8, 5.9, 1.4 Hz, 1H), 4.48 (t, *J* = 6.0 Hz, 1H), 3.03 (td, *J* = 6.7, 6.0 Hz, 2H), 2.24 – 2.16 (m, 2H), 1.70 (d, *J* = 1.3 Hz, 3H), 1.59 (d, *J* = 1.4 Hz, 3H); **$^{13}$C NMR** (151 MHz, $CDCl_3$) δ 143.70 (q, *J* = 1.9 Hz), 135.97, 134.32 (q, *J* = 33.1 Hz), 127.59, 126.26 (q, *J* = 3.8 Hz), 123.25 (q, *J* = 273.1, 272.5 Hz), 119.36, 43.05, 28.20, 25.73, 17.82; **$^{19}$F NMR** (376 MHz, $CDCl_3$) δ -65.77; **HRMS** (ESI-TOF) Calc'd for $C_{13}H_{17}F_3NO_2S^+$ [M+H] 308.0932, found 308.0933.

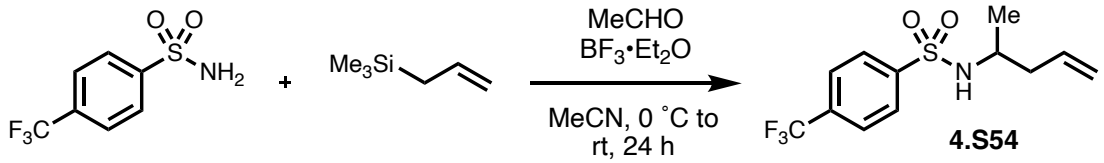


***Scheme 4.S3.*** Synthesis of α-methyl alkenyl sulfonamide **4.S54**. This compound was synthesized using an adapted version of a literature procedure describing the preparation of a similar compound.[12]

***N*-(pent-4-en-2-yl)-4-(trifluoromethyl)benzenesulfonamide (4.S54):** To a 4-mL dram vial equipped with a Teflon-coated magnetic stir bar were added acetaldehyde (0.28 mL, 5.0 mmol, 1 equiv), allyltrimethylsilane (0.95 mL, 6.0 mmol, 1.2 equiv), 4-(trifluoromethyl)benzenesulfonamide (1.13 g, 5.0 mmol, 1 equiv), and MeCN (8 mL). The reaction mixture was then cooled to 0 °C, and $BF_3$•$Et_2O$ (0.62 mL, 5.0 mmol, 1 equiv) was added in one portion. The mixture was stirred for 30 min at 0 °C, then allowed to warm to room temperature and left stirring overnight. After this time, water (100 mL) was added to the vial, and the reaction mixture was extracted with DCM (3 × 20 mL). The combined organic layers were dried over $Na_2SO_4$. The combined organic layers were dried over $Na_2SO_4$, and the solvent was removed *in vacuo*. Purification using silica gel column chromatography (20% EtOAc in Hexanes) gave the product as a colorless oil (529 mg, 36% yield). **$^1$H NMR** (600 MHz, $CDCl_3$) δ 8.01 (d, *J* = 8.1 Hz, 2H), 7.78 (d, *J* = 8.1 Hz, 2H), 5.56 (ddt, *J* = 17.3, 10.2, 7.2 Hz, 1H), 5.10–4.99 (m, 2H), 4.64 (d, *J* = 7.7 Hz, 1H), 3.45 (dh, *J* = 7.8, 6.5 Hz, 1H), 2.15 (ddt, *J* = 7.3, 6.2, 1.2 Hz, 2H), 1.11 (d, *J* = 6.6 Hz, 3H); **$^{13}$C NMR** (150 MHz, $CDCl_3$) δ 144.85, 134.42 (q, *J* = 33.0 Hz), 133.13, 127.69, 126.35 (q, *J* = 3.7 Hz), 123.38 (q, *J* = 272.9 Hz), 119.29, 49.73, 41.53, 21.47; **$^{19}$F NMR** (376 MHz, $CDCl_3$) δ -63.37; **HRMS** (ESI-TOF) Calc'd for $C_{12}H_{15}F_3NO_2S^+$ [M+H] 294.0776, found 294.0771.

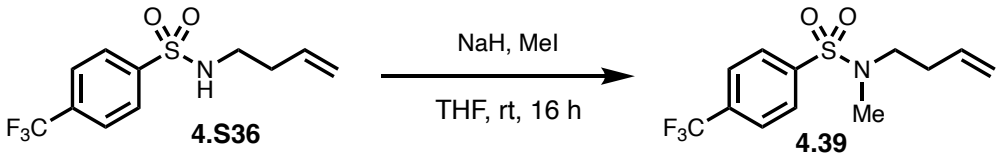


***Scheme 4.S4.*** Synthesis of *N*-methyl alkenyl sulfonamide **4.39**. This compound was synthesized using an adapted version of a literature procedure describing the preparation of a similar compound.[13]

***N*-(but-3-en-1-yl)-*N*-methyl-4-(trifluoromethyl)benzenesulfonamide (4.39):** To a 1-dram (4 mL) vial equipped with a Teflon-coated magnetic stir bar were added NaH (60% in mineral oil, 12 mg, 0.30 mmol, 0.6 equiv) and THF (1 mL). The vial was submerged in an ice bath, and a solution of the alkenyl sulfonamide **4.S36** (0.50 mmol, 1 equiv) in THF (2 mL) was subsequently added. The mixture was allowed to stir for at least 10 min, and then MeI (92 mg, 0.65 mmol, 1.3 equiv) was added dropwise. The reaction mixture was allowed to warm to room temperature and was stirred for 16 h. After this time, the reaction mixture was diluted with sat. aq. $NH_4Cl$ (10 mL) and extracted with EtOAc (3 × 1 mL). The combined organic layers were dried over $Na_2SO_4$, and the solvent was removed *in vacuo*. Purification using silica gel column chromatography (20% EtOAc in Hexanes) gave the product as a colorless oil (75 mg, 51% yield). **$^1$H NMR** (400 MHz, $CDCl_3$) δ 7.92 (d, $J$ = 8.1 Hz, 2H), 7.80 (d, $J$ = 8.2 Hz, 2H), 5.75 (ddt, $J$ = 17.1, 10.3, 6.8 Hz, 1H), 5.14–5.03 (m, 2H), 3.17–3.09 (m, 2H), 2.79 (s, 3H), 2.32 (tdd, $J$ = 8.2, 6.2, 1.4 Hz, 2H); **$^{13}$C NMR** (150 MHz, $CDCl_3$) δ 141.56 (q, $J$ = 1.5 Hz), 134.24 (q, $J$ = 33.2 Hz), 133.91, 126.24 (q, $J$ = 3.8 Hz), 123.27 (q, $J$ = 272.7 Hz), 117.46, 49.63, 34.73, 32.29; **$^{19}$F NMR** (376 MHz, $CDCl_3$) δ -63.33; **HRMS** (ESI-TOF) Calc'd for $C_{12}H_{14}F_3NO_2S^+$ [M+H] 294.0776, found 294.0779.

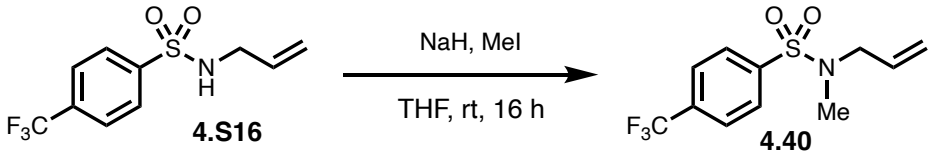


***Scheme 4.S5.*** Synthesis of *N*-methyl alkenyl sulfonamide **4.40**. This compound was synthesized using an adapted version of a literature procedure describing the preparation of a similar compound.[13]

***N*-allyl-*N*-methyl-4-(trifluoromethyl)benzenesulfonamide (4.40):** To a 20 mL scintillation vial equipped with a Teflon-coated magnetic stir bar were added NaH (60% in mineral oil, 40 mg, 1.00 mmol, 1 equiv) and THF (3 mL). The vial was submerged in an ice bath, and a solution of the alkenyl sulfonamide **4.S16** (265 mg, 1.00 mmol, 1 equiv) in THF (2 mL) was subsequently added. The mixture was allowed to stir for at least 10 min, and then MeI (75 µL, 1.20 mmol, 1.2 equiv) was added dropwise. The reaction mixture was allowed to warm to room temperature and was stirred for 16 h. After this time, the reaction mixture was diluted with sat. aq. $NH_4Cl$ (10 mL) and extracted with EtOAc (3 × 1 mL). The combined organic layers were dried over $Na_2SO_4$, and the solvent was removed *in vacuo*. Purification using silica gel column chromatography (20% EtOAc in Hexanes) gave the product as a white solid (166 mg, 60% yield). **$^1$H NMR** (400 MHz, $CDCl_3$) δ 7.93 (d, *J* = 8.1 Hz, 2H), 7.81 (d, *J* = 8.2 Hz, 2H), 5.71 (ddt, *J* = 17.5, 9.5, 6.3 Hz, 1H), 5.26–5.18 (m, 2H), 3.69 (dt, *J* = 6.5, 1.5 Hz, 2H), 2.73 (s, 3H); **$^{13}$C NMR** (150 MHz, $CDCl_3$) δ 141.40 (q, *J* = 1.4 Hz), 134.32 (q, *J* = 33.2 Hz), 131.97, 127.89, 126.27 (q, *J* = 3.6 Hz), 123.26 (q, *J* = 273.1 Hz), 119.61, 52.98, 34.17; **$^{19}$F NMR** (376 MHz, $CDCl_3$) δ -65.76; **HRMS** (ESI-TOF) Calc'd for $C_{11}H_{11}F_3NO_2S^-$ [M-H] 278.0463, found 278.0456.

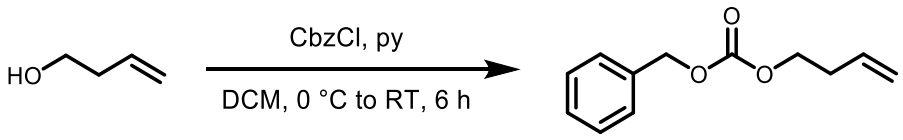


**Benzyl but-3-en-1-yl carbonate (4.S55):** But-3-en-1-ol (0.43 mL, 5 mmol) was charged into a 100-mL round-bottom flask containing DCM (25 mL) and pyridine (1.2 mL, 15 mmol) at 0 °C. Benzyl chloroformate (2.1 mL, 6.25 mmol) was added dropwise and the reaction was allowed to warm to room temperature. The reaction was stirred at room temperature for 6 h and then quenched with aq. HCl (2 M). The organic layer was dried over $Na_2SO_4$, concentrated *in vacuo*, and purified by column chromatography (5% EtOAc in Hexanes) to afford **4.S55** (877 mg, 85% yield) as a clear oil. **$^1$H NMR** (600 MHz, $CDCl_3$) δ 7.41–7.31 (m, 5H), 5.79 (ddtd, *J* = 17.0, 10.3, 6.7, 1.2 Hz, 1H), 5.18–5.07 (m, 4H), 4.20 (td, *J* = 6.8, 1.2 Hz, 2H), 2.43 (qd, *J* = 6.8, 1.4 Hz, 2H). **$^{13}$C NMR** (150 MHz, $CDCl_3$) δ 155.28, 135.42, 133.55, 128.73, 128.66, 128.48, 117.79, 69.70, 67.27, 33.20.

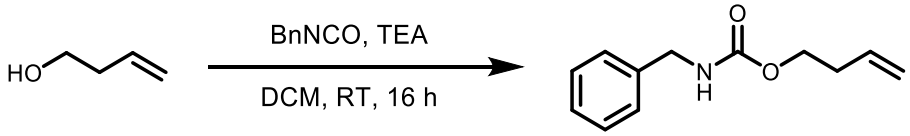


**But-3-en-1-yl benzylcarbamate (4.S56):** But-3-en-1-ol (0.43 mL, 5 mmol) was charged into a 100-mL RB flask containing DCM (50 mL) and triethylamine (3.5 mL, 25 mmol). Benzyl isocyanate (0.62 mL, 5 mmol) was added dropwise and the reaction was allowed to stir at room temperature overnight. The reaction was quenched with aqueous HCl (2 M). The organic layer was dried over $Na_2SO_4$, concentrated *in vacuo*, and purified by column chromatography (30% EtOAc in Hexanes) to afford **4.S56** (801 mg, 78% yield) as a yellow oil. **$^1$H NMR** (600 MHz, $CDCl_3$) δ 7.36–7.31 (m, 2H), 7.31–7.26 (m, 3H), 5.79 (ddt, *J* =

17.0, 10.2, 6.8 Hz, 1H), 5.16–5.04 (m, 2H), 5.04–4.92 (bs, 1H), 4.36 (d, *J* = 6.1 Hz, 2H), 4.15 (t, *J* = 6.8 Hz, 2H), 2.38 (qt, *J* = 6.7, 1.4 Hz, 2H); **$^{13}$C NMR** (150 MHz, $CDCl_3$) δ 156.71, 138.66, 134.37, 128.78, 127.65, 127.60, 117.22, 64.20, 45.17, 33.63.

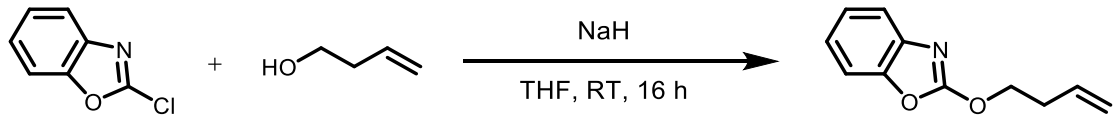


**2-(But-3-en-1-yloxy)benzo[d]oxazole (4.S57):** But-3-en-1-ol (0.86 mL, 10 mmol) was charged into a 100-mL round-bottom flask containing anhydrous THF (50 mL) and 60% w/w NaH in mineral oil (400 mg, 10 mmol). The reaction was allowed to stir at room temperature for 1 h and 2-chlorobenzoxazole (1.14 mL, 10 mmol) was added. The reaction was allowed to stir at room temperature overnight and then quenched with water and extracted with DCM (50 mL, ×3). The organic layers were combined, dried over $Na_2SO_4$, concentrated *in vacuo*, and purified by column chromatography (10% EtOAc in Hexanes) to afford **4.S57** (643 mg, 34% yield) as a pink oil. $^1$H NMR (600 MHz, $CDCl_3$) δ 7.48 (dd, *J* = 7.8, 1.5 Hz, 1H), 7.35 (d, *J* = 7.9 Hz, 1H), 7.26–7.22 (m, 1H), 7.20–7.15 (m, 1H), 5.88 (dddd, *J* = 18.3, 10.6, 7.3, 6.1 Hz, 1H), 5.21 (dt, *J* = 17.2, 1.6 Hz, 1H), 5.15 (dt, *J* = 10.3, 1.4 Hz, 1H), 4.61 (td, *J* = 6.7, 1.3 Hz, 2H), 2.64 (qd, *J* = 6.7, 1.4 Hz, 2H). **$^{13}$C NMR** (150 MHz, $CDCl_3$) δ 163.67, 148.55, 141.27, 133.10, 124.36, 122.92, 118.21, 118.04, 109.83, 71.22, 33.12.

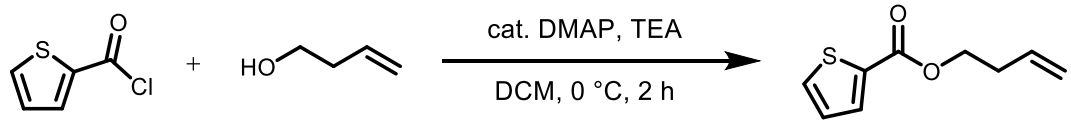

**But-3-en-1-yl thiophene-2-carboxylate (4.S58):** But-3-en-1-ol (0.57 mL, 6.6 mmol) was charged into a 100-mL round-bottom flask containing DCM (30 mL), 4-(dimethylamino)pyridine (73.3 mg, 0.6 mmol), and triethylamine (1.38 mL, 9.9 mmol). The mixture was cooled to 0 °C and 2-thiophenecarbonyl chloride (0.85 mL, 7.92 mmol) was added dropwise. The reaction was allowed to continue stirring at 0 °C for 2 h and then quenched with water and extracted with DCM (50 mL, ×3). The organic layers were combined, dried over $Na_2SO_4$, concentrated *in vacuo*, and purified by column chromatography (5% EtOAc in Hexanes) to afford **4.S57** (1.05 g, 87% yield) as a light brown oil. Characterization data match those of previous reports.[14]

**Diversification of Representative 1,2-Diarylated Products**

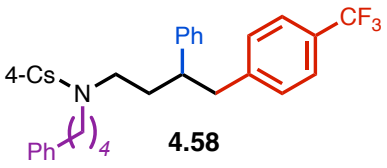


**4.58**

**4-cyano-*N*-(3-phenyl-4-(4-(trifluoromethyl)phenyl)butyl)-*N*-(4-phenylbutyl)benzenesulfonamide (4.58):** To a vial containing the starting material **4.57** (398 mg, 0.869 mmol, 1.00 equiv) was added triphenylphosphine (460 mg, 1.737 mmol, 2.00 equiv), 4-phenyl-1-butanol (273 µL, 1.737 mmol, 2.00 equiv), and dichloromethane (4.0 mL). The solution was stirred until homogeneous, then cooled in an ice water bath. A solution of DEAD (40 wt% in toluene, 791 µL, 1.737 mmol, 2.00 equiv) was added dropwise over 40 min. The mixture was warmed to room temperature and stirred for 1 h. The volatiles were removed *in vacuo*, and the crude residue was purified directly by flash column chromatography over silica gel (0 to 20% ethyl acetate in hexanes gradient) to afford the product as a thick, colorless oil (384 mg, 75%). **$^1$H NMR** (400 MHz, $CDCl_3$) δ 7.64–7.73 (m, 4H), 7.45 (d, $J$ = 8.1 Hz, 2H),

7.20–7.32 (m, 6H), 7.11 (d, $J$ = 7.1 Hz, 2H), 7.07 (d, $J$ = 8.0 Hz, 2H), 7.30 (d, $J$ = 6.8 Hz, 2H), 3.05 (t, $J$ = 7.4 Hz, 2H), 2.86–2.99 m, 3H), 2.74–2.84 (m, 2H), 2.54 (t, $J$ = 7.5 Hz, 2H), 1.84–1.99 (m, 2H), 1.48–1.55 (m, 2H), 1.30–1.38 (m, 2H); **$^{13}$C NMR** (100 MHz, $CDCl_3$) δ 143.9, 143.8, 142.6, 141.6, 132.8, 129.4, 128.6, 128.43 (q, $J$ = 32.3 Hz), 128.40, 128.3, 127.6, 127.5, 126.9, 126.0, 125.0 (q, $J$ = 3.7 Hz), 124.2 (q, $J$ = 272 Hz), 117.3, 116.0, 48.3, 46.5, 45.3, 43.4, 35.1, 34.6, 28.0, 27.6; **$^{19}$F NMR** (376 MHz, $CDCl_3$) δ -62.3; **HRMS** (ESI) Calc'd for $C_{34}H_{37}F_3N_3O_2S$ $[M+NH_4]^+$ 608.2553, found 608.2567.

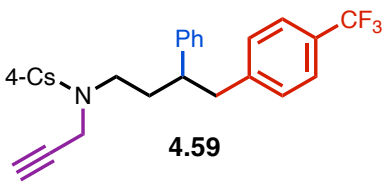


**4.59**

**4-cyano-*N*-(3-phenyl-4-(4-(trifluoromethyl)phenyl)butyl)-*N*-(prop-2-yn-1-yl)benzenesulfonamide (4.59):** To a 1-dram (4 mL) vial equipped with a Teflon-coated magnetic stir bar were added **4.57** (92 mg, 0.20 mmol, 1 equiv), $K_2CO_3$ (55 mg, 0.40 mmol, 2 equiv), and DMF (330 µL). After stirring for at least 5 min, propargyl bromide (80 wt % in toluene, 38 µL, 0.40 mmol, 2 equiv) was added, and the reaction mixture was left to stir at 100 ˚C under nitrogen for 24 h. After this time, the reaction mixture was cooled, diluted with water (10 mL) and extracted with EtOAc (3 × 1 mL). The combined organic layers were washed with sat. aq. NaCl, dried over $Na_2SO_4$, and concentrated *in vacuo* to leave a yellow residue. Purification using PTLC (20% EtOAc in Hexanes) gave the product as a colorless oil (65.2 mg, 66% yield). **$^1$H NMR** (400 MHz, $CDCl_3$) δ 7.81 (d, $J$ = 8.6 Hz, 2H), 7.72 (d, $J$ = 8.6 Hz, 2H), 7.45 (d, $J$ = 8.0 Hz, 2H), 7.28 (dd, $J$ = 8.1, 6.5 Hz, 2H), 7.25–7.19 (m, 1H), 7.13–7.08 (m, 4H), 4.01 (t, $J$ = 2.7 Hz, 2H), 3.14–2.84 (m, 5H), 1.99 (td, $J$ = 6.8, 3.7 Hz, 2H), 1.93 (t, $J$ = 2.5 Hz, 1H); **$^{13}$C NMR** (150 MHz, $CDCl_3$) δ 143.89 (d, $J$ = 1.1 Hz), 142.83, 142.75, 132.63, 129.46, 128.66, 128.45 (q,

$J$ = 32.2 Hz), 128.25, 127.66, 126.89, 125.11 (q, $J$ = 4.0 Hz), 124.28 (q, $J$ = 271.6 Hz), 117.33, 116.43, 75.72, 74.29, 44.97, 44.85, 43.33, 36.46, 33.14; **$^{19}$F NMR** (376 MHz, $CDCl_3$) δ -62.57; **HRMS** (ESI-TOF) Calc'd for $C_{27}H_{24}F_3N_2O_2S^+$ [M+H] 497.1511, found 497.1508.

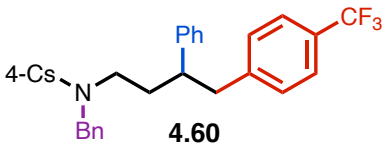


**4.60**

***N*-benzyl-4-cyano-*N*-(3-phenyl-4-(4-(trifluoromethyl)phenyl)butyl)benzenesulfonamide (4.60):** To a 1-dram (4 mL) vial equipped with a Teflon-coated magnetic stir bar were added a solution of **4.57** (69 mg, 0.15 mmol, 1 equiv) in DMF (200 µL), $K_2CO_3$ (55 mg, 0.40 mmol, 2 equiv), and 130 µL of DMF. After stirring for at least 5 min, benzyl chloride (51 mg, 0.40 mmol, 2 equiv) was added, and the reaction mixture was left to stir at 60 ˚C under nitrogen for 16 h. After this time, the reaction mixture was cooled, diluted with water (10 mL) and extracted with EtOAc (3 × 1 mL). The combined organic layers were washed with sat. aq. NaCl, dried over $Na_2SO_4$, and the solvent was removed *in vacuo* to leave a colorless residue. Purification using PTLC (20% EtOAc in Hexanes) gave the product as a white solid (61.8 mg, 75% yield). **$^1$H NMR** (400 MHz, $CDCl_3$) δ 7.76–7.69 (m, 4H), 7.41 (d, $J$ = 8.0 Hz, 2H), 7.27 (d, $J$ = 2.1 Hz, 1H), 7.25–7.18 (m, 5H), 7.08 (dd, $J$ = 7.7, 1.9 Hz, 2H), 6.96 (d, $J$ = 7.9 Hz, 2H), 6.92–6.87 (m, 2H), 4.28–4.16 (m, 2H), 2.98–2.88 (m, 1H), 2.83 (td, $J$ = 9.7, 9.2, 5.0 Hz, 1H), 2.79–2.74 (m, 2H), 2.66–2.56 (m, 1H), 1.80–1.63 (m, 2H); **$^{13}$C NMR** (150 MHz, $CDCl_3$) δ 143.89, 143.82 (q, $J$ = 1.2 Hz), 142.47, 135.41, 132.88, 129.33, 128.71, 128.61, 128.42, 128.32 (q, $J$ = 32.3 Hz), 128.18, 127.63, 127.54, 126.81, 125.22, 125.03 (q, $J$ = 3.8 Hz), 124.32 (q, $J$ = 272.0 Hz), 123.42, 117.33, 116.14, 52.39, 46.72, 45.14, 43.36, 33.93; **$^{19}$F NMR** (376 MHz,

$CDCl_3$) δ -62.56; **HRMS** (ESI-TOF) Calc'd for $C_{31}H_{28}F_3N_2O_2S^+$ [M+H] 549.1824, found 549.1826.

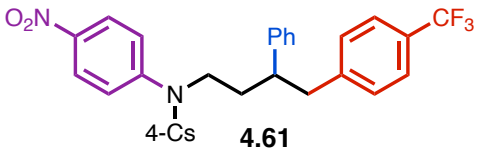


**4.61**

**4-cyano-*N*-(4-nitrophenyl)-*N*-(3-phenyl-4-(4-(trifluoromethyl)phenyl)butyl)benzenesulfonamide (4.61):** To a 1-dram (4 mL) vial equipped with a Teflon-coated magnetic stir bar were added **4.57** (92 mg, 0.2 mmol, 1 equiv), $K_2CO_3$ (55 mg, 0.40 mmol, 2 equiv), and DMF (330 µL). After stirring for at least 5 min, 1-fluoro-4-nitrobenzene (42 mg, 0.30 mmol, 1.5 equiv) was added, and the reaction mixture was left to stir at 100 ˚C under nitrogen for 23 h. After this time, the reaction mixture was cooled, diluted with water (10 mL), and extracted with EtOAc (3 × 1 mL). The combined organic layers were washed with sat. aq. NaCl, dried over $Na_2SO_4$, and concentrated *in vacuo* to leave a yellow residue. Purification using PTLC (20% EtOAc in Hexanes) gave the product as a yellow solid (88.7 mg, 77% yield). **$^1$H NMR** (600 MHz, $CDCl_3$) δ 8.11 (d, $J$ = 8.9 Hz, 2H), 7.70 (d, $J$ = 8.5 Hz, 2H), 7.53 (d, $J$ = 8.5 Hz, 2H), 7.41 (d, $J$ = 8.1 Hz, 2H), 7.29–7.24 (m, 2H), 7.24–7.20 (m, 1H), 7.08–7.00 (m, 6H), 3.55 (dt, $J$ = 13.7, 7.4 Hz, 1H), 3.33 (ddd, $J$ = 13.3, 7.7, 5.3 Hz, 1H), 2.88 (t, $J$ = 1.7 Hz, 3H), 1.91–1.77 (m, 2H); **$^{13}$C NMR** (150 MHz, $CDCl_3$) δ 146.75, 144.04, 143.76 (q, $J$ = 1.4 Hz), 143.75, 142.43, 141.36, 132.90, 129.37, 128.75, 128.49 (q, $J$ = 32.4 Hz), 128.44, 127.96, 127.58, 127.05, 125.11 (q, $J$ = 3.8 Hz), 124.53, 124.20 (q, $J$ = 271.5 Hz), 116.98, 48.73, 44.93, 43.29, 33.80; **$^{19}$F NMR** (376 MHz, $CDCl_3$) δ -62.56; **HRMS** (ESI-TOF) Calc'd for $C_{30}H_{25}F_3N_3O_4S^+$ [M+H] 580.1518, found 580.1523.

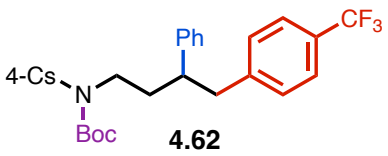


**4.62**

***tert*-butyl ((4-cyanophenyl)sulfonyl)(3-phenyl-4-(4-(trifluoromethyl)phenyl)butyl)carbamate (4.62):** To a 1-dram (4 mL) vial equipped with a Teflon-coated magnetic stir bar were added **4.57** (92 mg, 0.2 mmol), DMAP (2.4 mg, 20 µmol), and DCM (450 µL). After stirring for at least 5 min, di-*tert*-butyl dicarbonate (55 µL, 0.24 mmol, 1.2 equiv) was added, and the reaction mixture was left to stir at room temperature under nitrogen for 23 h. After this time, the reaction was diluted with water (10 mL) and extracted with EtOAc (3 × 1 mL). The combined organic layers were washed with sat. aq. NaCl, dried over $Na_2SO_4$, and concentrated *in vacuo* to leave a colorless residue. Purification using PTLC (20% EtOAc in Hexanes) gave the product as a colorless oil (72.6 mg, 65% yield). **$^1$H NMR** (500 MHz, $CDCl_3$) δ 7.95–7.90 (m, 2H), 7.76 (dd, $J$ = 8.5, 1.6 Hz, 2H), 7.45 (d, $J$ = 7.8 Hz, 2H), 7.31–7.25 (m, 2H), 7.21 (td, $J$ = 7.3, 1.5 Hz, 1H), 7.12 (t, $J$ = 6.9 Hz, 4H), 3.70–3.56 (m, 2H), 3.05–2.86 (m, 3H), 2.24–2.07 (m, 2H), 1.28 (d, $J$ = 1.5 Hz, 9H); **$^{13}$C NMR** (125 MHz, $CDCl_3$) δ 150.33, 144.00 (q, $J$ = 1.4 Hz), 142.46, 132.46, 129.46, 128.67, 128.48, 128.38 (q, $J$ = 33.2 Hz), 127.60, 126.89, 125.38, 125.07 (q, $J$ = 4.0 Hz), 124.31 (q, $J$ = 271.6Hz), 117.17, 116.89, 85.08, 46.36, 45.69, 43.64, 35.55, 27.81; **$^{19}$F NMR** (376 MHz, $CDCl_3$) δ -62.53; **HRMS** (ESI-TOF) for $C_{29}H_{30}F_3N_2O_4S^+$ [M+H] 559.1878, found 559.1888.

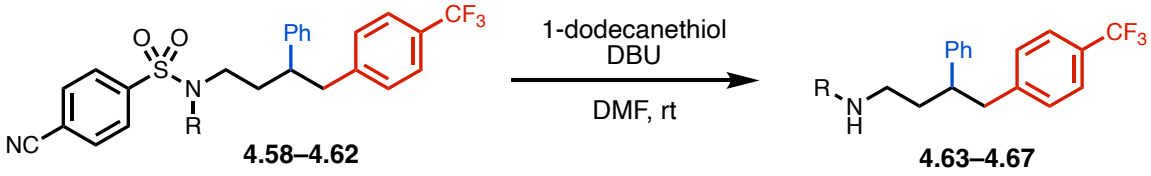


**4.58–4.62** **4.63–4.67**

***Scheme 4.S7.*** Synthesis of secondary alkyl amines **4.63–4.67**. These compounds were synthesized using adapted versions of literature procedures describing the preparation of similar compounds.

**General Procedure H:** A stock solution of 1-dodecanethiol in DMF was degassed by sparging with nitrogen for 20 min. Under a nitrogen atmosphere, the thiol solution was added to **4.58–4.62** in a reaction vessel equipped with a Teflon-coated magnetic stir bar, and the reaction mixture was stirred for 5 min. DBU was then added, at which point a light-yellow color developed, and the reaction mixture was stirred at room temperature for 21–24 h under nitrogen. After this time, the reaction mixture was diluted with water (10 mL) and extracted with EtOAc (×3). The organic layers were combined, and the solvent was removed *in vacuo* to leave an oil, which afforded pure product after silica gel column chromatography or PTLC.

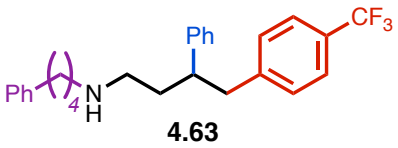


**4.63**

**3-phenyl-*N*-(4-phenylbutyl)-4-(4-(trifluoromethyl)phenyl)butan-1-amine (4.63):** The title compound was prepared from a 0.85 M stock solution of 1-dodecanethiol in DMF (3.25 mL, 2.75 mmol, 5.00 equiv), **4.58** (325 mg, 0.550 mmol, 1.0 equiv), and DBU (394 µL, 2.61 mmol, 4.75 equiv) with a reaction time of 24 h according to General Procedure H . After this time, the reaction mixture was diluted with water (10 mL) and extracted with ethyl acetate (3 × 10 mL). The crude oil was purified by silica gel column chromatography (0 to 10% MeOH in DCM gradient) to afford the product as a light-tan syrup (206 mg, 88%). **$^1$H NMR** (400 MHz, $CDCl_3$) δ: 7.44 (d, $J$ = 8.1 Hz, 2H), 7.23–7.30 (m, 4H), 7.13–7.22 (m, 4H), 7.07–7.13 (m, 4H), 2.84–3.01 (m, 3H), 2.58 (t, $J$ = 7.6 Hz, 2H), 2.51 (t, $J$ = 7.2 Hz, 2H), 2.39–2.48 (m, 2H), 1.82–1.95 (m, 2H), 1.53–1.64 (m, 2H), 1.42–1.51 (m, 2H); **$^{13}$C NMR** (100 MHz, $CDCl_3$) δ 144.4 (q, $J$ = 1.5

Hz), 143.6, 142.3, 129.4, 128.4, 128.3, 128.2, 128.16 (q, $J$ = 32.3 Hz), 127.5, 126.5, 125.7, 124.9 (q, $J$ = 3.7 Hz), 124.3 (q, $J$ = 272 Hz), 49.6, 47.8, 45.9, 43.7, 35.7, 35.5, 29.3, 29.0; **$^{19}$F NMR** (376 MHz, $CDCl_3$) δ -62.3; **HRMS** (ESI) Calc'd for $C_{27}H_{31}F_3N$ $[M+H]^+$ 426.2403, found 426.2414.

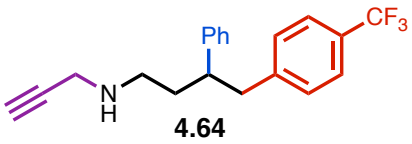

**4.64**

**3-phenyl-*N*-(prop-2-yn-1-yl)-4-(4-(trifluoromethyl)phenyl)butan-1-amine (4.64):** The title compound was prepared from a 1.65 M stock solution of 1-dodecanethiol in DMF (280 µL, 0.46 mmol, 2.7 equiv), **4.59** (85 mg, 0.17 mmol, 1 equiv), and DBU (123 µL, 0.815 mmol, 4.75 equiv) with a reaction time of 23 h according to General Procedure H. After this time, the reaction mixture was diluted with water (10 mL) and extracted with ethyl acetate (3 × 1 mL). The crude oil was purified by PTLC (20% EtOAc in Hexanes) to afford the product as a yellow oil (18 mg, 32% yield). **$^1$H NMR** (400 MHz, $CDCl_3$) δ 7.43 (d, $J$ = 7.8 Hz, 2H), 7.29–7.22 (m, 2H), 7.21–7.15 (m, 1H), 7.13–7.08 (m, 4H), 3.30 (t, $J$ = 2.3 Hz, 2H), 2.98–2.90 (m, 3H), 2.52 (t, $J$ = 7.3 Hz, 2H), 2.13 (t, $J$ = 2.4 Hz, 1H), 1.89–1.81 (m, 2H), 1.24 (s, 1H); **$^{13}$C NMR** (150 MHz, $CDCl_3$) δ 144.47 (q, $J$ = 1.4 Hz), 143.73, 129.42, 128.23 (q, $J$ = 32.2 Hz), 127.63, 125.00 (q, $J$ = 3.9 Hz), 124.34 (q, $J$ = 272.2 Hz), 82.11, 46.70, 45.67, 43.67, 35.64; **$^{19}$F NMR** (376 MHz, $CDCl_3$) δ -62.54; **HRMS** (ESI-TOF) Calc'd for $C_{20}H_{21}F_3N^+$ $[M+H]$ 332.1626, found 332.1632.

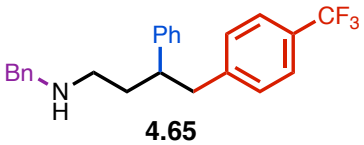

**4.65**

***N*-benzyl-3-phenyl-4-(4-(trifluoromethyl)phenyl)butan-1-amine (4.65):** The title compound was prepared from a 1.65 M stock solution of 1-dodecanethiol in DMF (220 µL, 0.36 mmol, 2.8 equiv), **4.60**

(70 mg, 0.13 mmol, 1 equiv), and DBU (91 µL, 0.61 mmol, 4.75 equiv) with a reaction time of 23 h according to General Procedure H. After this time, the reaction mixture was diluted with water (10 mL) and extracted with ethyl acetate (3 × 1 mL). The crude oil was purified by PTLC (20% EtOAc in Hexanes) to afford the product as a colorless oil (29 mg, 60% yield). **$^{1}$H NMR** (500 MHz, $CDCl_3$) δ 7.43 (d, *J* = 8.0 Hz, 2H), 7.30–7.16 (m, 8H), 7.08 (dd, *J* = 7.1, 1.8 Hz, 4H), 3.64 (q, *J* = 13.1 Hz, 2H), 2.92 (dd, *J* = 7.3, 4.2 Hz, 3H), 2.48 (t, *J* = 7.3 Hz, 2H), 1.93–1.80 (m, 2H), 1.45 (s, 1H); **$^{13}$C NMR** (150 MHz, $CDCl_3$) δ 144.54 (q, *J* = 1.3 Hz), 143.84, 140.17, 129.42, 128.47, 128.38, 128.20 (q, *J* = 33.4 Hz), 128.09, 127.64, 126.94, 126.48, 124.99 (q, *J* = 3.8 Hz), 124.35 (q, *J* = 271.7Hz), 123.45, 53.94, 47.40, 45.77, 43.70, 35.82; **$^{19}$F NMR** (376 MHz, $CDCl_3$) δ -62.52; **HRMS** (ESI-TOF) Calc'd for $C_{24}H_{25}F_3N^+$ [M+H] 384.1939, found 384.1943.

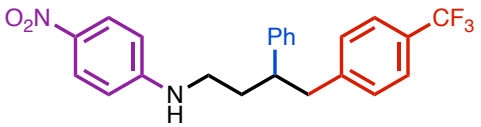


**4.66**

**2-nitro-*N*-(3-phenyl-4-(4-(trifluoromethyl)phenyl)butyl)aniline (4.66):** The title compound was prepared from a 1.65 M stock solution of 1-dodecanethiol in DMF (220 µL, 0.36 mmol, 2.7 equiv), **4.61** (78 mg, 0.13 mmol. 1 equiv), and DBU (96 µL, 0.64 mmol, 4.75 equiv) with a reaction time of 21 h according to General Procedure H. After this time, the reaction mixture was diluted with water (10 mL) and extracted with ethyl acetate (3 × 1 mL). The crude oil was purified by PTLC (20% EtOAc in Hexanes) to afford the product as a yellow oil (46 mg, 83% yield). **$^{1}$H NMR** (400 MHz, $CDCl_3$) δ 7.98 (d, *J* = 9.2 Hz, 2H), 7.44 (d, *J* = 7.8 Hz, 2H), 7.34–7.27 (m, 2H), 7.26–7.20 (m, 1H), 7.12 (ddd, *J* = 7.9, 4.2, 2.5 Hz, 4H), 6.30 (d, *J* = 9.2 Hz, 2H), 4.39 (t, *J* = 5.7 Hz, 1H), 3.11–2.89 (m, 5H), 2.07–1.92 (m, 2H); **$^{13}$C NMR** (150 MHz,

$CDCl_3$) δ 153.20, 144.02 (q, *J* = 1.4 Hz), 142.97, 137.75, 129.40, 128.86, 128.43 (q, *J* = 32.4 Hz), 127.55, 127.05, 126.38, 125.15 (q, *J* = 3.7 Hz), 123.40 (q, *J* = 272.0 Hz), 110.93, 45.81, 43.58, 41.66, 34.71; **$^{19}$F NMR** (376 MHz, $CDCl_3$) δ -62.49; **HRMS** (ESI-TOF) Calc'd for $C_{23}H_{22}F_3N_2O_2^+$ [M+H] 415.1633, found 415.1628.

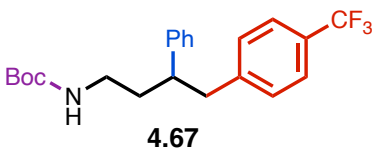


**4.67**

***tert*-butyl (3-phenyl-4-(4-(trifluoromethyl)phenyl)butyl)carbamate (4.67):** The title compound was prepared from a 1.65 M stock solution of 1-dodecanethiol in DMF (220 µL, 0.48 mmol, 5 equiv), **4.62** (54 mg, 97 µmol, 1 equiv), and DBU (69 µL, 0.46 mmol, 4.75 equiv) with a reaction time of 23 h according to General Procedure H. After this time, the reaction mixture was diluted with water (10 mL) and extracted with ethyl acetate (3 × 1 mL). The crude oil was purified by PTLC (20% EtOAc in Hexanes) to afford the product as a colorless oil (26 mg, 68% yield). **$^1$H NMR** (400 MHz, $CDCl_3$) δ 7.43 (d, *J* = 7.9 Hz, 2H), 7.29–7.22 (m, 2H), 7.18 (t, *J* = 7.2 Hz, 1H), 7.11–7.04 (m, 4H), 4.36 (s, 1H), 3.11–2.75 (m, 5H), 1.87 (ddd, *J* = 33.1, 14.7, 7.6 Hz, 2H), 1.40 (s, 9H); **$^{13}$C NMR** (150 MHz, $CDCl_3$) δ 155.85, 144.30 (q, *J* = 1.4 Hz), 143.27, 129.40, 128.60, 128.28 (q, *J* = 32.5), 127.58, 126.65, 125.00 (q, *J* = 4.0 Hz), 124.32 (q, *J* = 271.9 Hz), 123.42, 79.15, 45.54, 43.34, 38.92, 35.86, 28.39; **$^{19}$F NMR** (376 MHz, $CDCl_3$) δ -62.56; **HRMS** (ESI-TOF) Calc'd for $C_{22}H_{27}F_3NO_2^+$ [M+H] 394.1994, found 394.1999.

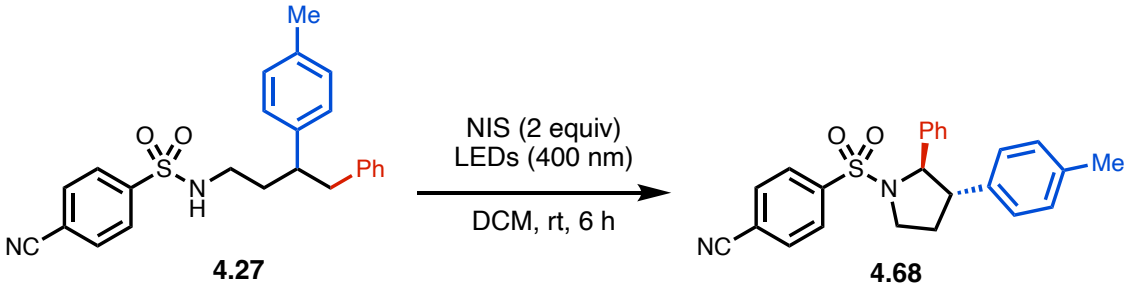


***Scheme 4.S8.*** Synthesis of 4-Cs protected pyrrolidine **4.68**. This compound was synthesized using an adapted version of a literature procedure describing the preparation of similar compounds.[12]

**4-((2-phenyl-3-(*p*-tolyl)pyrrolidin-1-yl)sulfonyl)benzonitrile (4.68):** Inside the glovebox, to a 1-dram (4 mL) vial equipped with a Teflon-coated magnetic stir bar were added **4.27** (38.7 mg, 96 µmol, 1 equiv) and NIS (43 mg, 0.19 mmol, 2 equiv). The vial was sealed with a screw-top cap, removed from the glovebox, and anhydrous DCM (2 mL, 0.05 M) was added. The reaction vessel was then irradiated with violet light (400 nm) via LEDs while stirring at room temperature for 6 h. After this time, the reaction mixture was washed with sat. aq. $Na_2S_2O_3$ (5 mL) and $NaHCO_3$ (5 mL) and extracted with DCM (3 × 1 mL). The combined organic layers were dried over $Na_2SO_4$, and the solvent was removed *in vacuo* to leave a colorless residue. Purification using PTLC (20% EtOAc in Hexanes) gave the product as a white solid (27.1 mg, 70% yield). **$^1$H NMR** (600 MHz, $CDCl_3$) δ 7.60 (s, 4H), 7.23–7.15 (m, 3H), 7.05 (d, $J$ = 6.7 Hz, 2H), 7.02 (d, $J$ = 7.8 Hz, 2H), 6.83 (d, $J$ = 8.1 Hz, 2H), 4.73 (d, $J$ = 6.9 Hz, 1H), 4.02 (ddd, $J$ = 10.4, 7.7, 4.1 Hz, 1H), 3.70 (ddd, $J$ = 10.4, 8.6, 6.4 Hz, 1H), 3.29 (dt, $J$ = 9.0, 6.7 Hz, 1H), 2.31 (s, 3H), 2.27 (ddd, $J$ = 12.8, 6.4, 4.1 Hz, 1H), 2.09 (dtd, $J$ = 12.7, 8.8, 7.8 Hz, 1H); **$^{13}$C NMR** (150 MHz, $CDCl_3$) δ 143.53, 140.50, 136.99, 136.55, 132.43, 129.41, 128.38, 127.65, 127.58, 126.95, 126.85, 117.48, 115.72, 71.21, 54.88, 49.19, 32.02, 21.01; **HRMS** (ESI-TOF) for $C_{24}H_{23}N_2O_2S^+$ [M+H] 403.1480, found 403.1478.

$^{1}$H-$^{1}$H NOESY was found to be ambiguous in determining *trans*/*cis* configuration since it is difficult to confidently assign the configuration of substituents of 5-membered rings from $^{3}J_{H,H}$ values.[15] However, the relative stereochemistry of **(±)-3f** could be assigned based on the $^{1}$H spectrum (specifically the chemical shift of the α-C(3°)–*H* atom and the *J*-values of the two benzylic H atoms), as described previously in the literature for 2,3-disubstituted pyrrolidines.[16]

# NMR Data for Chapter 5:

**General Procedure A:**

*$LiAlH_4$ reduction:* To a 250-mL round-bottom flask equipped with a Teflon-coated magnetic stir bar, were added dry THF (40 mL) and $LiAlH_4$ (10 mL, 2 M in THF, 2 equiv) under a $N_2$ atmosphere. The flask was placed in an ice bath, and the appropriate amino acid (10.0 mmol, 1 equiv) was added in portions. The reaction mixture was allowed to stir and warm to room temperature (approximately 1 h). Then, the flask was equipped with a reflux condenser and subjected to reflux in an oil bath heated to 80 °C while stirring under $N_2$ for 16 h. After this time, the heating was stopped, and the reaction mixture was allowed to cool to room temperature. The reaction was subsequently placed in an ice bath and initially quenched with 20% NaOH solution in a dropwise manner. Once quenched, copious amounts of 20% NaOH solution were added, the crude mixture was transferred to a separatory funnel, and the aqueous later was extracted with EtOAc (3 × 30 mL). The combined organic layers were then dried over $Na_2SO_4$ and concentrated *in vacuo* to afford an oil, which was used in the second step without further purification.

*Amide Coupling:* To a 48-mL bomb flask equipped with a Teflon-coated magnetic stir bar, were added dimethyl oxalate (5.0 mmol, 1 equiv), the amino alcohol from the previous step (10.0 mmol, 2 equiv), and toluene (17 mL). The flask was placed in an oil bath heated to 110 °C while stirring for 1 h. After this time, the heating was stopped, and the reaction mixture was allowed to cool to room temperature. Hexanes were added, the contents were filtered through a Büchner funnel, and the collected solid was washed with additional hexanes. Once dried, the collected solid was used in the third step without further purification.

*Cyclization:* To a 50-mL round-bottom flask equipped with a Teflon-coated magnetic stir bar, were added the diamide from the previous step (1.0 mmol, 1 equiv) and anhydrous DCM (10 mL). The flask was placed in an ice bath while stirring for approximately 5 min. Deoxo-Fluor (0.41 mL, 2.2 mmol, 2.2 equiv) was added dropwise, and the reaction was allowed to stir for 1 h. After this time, the reaction mixture was quenched with sat. $NaHCO_3$, allowed to warm to room temperature, and then transferred to a separatory funnel. The aqueous layer was extracted with DCM (3 × 10 mL). The combined organic layers were then dried over $Na_2SO_4$ and concentrated *in vacuo* to leave a yellow oil, which afforded pure product after silica gel column chromatography.

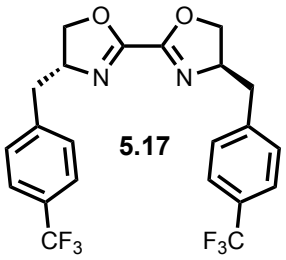


**(4*R*,4'*R*)-4,4'-bis(4-(trifluoromethyl)benzyl)-4,4',5,5'-tetrahydro-2,2'-bioxazole (5.17):** The title compound was prepared according to General Procedure A. Purification using silica gel column chromatography (80% EtOAc in Hexanes) gave the product as a white solid (237 mg, 52% yield for the last step). **$^{1}$H NMR** (400 MHz, $CDCl_3$) δ 7.57 (d, $J$ = 8.0 Hz, 4H), 7.35 (d, $J$ = 8.0 Hz, 4H), 4.68–4.58 (m, 2H), 4.44 (dd, $J$ = 9.7, 8.8 Hz, 2H), 4.18–4.11 (m, 2H), 3.23 (dd, $J$ = 14.0, 6.0 Hz, 2H), 2.85 (dd, $J$ = 14.0, 8.0 Hz, 2H); **$^{13}$C NMR** (150 MHz, $CDCl_3$) δ 155.19, 141.20 (q, $J_{C-F}$ = 1.6 Hz), 129.55, 129.22 (q, $J_{C-F}$ = 32.4 Hz), 125.62 (q, $J_{C-F}$ = 3.8 Hz), 124.16 (q, $J_{C-F}$ = 271.8 Hz), 72.63, 67.84, 40.89; **$^{19}$F NMR** (376 MHz, $CDCl_3$) δ –65.17; **HRMS** (ESI-TOF) Calc'd for $C_{22}H_{19}F_6N_2O_2^+$ [M+H] 457.1351, found 457.1348.

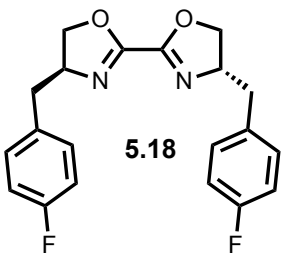


**(4*S*,4'*S*)-4,4'-bis(4-fluorobenzyl)-4,4',5,5'-tetrahydro-2,2'-bioxazole (5.18):** The title compound was prepared according to General Procedure A. Purification using silica gel column chromatography (80% EtOAc in Hexanes) gave the product as a white solid (133.5 mg, 38% yield for the last step). **$^{1}$H NMR** (400 MHz, $CDCl_3$) δ 7.18 (dd, $J$ = 8.3, 5.4 Hz, 4H), 7.00 (t, $J$ = 8.5 Hz, 4H), 4.58 (qd, $J$ = 8.6, 5.4 Hz, 2H), 4.40 (t, $J$ = 9.2 Hz, 2H), 4.14 (t, $J$ = 8.4 Hz, 2H), 3.17 (dd, $J$ = 14.0, 5.4 Hz, 2H), 2.74 (dd, $J$ = 14.0, 8.4 Hz, 2H); **$^{13}$C NMR** (150 MHz, $CDCl_3$) δ 161.82 (d, $J_{C-F}$ = 244.9 Hz), 155.10, 132.76 (d, $J_{C-F}$ = 3.1 Hz), 130.66 (d, $J_{C-F}$ = 7.8 Hz), 115.51 (d, $J_{C-F}$ = 21.1 Hz), 72.57, 68.17, 40.21; **$^{19}$F NMR** (376 MHz, $CDCl_3$) δ –118.84. **HRMS** (ESI-TOF) Calc'd for $C_{20}H_{19}F_2N_2O_2^+$ [M+H] 357.1415, found 357.1411.

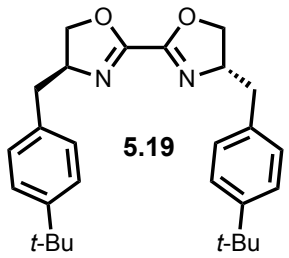


**(4*S*,4'*S*)-4,4'-bis(4-(*tert*-butyl)benzyl)-4,4',5,5'-tetrahydro-2,2'-bioxazole (5.19):** The title compound was prepared on a 4.0-mmol scale (last step) according to General Procedure A. Purification using silica gel column chromatography (80% EtOAc in Hexanes) gave the product as a white solid (635 mg, 33% yield for the last step). **$^1$H NMR** (400 MHz, $CDCl_3$) δ 7.33 (d, *J* = 8.3 Hz, 4H), 7.14 (d, *J* = 8.2 Hz, 4H), 4.65–4.55 (m, 2H), 4.42–4.35 (m, 2H), 4.21–4.15 (m, 2H), 3.25 (dd, *J* = 13.9, 5.0 Hz, 2H), 2.67 (dd, *J* = 13.9, 9.4 Hz, 2H), 1.31 (s, 18H); **$^{13}$C NMR** (150 MHz, $CDCl_3$) δ 155.12, 149.60, 134.14, 128.79, 125.62, 72.92, 68.32, 40.72, 34.43, 31.37; **HRMS** (ESI-TOF) Calc'd for $C_{28}H_{37}N_2O_2^+$ [M+H] 433.2855, found 433.2850.

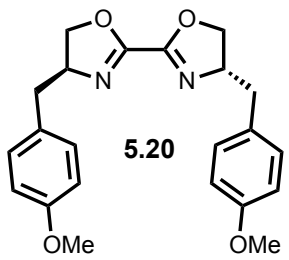


**(4*S*,4'*S*)-4,4'-bis(4-methoxybenzyl)-4,4',5,5'-tetrahydro-2,2'-bioxazole (5.20):** The title compound was prepared according to General Procedure A. Purification using silica gel column chromatography (80% EtOAc in Hexanes) gave the product as a white solid (100.6 mg, 26% yield for the last step). **$^1$H NMR** (400 MHz, $CDCl_3$) δ 7.13 (d, *J* = 8.3 Hz, 4H), 6.85 (d, *J* = 8.3 Hz, 4H), 4.55 (td, *J* = 8.8, 5.0 Hz, 2H), 4.36 (t, *J* = 9.1 Hz, 2H), 4.15 (t, *J* = 8.3 Hz, 2H), 3.79 (s, 6H), 3.20 (dd, *J* = 14.0, 5.0 Hz, 2H), 2.66 (dd, *J* = 13.9, 9.1 Hz, 2H); **$^{13}$C NMR** (150 MHz, $CDCl_3$) δ 158.46, 155.08, 130.14, 129.16, 114.12, 72.69, 68.43, 55.28, 40.21; **HRMS** (ESI-TOF) Calc'd for $C_{22}H_{25}N_2O_4^+$ [M+H] 381.1814, found 381.1809.

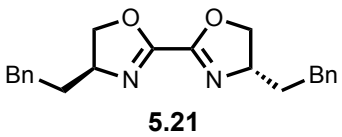


**5.21**

**(4*S*,4'*S*)-4,4'-diphenethyl-4,4',5,5'-tetrahydro-2,2'-bioxazole (5.21):** The title compound was prepared according to General Procedure A. Purification using silica gel column chromatography (80% EtOAc in Hexanes) gave the product as a white solid (182.5 mg, 52% yield for the last step). **$^1$H NMR** (400 MHz, $CDCl_3$) δ 7.29 (t, *J* = 7.6 Hz, 4H), 7.20 (d, *J* = 7.4 Hz, 6H), 4.50 (t, *J* = 9.1 Hz, 2H), 4.32 (p, *J* = 7.7 Hz, 2H), 4.05 (t, *J* = 8.4 Hz, 2H), 2.85 (ddd, *J* = 15.0, 9.5, 5.9 Hz, 2H), 2.80–2.69 (m, 2H), 2.12–1.99 (m, 2H), 1.89 (ddd, *J* = 15.9, 13.2, 6.5 Hz, 2H); **$^{13}$C NMR** (150 MHz, $CDCl_3$) δ 154.82, 141.22, 128.51, 128.45, 126.10, 73.34, 66.68, 37.13, 32.23; **HRMS** (ESI-TOF) Calc'd for $C_{22}H_{25}N_2O_2^+$ [M+H] 349.1916, found 349.1916.

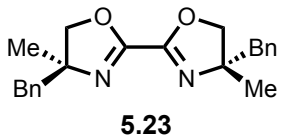


**5.23**

**(4*S*,4'*S*)-4,4'-dibenzyl-4,4'-dimethyl-4,4',5,5'-tetrahydro-2,2'-bioxazole (5.23):** The title compound was prepared according to General Procedure A. Purification using silica gel column chromatography (80% EtOAc in Hexanes) gave the product as a white solid (197.6 mg, 57% yield for the last step). **$^1$H NMR** (400 MHz, $CDCl_3$) δ 7.31–7.26 (m, 4H), 7.26–7.23 (m, 2H), 7.18 (dd, *J* = 7.8, 1.7 Hz, 4H), 4.35 (d, *J* = 8.5 Hz, 2H), 3.95 (d, *J* = 8.5 Hz, 2H), 2.95–2.86 (m, 4H), 1.38 (s, 6H); **$^{13}$C NMR** (150 MHz, $CDCl_3$) δ 153.55, 136.40, 130.40, 128.29, 126.76, 76.96, 46.33, 26.70; **HRMS** (ESI-TOF) Calc'd for $C_{22}H_{25}N_2O_2^+$ [M+H] 349.1916, found 349.1912.

**General Procedure B:**

To a round-bottom flask equipped with a Teflon-coated magnetic stir bar were added the alkenyl amine (1 equiv) and dry DCM (0.2 M). The flask was placed in an ice bath, and triethylamine (3 equiv) and DMAP (25 mol%) were subsequently added. The reaction

mixture was allowed to stir for at least 5 min. Lastly, the appropriate sulfonyl chloride (1.1 equiv) was added, and the reaction mixture was allowed to warm to room temperature and continue stirring for 16 h. After this time, the reaction mixture was transferred to a separatory funnel, washed with 1M HCl, and extracted with DCM (3×). The combined organic layers were then washed with brine, dried over $Na_2SO_4$, and concentrated *in vacuo* to afford a yellow oil, which provided pure product after silica gel column chromatography.

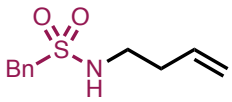

**5.S38**

***N*-(but-3-en-1-yl)-1-phenylmethanesulfonamide (5.S38):** The title compound was prepared from but-3-en-1-amine (71.1 mg, 1.00 mmol) and phenylmethanesulfonyl chloride (210 mg, 1.1 mmol), according to General Procedure B. Purification using silica gel column chromatography (20% Acetone in Hexanes) gave the product as a white solid (92 mg, 41% yield). **$^1$H NMR** (400 MHz, $CDCl_3$) δ 7.39 (s, 5H), 5.73–5.60 (m, 1H), 5.11–5.03 (m, 2H), 4.24 (s, 2H), 4.21 (t, $J$ = 6.3 Hz, 1H), 3.02 (q, $J$ = 6.4 Hz, 2H), 2.22 (qd, $J$ = 6.8, 1.3 Hz, 2H); **$^{13}$C NMR** (150 MHz, $CDCl_3$) δ 134.14, 130.63, 129.40, 128.84, 128.78, 118.20, 58.87, 42.65, 34.44; **HRMS** (ESI-TOF) Calc'd for $C_{11}H_{16}NO_2S^+$ [M+H] 226.0902, found 226.0894.

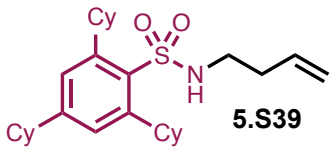

**5.S39**

***N*-(but-3-en-1-yl)-2,4,6-tricyclohexylbenzenesulfonamide (5.S39):** The title compound was prepared from but-3-en-1-amine (71.1 mg, 1.00 mmol) and 2,4,6-tricyclohexylbenzenesulfonyl chloride **5.S29** (423 mg, 1.1 mmol), according to General Procedure B. Purification using silica gel column chromatography (20% Acetone in Hexanes) gave the product as a white solid (375.5 mg, 82% yield). **$^1$H NMR** (500 MHz,

$CDCl_3$) δ 7.11 (s, 2H), 5.66 (ddt, *J* = 17.3, 10.4, 6.9 Hz, 1H), 5.14–5.07 (m, 2H), 4.28 (t, *J* = 6.2 Hz, 1H), 3.71 (s, 2H), 3.02 (q, *J* = 6.4 Hz, 2H), 2.49 (s, 1H), 2.27 (q, *J* = 6.7 Hz, 2H), 1.94–1.70 (m, 17H), 1.42 (td, *J* = 12.6, 8.8 Hz, 13H); **$^{13}$C NMR** (150 MHz, $CDCl_3$) δ 151.50, 148.98, 134.41, 132.28, 124.95, 118.40, 44.53, 41.51, 40.72, 35.24, 34.02, 33.70, 27.14, 26.75, 26.28, 26.05; **HRMS** (ESI-TOF) Calc'd for $C_{28}H_{44}NO_2S^+$ [M+H] 458.3093, found 458.3079.

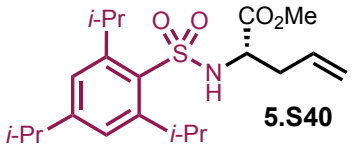

**5.S40**

**methyl (*S*)-2-((2,4,6-triisopropylphenyl)sulfonamido)pent-4-enoate (5.S40):** The title compound was prepared from alkenyl amine **5.S35** (1.29 mg, 10.0 mmol) and 2,4,6-triisopropylbenzenesulfonyl chloride (3.33 g, 11.0 mmol), according to General Procedure B. Purification using silica gel column chromatography (20% Acetone in Hexanes) gave the product as a white solid (2.94 g, 74% yield). **$^1$H NMR** (400 MHz, $CDCl_3$) δ 7.15 (s, 2H), 5.63 (ddt, *J* = 17.4, 10.6, 7.1 Hz, 1H), 5.15–5.03 (m, 3H), 4.10 (tt, *J* = 13.4, 6.5 Hz, 3H), 3.55 (s, 3H), 2.90 (hept, *J* = 7.0 Hz, 1H), 2.49 (dd, *J* = 7.3, 5.8 Hz, 2H), 1.30–1.22 (m, 18H); **$^{13}$C NMR** (150 MHz, $CDCl_3$) δ 171.64, 152.95, 150.26, 132.61, 131.49, 123.77, 119.65, 54.81, 52.36, 37.64, 34.17, 29.91, 24.85 (app-d), 23.59 (app-d); **HRMS** (ESI-TOF) Calc'd for $C_{21}H_{34}NO_4S^+$ [M+H] 396.2209, found 396.2200.

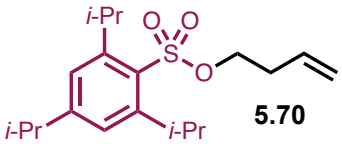

**5.70**

**but-3-en-1-yl 2,4,6-triisopropylbenzenesulfonate (5.70):** The title compound was prepared from but-3-en-1-ol (721.1 mg, 10.0 mmol) and 2,4,6-triisopropylbenzenesulfonyl chloride (3.33 g, 11.0 mmol),

according to General Procedure B. Purification using silica gel column chromatography (20% Acetone in Hexanes) gave the product as a white solid (2.79 g, 82% yield). **$^1$H NMR** (400 MHz, $CDCl_3$) δ 7.18 (s, 2H), 5.74 (ddt, *J* = 17.0, 10.2, 6.7 Hz, 1H), 5.15–5.06 (m, 2H), 4.13 (dt, *J* = 22.2, 6.8 Hz, 4H), 2.91 (hept, *J* = 7.0 Hz, 1H), 2.46 (qt, *J* = 6.8, 1.4 Hz, 2H), 1.26 (d, *J* = 6.8 Hz, 18H); **$^{13}$C NMR** (150 MHz, $CDCl_3$) δ 153.63, 150.79, 132.66, 129.50, 123.75, 118.18, 68.32, 34.25, 33.34, 29.57, 24.75, 23.56; **HRMS** (ESI-TOF) Calc'd for $C_{19}H_{31}O_3S^+$ [M+H] 339.1994, found 339.1988.

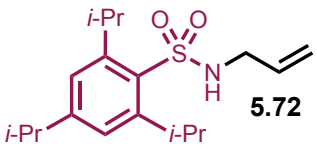

**5.72**

***N*-allyl-2,4,6-triisopropylbenzenesulfonamide (5.72):** The title compound was prepared from prop-2-en-1-amine (286 mg, 5.0 mmol) and 2,4,6-triisopropylbenzenesulfonyl chloride (1.67 g, 5.50 mmol), according to General Procedure B. Purification using silica gel column chromatography (20% Acetone in Hexanes) gave the product as a white solid (1.53 g, 95% yield). **$^1$H NMR** (500 MHz, $CDCl_3$) δ 7.17 (s, 2H), 5.82–5.72 (m, 1H), 5.23–5.09 (m, 2H), 4.37–4.28 (m, 1H), 4.16 (hept, *J* = 6.7 Hz, 2H), 3.60 (t, *J* = 6.2 Hz, 2H), 2.90 (hept, *J* = 7.0 Hz, 1H), 1.26 (dd, *J* = 6.8, 5.0 Hz, 18H); **$^{13}$C NMR** (150 MHz, $CDCl_3$) δ 152.83, 150.33, 133.23, 132.14, 123.83, 117.87, 45.53, 34.15, 29.63, 24.85, 23.58; **HRMS** (ESI-TOF) Calc'd for $C_{18}H_{30}NO_2S^+$ [M+H] 324.1997, found 324.1989.

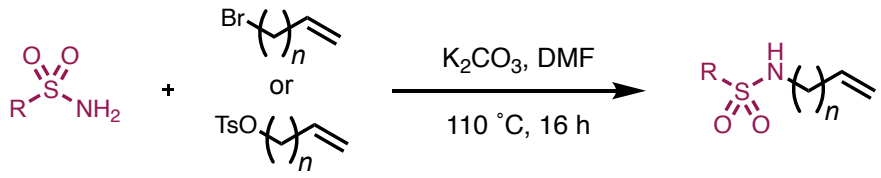


***Scheme 5.S3.*** Synthesis of alkenyl sulfonamides **5.S41–5.S45**, **5.71**, and **5.73–5.75**. These compounds were synthesized using adapted versions of literature procedures describing the preparation of similar compounds.[11]

**General Procedure C:** To a bomb flask equipped with a Teflon-coated magnetic stir bar, were added sulfonamide (1.2 equiv), the appropriate alkenyl bromide (1 equiv), $K_2CO_3$ (2 equiv), and DMF (0.3 M). The flask was placed in an oil bath, and the reaction mixture was allowed to stir at 110 °C for 16 h. After this time, the reaction mixture was cooled to room temperature. Then, water was added to the vial, and the reaction mixture was extracted with EtOAc (3×). The filtrate was concentrated *in vacuo* to afford a brown oil, which provided pure product after silica gel column chromatography.

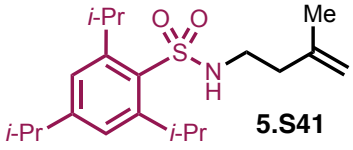


**5.S41**

**2,4,6-triisopropyl-*N*-(3-methylbut-3-en-1-yl)benzenesulfonamide (5.S41):** The title compound was prepared from alkenyl tosylate **5.S30** (10.69 g, 44.5 mmol) and 2,4,6-triisopropylbenzenesulfonamide (15.12 g, 53.4 mmol), according to General Procedure C. Purification using silica gel column chromatography (20% Acetone in Hexanes) gave the product as a white solid (7.50 g, 48% yield). **$^1$H NMR** (400 MHz, $CDCl_3$) δ 7.16 (s, 2H), 4.83 (s, 1H), 4.72 (s, 1H), 4.30 (t, $J$ = 6.2 Hz, 1H), 4.15 (p, $J$ = 6.8 Hz, 2H), 3.09 (q, $J$ = 6.5 Hz, 2H), 2.90 (p, $J$ = 7.0 Hz, 1H), 2.22 (t, $J$ = 6.7 Hz, 2H), 1.64 (s, 3H), 1.26 (dd, $J$ = 7.1, 3.8 Hz, 18H); **$^{13}$C NMR** (150 MHz, $CDCl_3$) δ 152.72, 150.35,

141.61, 132.14, 123.77, 113.27, 39.96, 37.36, 34.14, 29.65, 24.88, 23.58, 21.82; **HRMS** (ESI-TOF) Calc'd for $C_{20}H_{34}NO_2S^+$ [M+H] 352.2310, found 352.2307.

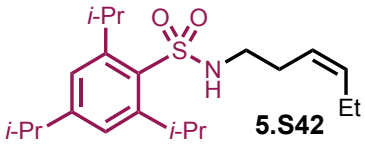

**5.S42**

**2,4,6-triisopropyl-*N*-(3-methylbut-3-en-1-yl)benzenesulfonamide (5.S42):** The title compound was prepared from alkenyl tosylate **5.S31** (10.69 g, 44.5 mmol) and 2,4,6-triisopropylbenzenesulfonamide (15.12 g, 53.4 mmol), according to General Procedure C. Purification using silica gel column chromatography (20% Acetone in Hexanes) gave the product as a white solid (1.99 g, 45% yield). **$^1$H NMR** (400 MHz, $CDCl_3$) δ 7.16 (s, 2H), 5.57–5.48 (m, 1H), 5.22–5.13 (m, 1H), 4.32 (t, *J* = 6.2 Hz, 1H), 4.15 (hept, *J* = 6.8 Hz, 2H), 2.98 (q, *J* = 6.6 Hz, 2H), 2.89 (h, *J* = 6.9 Hz, 1H), 2.30–2.22 (m, 2H), 2.06–1.96 (m, 2H), 1.26 (dd, *J* = 6.8, 3.9 Hz, 18H), 0.94 (t, *J* = 7.5 Hz, 3H); **$^{13}$C NMR** (150 MHz, $CDCl_3$) δ 152.68, 150.33, 135.67, 132.12, 124.14, 123.77, 42.32, 34.14, 29.62, 27.32, 24.89, 23.59, 20.62, 14.18; **HRMS** (ESI-TOF) Calc'd for $C_{21}H_{36}NO_2S^+$ [M+H] 366.2467, found 366.2464.

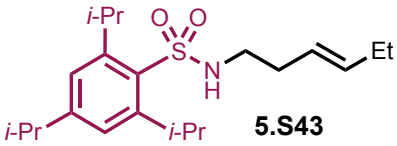

**5.S43**

**(*E*)-*N*-(hex-3-en-1-yl)-2,4,6-triisopropylbenzenesulfonamide (5.S43):** The title compound was prepared from alkenyl tosylate **5.S32** (10.69 g, 44.5 mmol) and 2,4,6-triisopropylbenzenesulfonamide (15.12 g, 53.4 mmol), according to General Procedure C. Purification using silica gel column chromatography (20% Acetone in Hexanes) gave the product as a white solid (873.6 mg, 28% yield). **$^1$H NMR** (400 MHz, $CDCl_3$) δ 7.16 (s, 2H), 5.54 (dtd, *J* = 15.4, 6.3, 1.4 Hz, 1H), 5.23 (dtd, *J* = 15.4, 7.0, 1.5 Hz, 1H), 4.38 (t, *J* =

6.2 Hz, 1H), 4.22–4.09 (m, 2H), 2.99 (q, $J$ = 6.5 Hz, 2H), 2.90 (hept, $J$ = 7.1 Hz, 1H), 2.20 (q, $J$ = 6.8 Hz, 2H), 2.03–1.94 (m, 2H), 1.30–1.22 (m, 18H), 0.94 (t, $J$ = 7.5 Hz, 3H); **$^{13}$C NMR** (150 MHz, $CDCl_3$) δ 152.63, 150.29, 136.23, 132.20, 124.52, 123.77, 42.15, 34.13, 32.49, 29.61, 25.54, 24.87, 23.58, 13.59; **HRMS** (ESI-TOF) Calc'd for $C_{21}H_{36}NO_2S^+$ [M+H] 366.2467, found 366.2467.

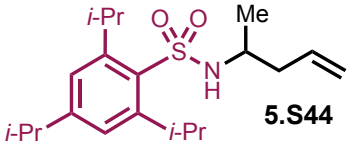

**5.S44**

**2,4,6-triisopropyl-*N*-(pent-4-en-2-yl)benzenesulfonamide (5.S44):** The title compound was prepared from alkenyl tosylate **5.S33** (3.80 g, 15.8 mmol) and 2,4,6-triisopropylbenzenesulfonamide (5.38 g, 19.0 mmol), according to General Procedure C. Purification using silica gel column chromatography (20% Acetone in Hexanes) gave the product as a white solid (333.8 mg, 6% yield). **$^1$H NMR** (400 MHz, $CDCl_3$) δ 7.15 (s, 2H), 5.68 (ddt, $J$ = 17.3, 10.3, 7.2 Hz, 1H), 5.11–5.01 (m, 2H), 4.24 (d, $J$ = 7.4 Hz, 1H), 4.14 (hept, $J$ = 6.8 Hz, 2H), 3.60–3.48 (m, 1H), 2.90 (hept, $J$ = 6.8 Hz, 1H), 2.28–2.14 (m, 2H), 1.29–1.23 (m, 18H), 1.08 (d, $J$ = 6.6 Hz, 3H); **$^{13}$C NMR** (150 MHz, $CDCl_3$) δ 152.60, 149.96, 133.72, 133.46, 123.76, 118.87, 48.78, 41.65, 34.12, 29.69, 24.87 (app-d), 23.60, 21.08; **HRMS** (ESI-TOF) Calc'd for $C_{20}H_{34}NO_2S^+$ [M+H] 352.2310, found 352.2311.

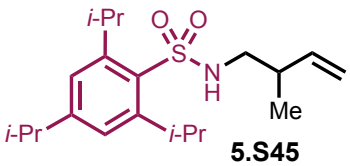

**5.S45**

**2,4,6-triisopropyl-*N*-(2-methylbut-3-en-1-yl)benzenesulfonamide (5.S45):** The title compound was prepared from alkenyl tosylate **5.S34** (2.40 g, 10.0 mmol) and 2,4,6-triisopropylbenzenesulfonamide (3.40 g, 12.0 mmol), according to General Procedure C. Purification using silica gel column chromatography (20% Acetone in

Hexanes) gave the product as a white solid (1.05 g, 30% yield). **$^1$H NMR** (400 MHz, $CDCl_3$) δ 7.16 (s, 2H), 5.56 (ddd, *J* = 17.7, 9.9, 7.9 Hz, 1H), 5.12–5.03 (m, 2H), 4.32 (dd, *J* = 8.0, 4.6 Hz, 1H), 4.13 (hept, *J* = 6.8 Hz, 2H), 2.98 (ddd, *J* = 11.9, 7.9, 5.3 Hz, 1H), 2.90 (p, *J* = 6.9 Hz, 1H), 2.76 (ddd, *J* = 11.9, 8.4, 4.6 Hz, 1H), 2.38 (dt, *J* = 13.9, 7.0 Hz, 1H), 1.30–1.21 (m, 18H), 1.00 (d, *J* = 6.8 Hz, 3H); **$^{13}$C NMR** (150 MHz, $CDCl_3$) δ 152.67, 150.27, 140.49, 132.19, 123.78, 116.46, 47.48, 38.06, 34.13, 29.66, 24.89, 23.58, 17.58; **HRMS** (ESI-TOF) Calc'd for $C_{20}H_{34}NO_2S^+$ [M+H] 352.2310, found 352.2303.

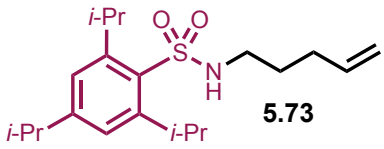

**5.73**

**2,4,6-triisopropyl-*N*-(pent-4-en-1-yl)benzenesulfonamide (5.73):** The title compound was prepared from 5-bromo-1-pentene (745 mg, 5.0 mmol) and 2,4,6-triisopropylbenzenesulfonamide (1.7 g, 6.0 mmol), according to General Procedure C. Purification using silica gel column chromatography (20% Acetone in Hexanes) gave the product as a white solid (1.31 g, 75% yield). **$^1$H NMR** (400 MHz, $CDCl_3$) δ 7.16 (s, 2H), 5.71 (ddt, *J* = 16.9, 10.7, 6.7 Hz, 1H), 4.99–4.91 (m, 2H), 4.30 (t, *J* = 6.4 Hz, 1H), 4.16 (hept, *J* = 6.8 Hz, 2H), 2.99 (q, *J* = 6.8 Hz, 2H), 2.89 (h, *J* = 6.9 Hz, 1H), 2.05 (q, *J* = 6.8 Hz, 2H), 1.60 (q, *J* = 7.2 Hz, 2H), 1.26 (ddd, *J* = 5.9, 4.8, 1.0 Hz, 18H); **$^{13}$C NMR** (150 MHz, $CDCl_3$) δ 152.69, 150.26, 137.24, 132.29, 123.79, 115.60, 42.29, 34.14, 30.81, 29.63, 28.86, 24.89, 23.59; **HRMS** (ESI-TOF) Calc'd for $C_{20}H_{34}NO_2S^+$ [M+H] 352.2310, found 352.2305.

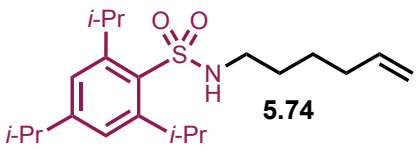

**5.74**

***N*-(hex-5-en-1-yl)-2,4,6-triisopropylbenzenesulfonamide (5.74):** The title

compound was prepared from 6-bromo-1-hexene (1.63 g, 10.0 mmol) and 2,4,6-triisopropylbenzenesulfonamide (3.4 g, 12.0 mmol), according to General Procedure C. Purification using silica gel column chromatography (20% Acetone in Hexanes) gave the product as a white solid (2.45 g, 67% yield). **$^1$H NMR** (400 MHz, $CDCl_3$) δ 7.16 (s, 2H), 5.71 (ddt, *J* = 16.9, 10.2, 6.7 Hz, 1H), 4.98–4.89 (m, 2H), 4.23 (t, *J* = 6.3 Hz, 1H), 4.15 (h, *J* = 6.8 Hz, 2H), 2.97 (td, *J* = 7.0, 6.3 Hz, 2H), 2.89 (h, *J* = 6.9 Hz, 1H), 2.04–1.95 (m, 2H), 1.54–1.44 (m, 2H), 1.44–1.32 (m, 2H), 1.26 (dd, *J* = 6.8, 4.4 Hz, 18H); **$^{13}$C NMR** (150 MHz, $CDCl_3$) δ 152.67, 150.25, 138.05, 132.27, 123.78, 114.96, 42.66, 34.14, 33.12, 29.62, 29.09, 25.85, 24.88, 23.59; **HRMS** (ESI-TOF) Calc'd for $C_{21}H_{36}NO_2S^+$ [M+H] 366.2467, found 366.2454.

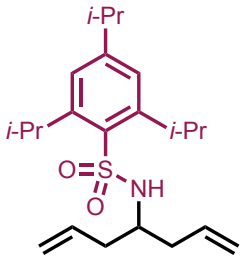


**5.75**

***N*-(hepta-1,6-dien-4-yl)-2,4,6-triisopropylbenzenesulfonamide (5.75):** The title compound was prepared from alkenyl tosylate **5.S36** (1.11 g, 4.17 mmol) and 2,4,6-triisopropylbenzenesulfonamide (1.42 g, 5.00 mmol), according to General Procedure C. Purification using silica gel column chromatography (20% Acetone in Hexanes) gave the product as a yellow oil (84 mg, 5% yield). **$^1$H NMR** (400 MHz, $CDCl_3$) δ 7.15 (s, 2H), 5.65 (ddt, *J* = 17.3, 10.4, 7.2 Hz, 2H), 5.10–5.00 (m, 4H), 4.32 (d, *J* = 7.4 Hz, 1H), 4.12 (hept, *J* = 6.8 Hz, 2H), 3.59–3.48 (m, 1H), 2.90 (hept, *J* = 6.9 Hz, 1H), 2.23 (t, *J* = 6.7 Hz, 4H), 1.26 (dd, *J* = 8.3, 6.8 Hz, 18H); **$^{13}$C NMR** (150 MHz, $CDCl_3$) δ 152.67, 149.95, 133.82, 133.40, 123.76, 118.86, 52.22, 38.56, 34.14, 29.80, 24.92, 23.60; **HRMS** (ESI-TOF) Calc'd for $C_{22}H_{36}NO_2S^+$ [M+H] 378.2467, found 378.2463.

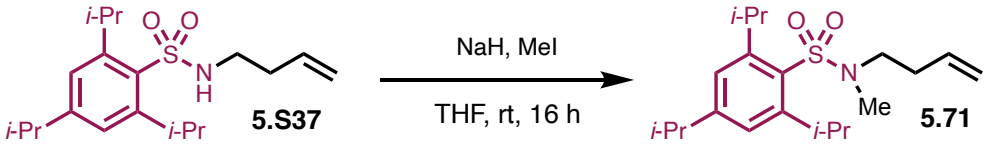


***Scheme 5.S4.*** Synthesis of *N*-methyl alkenyl sulfonamide **5.71**. This compound was synthesized using an adapted version of a literature procedure describing the preparation of a similar compound.[13]

***N*-(but-3-en-1-yl)-2,4,6-triisopropyl-*N*-methylbenzenesulfonamide (5.71):** To a 25-mL Schlenk tube equipped with a Teflon-coated magnetic stir bar, were added NaH (60% in mineral oil, 40 mg, 1.0 mmol, 1 equiv) and THF (2 mL). The vial was submerged in an ice bath, and a solution of the alkenyl sulfonamide **1a** (1.0 mmol, 1 equiv) in THF (3 mL) was subsequently added. The mixture was allowed to stir for at least 10 min, and then MeI (170 mg, 1.2 mmol, 1.2 equiv) was added dropwise. The reaction mixture was allowed to warm to room temperature and was stirred for 16 h. After this time, the reaction mixture was diluted with sat. aq. $NH_4Cl$ (10 mL) and extracted with EtOAc (3 × 1 mL). The combined organic layers were dried over $Na_2SO_4$, and the solvent was removed *in vacuo*. Purification using silica gel column chromatography (20% Acetone in Hexanes) gave the product as a white solid (316.6 mg, 90% yield). **$^1$H NMR** (400 MHz, $CDCl_3$) δ 7.15 (s, 2H), 5.74 (ddt, $J$ = 17.1, 10.2, 6.8 Hz, 1H), 5.13–5.00 (m, 2H), 4.16 (hept, $J$ = 6.8 Hz, 2H), 3.29–3.21 (m, 2H), 2.90 (hept, $J$ = 6.9 Hz, 1H), 2.73 (s, 3H), 2.42–2.32 (m, 2H), 1.25 (dd, $J$ = 6.9, 5.0 Hz, 18H); **$^{13}$C NMR** (150 MHz, $CDCl_3$) δ 153.01, 151.50, 134.86, 130.76, 123.83, 116.97, 47.77, 34.15, 33.32, 31.89, 29.25, 24.81, 23.58; **HRMS** (ESI-TOF) Calc'd for $C_{20}H_{34}NO_2S^+$ [M+H] 352.2310, found 352.2307.

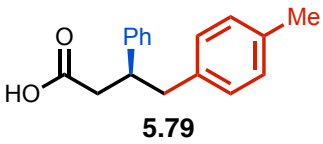


**5.79**

**(*S*)-3-phenyl-4-(*p*-tolyl)butanoic acid (5.79):** To an 8-mL round bottom glass tube equipped with a Teflon-coated magnetic stir bar, were added the 3-butenoic acid **5.78** (0.1 mmol), phenylboronic acid neopentylglycol ester **5.S1** (0.3 mmol), and (4*S*,4'*S*)-4,4'-dibenzyl-4,4',5,5'-tetrahydro-2,2'-bioxazole (**Bn-biOx**) (20 mol%). The tube was then equipped with a septum cap and introduced into an argon-filled glovebox antechamber. Once transferred inside the glovebox, anhydrous NaO*t*-Bu (0.3 mmol), and anhydrous isopropanol (0.9 mL) were added. The vial was sealed with a screw-top cap, removed from the glovebox, and was cooled while stirring to 0 °C in a Thermo Fisher Neslab CC 100 Immersion Cooler with an isopropanol bath. 4-Iodotoluene (0.3 mmol) in (0.1 mL anhydrous isopropanol) was added and the reaction mixture was stirred for 72 h at 0 °C. After this time, the reaction mixture was quenched with 2M aqueous HCl (1 mL) and EtOAc (1 mL) were added. The aqueous layer was further extracted with EtOAc (2 × 1 mL). Thereafter, the organic layers were combined, and the solvent was removed *in vacuo* to leave a yellow residue. Purification using PTLC (60:39:1 hexane:EtOAc:AcOH) gave the product as a white solid (5.1 mg, 20% yield, 92:8 e.r.). **$^1$H NMR** (500 MHz, $CDCl_3$) δ 7.32–7.22 (m, 2H), 7.18 (t, $J$ = 7.4 Hz, 1H), 7.14 (d, $J$ = 7.2 Hz, 2H), 7.02 (*d*, $J$ = 8.0 Hz, 2H), 6.93 (d, $J$ = 7.9 Hz, 2H), 3.41–3.31 (m, 1H), 2.86 (qd, $J$ = 13.6, 7.5 Hz, 2H), 2.65 (qd, $J$ = 15.9, 7.5 Hz, 2H), 2.28 (s, 3H). Spectral data match those previously reported.[17]

### 5.4.7. Deprotection of a Representative 1,2-Diarylated Product

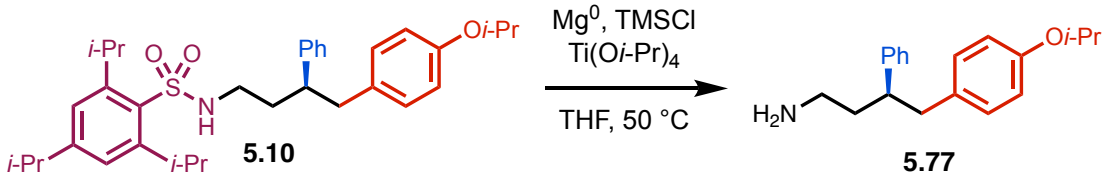


***Scheme 5.S5.*** Deprotection of representative product **5.10**.

**(*S*)-4-(4-isopropoxyphenyl)-3-phenylbutan-1-amine (5.77):** The title compound was prepared by an adapted literature procedure.[18] To an 8-mL round-bottom glass tube equipped with a Teflon-coated magnetic stir bar, were added **5.10** (0.1 mmol), Mg powder (12 mg, 0.5 mol), anhydrous THF (0.5 mL), Ti(O*i*-Pr)$_4$ (30 mL, 0.1 mmol), and TMSCl (19 mL, 0.15 mmol). The reaction mixture was stirred for 24 h at 50 °C. After this time, the reaction mixture was quenched upon addition of 1M aqueous NaOH (1 mL) and EtOAc (2 mL). The aqueous layer was further extracted with EtOAc (2 × 2 mL). Thereafter, the organic layers were combined, and the solvent was removed *in vacuo* to leave a yellow residue. Purification using PTLC (85:15 EtOAc:NEt$_3$) gave the product as a yellow solid (22.3 mg, 79% yield, 95:5 e.r.). **$^1$H NMR** (600 MHz, $CDCl_3$) δ 7.28 (t, $J$ = 7.5 Hz, 2H), 7.19 (t, $J$ = 7.4 Hz, 1H), 7.14 (d, $J$ = 7.0 Hz, 2H), 6.94 (d, $J$ = 8.5 Hz, 2H), 6.75 (d, $J$ = 8.6 Hz, 2H), 4.50 (hept, $J$ = 6.1 Hz, 1H), 2.94–2.74 (m, 3H), 2.61–2.48 (m, 2H), 1.87–1.66 (m, 2H), 1.33 (d, $J$ = 6.1 Hz, 6H); **$^{13}$C NMR** (150 MHz, $CDCl_3$) δ 156.05, 144.83, 132.43, 130.06, 128.32, 127.67, 126.15, 115.60, 69.84, 45.89, 43.15, 40.41, 39.22, 22.10; **HRMS** (ESI-TOF) Calc'd for $C_{19}H_{25}NO^+$ [M+H] 284.2014, found 284.2016.

**REFERENCES**

(1) Zhu, L.; Yu, H.; Xu, Z.; Jiang, X.; Lin, L.; Wang, R. Copper-Catalyzed Oxyazidation of Unactivated Alkenes: A Facile Synthesis of Isoxazolines Featuring an Azido Substituent. *Org. Lett.* **2014**, *16*, 1562–1565.

(2) Zhuo, L.-G.; Yao, Z. K.; Yu, Z.-X. Synthesis of *Z*-Alkenes from Rh(I)-Catalyzed Olefin Isomerization of β,γ-Unsaturated Ketones. *Org. Lett.* **2013**, *15*, 4634–4637.

(3) Katritzky, A. R.; Lang, H.; Wang, Z.; Zhang Z.; Song, H. Benzotriazole-Mediated Conversions of Aromatic and Heteroaromatic Aldehydes to Functionalized Ketones. *J. Org. Chem.* **1995**, *60*, 7619–7624.

(4) Zhan, G.; He, Q.; Yuan, X.; Chen, Y.-C. Asymmetric Direct Vinylogous Michael Additions of Allyl Alkyl Ketones to Maleimides through Dienamine Catalysis. *Org. Lett.* **2014**, *16*, 6000–6003.

(5) Toy, P. H.; Dhanabalasingam, B.; Newcomb, M.; Hanna, I. H.; Hollenberg, P. F. A Substituted Hypersensitive Radical Probe for Enzyme-Catalyzed Hydroxylations: Synthesis of Racemic and Enantiomerically Enriched Forms and Application in a Cytochrome P450-Catalyzed Oxidation. *J. Org. Chem.* **1997**, *62*, 9114–9122.

(6) Harding, K. E.; Burks, S. R. Applications of Intramolecular Amidomercuration. 2. Synthesis of Trans-5-Hydroxy-2-Propylpiperidine, (.+-.)-Pseudoconhydrine. *J. Org. Chem.* **1984**, *49*, 40–44.

(7) Han, B.; Yang, X.-L.; Fang, R.; Yu, W.; Wang, C.; Duan, X.-Y.; Liu, S. Oxime Radical Promoted Dioxygenation, Oxyamination, and Diamination of Alkenes: Synthesis of Isoxazolines and Cyclic Nitrones. *Angew. Chem. Int. Ed.* **2012**, *51*, 8816–8820.

(8) Motiwala, H. F.; Gülgeze, B.; Aubé, J. Copper-Catalyzed Oxaziridine-Mediated Oxidation of C–H Bonds. *J. Org. Chem.* **2012**, *77*, 7005–7022.

(9) Moss, M.; Han, X.; Ready, J. M. Zirconocene-Mediated Carbonylative Coupling of Grignard Reagents. *Angew. Chem. Int. Ed.* **2016**, *55*, 10017–10021.

(10) Ebule, R.; Mudshinge, S.; Nantz, M. H.; Mashuta, M. S.; Hammond, G. B.; Xu, B. A 5 + 1 Protic Acid Assisted Aza-Pummerer Approach for Synthesis of 4-Chloropiperidines from Homoallylic Amines. *J. Org. Chem.* **2019**, *84*, 3249–3259.

(11) Ebule, R.; Mudshinge, S.; Nantz, M. H.; Mashuta, M. S.; Hammond, G. B.; Xu, B. A 5 + 1 Protic Acid Assisted Aza-Pummerer Approach for Synthesis of 4-Chloropiperidines from Homoallylic Amines. *J. Org. Chem.* **2019**, *84*, 3249−3259.

(12) Noguchi, M.; Tsukimoto, A.; Kadowaki, A.; Hikata, J.; Kakehi, A. Stereocontrolled Intramolecular Nitrile Oxide Cycloaddition Reaction Using a Gauche–Gauche Interaction. *Tetrahedron Lett.* **2007**, *48*, 3539–3542.

(13) Dong, G. R.; Park, S.; Lee, D.; Shin, K. J.; Seo, J. H. Synthesis of 3-(Diarylmethylene)oxindoles via a Palladium-Catalyzed One-Pot Reaction: Sonogashira–Heck–Suzuki–Miyaura Combined Reaction. *Synlett* **2013**, *24*, 1993–1997.

(14) Kobayashi, T.; Ohmiya, H.; Yorimitsu, H.; Oshima, K. Cobalt-Catalyzed Regioselective Dehydrohalogenation of Alkyl Halides with Dimethylphenylsilylmethylmagnesium Chloride. *J. Am. Chem. Soc.* **2008**, *130*, 34–35.

(15) Napolitano, J. G.; Galvín, J. A.; García, C.; Norte, M.; Fernandez, J. J.; Daranas, A. H. On the Configuration of Five-Membered Rings: A Spin–Spin Coupling Constant Approach. *Chem. Eur. J.* **2011**, *17*, 6338–6347.

(16) (a) Pal, K.; Behnke, M. L.; Tong, L. A General Stereocontrolled Synthesis of *cis*-2,3

Disubstituted Pyrrolidines and Piperidines. *Tetrahedron Lett*. **1993**, *34*, 6205–6208. (b) Shang, M.; Feu, K. S.; Vantourout, J. C.; Barton, L. M.; Osswald, H. L.; Kato, N.; Gagaring, K.; McNamara, C. W.; Chen, G.; Hu, L.; Ni, S.; Fernández-Canelas, P.; Chen, M.; Merchant, R. R.; Qin, T.; Schreiber, S. L.; Melillo, B.; Yu, J.-Q.; Baran, P. S. Modular, Stereocontrolled $C_\beta$–H/$C_\alpha$–C Activation of Alkyl Carboxylic Acids. *Proc. Natl. Acad. Sci. USA.* **2019**, *116*, 8721–8727.

(17) Derosa, J.; Kang, T.; Tran, V. T.; Wisniewski, S. R.; Karunananda, M. K.; Jankins, T. C.; Xu, K. L; Engle, K. M. Nickel-Catalyzed 1,2-Diarylation of Alkenyl Carboxylates A Gateway to 1,2,3-Trifunctionalized Building Blocks. *Angew*. *Chem*., *Int*. *Ed*. **2020**, *59*, 1201–1205.

(18) Shohji, N; Kawaji, T.; Okamoto, S. Ti(O-*i*-Pr)$_4$/$Me_3SiCl$/Mg-Mediated Reductive Cleavage of Sulfonamides and Sulfonates to Amines and Alcohols. *Org*. *Lett*. **2011**, *13*, 2626–2629.

# APPENDIX III

KINETIC DATA

# Chapter 3 Kinetic Data

**General Procedure for Hammett Analysis:** To an 8 mL scintillation vial equipped with a Teflon-coated magnetic stir bar were added corresponding substrate (0.10 mmol), the corresponding aryl neopentyl boronate (0.30 mmol), and the corresponding aryl iodide (if solid) (0.30 mmol). The vial was then brought into the glovebox where it was evacuated/purged with $N_2$ (5 ×). $Ni(cod)_2$ (4.1 mg, 0.015 mmol) and DMFU (2.2 mg, 0.015 mmol) were added followed by anhydrous, degassed *i*-BuOH (0.2 mL) and the corresponding aryl iodide (if liquid) (0.30 mmol). A solution of NaOMe in *i*-BuOH (0.18 M, 800 µL) was then added, and the reaction stirred at 20 °C for 1 h. Aliquots (50 µL) were diluted into a solution of internal standard (4,4'-di-*tert*-butylbiphenyl in acetonitrile) over a set period of time and subject to UPLC analysis to determine the kinetics of the reaction. The product peaks were corrected by differences in response factors of the products. For the purposes of monitoring rates, we used the combined yield/concentration of both regioisomers.

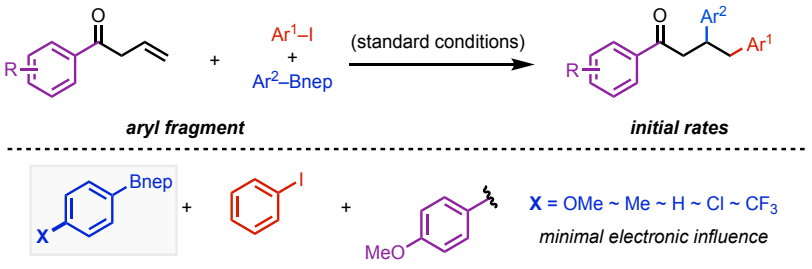


Raw data from kinetic experiments:

| substrate: | H | OMe | Cl | $CF_3$ | Me |
|---|---|---|---|---|---|
| time (min) | Product (mM) | Product (mM) | Product (mM) | Product (mM) | Product (mM) |
| 1 | 0.062 | 0.060 | 0.031 | 0.035 | 0.028 |

| | | | | | |
|---|---|---|---|---|---|
| 3.5 | 0.079 | 0.063 | 0.041 | 0.047 | 0.040 |
| 6 | 0.092 | 0.075 | 0.052 | 0.059 | 0.057 |
| 8.5 | 0.104 | 0.086 | 0.064 | 0.066 | 0.078 |
| 11 | 0.115 | 0.089 | 0.076 | 0.073 | 0.083 |
| 14 | 0.129 | 0.098 | 0.089 | 0.086 | 0.107 |
| 17 | 0.142 | 0.110 | 0.101 | 0.095 | 0.124 |
| 20 | 0.156 | 0.120 | 0.118 | 0.110 | 0.150 |
| 23 | 0.170 | 0.163 | 0.138 | 0.128 | 0.177 |
| 26 | 0.194 | 0.184 | 0.159 | 0.140 | 0.203 |
| 29 | 0.209 | 0.199 | 0.178 | 0.159 | 0.230 |
| 32 | 0.228 | 0.216 | 0.211 | 0.172 | 0.266 |

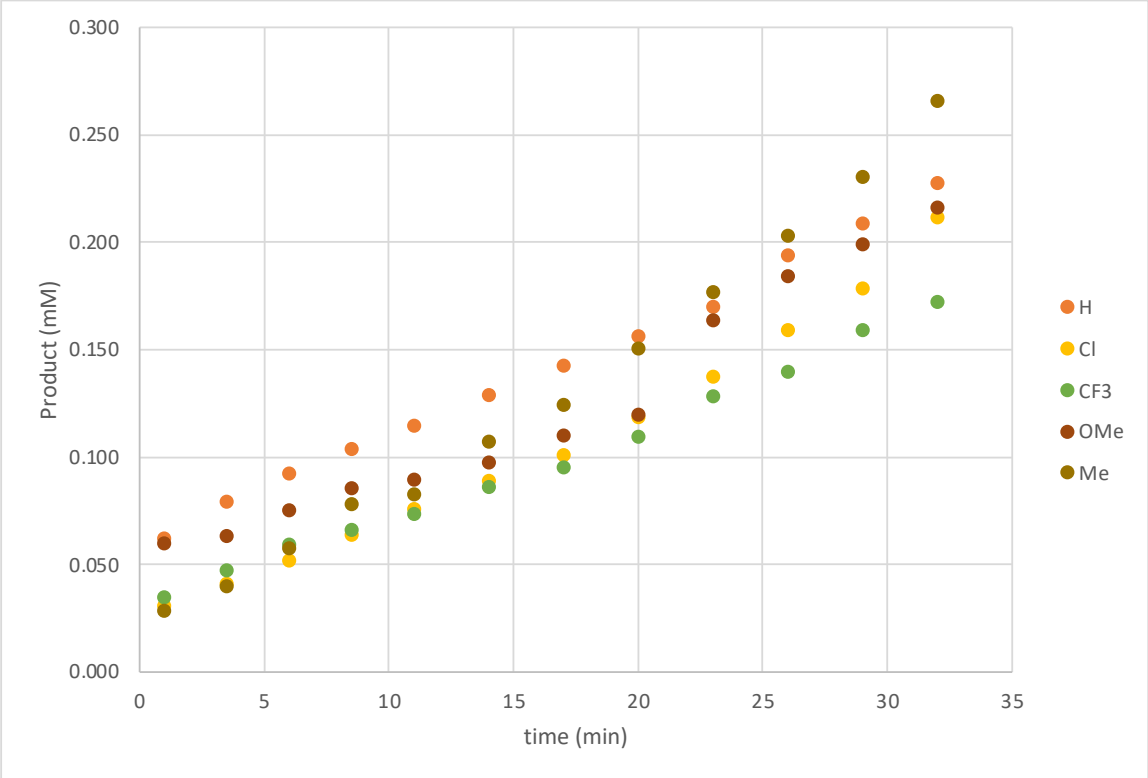


Section of kinetics for the Hammett study:

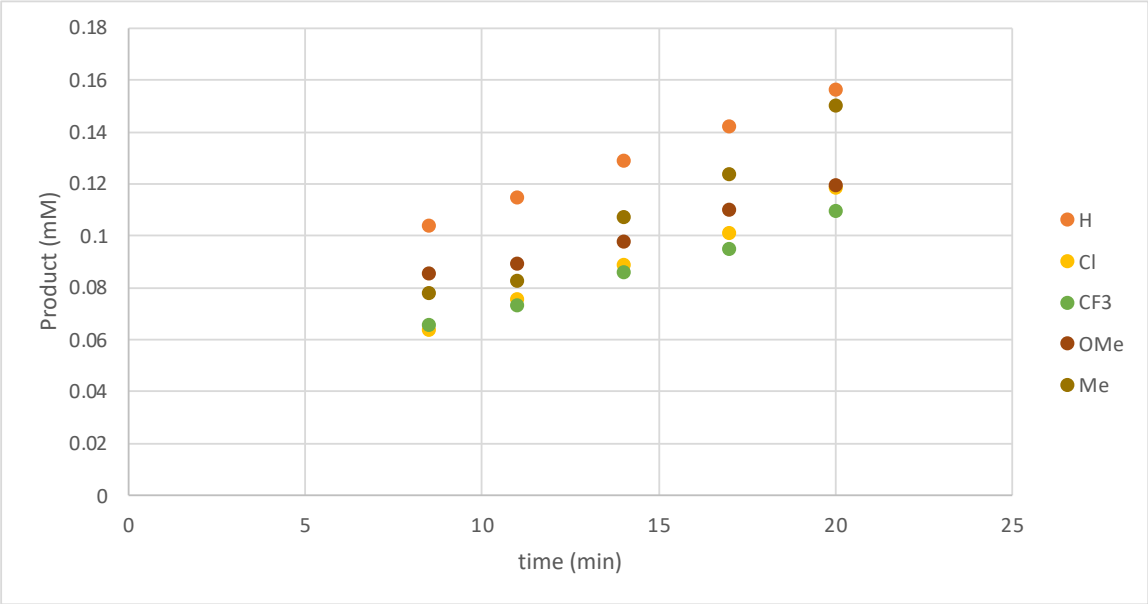


Comparison of computed kinetics vs actual:

| substrate: | H | | Cl | | $CF_3$ | | OMe | | Me | |
|---|---|---|---|---|---|---|---|---|---|---|
| time | (actual) | (computed) | (actual) | (computed) | (actual) | (computed) | (actual) | (computed) | (actual) | (computed) |
| 8.5 | 0.104 | 0.104 | 0.064 | 0.065 | 0.066 | 0.066 | 0.086 | 0.086 | 0.078 | 0.084 |
| 11 | 0.115 | 0.115 | 0.076 | 0.075 | 0.073 | 0.074 | 0.089 | 0.091 | 0.083 | 0.098 |
| 14 | 0.129 | 0.129 | 0.089 | 0.088 | 0.086 | 0.085 | 0.098 | 0.099 | 0.107 | 0.117 |
| 17 | 0.142 | 0.143 | 0.101 | 0.102 | 0.095 | 0.097 | 0.110 | 0.110 | 0.124 | 0.142 |
| 20 | 0.156 | 0.156 | 0.118 | 0.118 | 0.110 | 0.109 | 0.120 | 0.122 | 0.150 | 0.170 |

| Regression: | $R^2$ |
|---|---|
| H | 0.99 |
| Cl | 0.99 |
| $CF_3$ | 0.99 |
| OMe | 0.99 |
| Me | 0.97 |

Hammett Plot:

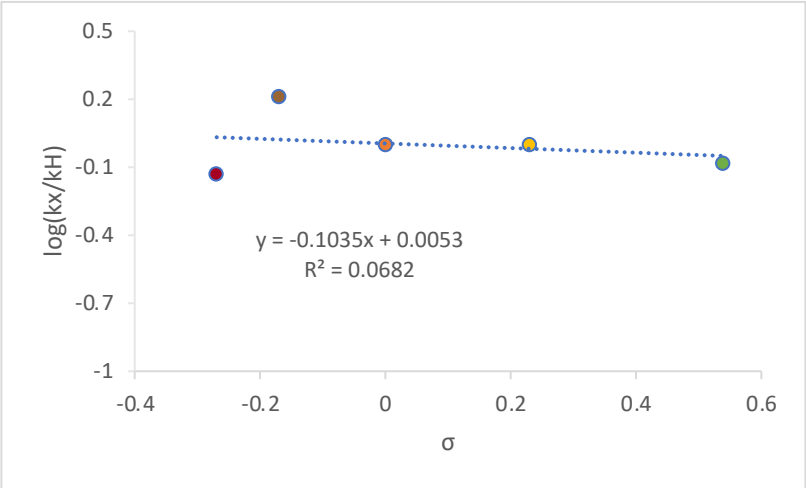


***Figure 3.S3.*** Effect of aryl boronate electronic properties on reaction rate. Initial rate data and Hammett plot.

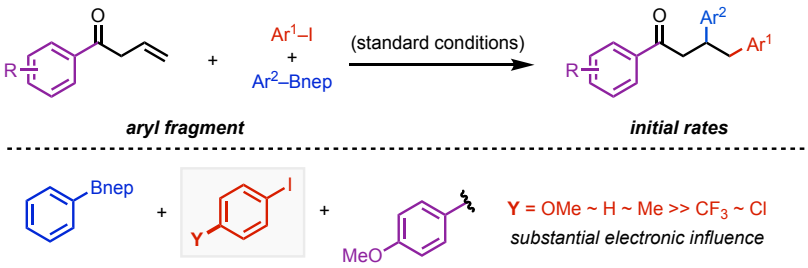


Raw data from kinetic experiments:

| substrate: | H | Cl | $CF_3$ | OMe | Me |
|---|---|---|---|---|---|
| time (min) | Product (mM) | Product (mM) | Product (mM) | Product (mM) | Product (mM) |
| 0.5 | 0.000259 | 6.33E-05 | 5.2E-05 | 0.00051 | 6.63E-05 |
| 2.5 | 0.033 | 0.015 | 0.006 | 0.080 | 0.052 |
| 4.5 | 0.032 | 0.018 | 0.007 | 0.084 | 0.054 |
| 6.5 | 0.033 | 0.021 | 0.008 | 0.087 | 0.058 |
| 9.5 | 0.039 | 0.027 | 0.009 | 0.105 | 0.076 |
| 12.5 | 0.043 | 0.033 | 0.011 | 0.119 | 0.091 |
| 15.5 | 0.048 | 0.037 | 0.012 | 0.126 | 0.104 |
| 23.5 | 0.053 | 0.038 | 0.014 | 0.141 | 0.123 |
| 26.5 | 0.058 | 0.042 | 0.016 | 0.142 | 0.128 |
| 30.5 | 0.059 | 0.041 | 0.015 | 0.151 | 0.130 |

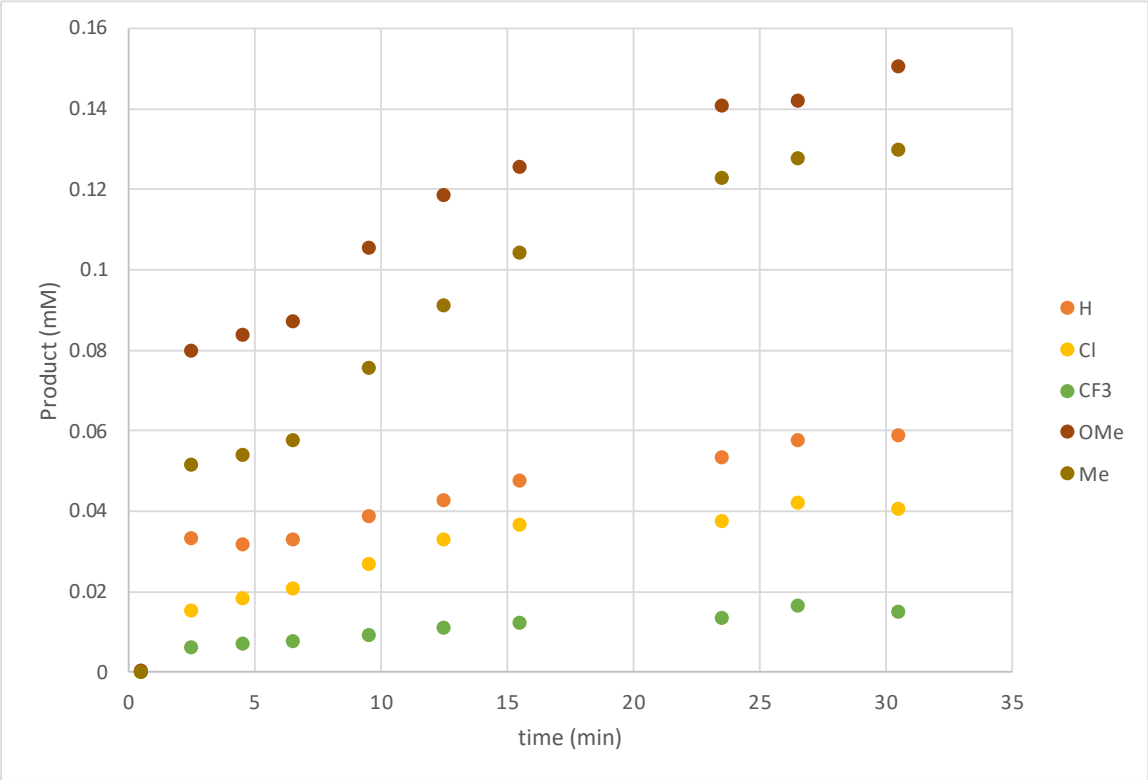


Section of kinetics for the Hammett study:

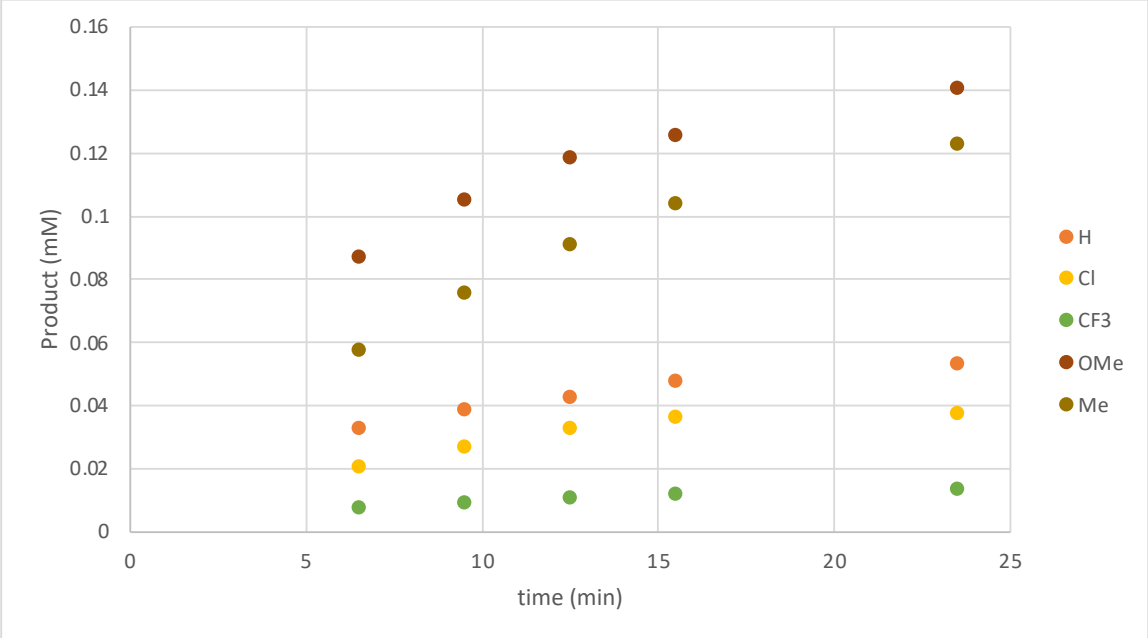

Comparison of computed kinetics vs actual:

| substrate: time | H (actual) | H (computed) | Cl (actual) | Cl (computed) | $CF_3$ (actual) | $CF_3$ (computed) | OMe (actual) | OMe (computed) | Me (actual) | Me (computed) |
|---|---|---|---|---|---|---|---|---|---|---|
| 6.5 | 0.033 | 0.033 | 0.021 | 0.018 | 0.008 | 0.008 | 0.087 | 0.088 | 0.058 | 0.057 |
| 9.5 | 0.039 | 0.039 | 0.027 | 0.024 | 0.009 | 0.009 | 0.105 | 0.104 | 0.076 | 0.076 |
| 12.5 | 0.043 | 0.043 | 0.033 | 0.028 | 0.011 | 0.011 | 0.119 | 0.117 | 0.091 | 0.091 |
| 15.5 | 0.048 | 0.047 | 0.037 | 0.030 | 0.012 | 0.012 | 0.126 | 0.127 | 0.104 | 0.104 |
| 23.5 | 0.053 | 0.053 | 0.038 | 0.028 | 0.014 | 0.014 | 0.141 | 0.140 | 0.123 | 0.123 |

| Regression: | $R^2$ |
|---|---|
| H | 0.95 |
| Cl | 0.99 |
| $CF_3$ | 0.99 |
| OMe | 0.99 |
| Me | 0.99 |

Hammett Plot:

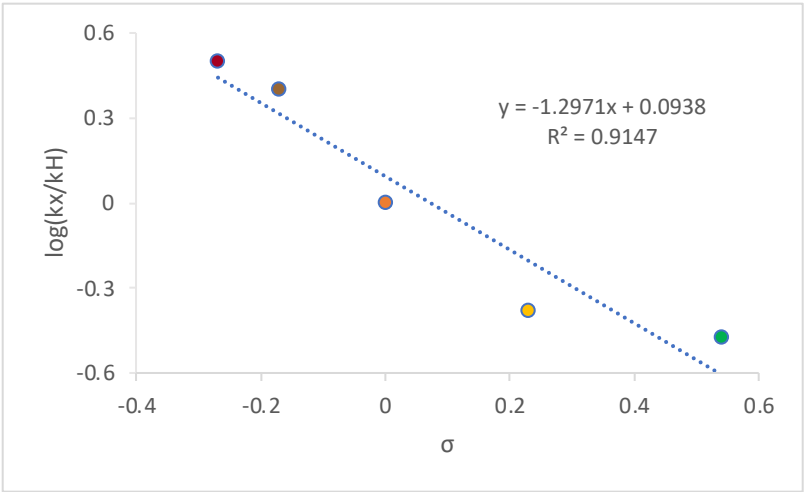


***Figure 3.S4.*** Effect of aryl iodide electronic properties on reaction rate. Initial rate data and Hammett plot.

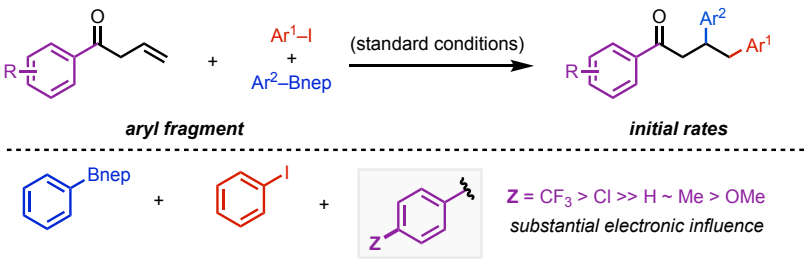

Raw data from kinetic experiments:

| substrate: | H | Cl | $CF_3$ | OMe | Me |
|---|---|---|---|---|---|
| time (min) | Product (mM) | Product (mM) | Product (mM) | Product (mM) | Product (mM) |
| 0.5 | 0.038 | 0.032 | 0.039 | 0.023 | 0.035 |
| 2.5 | 0.063 | 0.100 | 0.117 | 0.049 | 0.058 |
| 4.5 | 0.063 | 0.101 | 0.119 | 0.045 | 0.056 |
| 6.5 | 0.064 | 0.104 | 0.121 | 0.047 | 0.057 |
| 9.5 | 0.069 | 0.112 | 0.135 | 0.052 | 0.062 |
| 12.5 | 0.078 | 0.122 | 0.144 | 0.058 | 0.070 |
| 15.5 | 0.086 | 0.131 | 0.153 | 0.065 | 0.080 |
| 23.5 | 0.096 | 0.139 | 0.160 | 0.072 | 0.086 |
| 26.5 | 0.101 | 0.143 | 0.165 | 0.076 | 0.091 |
| 30.5 | 0.106 | 0.146 | 0.167 | 0.081 | 0.100 |

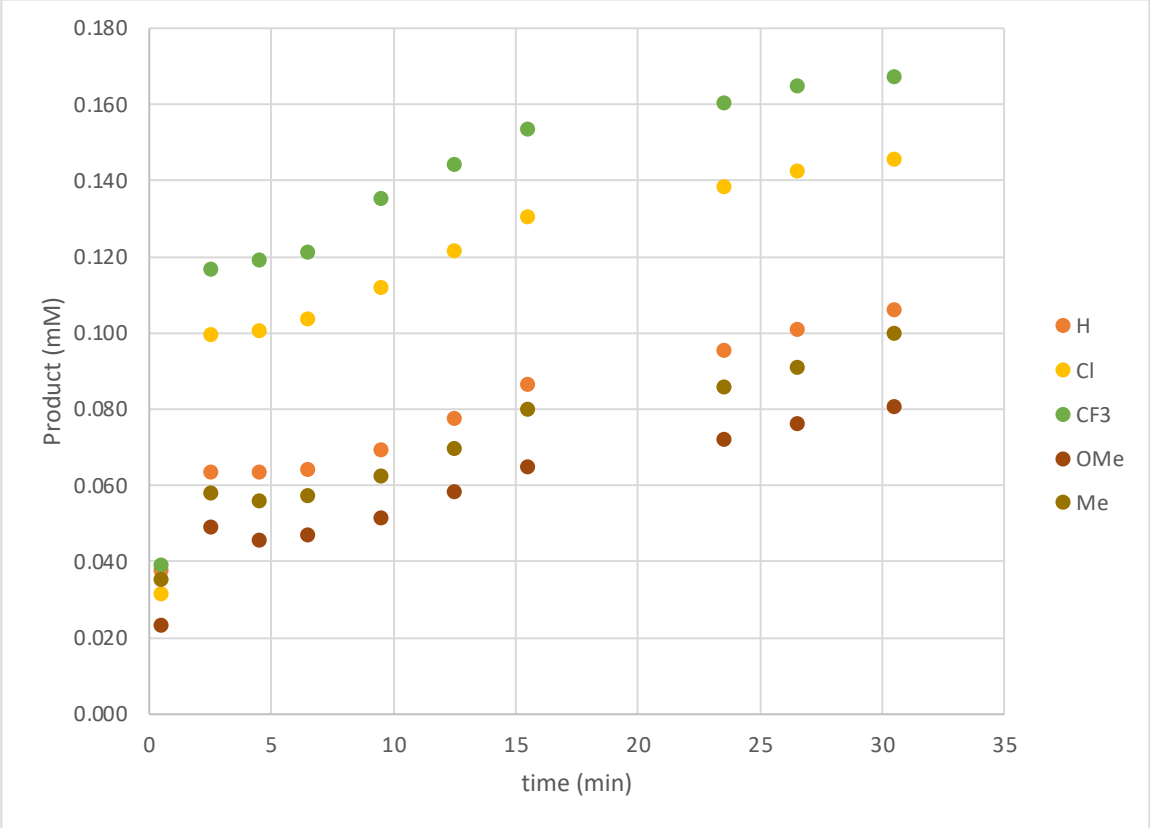


Section of kinetics for the Hammett study:

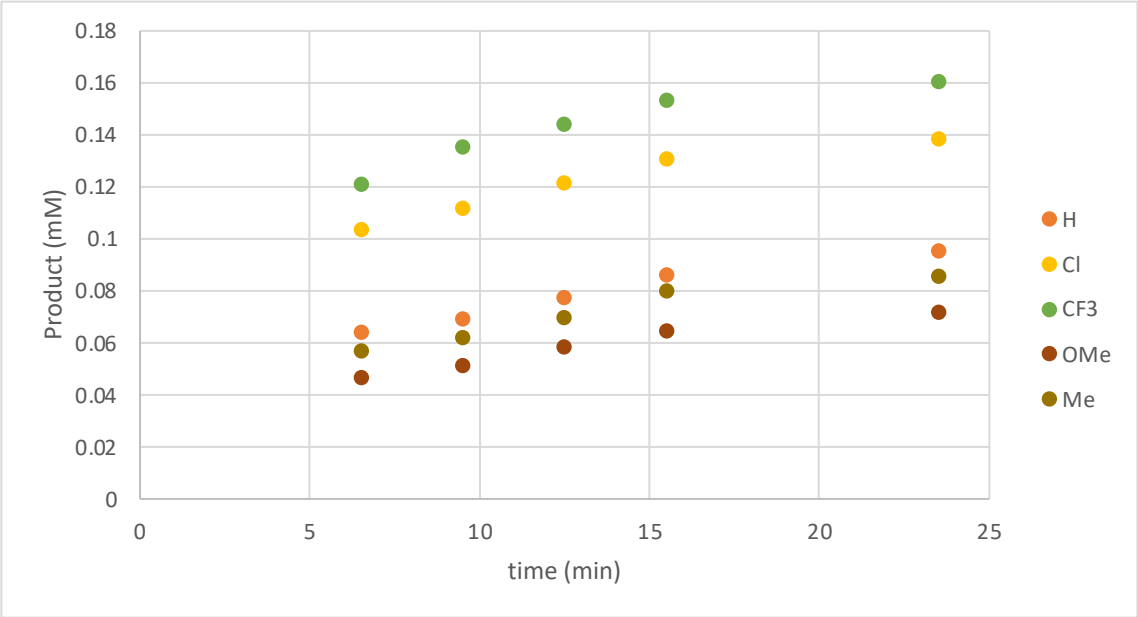


Comparison of computed kinetics vs actual:

| substrate: | H | | Cl | | $CF_3$ | | OMe | | Me | |
|---|---|---|---|---|---|---|---|---|---|---|
| time | (actual) | (computed) | (actual) | (computed) | (actual) | (computed) | (actual) | (computed) | (actual) | (computed) |
| 6.5 | 0.064 | 0.063 | 0.104 | 0.103 | 0.121 | 0.121 | 0.047 | 0.046 | 0.057 | 0.056 |
| 9.5 | 0.069 | 0.071 | 0.112 | 0.113 | 0.135 | 0.135 | 0.052 | 0.053 | 0.062 | 0.064 |
| 12.5 | 0.078 | 0.078 | 0.122 | 0.122 | 0.144 | 0.145 | 0.058 | 0.059 | 0.070 | 0.071 |
| 15.5 | 0.086 | 0.085 | 0.131 | 0.129 | 0.153 | 0.153 | 0.065 | 0.064 | 0.080 | 0.077 |
| 23.5 | 0.096 | 0.096 | 0.139 | 0.139 | 0.160 | 0.160 | 0.072 | 0.072 | 0.086 | 0.086 |

| Regression: | $R^2$ |
|---|---|
| H | 0.96 |
| Cl | 0.99 |
| $CF_3$ | 0.99 |
| OMe | 0.99 |
| Me | 0.97 |

Hammett Plot:

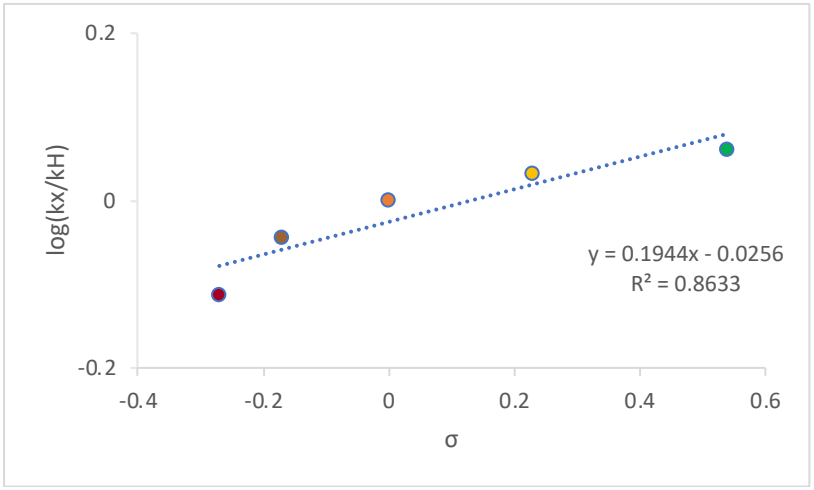


***Figure 3.S5.*** Effect of aryl ketone electronic properties on reaction rate. Initial rate data and Hammett plot.

# APPENDIX IV

SFC DATA

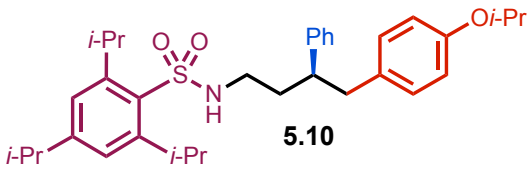


5.10

**SFC** (chiral column) The enantiomeric excess was determined by heart-cutting 2D LC-SFC. The LC dimension consisted of a Waters I-Class LC with a Waters BEH C18 column (1.7 µm, 2.1×100 mm) using a 0.1% aqueous formic acid:acetonitrile gradient (0.6 mL/min, 15–99% acetonitrile over 2.1 minutes) at 55 °C. The heart cut was performed at 2.62 minutes using a 6-port 2-position valve equipped with a 10 µL transfer loop. The SFC dimension consisted of a Waters UPC2 SFC with a Daicel IBN column (3 µm, 4.6×250 mm) using isocratic conditions (3.3 mL/min, 7% MeOH / $CO_2$, 1600 psi backpressure) at 30 °C. The enantiomers were detected by UV light (212 nm).

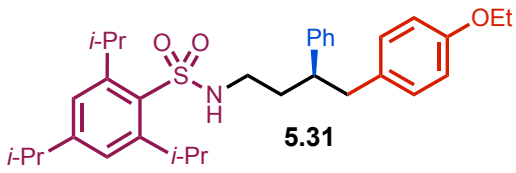


5.31

**(*S*)- *N*-(4-(4-ethoxyphenyl)-3-phenylbutyl)-2,4,6-triisopropylbenzenesulfonamide (5.31)**: **SFC** (chiral column) The sample was analyzed on a Waters UPC2 SFC with a Phenomenex CEL-1 column (3 µm, 4.6×250 mm) using isocratic conditions (3.3 mL/min, 20% IPA / $CO_2$, 1600 psi backpressure) at 30 °C. The enantiomers were detected by UV light (212 nm).

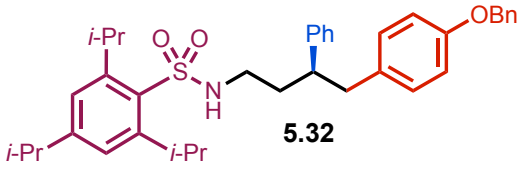


5.32

**SFC** (chiral column) The sample was analyzed on a Waters UPC2 SFC with a Daicel IC column (3 µm, 4.6×250 mm) using isocratic conditions (3.3 mL/min, 25% IPA / $CO_2$, 1600 psi backpressure) at 30 °C. The enantiomers were detected by UV light (212 nm).

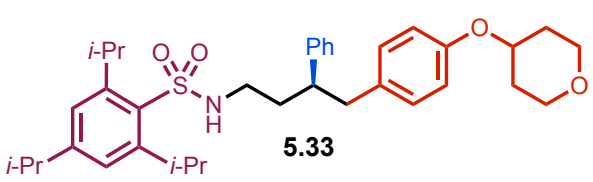


5.33

**SFC** (chiral column) The sample was analyzed on a Waters UPC2 SFC with a Daicel IBN column (3 μm, 4.6×250 mm) using isocratic conditions (3.3 mL/min, 15% MeOH / $CO_2$, 1600 psi backpressure) at 30 °C. The enantiomers were detected by UV light (212 nm).

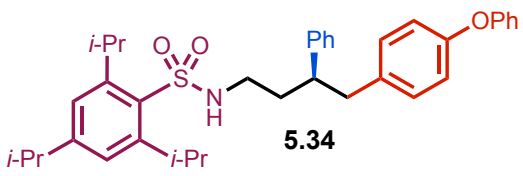


5.34

**SFC** (chiral column) The sample was analyzed on a Waters UPC2 SFC with a Phenomenex AMY-1 column (3 μm, 4.6×250 mm) using isocratic conditions (3.3 mL/min, 20% IPA / $CO_2$, 1600 psi backpressure) at 30 °C. The enantiomers were detected by UV light (231 nm).

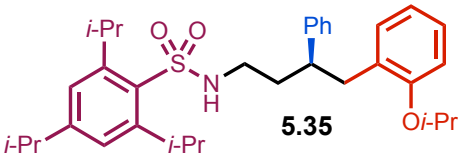


5.35

**SFC** (chiral column) The sample was analyzed on a Waters UPC2 SFC with a Phenomenex AMY-1 column (3 μm, 4.6×250 mm) under isocratic conditions (3.3 mL/min, 15% IPA / $CO_2$, 1600 psi backpressure) at 30 °C. The enantiomers were detected by UV light (228 nm).

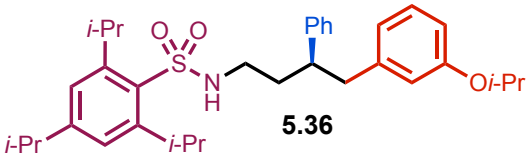


5.36

**SFC** (chiral column) The sample was analyzed on a Waters UPC2 SFC with a Diacel IBN column (3 μm, 4.6×250 mm) under

isocratic conditions (3.3 mL/min, 15% IPA / $CO_2$, 1600 psi backpressure) at 30 °C. The enantiomers were detected by UV light (228 nm).

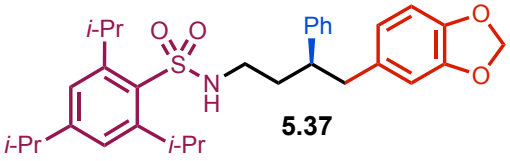


**5.37**

**SFC** (chiral column) The analysis was performed on a Waters UPC2 SFC with a Phenomenex CEL-1 column (3 μm, 4.6×250 mm) under isocratic conditions (3.3 mL/min, 10% MeOH / $CO_2$, 1600 psi backpressure) at 30 °C. The enantiomers were detected by UV light (212 nm).

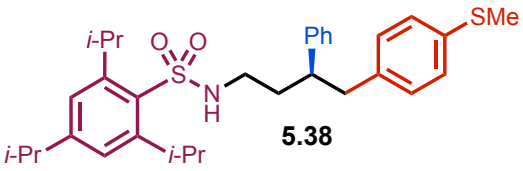


**5.38**

**SFC** (chiral column) The analysis was performed on a Waters UPC2 SFC with a Diacel IBN column (3 μm, 4.6×250 mm) under isocratic conditions (3.3 mL/min, 20% MeOH / $CO_2$, 1600 psi backpressure) at 30 °C. The enantiomers were detected by UV light (256 nm).

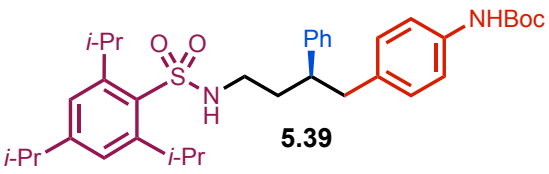


**5.39**

**SFC** (chiral column) The analysis was performed on a Waters UPC2 SFC with a Daicel IBN column (3 μm, 4.6×250 mm) using isocratic conditions (3.3 mL/min, 45% IPA / $CO_2$, 1600 psi backpressure) at 30 °C. The enantiomers were detected by UV light (235 nm).

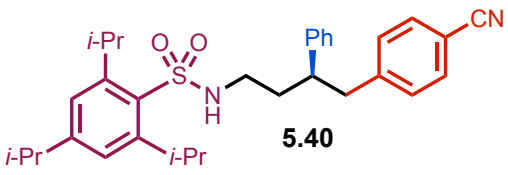


**5.40**

**SFC** (chiral column) The analysis was performed on a Waters UPC2 SFC with a Daicel IC column (3 μm, 4.6×250 mm) using isocratic conditions (3.3 mL/min, 30% IPA / $CO_2$, 1600 psi backpressure) at 30 °C. The enantiomers were detected by UV light (232 nm).

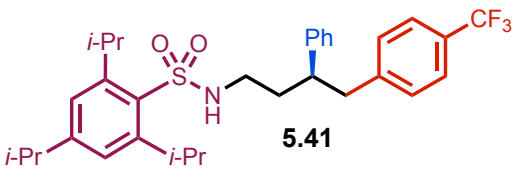


**5.41**

**SFC** (chiral column) The analysis was performed on a Waters UPC2 SFC with a Daicel IC column (3 μm, 4.6×250 mm) using isocratic conditions (3.3 mL/min, 15% IPA / $CO_2$, 1600 psi backpressure) at 30 °C. The enantiomers were detected by UV light (213 nm).

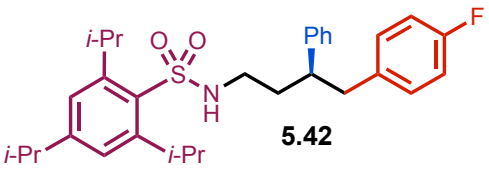


**5.42**

**SFC** (chiral column) The analysis was performed on a Waters UPC2 SFC with a Diacel IC column (3 μm, 4.6×250 mm) under isocratic conditions (3.3 mL/min, 25% IPA / $CO_2$, 1600 psi backpressure) at 30 °C. The enantiomers were detected by UV light (233 nm).

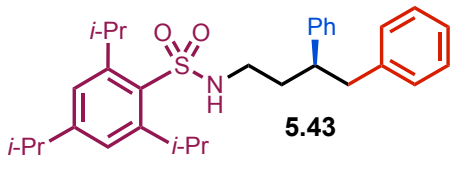


**5.43**

**SFC** (chiral column) The analysis was performed on a Waters UPC2 SFC with a Diacel IBN column (3 μm, 4.6×250 mm) under isocratic conditions (3.3

mL/min, 20% MeOH / $CO_2$, 1600 psi backpressure) at 30 °C. The enantiomers were detected by UV light (242 nm).

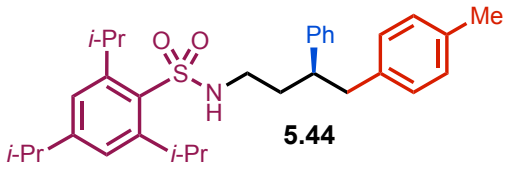


**5.44**

**SFC** (chiral column) The analysis was performed on a Waters UPC2 SFC with a Daicel IBN column (3 μm, 4.6×250 mm) using isocratic conditions (3.3 mL/min, 10% IPA / $CO_2$, 1600 psi backpressure) at 30 °C. The enantiomers were detected by UV light (212 nm).

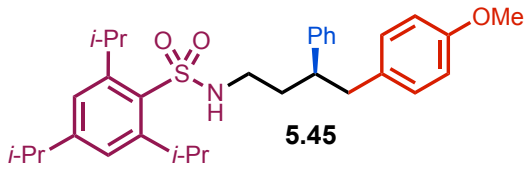


**5.45**

**SFC** (chiral column) The analysis was performed on a Waters UPC2 SFC with a Phenomenex AMY-1 column (3 μm, 4.6×250 mm) using isocratic conditions (3.3 mL/min, 5% IPA / $CO_2$, 1600 psi backpressure) at 30 °C. The enantiomers were detected by UV light (212 nm).

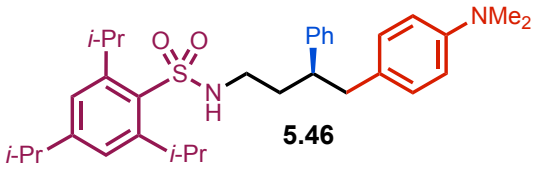


**5.46**

**SFC** (chiral column) The analysis was performed on a Waters UPC2 SFC with a Daicel IC column (3 μm, 4.6×250 mm) under isocratic conditions (3.3 mL/min, 40% IPA / $CO_2$, 1600 psi backpressure) at 30 °C. The enantiomers were detected by UV light (213 nm).

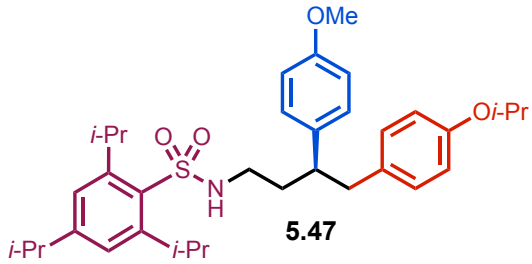


**5.47**

**SFC** (chiral column) The analysis was performed on a Waters UPC2 SFC with a Daicel IBN column (3 μm, 4.6×250 mm) under isocratic conditions (3.3 mL/min, 10% MeOH / $CO_2$, 1600 psi backpressure) at 30 °C. The enantiomers were detected by UV light (225 nm).

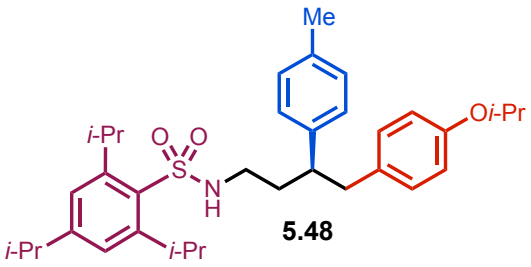


**5.48**

**SFC** (chiral column) The analysis was performed on a Waters UPC2 SFC with a Diacel IA column (3 μm, 4.6x250 mm) under isocratic conditions (3.3 mL/min, 15% IPA / $CO_2$, 1600 psi backpressure) at 30 °C. The enantiomers were detected by UV light (224 nm).

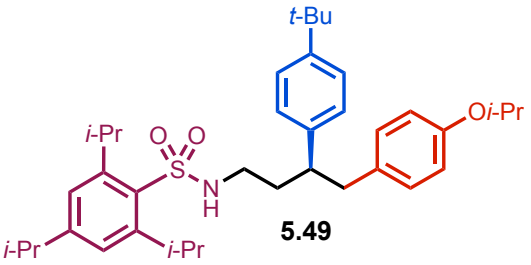


**5.49**

**SFC** (chiral column) The analysis was performed on a Waters UPC2 SFC with a Diacel IC column (3 μm, 4.6×250 mm) under isocratic conditions (3.3 mL/min, 10% MeOH / $CO_2$, 1600 psi backpressure) at 30 °C. The enantiomers were detected by UV light (216 nm).

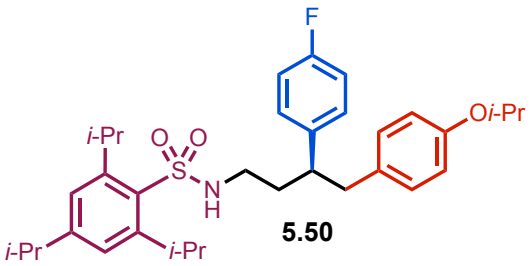


**5.50**

**SFC** (chiral column) The analysis was performed on a Waters UPC2 SFC with a Phenomenex AMY-1 column (3 μm, 4.6×250 mm) under isocratic conditions (3.3 mL/min, 20% IPA / $CO_2$, 1600 psi backpressure) at 30 °C. The enantiomers were detected by UV light (228 nm).

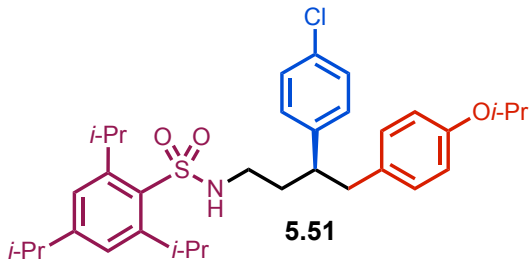


**5.51**

**SFC** (chiral column) The analysis was performed on a Waters UPC2 SFC with a Diacel IA column (3 μm, 4.6×250 mm) under isocratic conditions (3.3 mL/min, 15% IPA / $CO_2$, 1600 psi backpressure) at 30 °C. The enantiomers were detected by UV light (228 nm).

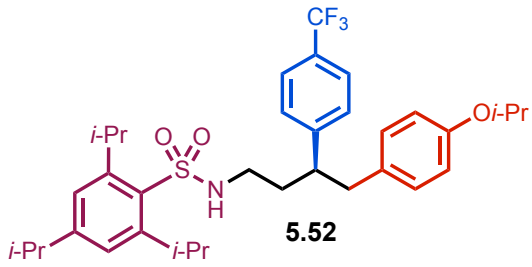


**5.52**

**SFC** (chiral column) The analysis was performed on a Waters UPC2 SFC with a Diacel IG column (3 μm, 4.6×250 mm) under isocratic conditions (3.3 mL/min, 15% IPA / $CO_2$, 1600 psi backpressure) at 30 °C. The enantiomers were detected by UV light (240 nm).

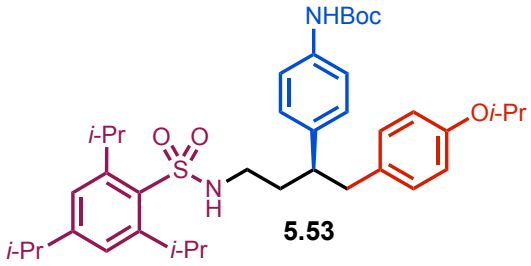


**SFC** (chiral column) The analysis was performed on a Waters UPC2 SFC with a Diacel IC column (3 μm, 4.6×250 mm) under isocratic conditions (3.3 mL/min, 35% MeOH / $CO_2$, 1600 psi backpressure) at 30 °C. The enantiomers were detected by UV light (236 nm).

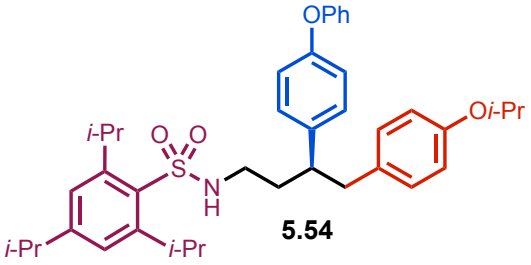


**SFC** (chiral column) The analysis was performed on a Waters UPC2 SFC with a Phenomenex AMY-1 column (3 μm, 4.6×250 mm) under isocratic conditions (3.3 mL/min, 20% IPA / $CO_2$, 1600 psi backpressure) at 30 °C. The enantiomers were detected by UV light (228 nm).

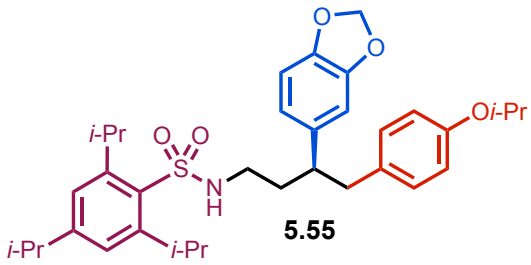


**SFC** (chiral column) The analysis was performed on a Waters UPC2 SFC with a Phenomenex AMY-1 column (3 μm, 4.6×250 mm) under isocratic conditions (3.3 mL/min, 20% IPA / $CO_2$, 1600 psi backpressure) at 30 °C. The enantiomers were detected by UV light (228 nm).

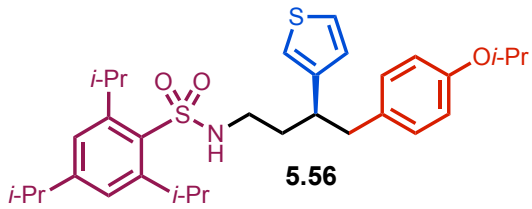


**5.56**

**SFC** (chiral column) The analysis was performed on a Waters UPC2 SFC with a Phenomenex AMY-1 column (3 μm, 4.6×250 mm) under isocratic conditions (3.3 mL/min, 20% IPA / $CO_2$, 1600 psi backpressure) at 30 °C. The enantiomers were detected by UV light (228 nm).

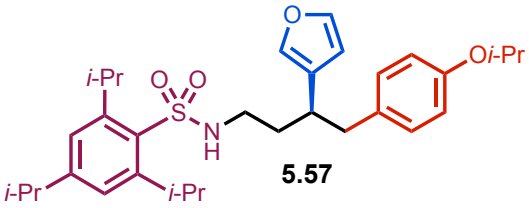


**5.57**

**SFC** (chiral column) The analysis was performed on a Waters UPC2 SFC with a Diacel IBN column (3 μm, 4.6×250 mm) under isocratic conditions (3.3 mL/min, 10% MeOH / $CO_2$, 1600 psi backpressure) at 30 °C. The enantiomers were detected by UV light (228 nm).

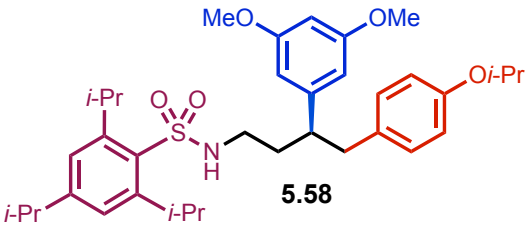


**5.58**

**SFC** (chiral column) The analysis was performed on a Waters UPC2 SFC with a Diacel IK column (3 μm, 4.6x250 mm) under isocratic conditions (3.3 mL/min, 30% IPA / CO2, 1600 psi backpressure) at 30 °C. The enantiomers were detected by UV light (226 nm).

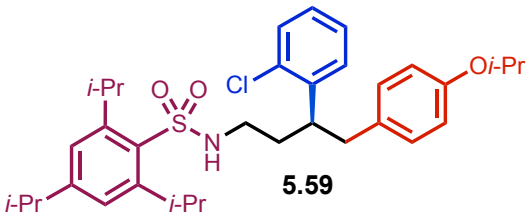


**5.59**

**SFC** (chiral column) The analysis was performed on a Waters UPC2 SFC with a Daicel IK column (3 μm, 4.6x250 mm) using

isocratic conditions (3.3 mL/min, 25% MeOH / $CO_2$, 1600 psi backpressure) at 30 °C. The enantiomers were detected by UV light (226 nm).

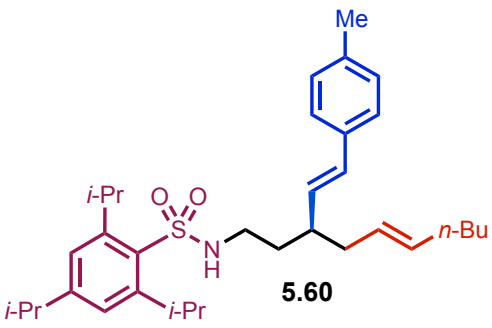


**5.60**

**SFC** (chiral column) The analysis was performed on a Waters UPC2 SFC with a Diacel IK column (3 μm, 4.6x250 mm) under isocratic conditions (3.3 mL/min, 10% IPA / CO2, 1600 psi backpressure) at 30 °C. The enantiomers were detected by UV light (212 nm).

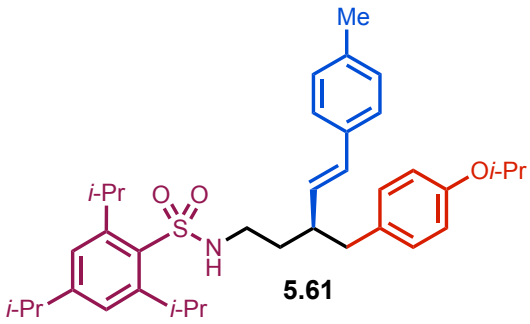


**5.61**

**SFC** (chiral column) The analysis was performed on a Waters UPC2 SFC with a Diacel IBN column (3 μm, 4.6×250 mm) under isocratic conditions (3.3 mL/min, 10% MeOH / $CO_2$, 1600 psi backpressure) at 30 °C. The enantiomers were detected by UV light (254 nm).

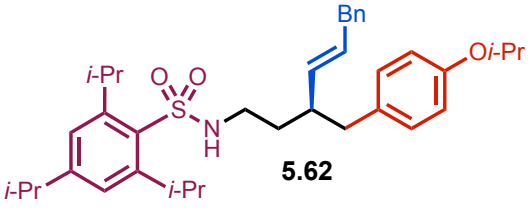


**5.62**

**SFC** (chiral column) The sample was analyzed on a Waters UPC2 SFC with a Phenomenex AMY-1 column (3 μm, 4.6×250 mm) under isocratic conditions (3.3 mL/min, 15% IPA / $CO_2$, 1600 psi backpressure) at 30 °C. The enantiomers were detected by UV light (225 nm).

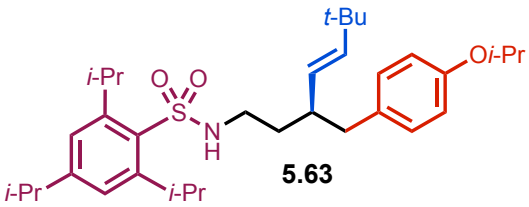


5.63

**SFC** (chiral column) The analysis was performed on a Waters UPC2 SFC with a Diacel IBN column (3 μm, 4.6×250 mm) under isocratic conditions (3.3 mL/min, 15% MeOH / $CO_2$, 1600 psi backpressure) at 30 °C. The enantiomers were detected by UV light (227 nm).

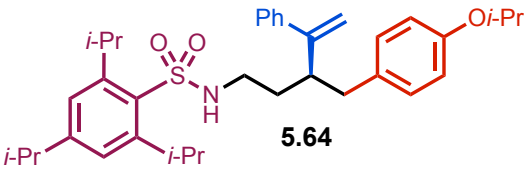


5.64

**SFC** (chiral column) The analysis was performed on a Waters UPC2 SFC with Phenomenex AMY-1 column (3 μm, 4.6x250 mm) under isocratic conditions (3.3 mL/min, 12% IPA / $CO_2$, 1600 psi backpressure) at 30 °C. The enantiomers were detected by UV light (225 nm).

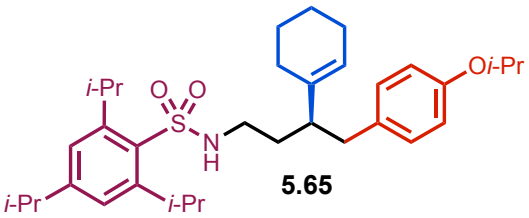


5.65

**SFC** (chiral column) The analysis was performed on a Waters UPC2 SFC with a Diacel IBN column (3 μm, 4.6×250 mm) under isocratic conditions (3.3 mL/min, 15% MeOH / $CO_2$, 1600 psi backpressure) at 30 °C. The enantiomers were detected by UV light (228 nm).

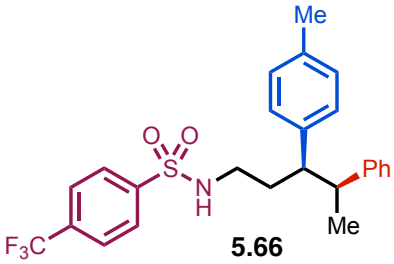


5.66

**SFC** (chiral column) The sample was analyzed on a Waters UPC2 SFC with a Phenomenex CEL-1 column (3 μm, 4.6x250 mm) under isocratic conditions (3.3 mL/min, 25% IPA / CO2, 1600 psi backpressure) at 30

°C. The enantiomers were detected by UV light (212 nm). **Preparative SFC** The major enantiomer was separated on a Waters Prep SFC 150 AP using a Phenomenex CEL-1 column (5 um, 21x250 mm). The purification was run under isocratic conditions (8% IPA / CO2, 100 mL/min, 1600 psi backpressure) at 35 °C. Fractionation was triggered by mass spec ($ESI^+$ on a Waters QDa, SIR channel m/z = 462.2).

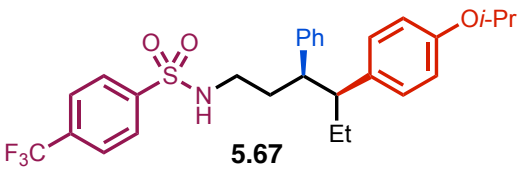


**5.67**

**SFC** (chiral column) The sample was analyzed on a Waters UPC2 SFC with a Diacel IBN column (3 μm, 4.6x250 mm) under isocratic conditions (3.3 mL/min, 15% MeOH / $CO_2$, 1600 psi backpressure) at 30 °C. The enantiomers were detected by UV light (225 nm).

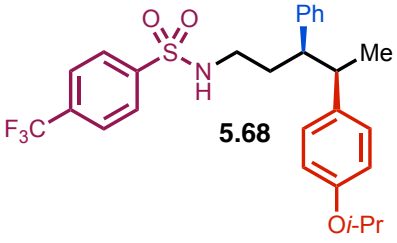


**5.68**

**SFC** (chiral column) The samples was analyzed on a Waters UPC2 SFC with a Daicel IK column (3 mm, 4.6x250 mm) using isocratic conditions (3.3 mL/min, 25% IPA / $CO_2$, 1600 psi backpressure) at 30 °C. The enantiomers were detected by UV light (226 nm).

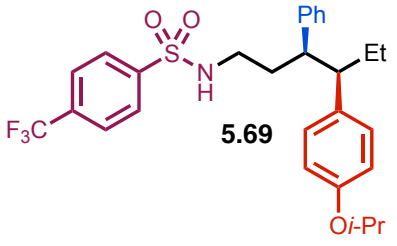


**5.69**

**SFC** (chiral column) The samples was analyzed on a Waters UPC2 SFC with a Diacel IBN column (3 μm, 4.6x250 mm) under isocratic conditions (3.3 mL/min, 20% MeOH / $CO_2$, 1600 psi backpressure) at 30 °C. The enantiomers were detected by UV light (225 nm).

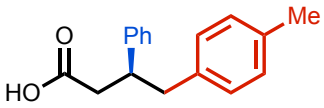


**2au**

**SFC** (chiral column) The sample was analyzed on a Waters UPC2 SFC with a Diacel IG column (3 μm, 4.6x250 mm) under isocratic conditions (3.3 mL/min, 7% MeOH with formic acid / $CO_2$, 1600 psi backpressure) at 30 °C. The enantiomers were detected by UV light (220 nm).

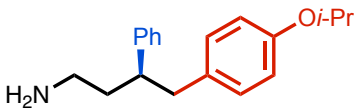


**5.77**

**SFC** (chiral column) The analysis was performed on a Waters UPC2 SFC with a Diacel IG column (3 μm, 4.6x250 mm) under isocratic conditions (10% MeOH containing 0.5 vol% 7M methanolic $NH_3$ / $CO_2$, 1600 psi backpressure) at 30 °C. The enantiomers were detected by UV light (228 nm).

# APPENDIX V

COMPUTATIONAL DATA

# Computational Data for Chapter 3:

**Substrate Coordination Modes:** Initially, the coordination mode of the ketone directing group to the nickel metal center was examined using **3.S12** as the model substrate. The migratory insertion step was evaluated as it was found to be the rate determining step. The transition states for the substrate binding as the ketone (**TS1**), the neutral enolate (**TS2, TS4, TS5**) and the anionic enolate (**TS3**) were located. The activation energy barrier for **TS1** was the lowest transition state indicating that the alkenyl ketone coordinates in the carbonyl form (Figure 3.S1).

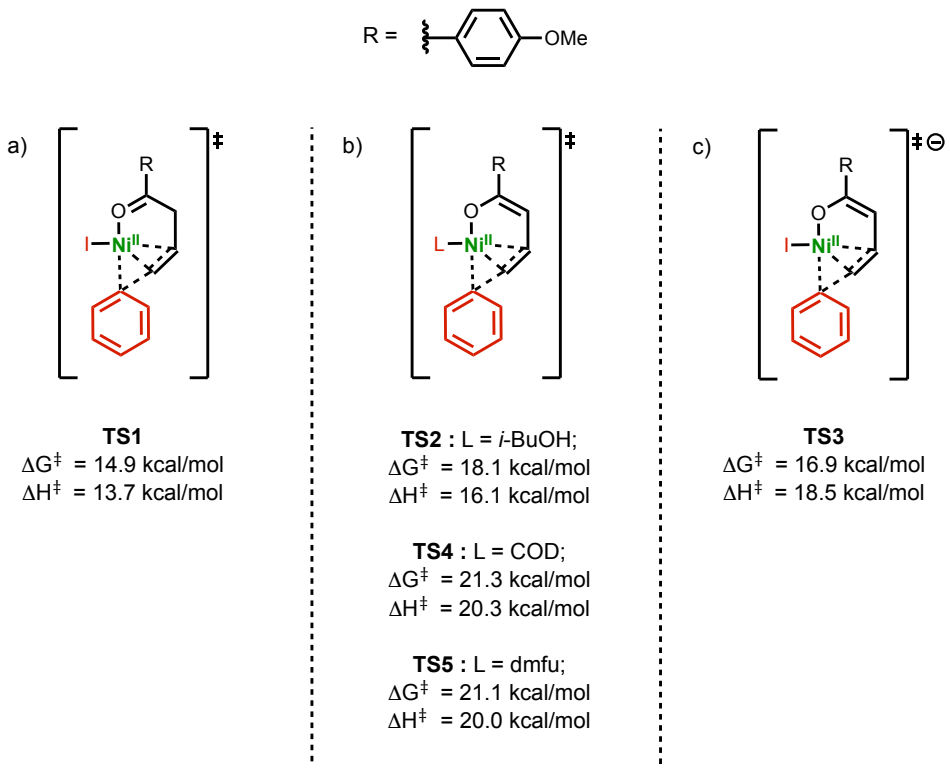


***Figure 3.S1.*** Comparison of the transition states for the substrate coordinating as the a) ketone (**TS1**), b) neutral enolate (**TS2, TS4, TS5**) and c) anionic enolate (**TS3**).

**The Role of the Conjugated Alkene in Reductive Elimination:** In our previously published 1,2-diarylation of alkenyl amides, DMFU was required for productive catalysis. The electron-deficient olefin (EDO) ligand played a crucial role by drastically reducing the activation energy barrier of the reductive elimination step. However, with alkenyl ketones, good reactivity was observed even without the use of DMFU. We think that the cause of this is that the ketone substrate in its isomerized form (conjugated alkenyl ketone) may act as an EDO ligand facilitating the reaction. We evaluated this possibility by locating the transition states of the reductive elimination step in the presence of the coordinated solvent; isobutanol (**TS6**), conjugated alkenyl ketone, (**TS7**) and electron-deficient olefin ligand; dimethyl fumarate (**TS8**) respectively (Scheme 3.S2). The binding mode of the conjugated alkenyl ketone lowers the activation barrier significantly (10.7 kcal/mol), compared to the solvent (36.2 kcal/mol).

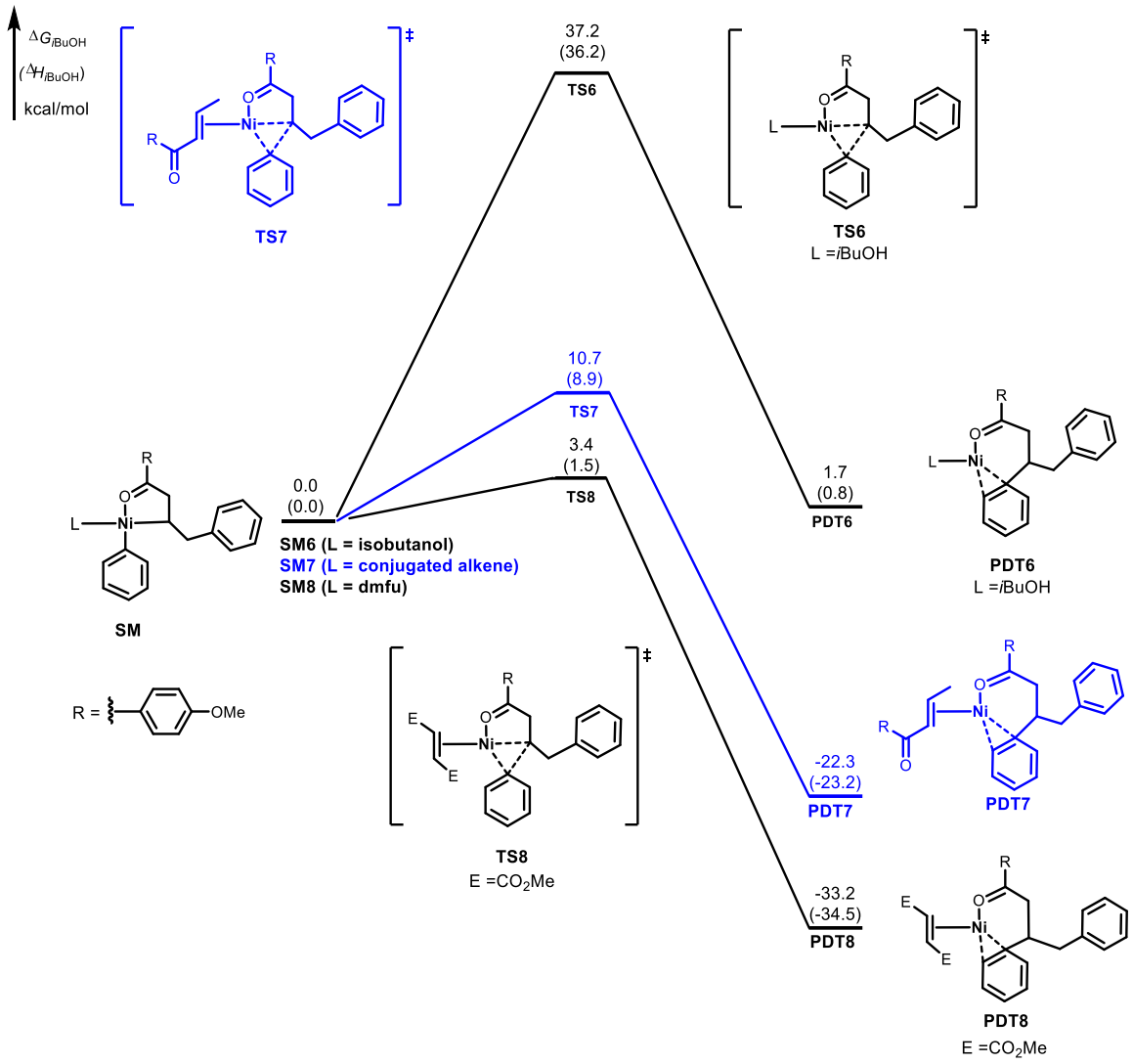


***Figure 3.S2.*** Computed energy profiles for reductive elimination.

# Computational Data for Chapter 5:

### Conformational Search of Migratory Insertion Transition States

Conformational sampling for the enantioselectivity-determining alkene migratory insertion transition states **TS2a** and **TS2b** was performed using the Conformer-Rotamer Ensemble Sampling Tool (CREST)[1a] program that uses the semiempirical tight-binding based quantum mechanical method GFN2-xTB[1b] to perform metadynamic sampling

(MTD) of conformers. In the CREST/GFN2-xTB conformational sampling for each transition state, the forming Ni–C and C–C bonds and the breaking Ni–C(Ph) bond were restrained at the same distances as DFT-optimized transition state geometries (1.95, 1.94, and 1.98 Å for the Ni–C, C–C, and Ni–C(Ph) bonds, respectively) with a force constant of 0.5 Hartree/Bohr$^2$.[2] The conformers were filtered by using a 0.5 Å root-mean-square-deviation (RMSD) and an energy window of 10 kcal/mol yielding 46 and 50 conformers for **TS2a** and **TS2b**, respectively. The conformers obtained from the CREST/GFN2-xTB conformational sampling were then fully optimized at the indicated DFT level. Similarities of the DFT-optimized TS conformers were then compared using GoodVibes package to identify duplicated conformers based on energies, rotational constants, and calculated frequencies (energy cutoff = 0.1 mHartree, RMS rotational constant cutoff = 0.1 GHz, RMS frequency cutoff = 10 wavenumbers, and maximum frequency difference = 10 wavenumbers).[3] After removing the duplicated conformers, we were left with 31 unique conformers for **TS2a** and 30 conformers for **TS2b**. Four lowest-energy conformers for **TS2a** and **TS2b** are shown in **Figure S5**. Although the benzyl group on the ligand and the trisyl group are both conformationally flexible, the trisyl group is always placed in proximity to the benzyl group on the undissociated arm of the biOx ligand, leading to steric repulsions. On the other hand, in two low-energy conformers of **TS2a** (**TS2a** and **TS2a-2**), the trisyl group is placed further away from the same Bn group because the trisyl is tilted towards the same direction as the ethylene group. It should be noted that in one of the low-energy conformers of **TS2a** (**TS2a-1**), the dissociated arm of biOx rotates to orient the oxygen atom rather than the nitrogen atom towards the nickel center. In this geometry, the benzyl group on the dissociated arm is placed away from the substrate. Therefore, the

favorable C–H/π interactions between the benzyl and the alkenyl C–H bonds are not present in this transition state conformer. On the other hand, in most low-energy TS conformers where the N atom on the dissociated biOx arm points towards the nickel center, C–H/π interactions between the Bn group on the dissociated biOx arm and the alkenyl C–H bonds are observed. The C–H/π distances in **TS2a** and **TS2a-2** ($d_{C–H/\pi}$ = 2.53 and 2.52 Å, respectively) are shorter than those in other TS conformers where steric repulsions with the trisyl are observed (*e.g.*, **TS2a-3**, **TS2b**, **TS2b-1**, **TS2b-2**, and **TS2b-3**, $d_{C–H/\pi}$ = 2.58~2.62 Å). Here, the steric repulsions with the trisyl lead to rotation of the biOx ligand that causes longer and less favorable C–H/π distances. In **TS2a-2** and **TS2b-1**, T-shaped π/π interactions between the benzyl group on the undissociated arm of the biOx ligand and the Ph group on the nickel (originally on the phenyl iodide electrophile). These T-shaped π/π interactions in both **TS2a-2** and **TS2b-1** are expected to be stronger with a more electron-deficient aryl iodide starting material, which would increase the amount of partial positive charge on the C–H bond of the benzene ring, leading to more favorable electrostatic interactions.[4] Because **TS2b-1** and **TS2a-2** are only 0.03 and 0.8 kcal/mol less stable than their corresponding lowest-energy conformer, **TS2b** and **TS2a**. In reactions with electron-deficient aryl iodides, **TS2b-1** and **TS2a-2** may become the lowest-energy conformers due to the T-shaped π/π interactions which are absence in **TS2a** and **TS2b**. Considering the energy difference between **TS2b-1** and **TS2a-2** ($\Delta\Delta G^{\ddagger}$ = 0.5 kcal/mol) is smaller than the energy difference between **TS2b** and **TS2a** ($\Delta\Delta G^{\ddagger}$ = 1.3 kcal/mol), these results are consistent with the experimental observation that reactions with electron-deficient aryl iodides lead to lower enantioselectivity.

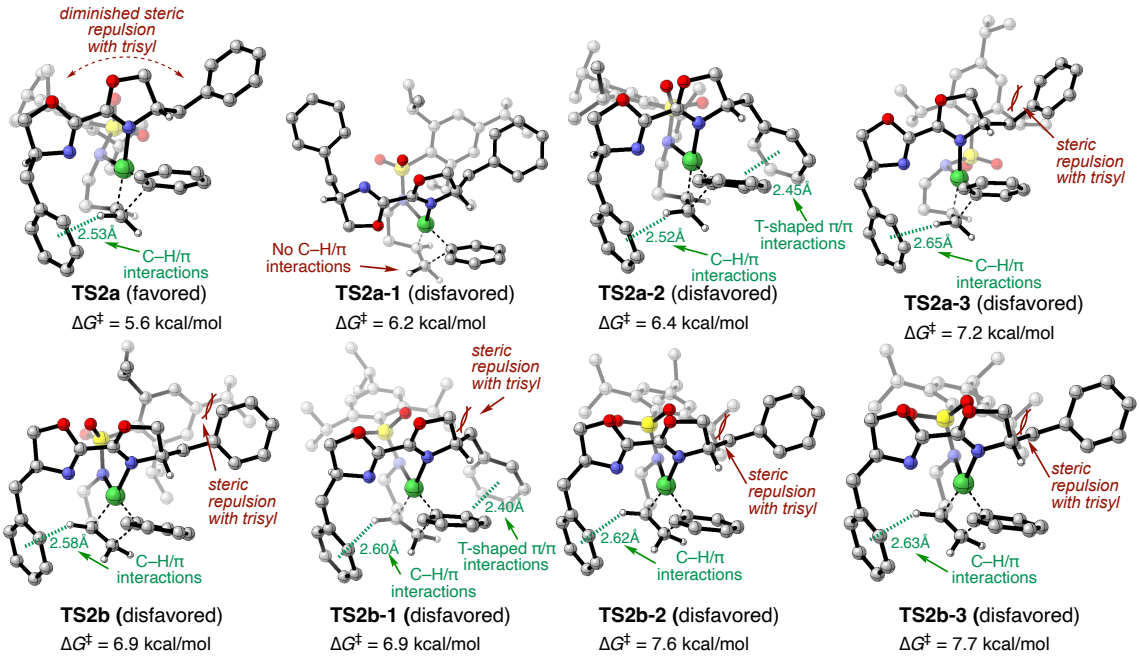


***Figure 5.S4***. Lowest-energy conformers of the migratory insertion transition states. Gibbs free energies are with respect to the arylnickel(II) intermediate **5.82**.

## Electronic Effects of Aryl Iodide Electrophile on Enantioselectivity

Experimentally, the enantioselectivity is slightly decreased when electron-deficient aryl iodide electrophiles, such as *p*-CN-PhI, were used (Table 5.4). To understand the electronic effects of the aryl iodide electrophile on the enantioselectivity, we computed the relative Gibbs free energies of the low-energy migratory insertion TS conformers using *p*-CN-PhI as the electrophile (Figure 5.S5). The *p*-CN substituent lowers the energies of both **TS2a-2_CN** and **TS2b-1_CN**, compared with corresponding TS conformers without the *p*-CN substituent (**TS2a-2** and **TS2b-1**, Figure 5.S4). Here, **TS2a-2_CN** and **TS2b-1_CN** are stabilized by stronger T-shaped π/π interactions between the Bn group on the ligand and the more electron-deficient aryl group with more positively charged C($sp^2$)–H bonds that lead to stronger electrostatic interactions.[5] In the reaction with *p*-CN-PhI, **TS2b-1_CN** becomes the most stable conformer of the migratory insertion TS leading to the minor

enantiomeric product. Therefore, the computed enantioselectivity of this reaction is diminished due to the smaller Gibbs free energy difference between **TS2b-1_CN** and **TS2a_CN** ($\Delta\Delta G^{\ddagger}$ = 0.82 kcal/mol) compared to the free energy difference between **TS2b** and **TS2a** ($\Delta\Delta G^{\ddagger}$ = 1.22 kcal/mol). These results are consistent with the experimental observation that reactions with electron-deficient aryl iodides lead to lower enantioselectivity.

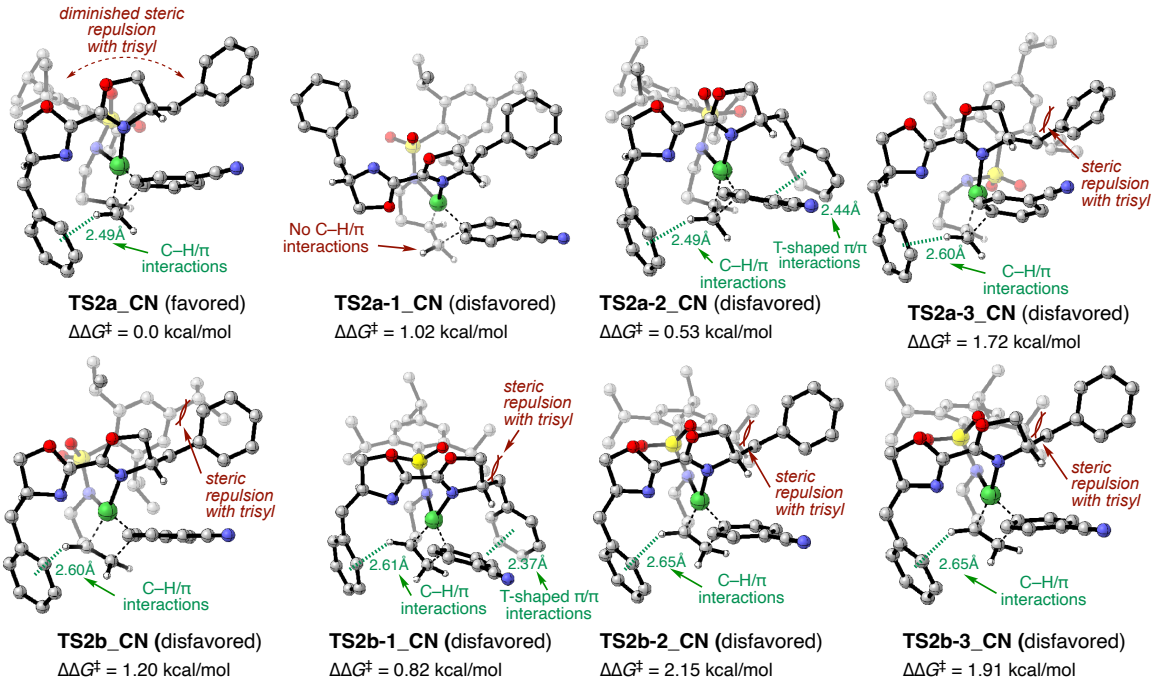


***Figure 5.S5***. Lowest-energy conformers of the migratory insertion transition states with 4-iodobenzonitrile. Gibbs free energies are with respect to the most stable transition state **TS2a_CN**.

## Enantioselectivity Calculations using Boltzmann-Weighted Averages of all Located Unique Transition State Conformers

Boltzmann weighting over all unique transition state conformers was used to compute the effective Gibbs free energy ($\Delta G_{\text{eff}}$)[5] for **TS2a** and **TS2b:**

$$\Delta G_{eff} = -RTln\left(\sum_{i}^{conformers} e^{-\Delta G_i/RT}\right)$$

where R is the ideal gas constant, T is the temperature (263.15 K) and $\Delta G_i$ is the migratory insertion activation barrier for each conformer with respect to **5.82**, the Ni(II) resting state prior to migratory insertion (Table 5.S6). The effective Gibbs energy is used to take the contribution of all unique conformers into account. The computed $\Delta G_{eff}$ values of **TS2a** and **TS2b** are 5.35 kcal/mol and 6.36 kcal/mol, respectively. Since the migratory insertion is the enantioselectivity-determining step, the e.r. was computed from the effective Gibbs free energies using the Eyring equation and determined to be 87:13 favoring the (*S*) enantiomer of the product, which is in agreement with the experimental enantioselectivity (e.r. = 88:12).

***Table 5.S6.*** Migratory insertion energy barrier values for all unique conformers computed at the DFT level.

| **TS2a** conformers | $\Delta G_i$ (kcal/mol) | **TS2b** conformers | $\Delta G_i$ (kcal/mol) |
|---|---|---|---|
| **TS2a** | 5.63 | **TS2b** | 6.85 |
| **TS2a-1** | 6.18 | **TS2b-1** | 6.89 |
| **TS2a-2** | 6.38 | **TS2b-2** | 7.61 |
| **TS2a-3** | 7.23 | **TS2b-3** | 7.71 |
| **TS2a-4** | 7.43 | **TS2b-4** | 8.40 |
| **TS2a-5** | 7.73 | **TS2b-5** | 8.54 |
| **TS2a-6** | 7.88 | **TS2b-6** | 9.04 |
| **TS2a-7** | 8.54 | **TS2b-7** | 9.11 |
| **TS2a-8** | 8.88 | **TS2b-8** | 9.19 |
| **TS2a-9** | 8.91 | **TS2b-9** | 9.19 |

| | | | |
|---|---|---|---|
| **TS2a-10** | 9.03 | **TS2b-10** | 9.26 |
| **TS2a-11** | 9.19 | **TS2b-11** | 9.28 |
| **TS2a-12** | 9.33 | **TS2b-12** | 9.53 |
| **TS2a-13** | 9.47 | **TS2b-13** | 9.54 |
| **TS2a-14** | 9.57 | **TS2b-14** | 9.63 |
| **TS2a-15** | 9.84 | **TS2b-15** | 10.23 |
| **TS2a-16** | 10.10 | **TS2b-16** | 10.86 |
| **TS2a-17** | 10.51 | **TS2b-17** | 10.89 |
| **TS2a-18** | 11.16 | **TS2b-18** | 10.94 |
| **TS2a-19** | 16.67 | **TS2b-19** | 12.07 |
| **TS2a-20** | 19.94 | **TS2b-20** | 13.76 |
| **TS2a-21** | 20.69 | **TS2b-21** | 15.22 |
| **TS2a-22** | 20.93 | **TS2b-22** | 15.28 |
| **TS2a-23** | 21.78 | **TS2b-23** | 16.10 |
| **TS2a-24** | 22.01 | **TS2b-24** | 16.47 |
| **TS2a-25** | 22.01 | **TS2b-25** | 16.49 |
| **TS2a-26** | 22.62 | **TS2b-26** | 16.63 |
| **TS2a-27** | 23.78 | **TS2b-27** | 17.91 |
| **TS2a-28** | 23.92 | **TS2b-28** | 19.72 |
| **TS2a-29** | 24.24 | **TS2b-29** | 20.60 |
| **TS2a-30** | 26.67 | | |

**Alternative Transmetalation and Reductive Elimination Pathways**

Several alternative transmetalation and reductive elimination transition states were considered computationally (Figure 5.S7). An alternative transmetalation transition state, **TS3a**, in which the Bn-biOx ligand does not completely dissociate from the nickel center is 23.8 kcal/mol less stable than **TS3**. The dissociation of the directing group in the reductive elimination transition state (**TS4a**) is 7.4 kcal/mol less favorable than the transition state with the directing group bound to the nickel center (**TS4**).

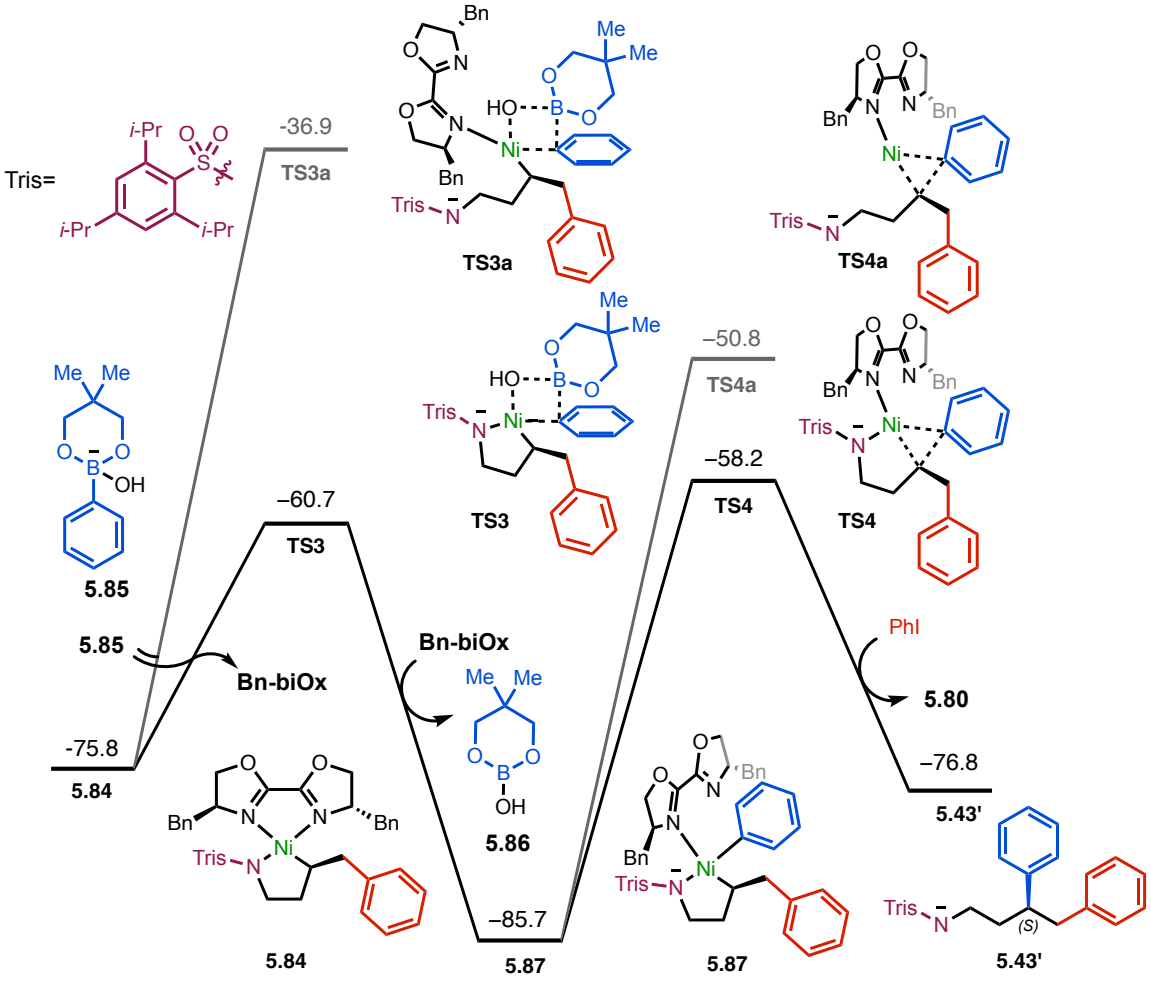


***Figure 5.S6.*** Alternative transmetalation and reductive elimination pathways.

Since $Ni(cod)_2$ is used as a precatalyst, we investigated the possibility of reductive elimination transition states with COD replacing the Bn-biOx ligand (**TS4b**) or with both the COD and Bn-biOx ligands coordinated to the nickel (**TS4c**). These reductive elimination transition states are less favorable than **TS4** supported by the Bn-BiOx ligand.

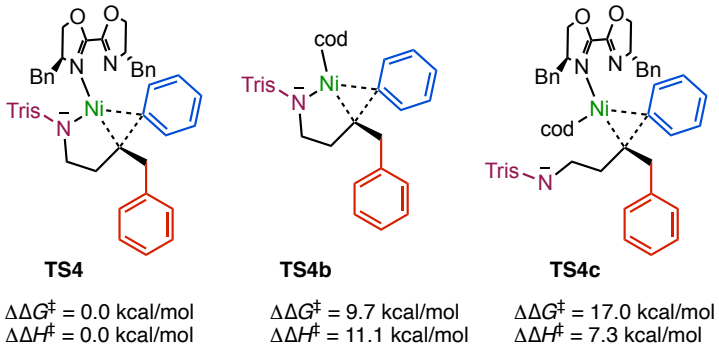


***Figure 5.S7.*** Other possible reductive elimination transition states. All Gibbs free energies and enthalpies are with respect to the most stable transition state **TS4**. The COD ligand has a monodentate coordination in **TS4b** and **TS4c**.

### Transmetalation with Phenylboronic Acid

The reactivity difference of phenylbronic acid and phenylboronic ester [PhB(nep)] in transmetalation was investigated computationally (Figure 5.S8). Transmetalation with (trihydroxy)phenylboronate **8.85'** via **TS5** requires a 1.3 kcal/mol higher barrier than the transmetalation with the phenylboronate ester **8.85** via **TS3.**

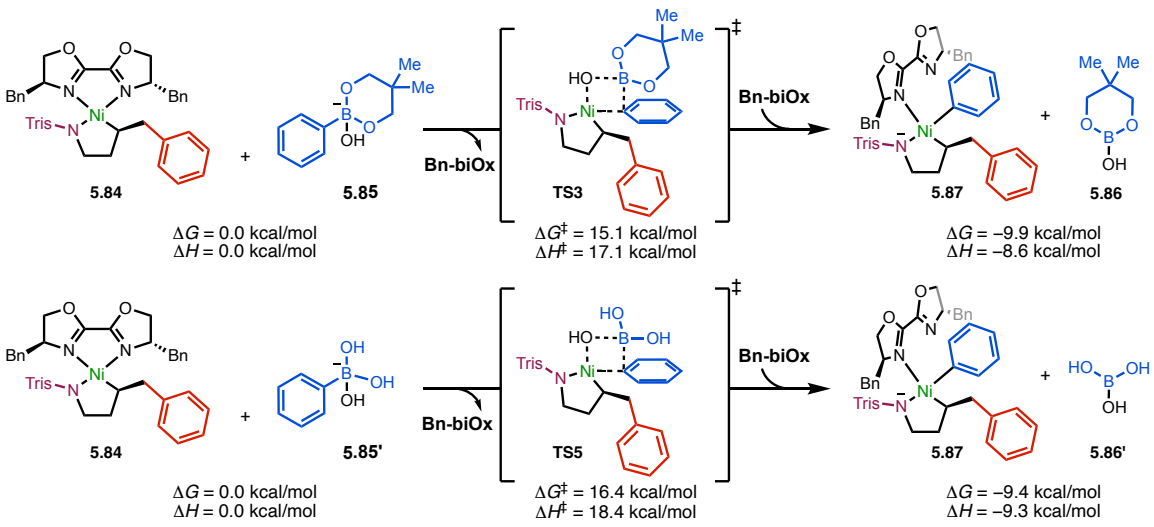


***Figure 5.S8.*** Computed transmetalation pathways with boronic acid and boronic ester. All Gibbs free energies and enthalpies are with respect to Ni(II) complex **5.84**.

## Isomers of the Reactant Oxidative Addition Complex

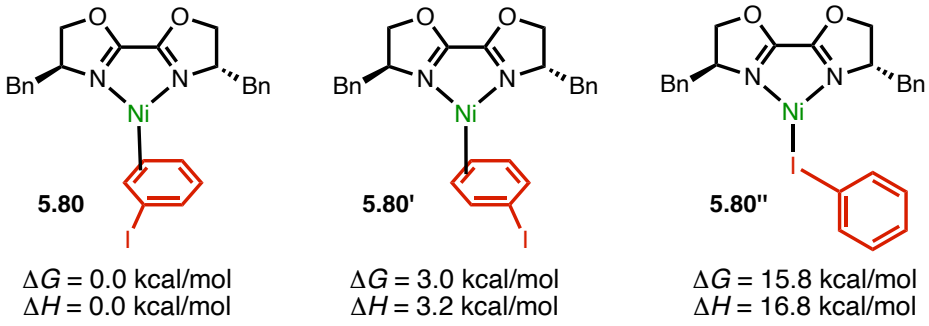


***Figure 5.S9.*** Isomers of the phenyl iodide–Ni(0) reactant complex.

## REFERENCES

(1) (a) Pracht, P.; Bohle, F.; Grimme, S. Automated Exploration of the Low-Energy Chemical Space with Fast Quantum Chemical Methods. *Phys. Chem. Chem. Phys.* **2020**, *22*, 7169–7192. (b) Bannwarth, C.; Ehlert, S.; Grimme, S. GFN2-xTB–An Accurate and Broadly Parametrized Self-Consistent Tight-Binding Quantum Chemical Method with

Multipole Electrostatics and Density-Dependent Dispersion Contributions. *J. Chem. Theory Comput.* **2019**, *15*, 1652–1671.

(2) For a computational study using a similar conformer sampling approach, see: Yepes, D.; Neese, F.; List, B.; Bistoni, G. Unveiling the Delicate Balance of Steric and Dispersion Interactions in Organocatalysis Using High-Level Computational Methods. *J. Am. Chem. Soc.* **2020**, *142*, 3613–3625.

(3) Luchini, G.; Alegre-Requena, J. V.; Funes-Ardoiz, I.; Paton, R. S. GoodVibes: Automated Thermochemistry for Heterogeneous Computational Chemistry Data. F1000Res. 2020, 9, 291. Version 3.0.2.

(4) Sinnokrot, M. O.; Sherrill, C. D. Substituent Effects in π−π Interactions: Sandwich and T-Shaped Configurations. *J. Am. Chem. Soc.* **2004**, *126*, 7690–7697.

(5) Guan, Y.; Ingman, V. M.; Rooks, B. J.; Wheeler, S. E. AARON: An Automated Reaction Optimizer for New Catalysts. *J. Chem. Theory Comput.* **2018**, *14*, 5249–5261.

# Omar Apolinar

oapoli@scripps.edu

**Current Address**
The Scripps Research Institute
10550 N. Torrey Pines Rd.
La Jolla, CA 92037

**Permanent Address**
507 Rush Dr. Apt 39
San Marcos, CA 92078
760.402.0272

## Education:

**University of Oxford**, Lincoln College, Oxford, UK.
D.Phil. in Biochemistry, August 2019–November 2024 (expected)
Research Advisors: Simon Aldridge, D.Phil. and Veronique Gouverneur, Ph.D. (co-supervisor)

**The Scripps Research Institute**, Skaggs Graduate School of Chemical and Biological Sciences, La Jolla, CA, USA.
Ph.D. in Chemistry, August 2019–November 2024 (expected)
Research Advisor: Keary M. Engle, Ph.D., D.Phil.

**California State University San Marcos**, San Marcos, CA, USA.
B.S. in Biochemistry, May 2019 (*summa cum laude*)
Research Advisor: Robert G. Iafe, Ph.D.

**San Marcos High School**, San Marcos, CA, USA.
Graduated in June 2015

## Academic Honors and Awards:

**National Science Foundation Graduate Research Fellowship** 2019
Awarded to outstanding young scientists pursuing doctoral studies.

**Skaggs–Oxford Scholarship**
Provides funding for a joint 5-year program dual degree program at Scripps Research and Oxford 2019

**CSUSM Department of Chemistry & Biochemistry Outstanding Faculty Student Collaboration Award** 2019
Awarded for outstanding faculty and student scholarly collaborations.

**CSUSM Department of Chemistry & Biochemistry Outstanding Senior in Biochemistry** 2019
Awarded to the top graduating senior in biochemistry.

**CSUPERB President's Commission Scholar Award**
Awarded to 11 CSU undergraduates in support to kickstart biotechnology-related research experience. 2017

## Mentored Publications (Undergraduate and Graduate):

12. **Apolinar, O.**; Struijs, J. J. C.; Sarkar, D.; Gouverneur, V.; Aldridge, S. "Nucleophilic Fluoride Anion Delivery from Triazacyclononane-Supported Molecular Ca–F Complexes." *Angew. Chem. Int. Ed.* **2024**, e202414790.
11. Kang, T.[†]; **Apolinar, O.**[†]; Engle, K. M. "Ni- and Pd-Catalyzed Enantioselective 1,2-Dicarbofunctionalization of Alkenes," *Synthesis* **2024**, *56*, 1–15. ([†]Authors contributed equally)
10. **Apolinar, O.**[†]; Kang, T.[†]; Alturaifi, T. M.; Bedekar, P. G.; Rubel, C. Z.; Derosa, J.; Sanchez, B. B.; Wong, Q. N.; Sturgell, E. J.; Chen, J. S.; Wisniewski, S. R.; Liu, P.; Engle, K. M. "Three-Component Asymmetric Ni-Catalyzed 1,2-Dicarbofunctionalization of Unactivated Alkenes via Stereoselective Migratory Insertion," *J. Am. Chem. Soc.* **2022**, 144, 19337–19343. ([†]Authors contributed equally)
9. Li, Z.-Q.; **Apolinar, O.**; Deng, R.; Engle, K. M. "Directed Markovnikov Hydroarylation and Hydroalkenylation of Alkenes Under Nickel Catalysis."*Chem. Sci.* **2021**, *12*, 11038–11044.
8. Kleinmans, R.[†]; **Apolinar, O.**[†]; Derosa, J.; Karunananda, M. K.; Li, Z.-Q.; Tran, V.T.; Wisniewski, S. R.; Engle, K. M. "Nickel-Catalyzed 1,2-Diarylation of Alkenyl Ketones: A Comparative Study of Carbonyl-Directed Reaction Systems." *Org. Lett.* **2021**, *23*, 5311–5316. ([†]Authors contributed equally)
7. Liu, M.; Tang, T.; **Apolinar, O.**; Matsuura, R.; Bussaca, C. A.; Qu, B.; Fandrick, D. R.; Zatolochnaya, O. V.; Senanayake, C. H.; Song, J. J.; Engle, K. M. "Atom-Economical Cross-Coupling of Internal and Terminal Alkynes to Access 1,3-Enynes." *J. Am. Chem. Soc.* **2021**, *143*, 3881–3888.
6. Kim, N.; Tran, V.T.; **Apolinar, O.**; Eastgate, M. D.; Wisniewski, S. R.; Engle, K. M. "Ni(COD)(DMFU): A Heteroleptic 16-Electron Precatalyst for 1,2-Diarylation of Alkenes." *Synlett* **2021**, 32, 1570–1754.
5. Wethman, R.; Derosa, J.; Tran, V.T.; Kang, T.; **Apolinar, O.**; Abraham, A.; Kleinmans, R.; Wisniewski, S. R.; Coombs, J. R.; Engle, K. M. "An Under-Appreciated Source of Reproducibility Issues in Cross-Coupling: Solid-State Decomposition of Primary Sodium Alkoxide Salts." *ACS Catal.* **2021**, *11*, 502–508.
4. **Apolinar, O.**; Tran, V.T.; Kim, N.; Schmidt, M. A.; Derosa, J.; Engle, K. M. "Sulfonamide Directivity Enables Ni-Catalyzed 1,2-Diarylation of Alkenyl Amines." *ACS Catal.* **2020**, *10*, 14234–14239.
3. Derosa, J.; **Apolinar, O.**; Kang, T.; Tran, V. T.; Engle, K. M. "Recent Developments in Nickel-Catalyzed Intermolecular Dicarbofunctionalization of Alkenes." *Chem. Sci.* **2020**, *11*, 4287–4296.

2. Tran, V. T.; Li, Z.; **Apolinar, O.**; Derosa, J.; Wisniewski, S. R..; Eastgate, M. D.; Engle, K. M. "Ni(COD)(DQ): An Air-Stable 18-Electron Ni(0)–Olefin Precatalyst."*Angew. Chem. Int. Ed.* **2020**, *132*, 7095–7100.
1. Nimmagadda, S. K.; Liu, M.; Karunananda, M. K.; Gao, D.-W.; **Apolinar, O.**; Chen, J. S.; Liu, P.; Engle, K. M. *Angew. Chem. Int. Ed.* **2019**, *58*, 3923–3927.

## Presentations (Undergraduate and Graduate):

**Poster Presentations:**

| | |
|---|---|
| 257th ACS National Expo & Meeting, Orlando, FL | 2019 |
| 31st Annual CSU Biotechnology Symposium, Anaheim, CA | 2019 |
| Southern California Conferences for Undergraduate Research (SCCUR), Pasadena, CA | 2018 |
| Scripps Research Student Poster Symposium, La Jolla, CA | 2018 |
| 21st Annual UW McNair Conference, Seattle, WA | 2018 |
| 30th Annual CSU Biotechnology Symposium, Santa Clara, CA | 2018 |

## Mentored Research Activities:

**Synthesis and Reactivity of Nucleophilic Ca–F Complexes with Oxygenic Ligand Frameworks**, August 2022–Current.
*Department of Chemistry, The University of Oxford, Oxford, UK.*

Effectuated main group organometallic chemistry in the research group of Professor Simon Aldridge (co-supervised by Professor Veronique Gouverneur) with the goal of attaining a solubilized Ca–F complexes that would be a molecular chemical analogue of $CaF_2$ and then explore its reactivity to synthesize organofluorine compounds. Specific aims included synthesizing a variety of ligands and Ca complexes using air-sensitive techniques and developing crystallizing methods for purification or single crystal X-ray diffraction. Other specific aims included reactivity studies of furnished Ca–F complexes with detailed analysis via NMR spectroscopy.

**Ni-Catalyzed Alkene Difunctionalization Utilizing Substrate Directivity**, August 2019–July 2022.
*Department of Chemistry, The Scripps Research Institute, La Jolla, CA, USA.*

Developed organometallic methodology in the research group of Professor Keary M. Engle using native directing groups for 1,2-dicarbofunctionalization of non-conjugated alkenes under nickel catalysis. Specific aims included synthesizing and analyzing new synthetically useful directing groups for increased reactivity and enantioselectivity.

## Work Experience:

**Discovery Process Chemistry Research Intern**, June 2019–August 2019
*Department of Discovery Process Chemistry, Janssen, La Jolla, CA, USA.*

Optimized an asymmetric hydrogenation method of heteroaryl ketones and evaluated substrate scope.

**STEM Peer Educator**, January 2017–May 2019.
*California State University San Marcos, San Marcos, CA, USA.*

Guided students in achieving independent learning in core undergraduate biology, chemistry, and physics courses.

## Volunteer and Outreach Experience:

**ACS Chemistry Expo: Marvelous Metals**, October 2019
*San Diego Miramar College, CA, USA.*

Helped run a chemistry demonstration exposing youth in San Diego to chemistry.

**St. Mark's Food Pantry Co-lead,** June 2013–July 2019
*St. Mark's Catholic Parish, San Marcos, CA, USA.*

Led volunteer training and general operation of the food pantry.

## Professional Organizations, Honorary Societies, and Affiliations:

**American Chemical Society**, Member
**Ronald E. McNair Postbaccalaureate Achievement Program**, McNair Scholar

## Personal Information:

**Ethnicity**: Hispanic
**Languages**: English (fluent), Spanish (fluent).
**Interests**: Athletics (soccer)

## References:

**Keary M. Engle**, Ph.D.
Professor, Department of Chemistry
The Scripps Research Institute
10550 N. Torrey Pines Road
BCC-169

La Jolla, CA 92037
keary@scripps.edu
(858) 784-7885

**Simon Aldridge**, DPhil
Professor, Department of Chemistry
University of Oxford
Chemistry Research Laboratory
Mansfield Road, Oxford OX1 3TA, UK
simon.aldridge@chem.ox.ac.uk
+44 01865 285201

**Veronique Gouverneur**, Ph. D.
Professor, Department of Chemistry
University of Oxford
Chemistry Research Laboratory
Mansfield Road, Oxford OX1 3TA, UK
Veronique.gouverneur@chem.ox.ac.uk
+44 01865 275644

**Brett Allison**, Ph.D.
Senior Scientist, Discovery Process Research
The Janssen Pharmaceutical Companies of Johnson & Johnson
3210 Merryfield Row,
San Diego, CA 92121
BAllison@its.jnj.com
(858) 320-3339

**Dan Pippel**, Ph.D.
West Coast Regional Head, Discovery Process Research
The Janssen Pharmaceutical Companies of Johnson & Johnson
3210 Merryfield Row,
San Diego, CA 92121
DPippel@its.jnj.com
(858) 784-3249